National Technical University of Athens

Doctoral Thesis

Thermophysical Modelling of Cryogenic ^4He, ^3He and mixtures. Modelling of cryocoolers near absolute zero.

Author: George-Rafael Domenikos

Supervisor:Prof. Emmanouil Rogdakis

A thesis submitted in fulfillment of the requirements for the degree of Doctor of Philosophy

in the

Laboratory of Applied Thermodynamics
School Mechanical Engineering

Declaration of Authorship

I, George-Rafael DOMENIKOS, declare that this thesis titled, Thermophysical Modelling of Cryogenic ^4He, ^3He and mixtures. Modelling of cryocoolers near absolute zero. and the work presented hereto, is my own. I confirm that:

- This work was done wholly or mainly while in candidature for a research degree at this University.
- Where any part of this thesis has previously been submitted for a degree or any other qualification at this University or any other institution, this has been clearly stated.
- Where I have consulted the published work of others, this is always clearly attributed.
- Where I have quoted from the work of others, the source is always given. With the exception of such quotations, this thesis is entirely my own work.
- I have acknowledged all main sources of help.

Signed:

Date:

The universe is bound to end in absolute cold and silence.
For now let's get to know the cold...

NATIONAL TECHNICAL UNIVERSITY OF ATHENS

Abstract

Thermal Engineering Sector
School Mechanical Engineering

Doctor of Philosophy

Thermophysical Modelling of Cryogenic ^4He, ^3He and mixtures. Modelling of cryocoolers near absolute zero.

by George-Rafael DOMENIKOS

The aim of the author of this thesis has been to provide a theoretical foundation for the workings of fluids and superfluids at temperatures close to absolute zero, with an added emphasis on the physical and thermodynamical behavior of Helium in its two isotopes, while offering new knowledge and explaining some of the phenomena occurring at these temperatures. The existing knowledge about the behaviors of superfluids has been documented, giving an up-to-date understanding of their workings. New equations of state that have been in greater agreement with the available experimental data have been established for both isotopes. A different approach to the explanation of superfluidity has been formed as a part of this work, where by splitting the partition function into an ideal and non-ideal part, a macroscopic connection between the phenomena of superfluidity and the Bose-Einstein condensation is presented. This approach has been used in conjunction with the previously defined EOS to showcase its validity when compared with the experimental data and then used to extend the reach of these EOS below their limiting threshold of the lowest values of the experimental data.

This theoretical work has been the foundation for the development of applications in the forms of novel cryocooler designs and their simulation in CFD environments for achieving temperatures near absolute zero. A modelization of a Superfluid Stirling Refrigerator (SSR) reaching temperatures down to 0.3K has been established, where 1D and 3D simulations for this design have been carried out. In particular, a model for handling superfluids within the ANSYS Fluent software has been established, which showcases how the presented EOS can be inserted in the program. Furthermore, it displays the application of superfluids in a CFD environment for the first time. By this simulation there has been no need for the usual simplifications used in models relating to supefluids, neglecting many of their behaviors. Thus, the results that have been produced seem to be in better agreement with the existing experimental data. This model has also been used to find the optimal working conditions of this type of cryocoolers as well as to present their cooling power-to-rpm and efficiency-to-rpm behaviors.

Acknowledgements

This work has been the outcome of a long and zealous endeavor. However, finalizing this work is not only a personal achievement, but it is also attributed to a great extent to the people that have helped me and guided me through my years of study. Since a early age I have had a certain affinity and curiosity towards more peculiar and exotic parts of science, which back then looked to my eyes like magic. Cryogenics is possibly the closest to be reached in order to see and directly interact with the unfathomable chaos of the microscopic quantum world in our macroscopic world. For this reason, I have always been interested in pursuing it, not only as my Ph.D. topic, but as a diploma thesis prior to that.

I am extremely grateful to my supervisor Professor Emmanouil Rogdakis for his much valued support and assistance in order to complete this research. He is also the one who gave me the opportunity to engage myself into this unique subject and try to merge thermodynamics, physics and engineering in one undertaking. His vast knowledge and experience has been obvious in every part of this project. Moreover, I should not fail to mention his vast knowledge of all scientific endeavors even beyond his specialty (including theoretical physics and mathematics). Professor Rogdakis' knowledge and guidance have been of paramount importance and will always be an integral part of me as a scientist and a person. Additionally, I have to thank my mother, Aimilia Eleftheriou, Director of Arsakeio Tositseio School, and my father, Dr. Harris Domenikos, Mechanical Engineer NTUA, both of who have given me the opportunity to understand the importance of the constant and unending pursuit of knowledge through one's lifetime. My father has been the one to set the cornerstones for all my scientific achievements, as he first led me into the workings of science and mathematics.

Moreover, a special place in the acknowledgements of this work needs to be given to my colleagues during my Ph.D. years, Dr. George Dogkas and Dr. Panagiotis Bitsikas, to Dr. George Antonakos and Dr. Neofytos Komninos, as well as to Professor Irene Koronaki, who have all provided me with great help and insight of utmost importance for the completion of many parts of the current work. I am also grateful to my high school physics teacher Ioannis Vakalopoulos, who inspired me into pursuing the sciences and actually introduced me to my current field of specialty, Thermodynamics.

Contents

Dedicated to my Father

Chapter 1

Introduction

1.1 Low Temperature Thermodynamics

Since the very beginning of science many have searched into the concept of temperature even as early as Aristotle who, through his works *Meteorology* ($Μετεορολογικα$) and *On the Universe* ($Περι\ Κοσμου$), tried to set an understanding about the nature of temperature. Of course, these first tries in explaining the mysteries of temperature were flawed in many areas, but do provide great insight on how a human interacts with such concepts. For centuries only empirical scales of temperature could be used, which while helpful in the everyday life and many applications, lacked the ability to conceive many hidden phenomena in the nature of temperature. The first absolute temperature scale was offered by Lord Kelvin [1] when the nature of absolute zero was theoretically shown and as such for the first time humanity acknowledged one of the limits of temperature. The Kelvin temperature scale differed in its core from the previous temperature scales as it had been the first one that was defined through the kinetic theory of particles rather than macroscopical observations of materials. Much more recently, it was shown that temperature also has a highest limit in the form of the Planck Temperature (10^{32}K), after the discovery of quantum mechanics and relativity, though these higher temperatures are not within the scope of this research.

In the late 19^{th} and early 20^{th} centuries, after this establishment of the absolute temperature a "race" to absolute zero began with many scientists and researchers trying to achieve lower and lower temperatures by the liquefaction of different gases. Zygmunt Florenty Wróblewski was the one to liquefy Nitrogen in 1883 and Hydrogen in 1885 and Heike Kamerlingh Onnes being the first to liquefy Helium in 1908. Helium had been known even at that time to be the element with the lowest boiling point of all. After the creation of liquid Helium, attempts were made to reach even lower temperatures with it and maybe achieve absolute zero or its solidification. When further attempts to cool Helium were made it was quickly discovered that below a certain temperature, liquid Helium did not behave as a normal fluid. This different behavior was first discovered by Pyotr Kapitsa [2], John F. Allen, and Don Misener [3] in 1937. This was the phenomenon of superfluidity, a phenomenon for which many different theories and models were formed over the 20^{th} century as to finally reach a mathematical and physical explanation of its behaviors. This phenomenon has so far been observed only in the two isotopes of Helium and has also been theorized to be true in parahydrogen (spin isomer of Hydrogen) without thus far having an experimentally proven existence in this element.

The phenomenon of superfluidity was quickly thought of having some relation with the theoretical state of matter being the Bose-Einstein condensate (BEC). This theoretical, up to that point of time, state of matter had been predicting that at low enough

temperatures all the particles of an ideal gas, obeying the Bose-Einstein statistics, would be at the same energy state. This means that being quantum particles they are governed by the same wave function, and therefore they all behave in a singular but quantum way. Accordingly, one would expect that if such a BEC was ever to be formed quantum behaviors could be observed macroscopically in the system. Some of these quantum behaviors include the free flow of the particles of the fluid, given the no interactions between them as they all are at the ground state. Hereto, this fact in combination with the low temperature restriction in both cases seemed to be directly connecting superfluidity with Bose-Einstein condensation. However, this connection was only theoretical, since the rest of the criteria for a BEC were not met by Helium, as even at its superfluid state interatomic interactions do take place. A different degenerated model based on the ideal of Bose-Einstein condensates needed to be formed. The existence of BECs had for nearly all the 20^{th} century been only theoretical, only to be experimentally proven by Anderson et al [4] in 1995. In their work it was for the first time proven that a BEC does occur as they experimentally showed by cooling dilute alkaline gases in the temperature range of pK. This was a remarkable achievement in the field of cryogenics as now the fifth state of matter, namely the BEC, was experimentally verified to exist for the first time. The BECs that have been produced to this day have achieved temperatures even lower, with the current lowest achieved temperature being at $38pK$ [5]. Those experiments, in addition to great theoretical insight about the behaviors near absolute zero, also provided the technical knowledge about achieving these temperatures by the use of laser trapping, an unprecedented method able to cool a few thousands of atoms to such low temperatures [6].

In the second half of the 20^{th} century more research was put into the thermodynamic behaviors of cryogenic elements and materials as many applications in need of these temperature ranges began to arise. One of the most important of such applications has been superconductivity. Superconductors are metals that, when at a low enough temperature, exhibit zero electric resistance. Elemental superconductors such as copper enter their superconducting phase at around 1.8K. Thus, a lot of research was put into both understanding the mechanics and the physics behind the phenomenon of supercoductivity and its possible relation with superfluidity. Furthermore, scientist and engineers also worked towards the development of cryocoolers that could achieve those temperatures for being able to capitalize on the phenomenon of superconductivity. Other applications that present the need for such low temperatures include particle detectors, as the levels of accuracy needed are so high that even the thermal noise of higher temperatures is orders of magnitude higher than the values themselves. Lastly, one modern application that actually requests the existence of nearly the lowest possible temperatures is the quantum computer. The chipset of a quantum computer works with q-bits (or quantum bits) that need to keep their quantum nature in order to be able to use the phenomenon of superposition. Using this attribute, the q-bits can participate in multiple calculations at the same time, which makes this type of computers infinitely faster than current supercomputers. To achieve the aforementioned behavior the wavefunction of the q-bits cannot be allowed to collapse by having any interaction whatsoever with outside forces, including thermal interactions. For this reason, the chipset of quantum computers needs to be held at temperatures lower than $1mK$.

1.2 Helium

Helium is the substance with the lowest known boiling point, at 4.2K, and is known to form a superfluid. Also, Helium does not solidify ever under atmospheric pressure. Solid Helium can form but this can only be achieved at pressures of around $22atm$. Thus, Helium is the only known substance to not have a triple point. The fact that it remains a liquid at such low temperatures gives it the ability to form a superfluid. Also, the existence of a supersolid has been theorized and some experimental data that support its existence exist. This is something that is still very controversial and many researchers on the subject disagree about its existence. The superfluid has some unique behaviors that differentiate it from a normal fluid, but not so far as for it to be described as new state of matter. The most obvious difference in the behavior of the superfluid is that it has zero viscosity, meaning that it can flow freely only under the force of its own inertia and surface tension.

Superfluidity as a phenomenon in Helium is a major part of this thesis, but a brief introduction to the nature and study of superfluidity over the years will also be provided here. From the beginning of the discovery of superfluidity in Helium-4 it was suggested that the nature of the phenomenon ought to be closely related to the Bose-Einstein condensation. The first explanations by Tisza [7] tried to introduce a two fluid model, where one part of the liquid Helium-4 (referred in this approach as the superfluid part) was behaving like a BEC and the rest of the liquid behaved like a normal fluid. While this theorization had merit as an idea, it failed to mathematically comply with the requirements of Bose-Einstein condensation given the interatomic interactions in Helium and as such no complete theory, nor equation of state was produced following this approach. The great insight on the behavior and physics of superfluids came by London and Landau, who showed that superfluidity as a phenomenon can be explained by studing the quantum excitations of the liquid. They also showcased that beyond a temperature threshold not enough energy exists in parts of the fluid for a percentage of the particles to achieve any excitation levels above the ground state and thus be able to interact. The thermodynamic behavior of the superfluid is attributed only to its excitations, which are formulated as different particles, called quasiparticles. Hence, this approach is sometimes for the sake of time referred to as the quasiparticle approach. This approach has been massively more successful than the two-fluid approach, as it is able to describe the exact physical behavior of superfluid Helium-4 and through experimental values for the energies of the quasiparticles it can produce the equations of state for Helium-4, currently used in most cryogenic applications. The only drawback that one might point out in this theory is its relative failure to directly connect superfluidity with Bose-Einstein condensation, although some might argue that this entire method is nothing more than a degenerated Bose-Einstein condensation theory for strongly interacting fluids. In this work a possible theory directly connecting the phenomenon of superfluidity with a theoretical non-degenerated Bose-Einstein condensation will be presented in following sections.

In all of the above Helium-4 is kept in mind as the sole isotope of Helium due to its overwhelmingly higher natural abundance [8], with it accounting for more than 99.9% of all natural Helium. Despite this, a second naturally stable isotope of Helium exists, Helium-3. This isotope has very different properties and has been seen to also have massive importance in cryogenic applications. Helium-3 consists of two protons and one neutron in its core. Given the half-integer spin of these hadrons the Helium-3 isotope

also has half-integer spin and therefore obeys the Fermi-Dirac statistics instead of the Bose-Einstein statistics that the Helium-4 does. This means any ideas about connections theoretical or practical to Bose-Einstein condensation needed to be heavily reworked upon. To understand the nature of superfluidity in Helium-3, knowledge from the subject of superconductivity was drawn. In a few words, for a metal to become a superconductor, the electron gas within it forms a Bose-Einstein condensate. The electrons also have half-integer spin. To overcome this problem the BCS theory of Cooper pairs was formed [9]. In this theory, simply put, pairs of fermions are considered to be entangled, giving the pair an integer spin, and making it behave as a boson. Using this fact, the Bose-Einstein condensation of these pairs is derived showing that a BEC indeed forms in the electron gas. A similar approach to this has been used to explain the behavior in Helium-3 although mathematically it has not been so rigorously studied as the superfluidity in Helium-4. In this study a more in-depth mathematical approach about this Bose-Einstein condensation in Helium-3 will be presented, showcasing that in Helium-3 too a theoretical connection between Bose-Einstein condensation and superfluidity can be established.

This difference in the statistical/physical behavior of Helium-3 means that its thermodynamic behaviors are also very different than the ones of Helium-4. The lambda transition to superfluidity in Helium-3 is in the order of $10^{-3}K$ in comparison to the $2.17K$ lambda temperature of Helium-4. This has great significance in cryogenic applications and cooling cycles. The excitations in Helium-4 have been almost completely eradicated below 1 K, meaning that its potential to be used as a cooling medium has been completely depleted. This is not the case for Helium-3 which remains a normal fluid until much lower temperatures. Thus, for cooling devices concerning temperatures below 1 K the use of Helium-3 is almost mandatory.

In addition to the two pure isotopic liquids of Helium, their mixture is also commonly used in cryogenic apparatuses. The difference between the lambda temperatures of the two isotopes means that in the mixture there are bound to be at least 3 phases. The first phase will be with both isotopes being in a normal fluid form, the second for the mixture to be below the lambda line of Helium-4 (with the Helium-4 part being a superfluid and the Helium-3 being a normal fluid) and a third case where both are superfluids. Due to the extremely low temperature requirements for Helium-3 to become a superfluid the mixture is never used when superfluid Helium-3 temperatures are reached. Near the lambda line of Helium-3, the Helium-4 will have been thermodynamically inert for three orders of magnitude in the temperature scale. Experiments have shown that added to these regions, one other region exists, referred to as the forbidden region. In this region the mixture cannot form and it is split into two different parts of some fixed available consistencies, a phenomenon that actually proves to be of great use in many applications. The behavior of the mixture will be studied extensively in following chapters.

1.3 Cryocoolers

In modern years a need for temperatures close to absolute zero in many applications has arisen. Applications of common use (like MRI scanners) to extremely high tech ones (like the CERN supercollider) require very low temperatures to operate. For these temperatures to be achieved many scientists have worked towards creating cooling machines, which, with their corresponding working media, are able to create such low temperature

environments. This field of cooling to low temperatures is generally referred to as cryogenics, including anything from liquid air to superfluid Helium. In this thesis the term cryogenics is going to be used when referring to temperatures of liquid Helium and below, as even liquid nitrogen, one of the most well known cryogenic media, actually exists in temperatures nearly two orders of magnitudes higher than superfluid Helium-4 [10].

For temperatures down to the lambda point of Helium-4, $\approx 2.18K$, usual cooling methods and thermodynamic cycles can apply like the Joule-Thomson expansion [11], the reverse Brayton cycle [12], mixed processes like the Claude cycle [13] etc. At temperatures below the lambda line of Helium-4 a lot of differentiations need to be made for the different thermodynamic cycles and traditional cooling methods to apply, due to the significantly different behaviors of the superfluid compared to the normal fluid as a working medium. One key feature that all the cooling machines below the lambda point must take into account is the zero viscosity of the superfluid and as such extreme care must be taken in order to prevent it from leaking. Additionally, from a thermodynamics point of view, the diminishing effectiveness of the superfluid needs to be accounted for, especially below 1 K, where despite Helium-4 remaining in a liquid form it is actually very close to being thermodynamically inert. Usual cycles for cooling apparatuses below the lambda point include the Joule-Thomson expansion, with little modification due to its nature as a process, the superfluid Stirling refrigerators (SSR), the dilution cycles and some other applications of lesser use. The superfluid Stirling refrigerator is an apparatus similar to a standard Stirling refrigerator with a specific difference in the design of the piston. At each piston a superleak is introduced, allowing only the superfluid part of the Helium to flow through it and therefore altering the distribution and consistency of the working medium at each step of the cycle. This procedure is used with a mixture of Helium-3 and Helium-4, for establishing a constant working medium in the form of Helium-3, which is not a superfluid in these temperature ranges. The SSR cryocoolers can achieve temperatures of around 0.3 K. For temperatures below this threshold the dilution cycle is generally used. The dilution cycle uses a Helium 3-4 mixture capitalizing on the inability of the mixture to exist in the forbidden region and creating cooling by the split of the two isotopes. Dilution comes the closest from all the traditional thermodynamic procedures to absolute zero with it being able to reach temperatures in the spectrum of 10^{-3}K or 10^{-4}K in some applications.

While the apparatuses like the SSRs and Joule-Thompson coolers are mostly used for larger scale cryogenic cooling, usually implemented to superconductors or large scale detectors, the dilution cycle is used for smaller applications. These smaller in size applications are to be of key importance in the years to come. The main application that the dilution cooler applies to is the cooling of quantum computers with all the current experimental ones running dilution refrigerators as their coolers.

Achieving temperatures below even the capabilities of dilution cooling is possible but requires completely different approaches and currently cannot be achieved for larger scales. According to the current literature no industrial or marketable need exists for such low temperatures, with the only applications of them being in experimental physics and especially in the formation of pure Bose-Einstein condensates, at temperatures in the millionths or lower of a K. These temperatures are achieved by the method known as laser cooling [6]. In laser cooling a laser trap is set and a few thousands of atoms are enclosed within it. Then the bounds of the trap are progressively lowered allowing only the higher energy atoms to escape from the trap. This procedure leads, when the bounds are lowered

enough, to a small percentage of the initial particles still remaining in the trap. These particles are the ones of the lowest temperature. The temperatures that can be achieved by this method are so low that the remaining particles are in the 5th state of matter, being a Bose-Einstein condensate. This technology is very interesting but given that these temperatures have no real applications and are not within the scope of an engineer, it will not be discussed further in this work.

1.4 Aim and Format of this study

Through this study the reader will receive a comprehensive description of the modelling of cryogenic Helium in both its pure isotopic forms and as a mixture, as well as be presented with the workings of Helium as a cryogenic cooling medium in applications aiming to achieve temperatures close to absolute zero. The sequence of the chapters is such as for the reader to be able to comprehend the workings of the models without much prior knowledge about cryogenic thermodynamics and physics.

For the description of any cooling apparatus to be initiated the first step is to have a clear view and understanding for the working medium. Thus, this study sets off to describe the behaviors of Helium at low temperatures. After the equations of state are derived, the models for the cryocoolers are developed and their results are shown. The thought sequence and methodology used in this work is briefly discussed below showcasing the main points of each of the chapters.

Chapter 2 - Physics of Superfluids
In Chapter 2 an initial explanation of the phenomenon of superfluidity is given, aiming for the reader to acquire an introductory understanding about the different approaches that have been used to describe superfluids and for them to comprehend the strengths and weaknesses of each theory. The two fluid-approach is discussed mathematically in this chapter and the equivalent Appendix A, while the mathematical description of the quasiparticle approach will be discussed in much greater detail in a later part of the study.

Chapter 3 - Helium 4
In Chapter 3 the presentation of the equations of state for Helium is initiated, describing the EOS of Helium-4 in this chapter. Firstly, an analysis of the quasiparticle approach based on the neutron scattering data of Brooks and Donnelly [14] is presented. Through this analysis equations describing the energies of the quasiparticles are developed which are shown to be of much greater accuracy compared to the ones of the literature. Following this, the thermodynamic variables are calculated through the energies of the quasiparticles using models statistical mechanics. These values are compared to the NIST database, where it is seen that this approach does not provide results of adequate accuracy. For this reason, a complete dataset for the data of Helium-4 is created based on connecting the data from different phases of many studies. Then an extensive code is developed to create a dynamic equation of state able to describe Helium-4 at cryogenic temperatures through all of its phases with an accuracy higher than other models published in the literature and being in the form of a continuous equation that is accurate in both values and derivatives able to correlate and thermodynamic variables with one-another. Using this, the first multiphase thermodynamic maps of Helium-4 are presented.

Chapter 4 - Entropic Lambda Transition
Over chapters 2 and 3 one will be able to understand two basic problems with the current understanding of superfluid Helium-4. Firstly, there is a general lack of a macroscopic and useful description of superfluidity in Helium and that due to this reason the available data and the presented equations of state of other studies have been limited to the experimental available data only, meaning that there is currently no description of Helium-4 below the temperature of 0.1K. These two issues are addressed in Chapter 4. In this chapter, a novel model connecting the macroscopical and microscopical view of the system is created and presented. Through this model two key observations can be made. Firstly, that by splitting the partition function into two parts, an interacting and an ideal, the superfluid transition in the overall Helium-4 to a theoretical Bose-Einstein condensation of the ideal part can be directly correlated. Then by calculating also the interacting part through the energies of the interactions one can have a theoretical description for the thermodynamic values of superfluid Helium-4 based on the values of the entropy calculated theoretically and as such being able to describe values going down even to absolute zero. Throughout this part it is shown that the behaviors of the model down to absolute zero have been the ones expected, as it predicts the coinciding of the isothermal and the isentropic lines, the zero entropy of the ideal part, which will have been totally condensed at 0K, as well as the existence of an interatomic potential at absolute zero, which has been theorised previously by London. Given this approach the data for below 0.1K have been created and inserted to the EOS of chapters 3 and later in 6.

Chapter 5 - Helium 3
Following the study of Helium-4 the study of the other stable isotope of Helium is presented, Helium-3. In Chapter 5 initially an equation of state of liquid Helium-3 is presented. Following the equation of state, the approach for the superfluid transition view through the partition function and the entropy is implemented on Helium-3. Unfortunately due to the scarcity of Helium-3 as a substance not a lot of experimental data are available and as such the implementation in Helium-3 with the available data cannot be as comprehensive as the one done in Helium-4. Despite this, through this method, the matching of the BEC temperature of the ideal part of the Helium-3 with the lambda transition point to superfluidity is shown. Additionally, during this process the BCS theory of Cooper pairs is implemented on Helium-3, where it is shown that the R2 universal constant of superconductivity holds true, meaning that the application of this theory holds sense in Helium-3.

Chapter 6 - Helium 3-4 Mixture
Having completed the equations of state of the two Helium isotopes and explained the physical differences between them, the equation of state and thermodynamic maps of the Helium 3-4 mixture are set as the aim of the next chapter, Chapter 6. In this chapter firstly the different phases that the mixture can exist in while at cryogenic temperature are explained. Then, by combining the data from the literature and using the equations of state for the pure isotopes from the previous chapters, a full database for the values of the different thermodynamic values is formed. Based on this form, a set of equations is derived for each of the variables, with the full code being presented in Appendix C. It can be seen that the accuracy of these equations is very high, and based on them a full set of thermodynamic maps of the Helium 3-4 mixture is presented. Due to the 3 independent

variables being the temperature, pressure and concentration of the mixture, an actual map would be 4-dimensional, something that is difficult to be presented in 2D in this study. For this reason, it is depicted as a series of 3D and 2D contour plots, some aiming to give the exact values and some others focusing on showcasing the overall behavior of the mixture. Additionally, while working on the mixture, the equation of the osmotic pressure is derived, which will end up being a very important part of the applications in cryocoolers using Helium 3-4 mixture as their working medium. Lastly, to aid in simulations using a cryogenic Helium 3-4 mixture the correlation between the overall volume of the mixture and the sum of the volumes of the two isotopes was found, where it was shown that this correlation is small, a fact that is heavily capitalized upon in the CFD simulations of the next chapters.

Chapter 7 - Solid Helium
In the previous chapter the research and models were focused on the fluid phases of Helium. A solid phase of Helium also exists, forming at pressures around 25 atm. Since the early days of the discovering of superfluidity people have questioned about the existence of other phases in Helium. The most commonly discussed is supersolid Helium. Up to this point it is not certain in the scientific community whether supersolidity is an actual phenomenon in Helium or a misinterpretation of some experimental results. Two experiments claim to have actually produced a supersolid. The first experiment in 2004 by Kim [15] was seen under great doubt in the scientific community and supersolidity remained a very questionable phenomenon. More recently in 2018 a second experiment was performed [16] which also showcased the existence of supersolidity. This experiment has been more widely accepted, though the uncertainty for the phenomenon still exists. This research does not take part in trying to determine whether supersolidity exists or not, but a theory is offered about the explanation of supersolidity if it is found to actually exist. In this theory the difference of the moment of inertia of the supersolid is explained as a superfluid of the vacuums of the crystal lattice of solid Helium. Inverse particles to the Helium atoms are theorized and then their BEC condensation temperature is calculated, showing that this would lead to a drop of the moment of inertia similar to the one shown in the experiments. This is not a complete theory of supersolidity by any sort but the calculations done under it so far have shown promise and given the latest experimental results, it seems to be worth pursuing further.

Chapter 8 - Superfluid Stirling Refrigerator 1D
Having established the equations of state for both the Helium-3 and Helium-4 isotopes now different cooling apparatuses that aim to achieve cryogenic temperatures can be studied and simulated. The main focus of this research will be around superfluid Stirling refrigerators. The superfluid Stirling refrigerator is similar to a standard Stirling cooler with some key differences considering the handling of the superfluid, as they will be discussed in greater detail in Chapter 8. Studying the literature, one will be able to see that the simulation and experimental data given for these apparatuses are scarce and most importantly in those simulations of the cryocoolers many simplifications are done in order to bypass the problems created from working with superfluids. Such simplifications include not working with the full EOS for the Helium mixture and assuming Helium-3 to be an ideal gas and the only cooling medium of the system, while the effects of the Helium-4 are neglected and it is considered totally thermodynamically inert. In this research I will

initiate from these assumptions and move forward towards much more realistic models working with the full equations of the Helium mixture and considering all the phenomena like the osmotic pressure and the superfluid ratio of the mixture. Firstly, a simplified model of an 1D single Stirling cooler is used with the medium being solely the Helium-3, using the isothermal model. This is done to compare to the existing simulations. Then, it is investigated how much deviation occurs between the isothermal model and the adiabatic model of the cooler, where it is seen that indeed the two models provide almost identical results. Then, conforming with the needs that have arisen in other studies as well, due to the lack of knowledge of the regenerative properties of the materials, a model of a dual Stirling refrigerator is developed and presented. In this model the regenerator is replaced with a common heat exchanger between two Stirling coolers, referred to as the recuperator. In the first attempt the approach of only the Helium-3 as an ideal gas for the working medium is used, and based on this the ideal phase difference between the two coolers and the cooling power and efficiency are calculated. Then, the procedure of developing models using the full equations of state of the mixture and the isotopes is developed. Firstly, again the 1D single cryocooler code is designed using the full EOS. It is seen in this that the phenomena are much more complex and due to this the code developed is much more elaborate and CPU bound, because it has to solve using the very extensive equations of the EOS. Lastly, the most accurate 1D simulation for the dual superfluid Stirling refrigerator with the full EOS is developed and shown. Through the models working with the EOS of the mixture, interesting results occur, such as the ovaloid behavior of the concentration of the mixture compared to the pressure or volume and the increase of the concentration value simultaneously in all the volumes of the machine. Also the efficiency and the cooling power are again calculated showing the effect of previously undocumented phenomena like the osmotic pressure and the dependency on the mixing properties of the two isotopes.

Chapter 9 - Superfluid Stirling Refrigerator 3D
The last major chapter of this study is Chapter 9. In this chapter to try and model the superfluid Stirling refrigerator in the best possible way a full 3D simulation was developed in ANSYS Fluent, where multiple cases were run in order to describe the full behavior of the machine and cross-validate with the 1D results. This has been to our knowledge the first published model of a superfluid description in a CFD environment. To achieve, this firstly a 3D schematic of the apparatus is drawn and then the important part of introducing the EOS to the ANSYS software is addressed. This is done in different steps, as it is explained in chapter 9, with the main idea being to use the small dependence of the volume to the consistency so as to find this consistency of the mixture, given the temperature and pressure, and then find in this way the energy values for that point. Through this, multiple cases are run where the optimal phase difference is found, being shown that it is close to the optimal phase difference produced by the 1D model. Also, it was established that the behavior of the flows was very similar in both models. Having established the optimal phase difference, an optimization for the rotational speed of the cooler was done, where a frequency of around 10Hz has been shown to produce the optimal results for efficiency and cooling power. Based on these cases the cooling power-to-frequency and efficiency-to-frequency have also been calculated and presented.

Chapter 2

Physics of Superfluids

Before one sets off to explain the superfluidity in Helium, first the basic mathematical concepts of superfluidity need to be explained to a certain depth, as for the reader to be able to understand the new concepts that will be introduced later in this study.

2.1 The two approaches to superfluidity

2.1.1 The two-fluid approach

In an effort to understand the peculiar behavior of liquid Helium below the lambda temperature the physicists, London and Tisza, established the idea that the superfluid has a direct connection to Bose-Einstein condensation. This idea was first proposed by London [17], who suggested that there was a direct connection between superfluidity and Bose-Einstein condensation. This idea was then further endorsed by Tisza in his works [7, 18, 19]. This connection between the two phenomena was phrased differently by the two scientists, with them agreeing on the central idea but not getting to the same conclusions. Tisza strongly suggested that a real Bose-Einstein condensate formed inside the superfluid, where one part of the liquid was in a BEC state and a second one remained a normal fluid. The position of London was to suggest that the superfluid itself was actually a degenerated form of a BEC. After years of many more scientists contributing to this matter, it is now known that the idea of London is much closer to reality than the suggestions of Tisza. In his later works London [20, 21] presented his finalized theory in the workings of superfluid Helium.

To understand the procedure of London one must first not work with Helium directly but refer to the ideal Bose gas, as this is the only possible candidate for the formation of a BEC. An ideal gas has the property of having no interatomic interactions. Ideal gases can be of two forms, the Fermi-Dirac ideal gas and the Bose-Einstein ideal gas . In the first case, due to the Pauli exclusion principle, a continuous behavior is followed going towards absolute zero, whilst in the case of Bose-Einstein ideal gases it is seen that a discontinuity appears in a specific temperature. This temperature, Tc, is the temperature of the formation of a Bose-Einstein condensate, and through its calculation one can further understand the physics of this state of matter. This Tc is:

$$Tc = \frac{h^2}{2\pi mk}\left(\frac{N}{2.612V}\right)^{\frac{2}{3}} \tag{2.1}$$

The calculation of this temperature, as well as the definitions and behaviors of the Bose-Einstein and Fermi-Dirac statistics are shown in Appendix A.

As shown in the calculations presented in Appendix A the distribution of the particles will be:

$$N = \frac{2\pi V}{h^3}(2m)^3 \int_0^\infty \frac{\sqrt{E}}{e^{(\frac{E}{kT}+\mu)}-1} dE = V(\frac{2\pi mkT}{h^2})^{\frac{3}{2}} F_{\frac{3}{2}}(\mu) \tag{2.2}$$

with F being a modified Riemann zeta function defined as:

$$F_x(y) = \frac{1}{\Gamma(x)} \int_0^\infty \frac{u^{x-1}}{e^{u+y}-1} du$$

with Γ being the standard gamma function $\Gamma(x) = \int_0^\infty e^{-y} y^{x-1} dy$. The F function is seen to be matching the ζ-function when the x=0.

So the distribution function can be re-written as:

$$N = \frac{1}{e^{\mu}-1} + N(\frac{T}{Tc})^{\frac{3}{2}} \frac{F_{\frac{3}{2}}(\mu)}{F_{\frac{3}{2}}(0)}$$

Therefore, one can now differentiate the thermodynamic behaviors of the ideal Bose gas according to the Tc. Below the critical temperature (T<Tc) the occupational number is:

$$n = n_0 = N[1 - (\frac{T}{Tc})^{\frac{3}{2}}]. \tag{2.3}$$

Above the critical temperature one can find the occupational number by using the formulation $F_{\frac{3}{2}}(\mu) = \zeta(\frac{3}{2})(Tc/T)^{\frac{3}{2}}$ into Eq. 2.2.

Similarly, with the calculations for the occupational numbers, as seen in the work of London [20], the rest of the thermodynamic variables like the specific heat or the free energy can be calculated to be different above and below the critical temperature.

This approach provides an understanding about the behavior of an ideal Bose gas near and below its critical temperature, and is the foundation for the work of London on the subject. Despite this, Helium in either of its two isotopic forms, is not an ideal gas and this method cannot apply. Tisza and London applied great effort to try and directly connect the phenomenon of superfluidity with Bose-Einstein condensation to no avail. Their work, however, provided an excellent mathematical insight to the workings of superfluid Helium and it was able to predict behaviors such as the second sound (Helium due to superfluidity exhibits multiple forms of sound).

2.1.2 The quasiparticle approach

The second and nowadays accepted method of describing superfluids was put forward by Landau [22, 23]. In this theory the behavior of superfluid Helium is explained by studying the quantum interactions between the particles and forfeiting any connections with Bose-Einstein condensation. In fact, Landau in his work was emphatically denying the existence of Bose-Einstein condensation within the superfluid. The quasiparticle approach is based on the excitations of the Helium atoms which are then described as different quantum particles. This theory draws heavily from the theory of phonons in crystals [24]. A phonon is nothing more than an oscillation, or a standing wave, within the lattice of any material. This wave has a specific wavefunction and energy. In the quantum realm the particles

are described by these two factors, their energy and their wavefunction. Therefore, one could readily assume the properties of a particle for these waves. (From an engineer's perspective such an assumption might seem farfetched but within the science of quantum mechanics this kind of assumptions are solid and ubiquitously used, constantly providing experimental results verifying their validity.) Landau used the phonons to describe the linear interactions of the particles of the system, but Helium being a fluid and not a solid, could not be completely defined by those linear interactions. In any liquid non-laminar flow occurs, forming vortices. This is something that also happens in superfluid Helium as well, although in the case of superfluids vortices are vastly different than the typical ones someone might expect knowing from the fluid mechanics of regular fluids [1]. To account for this extra degree of freedom in the lattice waves of the superfluid, Landau coined the idea of rotons. Rotons are also theoretical particles associated this time with the rotational movements within the fluid. Lastly, one can readily understand that occasions where both kinds of movements occur will take place in the system. For these instances Landau introduced the maxons, the kind of quasiparticles with the highest energies of the three. Based on the energy of the quasiparticles this approach has been extremely effective in describing the behaviors of superfluid Helium-4, as all the modern EOSs used are based on this method. The procedure to gain the thermodynamic values from the quasiparticles is based on the distribution of their energies and it will be shown in detail in following chapters. The basis of this method has been the energies of the quasiparticles, which can be experimentally measured.

Chapter 2 - Nomenclature

Tc	Bose-Einstein Condensation Temperature
h	Plank's constant
m	Atomic mass
k	Boltzmann constant
N	Number of atoms
V	Volume
E	Energy
μ	Chemical potential
F(x)	Modified Riemann Zeta function
$\Gamma(x)$	Gamma function
n	Occupational number

[1] In a superfluid quantum vortices occur, meaning that they behave like point vortices moving through the superfluid and not like a total vortice incorporating all the fluid, even if rotational velocity is given to the entire system [25]

Chapter 3

Helium 4

3.1 Theoretical Equation of State

In this chapter the Equation of state for Helium 4 below its boiling point will be established. The multiple approaches towards the EOS are going to be presented based either on the theoretical quasiparticle approach or on the existing experimental data. The theoretical quasiparticles approach of the EOS is to be based on the works of Landau [22] and Brooks et al [14]. Also, the works of McCarty in [26, 27] and Arp [28, 29] have been used to provide reference data for the EOS and the produced results.

3.1.1 Quasiparticle model

The boiling point of Helium 4 is at 4.2 K, but the lambda point is around 2.18 K depending on the pressure. Below the lambda point is where the superfluid begins forming. Below this point to describe the thermodynamic properties of the superfluid the quasiparticle approach is implemented, where the excitations of the particles are used to define the macroscopical thermodynamic data. These quasiparticles have been seen experimentally to follow an energy spectrum in the form shown below in figure 3.1.

The goal of this figure, which has been verified further since its first appearance by more modern experimental procedures and results, is to showcase the energy of the quasiparticles in a way that can be capitalized upon by using models of statistical physics in order to compute the thermodynamic data of the superfluid. Another reason why this kind of figure is highly successful in that undertaking is that, as it will be presently shown, it can be used to directly correlate the energy of the quasiparticles, and therefore all the thermodynamic values being byproducts of this, to the temperature and pressure.

The data used for the figure of Donnelly and Brooks as presented have been based on the tables of Wilks [30], but since their first publication the authors have suggested for this procedure to be adjusted and redone when more recent and accurate data become available. Thus, one of the aims of this chapter is to use the modern data from NIST to replicate this work and create a more accurate equation of the energies of the quasiparticles. The data that will be used to verify the values of the energies of the quasiparticles are taken from the most recent data from NIST [31] and the work of Donnelly [32] in 1998.

3.1.2 Theoretical approach of the quasiparticles

Studying the excitations in Helium 4 as described by Landau and the rest of the researchers of the quasiparticle theory it can be safely assumed that these excitations, being based

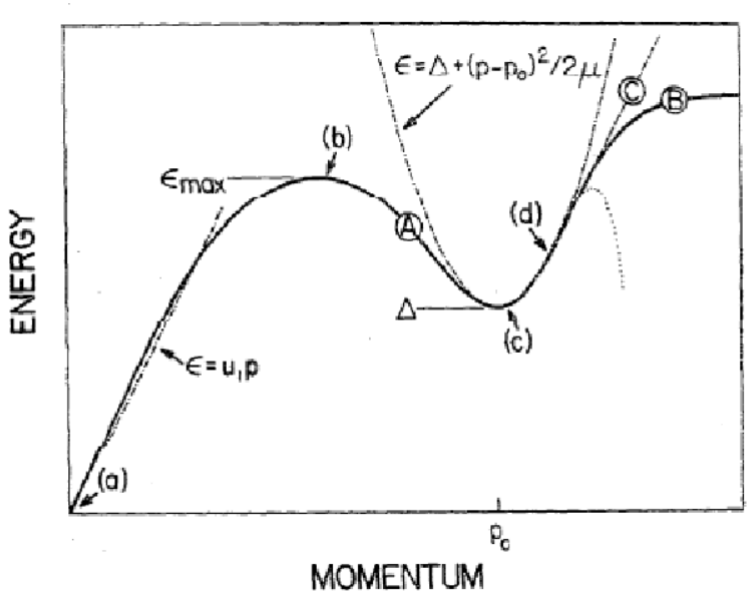

FIGURE 3.1: The energy of the quasiparticles to the their momentum is shown schematically. (a) is the phonon region, (b) the maxon peak, (c) the roton minimum. Source [22]

on weakly-interacting Helium-4 atoms, obey the Bose-Einstein statistics.

$$n(p,T,P) = \frac{1}{h^3} e^{-(\frac{E(p,T,P)}{T}-1)^{-1}}, \tag{3.1}$$

with n being the occupational number, p the momentum, T the temperature, P the pressure and h the Planck's constant. From this equation it can be seen that there is a direct connection between the occupational number and the energy of the quasiparticles. The quasiparticles have been categorized according to their energies into three classes.

Phonon energy

In Fig. 3.2 the first linear area of the graph is the phonon line, then there is the maxon peak followed by the roton minimum. From the roton minimum onward the number density of the excitations gets very high and it can be shown that the Bose-Einstein statistics actually degenerate to Maxwell-Boltzmann statistics (as shown in A.1). The study of the experimental data for the quasiparticles will initiate with the phonon line. With the momentum closing to zero. Based on the theoretical predictions of Freenberg [34] it can be seen that the correlation between the energy and the momentum is linear with:

$$\lim_{p\to} E(p,T,P) = u_1 p$$

with u_1 being the speed of sound (more specifically the speed of the first sound), the value of which can be found using the distribution function at zero if one new perfectly the distribution function, or by the use of experimental data as done in this work. It needs to be stated at his point that this linearity of the phonon energy might be problematic in higher temperatures and as such this will be addressed when the new distribution

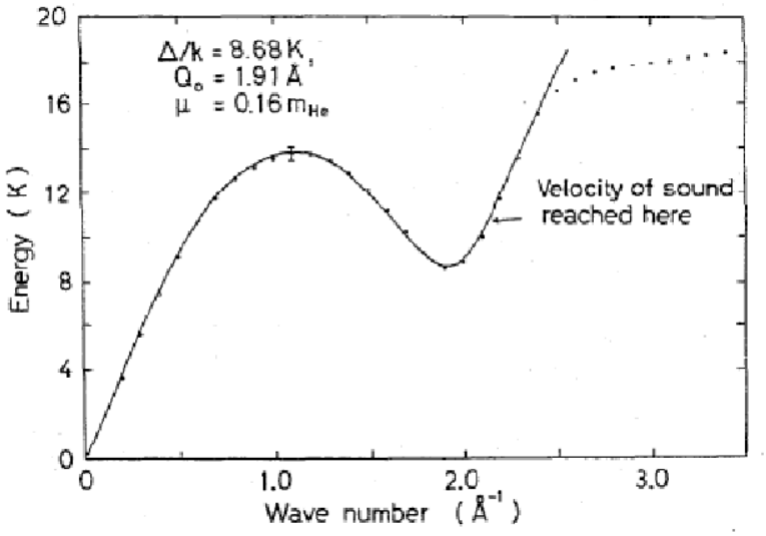

FIGURE 3.2: The energy of the quasiparticles in K to their momentum in $Å^{-1}$. The energies of the quasiparticles are given by the work of Yarnell et al [33] by using neutron scattering to verify the energies of the excitations. Source [14]

function is made by not forcing a linearity but by only introducing the equivalent boundary conditions to the system and let it free.

Maxon energy

Moving from the phonon line the maxon peak ought to be studied. Donnelly and Brooks in [14] provide a simple equation describing the maxons:

$$E\rho = E_0 + E_1\rho + E_2\rho^2 + E_3\rho^3 \tag{3.2}$$

with ρ referring to the density and the values $E_0 ... E_3$ given in Table.3.1

E_0	E_1	E_2	E_3
-216.5672	3998.6005	-23028.6027	44199.7232

TABLE 3.1: Values for eq.3.2 coefficients from [14]

This equation given by Donnelly and Brooks is capable of roughly describing the energy data for the maxons but when compared to the experimental data [14] it is seen that discrepancies occur and a better overall equation can be constructed having a higher accuracy as it will be shown.

Using the data for the maxon energies a polynomial equation of the following form is established:

$$E_{maxon} = \sum_{i=0}^{6}\sum_{j=0}^{6}(Cm_{i+1,j+1}T^iP^j) + E_{min} \tag{3.3}$$

with Cm being the coefficients given in table B.1. The temperature must be inserted in K and the pressure in atm for the product of the function to be in K.

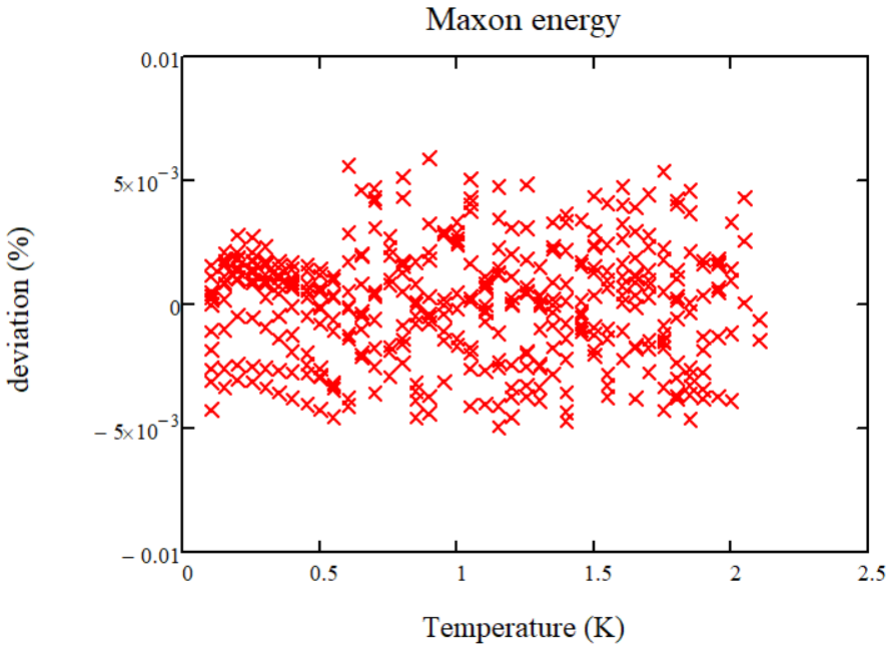

FIGURE 3.3: The deviations of the values of eq. 3.3 compared to the values of NIST [14]
. The mean deviation is found to be $8.113E-08\%$, the correlation coefficient is $r = 0.9999996207$ and the coefficient of determination $r^2 = 0.9999992413$

To verify the validity of this equation the deviation of its values to the experimental values is shown in Fig. 3.3

The accuracy of this equation is deemed excellent and much higher than the accuracy of eq.3.2 when compared to the same data set. Thus, the eq.3.3 will be used for the energy of the maxons.

Roton energy

Following this the rest of the energy spectrum needs to be defined. The roton minimum as it had been theorized by Landau and was seen experimentally, ought to be adequately described by a parabola.

$$E_{roton} = \Delta + \frac{(p - p_o)^2}{2\mu} \tag{3.4}$$

with Δ being the minimum energy of the rotons, μ the apparent mass of the rotons near that energy and p_o the momentum near that minimum point. These three are referred to as the Landau parameters and define the roton minimum. The p_o according to Dietrich's study [35] on neutron scattering is initially dependent only on the density:

$$p_o(\rho) = 3.64\hbar(\rho 10^{-3})^{\frac{1}{3}} \tag{3.5}$$

the p_o is calculated in Å^{-1} and the density must be inserted in g/cm^3. The Δ and μ can be correlated according to Dietrich's work as:

$$\Delta 0 = k(973.6969\rho)$$

$$\mu 0 = (0.32 - 1.103\rho)$$

with the $\Delta 0$ and $\mu 0$ being the values for T=0 K, and they can be correlated to higher temperatures as using the formulation:

$$\frac{\mu(\rho, T)}{\mu 0(\rho)} = \frac{\Delta(\rho, T)}{\Delta 0(\rho)}$$

The roton minimum Δ can also be directly calculated given some macroscopic variables of the medium by:

$$\Delta(\rho, T) = \Delta 0(\rho) - kT\frac{\rho_n}{\rho}(1 - \frac{a'Nr}{T}), \tag{3.6}$$

with Nr being the roton number density, ρ_n the normal fluid density (it will be shown later in this study that not all Helium 4 instantly becomes a superfluid when the lambda point is past and as such the differentiation between the normal fluid density and the superfluid density) and $a' = 8.75 \times 10^{-}23\, Kcm^3$ (a modified Avogadro's number to fit the units of the equation).

The equations above have been studied by Donnelly and Brooks and have been found to have deviations of the order of 20%. For this reason, in their work [14] they have created a least square regression to the data for better results on the energy of the rotons. The equations of [14] on the rotons are not presented in this work and one should refer to the original paper for their exact formation but their errors against the experimental data are being checked and have been seen to be accurate at temperatures below 1K but have a much greater loss of accuracy going towards the lambda point as it can be seen from the equivalent graphs 3.4.

It can be seen that while the deviations are lower than Dietrich's 20% it is certainly possible to improve on this equation. Thus, a polynomial regression is undertaken for the experimental data in the following form:

$$\Delta = \sum_{i=0}^{6}\sum_{j=0}^{6}(C_{\Delta i+1,j+1}T^iP^j) \tag{3.7}$$

$$\mu = \sum_{i=0}^{6}\sum_{j=0}^{6}(C_{\mu i+1,j+1}T^iP^j) \tag{3.8}$$

The values for the C_Δ and C_μ are shown in appendix B. From the figure below it can be seen that this set of equations provides a much higher accuracy than the original least square ones.

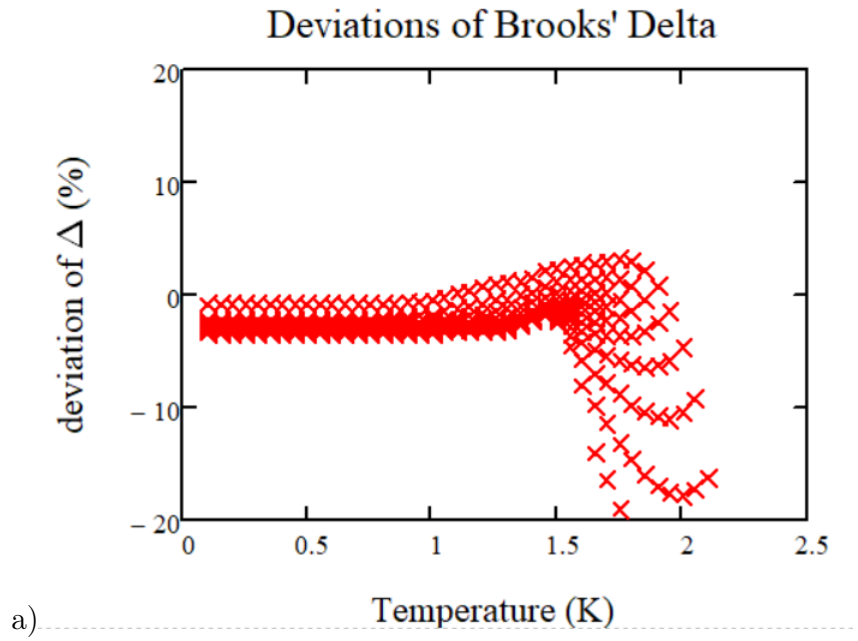

a)

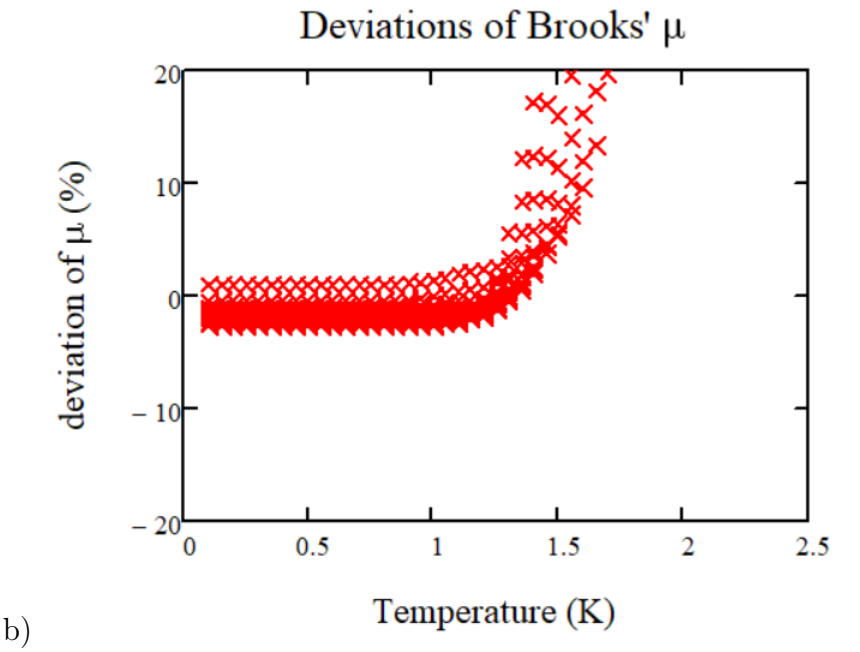

b)

FIGURE 3.4: (a) deviations of [14] least square approximation for the roton energy gap. The mean deviation for the energy gap is -4.583%. (b) deviations of [14] least square approximation for the roton mass. The mean deviation for the roton mass is 61.58%. This high deviation is mostly seen at higher temperatures where the roton population much more scarce, at lower temperatures the equation behaves better although it can still be seen to have relatively high deviations. The correlation coefficients for the energy gap and the roton mass are $r = 0.8759$ and $r = -0.4820$ respectively, while the determination coefficients are $r^2 = 0.7672$ and $r^2 = 0.2323$

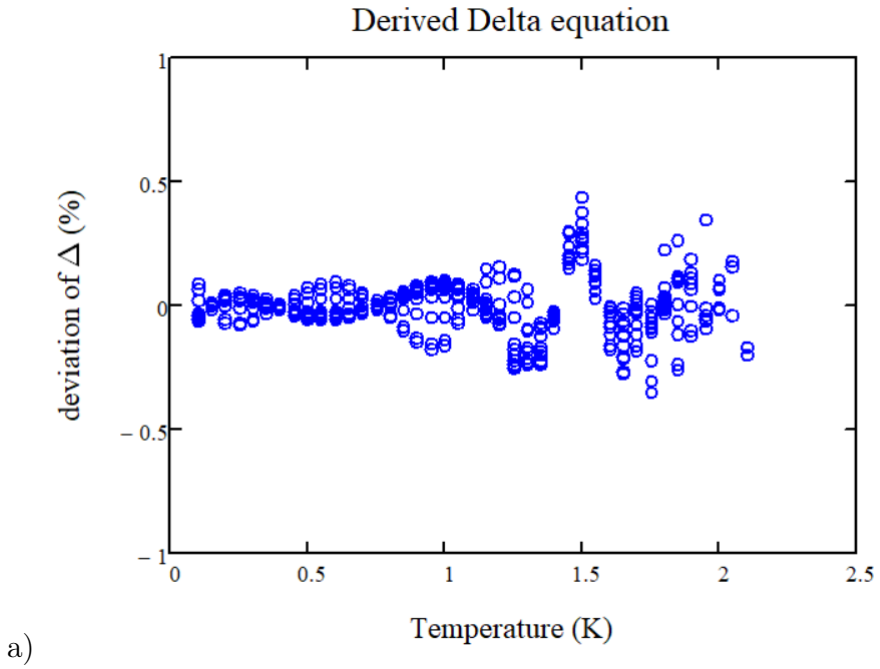

a)

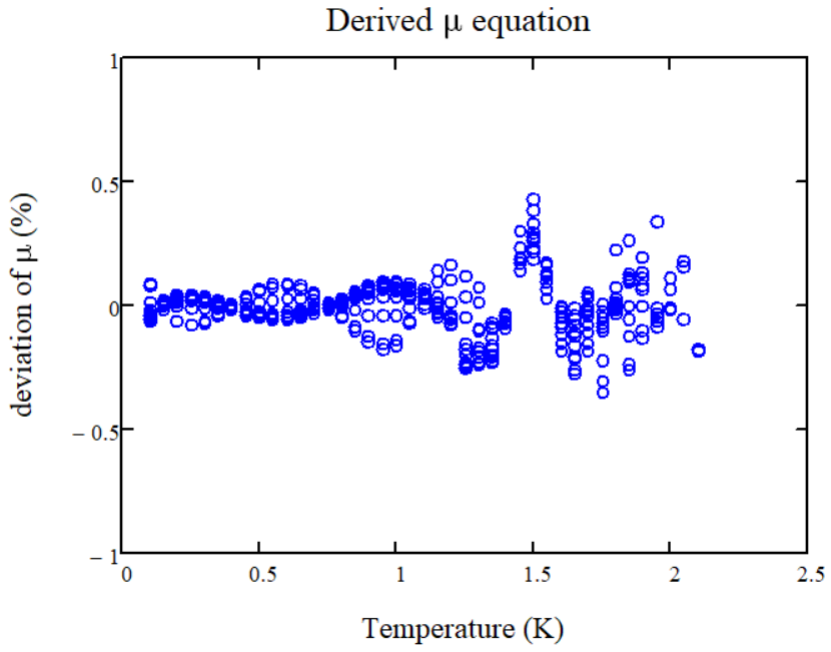

b)

FIGURE 3.5: (a) deviations of eq.3.7 regression for the roton energy gap. The mean deviation is seen to be $1.173E-04\%$, with the relative standard error being $5.243E-03\%$. (b) deviations of eq.3.8 regression for the roton mass. The correlation coefficients for the energy gap and the roton mass are $r = 0.99988$ and $r = 0.99989$ respectively, while the determination coefficients are $r^2 = 0.99976$ and $r^2 = 0.99978$

Comparing the figures 3.4 and 3.5 it can be seen that the equations provided in this work provide an accuracy that is orders of magnitudes better than the original equations. Thus these much improved equations are used in the calculations.

Following this one can now calculated with very good accuracy the values for the roton energy gaps and the roton mass as they are presented in below:

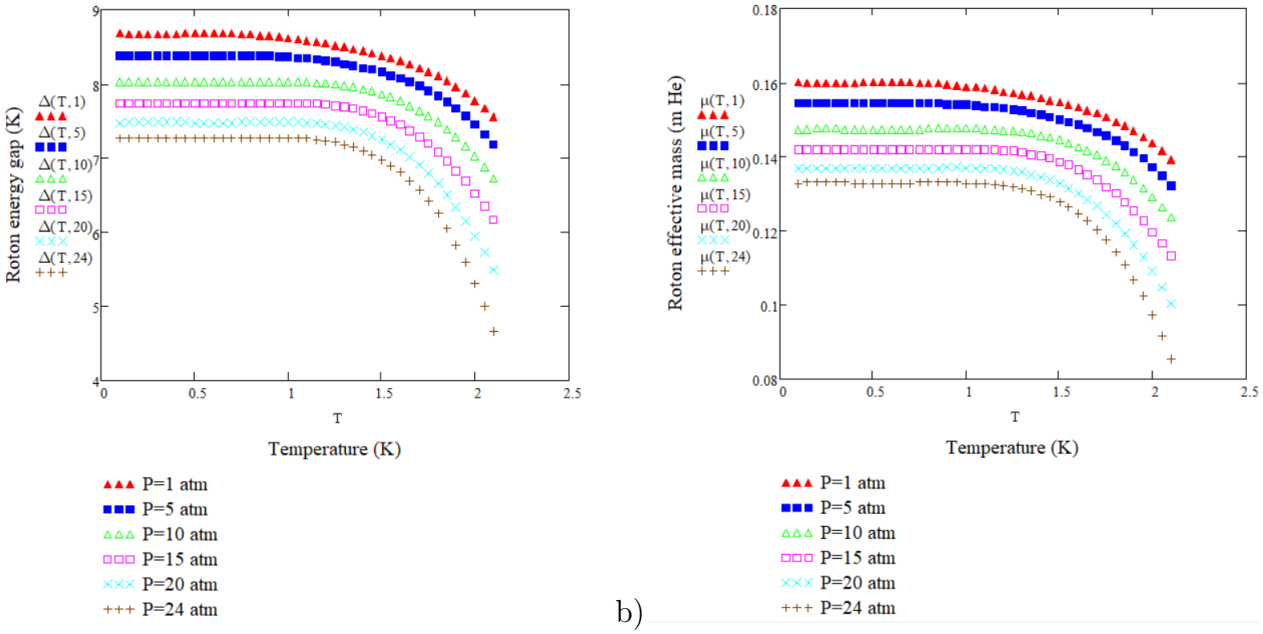

a) b)

FIGURE 3.6: (a) roton energy gap from eq.3.7 for pressures from 1 to 24 atm. (b) roton effective mass from eq.3.8 for pressures from 1 to 24 atm.

Total energy spectrum

Having now the equations for the energies of all the three types of quasiparticles one can initiate the formation of the entire energy spectrum.

According to Donnelly and Brooks the energy dissipation will be increasing by a lessening degree until reaching the double Δ value with a momentum p'.

$$E_p(p) = 2\Delta - \alpha e^{\frac{-a}{p'-p}}$$

with a and α constants that need to be found. By reviewing even the latest data for the energy of the quasiparticles it can be seen that the region above the roton minimum around 2.15 Å^{-1} is of very little importance for the thermodynamic data as if one sees the distribution function of the system they would observe directly that nearly no particles are in this energy condition. As such, it is supposed that a linear behavior is followed from the point where the function reaches a derivative equal to the velocity of the first sound. To describe the full energy spectrum of the quasiparticles the presented method is loosely based on the method of Brooks in [14] but with the new equations for the individual energies and resetting the boundary conditions and data to fit the latest experimental values from NIST. The function to describe the energy will be an 8th degree polynomial based on the momentum with its coefficients depending on the temperature and pressure of the system.

$$E(p,T,P) = u_1(T,P)p + a_3(T,P)p^3 + a_4(T,P)p^4 + a_5(T,P)p^5 + a_6(T,P)p^6 + a_7(T,P)p^7 + a_8(T,P)p^8 \tag{3.9}$$

The a_i are coefficient functions that will be determined during the solution of the system. The u_1 being the velocity of sound has been measured experimentally. Its values from [31, 27, 14] are combined to an overall set of data that are self consistent and cover all

the temperature and pressure spectrum. Based on this data an equation for the velocity of the first sound is derived:

$$u_1 = \sum_{i=0}^{6}\sum_{j=0}^{6}(C_{u1i+1,j+1}T^iP^j) \tag{3.10}$$

with the values of the C_{u1} are given in Appendix B, giving values in m/s for the velocity. Again when comparing to the experimental data it can be seen that this equation has great accuracy as seen below:

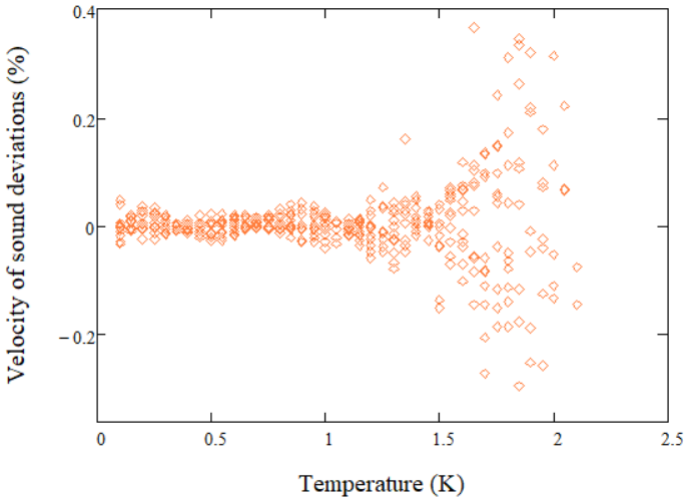

FIGURE 3.7: Deviation of eq.3.10 against the experimental data from [31, 27, 14]. The correlation coefficient is $r = 0.9912$ and the determination coefficient is $r^2 = 0.9824$

When noticing this graph, it is interesting to see that higher deviations are observed at higher temperatures which is counter-intuitive at first glance. Firstly, one needs to also see that even these higher deviations are extremely small with most being less than 0.2%. The reason that this happens is that the speed of sound has more diverging values as the temperature increases and the interactions between the Helium-4 atoms also increase due to the phonon-roton interactions. Having now the values for the speed of sound one can continue to solve for the coefficients of the energies of the quasiparticles. The boundary conditions of the are the following:

1) the linearity of the phonon energy at zero

$$\frac{d}{dp}E(0,T,P) = u1(T,P)$$

2) the energy of the phonons being zero when they are stationary

$$E(0,T,P) = 0$$

3)The maxon peak being located at $p_m = 1.1\text{Å}^{-1}$

$$E(p_m,T,P) = E_{maxon}(T,P)$$

$$\frac{d}{dp}E(p_m, T, P) = 0$$

4) the roton minimum being located at p_o

$$E(p_o, T, P) = \Delta(T, P)$$

$$\frac{d}{dp}E(p_o, T, P) = 0$$

$$\frac{d^2}{dp^2}E(p_o, T, P) = \frac{1}{\mu}$$

5) linearity after the roton minimum

$$\frac{d}{dp}E(p_c, T, P) = u_1(T, P)$$

with p_c being:

$$p_c(T, P) = \mu(T, P)u_1(T, P)m_{He4}\hbar^{-1}10^{-10} + p_o(T, P) \tag{3.11}$$

in Å^{-1}. For consistency within the calculations the units of the speed of sound need to be changed: $u_1''(T, P) = u_1(T, P)\frac{\hbar}{k}10^{10}$ from $[m/s]$ to $[K\text{Å}^{-1}]$. Thus, the overall system of equations can be written as:

$$p_m u_1''(T,P)+a_3p_m^3+a_4p_m^4+a_5p_m^5+a_6p_m^6+a_7p_m^7+a_8p_m^8=E_{maxon}(T,P)$$

$$u_1''(T,P)+3a_3p_m^2+4a_4p_m^3+5a_5p_m^4+6a_6p_m^5+7a_7p_m^6+8a_8p_m^7=0$$

$$p_o(T,P)u_1''(T,P)+a_3p_o(T,P)^3+a_4p_o(T,P)^4+a_5p_o(T,P)^5+a_6p_o(T,P)^6+a_7p_o(T,P)^7+a_8p_o(T,P)^8=\Delta(T,P)$$

$$u_1''(T,P)+3a_3p_o(T,P)^2+4a_4p_o(T,P)^3+5a_5p_o(T,P)^4+6a_6p_o(T,P)^5+7a_7p_o(T,P)^6+8a_8p_o(T,P)^7=0$$

$$6p_o(T,P)a_3+12p_o(T,P)^2a_4+20p_o(T,P)^3a_5+30p_o(T,P)^4a_6+42p_o(T,P)^4a_7+56p_o(T,P)^6a_8=\frac{1}{\mu(T,P)}$$

$$u_1''(T,P)+3a_3p_c(T,P)^2+4a_4p_c(T,P)^3+5a_5p_c(T,P)^4+6a_6p_c(T,P)^5+7a_7p_c(T,P)^6+8a_8p_c(T,P)^7=u_1''(T,P)$$

For this system to be solved it is written in a matrix form:

$$A(T,P) = \begin{bmatrix} p_m^3 & p_m^4 & p_m^5 & p_m^6 & p_m^7 & p_m^8 \\ 3p_m^2 & 4p_m^3 & 5p_m^2 & 6p_m^5 & 7p_m^6 & 8p_m^7 \\ p_o(T,P)^3 & p_o(T,P)^4 & p_o(T,P)^5 & p_o(T,P)^6 & p_o(T,P)^7 & p_o(T,P)^8 \\ 3p_o(T,P)^2 & 4p_o(T,P)^3 & 5p_o(T,P)^2 & 6p_o(T,P)^5 & 7p_o(T,P)^6 & 8p_o(T,P)^7 \\ 6p_o(T,P) & 12p_o(T,P)^2 & 20p_o(T,P)^3 & 30p_o(T,P)^4 & 42p_o(T,P)^4 & 56p_o(T,P)^6 \\ 3p_c(T,P)^2 & 4p_c(T,P)^3 & 5p_c(T,P)^2 & 6p_c(T,P)^5 & 7p_c(T,P)^6 & 8p_c(T,P)^7 \end{bmatrix} \tag{3.12}$$

$$B(T,P) = \begin{bmatrix} E_{maxon}(T,P) - u_1''(T,P)p_m \\ -u_1''(T,P) \\ \Delta(T,P) - p_o(T,P)u_1''(T,P) \\ -u_1''(T,P) \\ \frac{1}{\mu(T,P)} \frac{\hbar^2 10^2 0}{k\, m_{He4}} \\ 0 \end{bmatrix} \tag{3.13}$$

Thus, the solution of this system is given by:

$$R(T,P) = A(T,P)^{-1} B(T,P) \tag{3.14}$$

and the overall solution for the energies of the quasiparticles will be calculated by:

$$E(p,T,P) = u_1''(T,P) + \sum_{i=3}^{8} (p^i\ R(T,P)_{i-2}) \tag{3.15}$$

Observing the behavior of this equation in the following figure it can be seen that while the function behaves as expected in most of the spectrum there is no linearity after the roton minimum beyond the point of reaching the speed of sound.

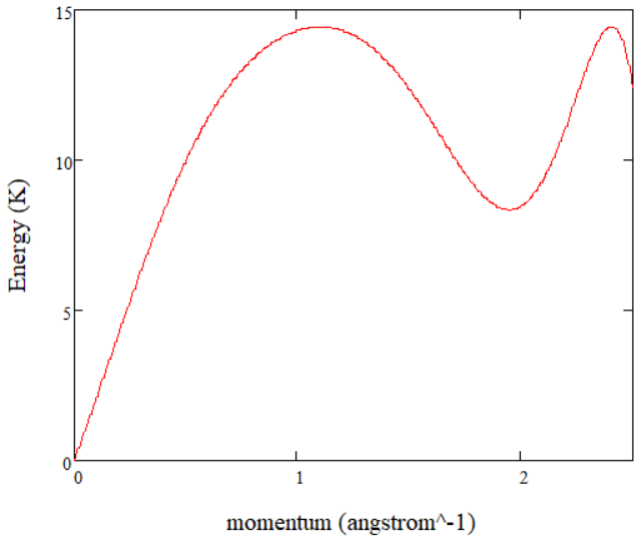

FIGURE 3.8: Energy to momentum diagram for the quasiparticles for T=1 K and P=5 atm without including the linearity corrections beyond the roton minimum

To overcome this the previous equation is re-written as:

$$E(p,T,P) = \begin{cases} u_1''(T,P)p + \sum_{i=3}^{8} (p^i\ R(T,P)_{i-2})\ if\ p < p_c(T,P) \\ u_1''(T,P)(p - p_c(T,P)) + (u_1''(T,P)p_c(T,P) + \sum_{i=3}^{8} (p_c(T,P)^i\ R(T,P)_{i-2}))\ otherwise \end{cases} \tag{3.16}$$

This equation when compared to the provided equation by Brooks et al in [14] offers multiple advantages. Firstly it is shown that the energies of the phonons the maxons

and the rotons are much closer to the real experimental values than the ones in the work of Brooks. Additionally, when Brooks et al solve their equivalent system for the coefficients they supposed fixed coefficients and solved the system multiple times providing the solutions for these coefficients. In this method the set of equations and the equivalent code provides a solution to every set of temperatures and pressures without the need for any interpolation between the values of the coefficients. Below the diagrams of the solutions of the energies of the quasiparticles at different temperatures and pressures are presented.

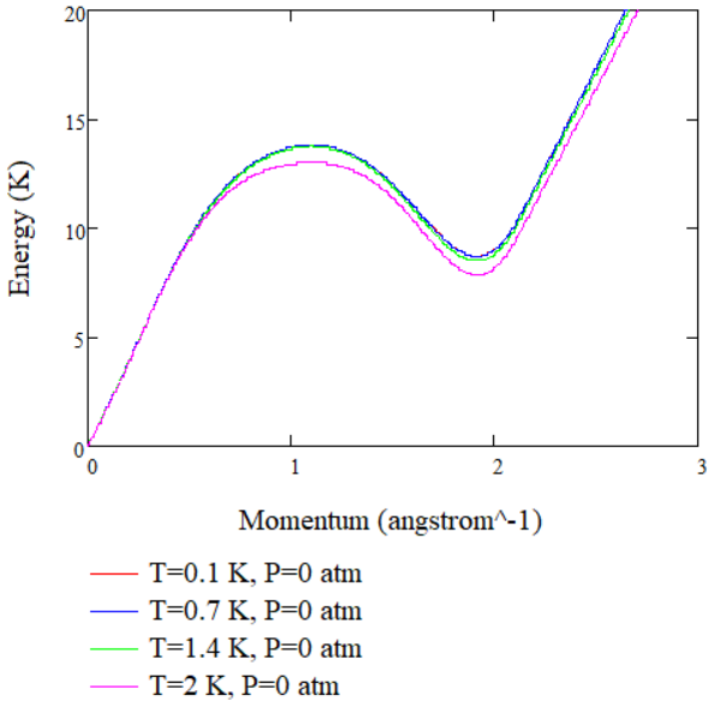

FIGURE 3.9: Energy to momentum diagram for the quasiparticles P=0 atm

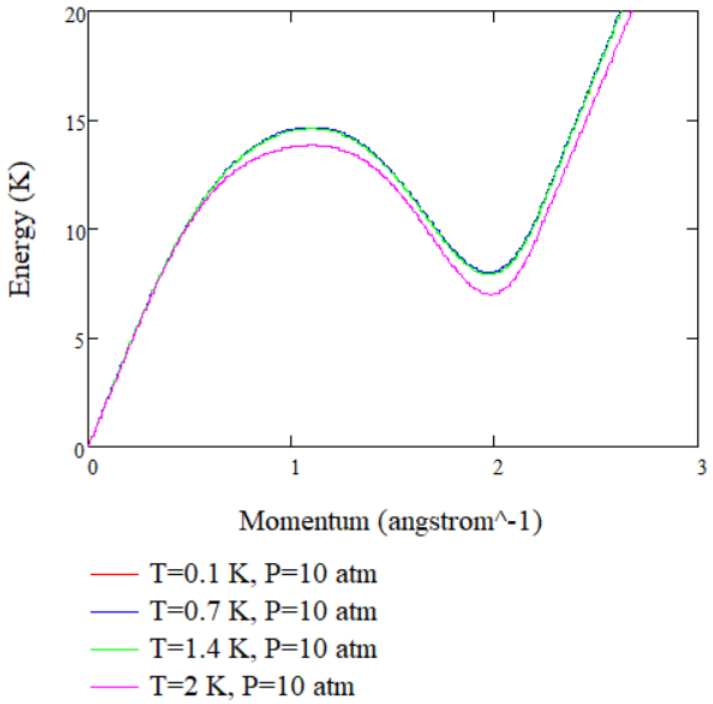

FIGURE 3.10: Energy to momentum diagram for the quasiparticles for P=10 atm

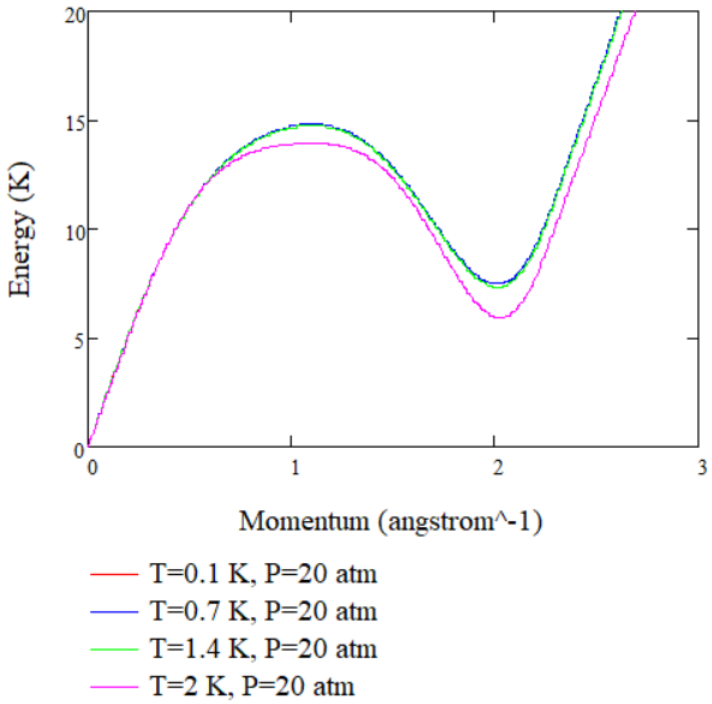

FIGURE 3.11: Energy to momentum diagram for the quasiparticles for P=20 atm

3.1.3 Theoretical Thermodynamic Properties

Having the values for the energy of the quasiparticles, now the derivation of the thermodynamic data can be initiated. Firstly, some properties at the vapor pressure of the Helium-4 are used from the work of Donnelly and Barenghi [32]. The procedure for the properties directly taken from the work of Donnelly is included in Appendix B.

Having the vapor pressure density and the isobaric expansion coefficient from the eq.B.1 and eq.B.5 respectively the following diagrams present their values.

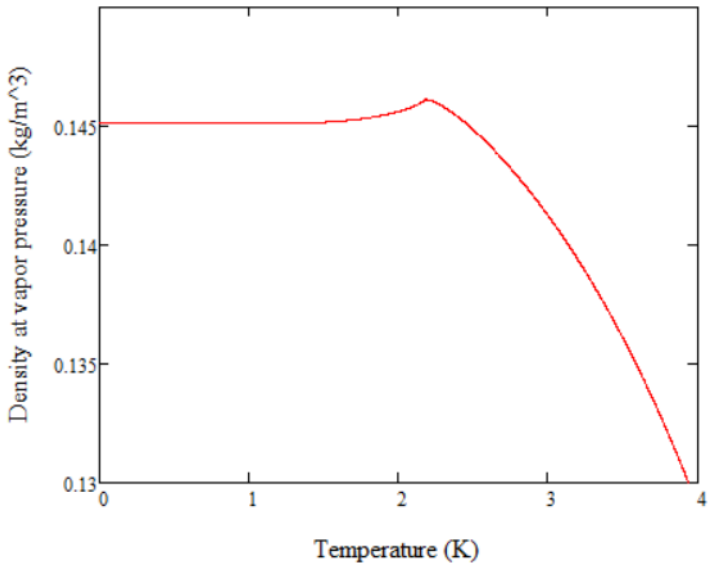

FIGURE 3.12: The vapor pressure density according to eq.B.1 from the work of [32]

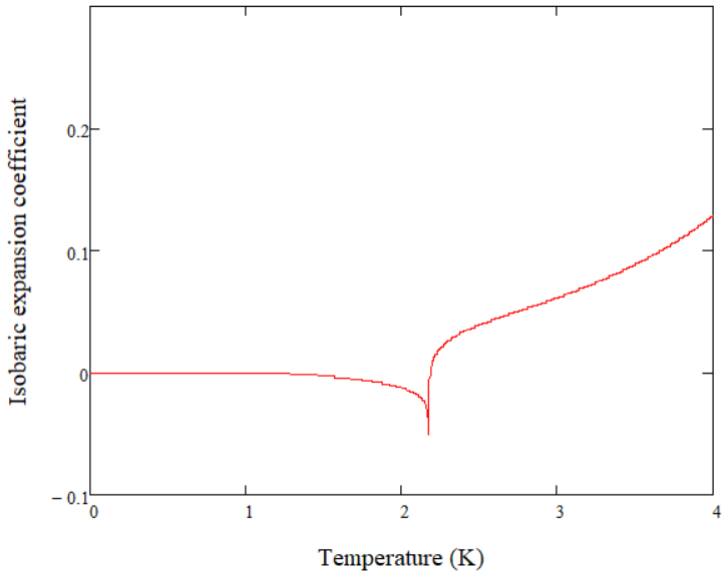

FIGURE 3.13: The isobaric expansion coefficient according to eq.B.5 from the work of [32]

Having the isobaric expansion coefficient at the vapor pressure in order to compute the density outside of the vapor pressure the additional variable of the isothermal compressibility is needed. For this variable experimental data exist from NIST [14], upon which a regression is made to provide and equation for this coefficient.

$$k_t(T,P) = \sum_{i=0}^{6}\sum_{j=0}^{6}(C_{k_t i+1,j+1}T^i P^j) \tag{3.17}$$

with the C_{k_t} coefficients given in Appendix B with values of the isothermal compressibility factor being in $cm^2\ dyn = 10m^2/N$. From the tables of [26, 27, 14] it can be seen that below around 1.5 K the density can be considered to be a factor only of pressure and not of temperature. This fact will be further showcased in a next part of this work where the full equations and maps from the experimental data are presented. Initiating from

$$dv = \frac{dv}{dT}dT + \frac{dv}{dP}dP$$

it can be transformed to

$$dv = a\ v\ dT - P\ k_t\ dP$$

with $a = \frac{1}{V}\frac{dV}{dT}$. If one now assumes the volume only as a product of pressure for a steady temperature it would be:

$$dV(P) = -P\ k_t\ dP$$

so the volume in terms of the pressure would be:

$$V(P) = -\int_0^P P\ k_t\ dp$$

For the specific volume in terms of both the temperature and pressure one can make use of both the variables of the isothermal compressibility and the isobaric expansion as:

$$v(T,P) = \frac{1}{\rho(T)}e\left(\frac{\int_0^T a(T)dT}{\int_0^P k(T,P)dP}\right) \tag{3.18}$$

One can now calculate the deviation of this theoretical equation for the specific volume against the experimental data from NIST.

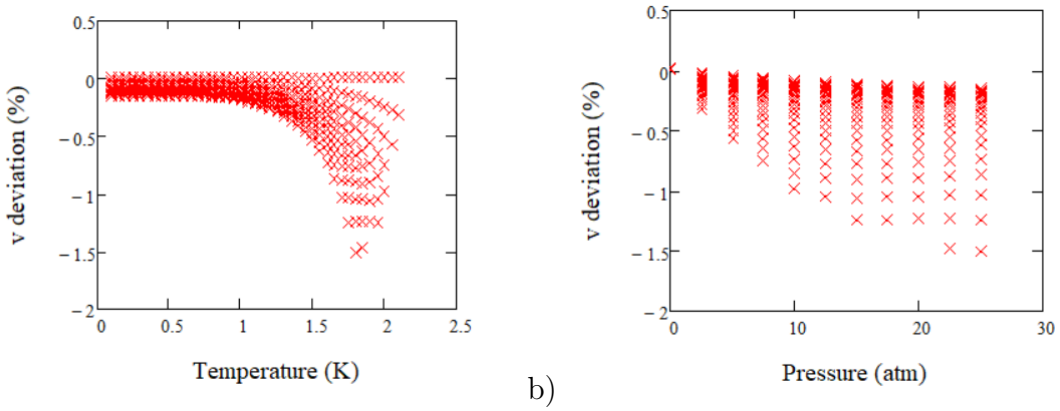

a) b)

FIGURE 3.14: The deviations of the values calculated from eq.3.18 against the experimental NIST data, in terms of T in (a) and P in (b). The correlation coefficient is $r = 0.99897$ and the determination coefficient is $r^2 = 0.99794$

From the Fig.3.14 it can be seen that despite the theoretical nature of this equation it is capable of describing in very high accuracy the values of the specific volume of the actual Helium-4.

Now, having the equations for the energy of the quasiparticles and the equation for the density of Helium-4 by using the equations of statistical mechanics as first mentioned by Landau [22].

$$S = \frac{V\,k}{2\pi^2}\int_0^\infty \left(\frac{n(q,T,P)E(q,T,P)}{kT} + ln(1+n(q,T,P)\right) q^2 dq \tag{3.19}$$

$$Cv = \frac{V}{2\pi^2}\int_0^\infty \left[E(p,T,P)\left((\frac{\partial n(p,T,P)}{\partial T})_{P,q} - a(T,P)\frac{q}{3}(\frac{\partial n(p,T,P)}{\partial q})_{P,T}\right)\right] q^2 dq \tag{3.20}$$

In the work of Donnelly and Brooks [14] more similar equations are used to describe the rest of the thermodynamic properties, but they have a form relying to values at zero temperature that needs to be established first. For this reason in this work the theoretical part of the thermodynamic properties is to be established by just using the equations 3.19 and 3.20 based on the density and the energy of the quasiparticles which are already known.

By using the standard thermodynamic relations from these two equations one can derive a fundamental equation for Helium-4. Firstly, the enthalpy can be defined as:

$$dH = TdS + VdP$$

and then the Gibbs free energy can be written as:

$$G(T,P) = H(T,P) - T\,S(T,P) \tag{3.21}$$

As such one has derived the G(T,P) function, which is a fundamental equation and can be used to derive all the remaining thermodynamic properties. Now the accuracy of these equations needs to be checked against the experimental values to verify its validity.

First the validity of eq.3.19 is seen through plotting it against the experimental data from NIST in a normal and a log scale and presenting its deviation values.

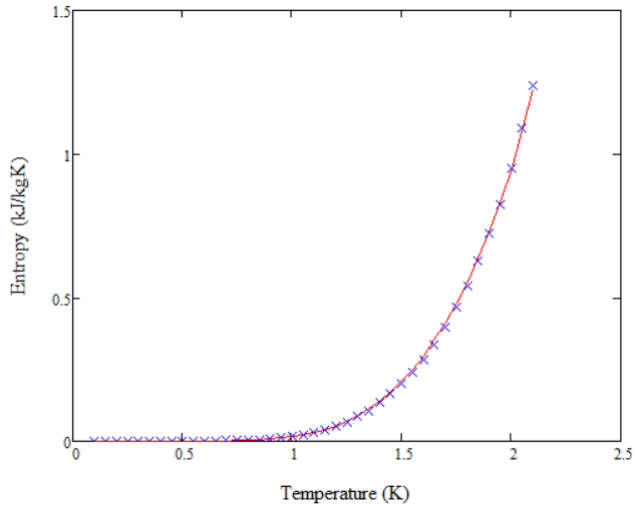

FIGURE 3.15: eq.3.19 results against the NIST data from [14, 26, 28]

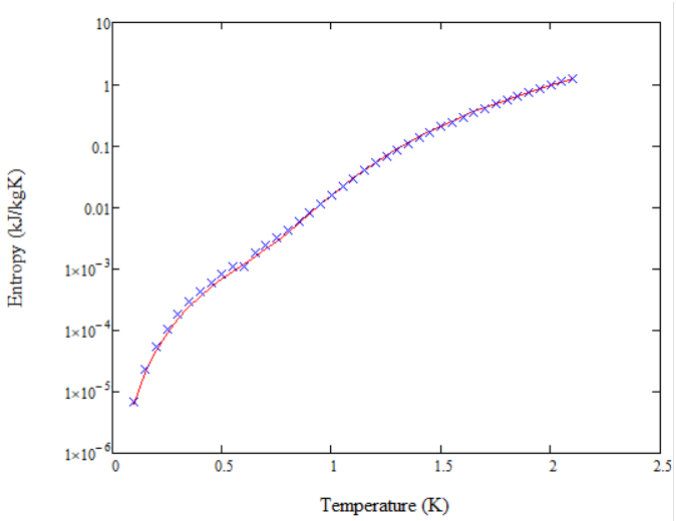

FIGURE 3.16: eq.3.19 results against the NIST data from [14, 26, 28] in logarithmic scale

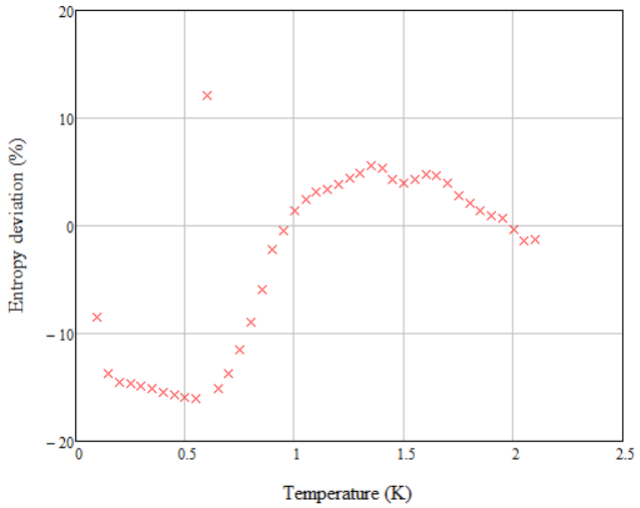

FIGURE 3.17: % deviations eq.3.19 results against the NIST data from [14, 26, 28]. The mean deviation is -7.86%. The correlation coefficient is $r = 0.842$ and the determination coefficient is $r^2 = 0.7089$.

The values that the entropy of Helium-4 changes in the couple of degrees between 0.1 and 2.1 K, as it can be seen from the graphs, are within 8 orders of magnitude. Given this one could suggest that the results of these equations are accurate enough to represent the data for the entropy. In higher temperatures, above 1K, it is seen through figures 3.15 and 3.17, that the provided equation has results that are adequate to describe the entropy of superfluid Helium-4. At lower temperatures one can see through figures 3.16 and 3.17 that the results of eq.3.19 do not so strictly adhere to the NIST data and deviations a little higher than 10% occur. Overall, the behavior of the equation of the entropy, given the difference in the orders of magnitude, is considered to be acceptable. However, to validate this method, one must not forget that the entropy has been directly computed, and other values that are then derived from it would lead to possibly higher deviations. For this reason the behaviors and the deviations of the Gibbs free energy are also checked.

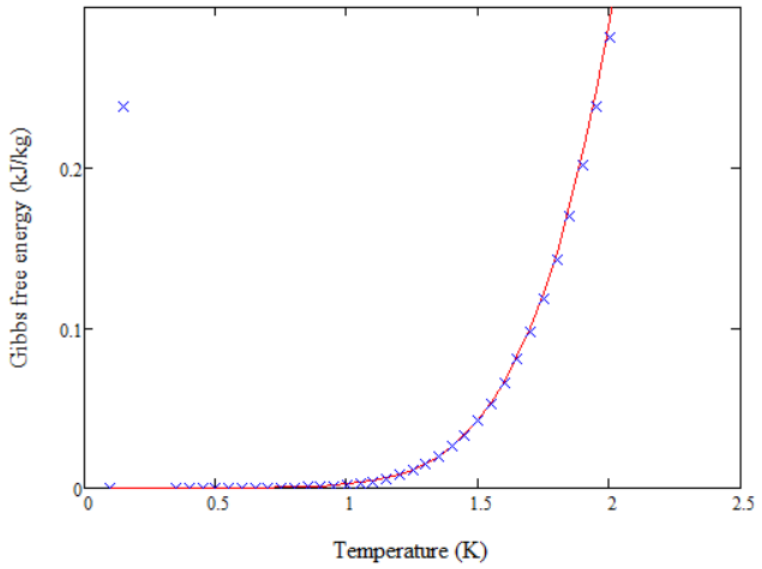

FIGURE 3.18: eq.3.21 results against the NIST data from [14, 26, 28]

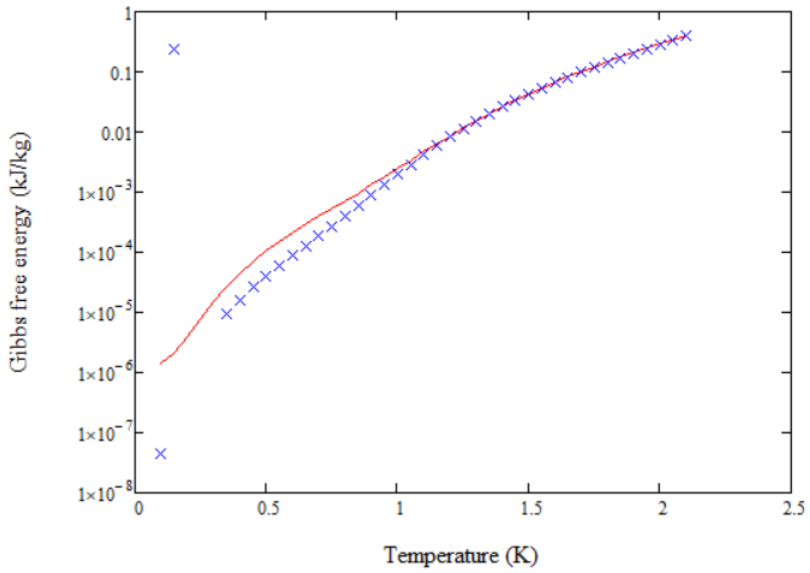

FIGURE 3.19: eq.3.21 results against the NIST data from [14, 26, 28] in logarithmic scale

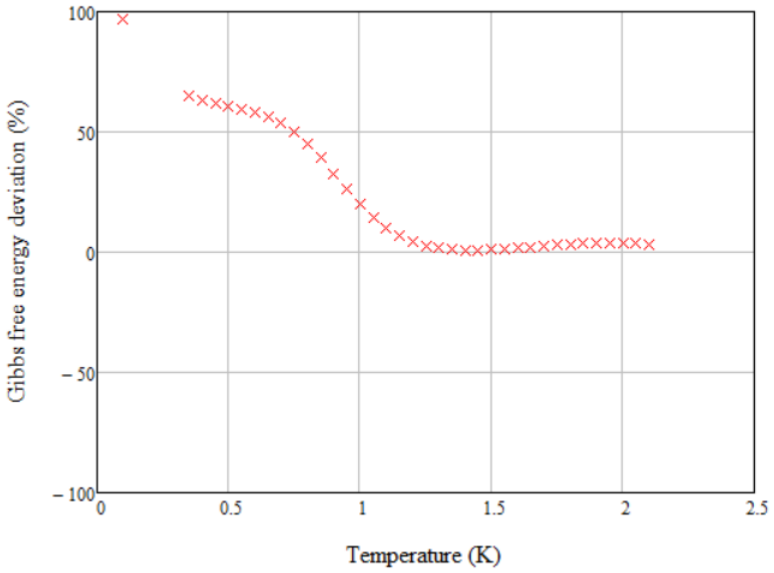

FIGURE 3.20: % deviations eq.3.21 results against the NIST data from [14, 26, 28]. The mean deviation is 39.24%.

Observing the figures 3.18, 3.19 and 3.20 a similar behavior to the entropies can be seen but intensified. The values change again 8 orders of magnitude from 0.1 to 2.1 K with eq.3.21 providing excellent results above 1 K but results that one would have to be extra careful when using it below that threshold. One can see that this equation can be used at a certain degree to provide accurate data for the Gibbs free energy given some care about not exceeding temperatures below 1 K but as a fundamental equation one also needs to check its potential to derive the rest of the thermodynamic data then the errors mean that its use must be limited to understanding the behaviors of the system and not at describing the exact values.

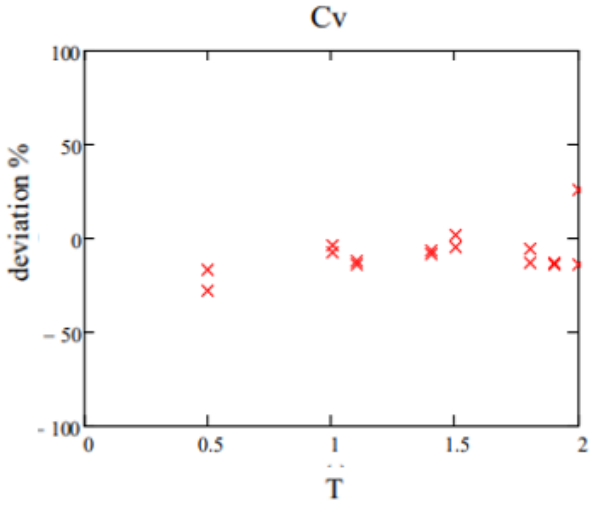

FIGURE 3.21: % deviations of applying the eq.3.19 to find the specific heat as $Cv = T\frac{\partial}{\partial T}S$ and checking its results against the NIST data from [14, 26, 28]. The mean deviation is -19.2%

This trend follows on the rest of the thermodynamic variables like the Helmholtz free energy and the enthalpy.

3.2 Numerical Equation of State

The inability to theoretically deduce the thermodynamic variables of the superfluid Helium-4, especially going towards absolute zero, is a fact that has been known to the researchers of the subject for many years. Even noble tries with extensive codes like the HEPAK from NIST [36] have been known to have a limiting value well above 1 K for the data they produce. For this reason, within this work a new and extensive code has been developed and published in [37].

The main goal of the code developed and presented in this chapter has been to create a very accurate and continuous equation of state for Helium-4 below 4.2 K. This equation of state must be accurate at all regions and additionally must be continuous and not be split up into different equations for different regions. This last part is of great importance for the applications of this equation. Through many cryogenic applications it can be seen that the lack of a continuous and accurate EOS for cryogenic Helium-4 in the literature leads to many assumptions being made and simulations not being able to cover different phases of the substance.

For this kind of equation to be established, a total data set for trustworthy values of all the thermodynamic values of Helium-4 needed to be established first. For this reason the data from the works of [38, 26, 27, 28, 36, 31, 14, 32] have been collected, cross referenced and transformed to be in the same units covering overall all the areas from 0 to 4.2 K. The procedure for acquiring the values below 0.1 K will be extensively shown in a following chapter of this work based on the previously published work of the author in [38], while their values have been already incorporated to the numerical code presented in this chapter.

This set of data will be shortly utilized to form all the values for the equation of state. Before undertaking this procedure though, firstly the bounds between the different phases need to be set.

3.2.1 Lambda Line

Through the literature many equations for the Lambda line exist, the most notable ones being the ones of Arp and McCarty [29, 31], as they are the ones most widely used depending on the needed variables. At this point of the study the equation of McCarty would make more sense to be used as it is defined in terms of pressure, while Arp's equation is in terms of density. Studying the equation given by [31] compared to the actual values it is seen that while this equation is of good quality and accuracy the authors determined that a better one could be established of the form:

$$T_\lambda(P) = a + b\, cos(c\, P + d) \tag{3.22}$$

a	1.759438110219911
b	5.237757610459909 -01
c	2.988936852213499 -02
d	6.435211650071271 -01

TABLE 3.2: Coefficients for eq.3.22

The pressure is in atmospheres and the coefficients are given in Table.3.2. Below the deviations from the NIST values of this equation compared to McCarty's equation are shown.

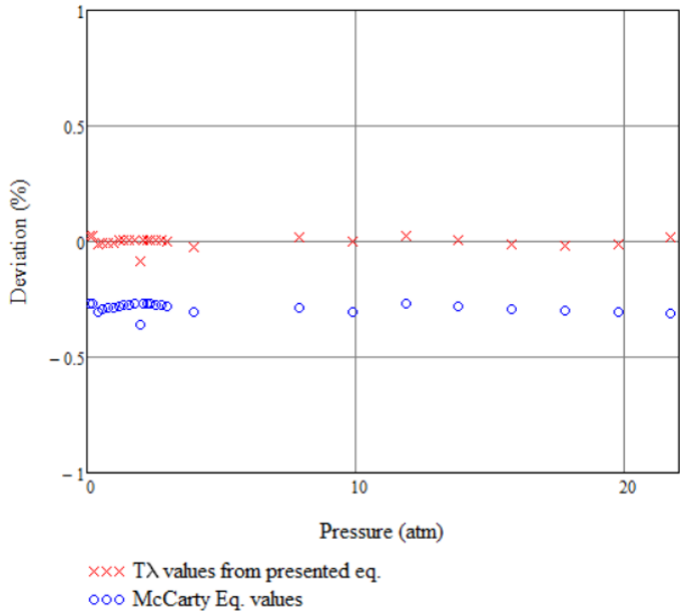

FIGURE 3.22: The deviations of the equations of the lambda line from [29, 31] respectively

3.2.2 Vapor Line

Considering the border between the liquid and the gas phase of Helium-4 one can study the works of McCarty [27] or Ortiz Vega [39]. In this work a different approach was used but utilizing the Wagner equation [40] for the vapor pressure and conforming it to McCarty's NIST data. The critical point of Helium-4 is at $T_c = 5.1953K$ and $P_c = 0.22746atm$ (referring to the classical thermodynamical critical point, not the Tc of the Bose-Einstein condensation). According to the Wagner equation:

$$F(T) = a_1(1-T) + a_2(1-T)^{1.5} + a_3(1-T)^{1.25} + a_4(1-T)^{2.8} \tag{3.23}$$

$$dF(T) = a_1 + 1.5a_2(1-T)^{0.5} + 1.25a_3(1-T)^{0.25} + 2.8a_4(1-T)^{1.8} \tag{3.24}$$

with the a_i values given in Table.3.3

a_1	-3.8357
a_2	1.7062
a_3	-0.71231
a_4	1.0862

TABLE 3.3: Coefficients for eq.3.23

The coefficients of Table.3.3 have been derived from using Wagner's equation against McCarty's data [31]. So, following the known procedure for acquiring the vapor pressure:

$$ln(Pr) = \frac{F(T)}{T}$$

$$dln(Pr) = \frac{dF(T)T - F(T)}{T^2}$$

$$P_{sr}(T) = e^{(\frac{F(T)}{T})}$$

and so, the vapor pressure according to the Wagner equation can be written as:

$$Ps(T) = P_{sr}(\frac{T}{T_c})P_c \tag{3.25}$$

with its behavior being the expected one as seen in the following figure:

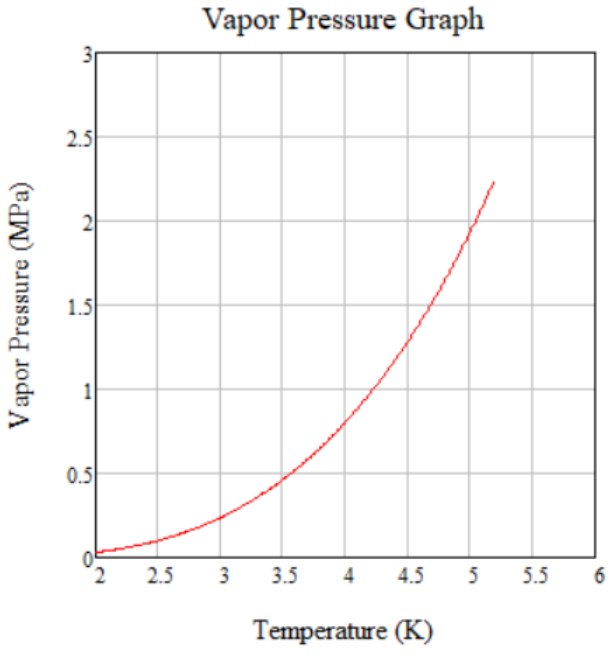

FIGURE 3.23: Vapor pressure values according to Wagner's equation

Now to verify the validity of this equation a comparison with the NIST data is made where the deviations are presented as following:

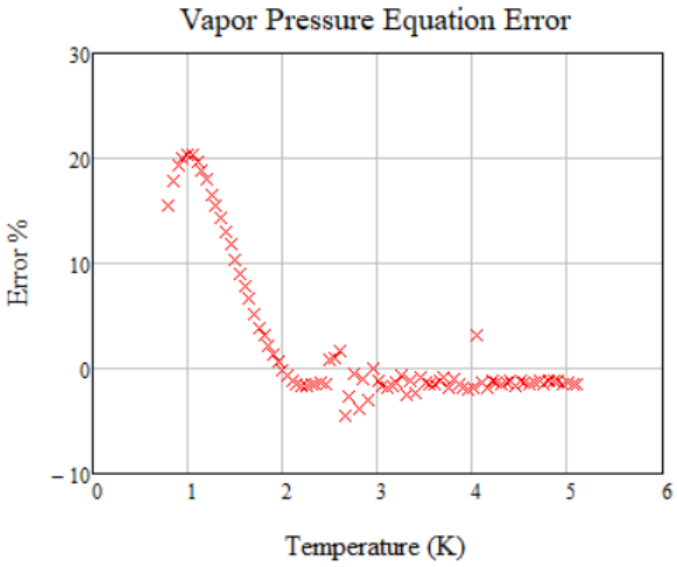

FIGURE 3.24: Vapor pressure errors according to equation eq.3.25 against the NIST [31] data, with the mean deviation being 3.77%

As it can be seen from the figure 3.24 the equation has an overall very good behavior, with some slightly higher error values below 2K. This fact is not concerning as for Helium-4 to be in a gaseous state below this temperature the pressure must be extremely low, something that is not realistic in any application or scenario.

3.2.3 Melting Line

The next boundary phase of the Helium-4 map is the solid to liquid line, or the melting line. This line has been studied and an equation for its produced by McCarty in 1998 [31] which is deemed to have great accuracy and therefore is being used in this work as well.

$$P_{melt}(T) = \alpha + \frac{\theta\, T^{\eta}}{\kappa^{\eta} + T^{\eta}} \tag{3.26}$$

with the coefficients being given in the Table.3.4

α	$2.384032197235548\times10^{1}$
θ	$7.3637042310090629\times10^{1}$
η	6.025643026329004
κ	2.573459220492934

TABLE 3.4: Coefficients for the melting line equation 3.26

3.2.4 Superfluid Equations

The formation of the total equation of state will initiate by forming different equations for the different phases of the Helium-4 and then these equations will be connected to a single continuous one capable of describing all the different phases.

Especially in the superfluid region it is exceedingly difficult to describe directly all the values of the thermodynamic variables without any loss of accuracy since the different

variables like the entropy or the Gibbs free energy are seen to change around 8 orders of magnitude within 1.5 K temperature difference. The equation of state that is to be formed will have the pressure and temperature as independent variables as these are usually the variables that are known in the different systems that this equation might be expected to describe.

The data that are available for this equation to be based upon in terms of temperature and pressure are with small enough intervals that a regression can be tried out, but the difference in the orders of magnitudes negates any ability of using a single regression for the whole range (0.1K to the lambda line).

This code aims to be able to describe with great accuracy both the values and the derivatives of all the properties of cryogenic Helium-4. Going towards absolute zero all the energy variables have an exponential behavior which leads to their orders of magnitude to be drastically changing. For this reason, it is not possible to describe with a single equation any of the energy variables through the entire range of cryogenic Helium, both above and below the lambda line, with adequate accuracy. Thus, a dynamic code has been created. In this code the combined set of the data is used and when the user requests a value from the equation, then the code creates the equation of state in the neighborhood of the requested point, achieving very high accuracy as well as continuity. To do that the code does two consecutive regressions, one over the pressure and one over the temperature in terms of which it takes multiple neighboring isobaric lines of data in terms of temperature. Then, in every isobaric line, it creates a new equation to create new points on the wanted isothermal line. Afterwards, it uses those points and creates a second equation of constant temperature in terms of pressure which is then used to create the wanted value. After this, the derivatives are checked to verify the smoothness of the function made for the neighborhood. If the derivatives are seen not to be in agreement with their respectively correlated thermodynamic values then the code redoes the procedure opting for polynomials of lesser degrees to achieve better smoothness. The full code is presented in Appendix B section B.2. The results of the aforementioned code are presented below:

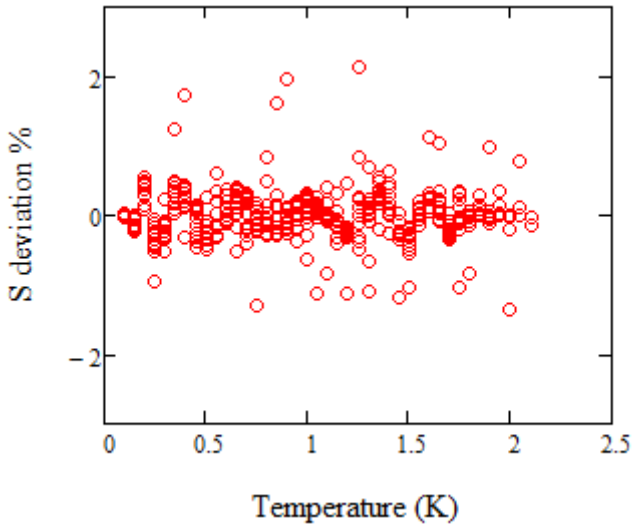

FIGURE 3.25: The deviations of the calculated entropy compared to the NIST values for the superfluid. The mean deviation is $7.495E-03\%$

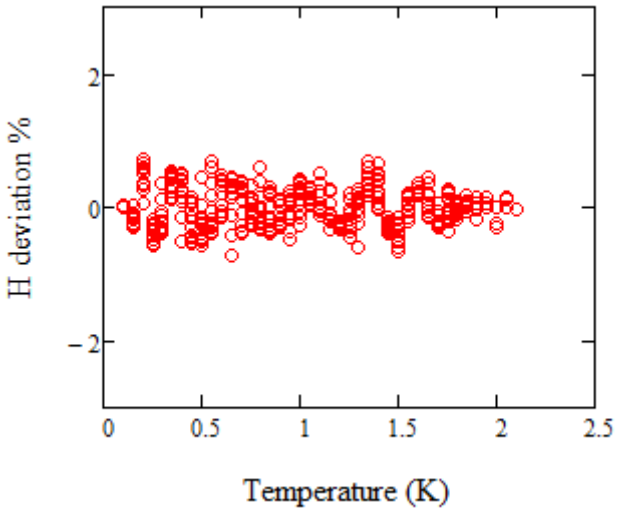

FIGURE 3.26: The deviations of the calculated enthalpy compared to the NIST values for the superfluid. The mean deviation is $3.978E-04\%$

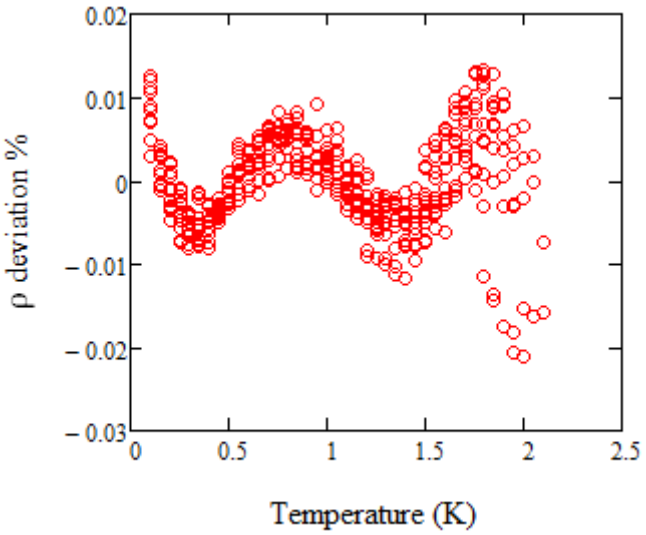

FIGURE 3.27: The deviations of the calculated density compared to the NIST values for the superfluid. The mean deviation is $1.627E-07$

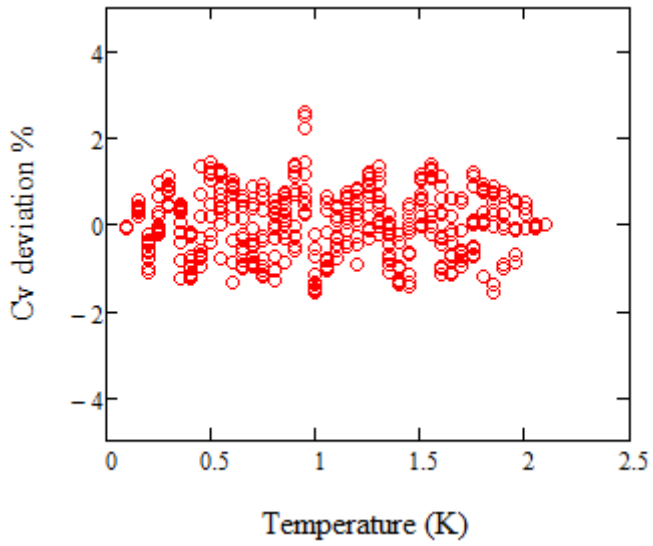

FIGURE 3.28: The deviations of the calculated specific heat under constant volume compared to the NIST values for the superfluid. The mean deviation is $2.795E-03$

From the graphs above it can be seen that the provided code offers a great accuracy with errors $<2\%$ the range of the values. Despite this apparent accuracy for an equation of state to hold validity it must be able to cross-correlate the resulting values between them. For this reason, the equation of the entropy and Gibbs free energy is used as a basis for the enthalpy and the specific heat under constant volume to be recalculated to then be compared to the original data and the ones directly calculated by the code.

The specific heat is calculated as:

$$Cv = T\frac{dS}{dT} \tag{3.27}$$

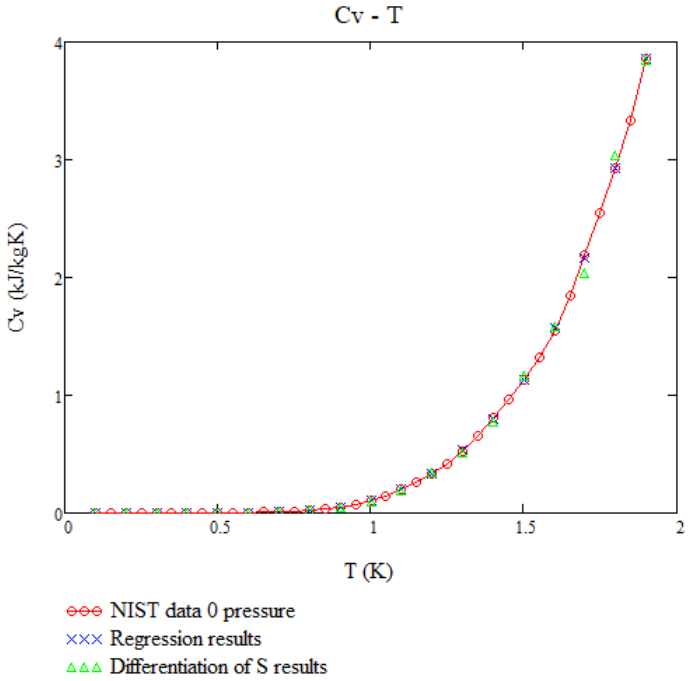

FIGURE 3.29: Comparison of the NIST values to the values provided by the code and the values as calculated by 3.27. The mean deviation is -0.064%, the correlation coefficient is $r = 0.99932$ and the coefficient of determination is $r^2 = 0.99864$

The enthalpy is calculated as:

$$H = G + T\,S \tag{3.28}$$

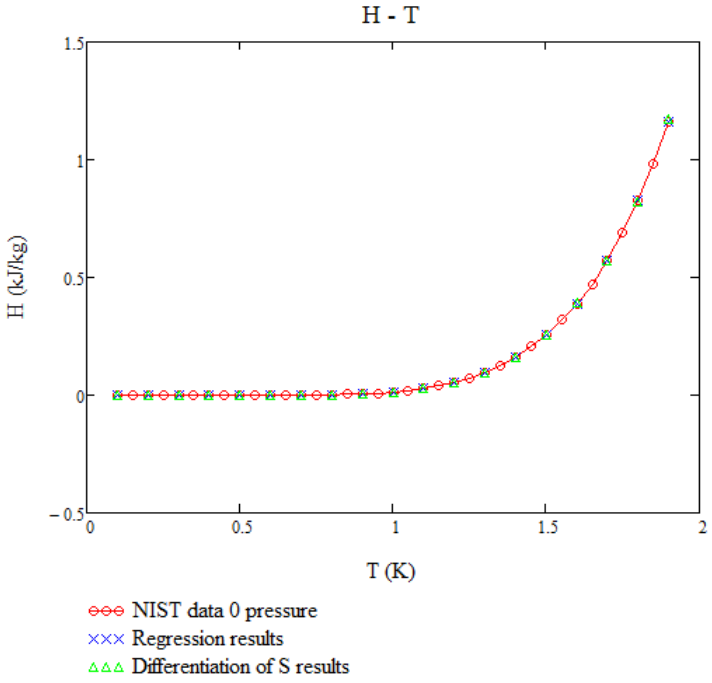

FIGURE 3.30: Comparison of the NIST values to the values provided by the code and the values as calculated by 3.28, the correlation coefficient is $r = 0.99996$ and the coefficient of determination is $r^2 = 0.99991$

From the figures 3.29,3.30 it can be seen that this set of provided equations are able to not only calculated the data points of the superfluid with great accuracy but also provide an excellent correlation between the different thermodynamic properties enabling the calculations of each one using other through the standard the thermodynamic equations and the Maxwell relations.

3.2.5 Normal Fluid Equations

The following region whose equations are needed to be calculated is the normal fluid region. This region might seem initially to be of a simpler nature than the superfluid region as it is closer to the thermodynamic behaviors of usual media, but one need not forget that near the lambda line many properties like the specific heat are exhibiting exceedingly high values and cause a discontinuity, something that is then observed to all the rest of the thermodynamic variables as well. For this reason, a similar code to the one described in the previous section is used as to achieve the maximum possible accuracy.

Below are presented the results of the code compared to the NIST data for two different pressures:

For a lower pressure of 1 atm:

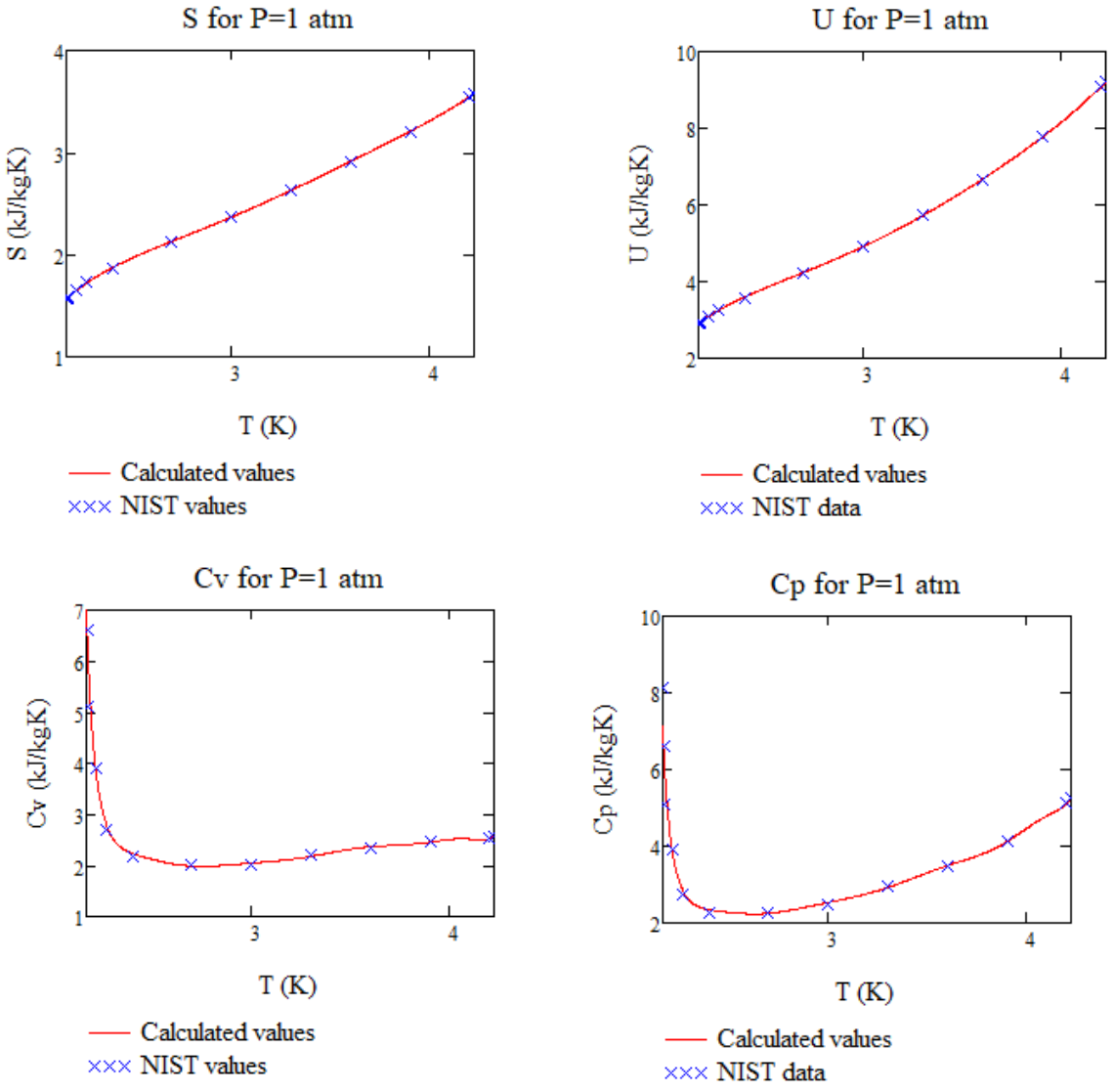

FIGURE 3.31: The deviations of the calculated values compared to the NIST values for the normal fluid at a pressure of 1 atm

For a higher pressure of 8 atm:

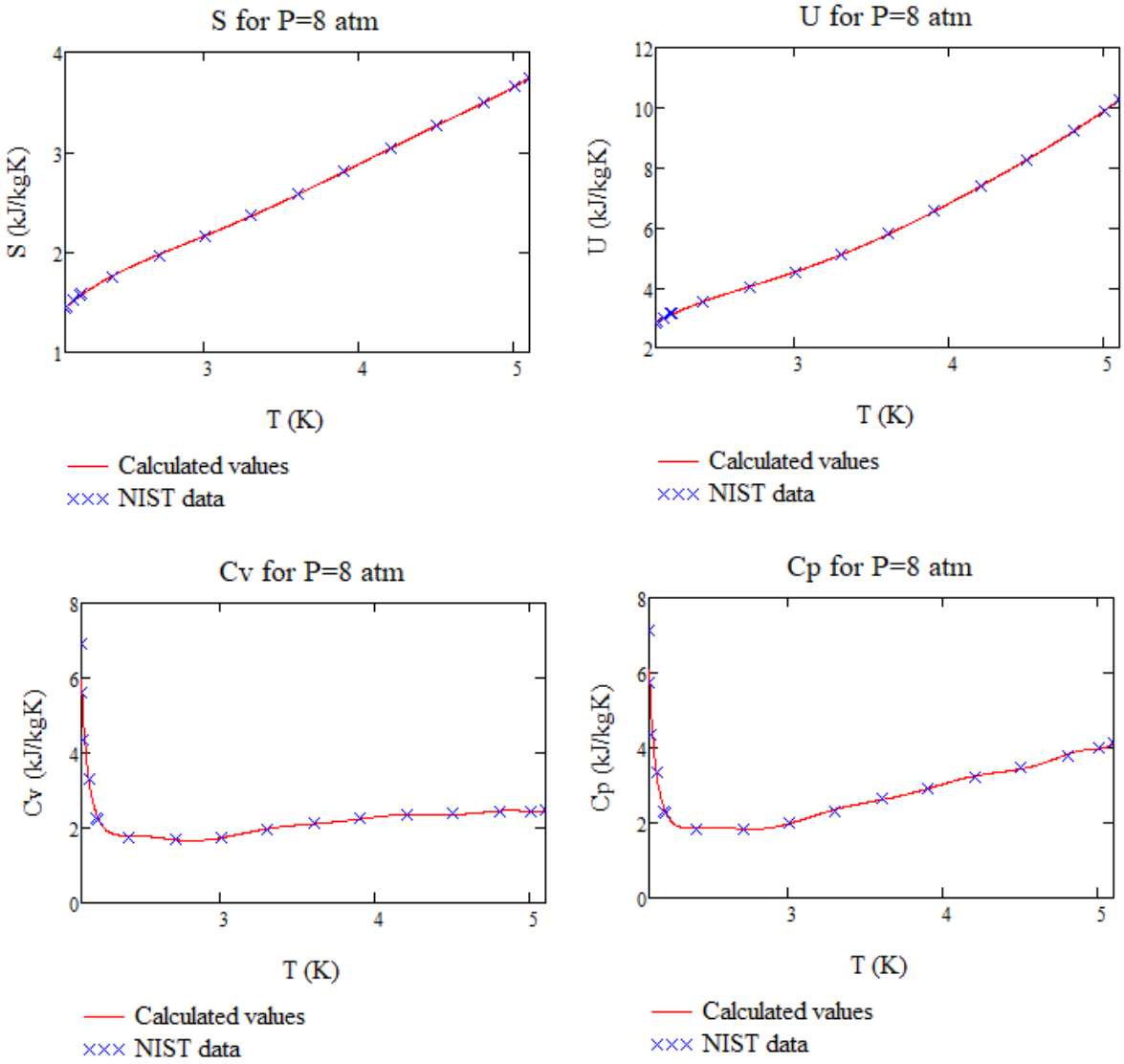

FIGURE 3.32: The deviations of the calculated values compared to the NIST values for the normal fluid at a pressure of 8 atm

From the graphs of the figures 3.31,3.32 it is seen that through this code a direct replication of the data points is achieved.

Again, the cross correlation between the different thermodynamic variables ought to be checked. For this the specific heat under constant volume is checked as the most ill behaving of all the variables given its tendency to extremely high values near the lambda point.

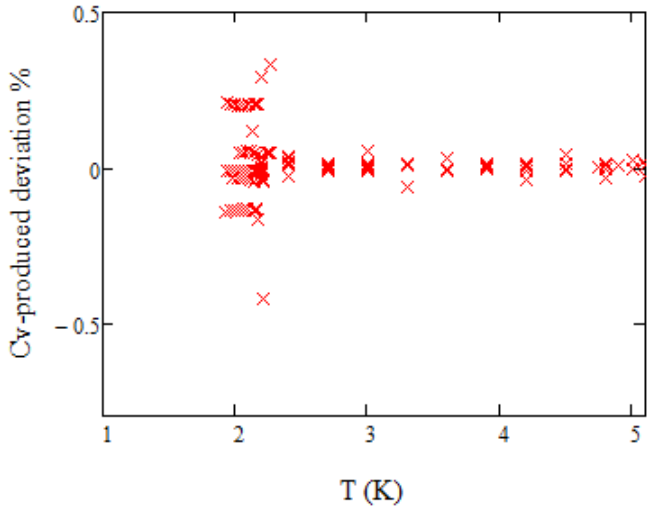

FIGURE 3.33: Comparison of the NIST values to the values provided by the code and the values as calculated by 3.27 for the normal fluid

As it can be seen through the figure 3.33 the accuracy of even the calculated from the entropy Cv values is extremely high verifying the validity of the results of the current equation of state.

3.2.6 Combined equations

Having the specific equations for the Helium-4 in the different sections is key in being able to understand and model its behavior, but for many applications and in the uses of many apparatuses the Helium-4 transitions between one or more of its phases need to be also described. For this reason, it is of great significance to create an overall system of continuous and derivable equations that bridge the existing gaps between the phases in the literature.

To achieve this unification a code has been developed where a function is dynamically created for each wanted temperature conforming to the values and derivatives above and below the lambda line. This dynamic setting of the equations ensures that there is a great accuracy at every case since the created equation is 2D instead of 3D, which is what would have to be in the case that the code was not dynamic and there would be a much greater loss of accuracy compared to the values. The code for the unification of the thermodynamic values above and below the lambda line is presented in B.

By using this created code one can provide the overall results and compare the accuracy with the experimental values by NIST.

For the presented plots below, because no data were available to the exact same pressures for the superfluid and the liquid, it was decided to plot the data for the pressure of the superlfuid and then include in the graph the values for the closest available pressure for the liquid. In the deviation diagrams the exact pressures have been used for both the liquid and the superfluid as different deviation graphs are given and as such the exact results for the deviations of the overall equation in each of the areas can be seen there. Two cases are presented for all the thermodynamic data, one of a lower pressure of 2.5 bars and one of a higher pressure of 20 bars to showcase the efficacy of this code in both ends of the pressure spectrum.

For the pressure of 2.5 bar

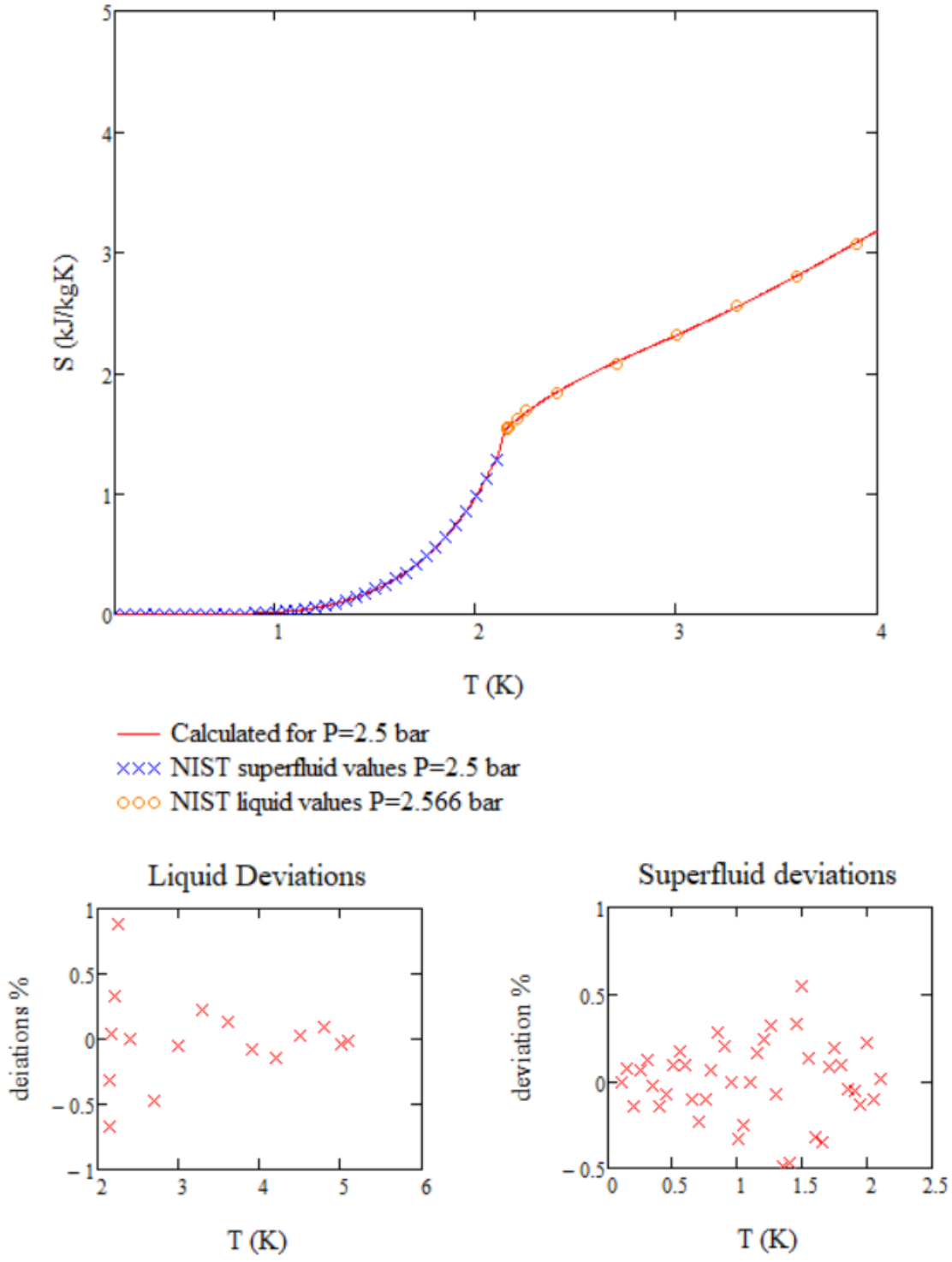

FIGURE 3.34: Calculated entropy compared to the NIST values

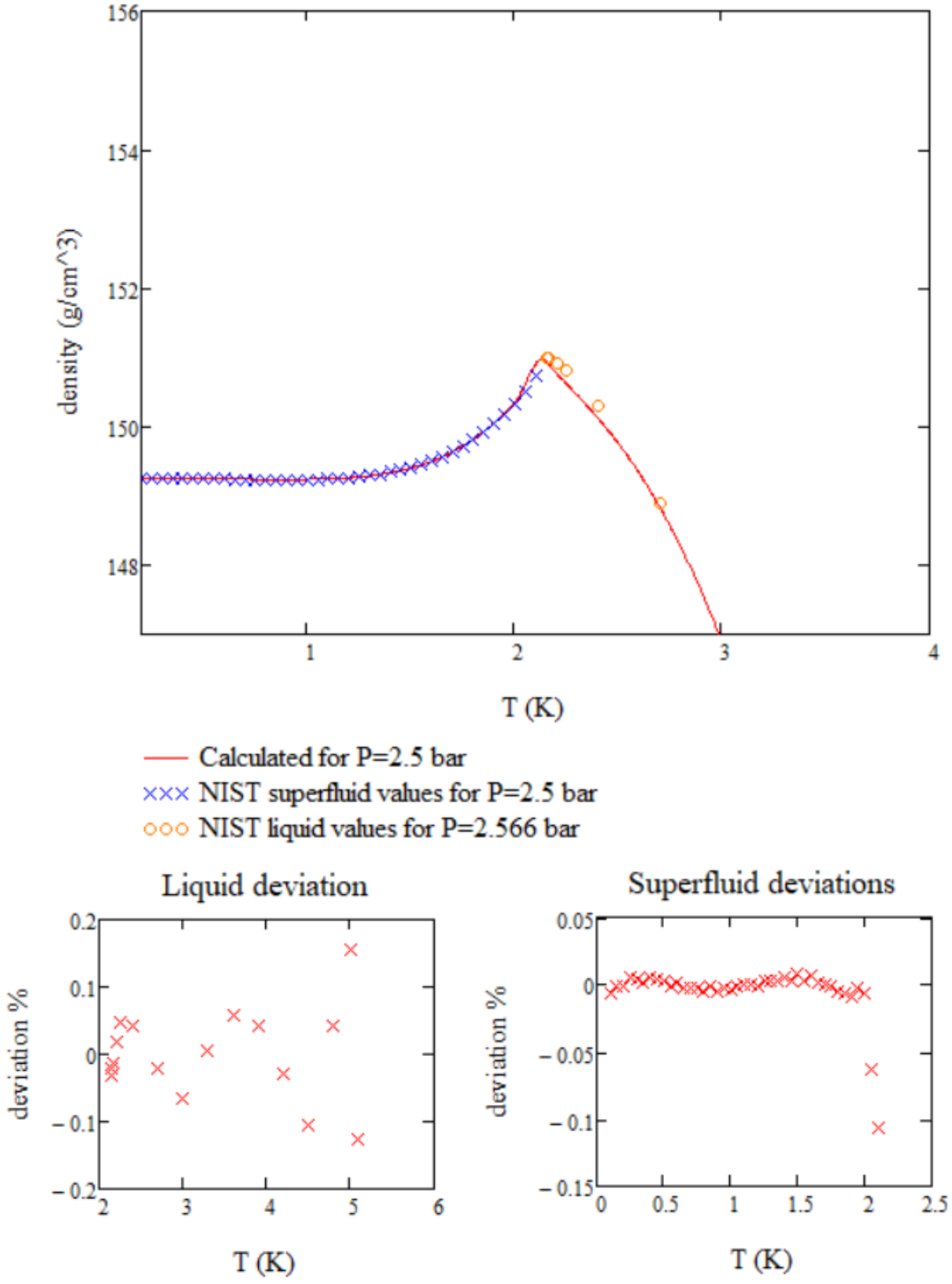

FIGURE 3.35: Calculated density compared to the NIST values

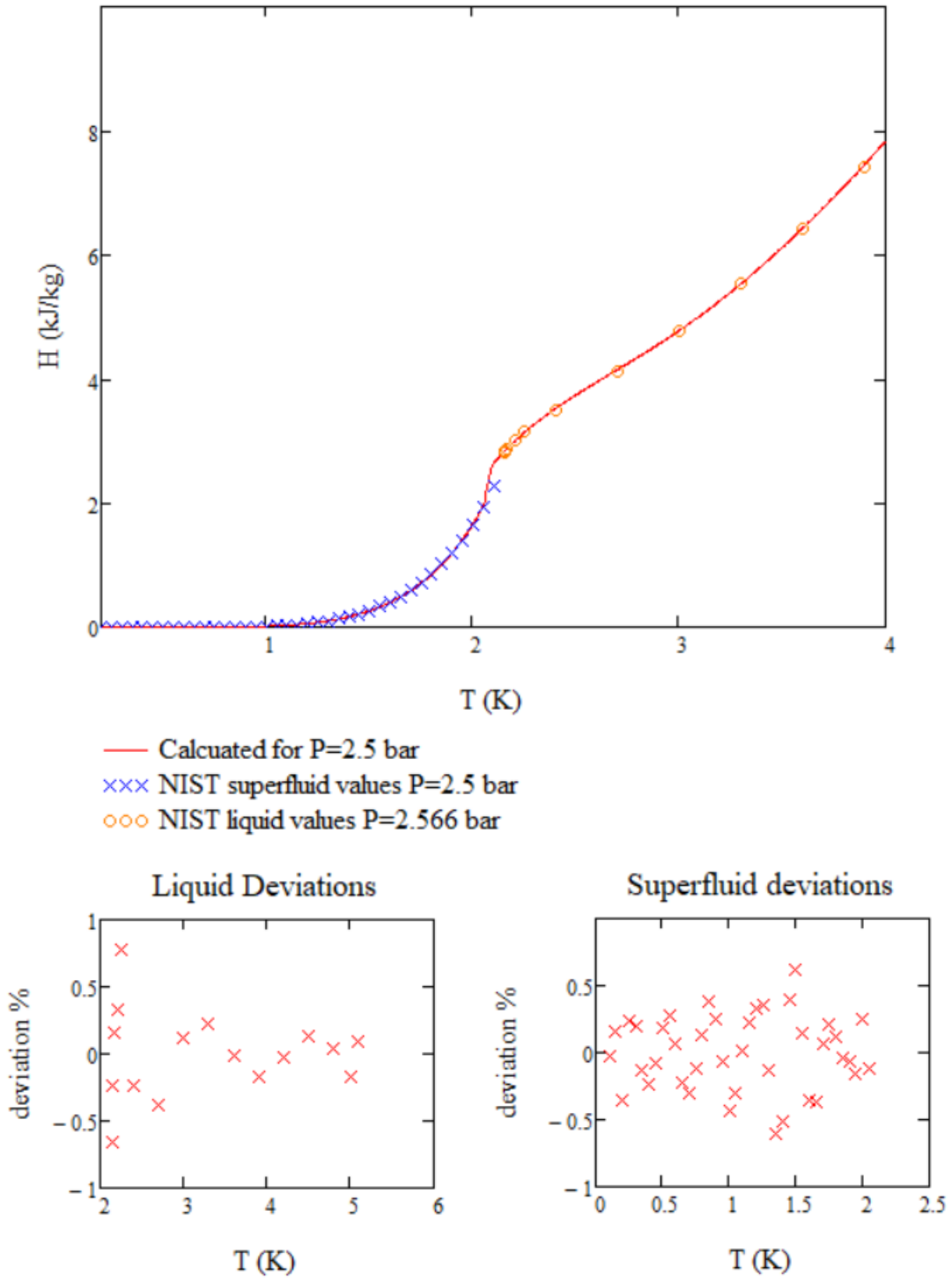

FIGURE 3.36: Calculated enthalpy compared to the NIST values

For the pressure of 20 bar

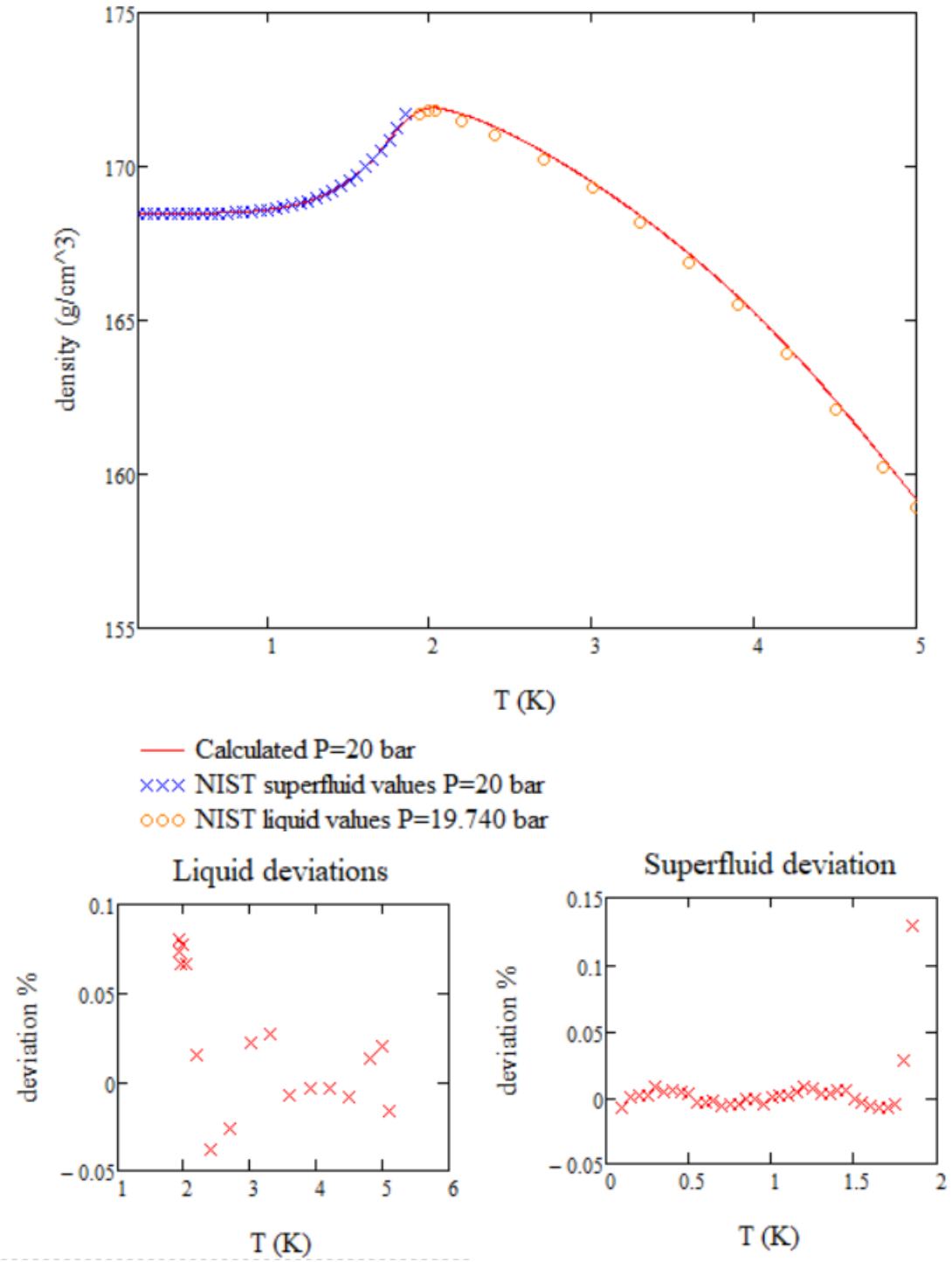

FIGURE 3.37: Calculated density compared to the NIST values

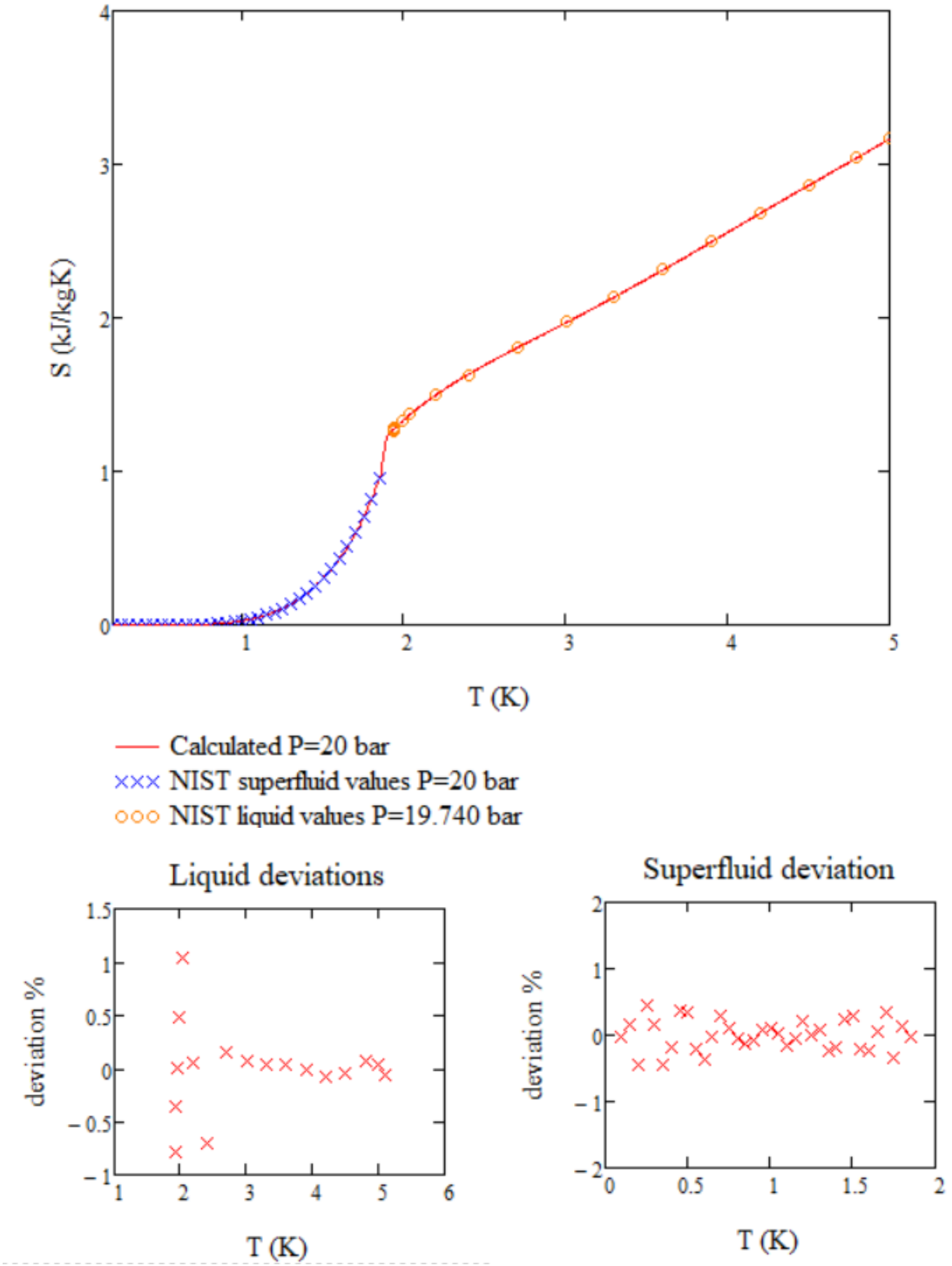

FIGURE 3.38: Calculated entropy compared to the NIST values

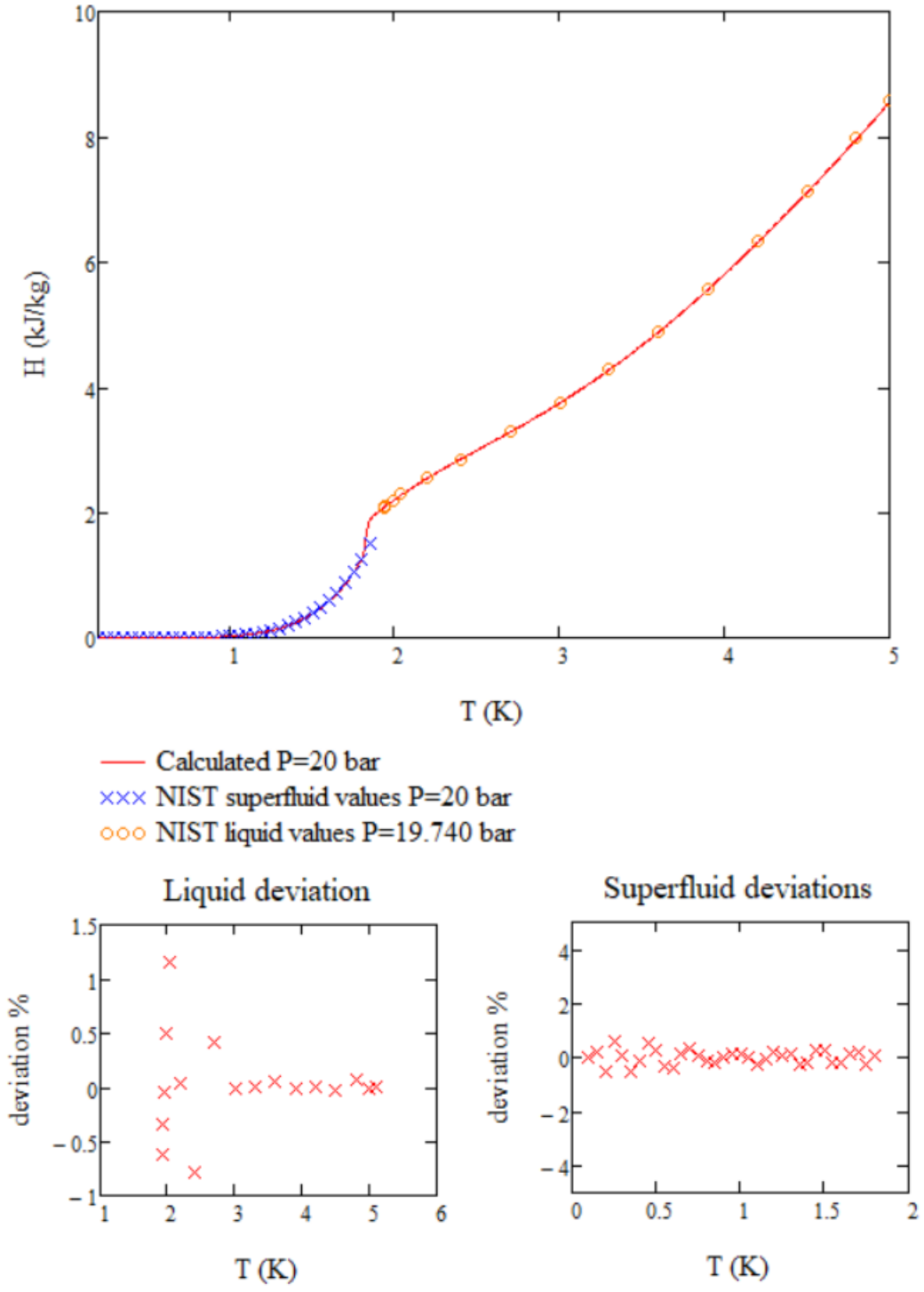

FIGURE 3.39: Calculated enthalpy compared to the NIST values

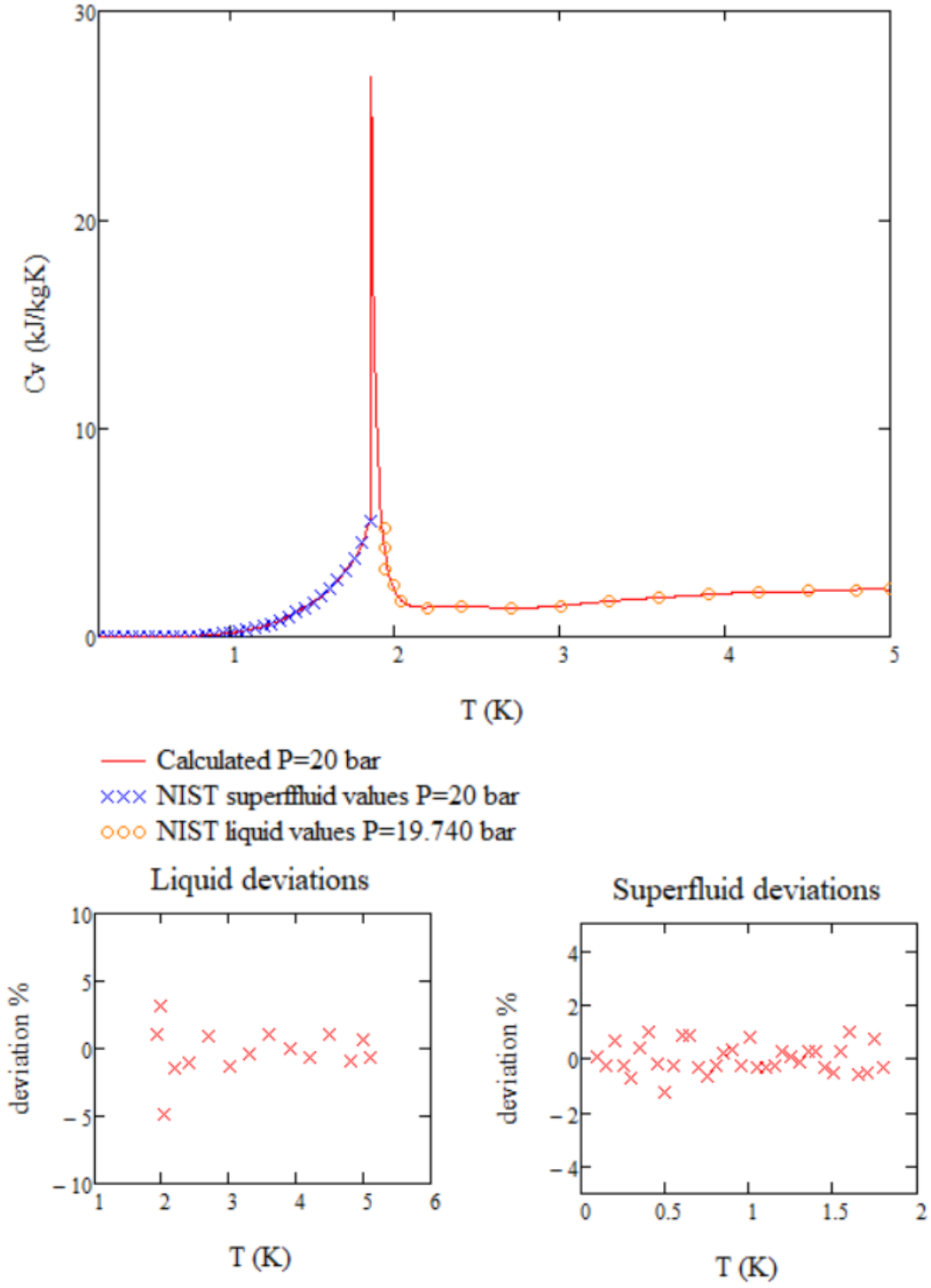

FIGURE 3.40: Calculated Cv compared to the NIST values

For the rest of the pressure spectrum the data is also calculated and presented in Appendix B. As it can be seen from these graphs as well as the graphs of the appendix is that the accuracy of the provided EOS is very high and it can be used for applications that require extremely small margins of error especially given the extreme difference in the in the orders of magnitudes of the values especially at lower temperatures. The mean deviations, the correlating coefficients and the coefficients of determinations for all the

variables for different pressures are shown in the table below.

Mean Deviations (%)	P=2.5 atm		P=10 atm	
	Superfluid	Liquid	Superfluid	Liquid
Density	-4.48E-03	-7.55E-05	9.82E-03	7.26E-03
Entropy	-2.34E-04	-1.97E-03	-4.49E-01	-2.42E-03
Enthalpy	-4.10E-01	-1.64E-03	-1.34E+00	-6.74E-03
Cv	2.44E-01	-5.78E-01	-5.60E-01	-5.10E-02
	P=17.5 atm		P=20 atm	
	Superfluid	Liquid	Superfluid	Liquid
Density	5.92E-03	9.65E-03	4.00E-03	2.10E-02
Entropy	-2.65E-04	6.42E-04	-2.74E-04	-3.05E-03
Enthalpy	-5.50E-01	-7.50E-02	-7.23E-01	2.30E-02
Cv	2.20E+00	-5.02E-01	2.28E+00	-5.86E-01

TABLE 3.5: Mean deviation (%) of the different thermodynamic variables against the NIST data for different pressures

	P=2.5 atm		P=2.566 atm	
	Superfluid		Normal Fluid	
	r	r^2	r	r^2
Density	0.99876	0.99752	0.99998	0.99997
Entropy	1	1	0.99998	0.99997
Enthalpy	0.99666	0.99333	0.99999	0.99999
Cv	0.92744	0.86014	0.97549	0.95158
	P=17.5 atm		P=17.760 atm	
	Superfluid		Normal Fluid	
	r	r^2	r	r^2
Density	0.99862	0.99723	0.99995	0.9999
Entropy	1	1	0.99997	0.99994
Enthalpy	0.99499	0.99	0.99999	0.99998
Cv	0.91982	0.84607	0.97202	0.94482

	P=10 atm		P=9.869 atm	
	Superfluid		Normal Fluid	
	r	r^2	r	r^2
Density	0.99683	0.99367	0.99998	0.99996
Entropy	0.99638	0.99277	0.99997	0.99994
Enthalpy	0.99139	0.98285	0.99999	0.99998
Cv	0.90456	0.81823	0.97521	0.95103
	P=20 atm		P=19.74 atm	
P=20 atm	Superfluid		Normal Fluid	
	r	r^2	r	r^2
Density	0.99928	0.99856	0.99993	0.99986
Entropy	1	0.99999	0.99997	0.99994
Enthalpy	0.99207	0.98419	0.99999	0.99998
Cv	0.89872	0.8077	0.97089	0.94263

TABLE 3.6: Correlation coefficients and coefficients of determination for the calculated data against the NIST values

3.2.7 Superfluid percentage in Helium-II

In addition to the thermodynamic properties of the fluid and the superfluid, one variable that is very important in any cryogenic engineering application is the percentage of superfluid below the Lambda line. Helium-4 does not all become a superfluid instantly at the lambda line, but it becomes a mixture of a superfluid and normal fluid. It is important for the exact superfluid percentage of the mixture to be known, as in any application that makes use of a superleak [41, 42, 43] only the superfluid part flows through and therefore is imperative to know its amount. Because the percentage of the superfluid does not directly correlate to the thermodynamic data, and for one to achieve such a correlation there would be a need to dive into the quantum mechanics of superfluidity, something that is out of the scope of this part of the study. Thus, the equation of the percentage of the superfluid presented here is a separate equation from the model created and should be used for its applications in engineering examples and not for deriving any deeper physical meanings. The equation form is based on the data of NIST as given in [14] and a sigmoid form was found to be the best for describing the data.

$$R(T,P) = \frac{a_1}{(1+e^{a_2-a_3T})(1+e^{a_4-a_5T})} \tag{3.29}$$

with the coefficients being:

a_1	$1.759438110219911\times10^{1}$
a_2	$5.237757610459909\times10^{-1}$
a_3	$2.988936852213499\times10^{-2}$
a_4	$6.435211650071271\times10^{-1}$

TABLE 3.7: Coefficients for the superfluid percentage equation 3.29

The results of the above equation are presented below.

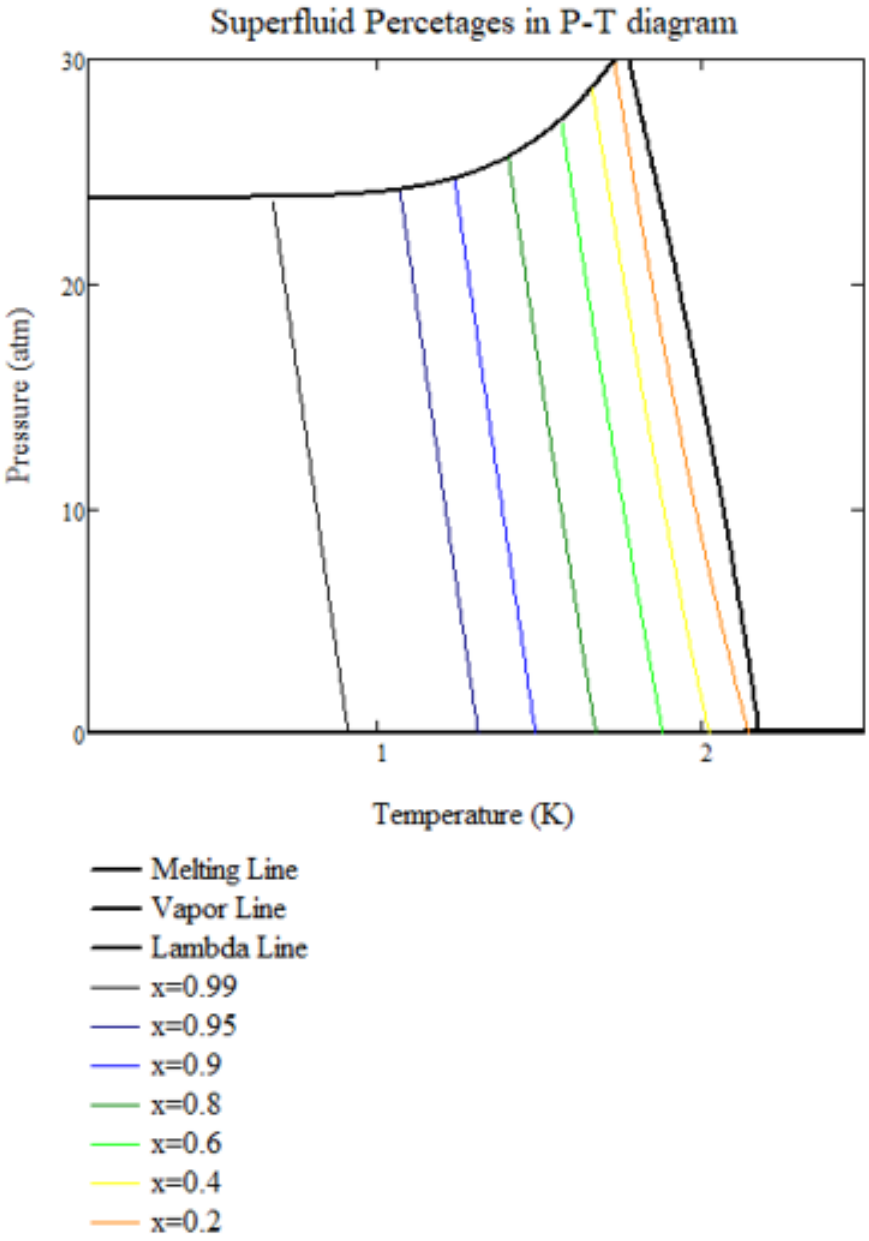

FIGURE 3.41: Superfluid percentage in Helium-II

The percentage of the superfluid increases while the temperature lowers, while reaching almost 100% when near the temperature of 1K. This phenomenon is very important and interesting both from a theoretical point of view as it will be discussed in the following chapter concerning the physics of superfluidity in Helium-4 and in the applications chapters especially for Superfluid Stirling Refrigerators.

3.2.8 Helium 4 Maps

Having completed the EOS for Helium 4 now the opportunity to create a full thermodynamic map for this working medium has arisen. Such a thermodynamic map does not exist in the literature due to the fact that there are no available full equations of state describing the Helium-4 through all of its phases. The maps that are to be presented are in terms of pressure and temperature. This is not usual in the presentations of thermodynamic maps, but it is chosen here for some important reasons. Firstly, through a P-T diagram the lambda line can be easily seen giving a connection to the lambda line graphs that one is used to studying when dealing with superfluid Helium. Additionally, if the more usual S-H diagram was chosen then the results would be very clattered as at these temperatures, and especially below the lambda line, as it will be seen the isenthalpic and isentropic lines, nearly converge.

In this map for Helium-4 (figure 3.42) one can clearly see the phases changes through the solidus and liquidus lines as well as the lambda transition through the lambda line. In addition, to these transitions the isochoric, isenthalpic and isentropic lines are being presented. As mentioned before, it can be seen that the isentropic and isenthalpic lines nearly converge especially below the lambda line. Moreover, one can notice that below around 1.5 K the behavior of the density seems to only be in terms of the pressure and has little to no correlation to the temperature. At the end of the book the full tables with the calculated data for Helium-4 are presented.

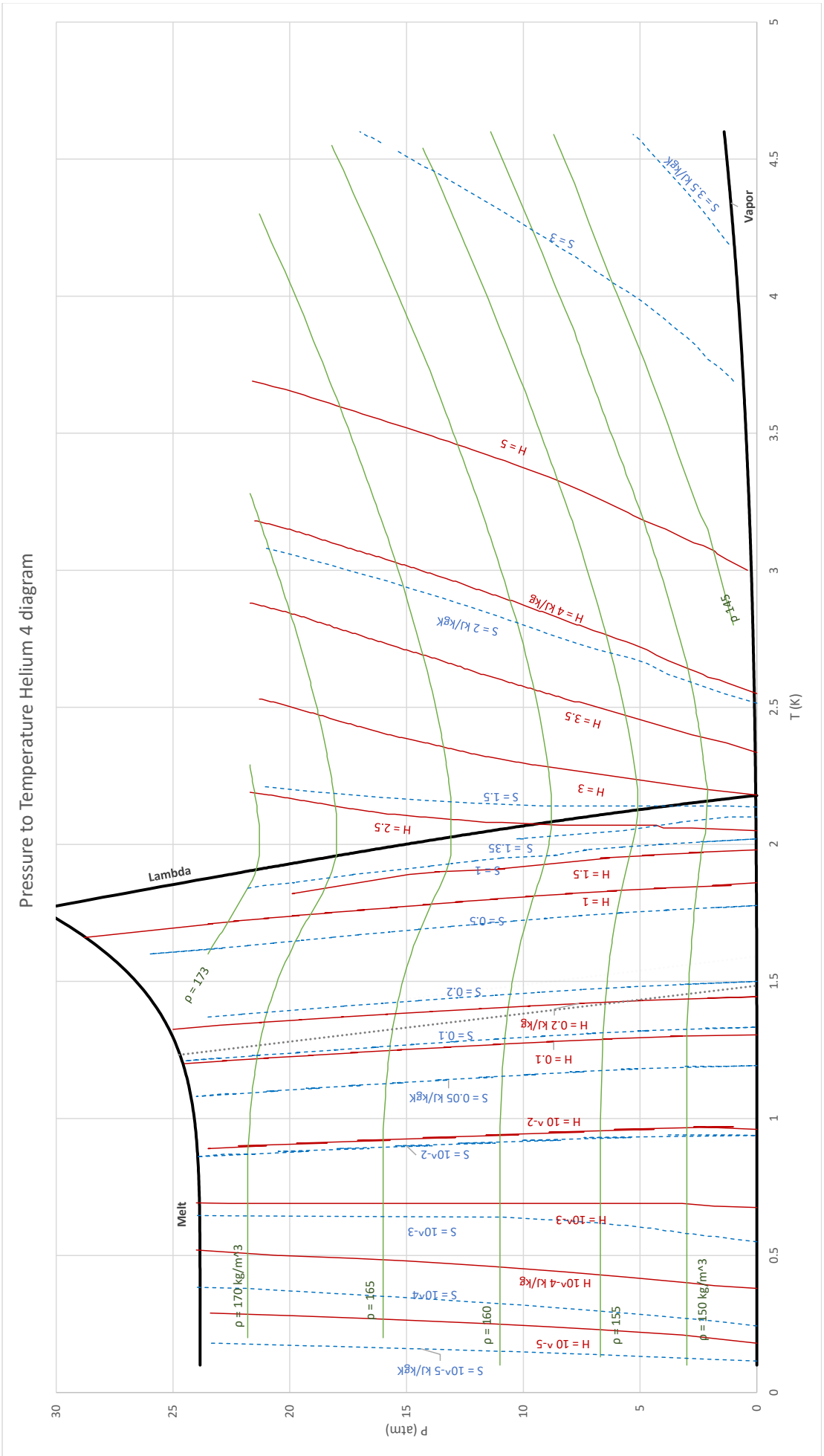

FIGURE 3.42: Helium-4 Thermodynamic Map

3.2.9 Polynomial Equation

This full code is designed as to be able to derive the properties of Helium with a very high accuracy through all of its phases, but as one can understand sometimes this much accuracy especially in applications with a wider temperature range is not needed, and the format of the code makes it mathematically extensive meaning that repeated calculations with it can require intense computing. This is something that can be overcome in smaller applications but in many CFD applications where computing power is of the essence and and this much accuracy is not required one could benefit more by using a less accurate but faster set of equations that can be more easily inserted to a CFD environment. For those reasons a polynomial equation is formed for the mostly used variables being the enthalpy, the density and the entropy.

The polynomials are of the following form:

$$S(T,P) = \sum_{i=0}^{6}\sum_{j=0}^{6} A_{i+1,j+1}\, T^i\, P^j \tag{3.30}$$

$$H(T,P) = \sum_{i=0}^{6}\sum_{j=0}^{6} B_{i+1,j+1}\, T^i\, P^j \tag{3.31}$$

$$\rho(T,P) = \sum_{i=0}^{6}\sum_{j=0}^{6} C_{i+1,j+1}\, T^i\, P^j \tag{3.32}$$

The values for the A, B, C are given in the tables of Appendix B. The convergence of the above equations is not as great as the resulting ones from the initial program these equations are able to describe the behavior of the system to an adequate degree with a standard error for eq. 3.30 for the entropy to be 0.081, for the eq. 3.31 for the enthalpy 0.067 and for the eq. 3.32 for the density to be 0.037. Due to this lesser accuracy of the polynomials compared to the extended code, it is advised that these polynomial equations are used in applications where temperature differences above 0.5K take place, as with these differences even an error of 10% would significantly affect the outcome due to the big differences between the values especially in lower temperatures. In cases where smaller temperature differences are achieved or where there is an emphasis on the behavior at temperatures below 0.5 K it is advised to directly use the full code with its much greater accuracy.

3.3 Conclusions of Helium 4 Chapter

In this chapter a comprehensive gathering of all the available data for Helium-4 at cryogenic temperatures has been undertaken. First of all, a theoretical equation of state has been developed based on the quasiparticle approach to superfluidity. Through this part of the study the equations for the energies of the quasiparticles are determined and presented, achieving greater accuracy to the experimental results compared to previous publications on the subject. In addition to this a full mathematical description for the energy model of the Helium-4 quasiparticles has been presented that does not require a direct input of the experimental data. Following this, the quasiparticle energy model is being used to calculate the thermodynamic variables of superfluid Helium-4. While

this is seen to be possible through using the equations provided by Donnelly, the overall outcomes are not accurate enough when compared to the experimental data to be able to be directly used in applications. In addition to this, the fact that this model requires the solution of multiple differential equations for its solution means that it is very time consuming (and CPU bound computationally) if it is to be used in any instances where a large number of data points is needed to be generated.

Given these shortcomings of the theoretical quasiparticle model, it is suggested that this model is used mainly to describe the physics of the system and a new numerical model is developed and presented in order to describe with much greater accuracy all the available data. This numerical model is such that is able to describe all the phases of Helium-4 below its liquefaction as well as the transitions between them. To achieve that the data points for both the fluid and the superfluid are cross-correlated a full and cohesive table of Helium data from different sources that are self consistent has been developed. Based on this set of data a new numerical code has been created to fit the data. One key aspect that needed to be solved in this part of the study is the very big differences in the orders of magnitude of the values when approaching absolute zero. Taking for example the entropy which experiences an 8 orders of magnitude drop from the lambda line to 0.1K. To overcome this hindrance, the code developed is dynamic, creating every time the EOS for the neighborhood of the requested point as to have great accuracy without the need of describing points far away that would be orders of magnitude larger or smaller and therefore lessen the accuracy of the system. This also means that since this code is based on the data from NIST, at any point in the future when newer or better data arise, one can simply insert these data in the code and proceed to have a very accurate equation of state for Helium-4 based on the new data. In addition to this code, a polynomial form of the EOS is also given which would be able to be used for applications requiring less accuracy. Those polynomials could be used a code that would work faster and without the need of handling all the data points for its use.

This work contains the so far fullest equation of state for cryogenic Helium-4 as it is the only one that is able to transverse between different regions, predict the transitions and have an overall accuracy that is higher than any previously published ones. In addition, the results of this EOS are cross-correlated with each other and it is shown that the provided values do not only achieve a mathematical accuracy but the derivatives are also accurate to a point where one could utilize one of the values like the Gibbs free energy with the temperature and pressure and create all the rest of the variables.

Using this equation of state the first full thermodynamic map of Helium-4 is created and presented.

Chapter 3 - Nomenclature

n	Occupational number
h	Plank's constant
p	Momentum
T	Temperature
P	Pressure
E	Energy of quasiparticles
u1	Speed of 1st sound
ρ	Density
Δ	Roton energy gap
μ	Roton mass
po	Momentum at Lambda point
k_t	Isothermal compressibility
v	Specific volume
S	Specific entropy
H	Specific enthalpy
Cv	Specific heat under constant volume
G	Specific Gibbs free energy
$T\lambda$	Lambda transition temperature
Ps	Vapor pressure
Pmelt	Melting line pressure
R	Superfluid ratio

Chapter 4

Entropic Lambda Transition

4.1 Low Temperature behavior of Helium

Helium is a substance that has been studied extensively during the last 100 years and it presents some very remarkable and interesting properties and behaviors in both high and low temperatures. At higher temperature its nature as an inert gas with a small atomic weight gives it properties that are very near to an ideal gas, to the point that at normal temperatures there is no need to differentiate its equation of state from the one of the ideal gas. At lower temperatures the behavior of Helium acquires even more interesting attitudes in many ways. Firstly, Helium is the only known substance that never solidifies under atmospheric pressure and has the lowest bowling point of any gas at 4.2 K under atmospheric pressure [44]. This means that Helium remains a liquid even at absolute zero under atmospheric pressure and only forms a solid at higher pressures [45]. The fact that a liquid exists so near absolute zero leads to some very different behaviors and characteristics compared to gases at normal higher temperatures. The key differentiation of Helium is that it undergoes the lambda transition and forms a superfluid. A superfluid is a phase where the liquid being in a superfluid form has zero viscosity [46], and presents interesting thermodynamic behaviors as well, like a major rise in the heat capacity and an abrupt slope change in the entropy at the lambda point [26]. Superfluid Helium has been a subject of many studies over the years, with various attempts to describe and explain its behavior. The first ideas considering the behavior of superfluid Helium have had a concern around its relation to Bose-Einstein condensates, with which a superfluid shares some properties. Like a Bose-Einstein condensate a superfluid can flow freely and it is thermodynamically inert below a certain temperature (however, it needs to be mentioned here that whereas the Bose-Einstein condensate can be described as completely thermodynamically, inert the superfluid can be considered, especially at its higher temperature ranges, only as approximately thermodynamically inert).

The first physical explanation for the phenomenon of superfluidity was the two-fluid approach by Tisza [7]. This approach stated that the superfluid consisted of two parts, one part that was the completely inert and free-flowing superfluid (very similar to a Bose-Einstein condensate in concept) and the second part was a normal fluid. The mixture of the two made up the Helium-II, which is what the phase below the lambda line in Helium-4 is referred to. This approach had great merit in explaining the behaviors of the superfluids and giving an adequate physical explanation of their formation, but its mathematical model seemed unable to provide an equation of state that described the experimental values of the superfluid. Then a second approach, by London [17], forwent the assumption of the two fluids and described the behavior of superfluid Helium both physically and mathematically through the quasiparticle approach. Landau [22] described

the thermodynamic behaviors of the superfluid in a quantum manner, with the quasiparticles being the excitations within the fluid. By studying these excitations of the different types of quasiparticles this approach has been seen to be able to fully describe the behavior of Helium in its superfluid form mathematically. The only apparent drawback of this approach is that due to its affinity in the quantum realm it provides an explanation that is more difficult to understand macroscopically and completely forgoes any connection with Bose-Einstein condensation.

While Bose-Einstein condensation is a phenomenon that is not directly used in the quasiparticle approach of describing superfluidity, this approach is also based on the fact that when the system does not have enough energy for its particles to overcome the energy gap and get to an excited state from the ground state then these particles do not interact with their neighboring ones. As such for the superfluid, the particles within the energy distribution of a given temperature that are able to get to excited states do interact with others and thus form the quasiparticles (the quasiparticles are nothing more than particles describing the different kinds of interactions between the Helium atoms). This phenomenon of particles staying in the ground state, while not directly correlated with Bose-Einstein condensation, gave the authors the idea for this study where a model is presented that correlates the superfluid transition with the Bose-Einstein condensation that ought to happen if only the non-interacting part of the liquid existed.

This procedure demands a framework of the equations that govern the statistical behavior of Helium. Helium has two stable isotopes, being Helium-3 and Helium-4 [8], which due to their different spins have vastly different statistical behaviors with one being a fermion and the other a boson. Thus, the statistical models for the two isotopes have to be very different. Especially in the case of Helium-3, given its fermionic nature the model that is used to described its thermodynamic statistical behavior is heavily based on the BCS theory [9] of a pair of fermions getting entangled and forming a Cooper pair with properties similar to a boson, obeying Bose-Einstein statistics. Through this approach it is shown in this work that the lambda transitions in both Helium-4 and Helium-3 match to a great degree the Bose-Einstein condensation temperatures of their non-interacting parts.

4.2 Defining the Statistical Mechanics of the System

Before setting off to provide the reader with the model for the statistical behavior of the isotopes of Helium it is deemed helpful to provide a concise subsection defining the variables and their nature used in the model. This statistical description has been based on the courses of Prof. Leonard Sussking of Calc.Tech.

Assume a system having i possible states (as a state one can consider any possible outcome of the system), with $i = 1 \dots n$. $P(i)$ will be the possibility of the system appearing in the i state, with $P(i) \geq 0$ with the sum of all the probabilities being equal to 1. $\sum_i P(i) = 1$.

According to these probabilities one can define the entropy for the information of the system. The entropy, statistically speaking, is only a measure that corresponds with the ignorance on the system, the higher the ignorance the higher the entropy. One very basic definition of the entropy can be: $S = log(M)$, where M is a variable representing our ignorance of the system. A more robust definition of the informational entropy is given by the Shannon entropy [47] where the entropy is defined as:

$$S = -\sum_i P(i) ln P(i) \tag{4.1}$$

This approach to entropy is mostly used in areas of information theory. In the physics realm the possibilities are rarely this discreet or dependent to only one variable. A more physical approach to this definition would be define the entropy in a phase-space.

$$S = \int P(p,x) ln P(p,x) \tag{4.2}$$

where P(p,x) is the probability of a particle being in a specific state in the phase space of position x and momentum p.

In even very simple physical or thermodynamical systems the large amounts of possibilities leads for the integral of the entropy to get to extremely high values making its use cumbersome in applications. For this reason, the Carnot entropy which is defined using the Boltzmann's constant as:

$$S_{Carnot} = kS = -k\sum_i P(i) ln P(i) = -k ln\Omega \tag{4.3}$$

Based on the definition of the probability distribution and on the fact that it is by default normalized it can be seen that $\sum P(i)E_i = E_i$ where E_i is the energy distribution. Now the problem that needs to be tackled at this point is to be able to find the probability distribution in terms of the entropy. For this reason, the method of the Lagrange multipliers is to be used.

Mathematically this correlation between the entropy and the probability distribution can be seen through the system of:

$$S(P_1, P_2, \dots) = -\sum_i P_i ln P_i$$

$$\sum P(i) = 1$$

$$\sum P(i)E_i = E_i$$

and with the Lagrange multipliers implemented this system can be transformed as:

$$S(P_1, P_2, \dots) = -\sum_i P_i ln P_i$$

$$G_1 = \sum P(i) - 1$$

$$G_2 = \sum P(i)E_i - E_i$$

Now, minimizing the entropy in terms of the probability distribution one can write:

$$S^*(P) = S(P) + \alpha\, G_1 + \beta\, G_2$$

$$S^* = \sum_i P_i ln P_i + \alpha \sum_i P_i + \beta \sum_i P_i E_i$$

by differentiating the above, according to Fermat's theorem of stationary points it would be equal to zero at the minimal value:

$$\frac{\partial S^*}{\partial P_i} = ln P_i + 1 + \alpha + \beta\, E_i = 0$$
$$ln P_i = -(1+\alpha) - \beta E_i$$
$$=> P_i = e^{-(1+\alpha)} e^{-\beta E_i}$$

Now we write $Z = e^{1+\alpha}$, and therefore the probability distribution can be written as:

$$P_i = \frac{1}{Z} e^{-\beta E_i} \tag{4.4}$$

In addition to this we know that $\sum_i P_i = 1$, so:

$$Z(\beta) = \sum_i e^{-\beta E_i}, \tag{4.5}$$

is defined as the partition function. Also we had that $\sum_i P_i E_i = E_i$ and as such:

$$\sum_i \frac{1}{Z} e^{-\beta E_i} E_i = E$$

By differentiating 4.5 over β:

$$\frac{dZ}{d\beta} = \frac{d \sum_i e^{-\beta E_i}}{d\beta}$$
$$\frac{1}{Z}\frac{dZ}{d\beta} = -\sum_i \frac{1}{Z} e^{-\beta E_i} E_i \tag{4.6}$$

So overall we can write that:

$$E(\beta) = -\frac{\partial ln Z}{\partial \beta} \tag{4.7}$$

Applying this to the definition of the entropy we can get:

$$\begin{aligned} S &= -\sum_i P_i ln P_i = -\sum \frac{1}{Z} e^{-\beta E_i} ln(\frac{1}{Z} e^{-\beta E_i}) = \\ &= \sum_i \frac{1}{Z} e^{-\beta E_i} (\beta E_i + ln Z) = \\ &= \beta \sum_i P_i E_i + \frac{1}{Z} ln Z \sum_i e^{-} \beta E_i = \\ &= \beta E + ln Z \end{aligned} \tag{4.8}$$

Differentiating the result of 4.8 one gets:

$$dS = \beta dE + Ed\beta + \frac{dlnZ(\beta)}{d\beta}d\beta = \beta dE$$

So it comes that:

$$\beta = \frac{S}{E}, \tag{4.9}$$

but also we know that

$$dE = TdS \implies \frac{S}{E} = \frac{1}{T} \tag{4.10}$$

Thus, by combining equations 4.9 and 4.10 it is derived that:

$$\beta = \frac{1}{T} \tag{4.11}$$

By following the above procedure, the definitions for all the basic statistical variables have arisen as they are summed up in the table below:

$P_i = \frac{1}{Z}e^{-\beta E_i}$	Probability distribution
$Z = \sum_i e^{-\beta E_i}$	Partition function
$E = -\frac{\partial lnZ}{\partial \beta}$	Energy
$T = \frac{1}{\beta}$	Temperature
$S = \beta E + lnZ$	Entropy

TABLE 4.1: Definitions of fundamental variables of statistical mechanics

Having defined the basic functions and variables of the statistical mechanics to be used in this model, readily one can initiate their application in a model. Initiating, the above mechanics are to be applied in an ideal gas. This application of the statistical mechanics to an ideal gas might at first seem simplistic and not related to Helium which, especially at these temperatures, is not an ideal gas, but later in this chapter it will be showcased that the behavior of the ideal gas holds a very significant meaning in understanding and describing superfluidity in Helium.

Assume a collection of N particles in a 3 dimensional space V with their values being defined by their position and momentum. Thus, the partition function will be written as:

$$Z = \int e^{\beta \sum_{n=1}^{3N} \frac{p_n^2}{2m}} d^{3N}x \, d^{3N}p \tag{4.12}$$

The equation above can be transformed by changing the position integral as: $\int d^3x = \frac{V^N}{N!}$. The N! as the denominator is used as to not count the same particle multiple times.

$$Z = \frac{V^N}{N!}(\int e^{-\frac{\beta}{2m}p^2})^{3N}$$

calculating the integral one gets:

$$Z = \frac{V^N}{N!}(\sqrt{\frac{2m\pi}{\beta}})^{3N}$$

To simplify this formula, we can use the Stirling's approximation for the factorial and get:

$$Z = \frac{V^N}{N^N e^{-N}}(\sqrt{\frac{2m\pi}{\beta}})^{3N}$$

$$Z = (\frac{e}{\rho})^N(\frac{2m\pi}{\beta})^{\frac{3N}{2}} \tag{4.13}$$

with $\rho = \frac{N}{V}$ the particle density. Following this the energy can be calculated as:

$$E = -\frac{\partial lnZ}{\partial \beta} = \frac{3}{2}N\,T$$

So by this one can calculate the standard form of the energy of an ideal gas.

4.3 Calculation of the partition function of Helium

The model that is being shown in this study showcases a novel approach where by calculating the partition function of Helium it will be shown that the lambda transition can be seen to be very clearly manifesting in the ideal part of the system and correspond to a theoretical Bose-Einstein condensation of the system.

4.3.1 Partition Function of Real gas

The difference between a real gas and an ideal gas is based on the difference that in the real gas there are interactions between the particles while in the ideal gas this is not the case. So for a real system the energy is defined as the sum of the kinetic energy and the potential energy of the particles.

The energy for a single particle will be:

$$\epsilon(r,p) = \frac{\hat{p}^2}{2m} + U(r), \tag{4.14}$$

where it is seen that the kinetic part is based on the momentum operator $\hat{p}$ (with m being the atomic mass) and the potential part on the potential energy U in terms of the interatomic distance r. This is the case for a single atom, but to describe the entirety of the gas one would need to find the energy of all the particles, which is the sum of the individual energies as seen in Eq. 4.15:

$$E = \sum_{n=1}^{N}\frac{\hat{p}^2}{2m} + \sum_{n>m}U(|x_n - x_m|), \tag{4.15}$$

with N being the total number of atoms in the gas and $|x_n - x_m|$ being the distance between the n_{th} and the m_{th}.

Integrating over all the possible positions of the two particles one gets:

$$\int dx_1^3 dx_2^3 U(|x_1 - x_2|) = V\, U_o$$

So knowing the energy one can define the partition function based on 4.1. The sum of the partition function due to the large number of atoms in any gas can be transformed to a an integral, where one must integrate over all the i, where the i are the two independent variables of the system p-momentum and x-position so for three dimensions one must integrate three times to cover all of them. Thus, the partition function is written as:

$$Z = \int \frac{d^{3N}p\, d^{3N}x}{N!} e^{\beta \sum_n \frac{p^2}{2m}} e^{\beta \sum_{n>m} U(x)} \tag{4.16}$$

$$Z = \frac{1}{N!} \int e^{\beta \frac{p^2}{2M}} d^{3N}p \int e^{\beta U(d_n)} d^{3N}x$$

$$Z = \int \frac{V^N e^{-\beta \frac{p^2}{2m}}}{N!} d^{3N}p \int \frac{e^{-\beta U(r)}}{V^N} d^{3N}r. \tag{4.17}$$

Equation 4.17 is a key result, as one can see that the first term of the equation, being $\int \frac{V^N e^{-\beta \frac{p^2}{2m}}}{N!} d^{3N}p$, is the partition function of the ideal gas as it was calculated before and the second term, $\int \frac{e^{-\beta U(r)}}{V^N} d^{3N}r$ does not contain any kinetic parts and therefore only refers to the interacting part of the system.

As such the partition function can be written in the form:

$$Z = Z_{ideal}\, Z_{interacting} \tag{4.18}$$

and based on the definition of the entropy through 4.1 one sees that the entropy is written as:

$$S = S_{ideal} + S_{interacting} \tag{4.19}$$

4.3.2 Entropy of Bose-Einstein condensate

Generally, as mentioned before the reason why Bose-Einstein condensation is not a phenomenon directly applied to Helium is because Helium is not an ideal Bose gas and has interactions between its particles. If one stops thinking of Helium as one entirety but sees it as two different entities as it is seen through this demonstration of the partition function it can be seen that the equations 4.18, 4.19. These two are not suggested to be actual different fluids but this is used only as a mathematical method that gives some very key advantages into the description of the superfluid. The work presented below has already been published in the paper [38] by the author at IMECE2021, where it received the Edward F. Obert Award for outstanding paper in thermodynamics.

Studying the ideal part of the system one can readily reach a simple but important conclusion. This term represents an ideal gas and in this case being based in Helium its particles are bosonic. This means that this term represents an ideal Bose gas.

For describing of the Entropy and Partition Function of the ideal Bose gas the works of Svidinsky et al. and Kim et al. at [48, 49] are being used. Through the paper [48], also based on the work of Scully et al. [50], it has been described theoretically and

verified numerically that when referring to an ideal Bose gas below a point of the critical temperature (around 0.8 Tc based on the particle density) the Ground State of the system does not play a part in the entropy of the ideal system. This is being done by assuming the entropy of the ideal gas being first a aggregate of the entropies of each individual particle and the entropy of the correlations between the particles as:

$$S_{ideal} = S_{ind} + S_{corr} \tag{4.20}$$

Each individual particle can be thought of being either in the ground state or an excited state. Thus, their entropy will be the sum of the entropies of the ground state and the excited states.

$$S_{ind} = S_{ground} + S_{exc} \tag{4.21}$$

So overall the entropy can be written as:

$$S_{ideal} = S_{ground} + S_{exc} + S_{corr} \tag{4.22}$$

In a Bose-Einstein condensate all the particles are in the ground state and as such there are no correlations between them because they do not possess adequate energy to interact to their neighbors. This means that in the equation Eq. 4.22 the terms S_{exc} and S_{corr} must cancel out as not to have an effect on the overall entropy based on the physics of the system. This something that makes physical sense but can also be mathematically shown as done in the numerical calculations of [48], where in a Bose-Einstein condensate the entropy of the ground state particles is calculated and seen to cancel out with the entropy of the correlations, so in the term of this work it means that:

$$S_{ground} = -S_{corr} \tag{4.23}$$

When an ideal Bose-gas exists below its critical temperature then it forms a Bose-Einstein condensate. Not all the gas instantly goes through the transition and with equations 4.23, 4.22 one can calculate the entropy of the condensate through the entropy of the excitations. To evaluate this entropy on the ideal part the canonical ensemble method is going to be used. The Hamiltonian of the particles is:

$$\hat{H} = \sum_{i=1}^{N} \left(\frac{\hat{p}^2}{2m} + \frac{1}{2} m\omega^2 \bar{r}^2 \right), \tag{4.24}$$

with the potential energy of the particle in the ideal Bose gas being:

$$U(\mu, T, \omega) = kT \sum_{i,j,k} ln(1 - e^{\frac{\hbar}{T}\omega(i+j+k) + \frac{\mu}{kT}}) \tag{4.25}$$

with k being the Boltzmann constant, h being Planck's constant with $\hbar = \frac{h}{2\pi}$ and μ the chemical potential. Since we are referring to the ideal part of the system then that means that the chemical potential will be zero, $\mu = 0$. The i, j, k indices refer to the 3-dimensional space. For simplifying the potential equation the Bose function is used, defined as:

$$g_a(z) = \frac{1}{(a-1)!} \int_0^{+\infty} \frac{x^{a-1}}{z^{-1}e^x - 1} dx \tag{4.26}$$

with z being the fugacity and a referring to the dimensionality of the system. Thus, the entropy of the canonical ensemble of an ideal Bose gas will be:

$$S_{canonical} = k\left(\frac{kT}{\hbar\omega}\right)^3 (4g_4(z) - \frac{\mu}{kT}g_3(z)) \tag{4.27}$$

The critical temperature [51] of an ideal Bose gas, is calculated in this manner to be:

$$T_c = \frac{\hbar\omega}{k}(\frac{N}{g_3(1)})^{\frac{1}{3}}, \tag{4.28}$$

and the entropy below this temperature will be transformed from Eq. 4.27 as:

$$S_{BEC} = k(\frac{kT}{\hbar\omega})^3 g_4(1). \tag{4.29}$$

A Bose-Einstein condensate will be formed but this, as in normal gases, will not take place instantly in all the particles of this theoretical gas. Due to the inert nature of Bose-Einstein condensates the thermodynamic properties of the gas are mainly governed by the particles not in this state. The number of these particles will be:

$$N^* = (\frac{\hbar\omega}{kT})^3 g_3(1). \tag{4.30}$$

So by using the equations 4.27, 4.29 and 4.30 the full entropy of the ideal part of the system is calculated.

This entropy can also be described by using the grand-canonical ensemble of the system instead of the canonical ensemble by implementing some key differentiations. The entropy of the ground state will be excluded as it is expected to be zero and the chemical potential will again be zero. The fact that the entropy of the ground state needs to be neglected is explained physically by understanding that by referring to an ideal Bose gas below the Tc then the particles in the ground state will be condensed into a BEC and as such will all occupy the same state providing a zero entropy, or with the mathematical simulation offered by [48]. Thus, the entropy of the grand-canonical ensemble will be:

$$S_{GC} = -k\frac{\partial}{\partial T}(T\sum_{\nu=1}^{\infty} ln(1 - e^{-\frac{\epsilon_\nu}{kT}})) \tag{4.31}$$

One now expects that this entropy ought to be the same as the entropy of the excitations in the canonical ensemble calculated below the critical temperature Tc, but one should also consider the effect of Eq. 4.30. By performing the calculations for the two different model the results that arise can be seen in the Figure 4.1. This differentiation of the entropy of the excitations of the canonical ensemble to the entropy of the grand canonical ensemble has a very significant physical meaning. In the way that the equation for the entropy of the grand canonical ensemble is written it is assumed that the entropy of the ground state bares no significance. This is true for the entropy in the canonical ensemble as well but excluding the values of the N^* particles which are not in the BEC state yet. This effect is more prevalent near Tc and lessens when the temperature lowers. This behavior also relates to the behavior seen in the works of [50],[49] and [48] where it is shown that this relation between a similarly defined grand canonical ensemble and

entropy of excitations can be derived by running the numerical model for the entropy of the ground state of a Bose-Einstein condensate.

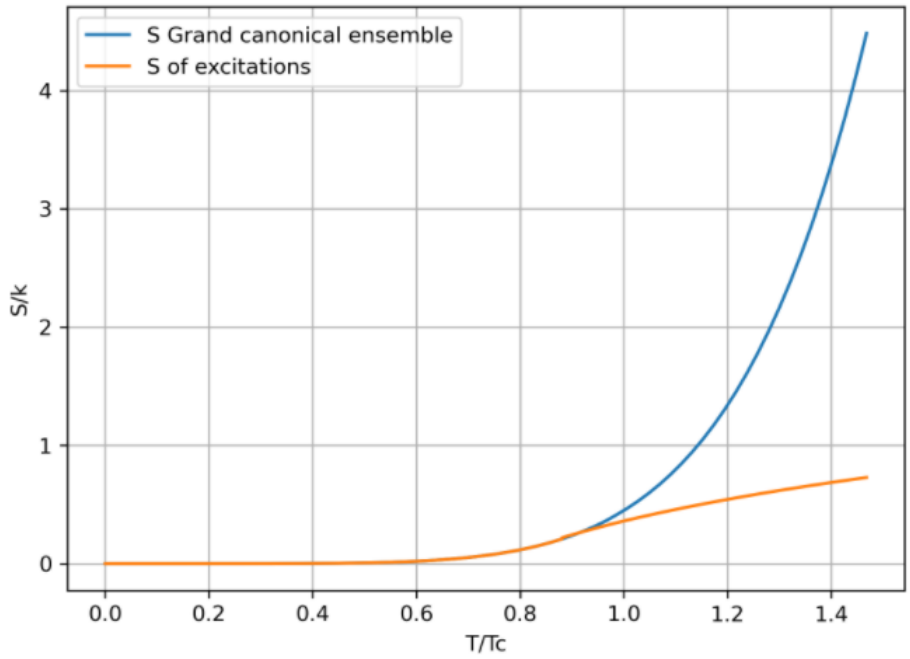

FIGURE 4.1: The entropy of the canonical ensemble for the excitations is shown in the blue line and the entropy of the modified grand canonical ensemble is shown in the orange line. It can be seen that they converge until around $\frac{T}{Tc} = 0.8$

This can also be viewed by observing the probability distribution function for the particles in the ground state being:

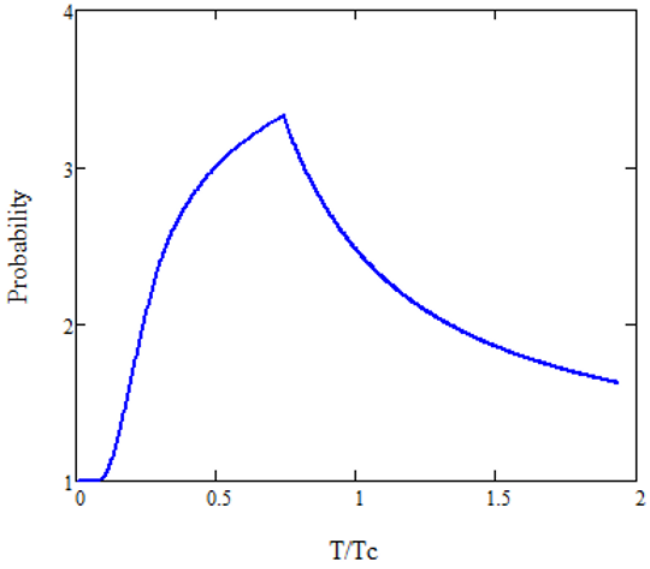

FIGURE 4.2: The probability distribution of the Ground State of the ideal Bose gas calculated from the equation Entropy of the Ground State

4.4 Combining the ideal and non ideal parts to Helium-4 and comparing to the experimental data

Through the provided calculations for the total entropy and the entropy of the ideal part one can expect that the ideal part will have an important effect on the overall thermodynamic behavior, especially considering the tendency of Helium to be a weakly interacting gas. To use the equations provided and apply them to Helium-4 they must first denormalised. For denormalising these equations one must first use the Bose-Einstein condensation temperature. One option would be for one to use the equation 4.28. Whilst this equation is sufficient to describe the behavior, the fact that it makes use of the number of particles N makes it troublesome in its thermodynamic uses for big and unknown numbers N. For this reason, the version A.1 will be used utilizing the particle density instead of the particles themselves. To remind the reader the used equation of the Tc is:

$$Tc = \frac{h^2}{2\pi mk}(\frac{N}{2.612V})^{\frac{2}{3}}.$$

Having the values for the particle density from the equation of state described in the previous chapter 3, one can readily calculate that the Tc will be in the range of 2.9-3 K depending on the temperature. On this point one can calculate the transition point as seen in 4.1 and through the mathematical models of [48] will be in the range of $0.8Tc \approx 2.2K$. This is a key result at this point as it showcases that the point where the ideal part transitions to the BEC in its ground state is very close to the lambda point of the full Helium-4. The result of this is that as far as the ground state of the ideal part is concerned, below this point the particles are on the ground state and obeying a Bose-Einstein distribution and as such they are condensed into a BEC. The forming of this condensate means that only the excited particles of the ideal part are responsible for the thermodynamic behavior. At this point one must be careful and not assume a formation of a BEC in the full Helium-4 as this is not the case. This BEC can be seen to be theoretically forming in the ideal part of the system and this can be used as a useful tool to study the transformation from normal fluid to superfluid with the energy transition of the ideal part of the gas.

Additionally, as it was shown in the figure 3.41 the transition to superfluidity is not something that happens instantly. This phenomenon is something that can also be clearly seen in the particles that enter the BEC phase in the ideal part as described by equation 4.30. From an energy state point of view this model counts on the property of the bosonic in nature particles of the system that allows them to exist simultaneously in the same state and when below the Tc in the ground state, to Bose-Einstein condense. Thus, by observing figure 4.2 one can see that the number of particles in the ground state transition very close to the lambda temperature of the full Helium-4, hence why the formation of the BEC initiates at around 0.8 of the Tc. In addition to this, not all particles are in the ground state which means that only a percentage of the properties of the ideal gas will amount to the properties of the full gas at each temperature.

Through this method it is seen that the contributing parts to the final entropy of the Helium-II are the entropy of the excitations of the ideal part and the entropy of the interacting part. The understanding of this is that the partition function and the entropy, and therefore all the thermodynamic variables, are based on the excitations of the crystallic structure of the system, them either being excitations of the individual

particles in the ideal part or interactions between different particles in the interacting part.

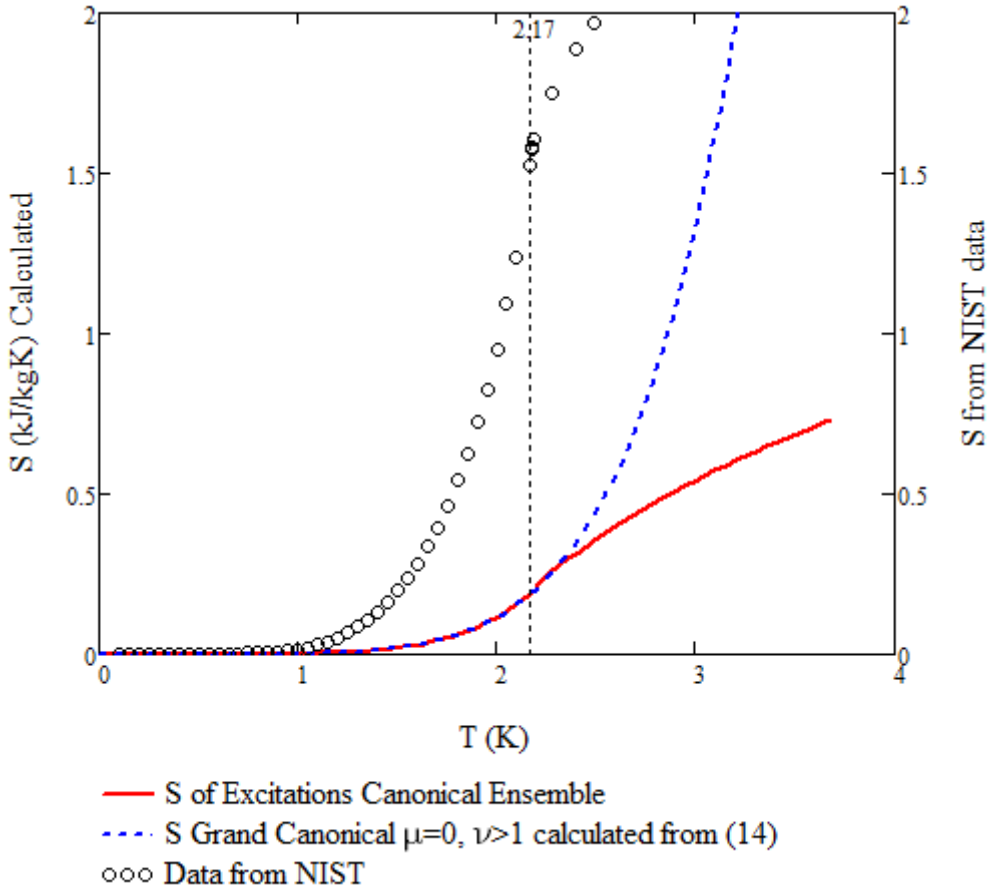

FIGURE 4.3: Comparison of the calculated values for the Entropy of ideal Bose Helium gas with the Entropy Values from NIST in order to highlight the common transition at around 2.2 K

As it can be seen and through the graph above the transitioning point of the entropy of the ideal part directly correlates to the lambda point of the superfluid. To get an even clearer view of this phenomenon and also verify the self-coherence of the mode the specific heat capacity under constant volume is being calculated for the ideal part and compared to the one for the superfluid from the provided equation of state based on the NIST data.

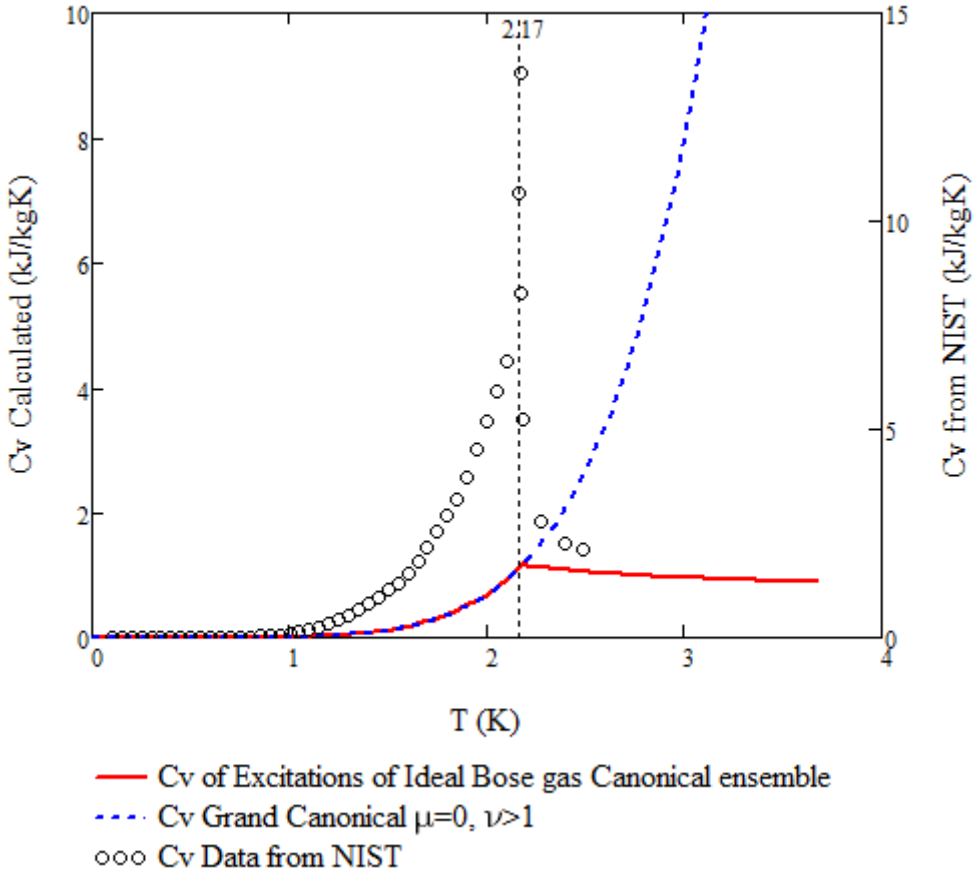

FIGURE 4.4: Comparison of the calculated values for the specific heat under constant volume of ideal Bose Helium gas with the Entropy Values from NIST in order to highlight the common transition at around 2.2 K

Through the figures 4.3 and 4.4 it is clear that there exist a significant correlation between the transition to superfluidity in the Helium-4 and the transition to a theoretical Bose-Einstein condensation in its ideal part.

4.5 Extrapolating the model to lower temperatures and deriving the interatomic potential

By having calculated the thermodynamic values for the full Helium-4 through the equation of state in the previous chapter based on the NIST data and now having calculated the entropy values for the ideal part of the system it is now straightforward to calculate the entropy of the interacting part of the system and through that find the results of the interatomic potential. Thus, through equation 4.19 one can get:

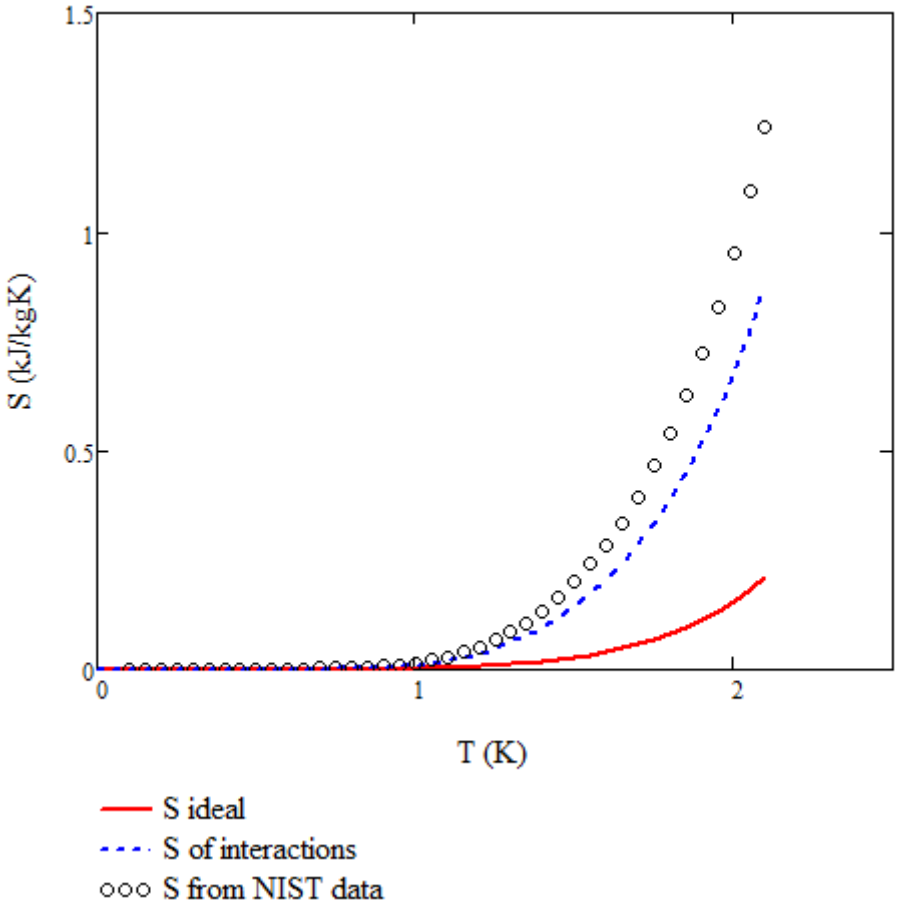

FIGURE 4.5: Entropies of interactions in 4He and excitations of the ground state compared to the overall Entropy from the EOS and the NIST data below the Lambda transition

Through having now the function and the values for the interacting part through the interatomic potential of Helium-4 the rest of the thermodynamic data below 0.1K, as missing from the NIST experimental values, can now be theoretically derived.

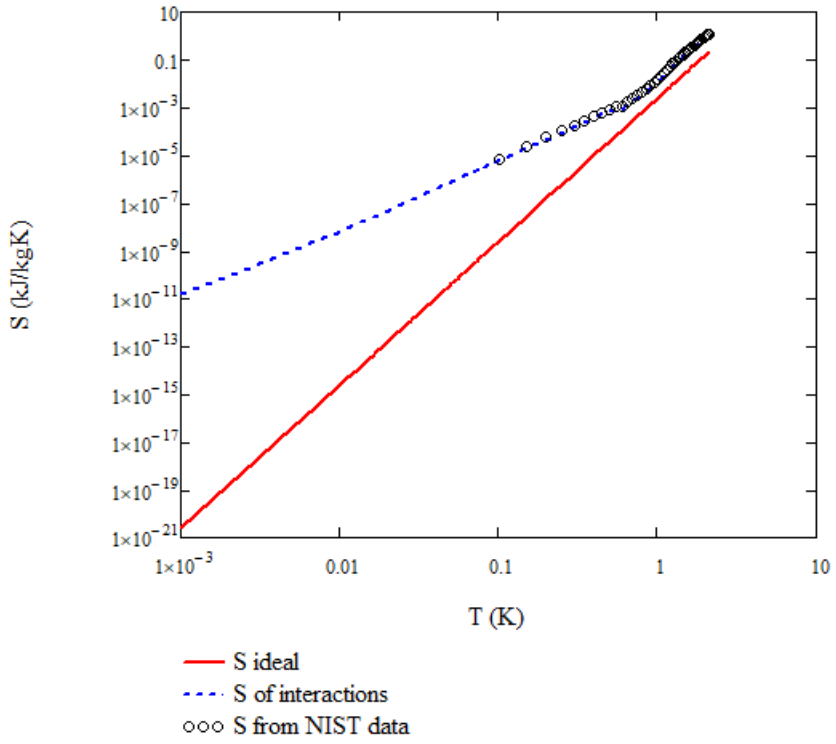

FIGURE 4.6: Equivalent to figure 4.5 with logarithmic axis for a clearer view going towards absolute zero

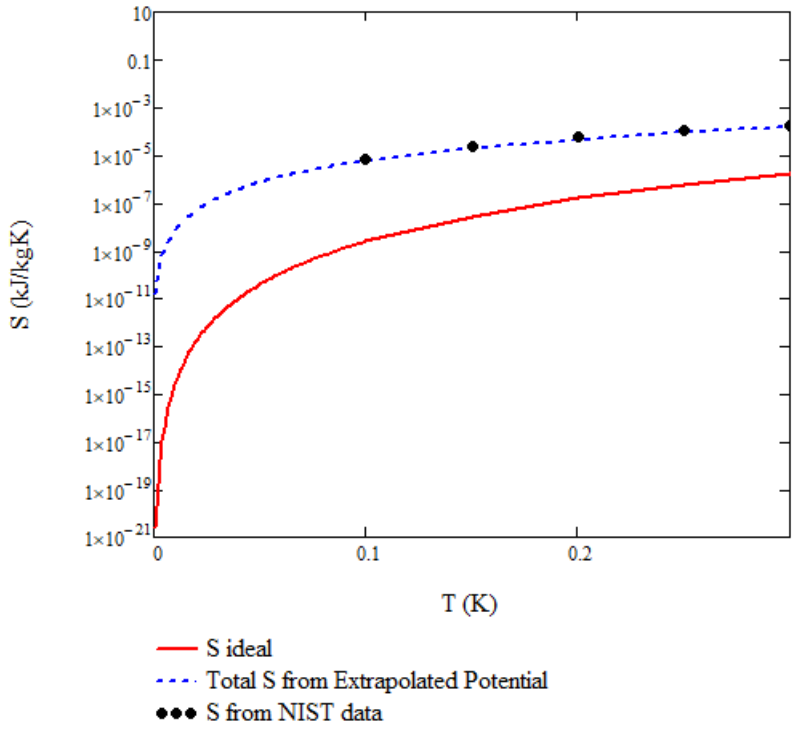

FIGURE 4.7: Equivalent to figure 4.5 with logarithmic x-axis centered towards the values closer to absolute zero

By plotting the entropy from the ideal part and the entropy through the potential of the interacting part it can be seen that the entropy and its derivative as closing to absolute zero are also zero, conforming to the 3rd law of thermodynamics and as such providing a further validation of this model which is seen to agree with both the experimental values at higher temperatures and the theoretically expected behaviors near absolute zero.

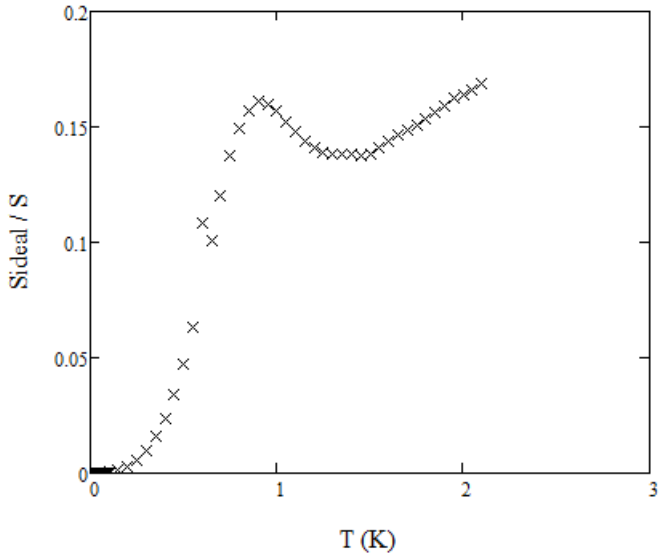

FIGURE 4.8: The percentage of contribution of the Entropy because of the ideal part over the total Entropy

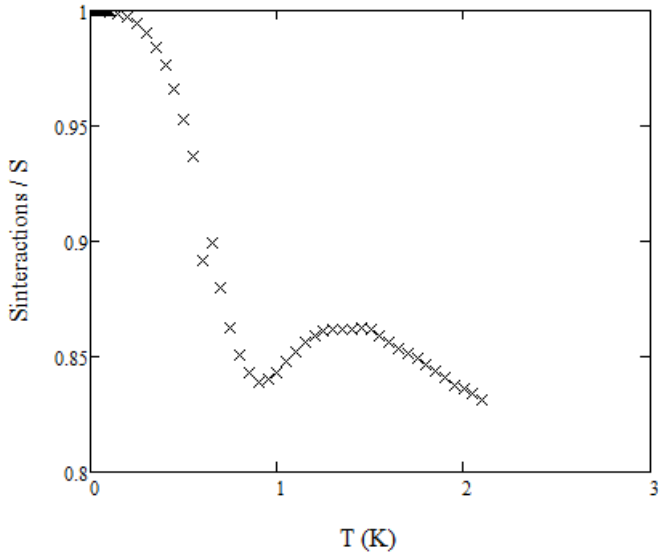

FIGURE 4.9: The percentage of contribution of the Entropy because of the potential over the total Entropy

T (K)	Entropy NIST data (kJ/kgK)	Entropy Calculated data eq. (9) (kJ/kgK)	Entropy Ideal eq.14 (kJ/kgK)	Entropy of Interactions (kJ/kgK)	Percentage ideal to total
1.00E-03	-	1.86E-11	0.00E+00	1.86E-11	1.31E-08
9.00E-03	-	5.90E-09	1.30E-15	5.90E-09	2.20E-05
1.70E-02	-	3.67E-08	5.89E-14	3.67E-08	1.61E-04
2.50E-02	-	1.13E-07	5.96E-13	1.13E-07	5.26E-04
3.30E-02	-	2.56E-07	3.15E-12	2.56E-07	1.23E-03
4.10E-02	-	4.87E-07	1.16E-11	4.87E-07	2.38E-03
4.90E-02	-	8.25E-07	3.38E-11	8.25E-07	4.09E-03
5.70E-02	-	1.29E-06	8.37E-11	1.29E-06	6.47E-03
6.50E-02	-	1.91E-06	1.84E-10	1.91E-06	9.63E-03
7.30E-02	-	2.70E-06	3.69E-10	2.70E-06	1.40E-02
8.10E-02	-	3.68E-06	6.89E-10	3.68E-06	1.90E-02
8.90E-02	-	4.87E-06	1.21E-09	4.87E-06	2.50E-02
9.70E-02	-	6.29E-06	2.03E-09	6.29E-06	3.20E-02
1.00E-01	-	6.89E-06	2.44E-09	6.89E-06	3.50E-02
3.00E-01	1.80E-04	1.80E-04	1.78E-06	1.79E-04	9.86E-01
5.00E-01	8.07E-04	8.07E-04	3.81E-05	7.69E-04	4.72E+00
7.00E-01	2.39E-03	2.39E-03	2.87E-04	2.10E-03	1.20E+01
9.00E-01	8.03E-03	8.03E-03	1.30E-03	6.73E-03	1.61E+01
1.10E+00	2.90E-02	2.90E-02	4.32E-03	2.50E-02	1.48E+01
1.30E+00	8.50E-02	8.50E-02	1.20E-02	7.30E-02	1.38E+01
1.50E+00	2.01E-01	2.01E-01	2.80E-02	1.73E-01	1.38E+01
1.70E+00	3.96E-01	3.96E-01	5.90E-02	3.37E-01	1.49E+01
1.90E+00	7.22E-01	7.22E-01	1.15E-01	6.07E-01	1.59E+01
2.10E+00	1.24E+00	1.24E+00	2.09E-01	1.03E+00	1.69E+01

TABLE 4.2: Showing the values and contributions of each part of the Entropy to the total Entropy at temperatures from 0.001K to near Lambda

By observing figures 4.8 and 4.9 and Table 4.2 one can see that going towards absolute zero the entropy the effect that the interacting part has to the total entropy is ever increasing leading to ever increasing values and eventually leading to representing 100% of the entropy near 0K. Through this one can see that the effect of the excitations diminishes as this is represented in the entropy of the ideal part, and completely disappears at 0K. This is physically sound as near absolute zero no excitations are expected to be existing and therefore no entropy could arise through them, something that this methodology seems to be inherently predicting and mathematically describing. Additionally, by following these results one can deduce that even at absolute zero an interatomic potential ought to exist between the particles of Helium-4. This is something that is also known to be true and conforms with the experiments and predictions of London.

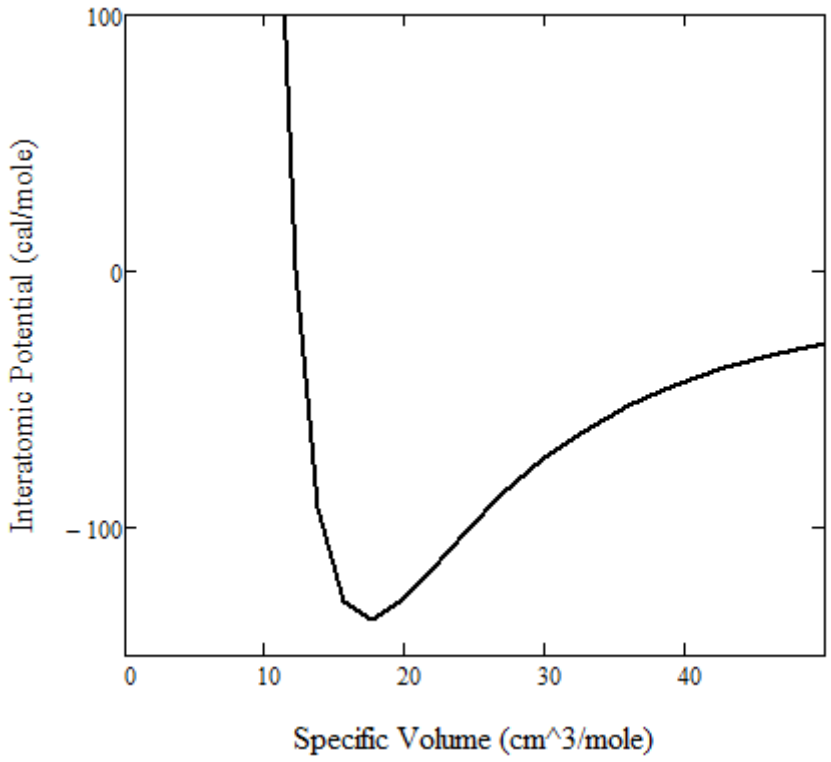

FIGURE 4.10: Interatomic potential for Helium-4 atoms based on the works of London [20, 17]

4.6 Conclusions of Entropic Lambda Transition Chapter

Through the above it was seen that finding the partition function of the Helium-4 near and below the lambda line and studying the effects of the superfluidity as a phenomenon on the partition function and the behavior of the entropy could greatly aid in the understanding of the phenomena themselves and provide a clearer macroscopical view of superfluidity without the need to dive too deeply in the quantum realm. By considering the interacting and ideal parts of Helium-4 as a product in the partition function and then transferring this to the entropy, one could now implement the Bose-Einstein statistics to the ideal part and figure out the Bose-Einstein condensation temperature. Through this, the entropy of the ideal part is derived and accordingly based on the existing EOS for the full Helium-4 the entropy of the interacting part was found. By following this method and splitting the partition function to an ideal and an interacting part one can study and predict the different behaviors of the two parts and how superfluid transition impacts their behaviors. The lambda transition on the superfluid was seen to be almost exactly matching the shift to Bose-Einstein condensation in the ideal part. This showcases that the connection between superfluidity and pure Bose-Einstein condensation is something that can be studied also through the macroscopic variables giving an advantage to its understanding for any engineering applications. By using this method one could model and predict the behavior of a superfluid by just using the thermodynamic variables of an ideal gas based on it and not have to extensively solve all the quantum mechanics of

the system. This approach by no means aim to replace existing theories of superfluidity in Helium-4 but it does offer a view that can be deemed very helpful in applications and an overall understanding between the macroscopical and the microscopical views of superfluids.

In addition to the fact that this method offers a more macroscopical view of superfluidity it can also be interpreted in a way that bridges the gap between the two-fluid approach and the quasiparticle approach to superfluids. In essence, by splitting mathematically the system into two parts, one being fully non-interacting and the second being interacting one can correlate this to the two-fluid model, where the Helium-II is considered to be a mixture of a non-interacting and an interacting liquid. Additionally, when calculating the entropies on this model it was shown that the entropy that arises is based on either the excitations of the individual particles or of their interactions. This can hint towards the quasiparticle approach as in both methods the thermodynamics of the system are only described through the excitations and state that the non-excited particles play no part in the overall system. The excitations of the single particles can be translated to the phonons, which are linear excitations of the lattice, with the interacting excitations of the system being the rotons (as when quantum vortices are created in the superfluid meaning an excitation that affects more than one particles interacting with each other). Overall, it can be seen that this macroscopical approach of the entropic transition to superfluidity provides an understanding which connects parts of both the existing theories of superfluidity.

So far this method has only been applied to superfluid Helium-4, but in later chapters it will be shown how this can be applied to other superfluids as well.

Chapter 4 - Nomenclature

S	Entropy
P(i)	Probability
p	Momentum
x	Position
k	Boltzmann constant
Ω	Macrostate
Ei	Energy of macrostate
G	Lagrange multiplier
Z	Partition function
β	Inverse temperature
T	Temperature
N	Number of atoms
V	Volume
m	Atomic mass
ρ	Density
ϵ	Energy of single atom
U	Potential energy
H	Hamiltonian
μ	Chemical potential
ω	Natural frequency
h	Plank's constant
ga	Bose function
N^*	Number of non-condensed particles

Chapter 5

Helium 3

As mentioned in previous chapters Helium as an element has two naturally occurring stable isotopes. The first and by far most common one is Helium-4 which has been studied extensively so far in this research. In addition to this isotope also Helium-3 exists. Helium-3 is a much rarer isotope being less than 0.001% of all natural Helium and an even smaller percentage on earth. Helium-3 consists of two protons and one neutron in its core. This means that Helium-3 has a total spin of $\frac{3}{2}$ being half-integer. As a particle with half-integer spin Helium-3 is a fermion in contrast to the bosonic Helium-4. Normally, the spin difference between the isotopes play no important role in the thermodynamic behavior of elements. This is because for all the rest of the elements the thermodynamics used are at significantly higher temperatures. Being at higher temperatures the Maxwell-Boltzmann statistics are used for their mechanics which do not differentiate on the spin. In the case of Helium, which remains a liquid near absolute zero where quantum interactions are having significant effects, one can no longer use the Maxwell-Boltzmann distribution and has to rely on the quantum distribution functions. The functions being the Bose-Einstein and the Fermi-Dirac (as shown in appendix A) are dependent on the spin of the particles. As such, this difference of the kind of spin between Helium-3 and Helium-4 leads to a vastly different behavior between them.

At higher temperatures due to the reliance on the Maxwell-Boltzmann distribution there is no differentiation between the two isotopes and as such at higher temperatures the equations of state do not differentiate between them.

At lower temperatures Helium-3 also forms a superfluid. This fact might initially seem as counter-intuitive as superfluidity is known to be a degenerated form of Bose-Einstein condensation. For a substance to form any kind of Bose-Einstein condensate or equivalent behavior it is given that it has to be made out of bosons. Helium-3 though, is fermionic. But Helium-3 does form a superfluid as the experiments have shown. The physics behind the formation of superfluids in fermionic gases and in general Bose-Einstein condensates of fermions are of great interest and a lot of work has been put over the years by many scientists to explain this behavior. In general, the idea behind the Bose-Einstein condensation in fermionic gases is based on the BCS theory of Cooper pairs [9],[52]. This theory has had great success in explaining the formation of BEC in electron gases explaining the phenomenon of superconductivity. In this work, in the later parts of this chapter, this theory is applied to Helium-3, where it is shown that when it is combined with the entropic approach as developed for Helium-4, it leads to results helping in a better understanding of superfluidity in Helium-3 as well.

While Helium-3 becomes liquid at the same temperature as Helium-4, it remains a normal liquid until very low temperatures, in the regions of 0.001K where its lambda transition occurs. Any superfluid is progressively more thermodynamically inert as its

temperature lowers. This means that Helium-4 at temperatures below 0.3-0.4K is almost completely thermodynamically inert and as such it cannot be used effectively as a working medium for cryocoolers below these temperatures. Because of the fact that Helium-3 has a significantly lower lambda temperature it can be used as a working medium for cooling apparatuses at temperatures as low as around 0.0005K. This is the working medium used for the lowest possible temperatures achieved through traditional thermodynamic processes without the need for exotic means like laser cooling

In recent years, other than its applications in cryogenics Helium-3 has found extensive applications as a fuel in nuclear fusion [53]. The reliance of all ultra low temperature cryogenic apparatuses to Helium-3, combined with its high demand as a fusion fuel and given its very low natural percentage means that it is an exceedingly rare element and its price has seen an extensive rise in recent years.

5.1 Equation of State for Liquid Helium-3

As with Helium-4 working with Helium-3 means that first of all a working equation of state needs to be established. In this case the available data for the thermodynamic behavior of Helium-3 are much more scarce than the ones for Helium-4.

The equation of state used at this part of the study is based on the works of Huang and Arp [54, 55]. For the full process behind the derivation and implantation of the mathematics of this model one is advised to read directly the references provided.

The based equation for the Helmholtz free energy is given by Huang and Arp as:

$$\begin{aligned}\frac{A}{RT_c}(\delta,\tau) &= C_1 ln(\delta) \\ &+ (C_2\delta^{-4}t^{-1} + C_3\delta^{-1}t^{-2} + C_4\delta^{-2}t^{-3} + C_5\delta^{-2}t^{-4}) \\ &+ \Big[(C_6 ln(\delta) + \sum_{i=7}^{13} C_i\delta^{i-6}) + (\sum_{i=14}^{19} C_i\delta^{i-14})\tau(ln(\tau)-1) \\ &+ (C_{20}\tau^3 + C_{21}\tau^5 + C_{22}\tau^8 + C_{23}\tau^9) \\ &+ \delta^{-2}(C_{24}\tau^2 + C_{25}\tau^4 + C_{26}\tau^6 + C_{27}\tau^8 + C_{28}\tau^9)\Big](e^{-\delta^2} - 1) \\ &+ C_{29}\delta^2\tau^4 e^{-(\delta^2+\tau^2)}\end{aligned} \tag{5.1}$$

where $\tau = \frac{T}{T_c}$ and $\delta = \frac{\rho}{\rho_c}$. The C values are given in the table 5.1 below.

i	C	i	C	i	C
1	-3.570E-01	11	8.840E-01	21	4.380E-01
2	-3.300E-03	12	-1.010E-01	22	-8.480E-01
3	9.971E-06	13	5.471E-03	23	5.790E-01
4	1.719E-06	14	-7.625E+00	24	1.579E+00
5	-2.651E-08	15	1.641E+01	25	1.095E+00
6	1.414E+01	16	-1.369E+01	26	-3.815E+00
7	8.332E+00	17	5.708E+00	27	6.720E+00
8	-2.133E+01	18	-1.187E+00	28	-4.020E+00
9	1.333E+01	19	9.800E-02	29	3.800E-02
10	-4.492E+00	20	-1.000E-01		

TABLE 5.1: coefficients for eq. 5.1

Based on this equation one can calculating the rest of the thermodynamic properties as following:

The atomic mass of Helium-3 is:

$$M = 3.016 \, \frac{g}{mol}$$

The critical temperature is:

$$T_c = 3.3157 \, K$$

The critical density is:

$$\rho_c = 41.191 \, \frac{kg}{m^3}$$

And the specific universal gas constant:

$$R_M = \frac{R}{M}$$

Thus, by using the Maxwell relations the rest of the thermodynamic values can be calculated as:

Helmholtz free energy:

$$A(\rho, T) = \frac{A}{RT_c}(\frac{T}{T_c}, \frac{\rho}{\rho_c})RT_c \tag{5.2}$$

Pressure:

$$P(\rho, T) = \frac{\rho^2}{1.01325 * 10^2}(\frac{d}{d\rho}A(\rho, T)) \tag{5.3}$$

Internal Energy:

$$U(\rho,T) = A(\rho,T) - T(\frac{d}{dT}A(\rho,T)) \tag{5.4}$$

Enthalpy:

$$H(\rho,T) = U(\rho,T) + \rho(\frac{d}{dT}A(\rho,T)) \tag{5.5}$$

Entropy:

$$S(\rho,T) = -(\frac{d}{dT}A(\rho,T)) \tag{5.6}$$

Gibbs free energy:

$$G(\rho,T) = H(\rho,T) - T\,S(\rho,T) \tag{5.7}$$

Isochoric specific heat:

$$Cv(\rho,T) = -T(\frac{d^2}{dT^2}A(\rho,T)) \tag{5.8}$$

Isobaric specific heat:

$$Cp(\rho,T) = Cv(\rho,T) + \frac{T}{\rho^2}\frac{(\frac{d}{dT}P(\rho,T)^2}{\frac{d}{d\rho}P(\rho,T)} \tag{5.9}$$

Gamma constant:

$$\gamma(\rho,T) = \frac{Cp(\rho,T)}{Cv(\rho,T)} \tag{5.10}$$

Speed of sound:

$$W(\rho,T) = [(2\rho\frac{d}{d\rho}A(\rho,T) + \rho^2\frac{d^2}{d\rho^2}A(\rho,T)\gamma(\rho,T)] \tag{5.11}$$

Compressibility factor:

$$z(\rho,T) = \frac{P(\rho,T)}{\rho\,R\,T} \tag{5.12}$$

To further validate the results of these equations their outcomes are checked against the existing data of [56, 57, 58, 59].

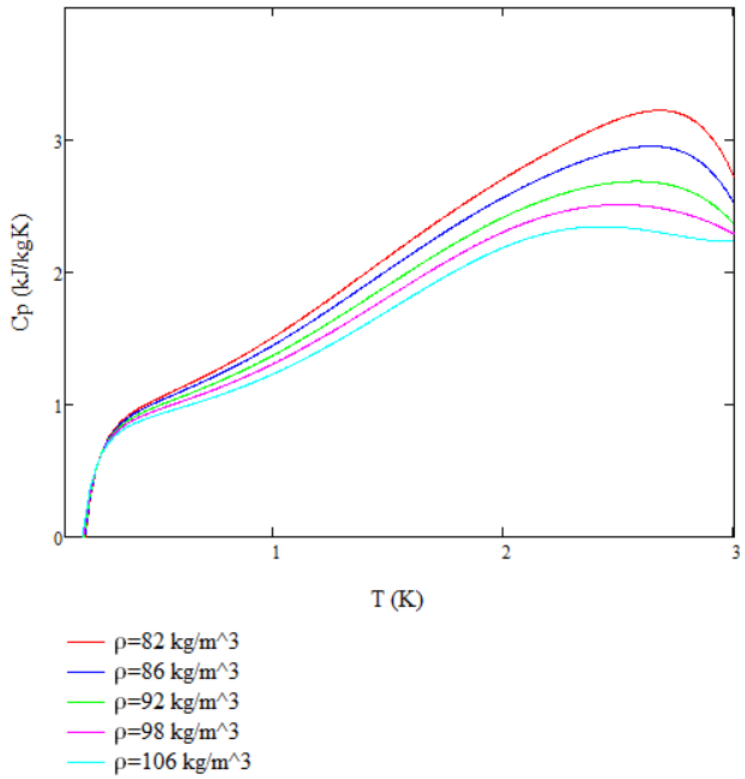

FIGURE 5.1: Cp values based on equation 5.9

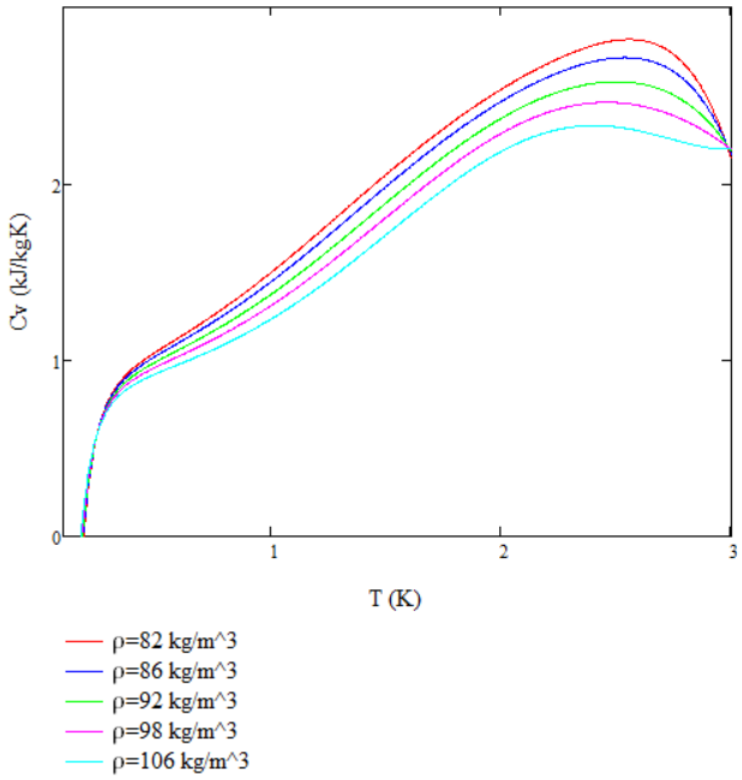

FIGURE 5.2: Cv values based on equation 5.8

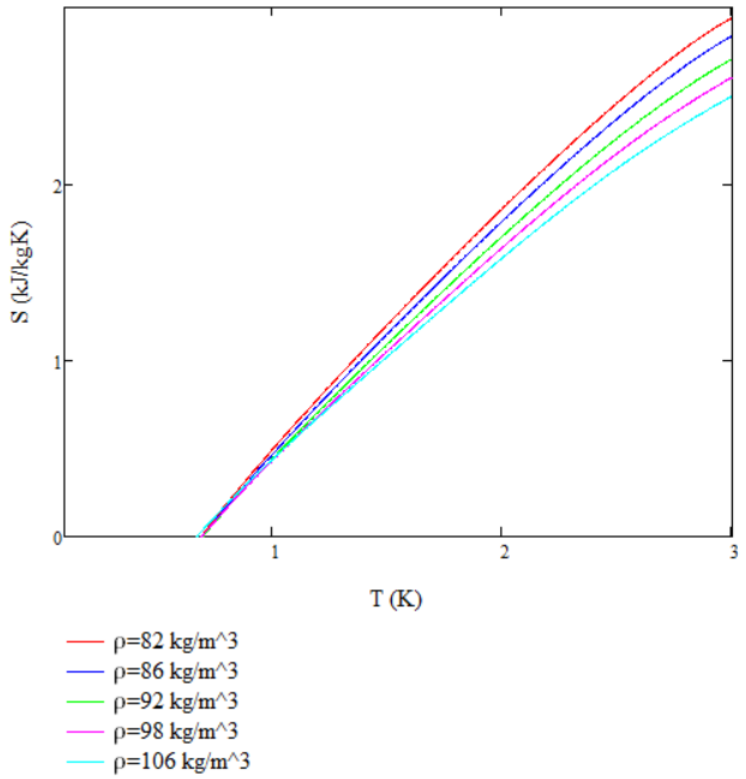

FIGURE 5.3: Entropy values based on equation 5.6

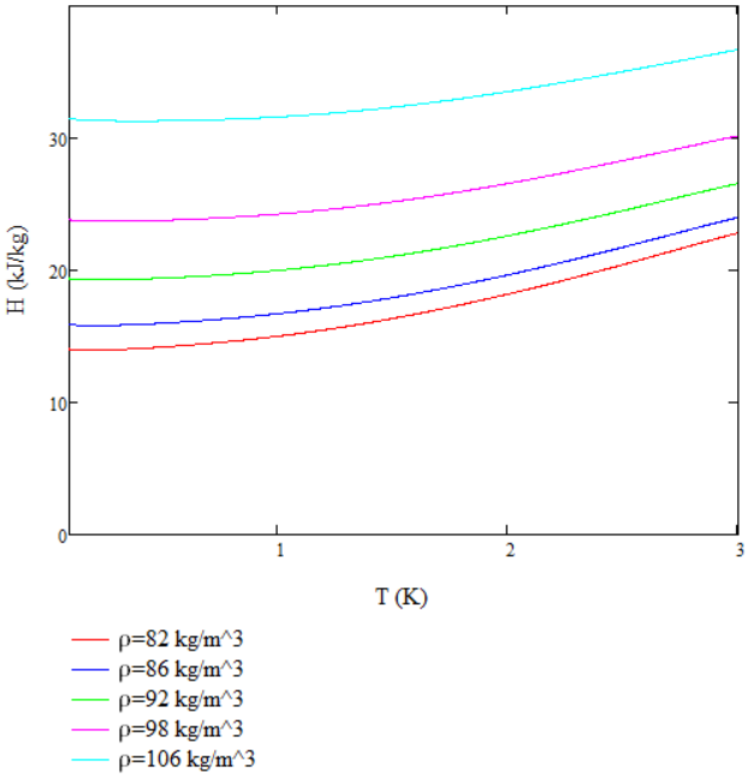

FIGURE 5.4: Enthalpy values based on equation 5.5

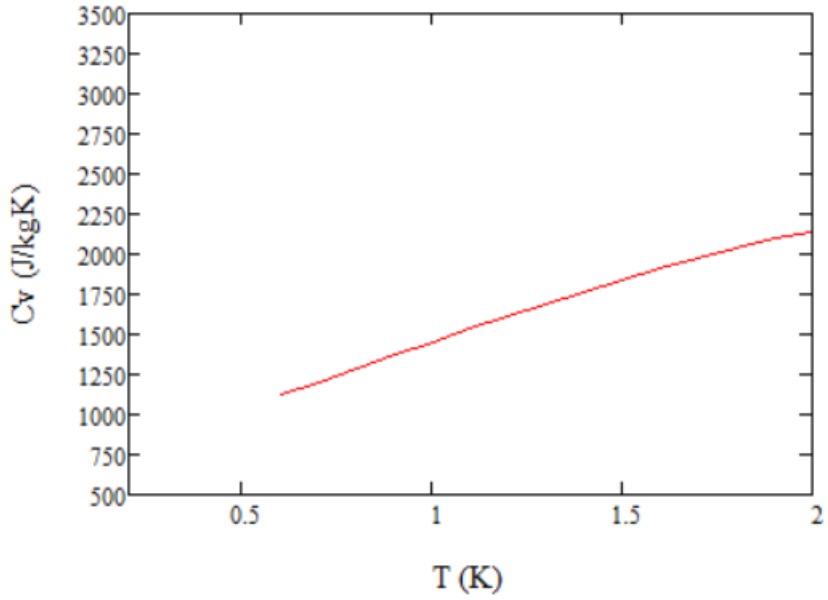

a)

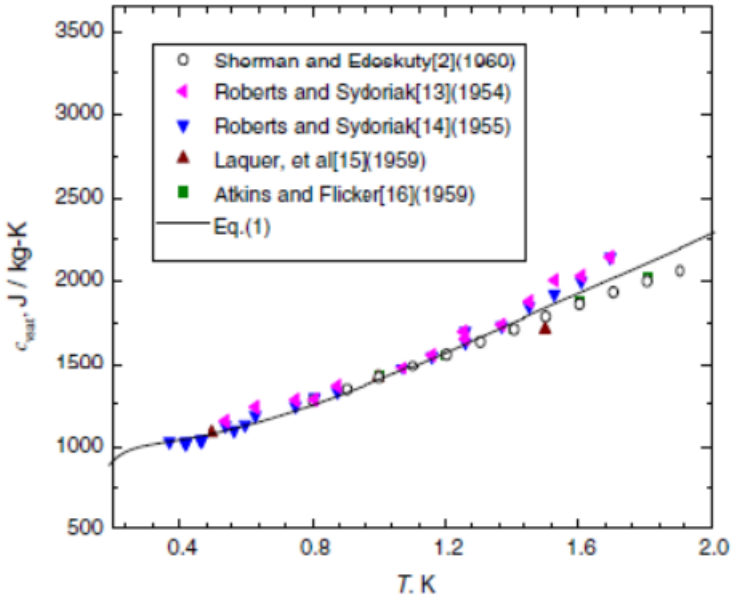

b)

FIGURE 5.5: Cv comparison to figure from Huang's work. Subfigure (b) is taken form Huang's work [54] for comparison reasons

In addition to the specific heat under constant volume the isobaric compressibility factor is calculated and checked as:

$$a_p(\rho,T) = \frac{\frac{d}{d\rho}\frac{d}{dT}A((\rho,T)}{2}(\frac{d}{d\rho}A(\rho,T)) + \rho\frac{d^2}{d\rho^2}A(\rho,T) \tag{5.13}$$

This equation is provided by [54] but when checked for its results directly it is seen that while it is theoretically correct the resulting values differ significantly from the expected ones. As such the isobaric compressibility is calculated in a different manner as:

$$a_p(T,P) = \frac{1}{v(T,P)}\frac{d}{dT}v(T,P) \tag{5.14}$$

Based on the equation 5.14 it can be seen that the behavior of the results is the expected one from the graph below:

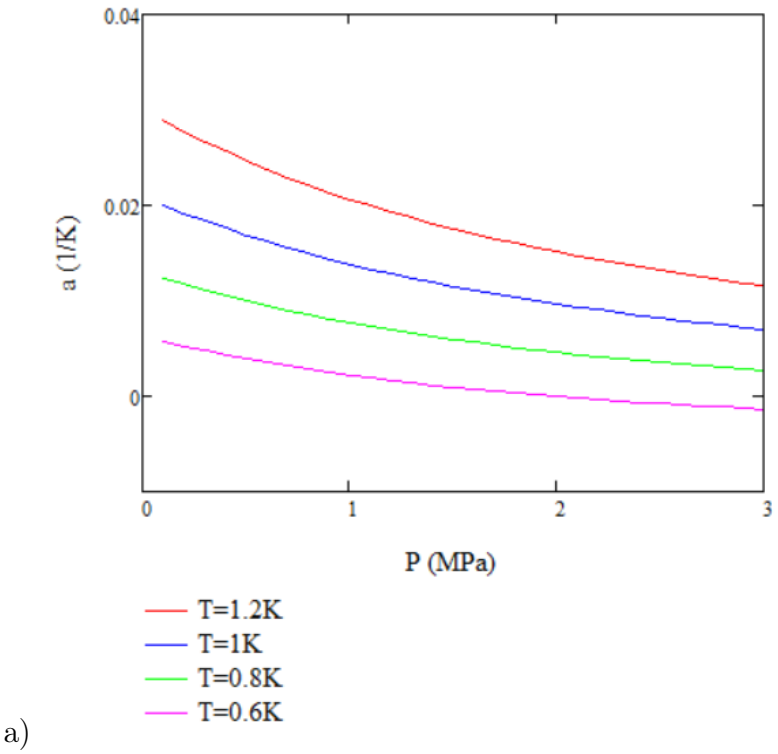

a)

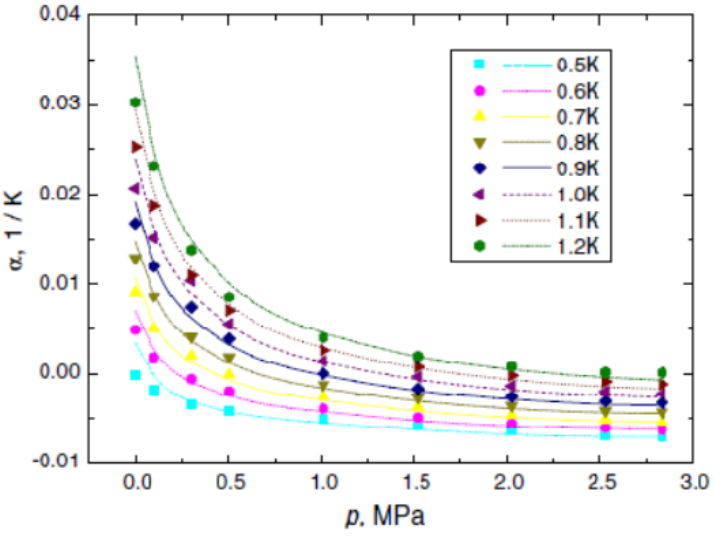

b)

FIGURE 5.6: Isobaric compressibility comparison to figure from Huang's work. Subfigure (b) is taken form Huang's work [54] for comparison reasons

5.2 Entropic Transition in Helium-3

In the previous chapter for Helium-4 a novel model was proposed for the description of its superfluidity based on the transition of the ideal part of the partition function and the entropy. This approach provided great results for Helium-4 and one can suppose that it provides an overall view for superfluidity if it can be seen to be applied with similar success to other superfluids as well. The only other known superfluid for which data exists is Helium-3. As such this split of the partition function approach will be implemented to Helium-3.

5.3 Basic Mathematics of BCS theory

For one to understand the nature of Bose-Einstein condensation in fermionic gases one needs to understand the BCS theory of Cooper pairs. A simplified model of the basic concepts of this theory is provided below, as for the reader to be able to mathematically understand and reconstruct the model for Helium that will be shown in the next section.

The BCS theory is based on the quantum mechanics problem of a Cooper pair. A Cooper pair can be any pair of fermionic particles. In the general literature Cooper pairs are mainly referred to pairs of electrons, but one can implement the same approach for any fermion, like a Helium-3 atoms. As such in this section the problem will be solved generally for a pair of generic fermions.

Consider two fermions in a potential well with its Schrodinger equation being:

$$[-\frac{\hbar^2\nabla_{x_1}^2}{2m} - \frac{\hbar^2\nabla_{x_2}^2}{2m + V(|x_1 - x_2|)}]\Psi(x_1, x_2) = E\Psi(x_1, x_2) \tag{5.15}$$

where Ψ is the wavefunction, x the positions of the two fermions and E the energy. To make the solution of the system easier, the equation is changed to the system of center mass, where it can be written as:

$$[-\frac{\hbar^2\nabla_R^2}{2m_{tot}} - \frac{\hbar^2\nabla_r^2}{2m_{reduced}} + V(r)]\Psi(R, r) = E\Psi(R, r) \tag{5.16}$$

with $R = 0.5(x_1 + x_2)$, $r = |x_1 - x_2|$, $m_{tot} = 2m$ and $m_{reduced} = \frac{m}{2}$, with m being the mass of the fermion. Easily it can be seen that the solution of the equation above will be of the form:

$$\Psi(R, r) = \psi(r)e^{iKR} \tag{5.17}$$

So by applying to the Schrodinger equation one can find the eigenvalues as:

$$[-\frac{\hbar^2\nabla_r^2}{2m_{reduced}} + V(r)]\psi(r) = (E - \frac{\hbar^2K^2}{2m_{tot}})\psi(r) \tag{5.18}$$

By applying the Fourier transform one gets a new modified wave-function as:

$$\Delta = (E - 2\epsilon)\psi \tag{5.19}$$

Based on the solutions of the equation above on can find the density of states per spin given the eigenvalues of the system as:

$$\rho(\epsilon) = \frac{m^{\frac{3}{2}}}{\sqrt{2}\hbar^3\pi^2}\sqrt{\epsilon} \tag{5.20}$$

and by as such the wavefunction can be written as:

$$\Delta = \frac{V_0 \Delta m^{\frac{3}{2}}}{\sqrt{2}\hbar^3\pi^2}\int_0^{\omega}\frac{\sqrt{\epsilon}}{2\epsilon - E} \tag{5.21}$$

By setting the $E = 0^-$ one can get the bound state of an attractive potential and get the minimum value for the potential as:

$$V_0 = \frac{\sqrt{2}\hbar^3\pi^2}{m^{\frac{3}{2}}\sqrt{\omega}} \tag{5.22}$$

By applying the above to a many fermion system one introduces the concept of the fermi density as:

$$1 = V_0\rho_F\int_0^{\hbar\omega}\frac{d\epsilon}{\sqrt{\epsilon^2 + \Delta_0^2}} \tag{5.23}$$

following this one can calculate the critical transition temperature as:

$$T_c = \frac{2e^{\gamma_E}}{\pi}\frac{\hbar\omega}{k}e^{-\frac{1}{V_0\rho_F}} \tag{5.24}$$

where γ is Euler's constant.

Now having these values one can calculate the R2 universal ratio for superconductors as:

$$R_2 = \frac{\Delta C}{\gamma T_c} = \frac{12}{7\zeta(3)} \approx 1.43 \tag{5.25}$$

5.4 BCS Theory on Helium-3

The second natural and stable isotope of Helium is Helium-3. Helium-3 has also been known to form a superfluid but its behavior has been experimentally seen to be different from Helium-4 especially considering the temperature of the Lambda transition to superfluidity. The reason for this different behavior of Helium-3 is that it is fermionic in contrast to the bosonic Helium-4 due to having one less neutron in its core. This means that the Bose-Einstein statistics cannot be used for the description of Helium-3. Despite this, Helium-3 does exhibit superfluidity. This again has been explained microscopically with the quasiparticle approach in Helium-3, but even less information exists about the correlation of Bose-Einstein condensation in Helium-3 compared to Helium-4. An attempt to showcase the relation between Bose-Einstein condensation and the superfluidity in Helium-3 will be attempted by combining the previous approach for Helium-4, referring to the split of the partition function and the entropy to an ideal and a non-ideal part, with the BCS theory of cooper pairs in the electrons of superconductors [9].

Again, in Helium-3 interactions exist between the particles and as such one cannot readily apply the cooper pairing solution to achieve Bose-Einstein condensation in the system, as such condensation cannot occur under these circumstances. But by splitting

again the partition function and the entropy using the same method as in the Eq. 4.22,4.17 one can derive a term for the ideal part of Helium-3 that has no interatomic interactions.

This term still cannot be considered an ideal Bose gas as its particles being fermions obey the Fermi-Dirac statistics. This will be addressed by applying the BCS theory of Cooper pairs, where a pair of fermions entangle and behave similarly to a boson. Therefore, the cooper pairs, being bosonic in their behavior and having no interactions between them form an ideal Bose gas. Thus, a temperature is found where this ideal Bose gas condenses into a BEC [60]. Without getting into very much detail about the different types of Cooper pairs [61] the simplest case of weak coupling will be assumed, with the mass of the pair being the $2m_{^3He}$ as shown to be the case with a deviation of less than 0.1% by [52].

Thus, following the method described for Helium-4, one can again derive and use the equations for the entropy and the partition function from the canonical or gran canonical ensemble with the differentiation of using the mass of a cooper pair of Helium-3 atoms instead of the mass of Helium-4. Also, now the number density ought to be established as it can no longer be directly derived from the density of Helium-3 but to calculate it one needs to take into account the density of the cooper pairs in the gas. The exact density of the cooper pairs in Helium-3 is difficult to be evaluated precisely, without a very extensive microscopical model (something that is deemed outside of the scope of this research) especially given the lack of published experimental data on the matter. However, a very good estimate of this density can be gained by studying the work of Matsuo in [62] for the density of cooper pairs of neutrons, where by assuming an energy 3 times higher than a neutron for a specific temperature, due to the atomic mass of Helium-3 being approximately 3 times the mass of a neutron, one can derive that the density of the cooper pairs in Helium-3 can be in the order of magnitude of $\rho/\rho_{^3He} \approx 10^{-4}$ compared to the normal density.

By applying the statistical model of chapter 4 and the data of chapter 5 one can derive, similarly to Helium-4, the temperature values for the transition of the ideal part to a theoretical state of Bose-Einstein condensate as:

$$Tc = \frac{2\pi\hbar^2}{\hat{m}k}\left(\frac{\hat{N}}{V\zeta(\frac{3}{2})}\right)^{\frac{2}{3}}, \tag{5.26}$$

where $\hat{N}$ is the number of cooper pairs in the gas, with the $\hat{N}/V$ term calculated from the spacial density of the cooper pairs from [62] with a used value of $\rho/\rho_0 \approx 10^{-4}$ (ρ being the spacial density for the cooper pairs in the ideal part of Helium-3 and ρ_0 the normal density of Helium-3) and $\hat{m} = 2m_{^3He}$ according to [52]. The density ρ for Helium-3 is taken from [54]. Despite [54] not offering data for temperatures near and below the lambda point as far as the density is concerned, one can safely say that at these temperatures the density has very little to no dependence on the temperature and is mainly defined from the pressure, something that can be seen if one observes the behavior of the temperature of Helium-4 from [14] from above the lambda point to near zero, where the density in the P-T diagram is seen to be represented by lines parallel to the temperature axis. So, the calculation has be done for a value of $\rho = 0.081 g/cm^3$. Thus, the result one gets from this calculation from Eq. 5.26 is a temperature of $Tc \approx 0.0023K$. This comes to match the order of magnitude of the $T\lambda \approx 0.0025K$ depending on the pressure [61]. Due to the limited available data for the thermodynamic values or a full equation of state for Helium-3 near and below the lambda point, one cannot present the graphs of

the entropies of the ideal and non-ideal parts as done in Helium-4. For the validation of the fact that in Helium-3 the lambda point co-exists with the point of Bose-Einstein condensation of its ideal part what can only be done so far is to rely on the calculation of the two temperatures.

In the field of superconductors the BCS theory predicts 3 universal ratios [63] that have been theoretically described and have been also experimentally verified for the different superconductors. Thus, for the theory that the ideal part of Helium-3 forms a theoretical Bose-Einstein condensate through the cooper pairs to hold merit, then the universal ratios of BCS should also apply in this case. The ratio R_2 from [63] is being examined with its definition being:

$$R_2 = \frac{\Delta C}{\gamma T c} = \frac{12}{7\zeta(3)} \approx 1.43, \tag{5.27}$$

where Δ is the energy gap, defined in [61] as $\Delta = kTc(1-\frac{T}{Tc})^{\frac{1}{2}}$, k the Boltzmann constant. The term γ a separate function defined as $\gamma = \frac{2\pi^2 k^2 \rho_F}{3}$ with ρ_F being the density of states per spin $\rho_F = \frac{m^{\frac{3}{2}}}{\sqrt{2}\hbar^3\pi^2}\sqrt{E_F}$ in terms of the Fermi energy $E_F = \frac{\hbar^2}{2m}(3\pi^2\frac{N}{V})$, and for this application we have $N = \hat{N}$ and $m = \hat{m} = 2m_{^3He}$. C is the specific heat whose value is given by [64].

Overall, by performing the calculations mentioned above we get a value of $R_2 = 1.382$. This value is not exactly the 1.43 expected for the R_2 universal ratio but it is within a margin of error that it is considered by the author acceptable given the small assumptions that had to be made during the calculations due to the lack of data for different values. Thus, it can be seen that when the BCS theory is applied to the ideal part of the Helium-3 isotope then, as with Helium-4, one can see the start of the formation of a Bose-Einstein condensate within the theoretical ideal part to co-exist and almost directly match the lambda transition (the transition from fluid to superfluid) of the real gas. Additionally, in Helium-3 it is seen that the BCS theory holds true for the ideal part of it as the universal constant that the BCS theory predicts is actually confirmed within a very small margin of error, meaning that the formation of cooper pairs and the formation of a BEC in this part of the gas holds true. The work of this chapter concerning the application of the etnropic transition to Helium-3 has been published by the author in [65].

5.5 Helium-3 Chapter conclusions

In this chapter a full model for Helium-3 has been presented. Firstly, the difference between the Helium-3 and Helium-4 isotopes is explained based on their spin difference. Continuing on the work of Huang [54] an equation of state for Helium-3 is being presented. The procedure initiates from the equation of Arp and Huang for the Helmholtz free energy and then the Maxwell relations and thermodynamic definitions are applied to this equation to create a full set of equations and data describing all the thermodynamic values for Helium-3.

The next step of the study of Helium-3 has been to apply to it the approach developed in the Entropic lambda transition chapter 4. The reasoning behind this is firstly to try and validate the theory by applying it to a second superfluid other than Helium-4 and secondly to define a theoretical model able to describe the behaviors of Helium-3 and superfluid Helium-3 at extremely low temperatures.

The model had to be significantly differentiated from its first application in Helium-4 due to the fermionic behavior of the isotope. To overcome this, knowledge from the field of superconductivity was used, where the BCS theory was implemented to showcase how the Helium-3 atoms could form Cooper pairs and behave like bosons. As such one is able to apply the entropic split to an ideal and a non-ideal part to Helium-3 and showcase that the ideal part, through the BCS theory of Cooper pairs, would Bose-Einstein condense very close to the lambda temperature of Helium-3 further validating the model, as it exhibits the same behavior as in Helium-4 despite the fermionic nature and the need for the application of the BCS theory.

In addition to predicting the lambda transition of Helium-3, this model has also been able to correctly predict the universal R2 ratio of superconductivity, showcasing the correct application of the BCS theory to the system. The only drawback of this application is that due to the very limited data of the thermodynamic values for Helium-3 one is not able to define the values for the interacting part of the entropy and the partition functions and as such the full theoretical model for the thermodynamic values going below 0.0001K, where the experimental data ends, is not possible. Despite this fact, the rest of the results have shown that this theory is viable in this system, and if in future these needed data arise, then this model would be able to predict the very low temperature behavior approaching absolute zero as done in Helium-4.

Chapter 5 - Nomenclature

A	Helmholtz free energy
R	Gas constant
Tc	Critical temperature
M	Molar mass
ρ_c	Critical density
α_p	Isobaric compressibility
m	Atomic mass
x	Position
h	Plank's constant
Ψ	Wavefunction
r,R	Distance
Δ	Fourier transformed wavefunction
ϵ,E	Energy
ω	Natural frequency
R2	Universal ratio of superconductivity
ζ	Riemann's zeta function
ρ_F	Fermi Density

Chapter 6

Helium 3-4 Mixture

The two stable isotopes of Helium are Helium-3 and Helium-4. Their physical and chemical properties are usually similar and in most application one equation of state is used for both isotopes. As it was discussed though in previous chapters at lower temperatures their behaviors significantly differ. The different behavior of the bosonic Helium-4 to the fermionic Helium-3 lead to some interesting overall behaviors when the two are combined. First of all, one needs to understand that the instances where one finds themselves working with a pure isotopic gas are rare and in most cases a mixture of the two isotopes is used. This is usually mitigated by the fact that the natural percentage of Helium-4 is around 99.9996% meaning that if one works with natural Helium, they need not care much about the Helium-3 percentage. In applications, though, where temperatures below 0.5K are required the use of Helium-3 is mandatory. Pure Helium-3 is exceedingly expensive and difficult to obtain and contain in its pure form due to its reliance to high vacuum apparatuses in order not to lose even small parts of this expensive substance. In reality the working medium that is used in most ultra low temperature refrigeration cycles is a Helium-3 Helium-4 mixture enriched in Helium-3. As it will be discussed in later chapters concerning those thermodynamic cycles the enrichment of the mixture can as low in values as 1-2% to much higher in the order of 30-40%.

Helium-4 undergoes the lambda transition at around 2.1 K while Helium-3 becomes a superfluid at around 0.001K. This means that when a mixture of the two exists in low temperatures, the two isotopes might be in different phases, which is really important to understand and describe for the study and use of the mixture. Due to this fact most models that exist in the literature, similarly to the models for the pure isotopes, limit themselves to specific regions staying clear of any phase transitions. This is a fact that is even more problematic for Helium 3-4 mixture at it is primarily used for cooling devices that work in different phases during their cycles. The usual approach to this, as it will be discussed further in the SSR chapter, is to consider Helium-4 completely inert and only work based on Helium-3. The approach is deemed problematic as it negates the ability to take into account the thermodynamic interactions of the superfluid Helium-4 due to the phonon-roton interactions at temperature above 0.8 K. For this reason, this study partially aims to develop a full EOS for the Helium 3-4 mixture that is continuous through the different phases and can be used to reproduce with high accuracy the experimental data and be of a form usable enough to be able to be inserted in CFD environments for simulations with the full mixture as the working medium.

6.1 Helium 3-4 Mixture phases

.

The different temperatures for the lambda transitions of the two isotopes lead into different phases of the mixture that give it very different properties depending on the phase it is in.

The regions are defined by the lambda line (λ) and the two sigma lines ($\sigma+$, $\sigma-$).These regions based on the phase transitions of the system are the following:

- Helium-3: Normal Fluid, Helium-4: Normal fluid. The area defined above the λ and $\sigma+$ lines, where both isotopes behave as normal fluids. This region is the easiest to understand and model as both of the two isotopes are above their lambda lines and behave like normal fluids. In this region the properties of both isotopes are not affected by their spin since they are above their lambda lines and therefore obey the Maxwell-Boltzmann statistics and thus the equation of state for this region is the most straightforward to derive.

- Helium-3: Normal Fluid, Helium-4: Superfluid. Above the $\sigma-$ and below the λ line exists the area where 3He is a normal fluid and 4He is a superfluid. This region exists below the lambda line of Helium-4 (2.1K) and above the lambda line of Helium-3 (0.001K). This is the most commonly used region for cryocoolers that work with the mixture as they capitalize on the fact that despite being at very low temperatures a part of the system is not in a superfluid phase and as such the mixture is much less thermodynamically inert than what pure Helium-4 would be at these temperatures.

- Helium-3: Superfluid, Helium-4: Superfluid. This is the area below the λ line of Helium-3, which by default means that the temperatures are below the λ line of Helium-4 as well. In this region both isotopes are superfluids. This region, though, is not generally of use. The temperatures are too low and the Helium-4 becomes only a problem on the system as it has absolutely no thermodynamic value. Thus, at temperatures of this magnitude (applications for which are very limited) pure Helium-3 is used and that only for cooling near the lambda line. In reality cryocoolers that want to achieve temperatures a lot lower than 0.001 K, forfeit the use of Helium altogether and opt for exotic types of cooling like laser trapping. For these reasons in most works in the literature this region is not mentioned at all.

- Forbidden region. This is the region below the $\sigma+$ and $\sigma-$ lines. While this is an area where one ought to technically expect the Helium 3-4 mixture to be able to exist, experiments have shown that the mixture actually cannot exist in this region and it gets separated into two parts with different consistencies in the end of the σ lines. This region is of great interest from an engineering point of view and its applications will be discussed more in following chapters especially considering superleaks and dilution cooling, due to the separation that it mandates on the system, which can be used effectively for types of cooling. This existence of the forbidden region is based on the conservation of the 3rd law of thermodynamics. The physics behind the formation of this forbidden region are of great interest but are not within the scope of this work to explore further, as they are deemed not to be able to provide engineering benefits since the outcomes of the phenomena are very well understood and extensively described.

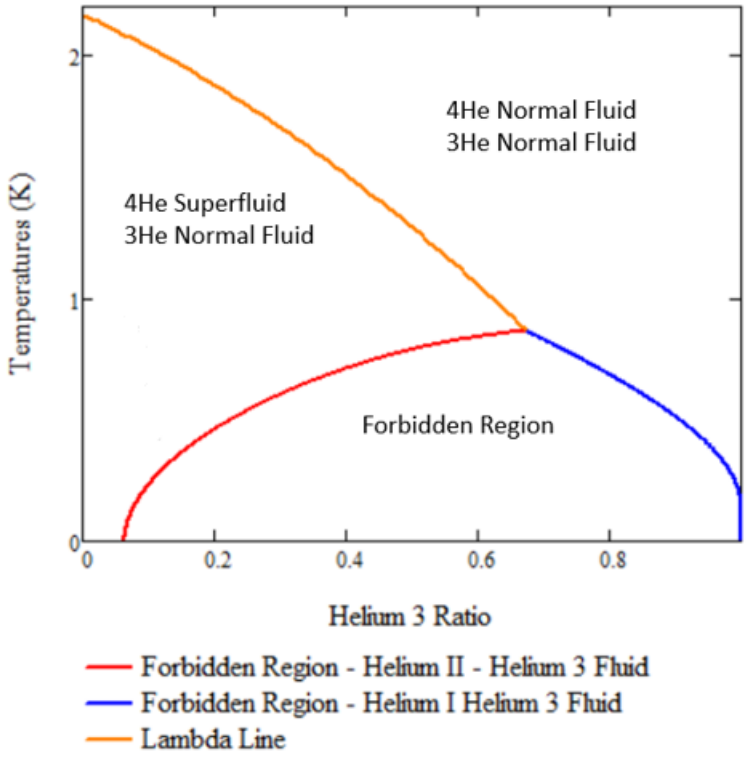

FIGURE 6.1: Region map of Helium 3-4 Mixture

The regions can be observed in the figure below:

6.2 Mixture Equation of State

6.2.1 Thermodynamic Data He3-4

The aim of this part of this work is to create a full equation of state of the mixture to be able to properly utilize it as a working media as one would for a normally behaving mixture like in [66]. This equation of state must achieve great accuracy on the existing experimental data covering all the regions of the cryogenic Helium 3-4 mixtures. To achieve that the first order of work would be to collect and unify all the reliable existing experimental and overall produced data on cryogenic Helium mixtures for all the regions.

Before setting off to use directly the data for the mixture, the data for the pure substances are to be used, as they will be needed greatly not only in the limit areas but also the mixture itself, as it will be shown through the equations later. The data for the Helium-4 are based on the equation of state provided in chapter 3 and published in the paper [37]. The data for Helium-3 are based on the equations developed on chapter 5 and on the data of Huang [54, 55].

Concerning the He3-4 mixture one of the earlier publications containing the thermodynamic data and the phase separation diagram are [67] with [68] describing the tri-critical point and [69] for the phase separation lines. For more dilute mixtures the data of [70]

are referenced and for higher pressures the study of [71] is used. Some of the aforementioned studies do include equations of state for one or more regions, especially the work of Chaurdy, but the extensively theoretical calculations used make these equations not ideal for engineering studies.

In addition to the thermodynamic data to adequately describe the Helium 3-4 mixture some other properties need to be mentioned as well, the most important of which is the osmotic pressure. The osmotic pressure is of great significance in all the apparatuses that make use of the Helium 3-4 mixtures and especially the ones that using superleaks, where the derivation of the osmotic pressure is mandatory as it will be shown in later chapters. The data from the osmotic pressure are based on the works of Arp and Salmela at [29] and [72].

The data gathered from all the sources mentioned are transformed and correlated in order to be in the same units and then checked for self-consistency with one-another. Based on this data a full set of equations is developed governing the Helium 3-4 mixture from 0.1 K to the Lambda line of Helium-4.

6.2.2 Zero Pressure equations

Before initiating the fitting of the data to the numeric code the thermodynamic values for the zero pressure are to be defined. The calculation of these data is based on the work of Chaudry [71]. A significant differentiation of this work to the work of Chaudry is that in order to achieve much better accuracy the EOS of state of the current work of chapters 3 and 5 are used, gaining significantly better results.

Firstly, the equations for the phase transitions are defined as:

$$x_d(T) = x_t - 0.209148\frac{T - T_t}{T - T_t - 0.080280} + 0.960222(T - T_t) + 0.549920(T - T_t)^2 \quad (6.1)$$

$$x_c(T) = x_t - 0.746805(T - T_t) - 0.180743(T - T_t)^2 + 0.316170(T - T_t)^3 \quad (6.2)$$

$$T\lambda(x) = T_t - 2.320259(x - x_t) - 1.023726(x - x_t)^2 \quad (6.3)$$

with $T_t = 0.867K$ and $x_t = 0.674$.

For given the equation of state for both the pure substances, one can use the following equation for the mixing term of the He3-4 mixture based on the work of Kuerten as:

$$V_r(x, T, P) = \sum_{i=0}^{3}\sum_{j=0}^{3}[x^i T^j(+Vr1_{1(i,j)}P^1 + Vr1_{2(i,j)}P^2 + Vr2_{i,j}\frac{1}{P + pvr}] \quad (6.4)$$

with Vr1 and Vr2 being:

$$Vr1_0 = \begin{pmatrix} 0.139 & -4.933 & -4.474 & -17.764 \\ -2.568 & 40.218 & 21.103 & -17.586 \\ 0.511 & -83.296 & 42.536 & -2.742 \\ 3.985 & 16.617 & 32.248 & -21.867 \end{pmatrix}$$

$$Vr1_1 = \begin{pmatrix} -0.071 & 2.043 & 1.971 & 1.212 \\ 0.898 & -13.571 & 1.238 & 0.334 \\ -0.199 & 18.304 & -9.101 & 7.526 \\ -1.372 & 2.396 & -18.727 & 7.804 \end{pmatrix}$$

$$Vr1_1 = \begin{pmatrix} 0.01 & -0.164 & -0.277 & 0.078 \\ -0.06 & 0.973 & 0.289 & -0.364 \\ -0.026 & -0.924 & -0.644 & 0.538 \\ 0.136 & -0.543 & 2.287 & -1.345 \end{pmatrix}$$

$$Vr2 = \begin{pmatrix} -1.165 & -8.229 & -5.791 & 62.108 \\ -4.505 & 24.649 & -104.817 & 8.141 \\ 10.159 & 31.641 & 29.678 & 4.32 \\ -11.354 & 4.229 & -81.74 & 32.624 \end{pmatrix}$$

So the overall molar volume for the mixture is calculated as:

$$v(x,T,P) = x\, v_3(T,P) + (1-x)v_4(T,P) + x(1-x)V_r(x,T,P) \tag{6.5}$$

where $v_3(T,P)$ is given by the inverse of eq.5.3 and $v_4(T,P)$ is given by eq.3.18. In both cases the relevant unit transformations need to be done as for the results to be given in molar volumes respectively by using the molar masses of Helium-3 and Helium-4.

6.2.3 Numeric Equations for He3-4 Mix EOS

To derive the equations for different thermodynamic variables code for fitting high degree polynomials in terms of the consistency, the temperature and the pressure is developed.The consistency and temperature and obligatory to be used in the equations, and as for the third variable the pressure was chosen instead of the specific volume or density as given the difference in the atomic weight of the two isotopes only molar variables could be given which would in turn would also have to rely on the consistency, leading to just using the pressure as a better overall solution.

The equations used are given in the Appendix C. The results of the numeric equations for the Helium 3-4 mixture are presented below.

The entropy is calculated as:

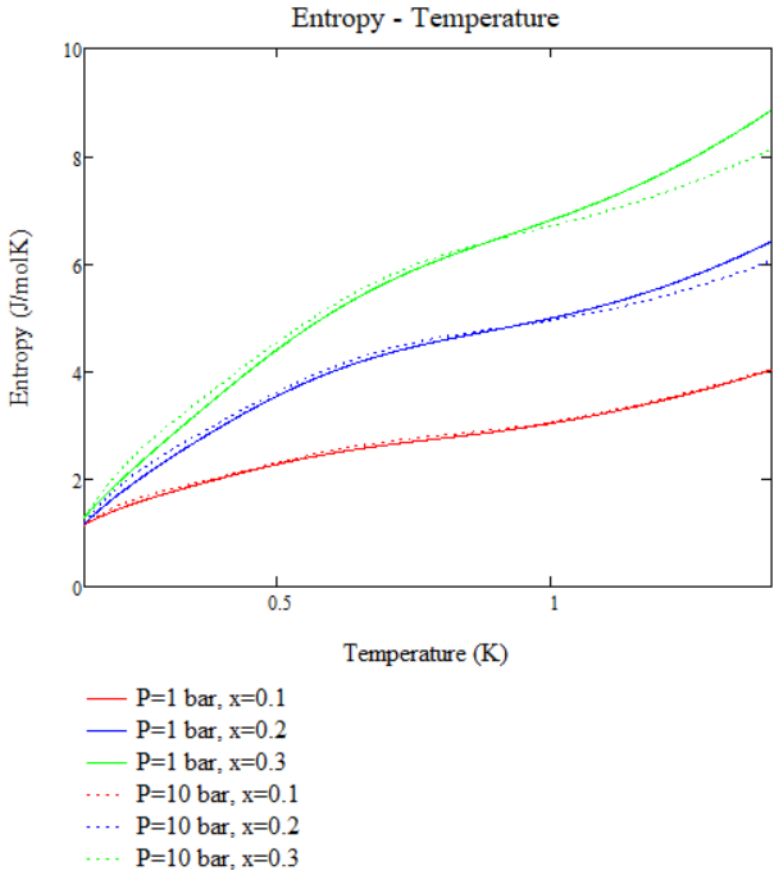

FIGURE 6.2: Entropy values for numerical mix equation at pressures of 1 and 10 atm.

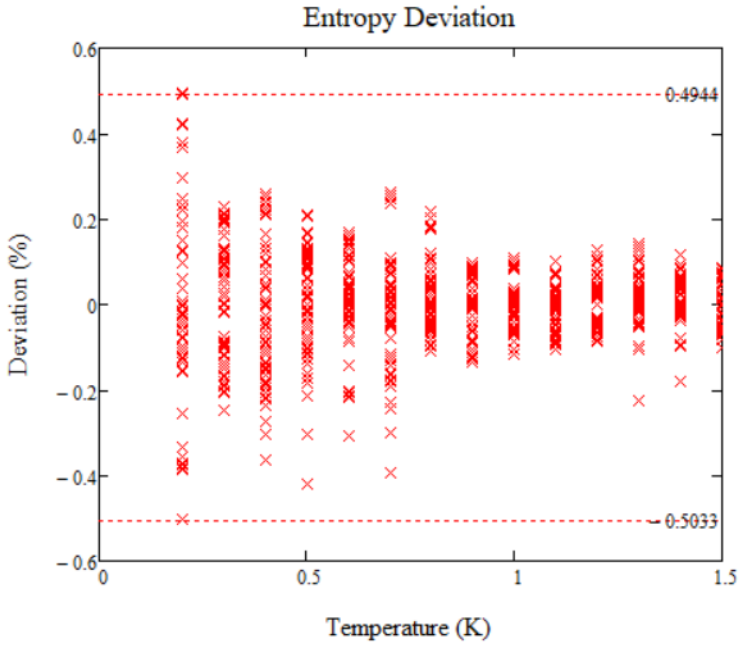

FIGURE 6.3: Entropy equation deviation from the used values.

The enthalpy is calculated as:

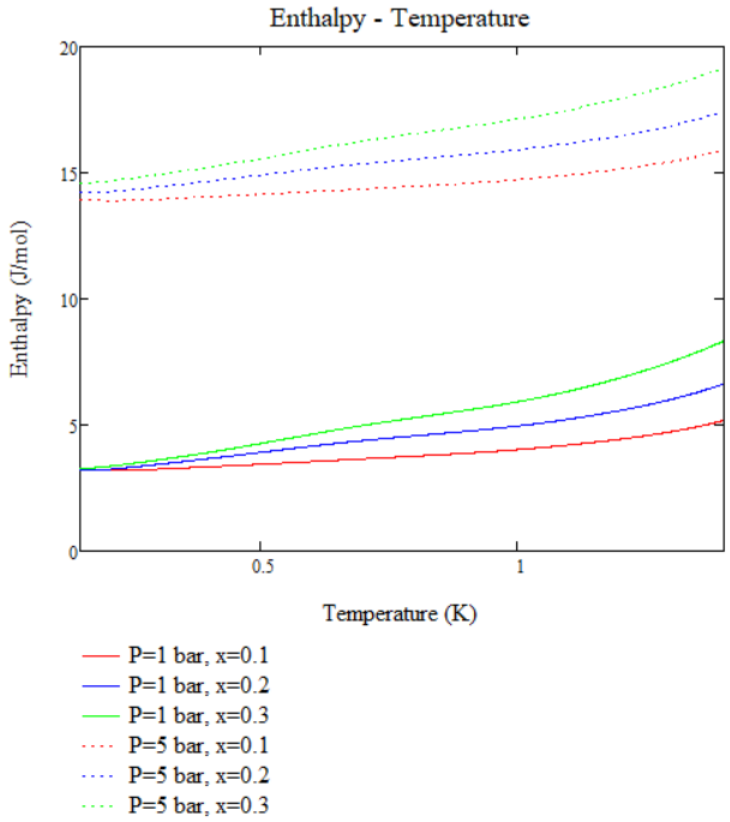

FIGURE 6.4: Enthalpy values for numerical mix equation at pressures of 1 and 10 atm.

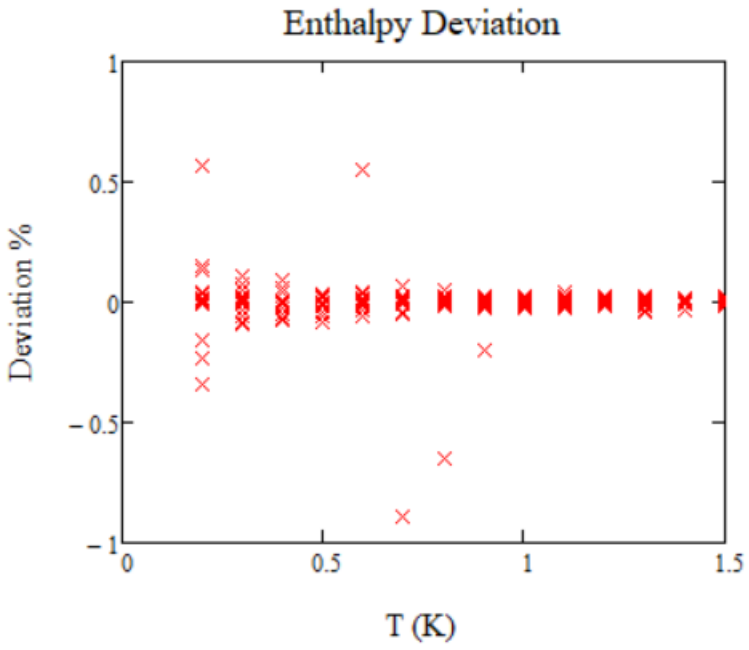

FIGURE 6.5: Enthalpy equation deviation from the used values.

The molar volume is calculated as:

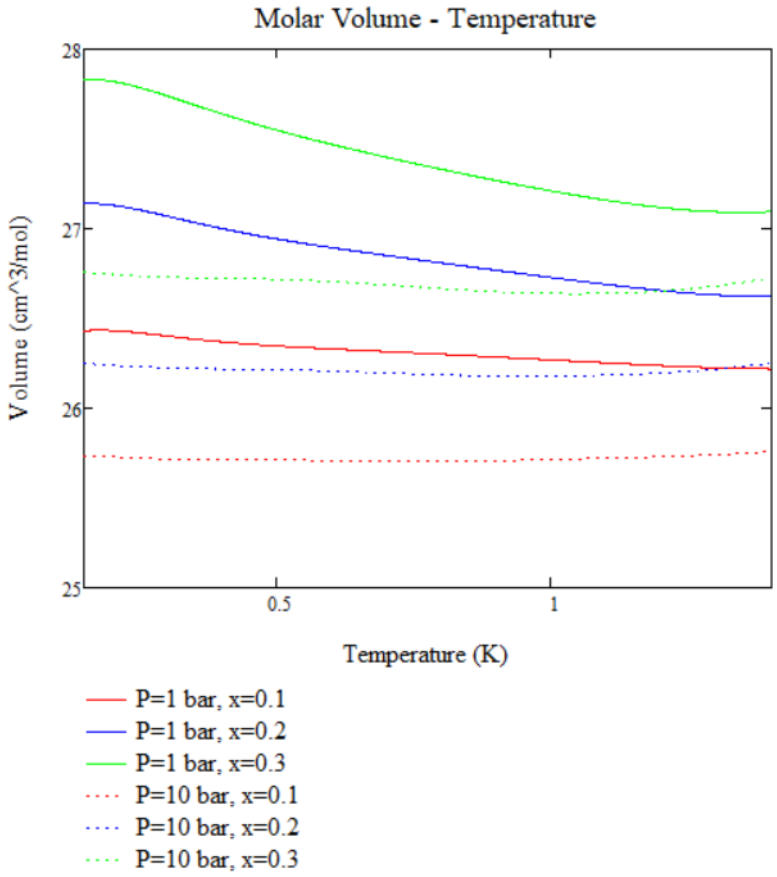

FIGURE 6.6: Molar volume values for numerical mix equation at pressures of 1 and 10 atm.

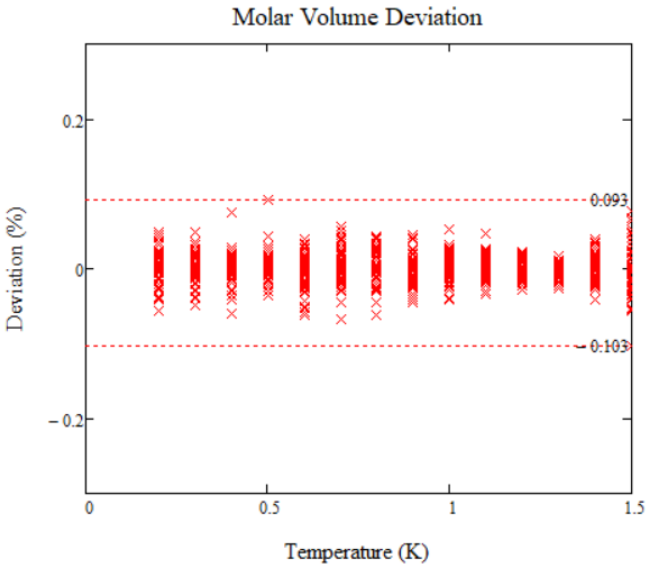

FIGURE 6.7: Molar volume equation deviation from the used values.

The accuracy of the equations provided is high and they can be suggested for use even in applications where very high levels of accuracy are needed.

6.2.4 Osmotic Pressure

The phenomenon of osmotic pressure is usually associated with mixtures that contain different substances. Isotopic mixtures usually present behaviors that resemble pure substances due to the similar behavior of their isotopes. The osmotic pressure describes the difference in pressure that occurs when a fluid is forced through a membrane where one of its substances is able to flow through but the others are not. The need of the system to retain an overall thermodynamic balance leads to this pressure difference based on the consistencies of the mixtures at the two sides. Usually, two isotopes of the same substance should always either pass or be blocked by the same membrane. Typically, at higher temperatures this also applies to Helium. But at low temperatures when the lambda point is reached then one of the isotopes of Helium (He4) becomes a superfluid. This transformation to superfluid means that Helium-4 will have no viscosity, meaning that it will be able to pass through porous media that would otherwise block its pass. The temperature difference of the two lambda lines leads to the Helium-3 part of the mixture still being a normal fluid. As such this part of the mixture would be unable to pass through the same porous medium that the superfluid Helium-4 passes through. As such when a Helium mixture at these temperatures is forced through such a medium and only Helium-4 passes through it means that a consistency difference between the two sides of the membrane will be formed and as such osmotic pressure occurs in the mixture. This phenomenon is very important in describing the thermodynamic and fluid mechanics behavior of low temperature Helium as many cryogenic apparatuses utilize the concepts of superleaks, which are exactly porous media allowing the superfluid part to pass through and blocking the normal fluid [73].

Based on the values given by Landau in [70] a numerical equation is formed describing the existing values with high accuracy as it will be displayed in the figure below.

A 3-variable polynomial interpolation of 4th degree is used with its coefficients given in C.

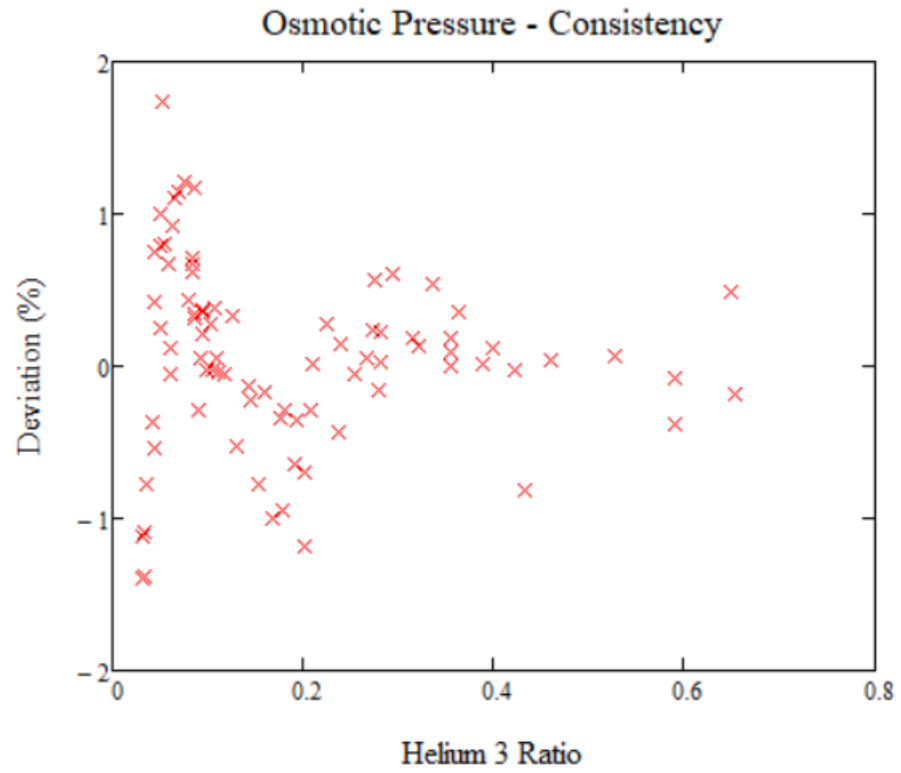

FIGURE 6.8: Osmotic Pressure deviations presented against Helium-3 ratio

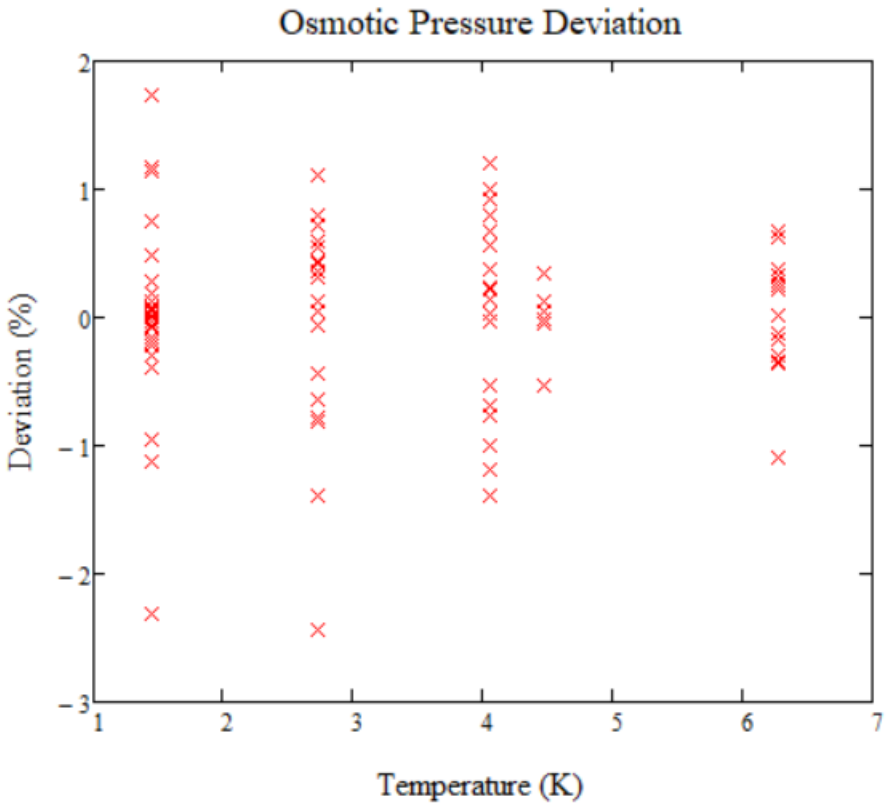

FIGURE 6.9: Osmotic Pressure deviations presented against Temperature

6.2.5 Volume dependence on consistency

In most engineering applications, especially in simulations done in CFD environments, finding the consistency of the mixture at each point of the simulation can prove to be exceedingly difficult if not impossible in some cases. In an apparatus that is simulated in a CFD environment the variable that is always known to the user is the volume of the apparatus. In applications where one uses a pure substance, by getting the variables of the pressure, the volume and the temperature from the CFD model the thermodynamic values can be calculated. In the case of a mixture, it is impossible to calculate the thermodynamic values if one does not know the consistency at each point of the simulation. In the cases of working with cryocoolers with a Helium 3-4 mix, besides the pressure and the temperature, what is also known is the total volume in the different regions of the machine. By knowing this total volume and knowing the available masses of Helium-3 in the system, it means that if one is able to show a low association of the molar volume with the consistency, then given the existing volumes of the apparatus and the Helium-3 mass one would be able to derive the consistency only by the volume. As it can be seen from the graph below, indeed the relation between the consistency and the volume is low. This is found by comparing the values for the total molar volume of the mixture to the sum of the molar volumes of the two substances.

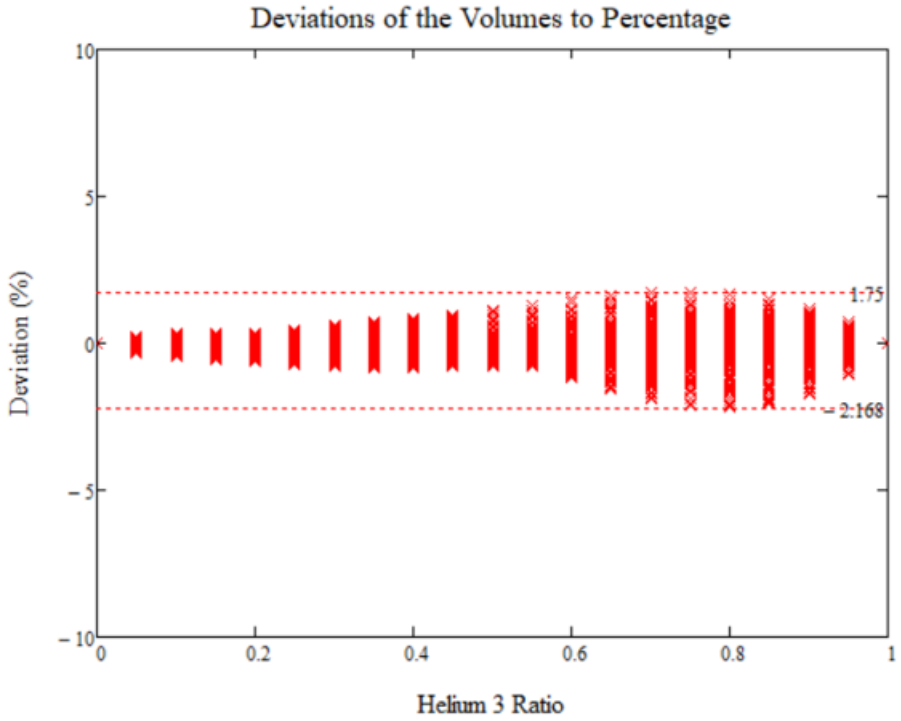

FIGURE 6.10: Showcasing the deviations between calculating the molar volume through the full equation and calculating it as the sum of the molar volume of the two pure isotopes 3He and 4He

Given these results, in applications concerning Helium mixtures with enrichment up to 25% it is observed that the mixing part of the equation is often neglected and the consistency variable is found directly from the sum of the pure molar volumes of the isotopes. This method based on the presented results ought to provide minimal errors

compared to using the full molar volume equation. A similar method to this is used in the paper of the author [42] where the results were shown to be consistent with the full theoretical model presented in [43].

6.3 Helium Mixture Thermodynamic Maps

For any set of Equations of state for a substance it is important and useful for the thermodynamic maps to be presented. This is something easily done in the cases of pure substances as there are only two independent variables on the systems. In a case of a mixture the number of independent variables is three. In the first case two independent variables lead to a 3D graph which can be properly defined in 2D as a contour plot. In the case of the mixtures with the 3 independent variables the occurring graph would be in 4D. Such a graph is difficult to be displayed in 2 dimensions. In this work the 4 dimensional thermodynamic maps of the Helium 3-4 mixture are to be presented in different ways.

Firstly, a sequence of contour plots of T and x axes for different pressures at each graph are presented. These kinds of displays can be beneficial for displaying parts of thermodynamic cycles.

This way of representing the 4D graph gives a good understanding about the numerical values but it lacks the ability to contain full thermodynamic cycles and showcase the dependency of all the energy derived variables to the pressure. For these reasons the maps are also presented in a different way.

A 4D diagram can also be represented as a 3D contour plot, meaning a surface with the coloring representing the 4th dimension. By doing this, one is able to showcase the dependence of all the thermodynamic variables on the temperature, pressure and consistency independent values. The 3D contour plot containing the enthalpy and the entropy is presented below:

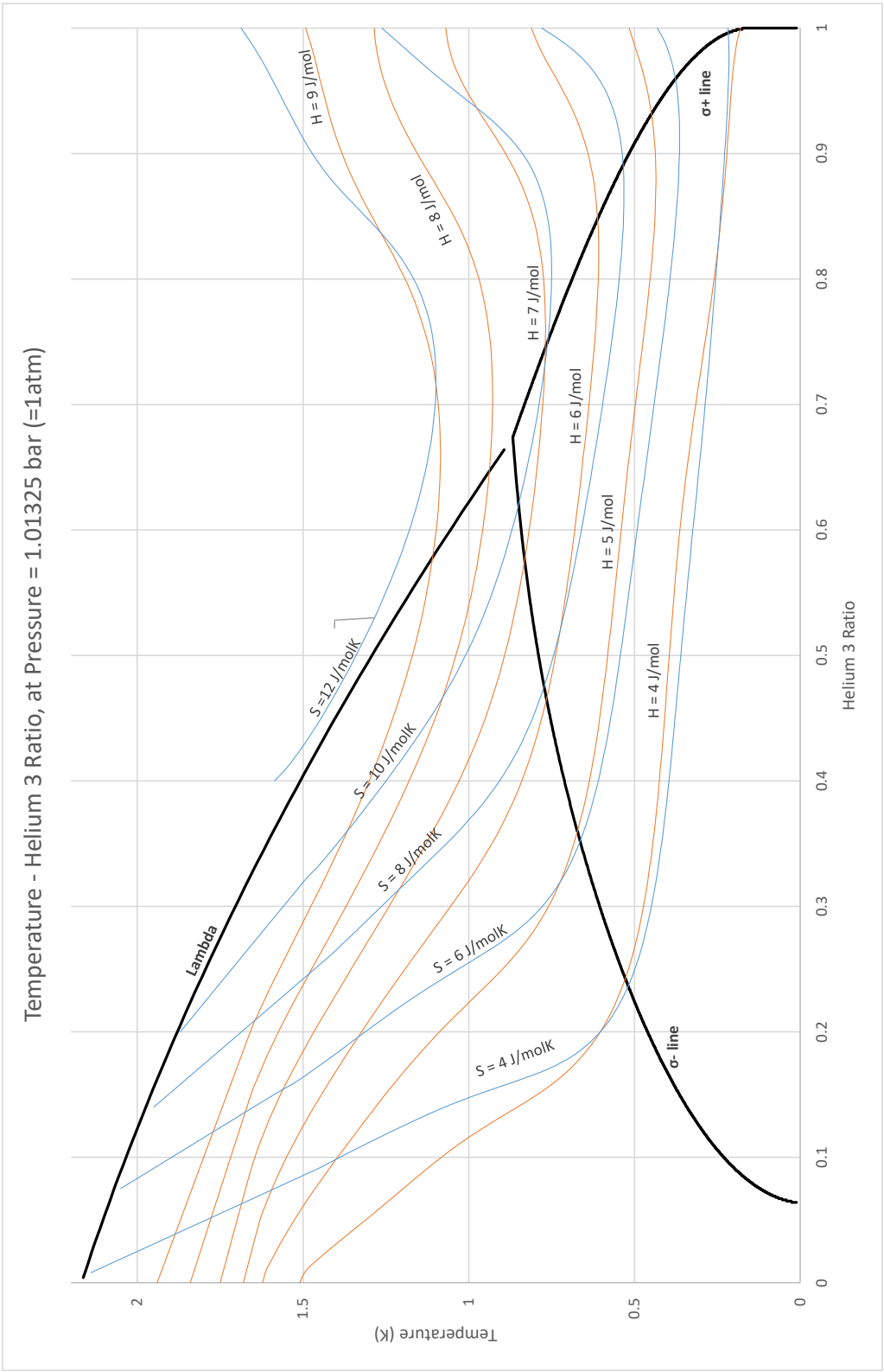

FIGURE 6.11: He3-4 mixture contour for P=1 bar

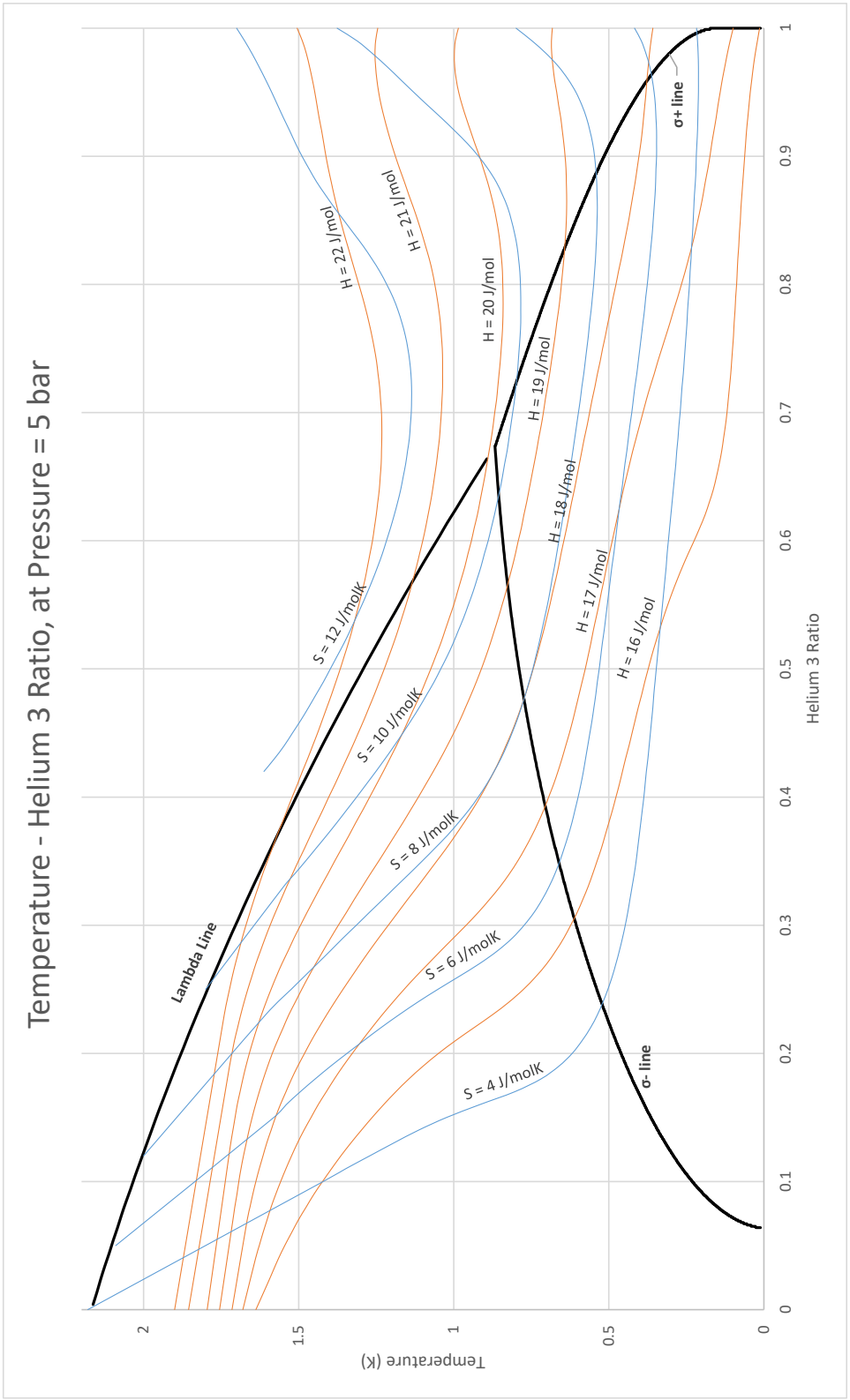

FIGURE 6.12: He3-4 mixture contour for P=5 bar

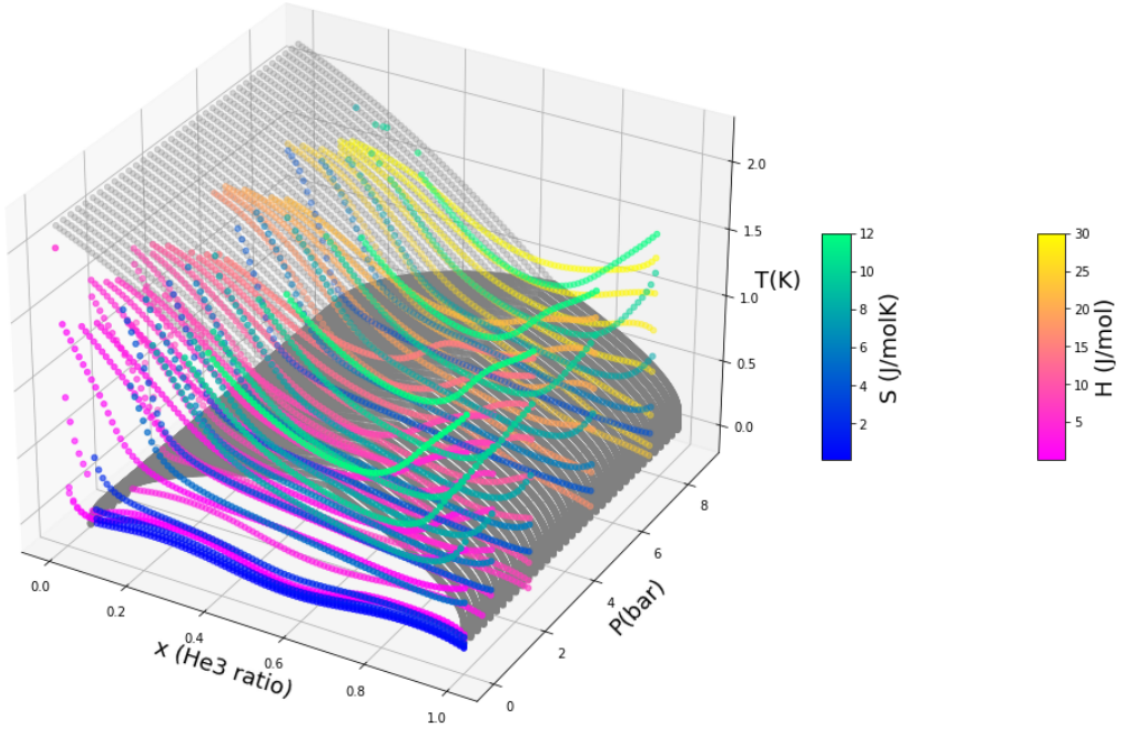

FIGURE 6.13: He3-4 mixture 3D contour map

In the previous graph one can see the different contour lines and their values through color of the enthalpy and entropy for some pressures. In addition, the lambda lines are also present on the graph for helping one understand how the enthalpy and entropy are affected through the transitions of the lambda lines.

Just by observing the values of the graphs compared to the values of the graphs of pure Helium-4 one can see that below the lambda line in the mixture the enthalpy and the entropy do not asymptotically go to zero, as they did in pure Helium-4, but their values remain significantly higher. This is to be expected because of the existence of Helium-3. As mentioned before Helium-3 does not become a superfluid until much lower in the temperature range and as such it creates a much higher thermodynamic activity potential compared to the nearly inert Helium-4 superfluid and the overall values remain significantly higher than Helium-4.

For one to understand even further the thermodynamic behavior of the mixture more 3D contour plots are presented below showcasing the behavior of the basic thermodynamic values with much higher sampling density for the pressure the consistency and the temperature.

6.3.1 Entropy Contours

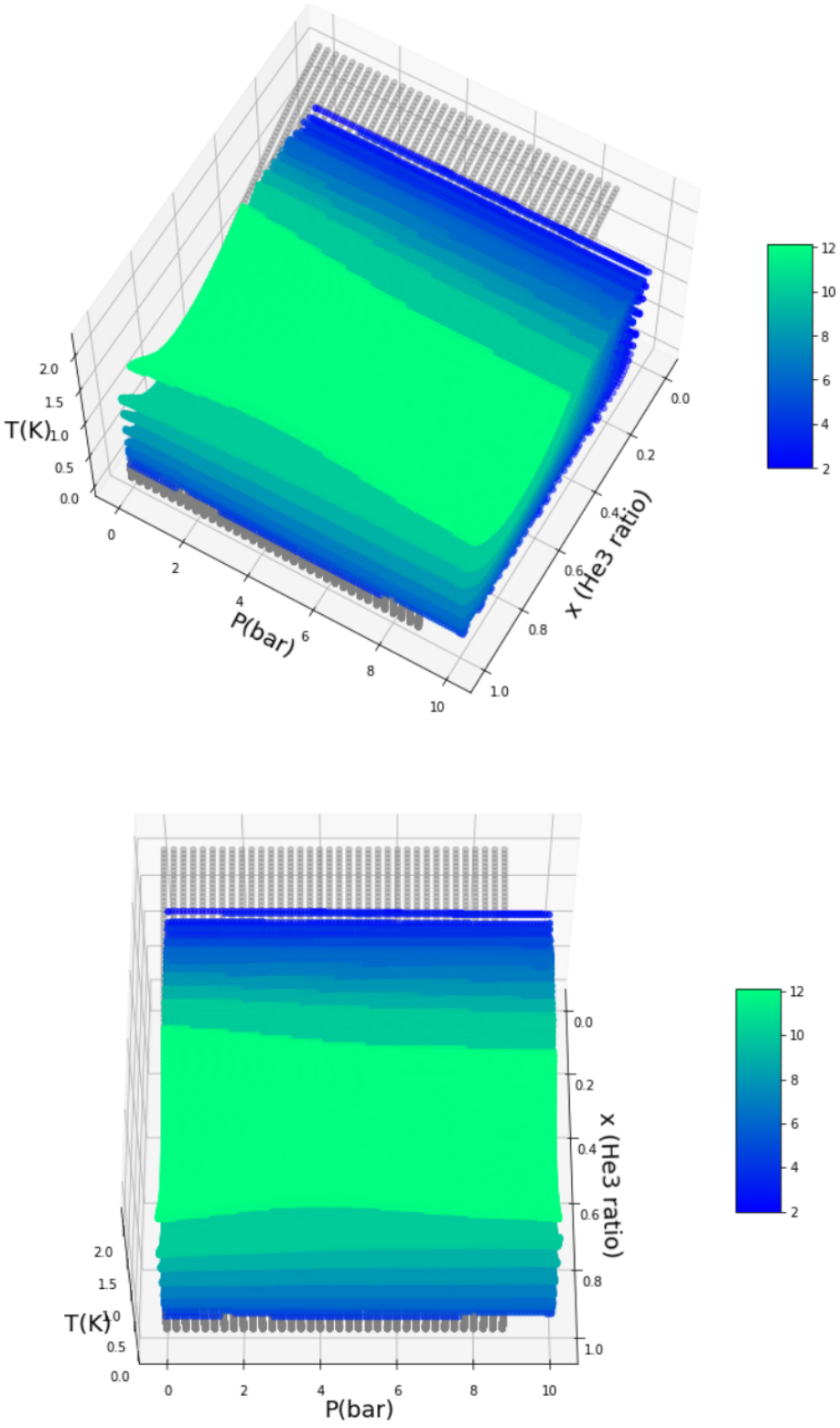

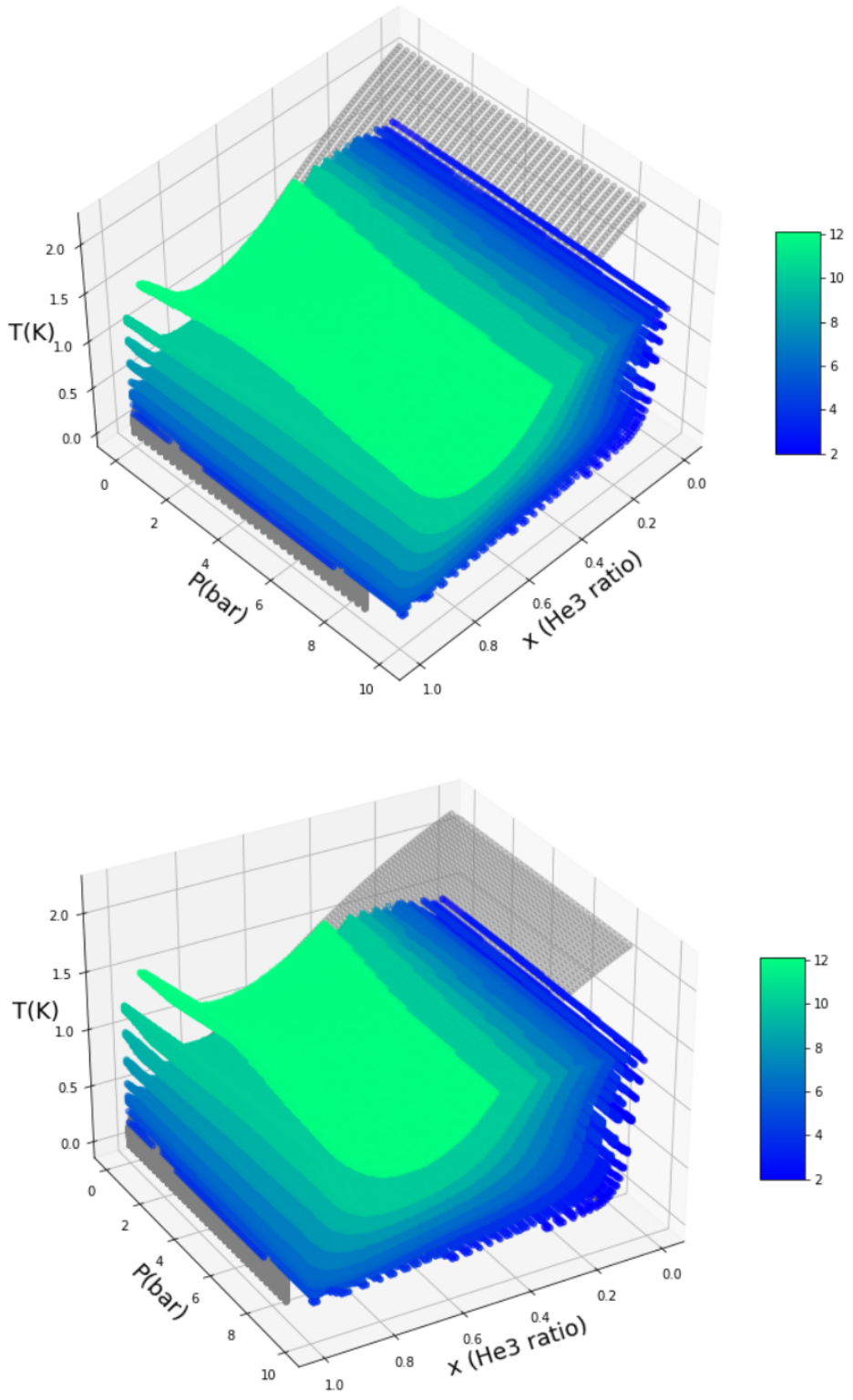

FIGURE 6.14: He3-4 mixture 3D map with contours of Entropy

Through the entropy diagrams it is seen that the entropy is heavily based on the temperature and much less on the pressure. This is consistent with the behavior of the pure substances and it is based on the fact that the entropies remain in the same range for all the different pressures. In addition to this it is seen that the entropy also has value that are a lot higher when it is close to the lambda line.

For a more detailed view of the entropy a series of 2D contours for different temperatures and pressures are presented where the isentropic lines are shown as for one to be able to get directly the values for the graph.

Firstly, the contours under constant pressure where the phase transition lines are presented:

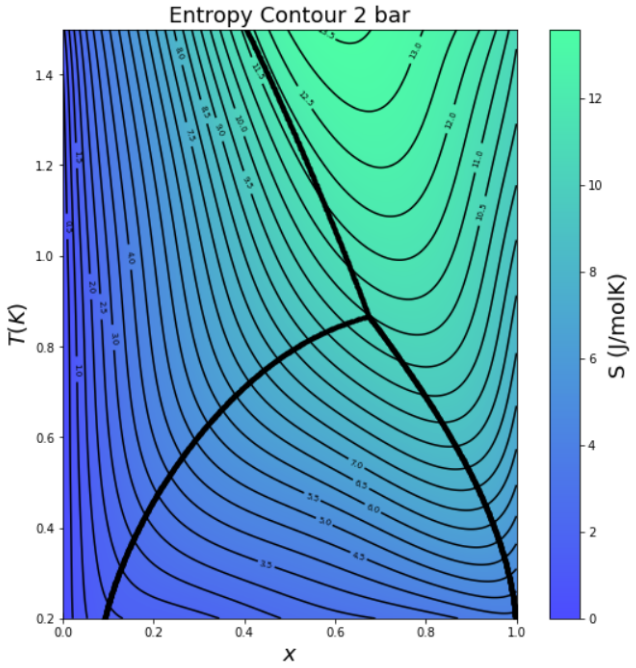

FIGURE 6.15: He3-4 mixture 2D contour of Entropy for P=2 bar

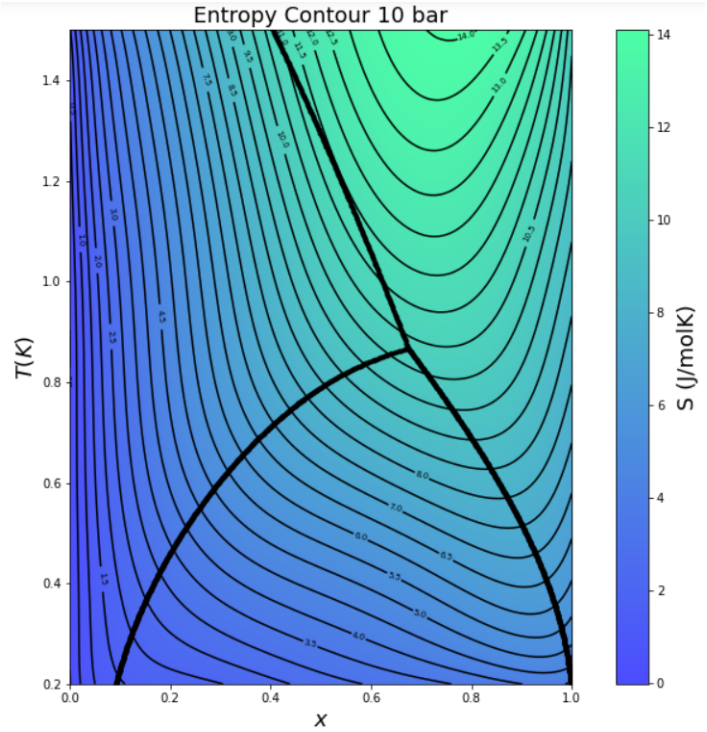

FIGURE 6.16: He3-4 mixture 2D contour of Entropy for P=10 bar

Also, the contours under constant temperatures are presented.

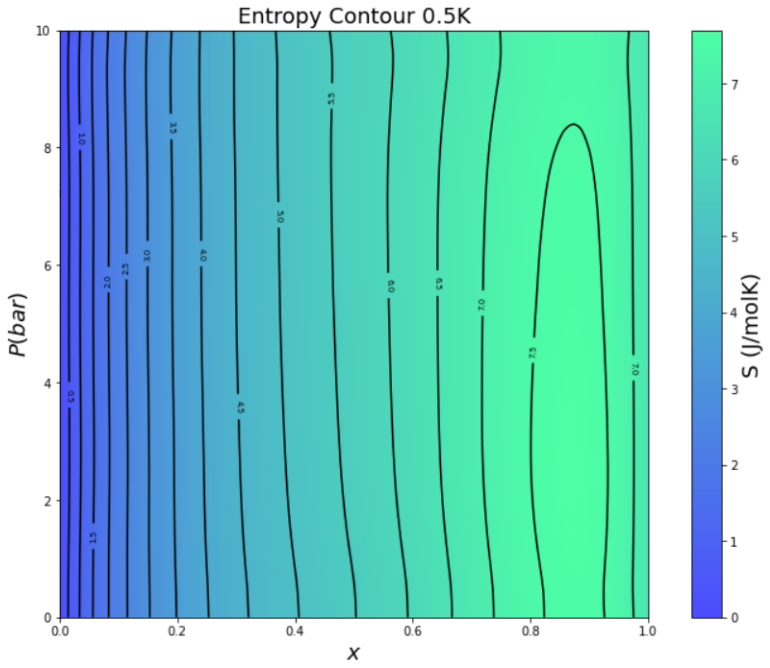

FIGURE 6.17: He3-4 mixture 2D contour of Entropy for T=0.5K

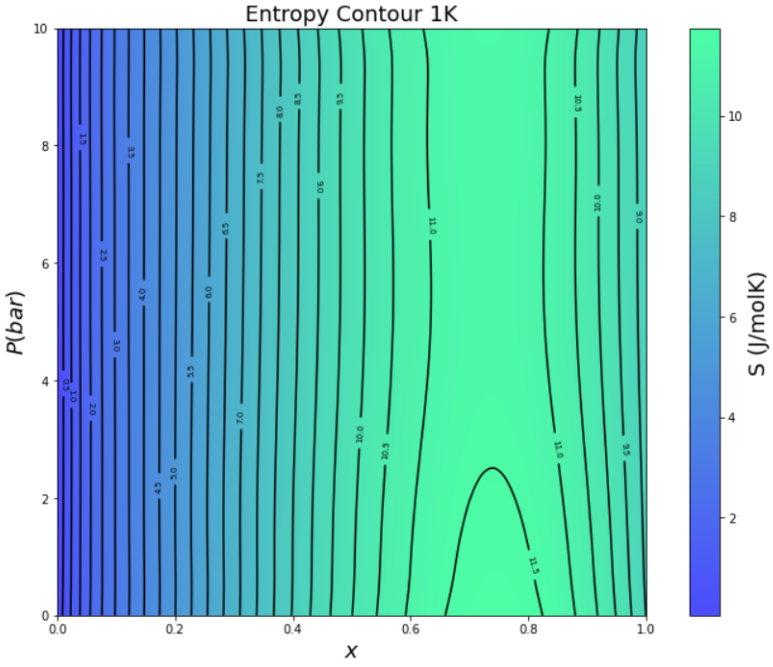

FIGURE 6.18: He3-4 mixture 2D contour of Entropy for T=1K

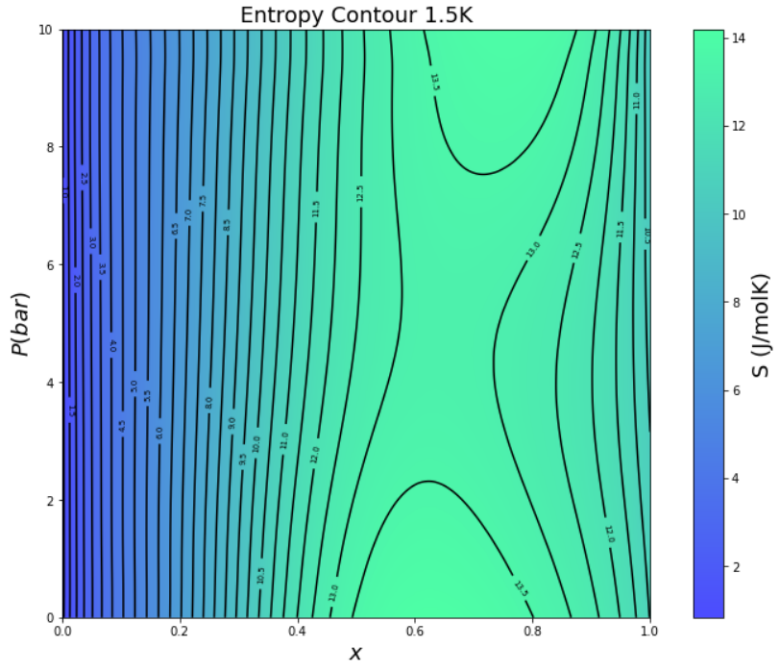

FIGURE 6.19: He3-4 mixture 2D contour of Entropy for T=1.5K

6.3.2 Enthalpy Contours

Enthalpy 3D contours

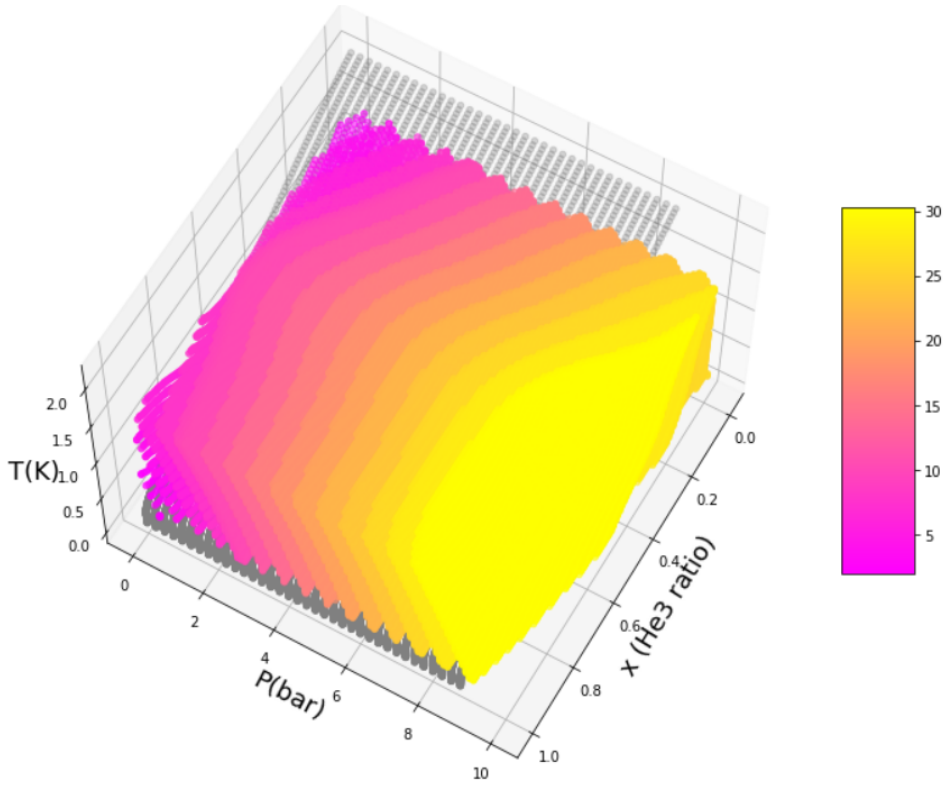

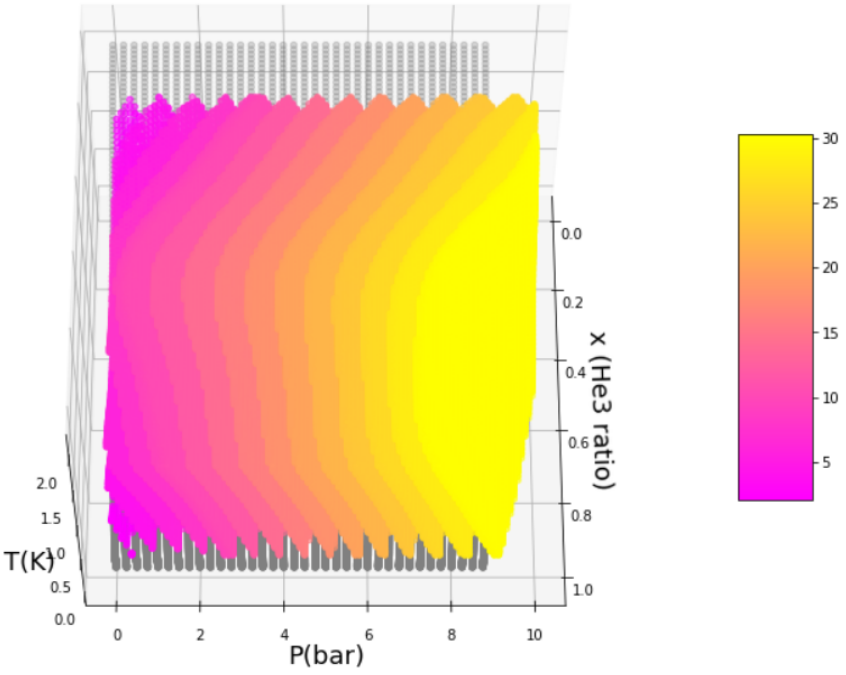
T(K)
P(bar)
x (He3 ratio)
0.0
0.5
1.0
1.5
2.0
0
2
4
6
8
10
0.0
0.2
0.4
0.6
0.8
1.0
30
25
20
15
10
5

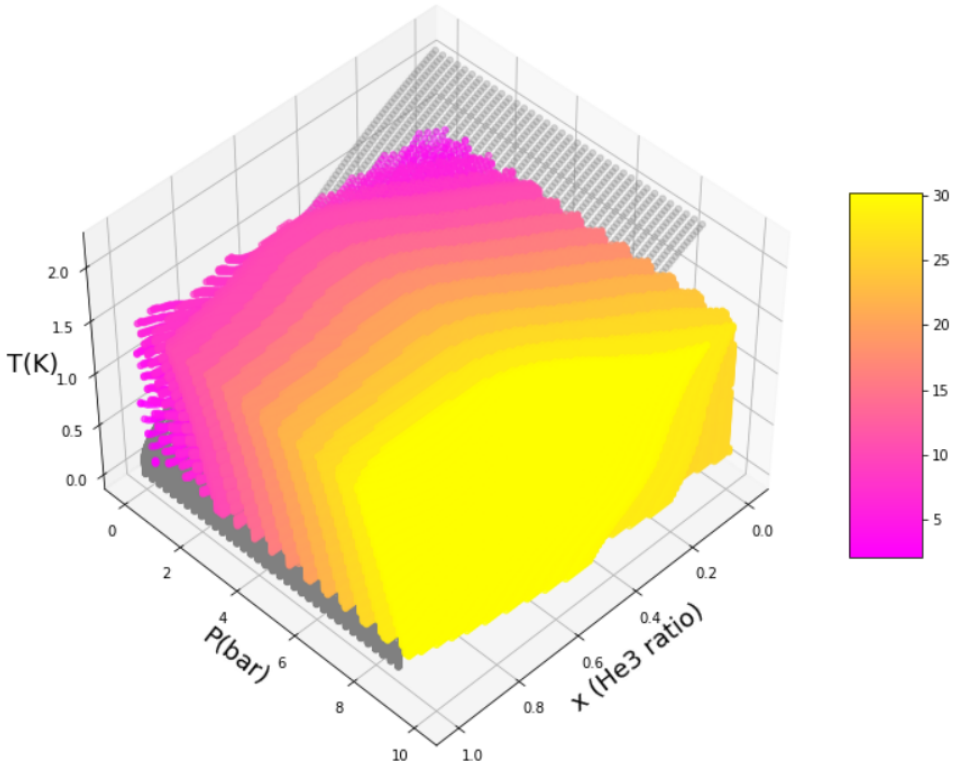
T(K)
P(bar)
x (He3 ratio)
0.0
0.5
1.0
1.5
2.0
0
2
4
6
8
10
0.0
0.2
0.4
0.6
0.8
1.0
30
25
20
15
10
5

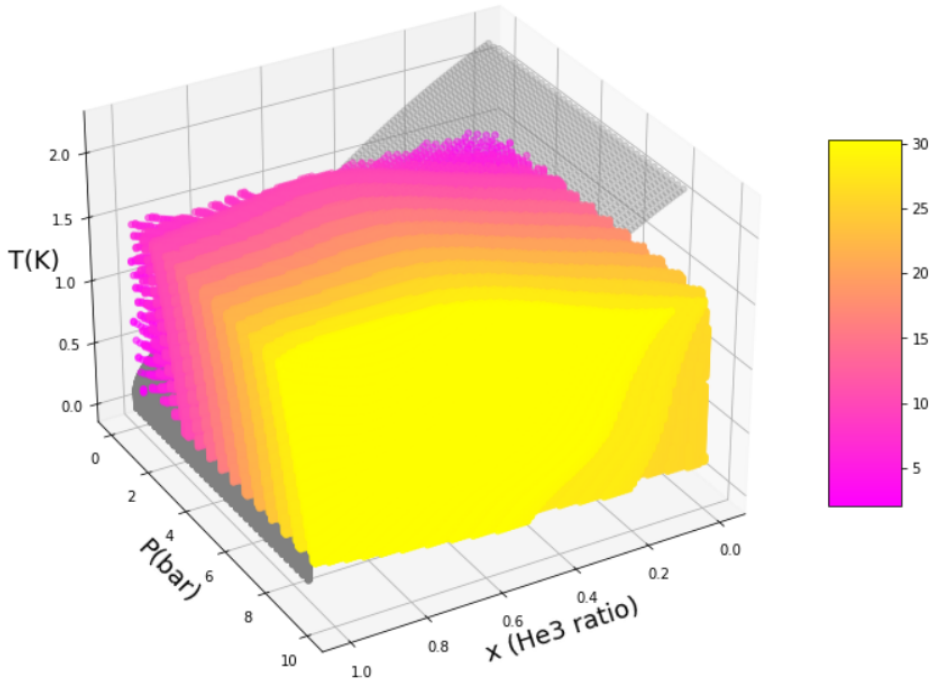

FIGURE 6.20: He3-4 mixture 3D map with contours of Enthalpy

In contrast to the entropy, the enthalpy is seen to be much more correlated to the pressure than it is to the temperature. The correlation to the temperature this time is less severe. When compared to the entropy it is seen that in both cases the difference in values on both the entropy and the enthalpy through the temperature range is similar in terms of percentage but while the entropy remains mostly consistent when the pressure changes, the enthalpy changes significantly with the pressure changes. This can be seen even more clearly through the detailed 2D contours for different temperatures and pressures presented below. (At the end of the book the full tables with the calculated data for Helium 3-4 mixture are presented.)

Firstly, the contours under constant pressure where the phase transition lines are presented:

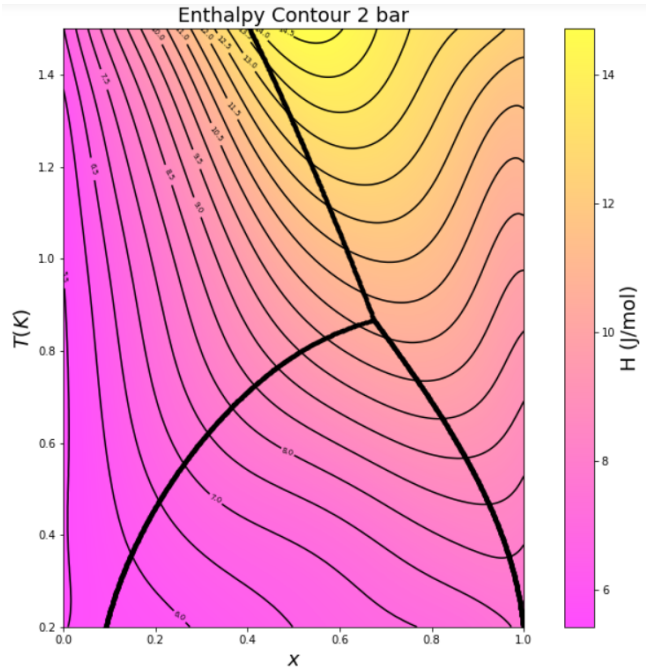

FIGURE 6.21: He3-4 mixture 2D contour of Enthalpy for P=2 bar

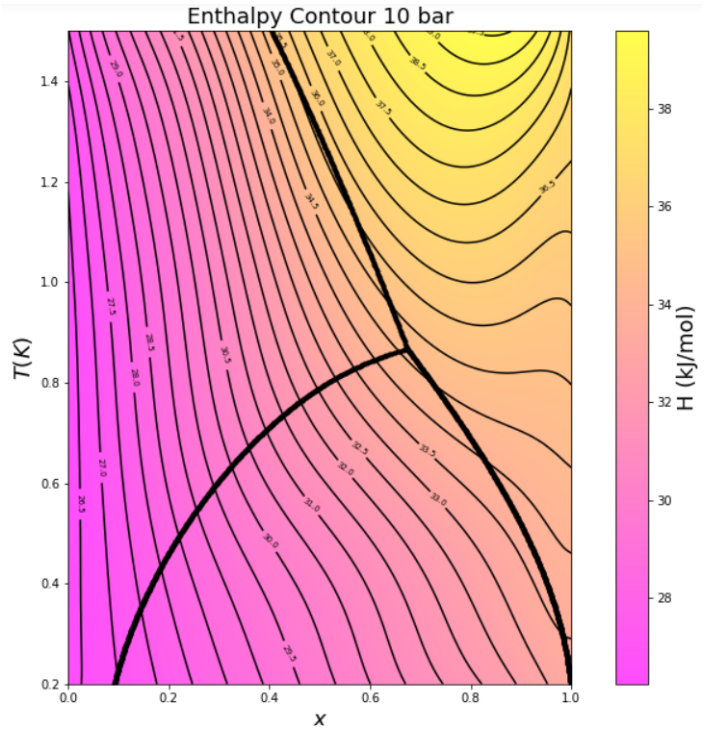

FIGURE 6.22: He3-4 mixture 2D contour of Enthalpy for P=10 bar

Also, the contours under constant temperatures are presented.

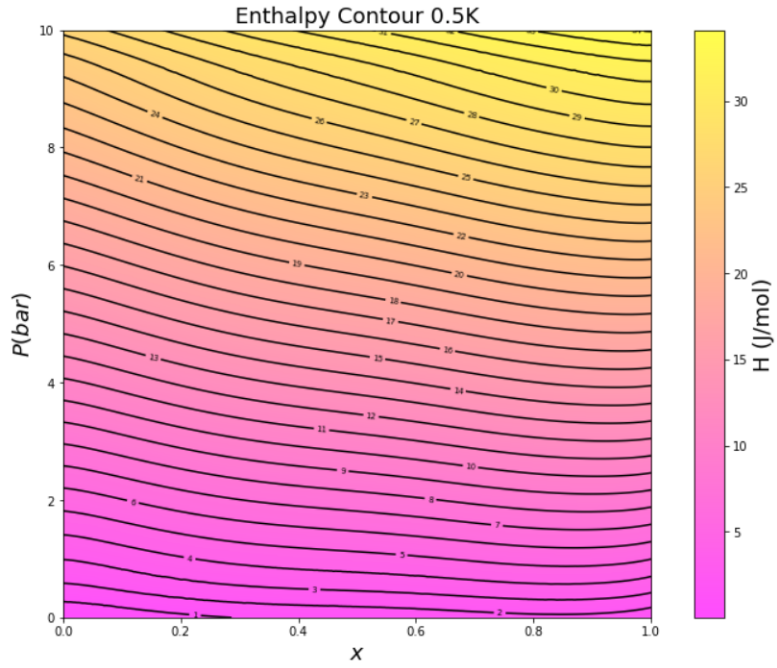

FIGURE 6.23: He3-4 mixture 2D contour of Enthalpy for T=0.5K

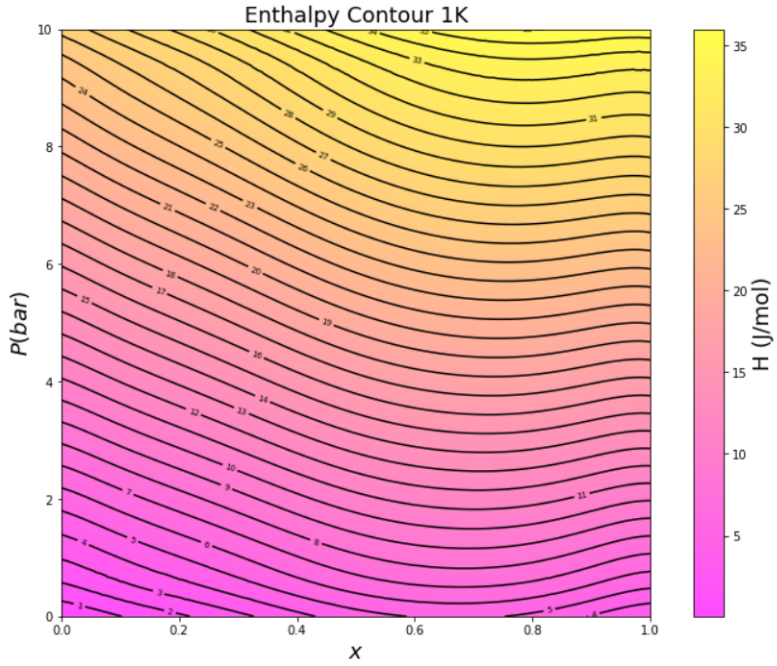

FIGURE 6.24: He3-4 mixture 2D contour of Enthalpy for T=1K

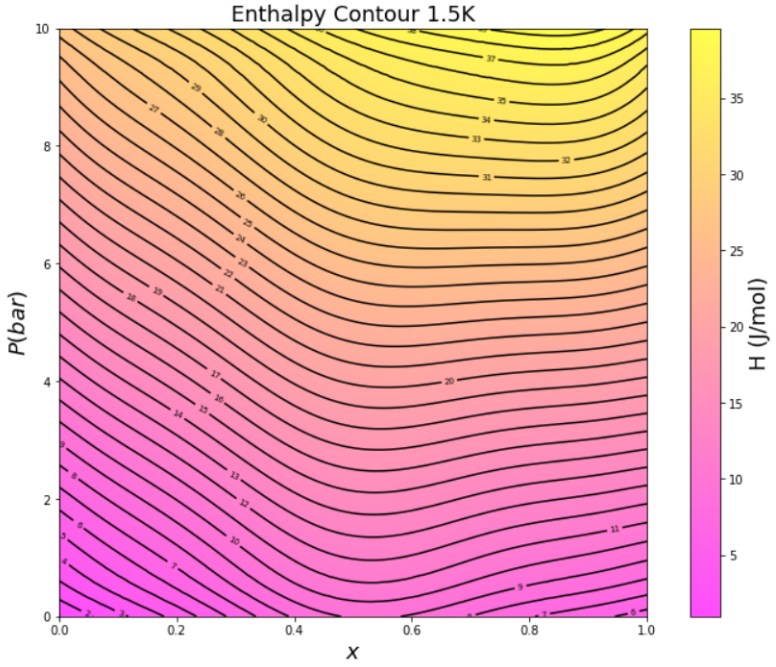

FIGURE 6.25: He3-4 mixture 2D contour of Enthalpy for T=1.5K

6.3.3 Molar volume contours

Molar volume 3D contour plots

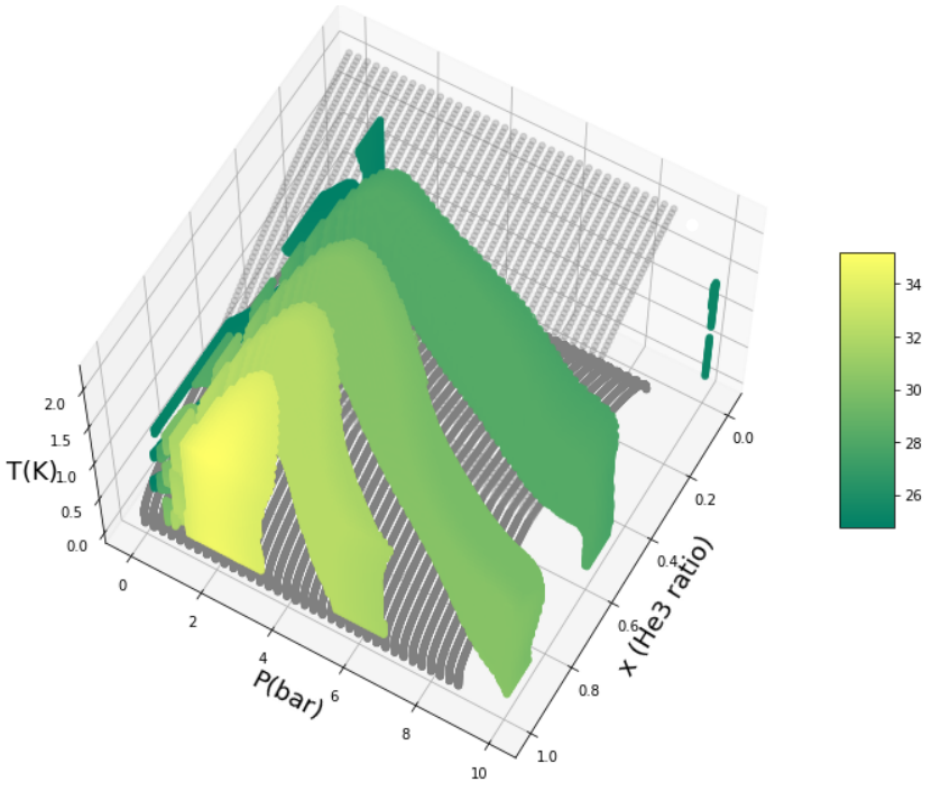

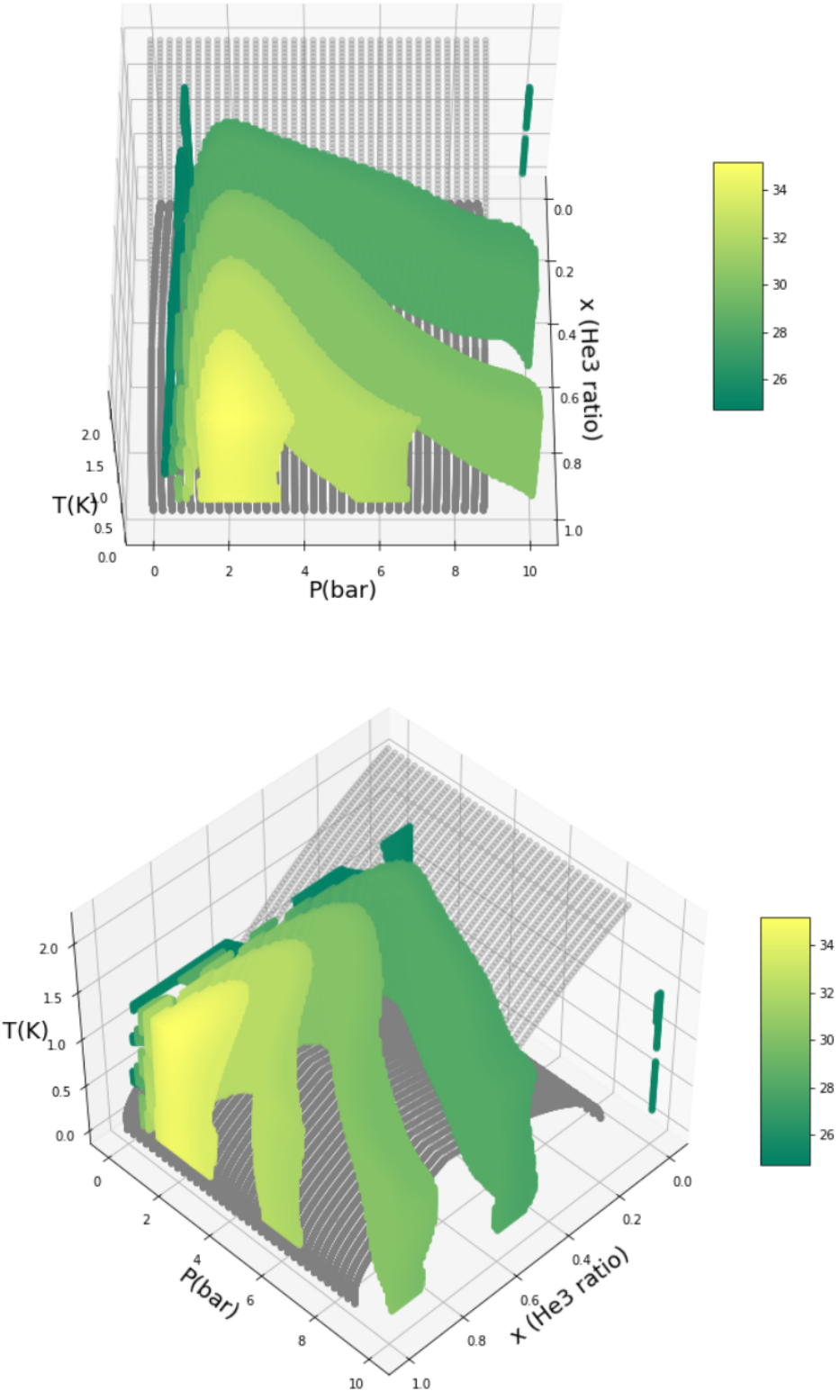
T(K)
P(bar)
x (He3 ratio)
34
32
30
28
26

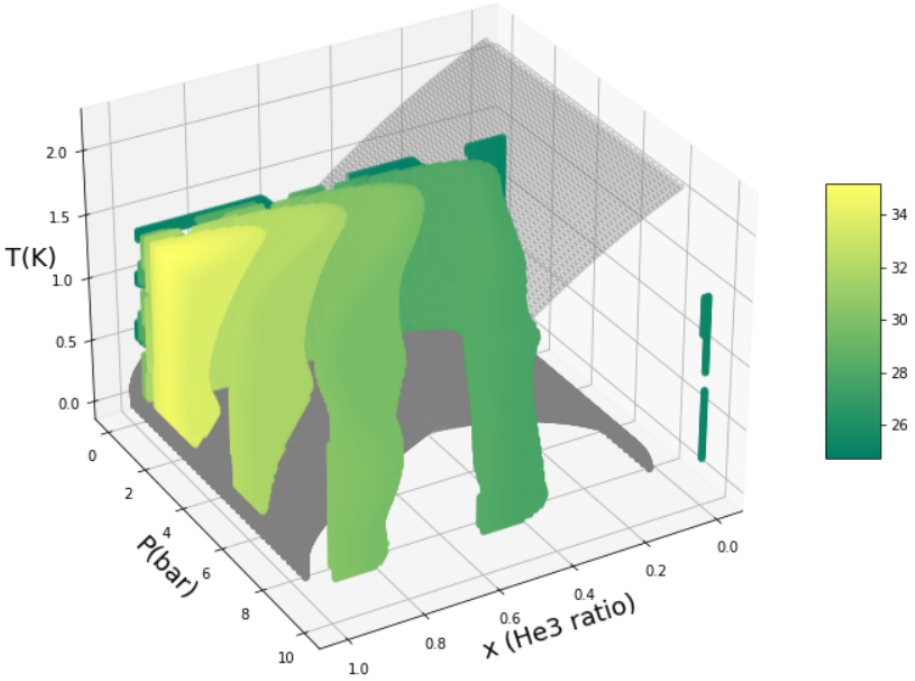

FIGURE 6.26: He3-4 mixture 3D map with contours of Molar volume

When studying the diagrams for the molar volumes it is seen that the values are strongly correlated to all three variables being highly dependent in the consistency, the temperature and the pressure.

Firstly, the contours under constant pressure where the phase transition lines are presented:

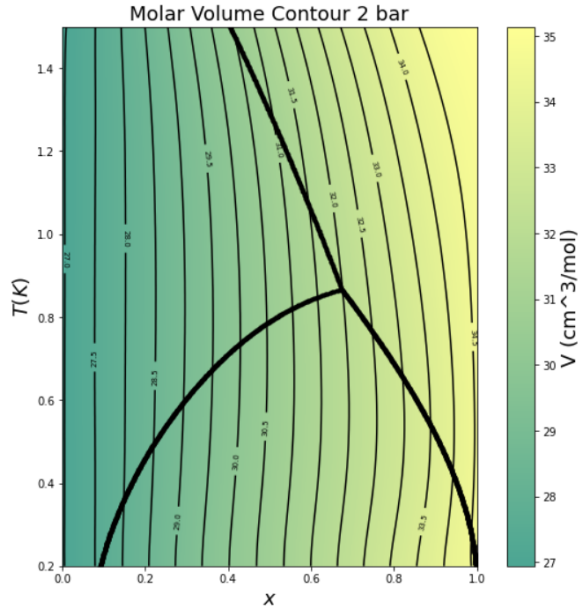

FIGURE 6.27: He3-4 mixture 2D contour of Molar Volume for P=2 bar

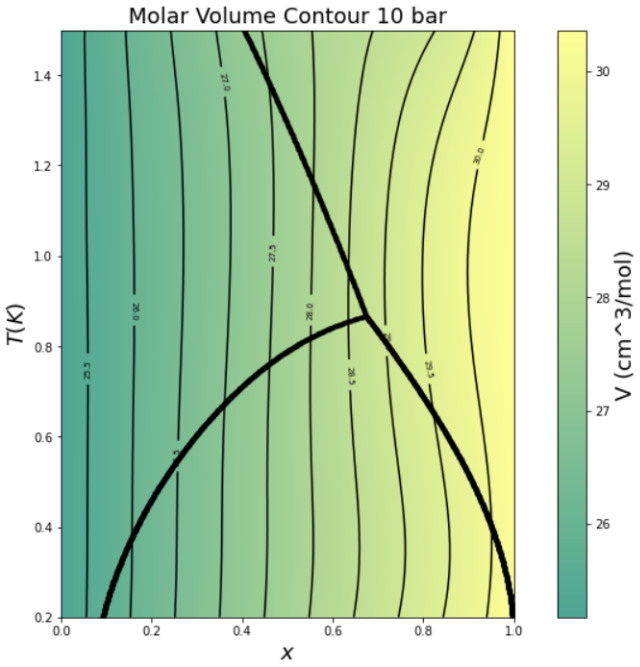

FIGURE 6.28: He3-4 mixture 2D contour of Molar Volume for P=10 bar

Also the contours under constant temperatures are presented.

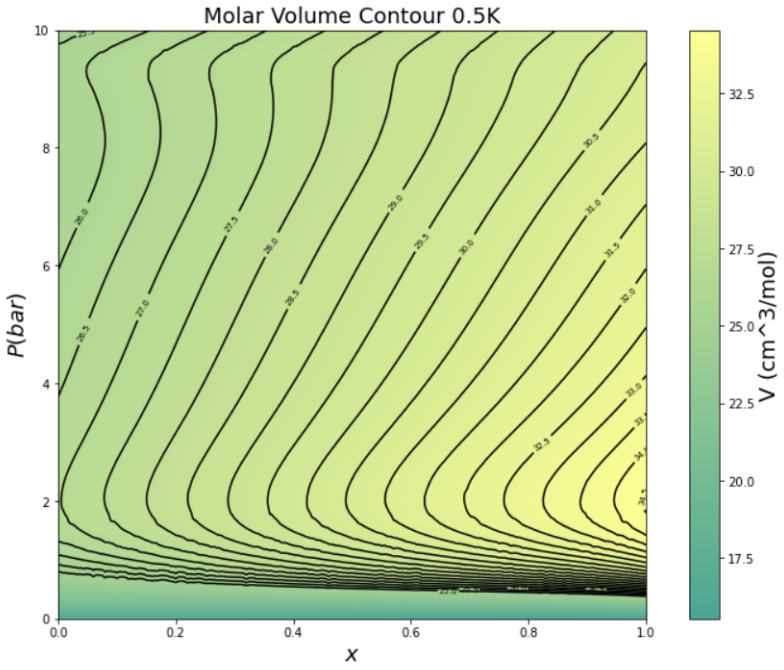

FIGURE 6.29: He3-4 mixture 2D contour of Molar Volume for T=0.5K

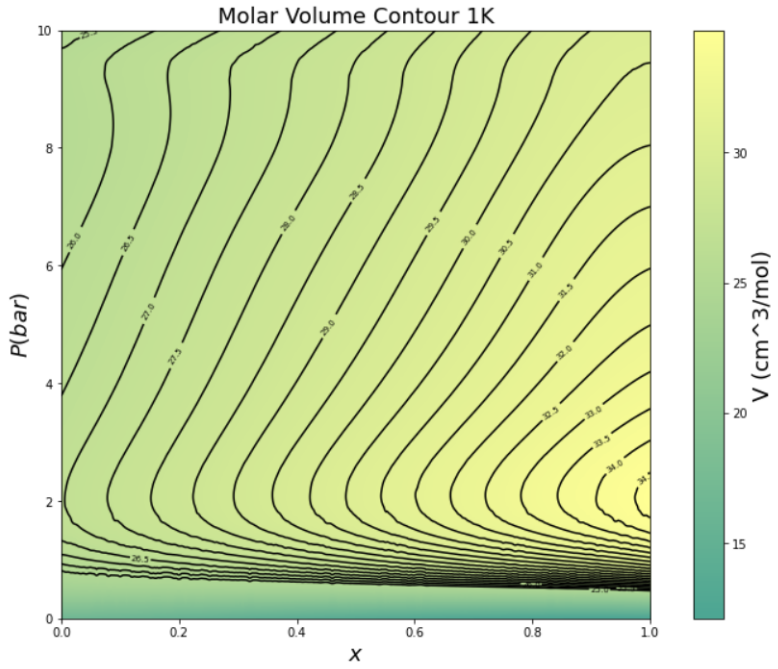

FIGURE 6.30: He3-4 mixture 2D contour of Molar Volume for T=1K

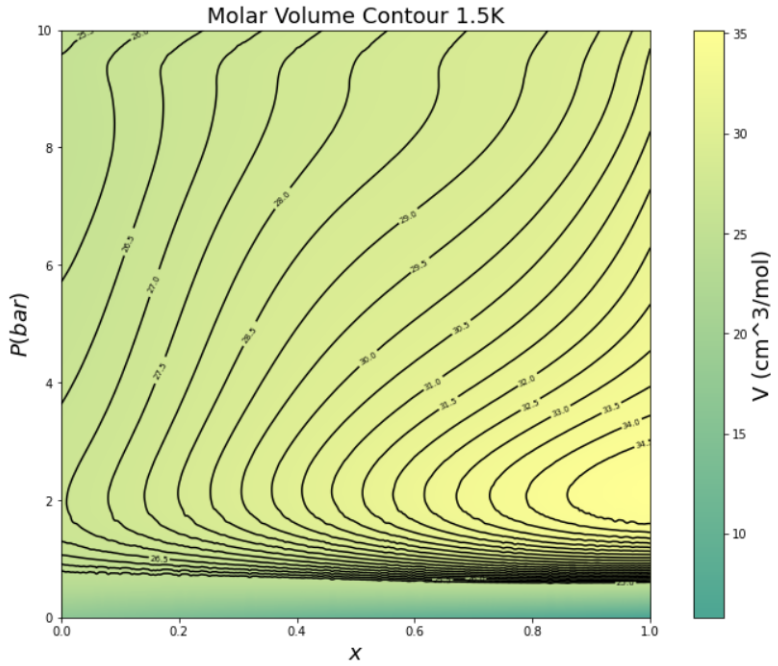

FIGURE 6.31: He3-4 mixture 2D contour of Molar Volume for T=1.5K

6.3.4 Chemical Potential

In addition to the energy variable and the volume another variable that is considered to be very useful in applications of Helium 3-4 mixtures is the chemical potential. In applications like the dilution coolers for instance where one has to solve the control volumes after the mixing chamber under a steady chemical potential [74, 75]. Thus, one need accurate

equations for the chemical potential as well. In a similar manner as the previous equations the equation for the chemical potential is created (its coefficients are given in Appendix C. Based on the provided equation the 4D maps seen as 3D contours are presented below.

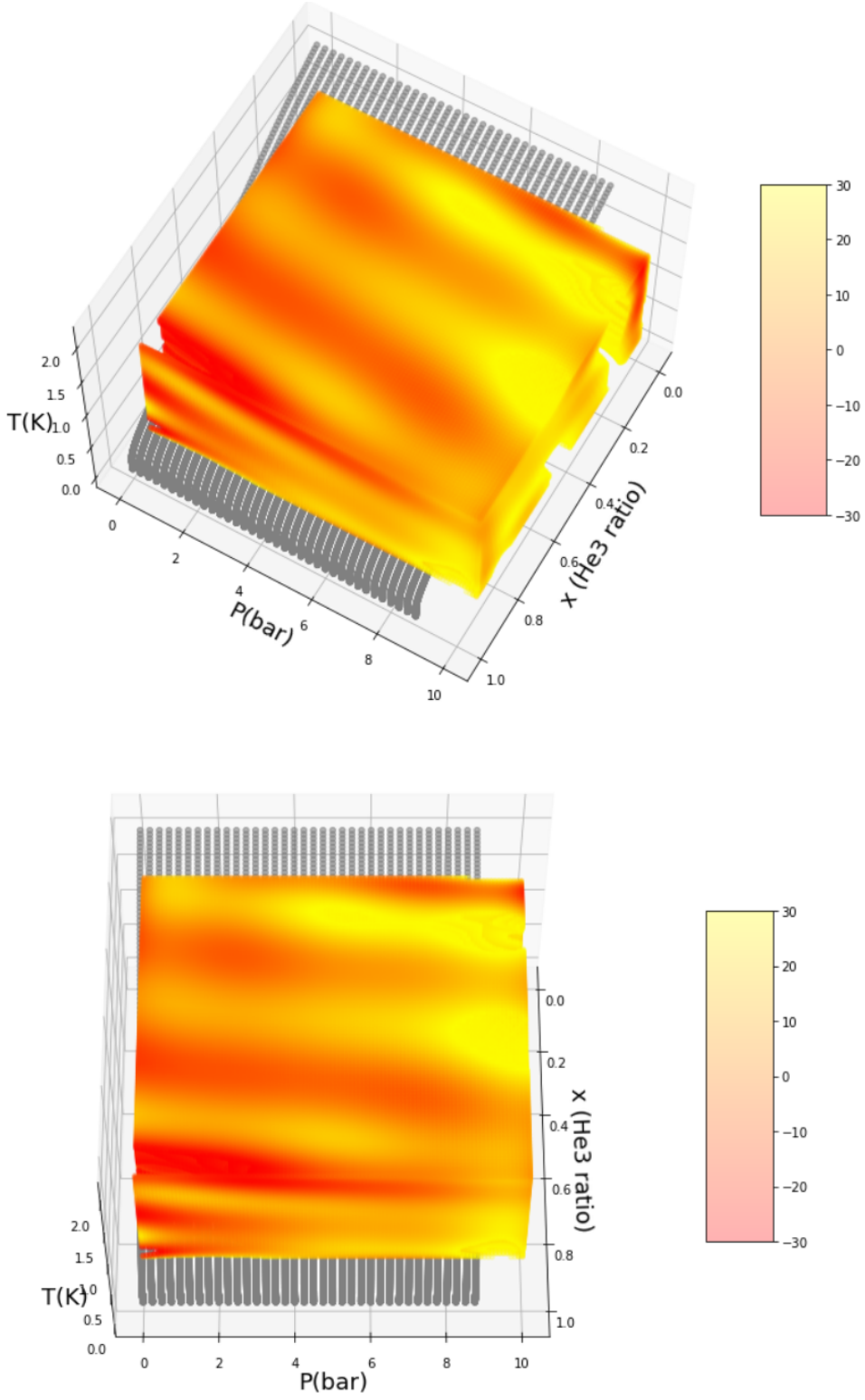

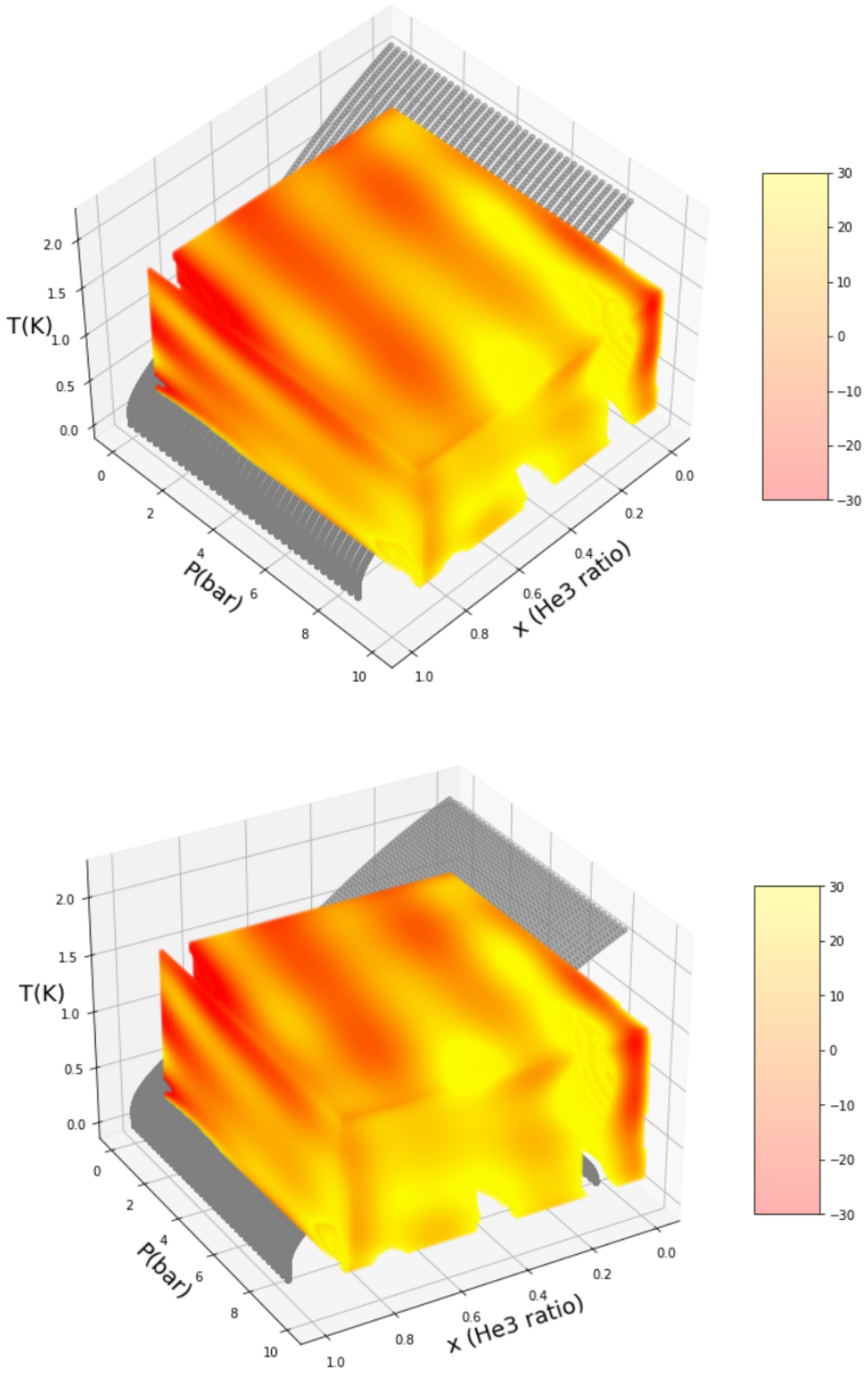

FIGURE 6.32: He3-4 mixture 3D map with contours of chemical potential

6.3.5 Full Helium 3-4 Mix Maps

Combining the equations from all the above one can create the full maps for the Helium 3-4 mixture as:

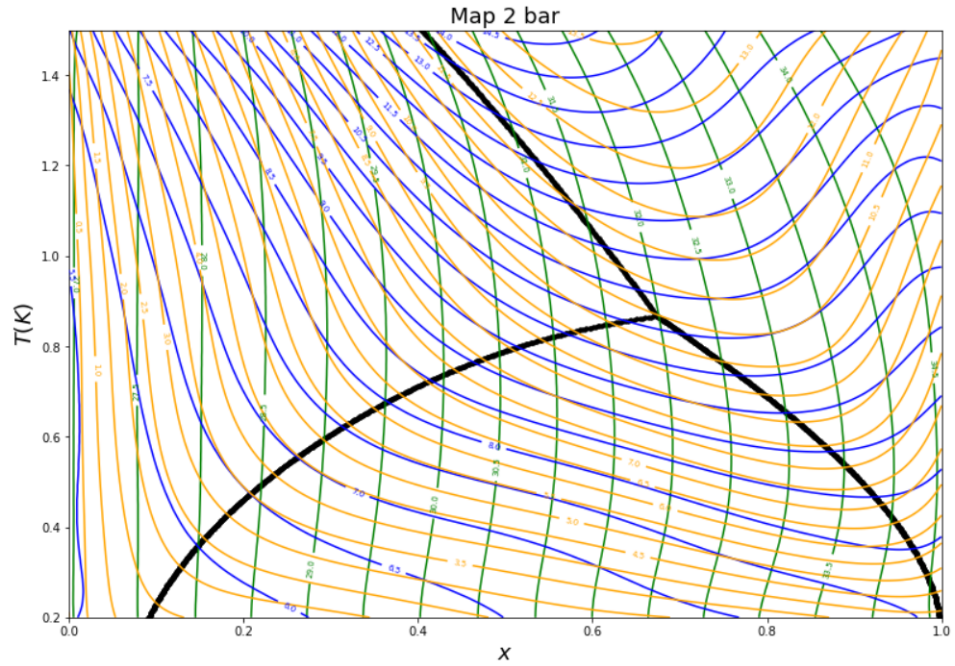

FIGURE 6.33: He3-4 mixture full contour map for P=2 bar. Green lines: Molar volume (cm3/mol), Yellow lines: Enthalpy (J/mol), Blue lines: Entropy (J/molK), Black lines: Phase transitions

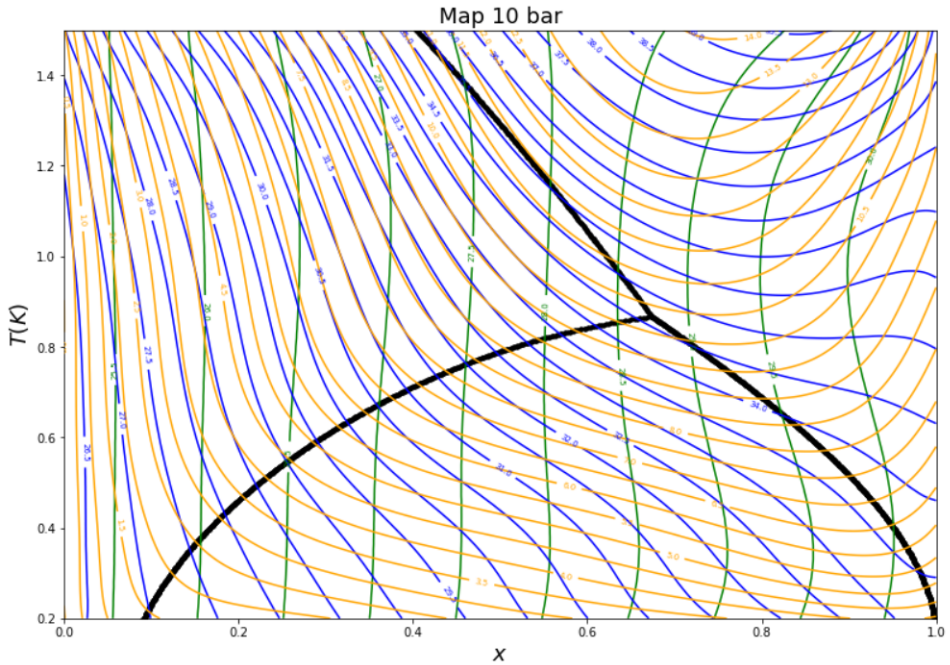

FIGURE 6.34: He3-4 mixture full contour map for P=10 bar. Green lines: Molar volume (cm3/mol), Yellow lines: Enthalpy (J/mol), Blue lines: Entropy (J/molK), Black lines: Phase transitions

6.4 Conclusions on Helium 3-4 Mixture chapter

In this chapter the behavior of the Helium 3-4 mixture is explained and described. First of all, its different regions are described showcasing the different phases that occur due to the different lambda transition temperatures of the two Helium isotopes.

As done in Helium 4, the aim of the study presented in this chapter has been to create a full, continuous and accurate equation of state describing the thermodynamical values of the mixture. Firstly, the thermodynamic data were collected from the different sources and combined to a single data set. Then, using this set of data in accordance with the equations of state for the two pure isotopes of Helium, a numerical model was created in order to describe the thermodynamic values of the system.

In addition to the standard thermodynamic values also the osmotic pressure has been evaluated. The values of the osmotic pressure are of great significance to the applications of the Helium 3-4 mixtures, as most cryogenic applications using it also make use of superleaks. These superleaks lead to a different concentration of Helium-3 in the two occurring mixtures, thus creating the osmotic pressure. As it will be seen in following chapters this pressure has very significant results in the behavior of cryogenic machinery working with Helium 3-4 mixture.

Moreover, when determining the values for the volume, some extra calculations were done to find out the dependence of the volume to the concentration of the mixture. This was done because in many applications it might be problematic to find the consistency of the mixture for the different parts of the machines used, but by showcasing this very low dependence of the volume on the consistency, one can evaluate the consistency inversely by using the volume of the two pure isotopes aggregated and getting a value nearly identical to the actual volume of the system.

For the numerical equations of the system a different difficulty arose than when compared to Helium-4. The existence of Helium-3 in the mixture means that even at very low temperatures the system is not in a total superfluid form and as such its thermodynamic values like the entropy and the enthalpy are significantly higher than the ones of pure Helium-4 and no very large changes in the orders of magnitude arise. The problem in this case is that the equation needs three independent variables instead of two. For this reason, a new fitting model had to be developed where polynomial equations with a big number of terms and high order were used. Utilising these equations, a full description of the Helium 3-4 mixture was achieved providing excellent results to the thermodynamic values as well as their derivatives needed for the correlations.

Using this equation of state full maps of the Helium 3-4 mixture have also been created and provided. A Helium 3-4 thermodynamic map would have to be 4 dimensional to account for the 3 independent variables. To account for that the provided maps are in two forms, one a sequence of 2D contours for different pressure and a 3D contour with the coloring showcasing the 4th value of the system.

Chapter 7

Solid Helium

Helium is the only known substance that remains a liquid even near absolute zero. Despite that, experiments have shown that at higher temperatures it is possible for Helium to form a solid. This offers another unique situation as it leads to an absence of a triple point, meaning that there is no single temperature and pressure point where the gaseous, liquid and solid phases can coexist [76].

As it can be seen from the thermodynamic map 3.42 of Helium-4, Helium forms a solid at really low temperatures at pressures of around 24 atm. Helium when solid forms a crystallic solid with different crystal formations (bcc, ecc, fcc) depending on the temperatures and pressures.

Since the first discoveries of superfluidity scientists have been theorizing about the existence of a possible supersolid. For nearly a century there had been no evidence for such a phase. Since beginning of the 21st century though, there has been a major shift as some experiments [15, 45] have occurred claiming to have achieved supersolidity. The cryogenic community has been greatly polarised on these results with many researchers refusing to accept the existence of supersolidity as a phase in Helium as a result of the 2004 experiment. Many different explanations have been implemented instead of supersolidity to explain the aforementioned results. Despite this, the scientists who initially authored the first paper and did the experiment remain strongly in their position stating that it is evidence of a supersolid phase. Explanations on these models have been given like in [77].

Personally I have also developed my own theory of supersolidity about an explanation of the given results of the 2004 experiments, and presented it as a technical presentation at the 27th - International Cryogenics Engineering Conference at Oxford, UK in 2018, where the reactions were mixed with some of the participants being in favor of the results and others declining the effort as they viewed the original experiment as false.

Unfortunately, the timing was not favorable as only a little while after this presentation was done a new experiment occurred and published in Physical Review [16] where even stronger evidence had been found supporting the existence of supersolidity. In this experiment a comparison was done between solid Helium-4 and Helium-3 and showcased that the difference in their behaviors was greater than the calculated one, meaning that the Helium-4 must have formed a supersolid.

At the present moment the consensus of the scientific community seems to be much more in favor of the existence of supersolidity in Helium-4. The model created to explain the supersolid in Helium-4 as a superfluid of the vacancies in the crystal is shown below. This work takes no part in proving or disproving supersolidity, but only aims to provide the basis of a viable supersolid theory of Helium-4 provided that a supersolid does actually form.

7.1 Supersolid Helium

In this part of the study the is aim to give a simple but adequate description of the mechanism that leads to the formation of a supersolid. The supersolid is a proposed state for helium, theorized since the early days of the studies of superfluidity and cryogenics of Helium. Despite this, supersolidity keeps being an elusive phenomenon that has only very recently observed in an experiment, with some critics even arguing that the results of the experiment might be able to be described by other phenomena, the main argument against this theory being the existence of vacancies at near zero temperatures. This experiment is the one conducted by Eun-Seong Kim and Moses Chan at Pennsylvania State University [45]. The proposed theory so far about the explanation of supersolidity attributes this behavior to the superflow of vacancies within the lattice form by the solid helium. This unobstructed flow leads to a differentiation of the moment of inertia of the solid helium, as the vacuums of the lattice move freely within it. This theory has been generally accepted to be the one to describe the supersolid phenomena, but its studies have not converged to a single mathematical theory known to explain this behavior. The current research points to mostly two different ways to approach this issue, either approaching it strictly macroscopically, or microscopically with extensive codes solving the quantum equations for all the particles. The presented point of view consists of the same theory, i.e. the movement of the vacancies to create a superfluid within the lattice, but the solution of the physical problem operates in a different way. The aim at the beginning of this research was to develop a way to describe the supersolid behavior through superfluidity, as the behavior of superfluid helium is already well defined and understood. The first hindrance faced, was that by following the two-fluid approach for superfluidity, i.e. the Bose-Einstein Condensate existing within the fluid and explaining its behavior, was that the vacancies could not be described with a straightforward wavefunction so as to solve the quantum problem for their Bose-Einstein Condensation. The idea behind this approach is the following. Each helium atom within the lattice can be readily described with a wavefunction. Therefore, the vacancies should be areas without a wavefunction. For a position with a vacancy, I assume that the zero wavefuction is not actually an absence of a wavefunction, but the overlay of the wavefunction of a particle that ought to have this spot, had the vacancy not been there, and another opposite wavefunction of a hypothetical particle, whose total sum is zero. By this train of thought we have those new hypothetical particles with the opposite wavefunction of the Helium ones in every place where there is a vacancy within the lattice. So, we have the information about their wavefunctions, hence being able to find their lambda temperature.

Formation of vacancies in the quantum lattice. The first part of our approach is to be able to describe the structure of the lattice in a quantum level. For that the first part is to be able to find the positioning and distance of the atoms relative to one another's. To achieve this, we use the known potential for the Helium as a Lenard-Jones potential, as provided in the work of Aziz et al [78].

So the potential will be of the form:

$$U(r) = 4\epsilon[(\frac{\sigma}{r})^{12} - (\frac{\sigma}{r})^{6}] \tag{7.1}$$

The above is the potential for one single Helium-4 atom. In this case more than one atoms partake in the system. In the overall lattice the local minima that will be formed will most often than not be the positions for the Helium atoms. As such, if one assumes

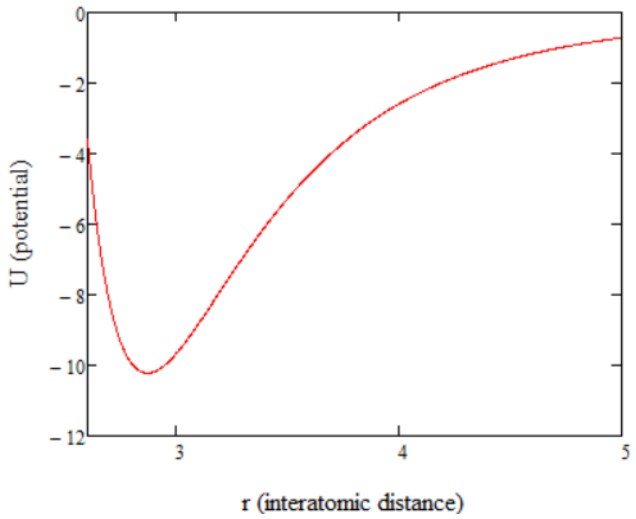

FIGURE 7.1: Lennard Jones Potential for Helium 4

a uniform structure in the solid then the potential that one atom would have to cross in order to move from one local minimum position to a neighboring one would be the same for all directions. As such a new potential needs to be formed that will be able to describe the two local minima locations. This potential will be a modified version of Aziz's Helium-4 potential having the following form:

$$U_{double}(r) = +\epsilon[(\frac{r_m}{r})^{12} - 2(\frac{r_m}{r})^6] + \epsilon[(\frac{r_m}{2r_m + d - r})^{12} - 2(\frac{r_m}{2r_m + d - r})^6] \tag{7.2}$$

where d is the interatomic distance of the structure, calculated by the density of the solid.

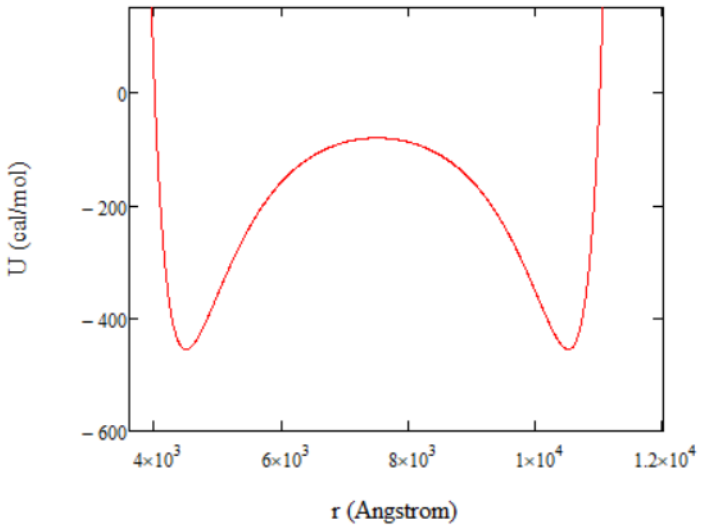

FIGURE 7.2: Double potential for Helium 4

Now having the potential one can proceed to solve the Schrodinger equation for the wavefunction of the system.

$$\frac{d^2}{dx^2}\Psi = (V(x) - E)\frac{2m}{\hbar}\Psi \tag{7.3}$$

Now some points on the potential need to be established as to showcase the possible locations of the particles and as such it is deemed better for the potential to centered around 0.

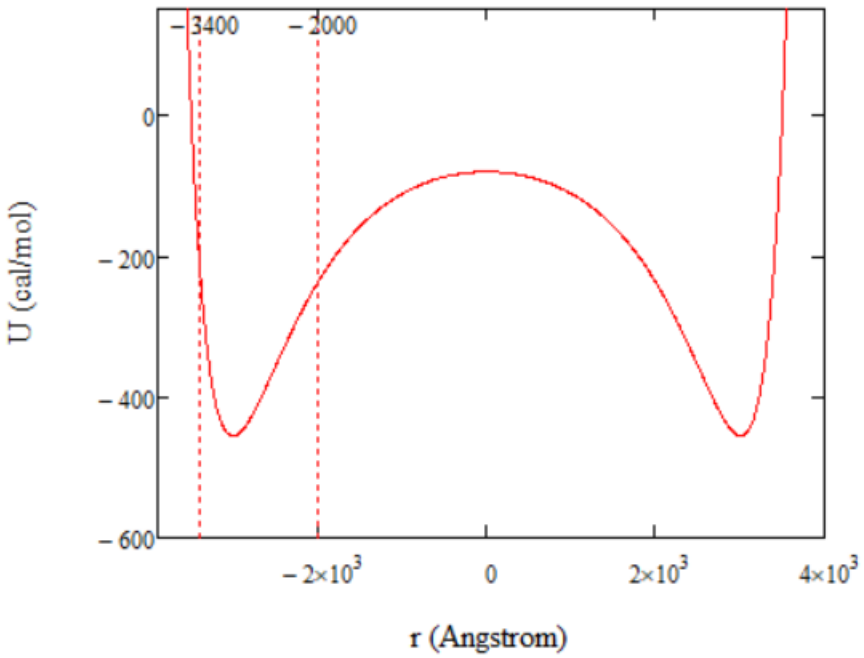

FIGURE 7.3: Centered Double potential for Helium 4

Now solving the Schrodinger equation one gets the following solutions:

$$\begin{aligned}\Psi_1 &= Ae^{i\,\alpha(x)x} + Be^{-i\,\alpha(x)x}\\ \Psi_2 &= Ce^{-\,\alpha(x)x}\\ \Psi_3 &= De^{i\,\alpha(x)x} + Ee^{-i\,\alpha(x)x}\end{aligned} \tag{7.4}$$

where Ψ_1 is the solution between -b and -a, Ψ_2 between -a and a and Ψ_3 between a and b, with a=2000 angstrom and b=3400 angstrom.

α is a function defined as:

$$\alpha = \sqrt{2m\frac{V(x) - E(T)}{\hbar^2}}$$

Now to proceed solving the equation one needs to adjust for the continuity of the wave function based on the following boundary conditions.

$$\Psi_1(-a) = \Psi_2(-a)$$
$$\frac{d}{dx}\Psi(-a) = \frac{d}{dx}\Psi(-a)$$
$$\Psi_2(a) = \Psi_3(a)$$
$$\frac{d}{dx}\Psi_2(a) = \frac{d}{dx}\Psi_3(a)$$
$$\Psi_1(-b) = \Psi_3(b)$$

Through solving this system one can get the wavefunctions of the different positions.

The formation of a supersolid is based on the idea that the vacancies in the matrix move in a certain manner which will be discussed shortly, but first one needs to find the vacancies in the crystal. The vacancies are expected to be formed in two ways, one through thermal excitations, and secondly, because this is a quantum system, also the formations through quantum tunneling need to be addressed, which is why the wavefunctions needed to have been evaluated. The thing that we now need to evaluate as the first part in our approach to supersolidity is the number of vacancies formed inside the lattice. For this part of the research we will assume no imperfections of Helium 3 in the crystallic structure. So, the way that imperfections form inside the crystal is due to the movement of atoms inside the potential of the lattice. As said, we assume that only the neighboring particle have an effect and with all the particles being the same the potential will be repetitive for each position of the crystal. The atoms inside the crystal can move in two different ways, first by thermodynamically acquiring enough energy in order to pass over the potential barrier, or by tunneling through the barrier.

The probability for vacancies to be formed thermally are calculated based on the temperature as given by [79]:

$$f_{thermal}(u,T) = 4\pi(\frac{M}{2\pi RT})^{\frac{3}{2}}u^2 e^{\frac{-Mu^2}{-2RT}} \tag{7.5}$$

And the probability of quantum tunneling occurring will be:

$$f_{tunnel} = \frac{\int_a^b \overline{\Psi_3(x,T)}\Psi_3(x,T)}{\int_a^b \overline{\Psi_1(x,T)}\Psi_1(x,T)} \tag{7.6}$$

The particles form a Maxwell-Boltzmann distribution as they themselves do not condense to a condensate state, so even if the Bose-Einstein distribution was used, it would degenerate to the same results for these energies. So, using the energy of the atoms and the barrier of the potential we calculate the number of atoms with an energy high enough to surpass it. Summing the two parts up, the total probability of vacancy formation is given as:

$$\xi(T) = f_{tunnel}(T) + f_{thermal}(T) \tag{7.7}$$

To have some numerical examples, for a temperature of 0.2K we have a percentage of 0.102.

Movement of the vacancies We want to calculate the properties, and especially the moment of inertia of the quantum crystal when it forms a supersolid. According to

most theories a supersolid forms as the vacancies of the crystal BE condense and move freely through the lattice. We first of all want to find the temperature at which the vacancies BE condense. In order to do so we must act as if the vacancies have a specific wavefunction. That generally is approached by viewing the wavefunctional behavior of the whole lattice and doing very intense calculations using difficult mathematical tools and time-consuming programs, without gaining much insight of the physical aspect of the problem. We will approach this problem in a different, more straightforward manner. We will first assume a crystallic matrix with no vacancies. Each particle of the matrix has each own wavefunction. In order then to create the vacancies we will assume particles with wave functions opposite to the ones of the Helium particle, hence when they are in the same space with the Helium atoms of the matrix then basically there will be a vacuum. These particles will move without any interference with the Helium atoms, but when they are not in a BE condensate phase they will be impaired by the [78] interatomic potential. That is supposed to mean that these particles are subjects of the interatomic forces by the potential, as are the Helium atoms, they have to move for these vacuums to be formed, but the potential itself is not changing by the appearance of these particles, nor do they attract or push any of the atoms of the matrix, they merely the make them nonexistent as long as they are in the same coordinates. So overall, we will have for these particles a potential well with infinite potential barriers at the end of the crystal, and the interatomic potential within the crystal, in an overlayed form, basically doing without the diverging terms. For a random position the wavefunction of the inverse particle would be the opposite of the $\Psi_1 + \Psi_3$ function of the particles above. We make the initial assumption that as the Ψ_3 wavefunction is already 1 order of magnitude smaller than the Ψ_1, in the case of a many particle system like the one pictured in the potential above, the particles that are further away will have a negligible wavefunction. So, the inverse particle will have to have the following wavefunction.

$$\Psi_{vac}(x,T) = -\Psi_1(x,T) - \Psi_3(x,T) \tag{7.8}$$

These particles are obliged to have the opposite properties of the particles of the matrix, being He4 atoms, therefore their spin would have to be also integer, so it can be safely said that they obey Bose-Einstein statistics. The system will Bose-Einstein Condense when an atom gets off the ground state for the first time so the critical temperature will be:

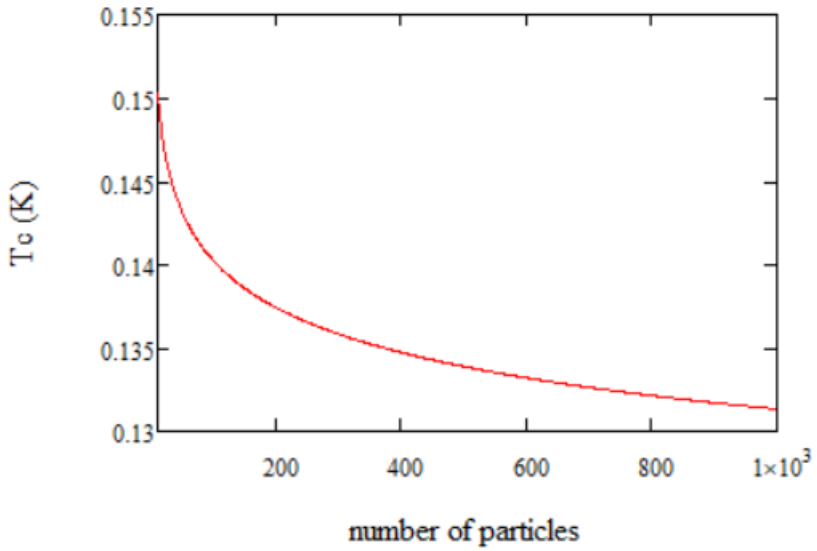

FIGURE 7.4: Relation of the Tc temperature to the number of particles

Having done the calculations above, we can see that for a given pressure the BE condensation temperature seems to be lessening as the number of particles increases, which seems counter intuitive. But we must take into account that with the current approach the number of particles is irrelevant to their interatomic distance, as this is derived earlier in the code and then the code runs with it as a constant. So, with that train of thought the fact that the BE temperature decreases with the number of particles makes sense as for a condensate to form with more particles, then the interatomic potential has a higher energy, which in turns means that the wavefunctions are with greater frequency, and therefore lower wavelength, so they need to be at an even lower energy for the condensate to form. Additionally, the approach must confirm the fact that with a smaller interatomic distance the BE condensation temperature has to be higher. In order to check that we have to run the code again, firstly by putting a lower pressure in the derivation of the interatomic distance, then solve again the S.Eq. for the wavefunction, and finally redo the BE condensation part, while carefully applying the term V(0,d(Nl,P)) as the potential numerically in order for the program to be able to proceed. Doing that we can see that with an increase in pressure there is a decrease in the BE condensation temperature as we would expect.

Comparison with the experimental results of [45]

The theory produced above, as seen, produces some logical results with values close to the ones that one would expect. But in order to be able to check the validity of the theory we want to compare it to the known experimental results. For this, we will use the results of Kim et al. paper [45]. For this part of the study, we will check the general validity of our results to check the deviation from the experiment, and not try to replicate the experimental results at this point, as it is not the point of this paper. Follow up work on this paper will be to fine tune all the inputs and replicate the exact results of Kim's experiment, if it found through this study that this theory is capable even at this early stage to produce results close to the experiment. The first order of business is to find out the percentage of the atoms that are below the critical temperature. The atoms have the same temperature of the hypothetical particles, so using this temperature we find the ξ number of vacancies about to be condensed.

Calculation of the zero point energy for n=1

$$E(n, L, d) = \frac{n^2\pi^2\hbar^2}{2m} - V_{center}(L, d)k \tag{7.9}$$

Also, we need to consider that each vacuum can condense with its neighboring ones. In this experiment a vycor crystal is used in the torsional pendulum to create a higher number of vacuums. A conservative estimate according to the literature should be sufficiently larger than the original number of vacancies. Also, we need to consider that a particle can only condense with a neighboring one, so assuming a BCC structure for this part of the research we find an 0.8 chance of having such a neighbor. For gathering the first results we assume that the superflow of the vacancies in the solid helium is such that we basically don't need to account for it at all in the moment of inertia. This means that replicating the oscillation with and without this difference in the moment of inertia we can find the difference in the periods and compare it to Kim's experimental results.

As such now the moment of inertia for the full Helium compared to the Helium minus the vacancy part are calculated as:

$$T_{full} = 2\pi\sqrt{\frac{I_{He} + I_{vycor}}{G}} \tag{7.10}$$

$$T^* = 2\pi\sqrt{\frac{I_{He} + I_{vycor} - I_{He}x_{vac}}{G}} \tag{7.11}$$

where x_{vac} is the percentage of the vacancies that are into a BEC state. Calculating the difference of the resonant period between the two we can see that their difference is around 1000ns and changing according to the temperature with the big incline being near the critical temperature. The results of these calculations are reassuring, despite being off the exact experimental values, as they are close enough to give us the green light to move forward with this idea to try in the future to exactly replicate this experiment. It seems that this point of view of the subject has a lot of merit, as it offers the ability to study with great detail and to use the existing knowledge of the superfluid helium thus making the study of the superflow easier. In future studies, we will further develop this approach and now that the theory is comprised, focused on the exact replication of the experimental result to see if this theory is confirmed or needs some alterations.

7.2 Conclusions on the Solid/Supersolid Helium chapter

In this chapter a brief dive into the physics of solid Helium has been presented. Solid Helium being probably one of the most exotic solids in existence has caused no small deal of controversy for its behaviors. Recent experiments have suggested that under the right circumstances solid Helium undergoes a phase transition and forms a new phase of matter, called a supersolid. This is not something that it is set in stone in the cryogenic and scientific community in general, but 2018 experiments greatly strengthened this position. In this chapter a model for the explanation of this supersolid behavior has been proposed.

The basic idea of a supersolid is that the vacancies that are formed in the lattice form some kind of superfluid that is able to freely move. To describe this superfluid in

this study the following method has been proposed. One needs to study the vacancies not as empty space but as superposition of a Helium atom and a hypothetical inverse Helium atom having the opposite wavefunction to the atom mentioned, so that the total wavefunction will be zero. By doing this, one is able to study these inverse particles on their own, and by them being mirror particles of Helium atoms and as such bosons, find their condensation temperature. So overall by finding an estimate for the number of vacancies of the system and applying the aforementioned method, results that resemble the ones of the experiments are seen to arise.

Chapter 7 - Nomenclature

U	Potential Energy
r	Distance
ϵ,E	Energy
Ψ	Wavefunction
V(x)	Potential
m	Atomic mass
h	Plank's constant
f,	probability of vacancy formation
T_{full}	Moment of inertia with no vacancies
T^*	Reduced moment of inertia

Chapter 8

Superfluid Stirling Refrigerator 1D

8.1 Introduction to Stirling cryocooling

As mentioned in previous chapters there are many uses that require extremely low temperatures for their applications. For this reason, there are many apparatuses that are used in order to cool down to temperatures approaching even absolute zero. Many cryogenic applications make use of nitrogen, oxygen of hydrogen. The above can be used to reach low temperatures that are used often in medical and material-processing applications but all of the aforementioned elements become solidified at temperatures not near absolute zero, negating then as candidates for closing to absolute zero and working on applications at this temperature range. The only known substance that remains in a non-solid form at temperatures this close to zero is Helium. In the previous chapters we have gone into great detail into explaining the working and behaviors of Helium throughout both its isotopes and their mixture as well as the different phases it exists in.

One of the main machines that is used for cooling Helium is Stirling coolers. Stirling coolers are used at higher temperatures as well working with Helium, but the can also work with liquid Helium and superfluid Helium as well. The effectiveness of Stirling refrigerators close to absolute zero is significant compared to other means of cooling, and in the past two decades some a new variation of Stirling engines has been introduced that can be used to more effectively cool Helium to temperatures down to near even 0.3 K.

8.1.1 The Stirling cycle

The Stirling cycle is one or the most basic cycles in thermodynamics and aims to be an implementation of the Carnot cycle. Stirling engines or coolers are comprised of 5 volumes in them. The expander, the cooler, the regenerator the heater and the compressor. The usual mechanical synthesis of a Stirling machine comprises of 2 opposed pistons connected to a crankshaft with the regenerator connecting the top of them. A simple view of the Stirling engine can be seen through the graph below.

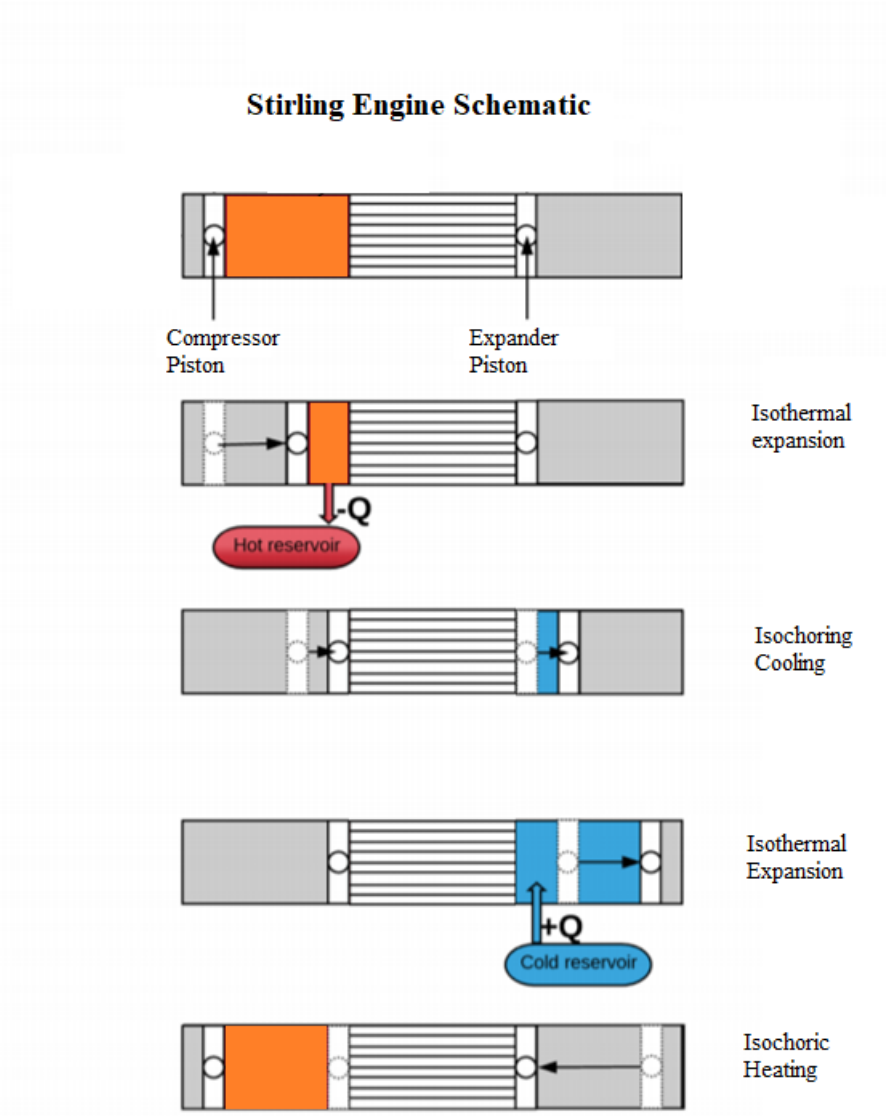

FIGURE 8.1: Schematic of basic Stirling refrigerator

The basic steps of the Stirling cooling cycle are the following.

- Isothermal compression: The compressor piston moves towards the regenerator while the expander piston remains close to the regenerator. The excess heat of the fluid is dumped into the hot reservoir.
- Isochoric Cooling: Both pistons move towards the right (in the view of the figure 8.1) and the fluid is being cooled leaving its heat in the regenerator.
- Isothermal expansion: The compressor piston remains close to the regenerator while the expander piston moves away from it. Heat is being drawn from the cold reservoir into the fluid.
- Isochoric Heating. Both pistons move towards the left with the fluid regaining the heat previously left in the regenerator.

.

8.1.2 The Superfluid Stirling Refrigerator

The standard Stirling engine is capable of cooling Helium down to its liquefaction point and even beyond that working with liquid Helium. Below the lambda temperature a standard Stirling refrigerator begins to quickly fail as a cooling apparatus. This is because below this temperature a superfluid begins to form, which due to its lack of viscosity, cannot be contained through the piston seals and escapes the cylinders.

The nature of the superfluid initially seems to hinder the potential of the Stirling apparatus as a cryocooler, but with some key modifications it can be show that the formation of the superfluid can be deemed as beneficial for the overall cycle. The initial models were presented by Brisson et al [80] and then implemented further in [81, 82, 83]. In this new formation of the Stirling cryocooler the idea is that a superleak [41] is included in each of the pistons. The working medium in such a machine is a Helium 3-4 mixture usually enriched in Helium-3. As the mixture exists in lower temperatures the superfluid Helium-4 part flows freely through the superleak while the normal fluid Helium is confined into the normal working volumes of the Stirling engines. This kind of cryocoolers initiate from temperatures below the lambda line and lead down to temperature in the range of 0.3 K. One key point that needs to be mentioned in this type of refrigerators is the importance of the Helium-3 part especially at lower temperatures. Because Helium-4 is in its superfluid form and is progressively more thermodynamically inert as it approaches absolute zero the bulk of the thermodynamic work is applied by the Helium-3 part. This is the reason why these apparatuses work with enriched Helium 3-4 mixtures. At temperatures above 1 K not all Helium-4 has become a superfluid and such as the interacting parts of it cannot freely pass through the superleak. This phenomenon while subtle is important to incorporate in the modelling of the systems. Most models that so far exist in the literature actually forgo the interactions of the Helium-4 part altogether but this is problematic especially when being above 1.2-1.3 K and nearing the lambda line. Lastly, the phenomenon of the osmotic pressure needs to be included in such a model, in addition to the difference in the composition of the mixture before and after the superleak lead to the formation of the osmotic pressure difference between them.

8.2 Single ideal gas isothermal Stirling cryocooler

The kind of cryocoolers can be simulated ranging from simpler models to much more elaborate ones. For starting of the study the simplest of the possible models is presented, describing a Single ideal gas isothermal Stirling cryocooler. This model includes assumptions that will be then re-evaluated on later models based on their behavior on this one. This work is part of the paper [43] of the author of this work.

Firstly, one needs to set the temperature range, that being from 0.4 to 1K. This temperature range is selected as to stay clear of the phonon-roton interaction temperature range for Helium-4. This will be something followed throughout the study of these cryocoolers.

In this case, the Helium-4 is considered to be completely thermodynamically inert and neglected as a part of the working medium and also that Helium-3 behaves like an ideal gas. Both of these assumptions are not too accurate representations but are able to provide results that help understand to a reasonable degree the behavior of the system. These exact assumptions have been also made by Patel and Brisson in their works.

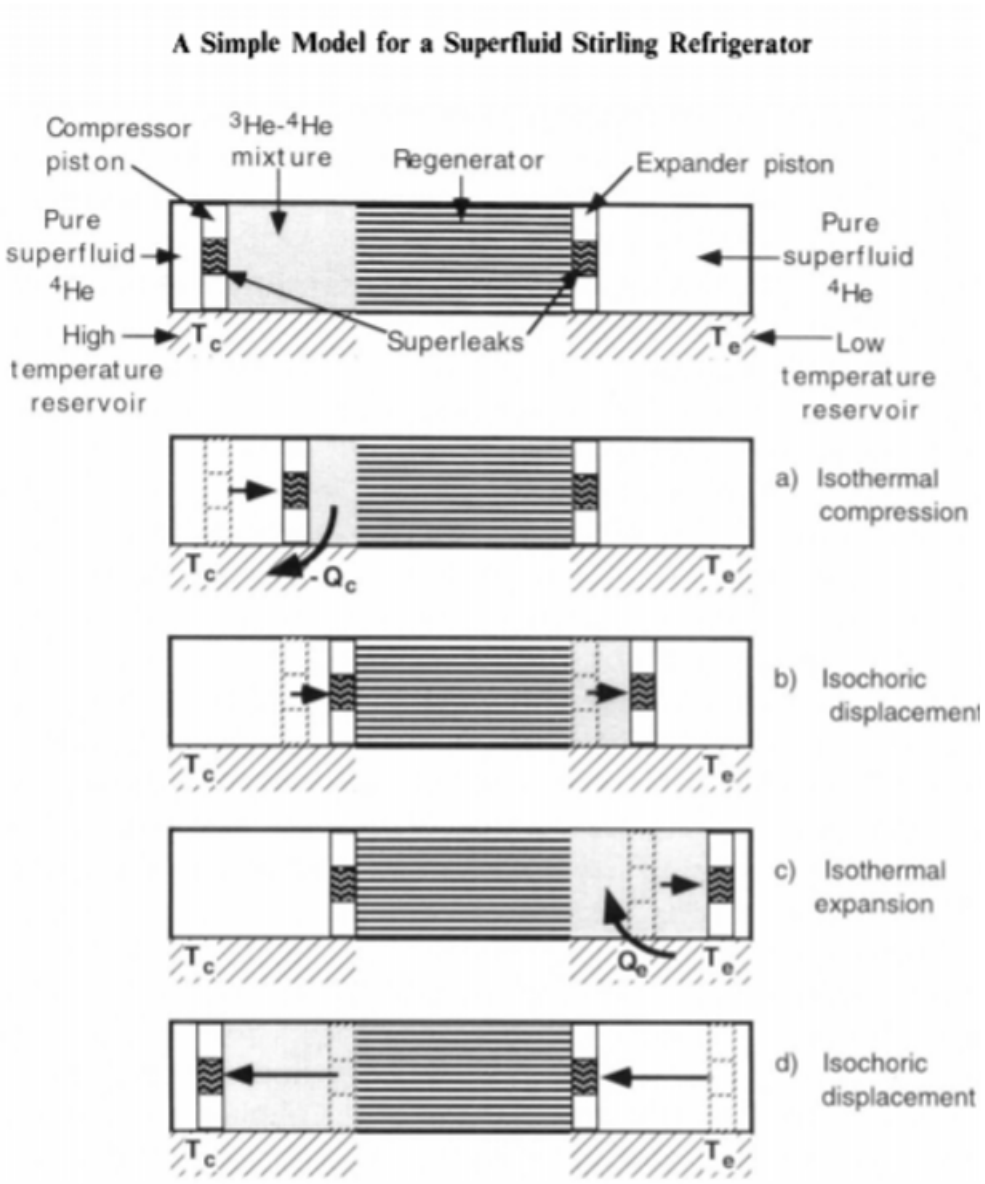

FIGURE 8.2: A simple schematic of a Superfluid Stirling refrigerator form Brisson's et al work in [81]

The sizing of the cooler is based on the following geometry:

V_{clc}	11.537 cm^3	compressor clearance
V_{cle}	8.061 cm^3	expander clearance
V_{swc}	18.744 cm^3	swept volume cooler
V_{swe}	35.48 cm^3	swept volume expander
V_k	35.48 cm^3	cooler
V_r	12.118 cm^3	regenerator
V_h	5.36 cm^3	heater

TABLE 8.1: Geometry of 1D single Stirling, the naming definitions are based on the standardized definitions of Urieli [84]

The equations of the different volumes are calculated as:

$$V_c(\theta) = V_{clc} + \frac{1}{2}V_{swc}(1 + cos(\theta)) \tag{8.1}$$

$$V_e(\theta) = V_{cle} + \frac{1}{2}V_{swc}(1 + cos(\theta + \frac{\pi}{2})) \tag{8.2}$$

$$V(\theta) = V_c(\theta) + V_e(\theta) + V_k + V_r + V_h \tag{8.3}$$

According to the ideal gas law the pressure can be calculated and normalised as:

$$\frac{P}{NR}(\theta) = (\frac{V_c(\theta)}{T_k} + \frac{V_r}{T_r} + \frac{V_e(\theta}{T_h}) \tag{8.4}$$

In the isothermal Stirling model the work being put into the system is equal to the cooling power of the cooler:

$$W_c(\theta) = \int_0^{2\pi} \frac{P}{NR}(\theta)\frac{d}{d\theta}V_c(\theta)d\theta \tag{8.5}$$

One of the most important parts of modelling Stirling coolers is the modelling of the regenerator. At this part of the study the simplest model is to be assumed where the regenerator is a single cell with a steady temperature being calculated as:

$$T_r = \frac{T_k - T_h}{ln(\frac{T_k}{T_h})} \tag{8.6}$$

To check these equations for an initial validity a run is being done and compared to [81, 82] with a temperature range of 1 to 3 K. (This temperature range is used only for comparison reasons and is overall deemed invalid for this work due to running through different phases of Helium without properly adjusting the model. In this particular case due to the Helium-4 being neglected and Helium-3 being thought of as an ideal gas these limitations could be neglected in the work of Patel and Brisson).

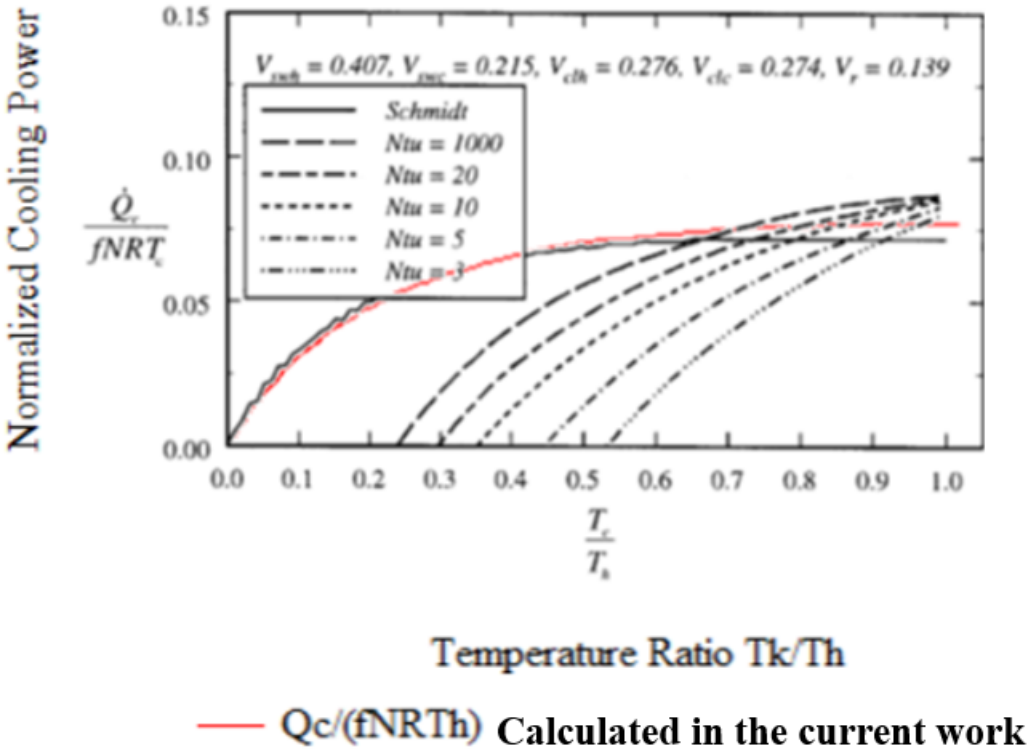

FIGURE 8.3: Comparizon of Normalised Cooling Power to Temperature Ratio results of this studies calculation and [82]

As it can be expected the gained behavior is identical to the work of Patel.

8.3 Single ideal gas adiabatic Stirling refrigerator

Given the description of the isothermal model now one needs to evaluate whether the assumption of a isothermal model is possible. To do that a more detailed description is underdone, using an adiabatic model for the cooler based on the works of Rogdakis et al [85, 86].

The geometry of the machine remains the same as described in Table8.1 with a frequency of f=1.6Hz

Given that so far no pressure losses are assumed the pressure will be the same for all the volumes of the machine at each angle of the crankshaft.

$$P(\theta) = \frac{M\ R}{\frac{V_c(\theta)}{T_k} + \frac{V_k}{T_k} + \frac{V_r}{T_r} + \frac{V_h}{T_h} + \frac{V_e(\theta)}{T_h}} \tag{8.7}$$

Based on the ROBOAN code developed in [87] by Rogdakis, Antonakos and Borbilas the behavior of the cycle is being determined. Through this analysis one can determine how the temperatures of the expander and the compressor are affected when their behavior is changed from being isothermal to being adiabatic.

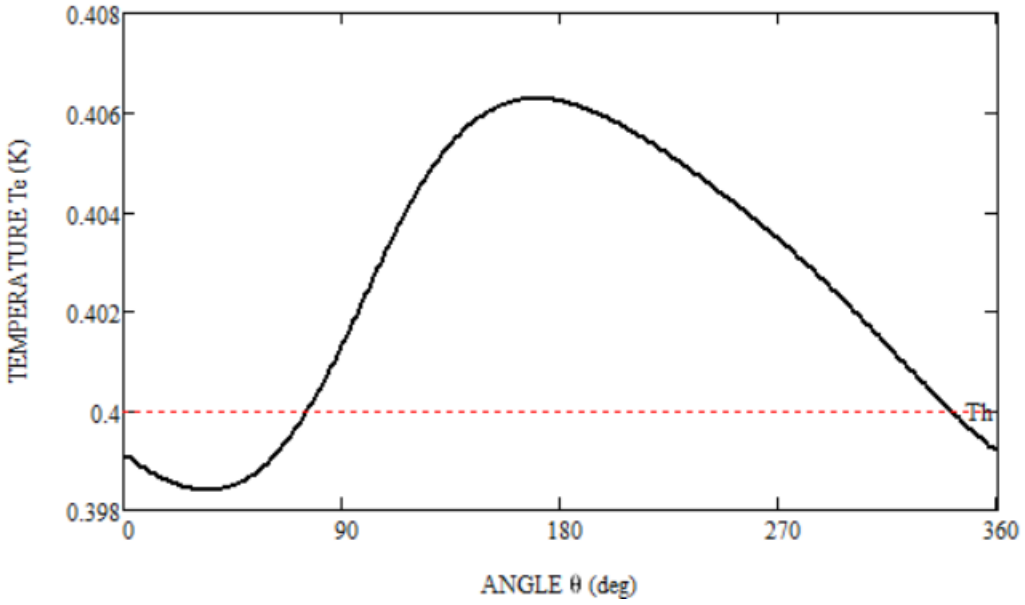

FIGURE 8.4: Hot piston temperature fluctuations

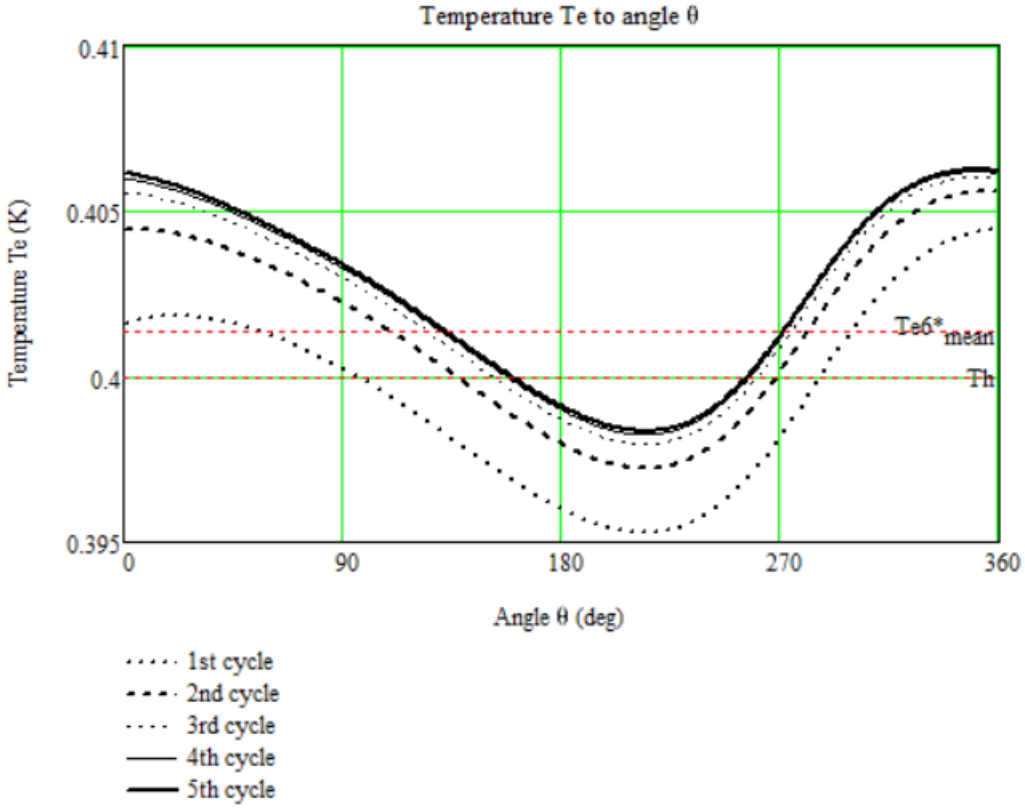

FIGURE 8.5: Hot piston temperature fluctuations evolution over 6 cycles

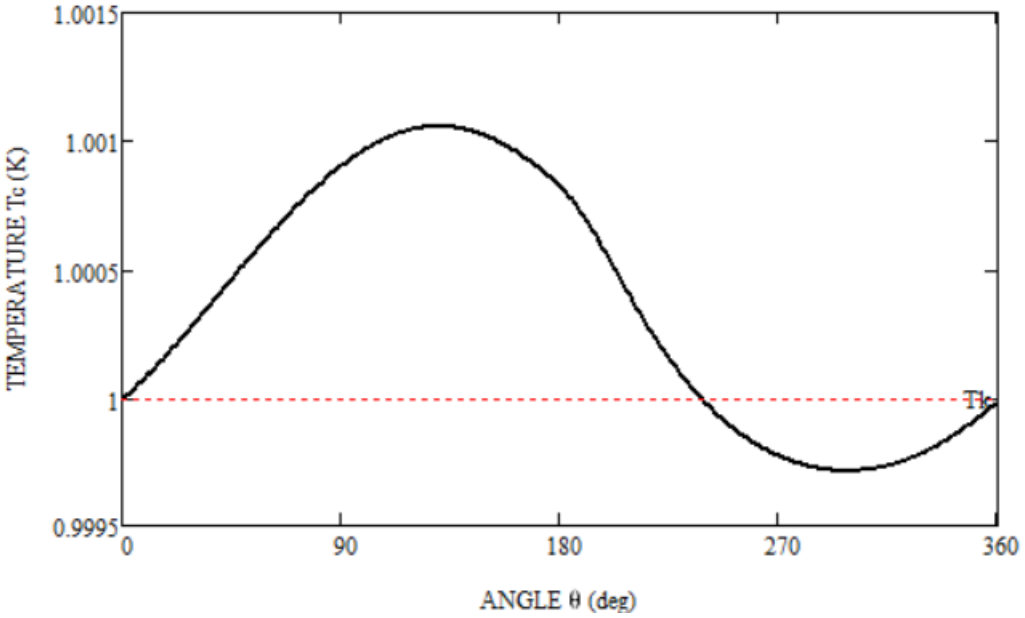

FIGURE 8.6: Cold piston temperature fluctuations

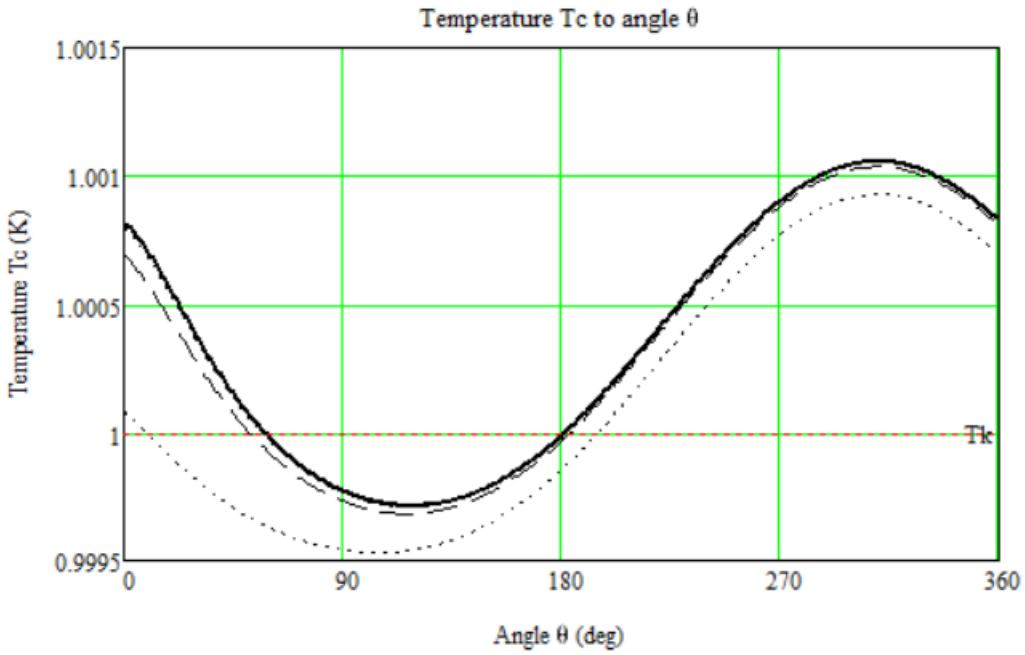

FIGURE 8.7: Cold piston temperature fluctuations evolution over 6 cycles

From the graphs above one can see that there are fluctuations of the temperatures of the pistons compared to their steady temperatures from the isothermal model. But if one is to investigate more closely the values, they would see that these fluctuations are extremely small, something that can be even more easily seen in the graph below plotting the high and low temperatures comparatively.

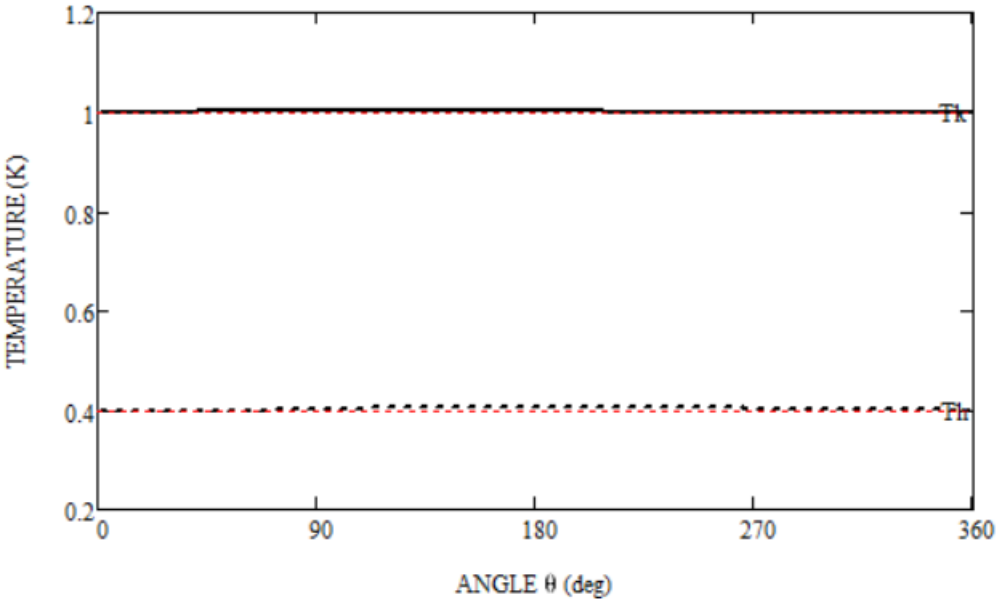

FIGURE 8.8: Piston temperature fluctuations plotted for both hot and cold piston

Overall, it can be seen from the above plots that the variation of the temperatures of the pistons compared to the temperatures of the isothermal model is minimal when compared to the variation of temperatures during the cycle. The fluctuations are of the order of 0.15%. Because of this negligible difference the cooling outcomes of both the isothermal and adiabatic models is the almost exactly the same. This behavior is believed to be based on two facts. One, the cycle has a relatively low frequency meaning that there is enough time for the pistons to reach thermal equilibrium with their environment and behave more like the isothermal model. Through some tests run in the same code it was seen that even if one was to drastically raise the frequency this behavior remains unchanged to a very significant degree. This behavior is attributed to the fact that at such low temperatures with a small temperature differentiation between the Th and the Tk the deviations of the temperature and the pressure are not enough to cause a substantial difference in the temperatures of the compressor and the expander. This fact can be easily understood if one runs the same model for the same geometry and frequency at higher temperatures. If Th=300K and Tk=1000K then with everything else remaining the same the fluctuations caused are of the order or 16%, or two orders of magnitudes larges than before.

For these reasons one concludes that the results of the isothermal and adiabatic model do not differ at such low temperatures and as such following this the isothermal model is to be used.

8.4 Dual Ideal gas Stirling refrigerator

One of the key points of Stirling coolers is the regenerator as it is responsible of doing most of the heat transfer on the working medium during the cycle. Usually when developing Stirling engine, a great deal of care is given into designing the best possible regenerator.

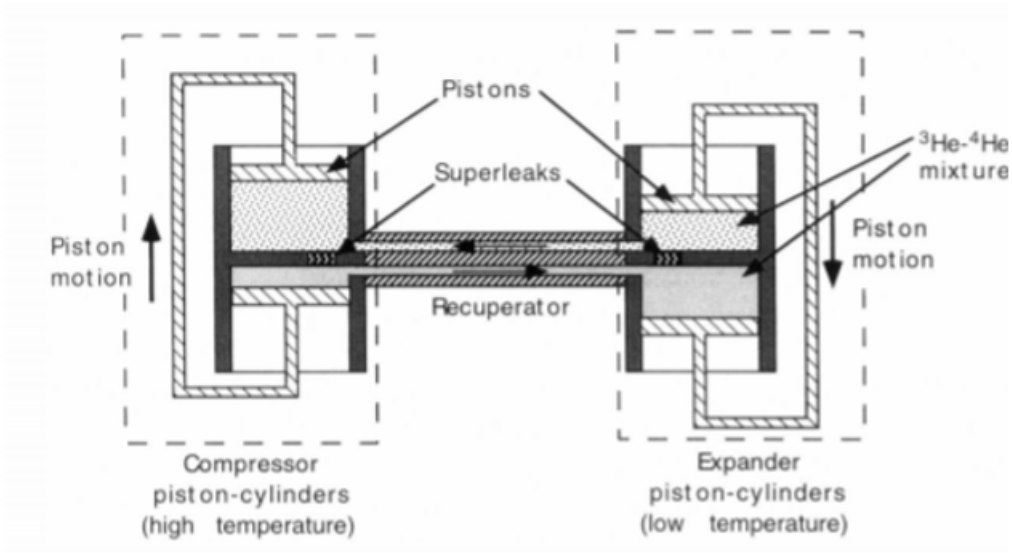

FIGURE 8.9: Dual Stirling schematic given by Brisson's work at [80]

In our case, the temperatures as such that the regenerative properties of most materials are not known to any significant degree. For this reason, a workaround is used to the use of a regenerator. What is available for these temperatures are the heat transfer properties for some materials. For this reason, to utilize this fact and overcome the lack of knowledge for the regenerative properties the designed machine consists of two conjoined Stirling coolers fused to have a common regenerator. This is not a regenerator anymore but only a heat exchanger. The two Stirling machines operate with a phase difference such that counter flow occurs during the cycle in the system and the two currents exchange their heats with each other negating the need for a regenerator. This heat exchanger will be from this point onward refer to as the recuperator.

The flows in the recuperator as one can understand are of the utmost significance for the good working of this apparatus and special care needs to be given when the phase difference between the two coolers is chosen. One can understand that three kinds of flow are possible in the recuperator.

- **Counterflow**: where the two sides of the recuperator from the two Stirling machines have opposite flows. This is the optimal working condition as one flow goes from the cold side towards the hot and the other from the hot to the cold, thus exchanging heats during their paths.

- **Neutral Parallel Flow**: This is the case where both currents flow from the cold side to the hot. In this scenario the two currents do not exchange significant amounts of heat with each other and they are eventually dumped with the cold box temperature in the hot side. This is easily addressed by introducing heat from the hot box, and given the ease of heating at these temperatures this occurrence while not ideal for producing cooling is of no negative importance to the overall workings of the apparatus.

- **Destructive Parallel Flow**: This is the scenario where both currents run from the hot side to the cold side and therefore deposit heat in the cold box. This is

catastrophic for the cycle as the heat dumped in the cold box for even a few degrees with this flow is able to completely cancel out and even reverse all the cooling power of the cycle, as the heat is deposited to the cold box. For this reason measures need to be taken to make sure that this kind of flow does not occur at all in the cycle.

It is clear through the description of this system that the two sides exchange heat with one another in order to complete the Stirling cycle. The amounts of heat exchanged, assuming for this point of the study the recuperator to be an ideal heat exchanger, must be equal. The mass flows that occur will be different at each side and thus one side will amount to the greater mass flow and lesser temperature difference, and the opposite (high temperature difference and lower mass flow) will occur on the opposite side. The side with the greatest of the two mass flows is not and cannot be determined from the previous conditions of the system, thus the code developed address has to address this issue. To surmount this problem, at every time step, a greater flow is assumed at one of the two sides and then the unknown exit temperature is found. If the temperature found is beyond of the temperature range of the isothermal model, then the initial assumption is wrong and therefore the opposite is used. Having the temperatures and mass flows the rest of the thermodynamic data of the cycle are determined. As far as the phase difference is concerned in their works Patel and Brisson assumed a 180 deg phase difference. This is going to be the initiating point of this study, and later this phase difference is to be optimised.

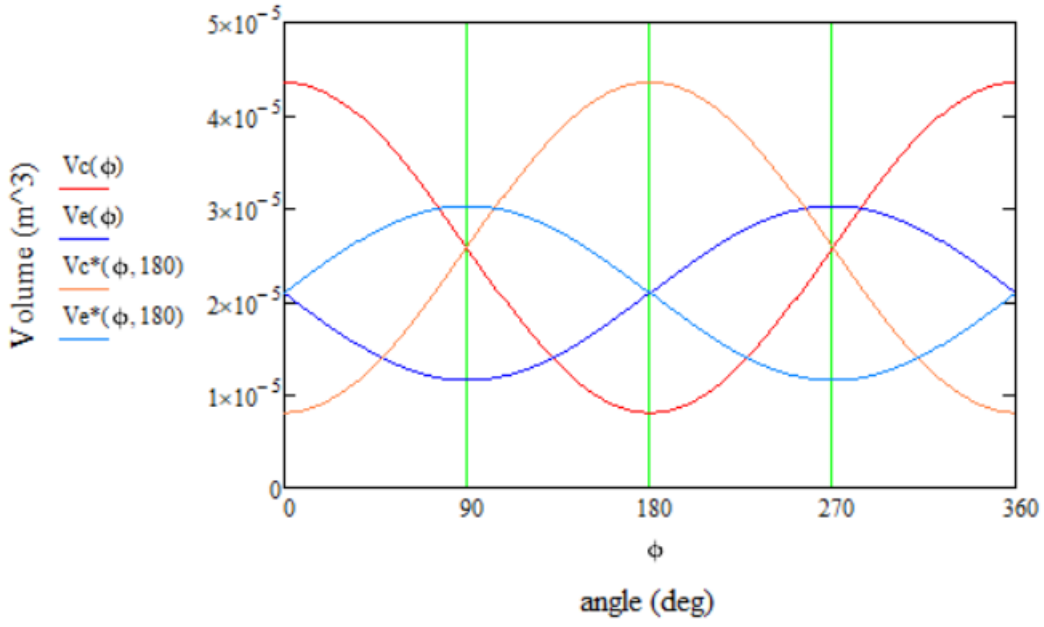

FIGURE 8.10: Volumes of the two coolers during the cycle for an 180 deg phase difference

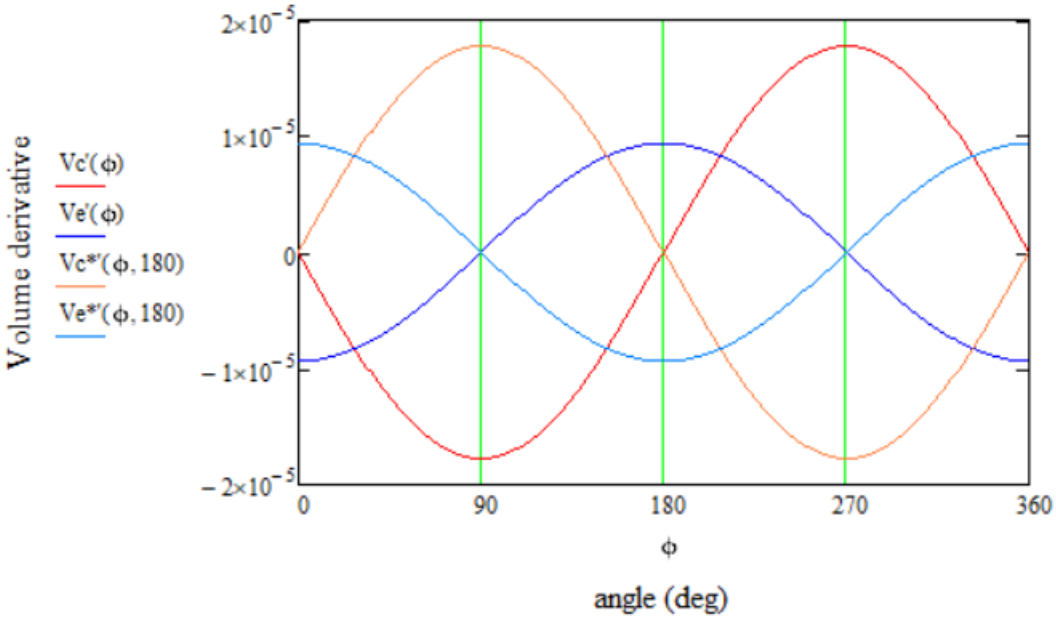

FIGURE 8.11: Derivatives of the volumes over the angle of the two coolers during the cycle for an 180 deg phase difference

Initiating the code from some known conditions for each point the pressure ration between it and the next needs to be found and it is determined as:

$$r_p(\theta, Tr_p, Tr_n) = \frac{\frac{V_c(\theta)}{T_k} + \frac{V_k}{T_k} + \frac{V_r}{Tr_p} + \frac{V_h}{T_h} + \frac{V_e(\theta)}{Th}}{\frac{V_c(\theta+1)}{T_k} + \frac{V_k}{T_k} + \frac{V_r}{Tr_n} + \frac{V_h}{T_h} + \frac{V_e(\theta+1)}{Th}} \tag{8.8}$$

and the pressure difference normalised to the pressure can be written as:

$$\frac{dP}{P}(\theta, Tr_p, Tr_n) = r_p(\theta, Tr_p, Tr_n) - 1 \tag{8.9}$$

Now the masses for the different volumes as well as the mass transfers need to be calculated:

For the compressor:

$$m_c(\theta, Tr_p, Tr_n) = \frac{\frac{V_c(\theta)}{T_k}}{\sum \frac{V_i}{T_i}(\theta, Tr_n)} \tag{8.10}$$

$$Dm_c(\theta, Tr_p, Tr_n) = m_c(\theta, Tr_p, Tr_n)(\frac{dP}{P}(\theta, Tr_p, Tr_n) + \frac{dV_c(\theta)}{V_c(\theta)}) \tag{8.11}$$

For the cooler:

$$m_k(\theta, Tr_p, Tr_n) = \frac{\frac{V_k}{T_k}}{\sum \frac{V_i}{T_i}(\theta, Tr_n)} \tag{8.12}$$

$$Dm_k(\theta, Tr_p, Tr_n) = m_k(\theta, Tr_p, Tr_n)(\frac{dP}{P}(\theta, Tr_p, Tr_n)) \tag{8.13}$$

For the heater:

$$m_h(\theta, Tr_p, Tr_n) = \frac{\frac{V_h}{T_h}}{\sum \frac{V_i}{T_i}(\theta, Tr_n)} \tag{8.14}$$

$$Dm_h(\theta, Tr_p, Tr_n) = m_h(\theta, Tr_p, Tr_n)(\frac{dP}{P}(\theta, Tr_p, Tr_n)) \tag{8.15}$$

For the expander:

$$m_e(\theta, Tr_p, Tr_n) = \frac{\frac{V_e(\theta)}{T_h}}{\sum \frac{V_i}{T_i}(\theta, Tr_n)} \tag{8.16}$$

$$Dm_e(\theta, Tr_p, Tr_n) = m_c(\theta, Tr_p, Tr_n)(\frac{dP}{P}(\theta, Tr_p, Tr_n) + \frac{dV_e(\theta)}{V_e(\theta)}) \tag{8.17}$$

By using the above the mass remaining on the normalised recuperator can be found:

$$m_r(\theta, Tr_p, Tr_n) = 1 - m_c(\theta, Tr_p, Tr_n) - m_k(\theta, Tr_p, Tr_n) - m_h(\theta, Tr_p, Tr_n) - m_e(\theta, Tr_p, Tr_n) \tag{8.18}$$

So overall the mass flows can be determined as:

$$gA_{ck}(\theta, Tr_p, Tr_n) = -Dm_c(\theta, Tr_p, Tr_n) \tag{8.19}$$

$$gA_{kr}(\theta, Tr_p, Tr_n) = -(Dm_c(\theta, Tr_p, Tr_n) + Dm_k(\theta, Tr_p, Tr_n)) \tag{8.20}$$

$$gA_{he}(\theta, Tr_p, Tr_n) = Dm_e(\theta, Tr_p, Tr_n) \tag{8.21}$$

$$gA_{rh}(\theta, Tr_p, Tr_n) = Dm_h(\theta, Tr_p, Tr_n) + Dm_e(\theta, Tr_p, Tr_n) \tag{8.22}$$

All the functions defined above are for the one of the two Stirling coolers, a similar set for the second cooler using its different volumes is defined.

Now that the functions have been defined the solution of the system can initiate:

For $\theta = 1$: $Tr_p = \frac{T_k - T_c}{ln(\frac{T_k}{T_c})}$

For $\theta = 2$:

Suppose that $m < m^*$. The exit temperature is found solving on the energy conservation in the recuperator when the flow is from the hot to the cold on cooler 1 and from the cold to the hot side on cooler 2. Cooler 1 functions are the regularly defined ones and cooler 2 are the ones with the * notation:

$$gA_{kr}(\theta, Tr_p, \frac{T_k - T_h}{ln(\frac{T_k}{T_h})}) + gA_{hr}(\theta, Tr_p, \frac{T_k - T_h}{ln(\frac{T_k}{T_h})}) + m_r(\theta, Tr_p, \frac{T_k - T_h}{ln(\frac{T_k}{T_h})}))(T_k - T_h) =$$
$$= \epsilon(T_{kout^*} - T_h)(gA_{kr^*}(\theta, Tr_p, \frac{T_{kout^*} - T_c}{ln(\frac{T_{kout^*}}{T_h})}) + gA_{hr^*}(\theta, Tr_p, \frac{T_{kout^*} - T_h}{ln(\frac{T_{kout^*}}{T_h})}) + m_{r^*}(\theta, Tr_p, \frac{T_{kout^*} - T_h}{ln(\frac{T_{kout^*}}{T_h})})) \tag{8.23}$$

The exit temperature is calculated and if it is higher than the high temperature for the cycle then the initial assumption was not valid and therefore the opposite assumption has to hold true. In this case the system that needs to be solved is the foollowing:

$$gA_{kr}(\theta, Tr_p, \frac{T_k - T_{hout}}{ln(\frac{T_k}{T_{hout}})}) + gA_{hr}(\theta, Tr_p, \frac{T_k - T_{hout}}{ln(\frac{T_k}{T_{hout}})}) + m_r(\theta, Tr_p, \frac{T_k - T_{hout}}{ln(\frac{T_k}{T_{hout}})}))(T_k - T_{hout})\epsilon =$$
$$= (T_k - T_h)(gA_{kr^*}(\theta, Tr_p, \frac{T_k - T_h}{ln(\frac{T_k}{T_h})}) + gA_{hr^*}(\theta, Tr_p, \frac{T_k - T_h}{ln(\frac{T_k}{T_h})}) + m_{r^*}(\theta, Tr_p, \frac{T_k - T_h}{ln(\frac{T_k}{T_h})})) \tag{8.24}$$

Now the two systems for the flows of the opposite direction need to be addressed, where the flow is from the cold to the hot side in cooler 1 and from the hot to the cold side in cooler 2.

Assuming $m < m*$:

$$gA_{kr}(\theta, Tr_p, \frac{T_k - T_h}{ln(\frac{T_k}{T_h})}) + gA_{hr}(\theta, Tr_p, \frac{T_k - T_h}{ln(\frac{T_k}{T_h})}) + m_r(\theta, Tr_p, \frac{T_k - T_h}{ln(\frac{T_k}{T_h})}))(T_k - T_h) =$$
$$= \epsilon(T_k - T_{hout^*})(gA_{kr^*}(\theta, Tr_p, \frac{T_k - T_{hout^*}}{ln(\frac{T_k}{T_{hout^*}})}) + gA_{hr^*}(\theta, Tr_p, \frac{T_k - T_{hout^*}}{ln(\frac{T_k}{T_{hout^*}})}) + m_{r^*}(\theta, Tr_p, \frac{T_k - T_{hout^*}}{ln(\frac{T_k}{T_{hout^*}})})) \tag{8.25}$$

and if the assumption is seen to be incorrect then the system solved will be:

$$gA_{kr}(\theta, Tr_p, \frac{T_{kout} - T_h}{ln(\frac{T_{kout}}{T_h})}) + gA_{hr}(\theta, Tr_p, \frac{T_{kout} - T_h}{ln(\frac{T_{kout}}{T_h})}) + m_r(\theta, Tr_p, \frac{T_{kout} - T_h}{ln(\frac{T_{kout}}{T_h})}))(T_{kout} - T_h)\epsilon =$$
$$= (T_k - T_h)(gA_{kr^*}(\theta, Tr_p, \frac{T_k - T_h}{ln(\frac{T_k}{T_h})}) + gA_{hr^*}(\theta, Tr_p, \frac{T_k - T_h}{ln(\frac{T_k}{T_h})}) + m_{r^*}(\theta, Tr_p, \frac{T_k - T_h}{ln(\frac{T_k}{T_h})})) \tag{8.26}$$

The energy conservation equations are solved at each step as to gain the temperatures of the system and then be able to calculate the pressure and the rest of the thermodynamic data. The X argument in the functions for the second cooler is implemented in the code signifying the phase difference so in later points, the optimal phase difference can be found. The code that has been used to solve this apparatus is presented in Appendix D.1

Using this code, the resulting exit temperatures for the two machines in an 180 deg phase difference can be seen in the graph below:

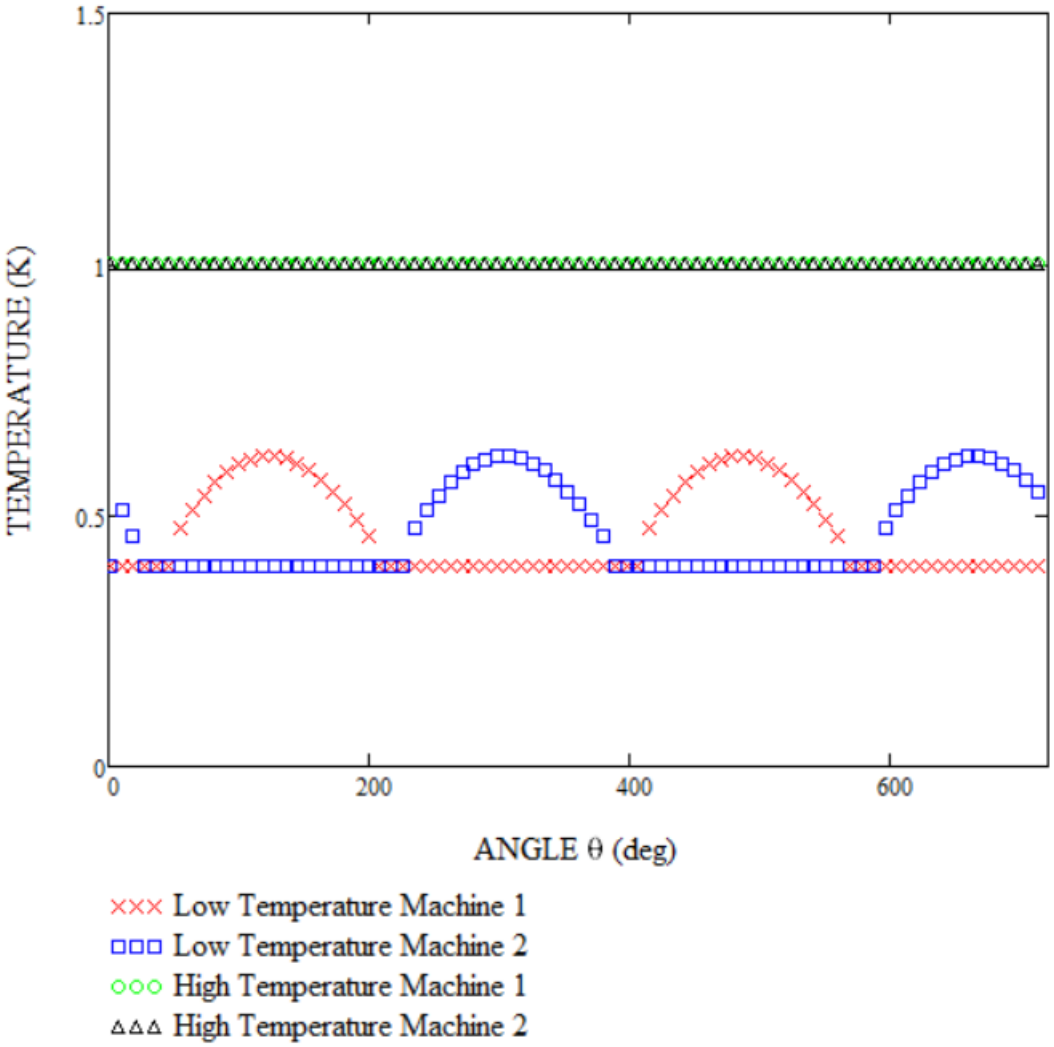

FIGURE 8.12: Exit temperatures of the recuperator

In the graph one can see that the exit temperatures fluctuate in the expected way, meaning that the exit temperature of the cold side is always higher than the Th, except for the two times in each cycle (seen between the valleys in the graphs above) where the first type of parallel flow occurs and the temperatures are set to Th and Tk.

Given these temperatures one can calculate the temperature of the recuperator.

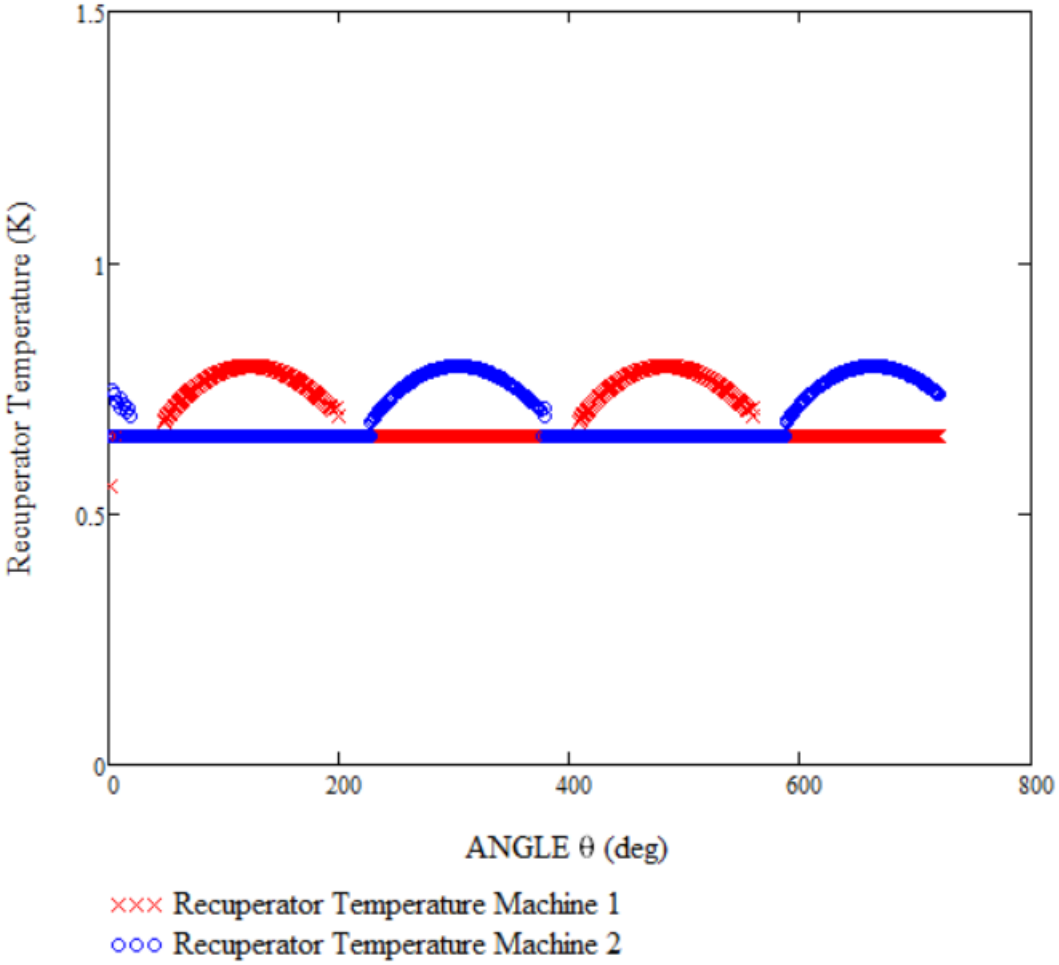

FIGURE 8.13: Temperature of the recuperator

The results of the code are understandable and expected but to further check the validity one can check the mass flows throughout the cycle and verify that the overall mass is preserved. In the graph below it can be seen that this is the case and the mass is preserved at every point of the cycle.

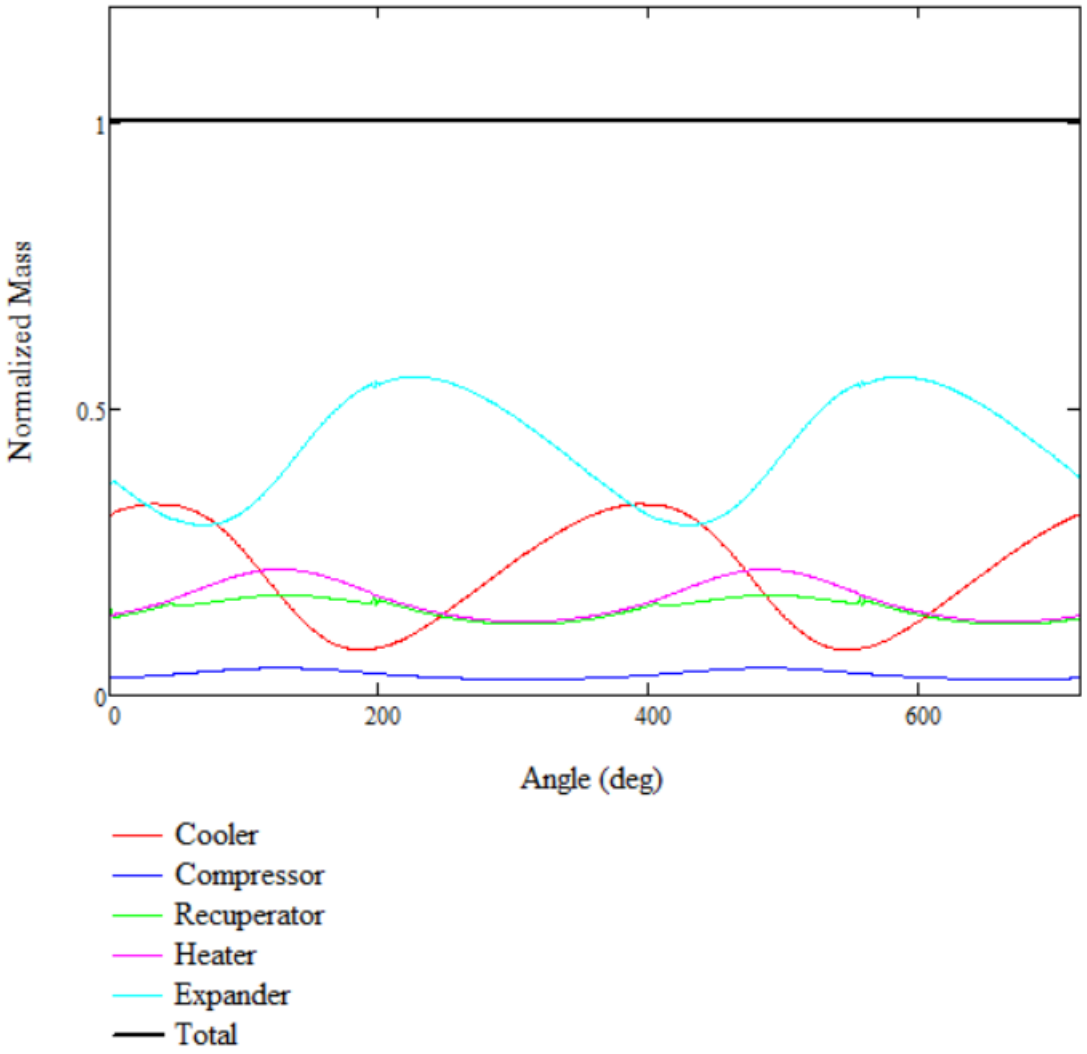

FIGURE 8.14: Normalized masses during the cycle

The pressure at each point of the cycle can be found as:

$$\frac{P}{M} = \frac{R}{\sum \frac{V_i}{T_i}(\theta, Tr)} \tag{8.27}$$

and the mean pressure would be:

$$\frac{P}{M} = \frac{\sum_{\theta=2}^{360} \frac{P}{M} M}{360} \tag{8.28}$$

To observe the behavior of the system better on can look into the mass flow rate graph for the recuperator.

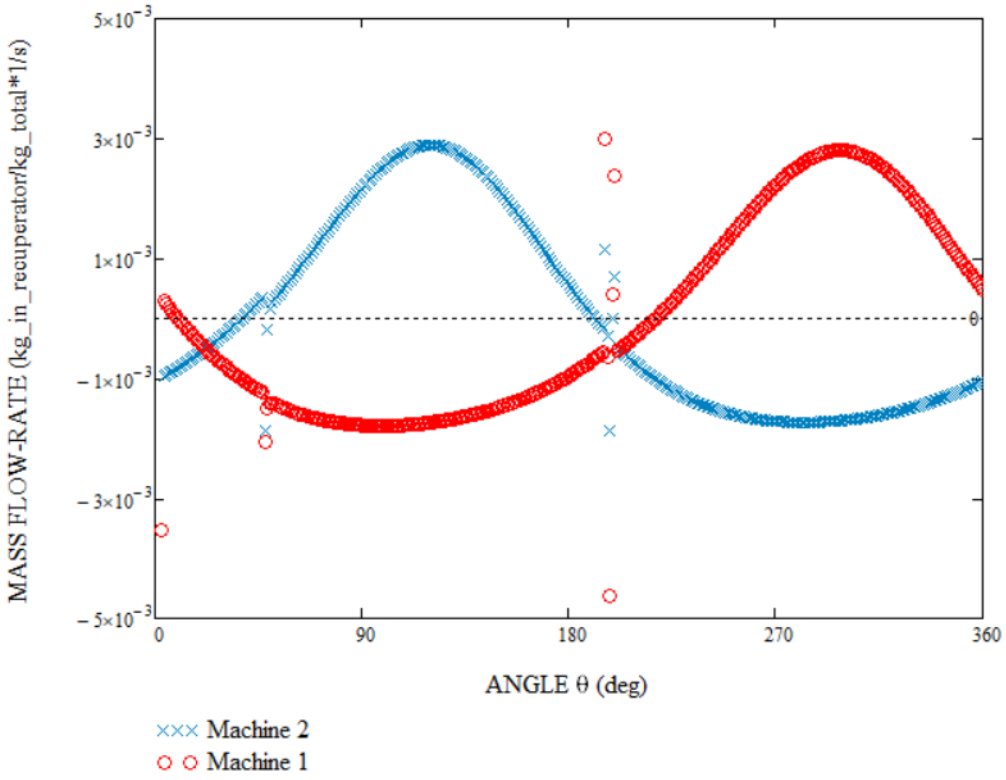

FIGURE 8.15: Mass flow rate for the recuperator for 18 deg phase difference

What can be seen from this graph, is that no destructive parallel flow occurs in the system.

The works of the pistons will be the same as the heats exchanged and are found as:

$$q_c = w_c = \sum_{\theta=2}^{360} \left(\frac{P}{M}\frac{dV_c}{\theta}(\theta)\right) \tag{8.29}$$

$$q_e = w_e = \sum_{\theta=2}^{360} \left(\frac{P}{M}\frac{dV_e}{\theta}(\theta)\right) \tag{8.30}$$

Now having the thermal behavior of the system, one is able to calculate its cooling power. To calculate this cooling power in a simple isothermal Stirling model one would simply use the work of the expander. But is this case, one has to take into account the cooling power lost for all the instances when the fluid exits the recuperator on the cold side with a temperature higher that the Th. For this reason, for all those cases the extra heat from the fluid is taken into account as if it has been dumped in the cold box. This lost cooling power is calculated as:

$$\begin{aligned}
&\text{qlost} := \left|\begin{array}{l}
q \leftarrow 0 \\
\text{for } \theta \in 3..360 \\
\quad \left|\begin{array}{l}
\text{qlost} \leftarrow -\left[gAr_{rh}\left(\theta, Tr_{\theta-1}, Tr_{\theta}\right)\cdot\left(Thout_{\theta} - Th\right)\cdot cp\cdot M\right] \text{ if } Thout_{\theta} \neq Th \\
q \leftarrow q + \text{qlost}
\end{array}\right. \\
q
\end{array}\right.
\end{aligned}$$

In addition to this lost cooling potential the code needs to also be able to account for the cooling potential lost in the cases when parallel flow might occur, thus a second loss must be calculated as:

$$\begin{aligned}
&q_{regen} := \left|\begin{array}{l}
q \leftarrow 0 \\
\text{for } \theta \in 3..360 \\
\quad \left|\begin{array}{l}
\text{qlost} \leftarrow \left[\left(gAr_{kr}\left(\theta, Tr_{\theta-1}, Tr_{\theta}\right) + gAr_{rh}\left(\theta, Tr_{\theta-1}, Tr_{\theta}\right)\right)\cdot cp\cdot M\cdot(Tk - Th)\right] \text{ if } Thout_{\theta} = Th \wedge Thout^{*}_{\theta} = Th \\
q \leftarrow q + \text{qlost}
\end{array}\right. \\
q
\end{array}\right.
\end{aligned}$$

So overall the cooling power for 180 deg phase difference will be:

$$q = q_e + q_e^* + q_{lost} + q_{lost^*} + q_{regen} + q_{regen^*} = 0.073 W/kg \tag{8.31}$$

And the COP of the system is found as:

$$COP = \frac{q_e + q_e^* + q_{lost} + q_{lost^*} + q_{regen} + q_{regen^*}}{w + w^*} = 45.66\% \tag{8.32}$$

As previously stated, the efficiency and overall behavior of the cycle depend to the phase difference of the two coolers. Thus, any phase difference where destructive parallel flow is being detected in the system needs to be excluded. The phase differences for which destructive parallel flow does not occur are between X=152. . . 209 deg. Within this range, the cooler will produce cooling power. Following this, the optimum phase difference is sought after based on achieving the best efficiency for the cooler. For that reason, the code has designed from the beginning to be able to work with a variable phase difference. One can see the behavior of the system based on the phase difference on the graph below.

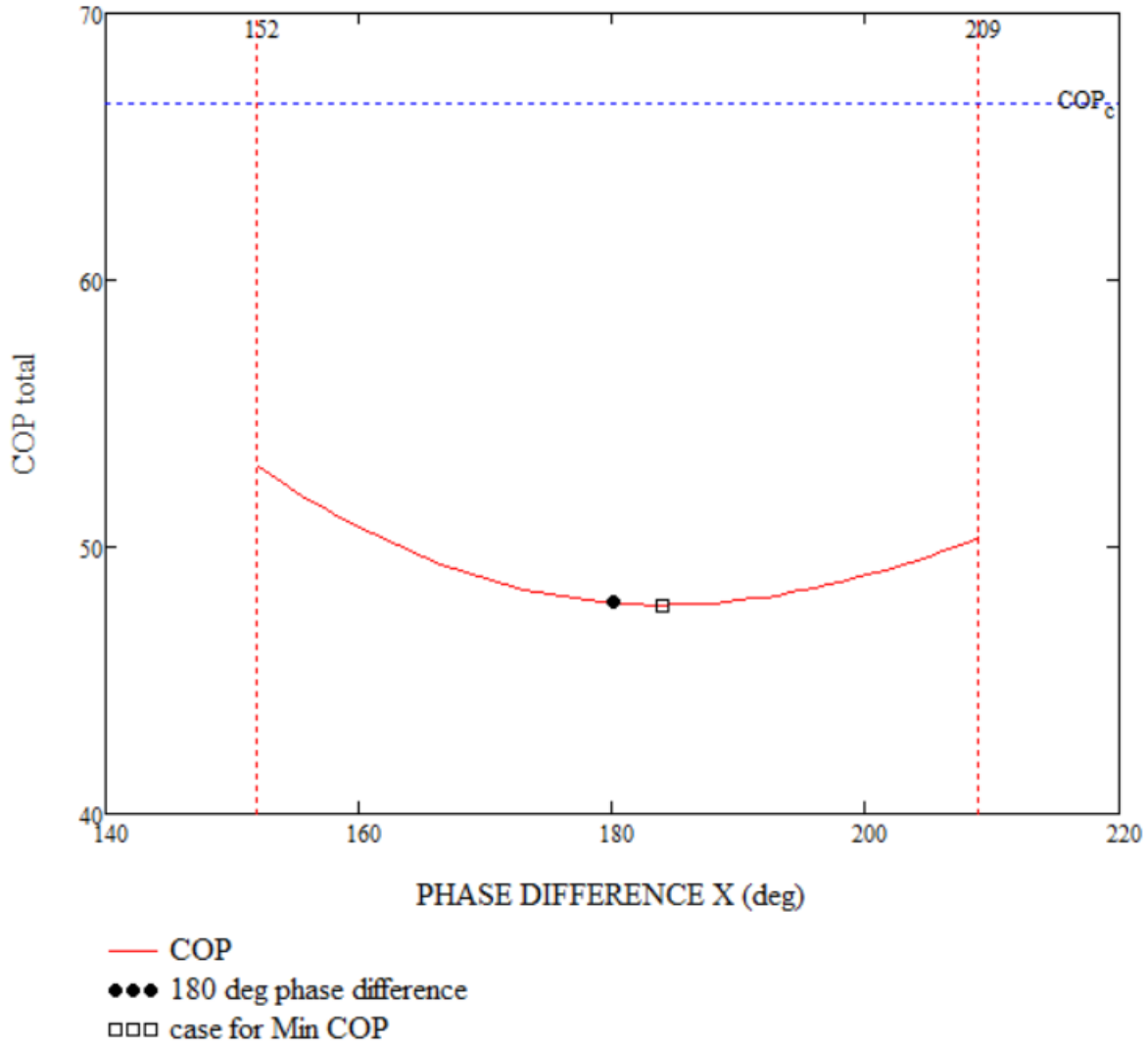

FIGURE 8.16: COP to phase difference graph. Beyond the red dash lines on the left and the right of the figure are the regions where destructive parallel flow occurs. The COP Carnot is also shown in the figure as the blue dashed line being $COP_{Carnot} = 66.6\%$

This graph showcases that the 180 deg phase difference is a safe choice when the flows are concerned but it is quite an ineffective solution as it is quite near the bottom of the COP curve. By choosing another phase difference one can achieve a significantly better efficiency for the system. The optimal value is seen to be at 152 deg where $COP(152^o) = 53.074\%$. As expected in all circumstances the COP is lesser than the COP of the Carnot cycle in this temperature range. At this point to make it easier for the reader to utilise these results and not have to run the entire code to get the results a polynomial is fitted to simulate the behavior of the COP to the phase difference.

$$COP_{tot}(x) = -1.5202 + 3.8188x - 4.6364x^2 + 2.0603x^3 - 3.0831x^4 \tag{8.33}$$

The calculations above as it can be seen in equations 8.23-8.26 contain an ϵ term that has not been explicitly discussed so far. This term is there to signify the losses from the materials in the recuperator acting as a heat exchanger. The recuperator of the modelled

system is made by a Kapton covered Epoxy. The heat conductivity of this material at cryogenic temperatures is given by Rondeaux and Barucci in [88, 89]. Using the NTU method the behavior of the system for a given efficiency is derived. Based on the data for the heat convectivity for Kapton-Epoxy and Helium at these temperatures, the efficiency of the recuperator is calculated to be $\epsilon = 98,7\%$. The equivalent NTU would be NTU=75 and the COP=53.024% for X=152 deg phase difference. For ease of use of the reader an polynomial regression of the COP to NTU correlation is also provided.

$$\begin{aligned} COP(NTU) = &-3.326 \times 10^{-10} NTU^4 + 4.11 \times 10^{-7} NTU^3 - 8.504 \times 10^{-5} NTU^2 \\ &+ 6.864 \times 10^{-3} NTU + 52.822 \end{aligned} \tag{8.34}$$

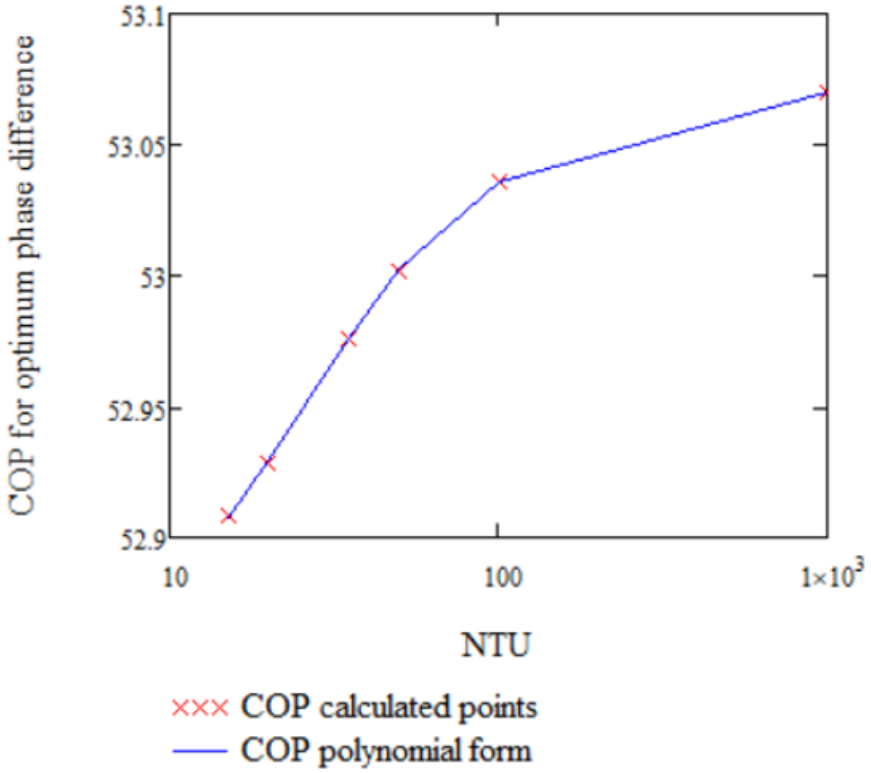

FIGURE 8.17: Optimum phase difference COP for different NTU

It can be seen from the graph that as the NTU increases so does the COP, until stabilizing near a final value for $\epsilon = 100\%$.

8.5 Single Superfluid Stirling Helium 3-4 Mixture

The previously presented model was comprehensive in the explanation of the machine and its behavior but it was very simplistic in the essence of the working medium. It assumed that Helium-4 is completely inert, that Helium-3 is an ideal gas, that they have no mixing interactions and it forgoes the phenomenon of the osmotic pressure. All these issues are important to be addressed. So far, no study from any other author has attempted to use a full model of Helium for such a modelling of an superfluid Stirling refrigerator. During this research, a first attempt had been made into describing the full model given the values for the Helium 3-4 mixture and published in [43]. That study presents a valid model for the behavior of Helium 3-4 mixtures based on the EOS of Chaudhry [71]. That equation of state though had not been ideal and the model had some limitations. Continuing that work the same model was then improved by using the full equation of state of the Helium 3-4 mixture as described in 6 and published in [90].

The geometry of the apparatus remains the same as before but this time using only one Stirling machine. The solution of the system is similar with some key differences that have arisen due to working with the mixture as they will be described below.

First of all two new volumes will have to be included in the system, being the regions behind the pistons where the superfluid Helium-4 can leak through. To find these volumes the swept volume of the piston is used and they are defined as:

$$V_c'(\theta) = V_c(0) - V_c(\theta) \tag{8.35}$$

$$V_e'(\theta) = V_e(270) - V_e(\theta) \tag{8.36}$$

So the volume in the inside of the system where all the Helium-3 and part of the Helium-4 exist is:

$$Vin(\theta) = V_c(\theta) + V_k + V_r + V_h + V_e(\theta) \tag{8.37}$$

Now the masses for the different volumes need to be established as:

$$m_c'(\theta, x, P) = \frac{V_c'(\theta)}{v_{He4}(T_k, P - P_{osm}(x, T_k, P))} \tag{8.38}$$

The v_{He4} is derived from the equation given by the code in B.4. The P_{osm} refers to the osmotic pressure though the eq. C.1.

$$m_c(\theta, x, P) = \frac{V_c(\theta) + V_k}{v(x, T_k, P)} \tag{8.39}$$

The $v(x, T, P)$ refers to the equation 6.5.

$$m_r(\theta, x, P) = \frac{V_r}{v(x, T_r, P)} \tag{8.40}$$

$$m_e(\theta, x, P) = \frac{V_e(\theta) + V_h}{v(x, T_k, P)} \tag{8.41}$$

$$m_e'(\theta, x, P) = \frac{V_e'(\theta)}{v_{He4}(T_h, P - P_{osm}(x, T_k, P))} \tag{8.42}$$

While the previous case was based on normalized values, in this case it is seen beneficial to work with actual values. A Helium 3-4 mixture with a 33% enrichment has been chosen (close to the 30% used by [83]) with m3=1.5 mol and m4=3 mol.

To find the pressure for a given state of concentrations of the system one uses the mass equation as:

$$m_3+m_4 = mc'(\theta, x_c, P)+mc(\theta, x_c, P)+mr(\theta, x_r, P)+me(\theta, x_e, P)+me'(\theta, x_e, P) \quad (8.43)$$

Now similar to the code presented in the previous section the following code is created and used based on a similar train of thought as before to solve the system for the full mixture. The full code is presented in Appendix D.2.

Given the developed code the machine is simulated produces the following results.

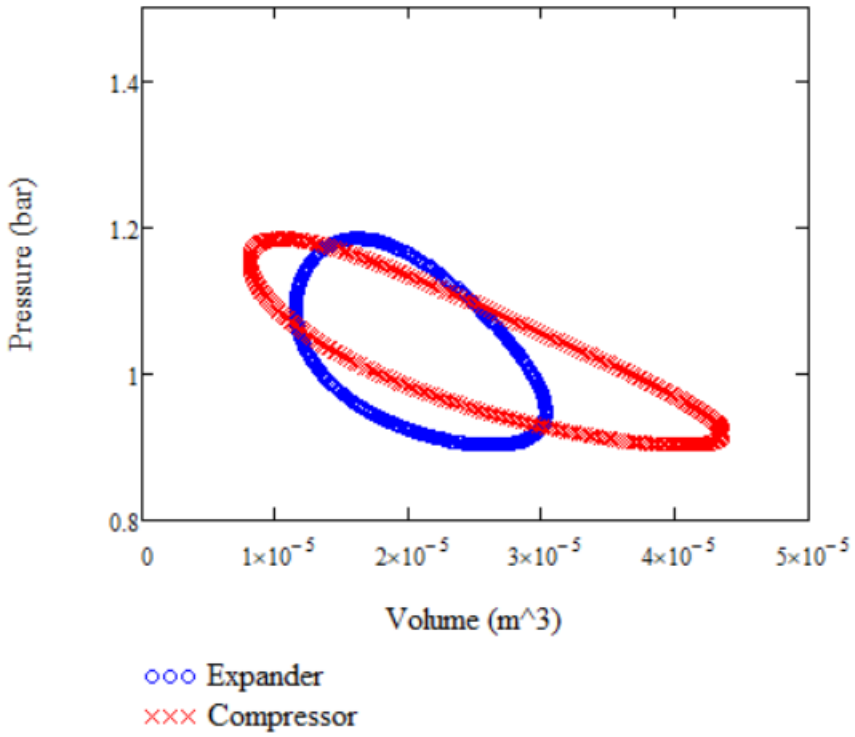

FIGURE 8.18: Volumes of the compressor and expander against the Pressure

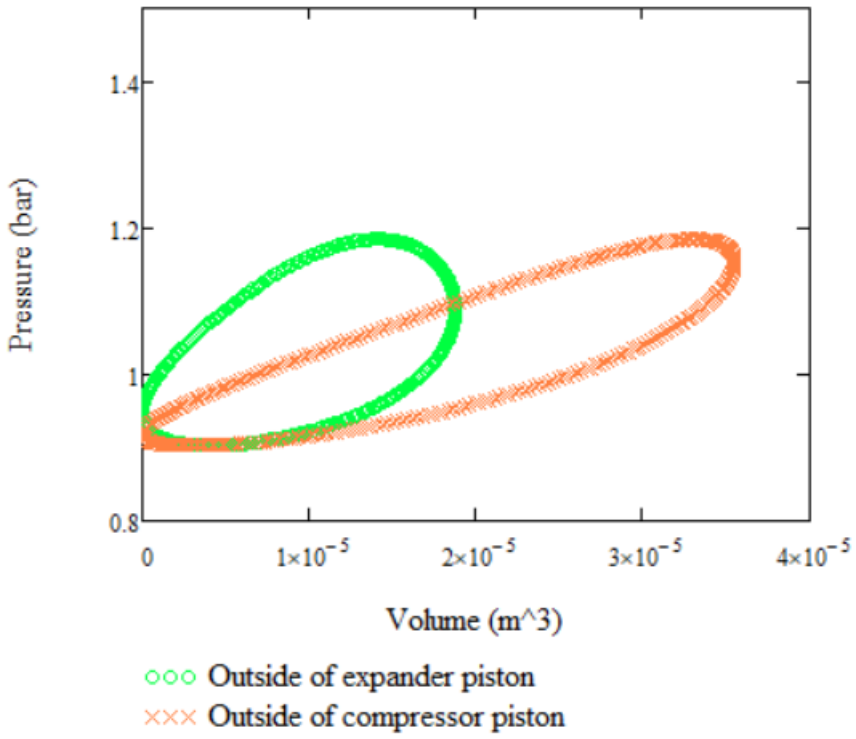

FIGURE 8.19: Volumes of the outside of the pistons against the Pressure

From these graphs it can be seen that despite the introduction of the different volumes and the superleaks the oval-shaped P-V diagram of the Stirling engines is still applied.

The above are behaviors that are expected and are present in all simulations of Stirling engines. One outcome that brings significant interest is the plot between the Helium-3 concentration and the volume. As seen in the figures below one can see that the oval shape presents itself on this kind of graph as well. This outcome is important as based on these results it seems to be describing a behavior present of any Stirling machine working with a mixture.

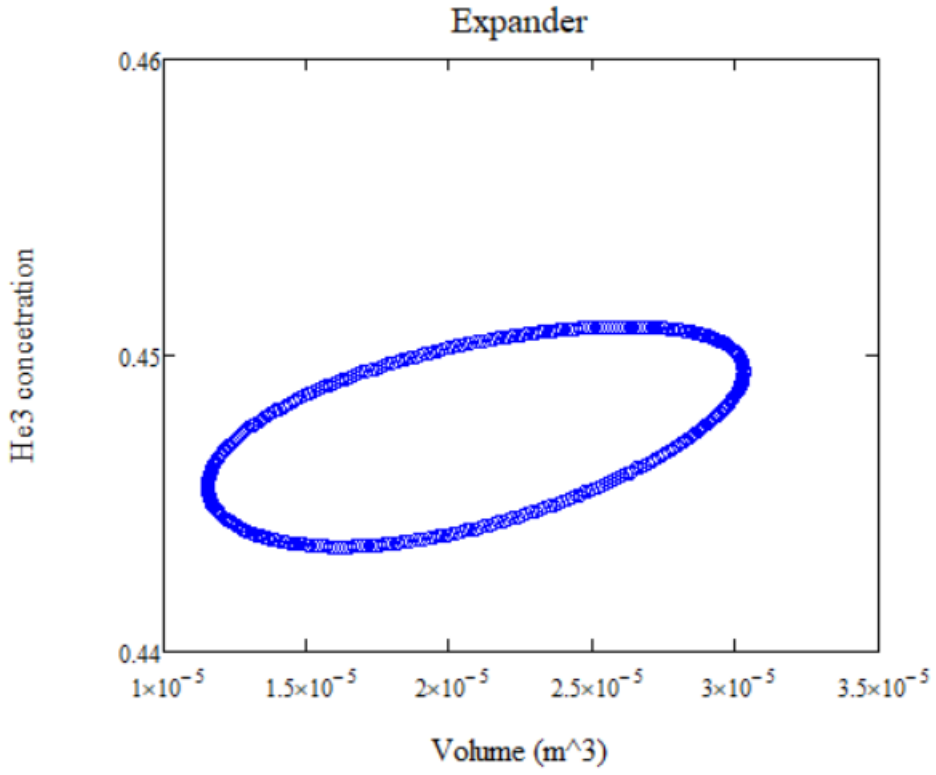

FIGURE 8.20: Helium-3 concentration against the volume in the expander

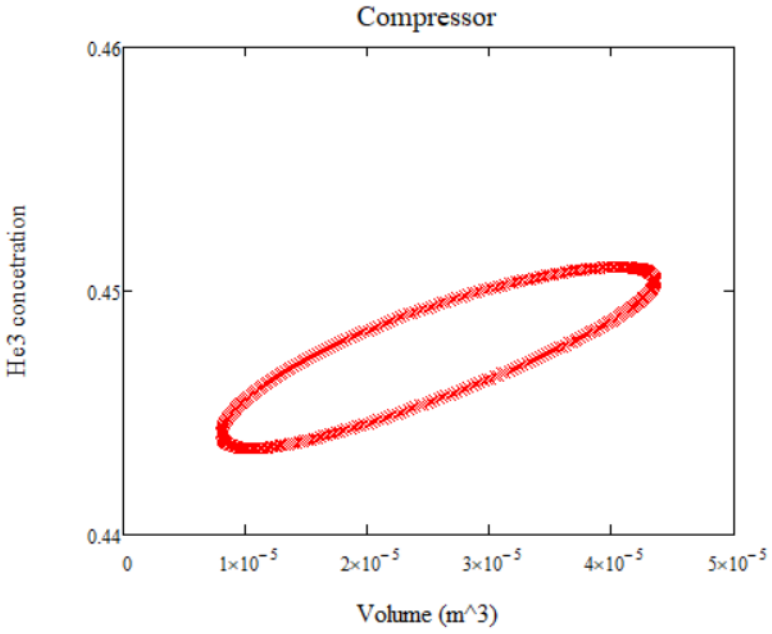

FIGURE 8.21: Helium-3 concentration against the volume in the compressor

Through the simulation one can see how the Helium-3 concentration and mass is evolving in the cycle.

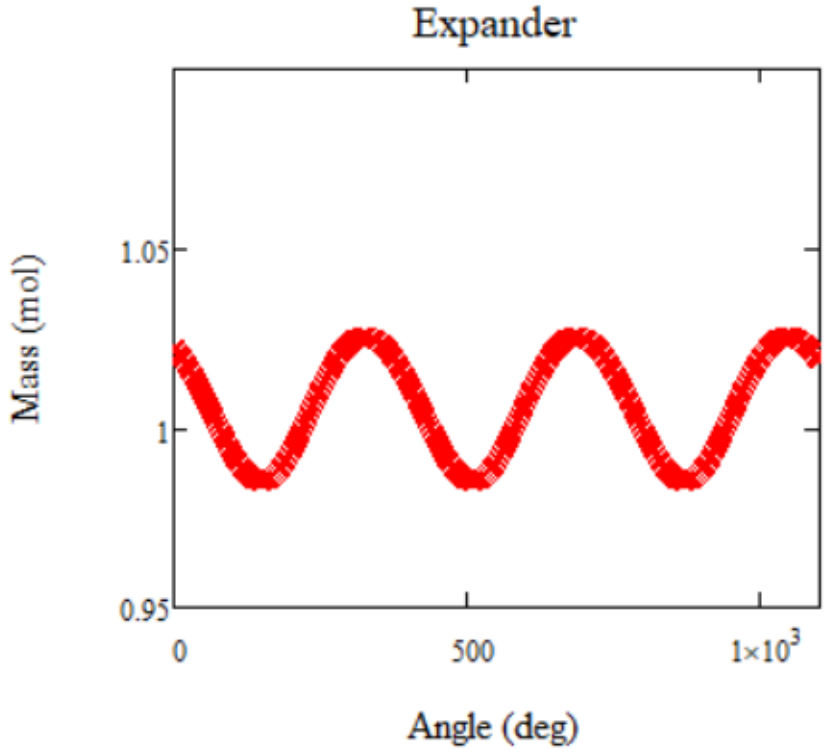

FIGURE 8.22: Mass in the expander

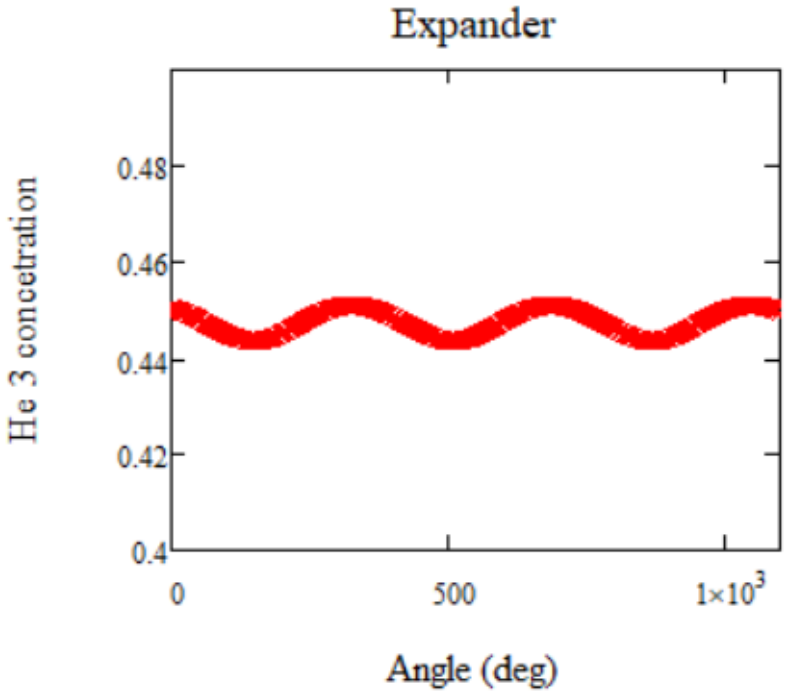

FIGURE 8.23: Helium-3 concentration in the expander

Now in codes simulating such machines usually it takes some cycles for the code to converge. This is usually the case as the numerical equations are not solved directly but

initial guesses are augmented until they are converged to the final value. The format of this code is such that this is not the case and the equations for the energy and mass in both the ideal and the full He3-4 mix codes are directly solved. This leads to the system directly converging to the correct values without the need of multiple cycles. This can be seen in even more clearly in the following plot where it is shown that even in the first three cycles there are no deviations between the values.

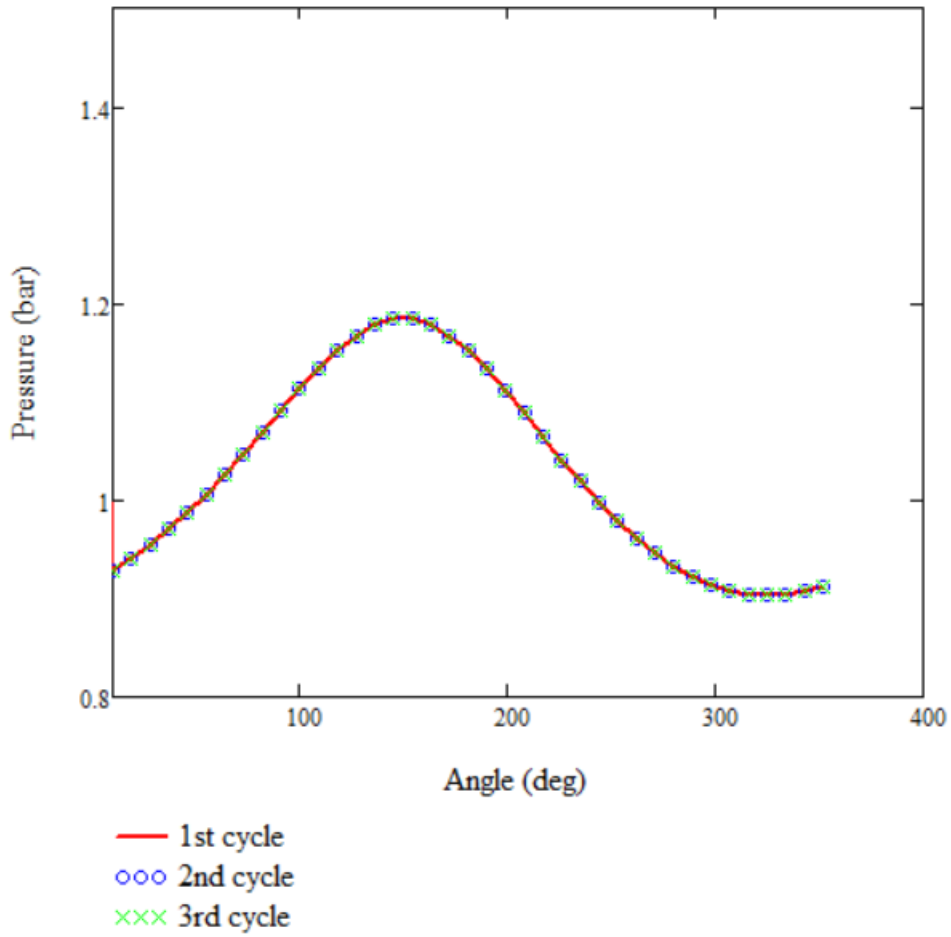

FIGURE 8.24: Convergence of the cycles of Helium 3-4 superfluid Stirling

In this case when one wants to calculate the energy values of the system the EOS again needs to be used and the different heat exchanges based on the enthalpy $H(x, T, P)$ given in eq. C.1.

$$Q_e = \sum_{\theta=3}^{362} (m_e(\theta)H(x_e(\theta), T_h, P(\theta)) - m_e(\theta-1)H(x_e(\theta-1), T_h, P(\theta-1)) \tag{8.44}$$

$$Q_k = \sum_{\theta=3}^{362} (m_c(\theta)H(x_c(\theta), T_k, P(\theta)) - m_c(\theta-1)H(x_c(\theta-1), T_k, P(\theta-1)) \tag{8.45}$$

$$Q'_c = \sum_{\theta=3}^{362} (m'_c(\theta)H(x'_c(\theta), T_k, P(\theta)) - m'_c(\theta-1)H(x'_c(\theta-1), T_k, P(\theta-1)) \tag{8.46}$$

$$Q_e = \sum_{\theta=3}^{362} (m_e(\theta)H(x_e(\theta), T_h, P(\theta)) - m_e(\theta-1)H(x_e(\theta-1), T_h, P(\theta-1)) \tag{8.47}$$

Based on the above the efficiency can now be evaluated similarly as before for a COP=29.2% and a cooling power of Q=2.4mW.

Through the results one can see that his application has values that are lower than the ideal model. This is expected though to be the case as in the previous simulation the phenomenon of the osmotic pressure and the interactions of the Helium-4 part had been completely neglected.

8.6 Dual Superfluid Stirling Helium 3-4 Mixture

Following the previous analysis, the next step is to implement the same EOS to the dual Stirling refrigerator.

The base difference between the code used here and the original code for the dual isothermal Stirling with the ideal gas is that the enthalpy is directly calculated through the equation of state and at each point other than the exit temperatures and the pressure also the concentration needs to evaluated at each of the volumes of the apparatus.

The $v(x, T, P)$ refers to the equation 6.5. The v_{He4} is derived from the equation given by the code in B.4. The P_{osm} refers to the osmotic pressure though the C.1. The enthalpy $H(x, T, P)$ is given in C.1.

The geometry of the engine is the same as given in table 8.1 applied to the two conjoined Stirling engines. The volumes outside the pistons are given as:

$$V'_c(\theta) = V_c(0) - V_c(\theta) \tag{8.48}$$

$$V'_e(\theta) = V_e(270) - V_e(\theta) \tag{8.49}$$

$$V_c(\theta) = V_{clc} + \frac{1}{2}V_{swc}(1 + cos(\theta)) \tag{8.50}$$

$$V_e(\theta) = V_{cle} + \frac{1}{2}V_{swc}(1 + cos(\theta + \frac{\pi}{2})) \tag{8.51}$$

$$V^{*\prime}_c(\theta) = V^*_c(0) - V^*_c(\theta) \tag{8.52}$$

$$V^{*\prime}_e(\theta) = V^*_e(270) - V^*_e(\theta) \tag{8.53}$$

$$V^*_c(\theta, X) = V_{clc} + \frac{1}{2}V_{swc}(1 + cos(\theta + X)) \tag{8.54}$$

$$V_e^*(\theta, X) = V_{cle} + \frac{1}{2}V_{swc}(1 + cos(\theta + \frac{\pi}{2} + X)) \tag{8.55}$$

where X is the phase difference between the two engines.

The masses of the volumes of the system are defined similarly as in equations 8.56, 8.57, 8.58, 8.59, 8.60 and thus they are not repeated. In addition to these equations their equivalent for the second Stirling engine are introduced as:

$$m_c^{*\prime}(\theta, x, P, X) = \frac{V_c^{*\prime}(\theta, X)}{v_{He4}(T_k, P - P_{osm}(x, T_k, P))} \tag{8.56}$$

$$m_c^*(\theta, x, P, X) = \frac{V_c^*(\theta, X) + V_k}{v(x, T_k, P)} \tag{8.57}$$

$$m_r^*(\theta, x, P, X) = \frac{V_r}{v(x, T_r, P)} \tag{8.58}$$

$$m_e^*(\theta, x, P, X) = \frac{V_e^*(\theta, X) + V_h}{v(x, T_k, P)} \tag{8.59}$$

$$m_e^{*\prime}(\theta, x, P, X) = \frac{V_e^{*\prime}(\theta, X)}{v_{He4}(T_h, P - P_{osm}(x, T_k, P))} \tag{8.60}$$

Now the mass differences for the volumes are defined as:

$$Dm_c(\theta, x_{cn}, P_n, x_{cp}, P_p) = m_c(\theta, x_{cn}, P_n) - m_c(\theta - 1, x_{cp}, P_p) \tag{8.61}$$

$$Dm_e(\theta, x_{en}, P_n, x_{ep}, P_p) = m_e(\theta, x_{en}, P_n) - m_e(\theta - 1, x_{ep}, P_p) \tag{8.62}$$

$$Dm_r(\theta, x_{rn}, P_n, Tr_n, x_{rp}, Tr_p, P_p) = m_r(\theta, x_{rn}, P_n, Tr_n) - m_r(\theta - 1, x_{rp}, Tr_p, P_p) \tag{8.63}$$

$$Dm_e'(\theta, P_n, P_p) = m_e'(\theta, P_n) - m_e'(\theta - 1, P_p) \tag{8.64}$$

$$Dm_c'(\theta, P_n, P_p) = m_c'(\theta, P_n) - m_c'(\theta - 1, P_p) \tag{8.65}$$

and with the equivalent in the second Stirling cooler being:

$$Dm_c^*(\theta, x_{cn}, P_n, x_{cp}, P_p, X) = m_c^*(\theta, x_{cn}, P_n, X) - m_c^*(\theta - 1, x_{cp}, P_p, X) \tag{8.66}$$

$$Dm_e^*(\theta, x_{en}, P_n, x_{ep}, P_p, X) = m_e^*(\theta, x_{en}, P_n, X) - m_e^*(\theta - 1, x_{ep}, P_p, X) \tag{8.67}$$

$$Dm_r^*(\theta, x_{rn}, P_n, Tr_n, x_{rp}, Tr_p, P_p, X) = m_r^*(\theta, x_{rn}, P_n, Tr_n, X) - m_r^*(\theta - 1, x_{rp}, Tr_p, P_p, X) \tag{8.68}$$

$$Dm_e'^*(\theta, P_n, P_p, X) = m_e'^*(\theta, P_n, X) - m_e'^*(\theta - 1, P_p, X) \tag{8.69}$$

$$Dm_c'^*(\theta, P_n, P_p, X) = m_c'^*(\theta, P_n, X) - m_c'^*(\theta - 1, P_p, X) \tag{8.70}$$

The mass flows between the volumes are defined as:
Through the hot piston:

$$gA_{oc}(\theta, P_n, P_p) = Dm_c'(\theta, P_n, P_p) \tag{8.71}$$

$$gA_{oc}^*(\theta, P_n, P_p, X) = Dm_c'^*(\theta, P_n, P_p, X) \tag{8.72}$$

From the compressor to the recuperator.

$$gA_{cr}(\theta, x_{cn}, P_n, x_{cp}, P_p) = Dm_c(\theta, x_{cn}, P_n, x_{cp}, P_p) + Dm_c'(\theta, P_n, P_p) \tag{8.73}$$

$$gA_{cr}^*(\theta, x_{cn}, P_n, x_{cp}, P_p, X) = Dm_c^*(\theta, x_{cn}, P_n, x_{cp}, P_p, X) + Dm_c'^*(\theta, P_n, P_p, X) \tag{8.74}$$

From the recuperator to the expander:

$$gA_{re}(\theta, x_{en}, P_n, x_{ep}, P_p) = Dm_e(\theta, x_{cn}, P_n, x_{cp}, P_p) - Dm_e'(\theta, P_n, P_p) \tag{8.75}$$

$$gA_{re}^*(\theta, x_{en}, P_n, x_{ep}, P_p, X) = -Dm_e^*(\theta, x_{en}, P_n, x_{ep}, P_p, X) + Dm_e'^*(\theta, P_n, P_p, X) \tag{8.76}$$

Through the cold piston:

$$gA_{oe}(\theta, P_n, P_p) = -Dm_e'(\theta, P_n, P_p) \tag{8.77}$$

$$gA_{oe}^*(\theta, P_n, P_p, X) = -Dm_e'^*(\theta, P_n, P_p, X) \tag{8.78}$$

For solving the system again, one needs to determine at each point the side where the greater mass flow occurs. To get this information the same method as the ideal dual Stirling is applied with assuming one having the greater flow and the confirming or rejecting the initial assumption based on the exit temperatures of the recuperator.

Assume that $m < m*$. A system of nine equations and nine variables is formed. The subscript "p" refers to the previous $\theta - 1$ step and "pp" to the double previous $\theta - 2$. The variables containing the "A" are the unknowns of the system that need to be found.

Energy conservation at the recuperator.

$$\begin{aligned} &gA_{cr}(\theta - 1, x_{cp}, P_p, x_{cpp}, P_{pp})H(PA, Tk, xrA) \\ &- gA_{re}(\theta - 1, x_{ep}, P_p, x_{epp}, P_{pp})H(PA, Th, xrA) = \\ &gA_{cr}^*(\theta - 1, x_{cp}^*, P_p^*, x_{cpp}^*, P_{pp}^*)H(PA^*, Tk, xrA^*) \\ &- gA_{re}^*(\theta - 1, x_{ep}^*, P_p^*, x_{epp}^*, P_{pp}^*)H(PA, ThoutA*, xrA*) \end{aligned} \tag{8.79}$$

Helium 3 conservation cooler 1.

$$m_3 = xcA\, m_c(\theta, xcA, PA) + xrA\, m_r(\theta, xrA, \frac{Tk - Th}{ln(\frac{Tk}{Th})}, PA) + xeA\, m_e(\theta, xeA, PA) \tag{8.80}$$

Helium 4 conservation cooler 1.

$$m_4 = (1 - xcA)\, m_c(\theta, xcA, PA) + (1 - xrA)\, m_r(\theta, xrA, \frac{Tk - Th}{ln(\frac{Tk}{Th})}, PA) + (1 - xeA)\, m_e(\theta, xeA, PA) + m'_c(\theta, PA) + m'_e(\theta, PA) \tag{8.81}$$

Helium 3 conservation cooler 2.

$$m_3 = xcA^* m^*_c(\theta, xcA^*, PA^*) + xrA^* m^*_r(\theta, xrA^*, \frac{Tk - ThoutA^*}{ln(\frac{Tk}{ThoutA^*})}, PA^*) + xeA^* m^*_e(\theta, xeA^*, PA^*) \tag{8.82}$$

Helium 4 conservation cooler 2.

$$m_4 = (1 - xcA^*)\, m^*_c(\theta, xcA^*, PA^*) + (1 - xrA^*)\, m^*_r(\theta, xrA^*, \frac{Tk - ThoutA^*}{ln(\frac{Tk}{ThoutA^*})}, PA^*) + (1 - xeA^*)\, m^*_e(\theta, xeA^*, PA^*) + m'^*_c(\theta, PA^*) + m'^*_e(\theta, PA^*) \tag{8.83}$$

Helium 4 mass conservation at expander cooler 1.

$$(1 - xeA)m_e(\theta, xeA, PA) - (1 - x_{ep})m_e(\theta - 1, x_{ep}, P_p) = m'_e(\theta, PA) - m'_e(\theta - 1, P_p) + (1 - xrA)m_r(\theta, xrA, \frac{Tk - Th}{ln(\frac{Tk}{Th})}, PA) - (1 - x_{rp})m_r(\theta - 1, x_{rp}, Tr_p, P_p) \tag{8.84}$$

Helium 4 mass conservation at compressor cooler 1.

$$(1 - xcA)m_c(\theta, xcA, PA) - (1 - x_{cp})m_c(\theta - 1, x_{cp}, P_p) = m'_c(\theta, PA) - m'_c(\theta - 1, P_p) + (1 - xrA)m_r(\theta, xrA, \frac{Tk - Th}{ln(\frac{Tk}{Th})}, PA) - (1 - x_{rp})m_r(\theta - 1, x_{rp}, Tr_p, P_p) \tag{8.85}$$

Helium 4 mass conservation at expander cooler 2.

$$(1 - xeA^*)m^*_e(\theta, xeA^*, PA^*) - (1 - x^*_{ep})m^*_e(\theta - 1, x^*_{ep}, P^*_p) = m'^*_e(\theta, PA^*) - m'^*_e(\theta - 1, P^*_p) + (1 - xrA^*)m^*_r(\theta, xrA^*, \frac{Tk - ThoutA^*}{ln(\frac{Tk}{ThoutA^*})}, PA^*) - (1 - x^*_{rp})m^*_r(\theta - 1, x^*_{rp}, Tr^*_p, P^*_p) \tag{8.86}$$

Helium 4 mass conservation at compressor cooler 2.

$$(1 - xcA^*)m^*_c(\theta, xcA^*, PA^*) - (1 - x^*_{cp})m^*_c(\theta - 1, x^*_{cp}, P^*_p) = m'^*_c(\theta, PA^*) - m'^*_c(\theta - 1, P^*_p) + (1 - xrA^*)m^*_r(\theta, xrA^*, \frac{Tk - ThoutA^*}{ln(\frac{Tk}{ThoutA^*})}, PA^*) - (1 - x^*_{rp})m^*_r(\theta - 1, x^*_{rp}, Tr^*_p, P^*_p) \tag{8.87}$$

Solving the above one gets the consistency of the mixture at each of the volumes $(x_c, x_r, x_e, x^*_c, x^*_r, x^*_e$, the exit temperature of the recuperator of cooler 2 $Thout^*$ and the

pressures of the two coolers P, P^*.

If the exit temperature is evaluated to be outside the temperature range then the initial assumption was wrong and the new system for $m > m*$ needs to be defined and solved.

Energy conservation at the recuperator.

$$\begin{aligned} &gA_{cr}(\theta-1, x_{cp}, P_p, x_{cpp}, P_{pp})H(PA, Tk, xrA) \\ &- gA_{re}(\theta-1, x_{ep}, P_p, x_{epp}, P_{pp})H(PA, Th, xrA) = \\ &gA^*_{cr}(\theta-1, x^*_{cp}, P^*_p, x^*_{cpp}, P^*_{pp})H(PA^*, Tk, xrA^*) \\ &- gA^*_{re}(\theta-1, x^*_{ep}, P^*_p, x^*_{epp}, P^*_{pp})H(PA, ThoutA*, xrA*) \end{aligned} \tag{8.88}$$

Helium 3 conservation cooler 1.

$$m_3 = xcA\, m_c(\theta, xcA, PA) + xrA\, m_r(\theta, xrA, \frac{Tk - ThoutA}{ln(\frac{Tk}{ThoutA})}, PA) + xeA\, m_e(\theta, xeA, PA) \tag{8.89}$$

Helium 4 conservation cooler 1.

$$\begin{aligned} m_4 &= (1-xcA)\, m_c(\theta, xcA, PA) + (1-xrA)\, m_r(\theta, xrA, \frac{Tk - ThoutA}{ln(\frac{Tk}{ThoutA})}, PA) \\ &+ (1-xeA)\, m_e(\theta, xeA, PA) + m'_c(\theta, PA) + m'_e(\theta, PA) \end{aligned} \tag{8.90}$$

Helium 3 conservation cooler 2.

$$m_3 = xcA^*\, m^*_c(\theta, xcA^*, PA^*) + xrA^*\, m^*_r(\theta, xrA^*, \frac{Tk - Th}{ln(\frac{Tk}{Th})}, PA^*) + xeA^*\, m^*_e(\theta, xeA^*, PA^*) \tag{8.91}$$

Helium 4 conservation cooler 2.

$$\begin{aligned} m_4 &= (1-xcA^*)\, m^*_c(\theta, xcA^*, PA^*) + (1-xrA^*)\, m^*_r(\theta, xrA^*, \frac{Tk - Th}{ln(\frac{Tk}{Th})}, PA^*) \\ &+ (1-xeA^*)\, m^*_e(\theta, xeA^*, PA^*) + m'^*_c(\theta, PA^*) + m'^*_e(\theta, PA^*) \end{aligned} \tag{8.92}$$

Helium 4 mass conservation at expander cooler 1.

$$\begin{aligned} &(1-xeA)m_e(\theta, xeA, PA) - (1-x_{ep})m_e(\theta-1, x_{ep}, P_p) = \\ &m'_e(\theta, PA) - m'_e(\theta-1, P_p) + (1-xrA)m_r(\theta, xrA, \frac{Tk - ThoutA}{ln(\frac{Tk}{ThoutA})}, PA) \\ &- (1-x_{rp})m_r(\theta-1, x_{rp}, Tr_p, P_p) \end{aligned} \tag{8.93}$$

Helium 4 mass conservation at compressor cooler 1.

$$\begin{aligned} &(1-xcA)m_c(\theta, xcA, PA) - (1-x_{cp})m_c(\theta-1, x_{cp}, P_p) = \\ &m'_c(\theta, PA) - m'_c(\theta-1, P_p) + (1-xrA)m_r(\theta, xrA, \frac{Tk - ThoutA}{ln(\frac{Tk}{ThoutA})}, PA) \\ &- (1-x_{rp})m_r(\theta-1, x_{rp}, Tr_p, P_p) \end{aligned} \tag{8.94}$$

Helium 4 mass conservation at expander cooler 2.

$$\begin{aligned}&(1-xeA^*)m_e^*(\theta,xeA^*,PA^*)-(1-x_{ep}^*)m_e^*(\theta-1,x_{ep}^*,P_p^*)=\\&m_e'^*(\theta,PA^*)-m_e'^*(\theta-1,P_p^*)+(1-xrA^*)m_r^*(\theta,xrA^*,\frac{Tk-Th}{ln(\frac{Tk}{Th})},PA^*)\\&-(1-x_{rp}^*)m_r^*(\theta-1,x_{rp}^*,Tr_p^*,P_p^*)\end{aligned}\tag{8.95}$$

Helium 4 mass conservation at compressor cooler 2.

$$\begin{aligned}&(1-xcA^*)m_c^*(\theta,xcA^*,PA^*)-(1-x_{cp}^*)m_c^*(\theta-1,x_{cp}^*,P_p^*)=\\&m_c'^*(\theta,PA^*)-m_c'^*(\theta-1,P_p^*)+(1-xrA^*)m_r^*(\theta,xrA^*,\frac{Tk-Th}{ln(\frac{Tk}{Th})},PA^*)\\&-(1-x_{rp}^*)m_r^*(\theta-1,x_{rp}^*,Tr_p^*,P_p^*)\end{aligned}\tag{8.96}$$

The code above it conceptually very similar to the one defined for the ideal dual Stirling. One issue that one faces when having to solve these systems of equations is that due to having to solve over the equations of state which are really complicated functions. This means that even by using different numerical models for the solution it is very difficult to gain correct and continuous results at every angle of the system. In the graphs presented below it will be seen that the overall behavior of the system is resembling the behavior of the dual ideal Stirling model but there is a lot of noise in the data as at many points the numerical algorithms fail for a solution.

The full code for the solution of the system is shown in Appendix D.3.

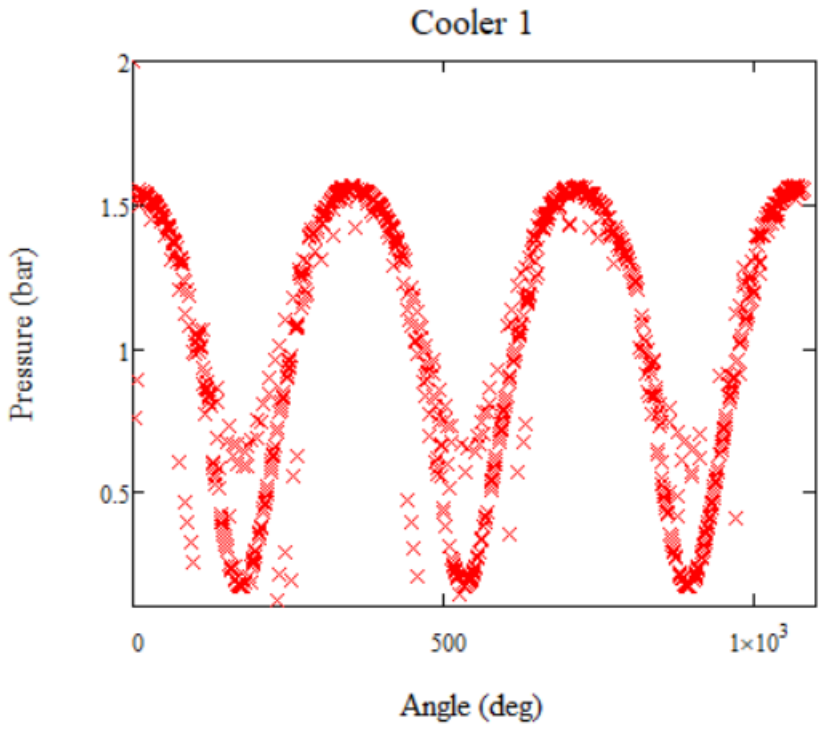

FIGURE 8.25: Pressure to total volume in 1D dual SSR with Helium 3-4 mix at cooler 1 with 180 deg phase difference

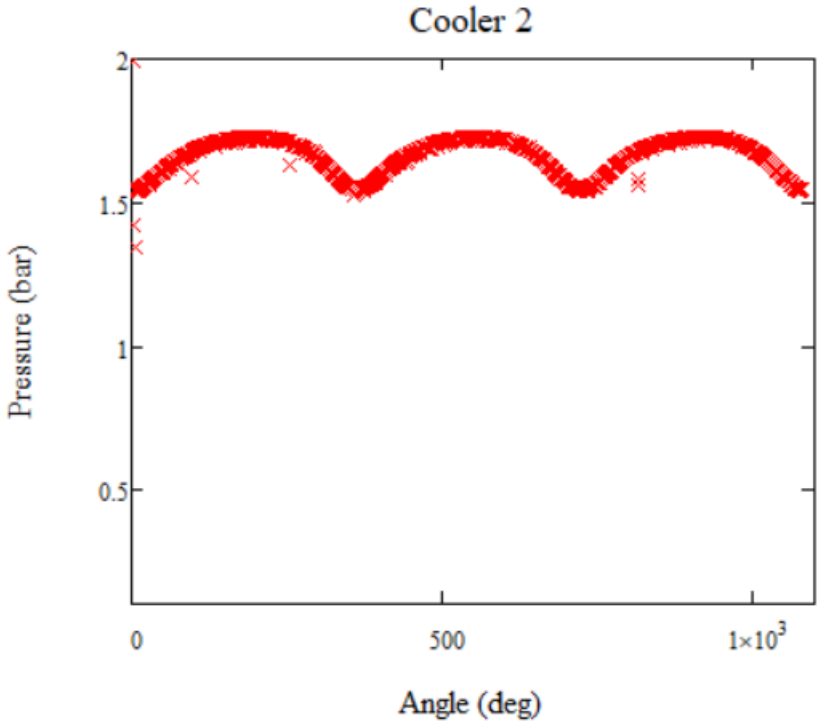

FIGURE 8.26: Pressure to total volume in 1D dual SSR with Helium 3-4 mix at cooler 2 with 180 deg phase difference

The two graphs above one can see that the typical structure of a Stirling machine exists, but the graph is a lot noisier than the previous examples. This is because the code cannot correctly solve the equations numerically at all points. Despite the noise if one is to observe these graphs as well as the following ones it can be seen that the overall behavior of the system is mostly correct.

To understand more about the behavior of the system one needs to further look into the evolution of the concentration of Helium-3 in the different parts of the system.

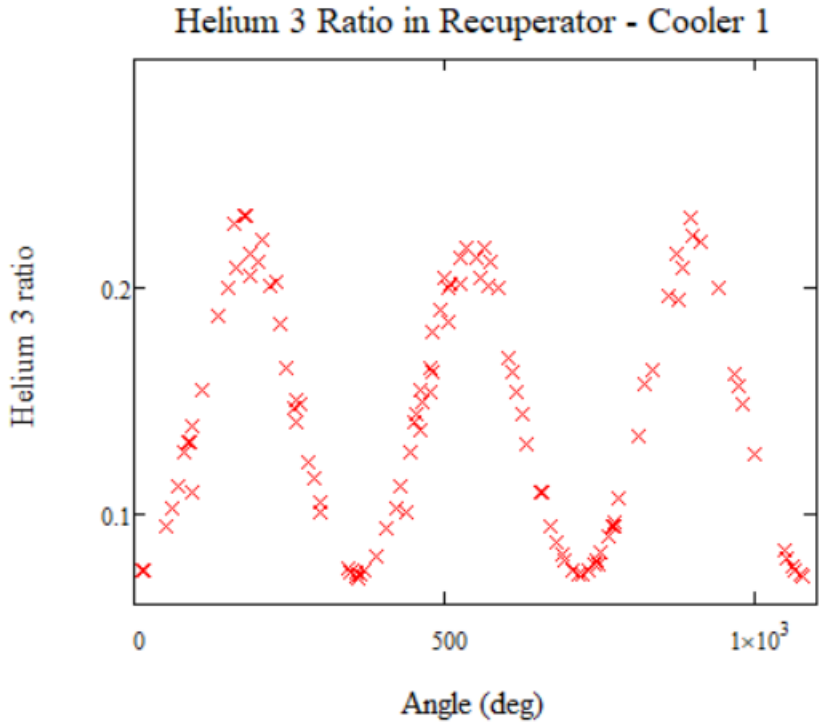

FIGURE 8.27: Helium-3 concentration to angle in 1D dual SSR with Helium 3-4 mix at cooler 1 with 180 deg phase difference

It can be seen that the Helium-3 ratio of the system increases and peaks ones at each cycle. This is the case not only in the recuperator but also on the expander and the compressor as well with the consistency peaking around the same values. At first this might sound counter intuitive as all the areas seem to be increasing their Helium-3 concentration at once. To understand this one needs to simply view this behavior in comparison with the volume. As seen in the graph depicting the Helium-3 consistencies at each of the regions as well as the volume as the cycle evolves, the concentrations are maximized when the total volume enclosed between the pistons is minimized. This now explains the behavior because as this volume is minimized more Helium-4 is out of this volume while all the Helium-3 is still concentrated there. As such this means that the overall concentration of Helium-3 in the system is expected to rise.

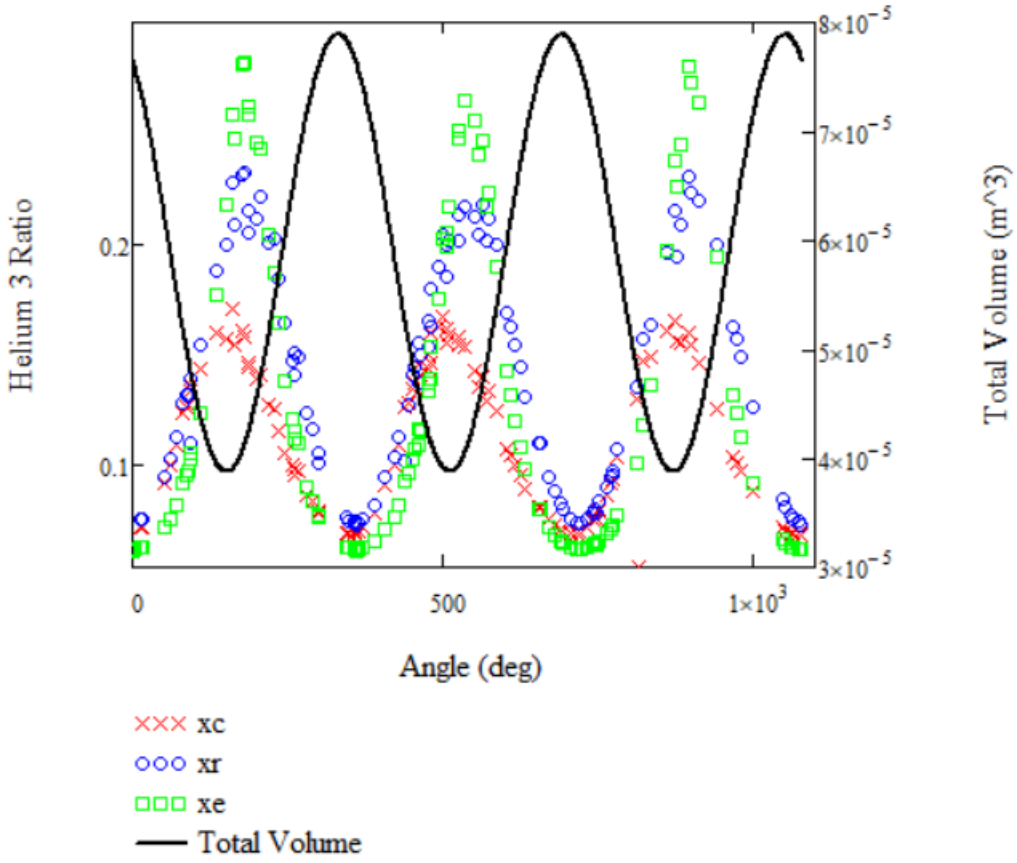

FIGURE 8.28: Helium-3 concentration in Y1 axis, Enclosed Volume between the pistons in Y2 axis against the angle in 1D dual SSR with Helium 3-4 mix at cooler 1 with 180 deg phase difference

Due to the difficulty of the code to provide exact solutions for all the points of the system, while the solution is adequate for one to understand the overall behavior the energy outcomes are not ideal to be based upon for the calculation of the cooling power as would have trouble calculate accurate values for the work given that the pressure has significant deviations. The best solution was gained by using the Levenberg-Marquardt method [91].

Working similarly to eq.8.31 and 8.32 the cooling power and the COP can be calculated in a similar manner to the previous chapter as they need to be established for the case of the mixture as well like in normal working media like in [92, 93]. The values gained by these calculations are: q=0.051 W/kg and COP=34.2%. These values are lower than the ideal model which is to be expected due to the losses due to the osmotic pressure and the overall better description of the system. In any case the outcomes of this code for the cooling power and the COP are not suggested to be directly used due to the difficulties of the solving the code. If a new numerical method is used to be able to solve all the equations for all the points, then it would be advised for the code to be re-run.

In the following chapter an even more accurate representation of the model is to be presented where a full CFD 3D analysis is proposed giving results that are much more accurate not only numerically but being able to describe more adequately all the physical phenomena as well.

8.7 Conclusions on the 1D Superfluid Stirling Refrigerator chapter

In this chapter the knowledge gathered in the previous parts of this study considering the EOS of Helium in its different forms is being applied to an important engineering application.

Stirling cryocoolers are used in many cryogenic applications able to reach very low temperatures. Usually Stirling engines work with Helium gas as working medium. Other than that, they can to work with fluid Helium as well. A problem, though, arises when the temperatures reach levels below the lambda temperature of Helium-4. At these temperature ranges Helium-4 becomes a superfluid. This is problematic for the working of the Stirling cooler as firstly the zero viscosity of the superfluid makes it able to escape the pistons and additionally as the temperature lowers the Helium-4 becomes more and more thermodynamically inert and as such more ineffective as a working medium. For this reason, a different variant of the Stirling refrigerator is studied.

The key differences of the two variants are based on the introduction of superleaks to the pistons and the use of an enriched in Helium-3 Helium mixture. At each of the pistons a superleak is introduced which enables the superfluid part of the mixture to flow through but blocks the normal fluid part. Usually this means that the Helium-3 is blocked by the vycor glass superleak and superfluid Helium-4 passes through. The enriched mixture is used as to give the machine more cooling potential even at temperatures that are well below 1K, where usually the Helium-4 would not be able to function at all as a cooling medium.

To describe this kind of Superfluid Stirling Refrigerator (SSR) multiple models have been established and presented in this study, considering all the different phenomena.

Firstly, the simplest case is described for a single Stirling cryocooler working based on the Schmidt model, where the working medium is simplified to superfluid Helium-4 being considered completely inert and the Helium-3 considered to be behaving like an ideal gas. These assumptions have been made in that subsection of the chapter basically to initiate the study of the problem and compare the setup to other such models of the literature which have all done similar assumptions in their description.

Then, trying to reduce the number of assumptions used in the model, the isothermal and adiabatic models are both simulated for the 1D ideal system. It is figured out that at these temperature ranges in the 1D model the adiabatic and isothermal model produce almost the same results with minimal deviations between them. As such, it is shown that in 1D Stirling models of these temperature ranges, irrespective of the rotational speed, the isothermal model is sufficient for describing the system.

Moving forward one needs to start accounting for the losses in the machine. In a typical Stirling machine, the regenerator is due for the largest parts of the losses. In this temperature range, though, the regenerative properties of materials are unknown and therefore no accurate regeneration models can be produced. For this reason, a dual Stirling setup is used, where two Stirling coolers are conjoined, connected in the area formerly of the regenerator which is now replaced by a heat exchanger, referred to as the recuperator. The two coolers are working with a phase difference so that counterflow occurs in the recuperator and the two streams exchange heat the same as to one stream would to a normal regenerator. Solving this model in 1D a code was developed that is able to find which side stream has the greater mass flow and which the higher temperature

difference. Based on this the full evolution of the cycle is produced. Then the cooling potential and the efficiency of the cycle are determined making sure to account for the losses due to the different kind of flows that occur during the cycle.

As mentioned, the two Stirling coolers work in a phase difference. In the literature this phase difference is always set to 180 deg. In this study, it was decided to investigate this phase difference and find its optimal value. By rerunning the simulation for various phase differences, the limits for the minimum and maximum phase difference are found as well as the optimal phase difference of the system. By doing this simulation it was seen that the 180 deg phase difference, while being a safe choice as it stayed well clear of any kind of destructive parallel flow, it actually produces a very low efficiency for the cycle and it is advised against using it in such cryocoolers.

All the existing models in the literature have worked with the aforementioned assumptions for the working medium. While these assumptions do produce an overall image for the behavior of the system, in all actuality, they are gross simplifications of the physics and thermodynamics of cryogenic Helium and as such it is considered that an accurate model would have to work with the full EOS for Helium. Thus, throughout this study, the first models of Superfluid Stirling Refrigerators have been implemented and published.

The equations of state used are the ones developed for Helium-3 Helium-4 and their mixtures in the previous chapters. Following a similar trend with the ideal model, firstly a single Stirling refrigerator is modeled. This model is presented mostly as to showcase the basic Stirling cooling behaviors working with the full Helium 3-4 mixture. The outcomes of this model are similar in their behavior to that of the ideal gas ones though their values are different, as now phenomena like the osmotic pressure and the interactions between the two isotopes are taken into account. In addition, by running this model one can see that the plot of the concentration of the mixture to the volume is of great interest at it presents an ovaloid behavior similar to the one expected by the pressure to volume diagram.

Following this the full model for the dual Stirling refrigerator with the full Helium 3-4 equation of state was produced and presented. This was a similar model in concept to the one developed for the ideal gas but it is seen to be much more mathematically intensive, as for each point of a cycle two 9x9 non linear systems need to be solved containing multiple terms of variables like the enthalpy, the density and the specific heat, which are defined by equations with more than 200 terms each respectively. This leads to some noise and clutter in the solution phase space, especially solving for the pressure. Despite this, one is more than able to acquire significant information about the working of the system from this model. The concentration of Helium-3 is seen to be increasing in all volumes at the same time, being correlated mostly to the overall volume enclosed between the pistons which hold all the available Helium-3. Overall, it can be seen that the efficiency and the cooling power of this apparatus when compared to the ones of the ideal model are lower to a degree which is expected because different losses like the ones from the osmotic pressure are now incorporated in the system.

Chapter 8 - Nomenclature

V	Volume
P	Pressure
N	Number of particles
R	Gas constant
Qc,Wc	Cooling power
θ	Angle of crankshaft
r_p	Pressure ratio
m_x	Mass in the x-volume
Dm_x	Mass difference in the x-volume
gA_{xy}	Mass flow between x and y volumes
COP	Coefficient of performance
x	Helium 3 concentration

Chapter 9

Superfluid Stirling Refrigerator 3D CFD

The superfluid Stirling models that have been provided thus far are able to describe the phenomena and provide an adequate understanding of the cooling power and efficiency of the system. Despite this, as it can be understood, being models in a single dimension they can never provide a full representation of the system.

To fully understand and validate the results of the modelling of such cryocoolers all the phenomena need to be incorporated in a simulation. Many phenomena especially considering the fluid dynamics of the system in three dimensions are not able to ever be properly described through an one dimensional model. In models of apparatuses working on higher temperatures empirical mathematical models exist for describing the flow in the regenerators etc, something that is absent in this temperature range.

For this reason, as the final part of the description of the Superfluid Stirling Refrigerator it was designed and simulated in a 3D CFD environment. The chosen software for undertaking such a project has been ANSYS Fluent. This software was chosen for multiple reasons. First of all, a lot of literature and knowledge exists in the design of normal Stirling coolers in ANSYS Fluent, something that was useful in many instances within the project. In addition, when compared to other software like Solidworks, it was seen that the ANSYS Fluent gave the user a greater freedom into introducing parts to the simulations through direct code in C++. That was very important as phenomena of superfluidity would need to be incorporated in the system, something not originally designed by the developers and as such the user interface would not be able to address.

So presented in this part of the study are the workings and the results of an SSR through the ANSYS Fluent CFD modeling software. As in the previous models the core principle of this system is the superfluid phase of Helium 4 at temperatures below the lambda line. The designed superfluid Stirling refrigerator works in the same manner as before, meaning like a typical Stirling cooler with the addition of superleaks at the piston-heads. These superleaks block normal Helium but let Superfluid Helium pass through freely. Again, because only Helium-4, due to their difference in the lambda temperature will be in its superfluid range and be the one passing through the superleaks.

In previous 1D models of other researchers an approximation has been made for simplicity, assuming that the Helium 4 being a superfluid, is totally thermodynamically inert and is of insignificant thermodynamical value to the system, while the Helium-3 is used as an ideal gas. These are assumptions that are addressed in this work and instead of using such simplifications more complete models of Helium are used. In this simulation also instead of a single Stirling engine, again based on the lack of knowledge for the recuperative properties of the material, a dual Stirling machine is designed.

9.1 Description of the 3D system

The designed apparatus is based on the dual cryocooler presented in chapter 8. Since this has been, to our knowledge, the first ever model containing superfluids in a CFD environment a simplified version of the recuperator was designed which consists only of two passages, one accounting for each machine. In designing this recuperator, special care was taken into keeping the volumes and the surface areas unchanged despite the changed geometry of the system. The reason behind choosing a simple over a more complex geometry for the recuperator, which might have provided better results, is that the fluid dynamics of the superfluids are very complex. In the current model a laminar flow was aimed for all of the flows in the recuperator. In superfluid turbulent flow is exceedingly difficult to model as it is described by the existence of quantum vortices, something that at this point was deemed unnecessary to be implemented in the CFD program. The simulated cryocooler is depicted in the figure below.

In schematic 9.1, the different volumes/spaces of the apparatus are shown, with black for the one cryocooler (Machine 1) and red for the other one (Machine 2). To provide an easier understanding of the system and in order to correlate its operation with that of a Stirling cryocooler, each of the two channels of the recuperator are indicated as a regenerator (R-1 and R-2) in this part of the study. In subfigure (b) of 9.1 a view of the front part of the engine, as well as a close view of the recuperator are shown in the two below sketches of Figure 1 (left and right respectively). The heat exchanger next to the expander is the heater, despite that it is of lower temperature compared to the cooler. This is because as for the terms of the cooler's geometry and operation to be in accordance with these of a standard Stirling Engine. Moreover, it can be thought of as describing the heat being drained from the cold box and transferred towards the system. As such, the terms "heater" and "cooler" do not strictly describe the temperatures of the two volumes but whether heat is absorbed from the environment or rejected from the cooler to the equivalent box. A simple design was chosen for the two heaters and the two coolers as their function is not complex. The fluid enters the recuperator from the heater or cooler through a passage.

The geometry of the system is presented in the following table. All the data, such as volumes and wet areas, are the same for the two machines so only one set of geometric data needs to be presented to describe the apparatus.

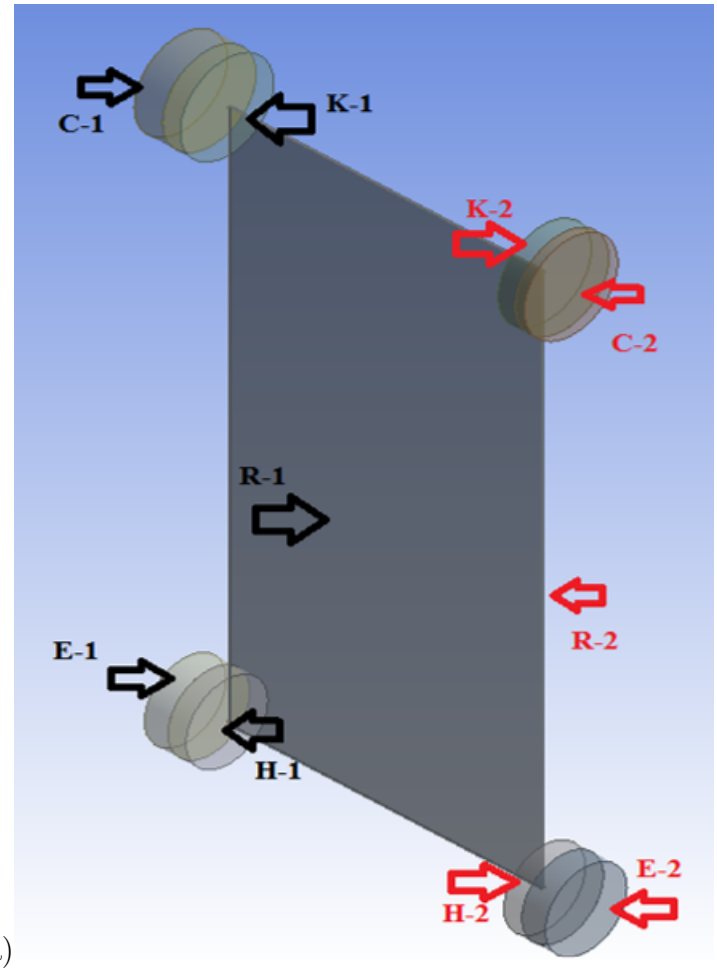

a)

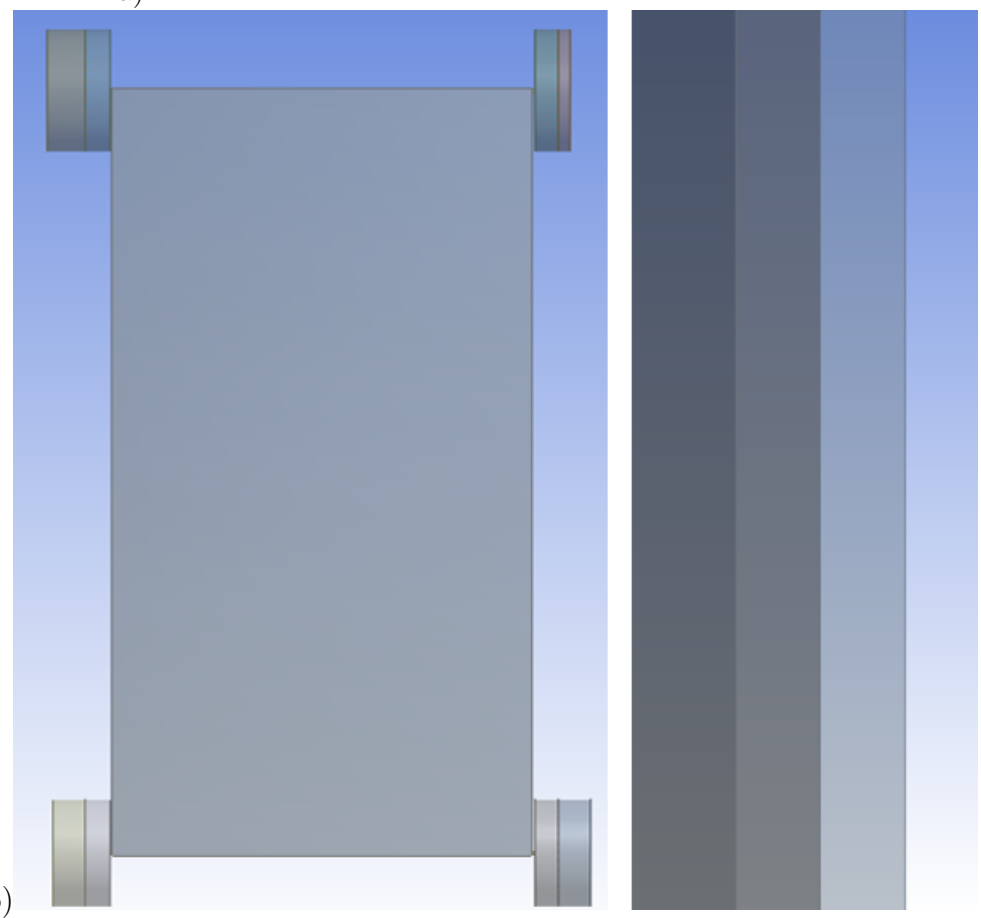

b)

FIGURE 9.1: Design of cryocooler system.

Compressor	
Swept volume	17.74 cm3
Clearance volume	8 cm3
Diameter	47.5 mm
Cooler	
Volume	15.88 cm3
Length	8.9 mm
Heater	
Volume	12.44 cm3
Length	9.1 mm
Expander	
Swept volume	9.39 cm3
Clearance volume	11.62 cm3
Diameter	41.6 mm
Recuperator channel - Regenerator	
Volume	21.18 cm3
Wetted area	101.6 cm2
Length	200 mm
Width	2.38 mm

TABLE 9.1: Geometry of the Stirling refrigerator

The volumes compressor and the expander are obviously changing throughout the cycle. The table above describes their initial values at the start of the cycle. For the values during the cycle the volumes are defined by user defined functions inserted in the system. The UDFs for the different runs of the system are a given in the Appendix E.

For the simplest case of a 180 deg phase difference between the two coolers the volumes are showcased below:

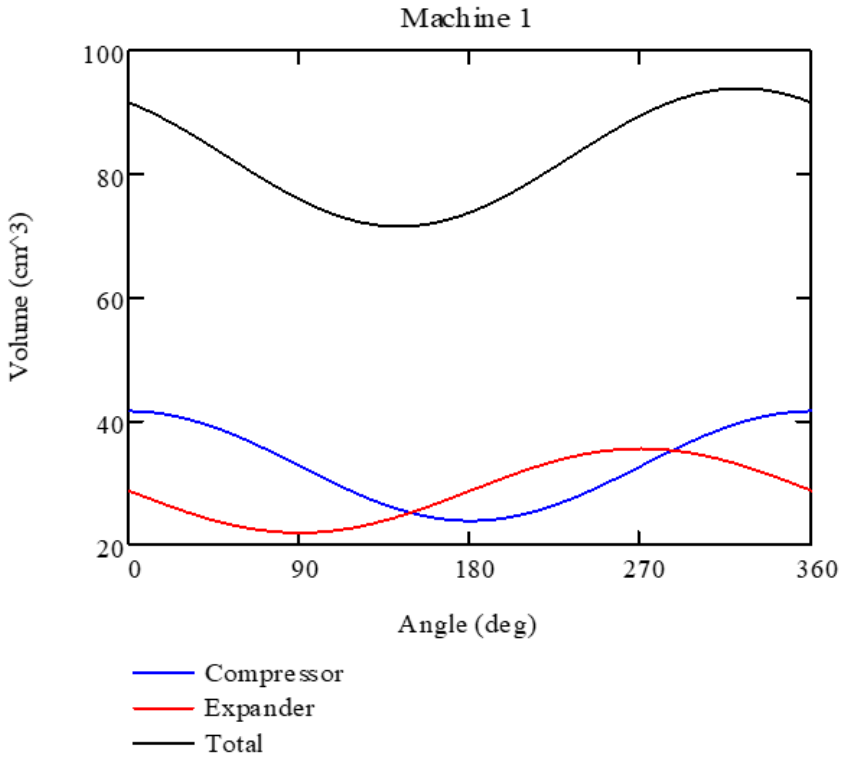

FIGURE 9.2: Volume fluctuations of cooler 1

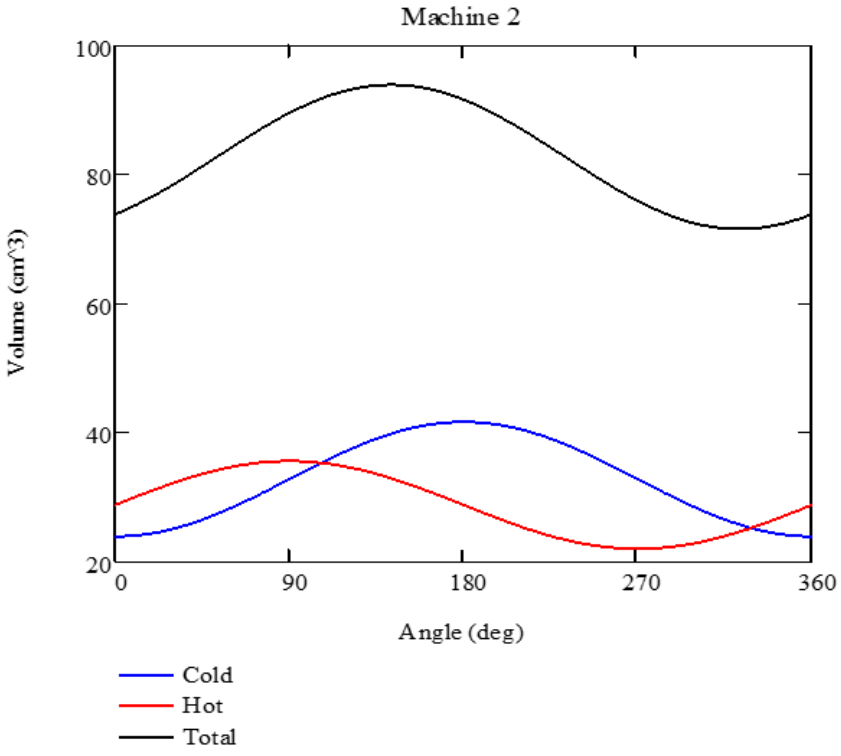

FIGURE 9.3: Volume fluctuations of cooler 2 with 180 deg difference

9.2 Setup and Simulation

To create the mesh of the system some in-built tools of the ANSYS Fluent software were used. By utilizing the different options, it was concluded that the best results are achieved by using the ANSYS Mesh calculator. The used grid consisted of about 4620000 nodes and 972000 elements, as seen in figure 9.4. The grid quality though has improved compared to the first publication of this study in [42], by using hexahedral elements on the pistons and the heaters and coolers, but not limiting the system in the recuperator. This ends up giving a grid quality of close to 84%, improved from the prior 75%. By previous work of the authors Rogdakis et al [94], these numbers are deemed satisfactory to produce noteworthy results.

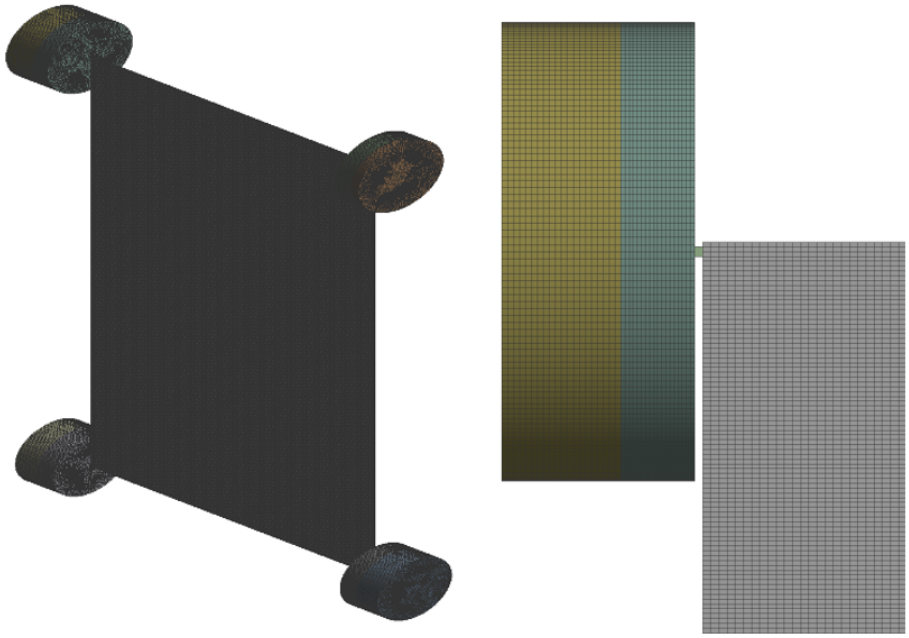

FIGURE 9.4: Generated computational mesh from ANSYS Fluent Mesh generator

The designed cooler of the simulation runs at a frequency of 1 Hz, or 60 rpm. In most of the CFD simulations related to Stirling Engines a turbulent model is suggested, due to the turbulent flow even at relatively low rotational speed [85]. However, as the operating frequency is very low in conjunction to the extremely low temperatures and the simplicity of the geometry the laminar model was selected. The high temperature of the cycle as before is Tk=1K and the low Th=0.4K. For the adjacent walls of the heat exchanges are set to have constant temperatures in the program equal to Tk and Th respectively. In order for the wall temperatures to be constantly in the desired values, external convection is applied to the system. The temperature of the respective freestream is equal to the desired temperatures (0.4 and 1 K for heaters and coolers respectively). A heat transfer coefficient of a large value is implemented between the heat exchanger wall and the external freestream (103-104 W/(m2·K)) for the temperature to steady. In addition, because of the cryogenic low temperatures the default properties for the working gas of the program cannot be applied. The viscosity, conductivity of He-3 was obtained by [71]. As for the heat capacity and the density tables created by the EOS defined

in chapter 6 were inserted in the program. All the solid parts (walls) we defined to be made of a Kapton Epoxy composite. The properties of Kapton and Epoxy in the studied temperatures were as previously defined by the values by [88] and [89]. Each cycle is divided in 5760 timesteps. This means that every degree of crank angle is divided into 16 timesteps. The timestep size is equal to 1.736E-04 s. Based on the work of Rogdakis, Bitsikas et al[94] it was deemed that smaller timesteps lead to faster convergence and more accurate solutions. Because of the low frequency, each cycle is divided in a high number of timesteps so that the timestep is kept to a small value. Results were obtained every 0.5 deg. The data, along with parameters related to the simulation are listed in the table below.

Model		Laminar
Freezing freestream temperature		0.4 K
Cooler freestream temperature		1 K
Frequency		1 Hz
Solver Type		Pressure-Based
Algorithm (Pressure-Velocity Coupling)		SIMPLE
Spatial Discretization	Gradient	Least Squares Cell Based
	Pressure	Second Order
	Momentum	Second Order Upwind
	Turbulent Kinetic Energy	First Order Upwind
	Turbulent Dissipation Rate	First Order Upwind
	Energy	Second Order Upwind
Time Step Discretization		Second Order Implicit
Residuals	Continuity	5E-04
	X-velocity	5E-04
	Y-velocity	5E-04
	Z-velocity	5E-04
	Energy	1E-08
	k	1E-03
	ϵ	1E-03
Number of time steps per cycle		5760
Time step		1.736E-04 sec
Iterations per time step		100

TABLE 9.2: Solution parameters

9.3 Optimization of the calculating procedure

The first runs for this case closely followed the initial trials presented in [42]. In these first runs a large number of steps and iterations had been chosen as to assure that the machine would be described and calculated for in enough detail. Each 360° cycle was decided to be divided in 5760 timesteps of 1.736E-04s each, with 100 computing iterations per time step. This setup, while it provided results very close to the expected ones from the 1D model, was extremely time consuming. Thus, for faster convergence of the steady state multiple initializations during different stages (leading to uncertainties about how many cycles would occur before the steady state would have been reached in a fully

simulated scenario) as running many cycles would be all but impossible due to the very time-consuming calculations. For this reason, now that many cases needed to be run, since accurate results existed from the full-scale time-consuming computation, it was decided that the calculating procedure ought to be optimized and made a faster. The mesh was initially changed but it was quickly seen that any simplification in the meshing would directly result in the divergence from the previous results and loss of mesh quality. Thus, the iterations and timesteps were investigated. Firstly, the convergence per iteration was studied and it was seen that typically 5 to 10 were enough to reach a convergence of more than 99% per timestep, therefore 10 timesteps were used for all calculations afterwards. Secondly the timesteps were the final part to be investigated. The variation of the timesteps, especially considering the changes in the speed of the machine that are going to be run in the different cases, had to be investigated per case, as to achieve both adequate convergence with the previous results but also make sure that as the speed is increased no negative volumes occur in the mesh causing the program to crash. Therefore, the timesteps used where from 10E-03 s to 5E-03s with the number of timesteps ranging from 500 to 2000 depending on the Hz of the case as to make sure that multiple cycles are computed, enough to reach the steady state of the system. Overall, this procedure provided results that were almost directly identical to the initial setup while taking a fraction of the time to compute reducing the overall duration of the calculations by over 80%.

9.4 Results and Phase difference optimization

The aforementioned model has been run for different phase differences in order to study the behavior and outcomes of the cycle and cross-validate the results of the 1D model for the optimal phase difference.

9.4.1 Case - 180 deg phase difference 1Hz

This is the initial case where the two Stirling coolers run one directly opposite of the other. This symmetry of the cycle though can be seen not to be directly translated to the mass flow or the mean pressure plots. The volumes of the different regions of the cooler as found as:

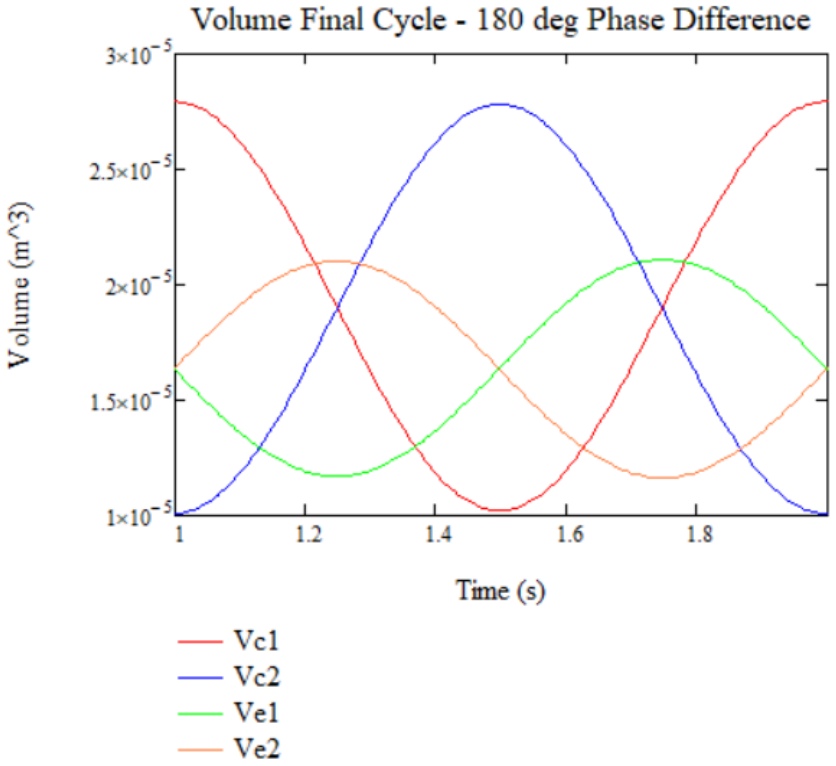

FIGURE 9.5: Volumes for 180 degree phase difference

The mean pressure of the system is:

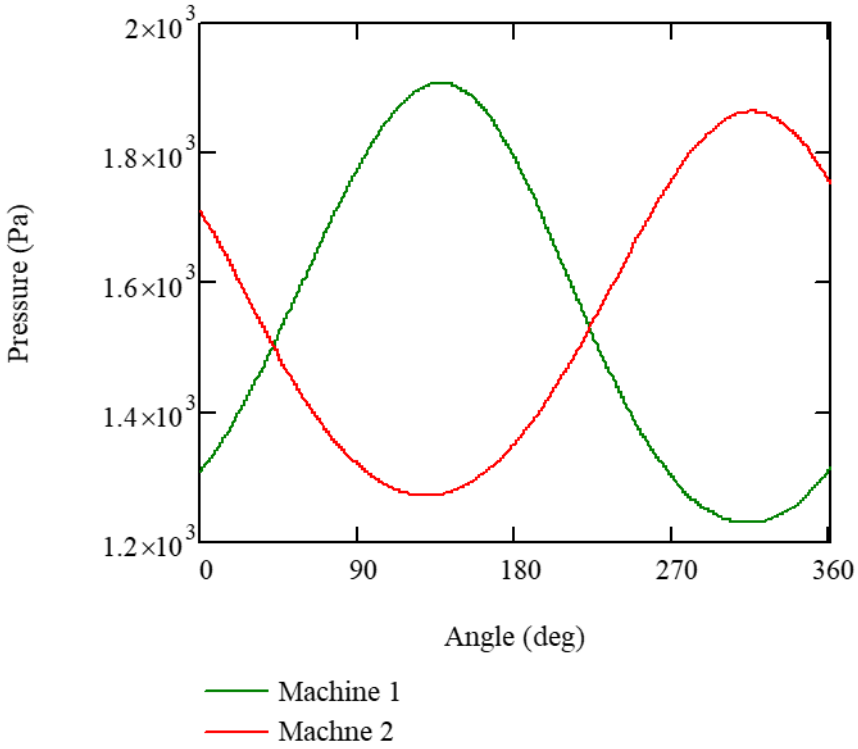

FIGURE 9.6: Mean pressure for the two coolers for 180 deg phase difference

While the pressure for the different part is:

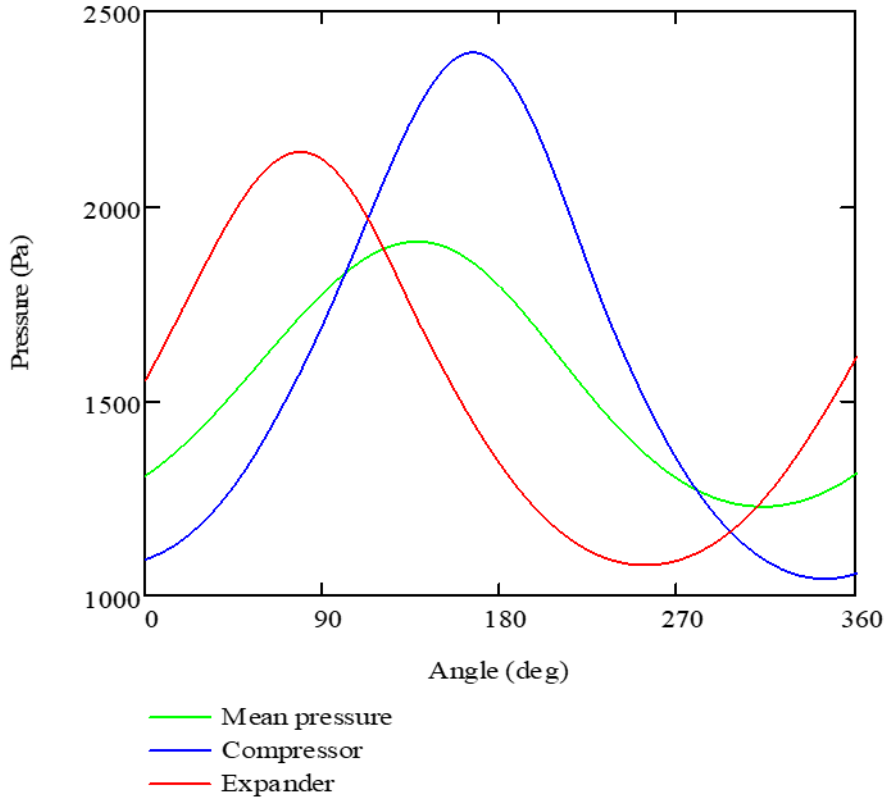

FIGURE 9.7: Pressure for the different volumes of cooler 1 for 180 degree phase difference

In addition to the pressure the pressure drop is also found for the run of the system.

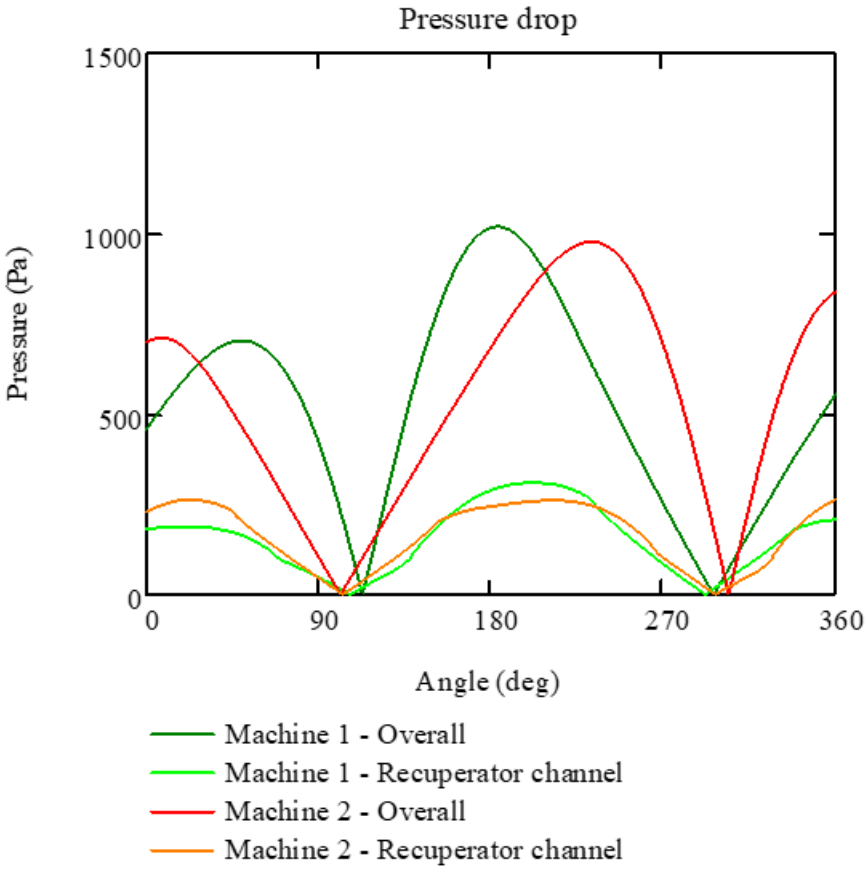

FIGURE 9.8: Pressure drop for 180 deg phase difference

The temperatures of the system can be seen to have a similar behavior to the 1D adiabatic example.

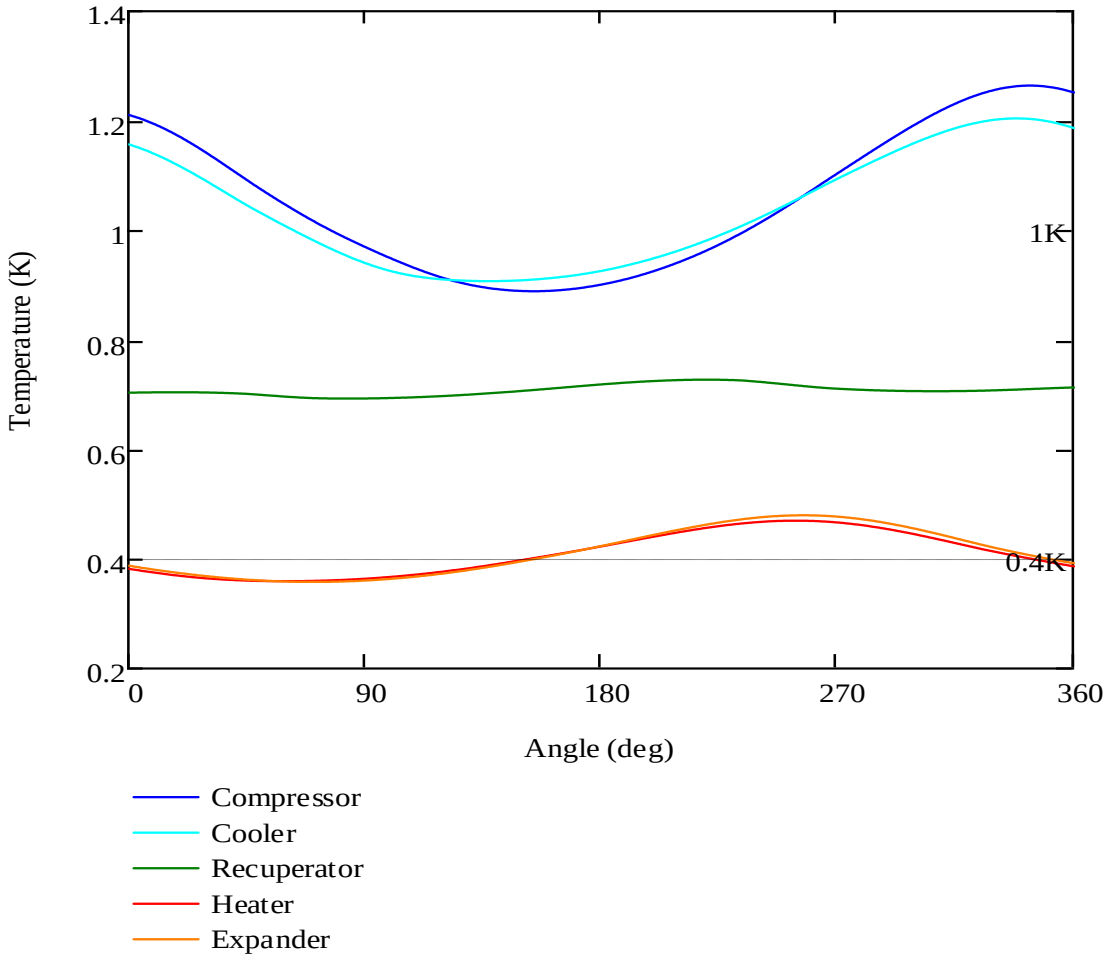

FIGURE 9.9: Temperatures of the apparatus for 180 deg phase difference

To understand the behavior of the system probably the most important values to look at on each of the cases is the mass flows. The mass flow for this plot can be seen as:

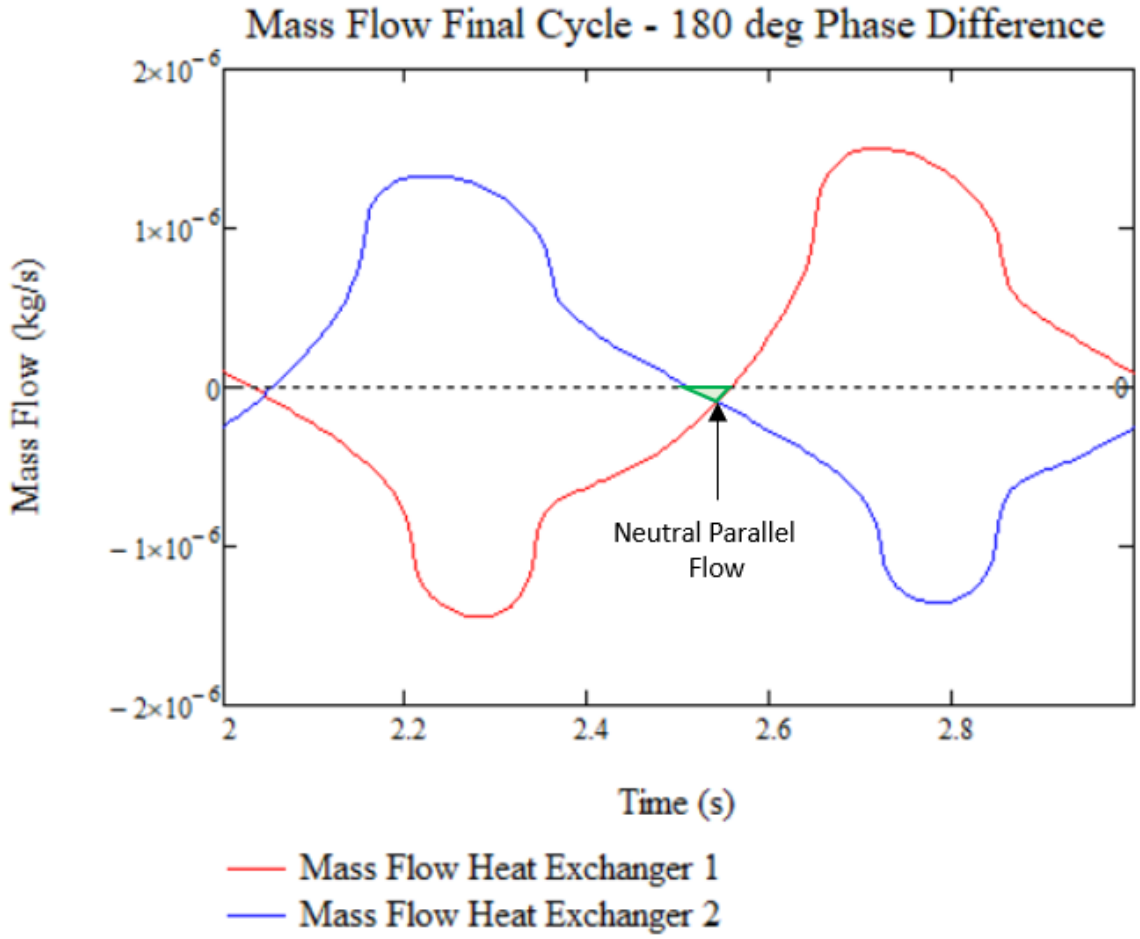

FIGURE 9.10: Mass flow rate in the recuperator for 180 degree phase difference

As it can be seen from this graph no destructive parallel flow occurs a result similar to the one of the 1D model.

The machine is seen to be converging after the first cycle and by getting the energy data from the program the cooling power and efficiency can be calculated.

$$COP(180deg, 1Hz) = \frac{Q_h}{W_{tot}} = 25.88\% \tag{9.1}$$

9.4.2 Case - 140 deg phase difference 1Hz

0.005s timestep duration, 1600 timesteps

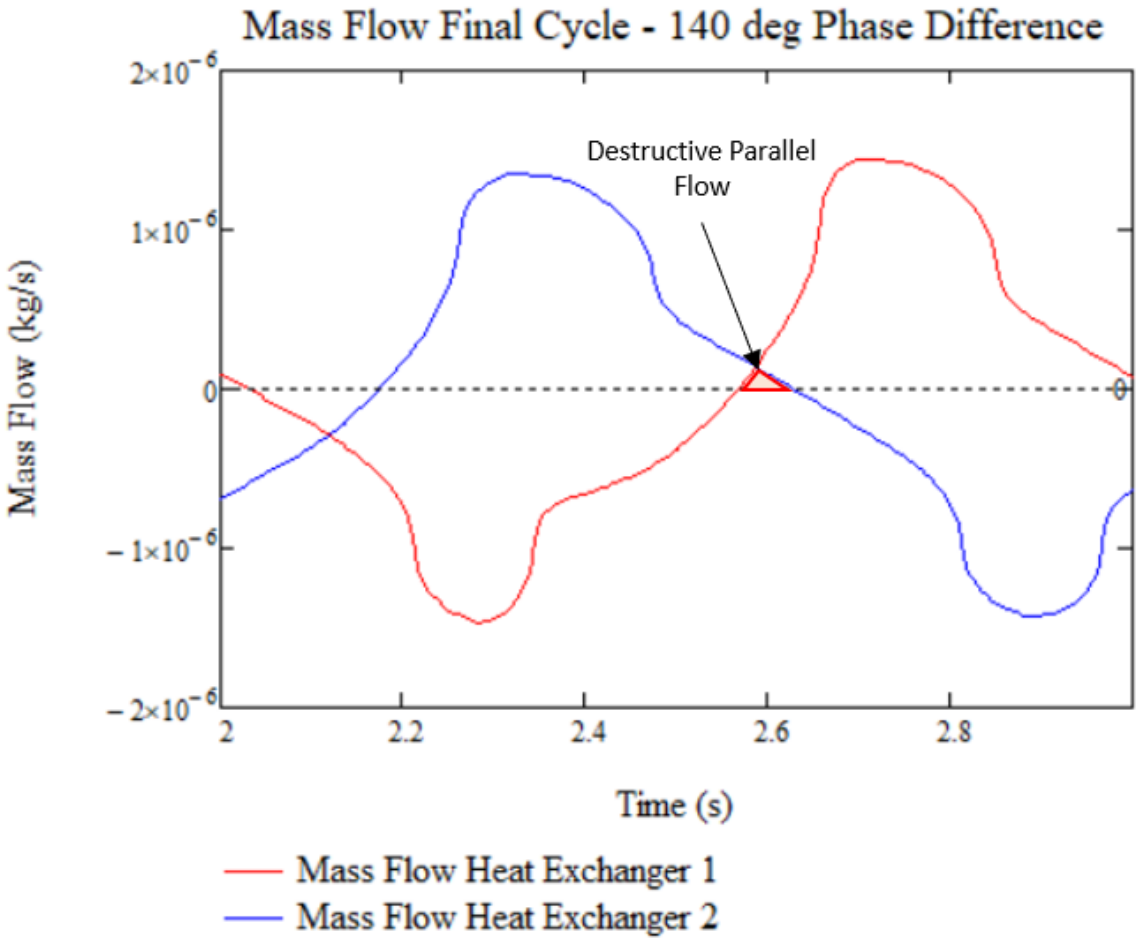

FIGURE 9.11: Mass flow rate in the recuperator for 140 degree phase difference

In this case, as it is expected from the 1D previous simulation destructive parallel flow occurs in the cycle and therefore the COP is expected to be much lower, as it is the case:

$$COP(140deg, 1Hz) = \frac{Q_h}{W_{tot}} = 11.2\% \tag{9.2}$$

This difference is to be expected as near the 2.6s point it can be seen that both flow rates are positive, meaning that the fluid in both coolers is moving from the hot side to the cold side and dumping ll the heat in the cold box, canceling a great part of the overall cooling power of the cycle.

9.4.3 Case - 152 deg phase difference 1Hz

0.005s timestep duration, 1600 timesteps.

In this scenario the 152 deg phase difference is checked. This particular case is checked as in the 1D simulation it was shown that at 152 deg phase difference the optimal COP appeared.

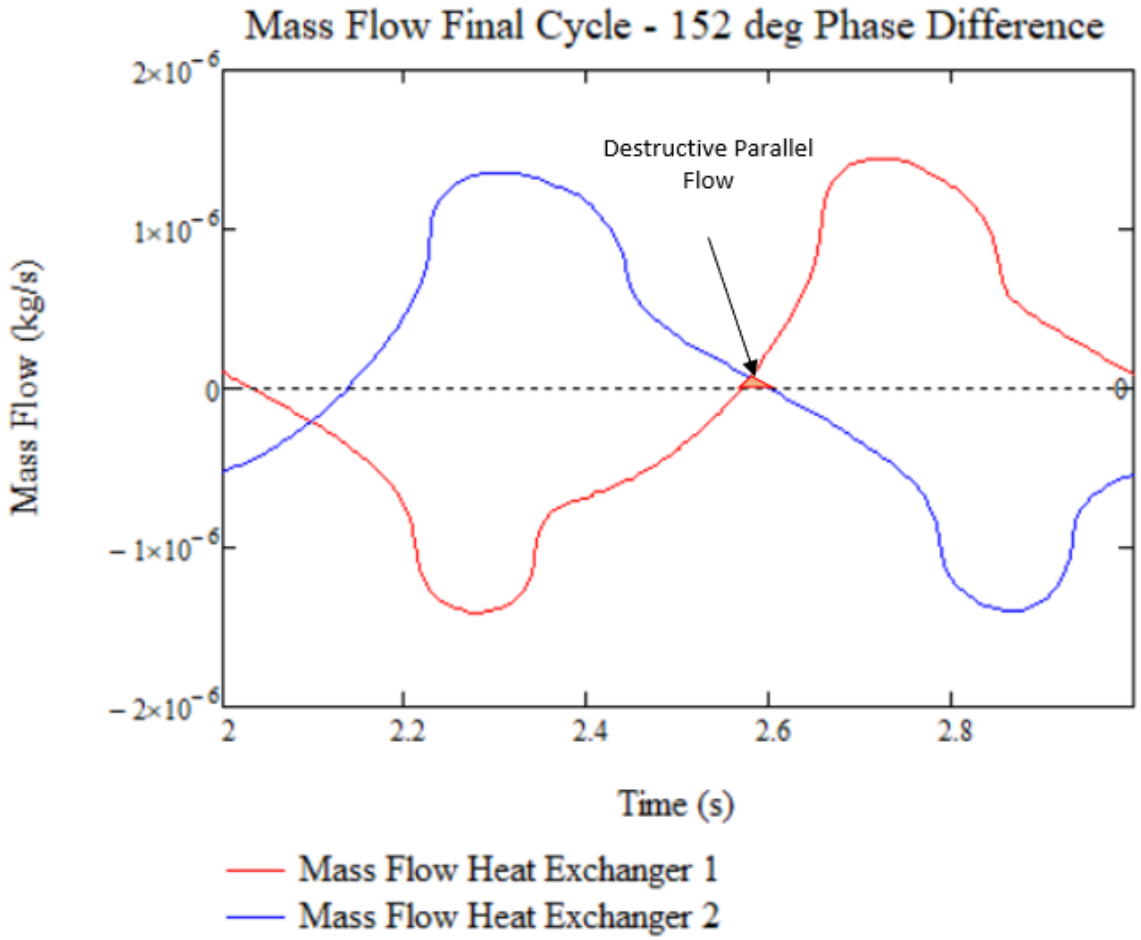

FIGURE 9.12: Mass flow rate in the recuperator for 152 degree phase difference

In the 3D simulation of this phase difference it can be seen that the behavior of the cycle is much better than the previous one of 140 degrees but in this cycle as well a very small amount of destructive parallel flow is detected again around the 2.6s point. This time the value. In this case the parallel flow is small enough that the system produces an adequate amount of cooling power despite this, but as it will be shown in the next cases when no parallel flow occurs the cooling power and efficiencies are even higher.

$$COP(152deg, 1Hz) = \frac{Q_h}{W_{tot}} = 26.4\% \tag{9.3}$$

9.4.4 Case - 160 deg phase difference 1Hz

0.005s timestep duration, 1600 timesteps

The next case of 160 deg phase difference raises the phase difference a bit to try and completely block any formation of the destructive parallel flow.

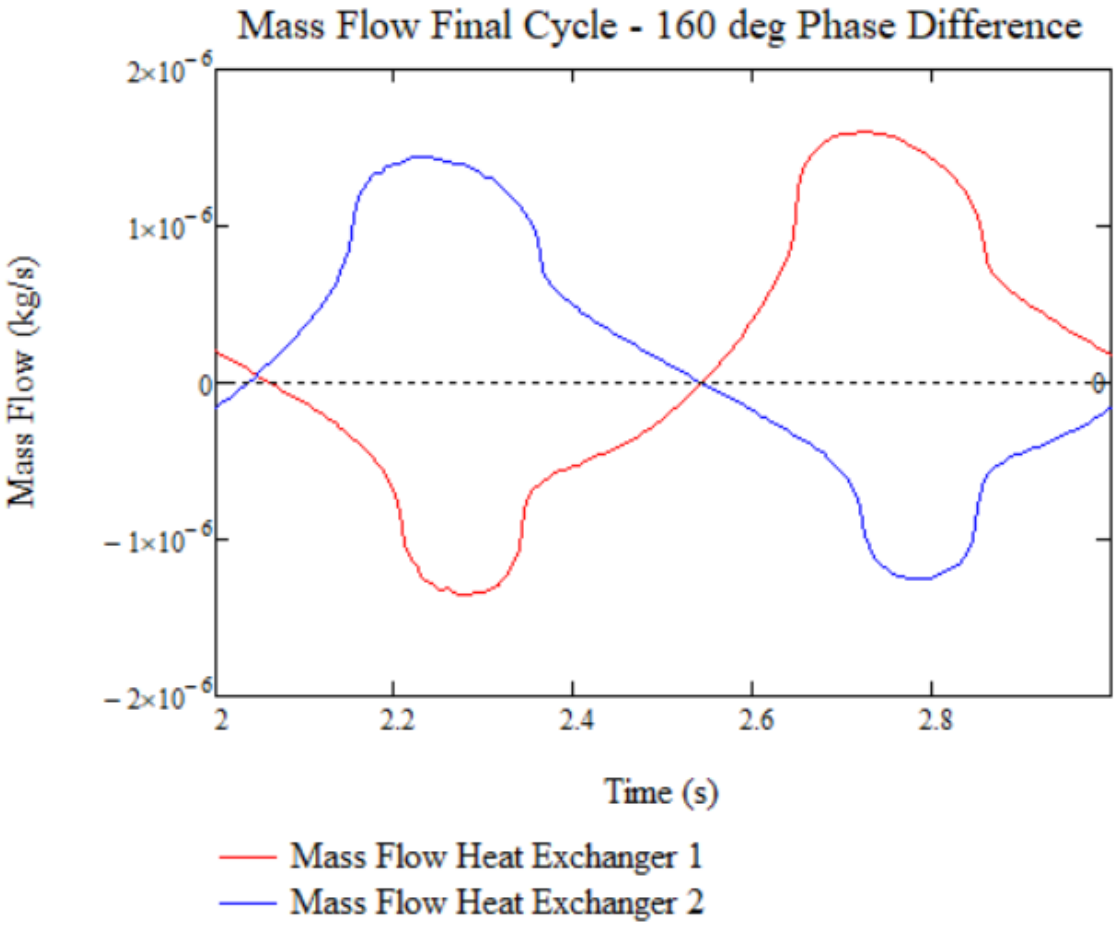

FIGURE 9.13: Mass flow rate in the recuperator for 160 degree phase difference

In this case it can be seen that absolutely no parallel flow occurs and therefore the cooling potential and the efficiency are seen to be greater than the previous cases.

$$COP(160deg, 1Hz) = \frac{Q_h}{W_{tot}} = 30.2\% \tag{9.4}$$

9.4.5 Case - 200 deg phase difference 1Hz

0.005s timestep duration, 1600 timesteps

When recalling on the behavior of the COP in the 1D model one remembers its parabolic behavior, centered around the 180 deg mark. As such, cases with phases difference higher than 180 deg need to also be checked.

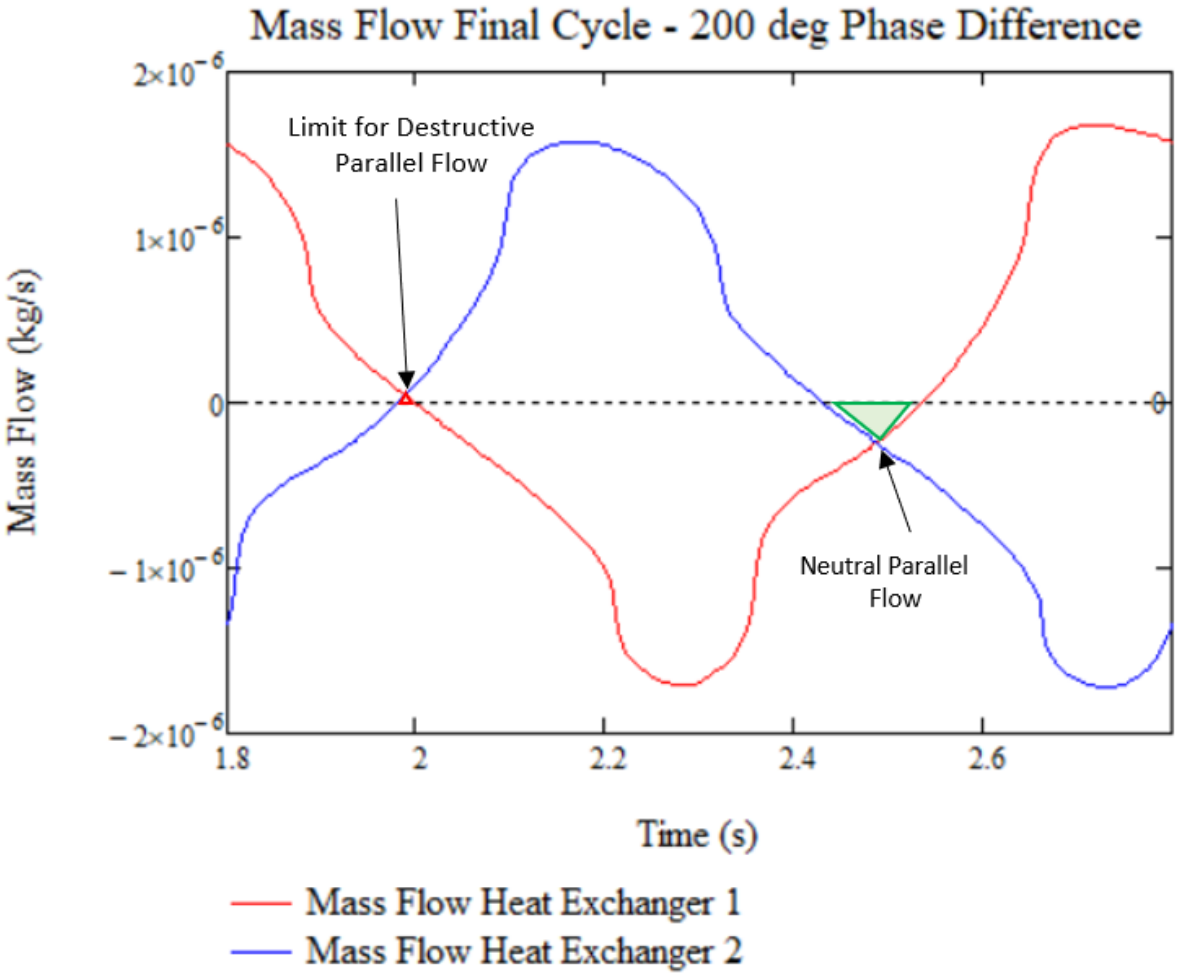

FIGURE 9.14: Mass flow rate in the recuperator for 200 degree phase difference

In this case it can be seen that neutral parallel flow occurs in the system.

$$COP(200deg, 1Hz) = \frac{Q_h}{W_{tot}} = 29.8\% \tag{9.5}$$

Through the calculation of the efficiency in this case one can clearly see that the effect of the nuetral parallel flow in the system is minimal.

9.4.6 Phase optimization results

Through the presented plots above one can see that the 180 deg phase difference produces a low overall efficient but as one too far away from it, where destructive parallel flow occurs. Thus, the parabolic trend keeps hold in the 3D simulation as it can be seen through the graph and the table below. Two differences here that ought to be mentioned between this model and the 1D simulation. The limits for the avoidance of the destructive parallel flow are smaller, from 152 to 160 deg and from 209 to 200 deg. Additionally, the efficiencies are quite a smaller than the 1D model. These differences are to be expected as in a 3D simulation all effects that have to do with the fluid dynamics and heat transfer are being calculated and accounted for, rather than the limiting view, or complete inability to predict in some cases, through the 1D model. Overall, the fact that the same type of curve for the COP arises is a result that is satisfactory as both models converge to it.

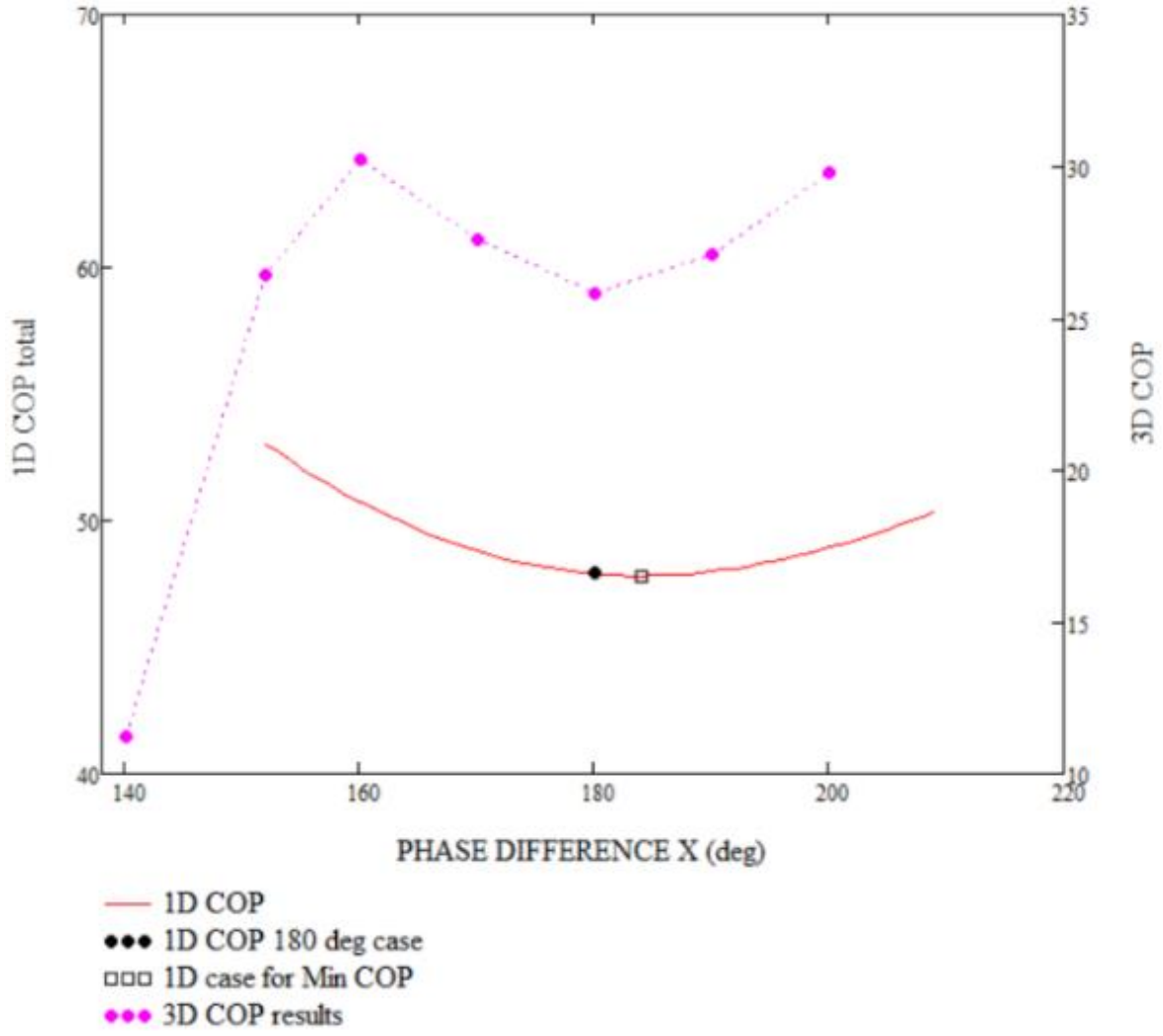

FIGURE 9.15: Comparison of the 1D results (red line and black dots) to the 3D results (purple dots) for the COP to the various Phase differences

Phase Difference (deg)	COP (%)
140	11.2
152	26.4
160	30.2
170	27.6
180	25.8
190	27.1
200	29.8

TABLE 9.3: Phase difference to COP values

9.5 Operational speed optimization

After finding the optimal phase difference for the 3D model, the next step of this study of the model is to evaluate rotation speed which the Stirling cooler is most effective at. For doing this, one has to take into account multiple criteria when calculating the different cases. First of all, as the speed increases, the system will behave closer to the adiabatic model instead of the isothermal, since generally with the increase of speed in Stirling engines one tends more to the adiabatic model than to the isothermal [84]. In the CFD model this is not an issue as, through the way that the system is modelled, its behavior is based on the adiabatic model from the beginning as seen in figure 9.9, where the standard adiabatic behavior is displayed, similar to 8.5 but with a higher temperature fluctuation.

This fact in most cases only has an impact on the COP of the cooler because of the different heat transfer in the heater and cooler, but in our case a more serious consideration arises. Helium 4, which is the bulk of the Helium in the machine, is said to be fluid-dynamically inert as a superfluid (meaning non-viscus and in the ground state) and despite being considered non-inert thermodynamically, the code still doesn't account for its fluid dynamics behavior as it is considered to be fully a superfluid. When the temperature gets higher and closer to the lambda line, the quasiparticles of the superfluid begin experiencing noticeable interactions and therefore the assumptions of superfluidity for the entirety of Helium-4 cannot hold true based on eq.3.29, and the whole system thermodynamically, as well as mechanically due to the superleaks, would have to be defined again and redesigned to account for these interactions.

Moreover, one must also be careful when applying the higher speeds as the turbulence might start occurring. If turbulence occurs, its description in the superfluid is increasingly difficult becoming even a point of study among researchers even today, as quantum vortices occur according to [94]. A description of such a phenomenon while theoretically possible, would be very difficult at this point to integrate into a CFD simulation and would add so much complexity that the solution by the program, if at all possible, through such a setup, would be extremely time consuming.

Based on the EOS of Helium-4 that has been presented in this study 3.41, one can see that even with the overreach of temperature from the Tk reaching up to nearly 1.3K, the superfluid ratio is around 95% there. Given the run simulations presented below it was established that in the region of up to 30Hz the temperatures do not exceed the value of 1.4K and therefore the effects of the phonon-roton interaction do not occur. This is because even at 1.4K the superfluid ratio is 94.2% for the given pressure from eq.3.29 and the working medium stays at a temperature range above 1.2K for a very small amount

of the cycle 9.9. For the case studies mentioned below the effect normal fluid part of Helium-II should be easily negligible. For operating speeds above 30Hz this should be checked again as the speed rises and so do the deviations of the temperature.

Moving on, different cases are again going to be simulated in order to find the optimal working speed of the machine regarding the COP as well as power. The previous study has shown the optimal phase difference to be 160 deg, and thus this is the one that is going to be used in the rest of the cases. Due to the different speeds of the pistons now, one has to alter the timesteps and iterations of every case in order to stay clear of negative volumes occurring in the matrix of the program during the evaluations and causing an error.

9.5.1 Case - 160 deg phase difference 2Hz

2Hz, 0.005 s timestep duration, 800 timesteps

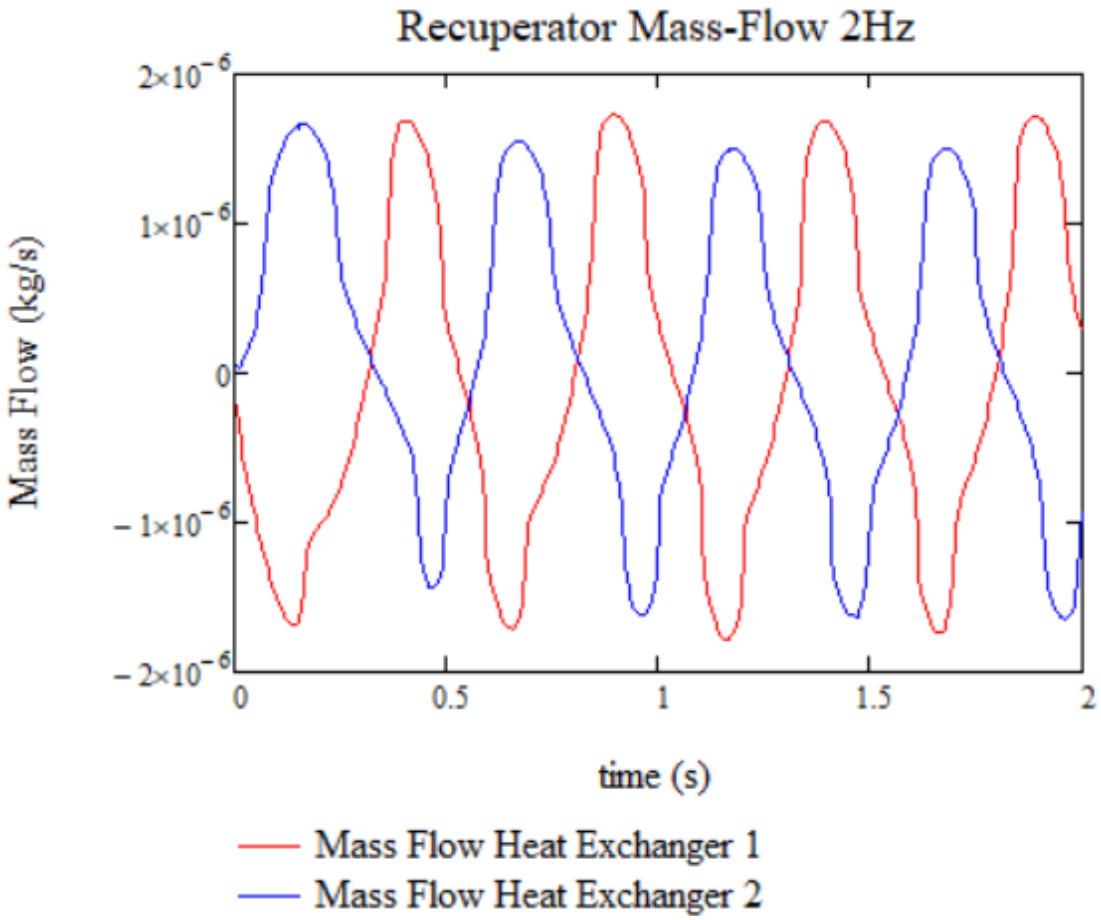

FIGURE 9.16: Mass flow rate in the recuperator for 160 degree phase difference at 2Hz

9.5.2 Case - 160 deg phase difference 10Hz

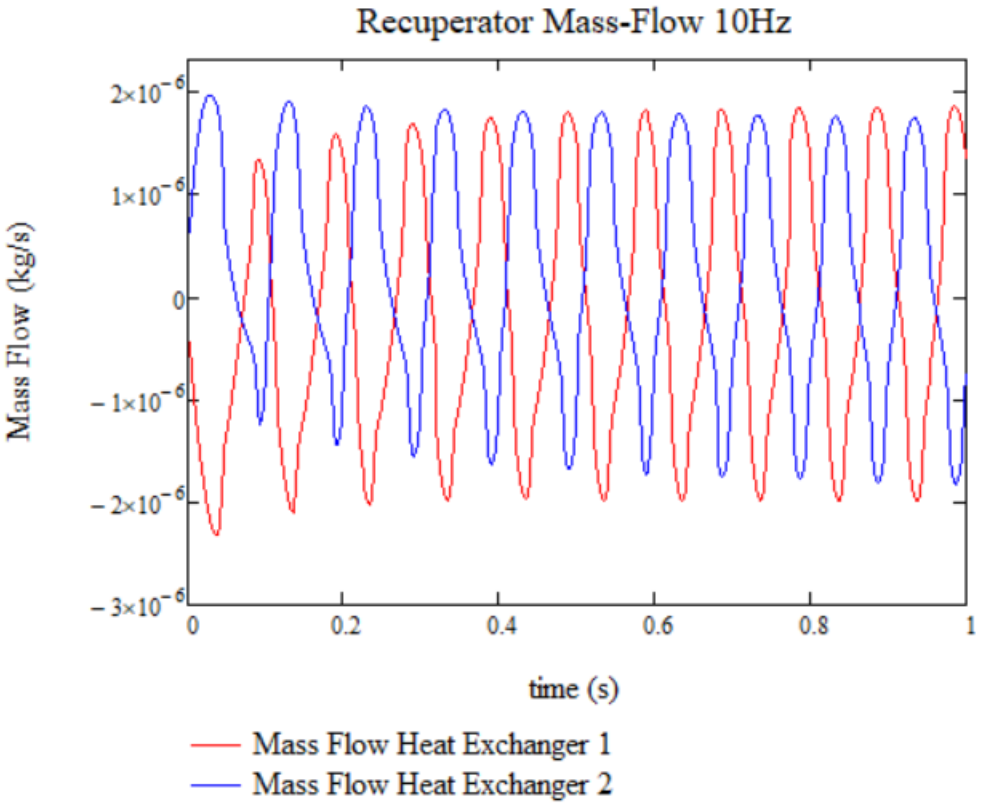

FIGURE 9.17: Mass flow rate in the recuperator for 160 degree phase difference at 10Hz

9.5.3 Case - 160 deg phase difference 15Hz

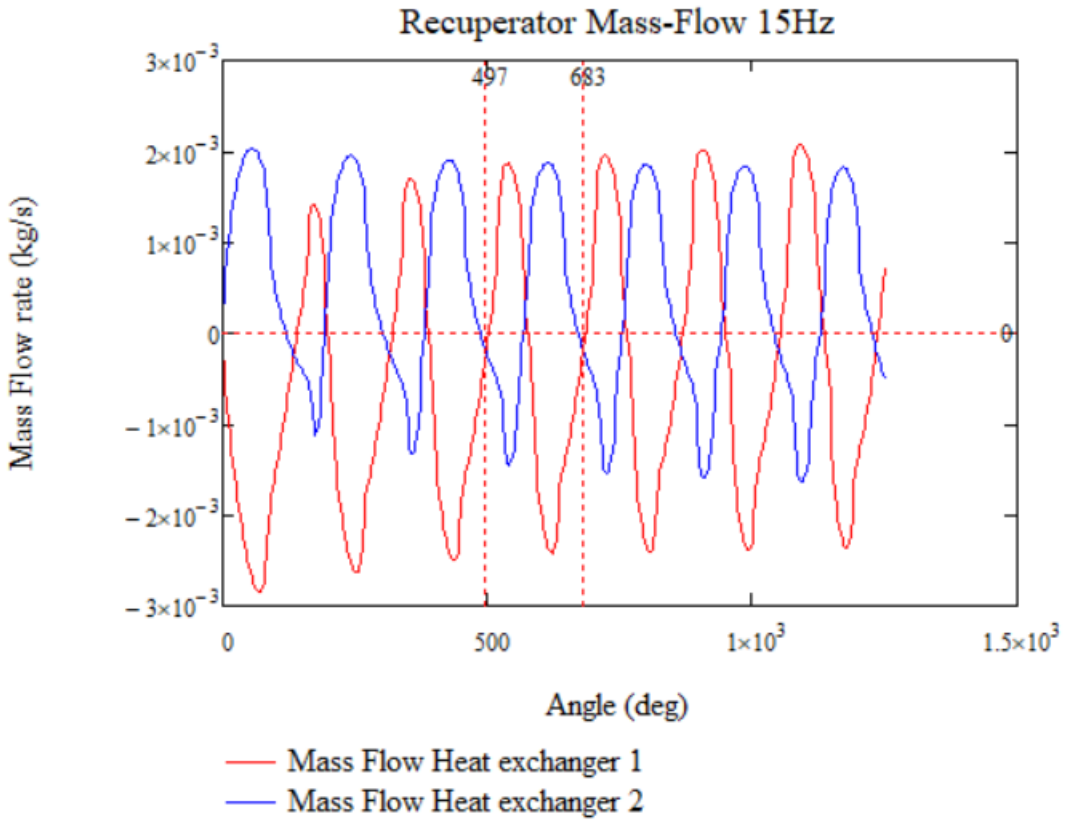

FIGURE 9.18: Mass flow rate in the recuperator for 160 degree phase difference at 15Hz

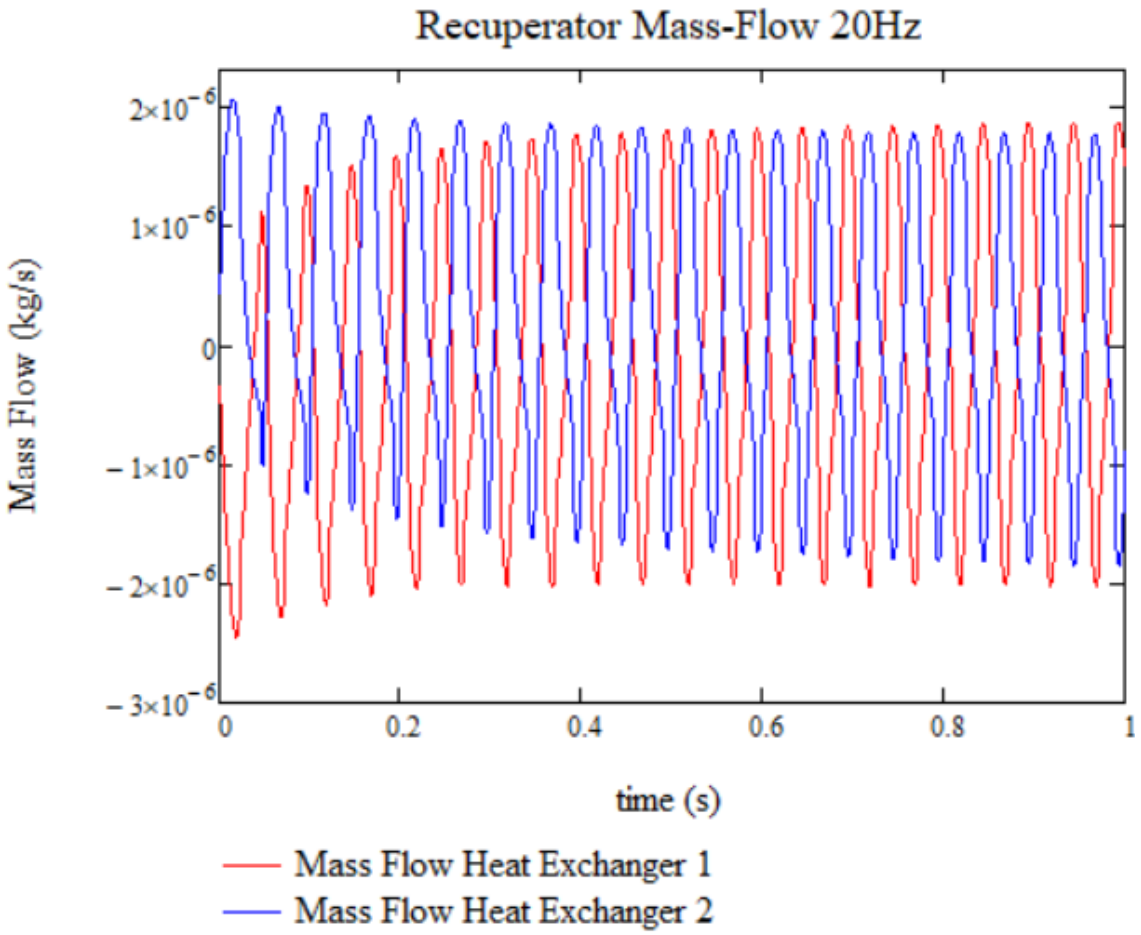

FIGURE 9.19: Mass flow rate in the recuperator for 160 degree phase difference at 20Hz

As it can be seen for the plots showcasing the mass flow of the different cases for the rotational speeds of the coolers the overall apparatus reaches a convergence quite quickly. In fact, one can observe that the convergence of the cycle seems to be always taking place around the 0.5s mark. While the number of cycles differs based on the rotational speed the overall time seems to be relatively constant for the convergence of the system.

9.6 3D simulation overall results

Based on all the run cases now one can observe the overall behavior of this cooler and find the optimum working conditions for it as well as the create the power and efficiency curves.

Speed (Hz)	COP (%)	Cooling Power (mW)
1	30.2	0.542
2	29.7	0.842
5	36	1.569
10	38.2	2.219
15	32	2.086
20	28.1	2.374

TABLE 9.4: Speed COP and Cooling power values for the different cases

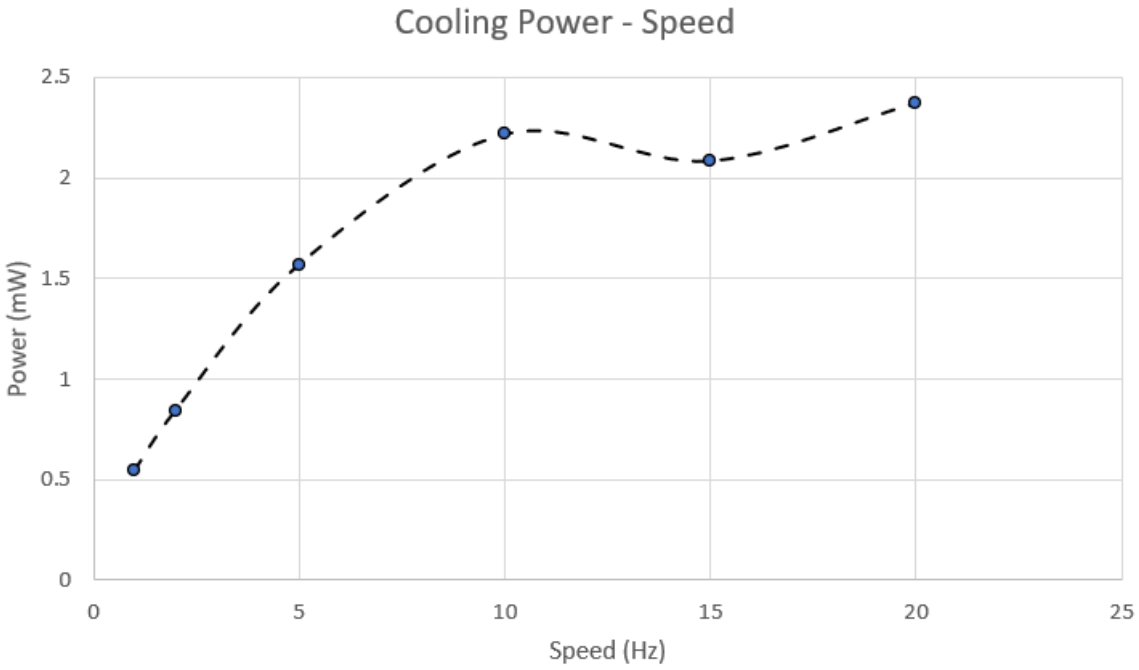

FIGURE 9.20: Cooling power to operational speed plot

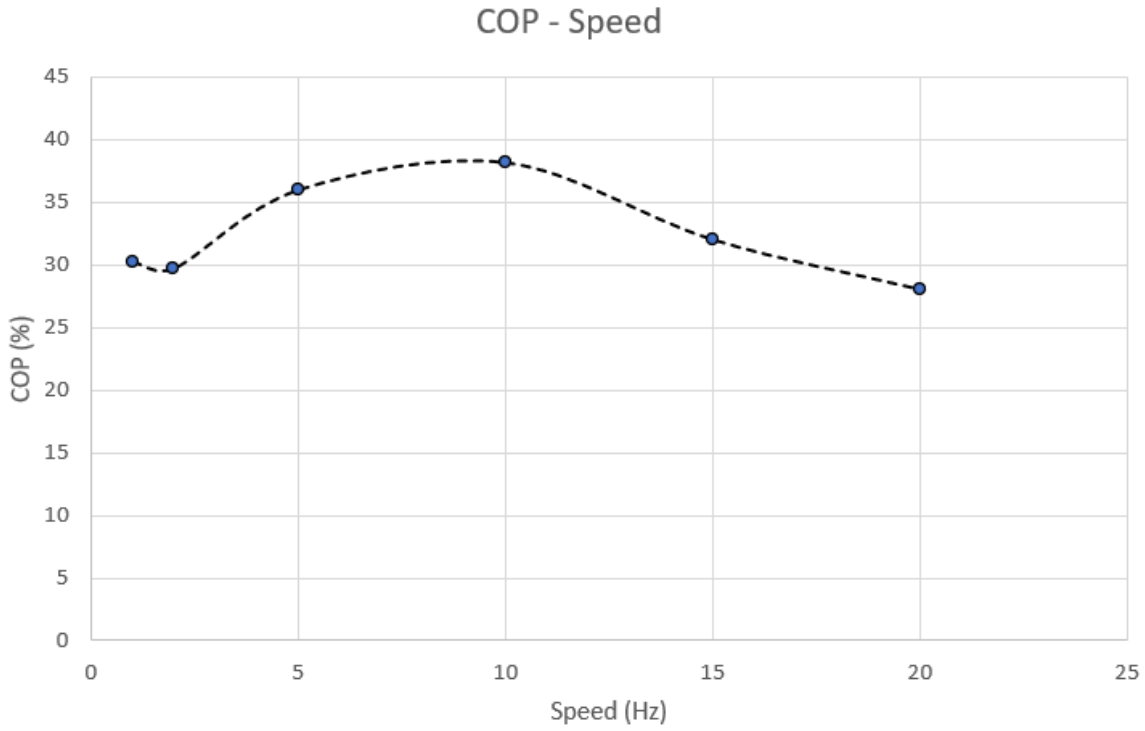

FIGURE 9.21: COP to operational speed plot

From the diagrams above, judging from the COP and power the optimal speed for the cryocooler is chosen to be at 10Hz, where the power is nearly at its maximum value and the COP, seeing it clearly from the trendline, is also at its maximum and decreasing rapidly as one increases the speed. As the COP reaches its maximum value at 10Hz and the power is at almost maximum as well at that speed it was chosen to not increase the operating to more than 20Hz as to also negate the danger of running into turbulent flows which, as mentioned, the current model is not able to simulate.

9.7 Conclusions of the 3D Superfluid Stirling Refrigerator chapter

In this chapter the work for simulating as accurately as possible the superfluid Stirling refrigerator is continued. No 1D model would ever be able to describe all the thermodynamical and fluid behavior in a apparatus. For this reason, it was decided for a full 3D CFD simulation of the system to be undertaken.

The ANSYS Fluent software was chosen to be used for designing and simulating the system. This software was chosen based on its ability to design and solve complex geometries and accept user defined functions used for incorporating the data for the description of the superfluid. To our knowledge currently this work and the publications of the author are the only published simulations of a system in a CFD environment with a superfluid as a working medium.

Over this project, first the geometry was designed and then the mesh and grid of the system were set. Having set the geometry, the moving parts are introduced with the UDFs, as well as the data for the thermodynamics of the superfluid. Additionally, using directly the program's interface, the heat transfer properties of the materials used were introduced.

Running this simulation, the values for the pressures and the temperatures throughout the system were gained, as well as the pressure drops. Overall, by using this data the cooling power and efficiency of the cycle were calculated. Through this scenario it was seen that at a 3D simulation the behavior of the system more closely resembles an adiabatic Stirling behavior than an isothermal one due to the fluctuations of the temperatures at the cooler and the heater.

Thus, a fully working design for the CFD analysis of an SSR was created and its values seem to be in general agreement with the expected ones. Using this design, it was decided to run some case studies in order to find the optimal phase difference and working conditions of the machine.

For doing this, firstly, different simulations were run for the various phase differences between the engines. The results of these runs were in excellent agreement with the 1D code validating both the parabolic behavior of the efficiency compared to the phase difference and the limits for the destructive parallel flow occurring and canceling out a large part of the cooling potential of the cycle. It was found that the optimal phase difference was at 160 deg, very close to the 152 deg predicted by the 1D model. Afterwards, more simulations were run considering the speed of the cooler. In the available literature all the 1D models that exist run at or near 1Hz. Thus, the initial simulation was also run at 1Hz. Following that it was decided to run the cooler at higher speeds and study its behaviors.

It was seen that at higher speeds it took the system more cycles to converge to a steady state, but it was also observed that the total amount of time needed to reach this steady state remained relatively unchanged in the order of 0.5s. Through these calculations the first Cooling power-to-Speed curve and COP-to-Speed curve of such an engine were produced. It was seen through them that the optimal rotational speed of the cooler is at around 10Hz. This is because at this speed the efficiency is near its maximum and the cooling power is of a value near the maximum, too. The simulations were capped at 20Hz and not moved to higher speeds as to avoid greater fluctuations of the temperatures something that would mean that the phonon-roton interactions would have to be taken

into account and turbulence might start to form in the system. Even so, it is seen through the efficiency to speed graph that the trendline suggests a lowering efficiency value with any further increase of the rotational speed and as such it is expected that even if one were to incorporate the aforementioned phenomena in the system, it would be seen that higher rotational speed would lead to a worse overall performance.

Chapter 10

Innovation Points of the study

This work has been in a large part basic research, as through it a lot of new knowledge was produced in order to bridge gaps in the existing literature and to create applied theoretical physics concepts in never attempted before engineering applications. In the first steps of this research the initial aim was to go through the equations of state for Helium and then using them to dive deeper in the engineering applications. It was quickly discovered, though, that despite the existing work in the study of Helium, the field of Helium cryogenics is not well defined and documented. Superfluidity as a phenomenon, while it is well documented in its macroscopical behaviors and also explained in a microscopical manner, lacks to a high degree a connection of the two. Additionally, when the EOS of the different Helium isotopes and their mixture is concerned, while a lot of knowledge exists, there has been no overall consistent equation of state governing the different phases of Helium, nor a physical statistical model that can be implemented to describe the behaviors of both the fluid and the superfluid. This can be seen even more clearly if one is to look into the literature for the thermodynamic maps at cryogenic temperatures. Despite the many existing EOS of state for the different regions one is not able to find an overall map based on an overall equation of state for either Helium-4 nor the Helium 3-4 mixture. For this reason a very big part of this research was dedicated to creating the needed models and equations and create an overall baseline for working with Helium at cryogenic temperatures.

In particular, the innovation points considering the thermophysical modelling of Helium in this research have been:

- Collecting and analysing all the available data for Helium-4 from the literature, cross-correlating them and developing a full set of reliable and self consistent data covering all the phases of Helium-4 below its liquefaction point.

- Creating an equation of state based on this dataset, which is accurate to a degree much higher than any previously published attempts and able to describe all the phases of Helium-4. This equation of state is consistent with not only the thermodynamic values but also the different derivatives, and therefore able to generate the fundamental equations for Helium-4.

- Using this equation of state to create the first thermodynamic map of cryogenic Helium-4, including properties like the superfluid ratio as for it to be in a useful form for engineering applications. The early stage of the work in the Helium-4 EOS has been presented in the International Cryogenic Engineering Conference - International Cryogenic Material Conference ICEC27-ICMC2018 (An improved Equation of State for Superfluid Helium 4). The later stages of this work containing the full

equation of state and thermodynamic maps have been presented at IMECE2021 and published by AMSE (Continuous Equation of State and Thermodynamic Maps for Cryogenic Helium 4)

- Creating a full statistical model cryogenic Helium-4 and describing the transition to superfluidity through the partition function and entropy giving a thermodynamic and statistical connection between the microscopic and macroscopic view of superfluidity as well as bridging the two-fluid approach with the quasiparticle approach of superfluidity. This work has been presented at IMECE2021 and published by ASME where it received the Edward F. Obert award for an outstanding paper in thermodynamics (Studying the Superfluid Transformation in Helium 4 through the Partition Function and Entropic Behavior).

- Creating a statistical model for superfluidity in Helium-3 by applying the BCS theory of Cooper pairs in conjunction with the entropic approach developed for Helium-4. The final version of the entropic approach to superfluidity of Helium-4 and the application to Helium-3 is published in the Journal of Energy Resourses Technology of the ASME (Thermodynamic Correlation of the Entropy of Bose-Einstein Condensation transition to the lambda points of Superfluids).

- Gathering all the available data for the Helium 3-4 mixture and creating an overall self-consistent dataset. Then based on this dataset a continuous EOS describing all the different phases and phenomena including the osmotic pressure able to be used in high accuracy applications has been created. Using this equation of state the first thermodynamic maps of Helium 3-4 mixtures have been created and published. This work has been presented at IMECE2021 and published by ASME (Thermodynamic Behavior and Equation of State for Cryogenic Helium 3-4 Mixtures)

- Developing a novel physical model for a different approach to supersolidity and describing up to a point the behaviors and the results of experiments claiming to have observed supersolidity in solid Helium. This work has been presented in the International Cryogenic Engineering Conference - International Cryogenic Material Conference ICEC27-ICMC2018 (A different approach at solid and supersolid Helium).

Through the above it can be seen that a considerable amount of basic research has been done and a significant amount of knowledge produced in the area of the thermophysical behavior of cryogenic Helium.

The second part of this dissertation is concerned with applying this knowledge to engineering applications. More specifically, different versions of cryocoolers have been designed and modeled aiming to achieve temperatures as low as 0.3K. The modelling of cryocoolers at these temperatures is an area with limited knowledge especially considering the full simulations, and in most cases grossly simplified models are used to describe them. As such a basic aim of this research has been to produce a model that is much more accurate than the existing ones and describe these cryocoolers to a more advanced degree. Emphasis has been given not only on the final results of the models and the behaviors of the Stirling cryocoolers but also to the in-depth description, understanding and application of different phenomena taking place in the realm of superfluids when applied to engineering applications and models. As such the innovation points and novel ideas and concepts of this research considering the cryocoolers have been:

- Showcasing that at these temperature ranges the isothermal models seem to be converging with the adiabatic ones of the Stirling cycle
- Creating a full model of a superfluid Stirling refrigerator in 1D incorporating the full equation of state of the Helium 3-4 mixture, including the phenomenon of the osmotic pressure at the superleaks.
- Finding the optimal phase difference for the superfluid Stirling refrigerator apparatus and give a thorough explanation through the flows and cooling outcomes of the model. This work has been presented in the IMECE2019 and published by ASME (Thermodynamic modelling of superfluid Stirling cryocoolers).
- Creating the first published 3D CFD simulation of a cryocooler with a superfluid as a working medium. Using the ANSYS Fluent software the Helium 3-4 mixture properties have been introduced to the system and with some key modifications, such as being able to find the concentration of the mixture using the low dependency of the volume on the consistency of the mixture, solving for the full cycle and convergence of the system. This work has been presented in IMECE2019 and published by ASME (Computational Analysis of Cryogenic Stirling Refrigerator).
- Using the ANSYS Fluent CFD software to run different models for superfluid Stirling cryocoolers and finding their optimal working conditions considering the phase difference as well as the rotational speed. Through these simulations the first cooling power-to-rpm and efficiency-to-rpm curves for a superfluid Stirling cryocooler have also been produced. This work is currently under submission for publication (Computational Analysis, 3D Simulation and Optimization of Superfluid Stirling Cryocooler).

Overall it can be seen that also in the area of crycoolers a significant amount of new knowledge has been gained from this research considering not only the direct applications of the models, such as showcasing a very accurate model of a Stirling cryocooler in a CFD environment able to reach temperatures for cooling type-II elemental superconductors or be part of a cryocooler for a quantum computer. Also some very key aspects and methods that one can utilize are showcased in order to work with superfluids as working media in low temperature engineering applications.

Chapter 11

Conclusions and Discussion

After reading this study the reader hopefully will have gained an in-depth understanding about cryogenic Helium, its physics, different phases and its applications as a working medium for cryocoolers. Through the first parts of this study the full equation of state for Helium-4 has been presented. It is seen that during this work equations for the energies of the quasiparticles have been derived that are of a much higher accuracy than the existing ones. All the available data have been interconnected into an overall self-consistent dataset. Based on this dataset a dynamic code for the equation of state is developed, where the provided accuracy is seen to be much higher than any existing equations in the literature and most importantly it covers all the different phases of cryogenic Helium-4.

While researching the behavior of superfluid Helium-4 a full statistical model for the thermodynamic behavior of it as superfluid has been developed. This novel model has given the opportunity to describe the phenomenon of superfluidity macroscopically and also it can be seen to bridge the two existing but separate theories of superfluidity, the two-fluid approach and the quasiparticle approach. Furthermore, as it was seen through this model, the connection between superfluidity and Bose-Einstein condensation has been shown as the lambda transition is seen to correspond with the Bose-Einstein condensation temperature of the theoretical ideal part of the Helium-4. Thus, the general idea stating that superfluidity is a degenerated form of Bose-Einstein condensation is seen to be confirmed in this way as the superfluid is described as an aggregate of a Bose-Einstein condensate part and an interacting part. Also, through this procedure the existence of an interatomic potential at absolute zero is shown confirming the predictions of London.

The same principles are applied to Helium-3, where using a different mathematical model the BCS theory of Cooper pairs is applied first and then the statistical behavior of the ideal and non-ideal parts of the Cooper pair gas are described. Based on this it is shown that the lambda transition of Helium-3 as well, can be predicted through this method and also the R2 universal constant of superconductivity is almost directly predicted, supporting the correctness of the application of this theory in Helium-3. Unfortunately, compared to Helium-4 there is a massive shortage of available data for Helium-3 due to its rarity. Thus, the full thermodynamic analysis of the model considering the entropic transitions cannot be at this point computed. When new data arises, this part of the research will be continued, in order to pursue further knowledge about the applications of the procedure to Helium-3 and if all the phenomena as in Helium-4 are conserved an escalation of this model to a full model for predicting superfluidity can be formed.

Superfluids have been an intricate and controversial area of study with great disagreements between respected scientists considering their workings and physical explanations. This controversiality about superfluidity has subsided as, microscopically, the

phenomenon has been explained in the past decades. An even more controversial issue in the cryogenic community of Helium has arisen in recent years, though, the issue of supersolidity. Supersolidity has been theorised for many years, but has only be proposed to have been experimentally observed in 2004. This experiment has had a great number of doubts placed upon it by members of the cryogenic community, while it has been seen as success by others. During this study a theory about supersolid Helium has been created and was presented by the author in the world's biggest cryogenic conference, causing some controversy there as well, where support was shown by some of the most esteemed scientists in the field, but also reactions saying that the theory is based on a wrong experiment were expressed. The timing was not been in our favor as only a few months after this presentation a new experiment had arisen which further supported the existence of supersolidity. The developed model has been presented in this study but due to the still high controversiality of the issue it was decided to leave the completion of the full model for a later date, when the waters around supersolidity will have settled. It is the opinion of the author that this time is not far, as the results of the latest experiments are such that leave little doubt about the supersolidity. Thus following this dissertation, the author will continue to pursue the explanation of superfluidity as a phenomenon and apply the theory to the results of the latest experiments to establish or maybe even disprove the efficacy of the theory. Thus far, the presented theory of supersolidity stating that a supersolid is formed due to the formation of a superfluid of the vacuums of the crystallic lattice of solid Helium-4 has shown promising results against the data of the 2004 experiment.

Natural Helium as it has been mentioned, consists of the two isotopes of Helium-3 and Helium-4. The two isotopes as it has been seen have vastly different behaviors. Also, they have vastly different natural percentages as well with Helium-4 being massively more abundant. Helium-3 becomes a superfluid at much lower temperatures and as such it is of much greater value for some applications. The number of applications that work with solely Helium-3 as their working medium are few and far between due to its prices. Also, its use as a fuel for nuclear fusion driving this price even higher means that there is a dire need to replace pure Helium-3 as a sole working medium in the cryogenic community. For this reason, mixtures of Helium enriched with Helium-3 are used and especially in applications below the lambda line of Helium-4 are highly dependent on Helium-3 to achieve their cooling power. Thus, in this research a thorough gathering, sorting and correlation of all of the available data for Helium 3-4 mixtures is done in order to develop a full set of equations of state and thermodynamic maps for mixture. This equation of state is not only based on the existing data for Helium 3-4 mixtures but also uses the previously developed equations of state for the pure Helium-3 and Helium-4 isotopes, achieving in this way much greater accuracy to the real values compared to other existing equations, while it is continuous through the various phases of the mixture. Special care was given to make this equation of state usable for simulations and CFD applications, where variables like the superfluid ratio, the chemical potential and the osmotic pressure have been included. Based on this equation the first full set of thermodynamic maps for Helium 3-4 mixtures have been created and published, where it has been presented in this study a sequence of 3D and 2D contour in order to depict a 4-dimensional picture in 2 dimensions.

At that point of the study the equations of state of both the isotopes and the mixture were established as well as the physical behaviors of the different substances. As such the final part of this study could be initiated, where these extended models, very accurately

describing the behavior of cryogenic Helium, could be implemented into applications. The chosen application that this study has focused on has been the superfluid Stirling refrigerator where a full and comprehensive analysis has been presented. The present analysis can also provide invaluable knowledge about how one can handle and model cryogenic Helium and superfluids in general in fluid mechanics simulations and introduce them in computing software like ANSYS or Solidworks.

The first part of the cryocooler simulations has been to follow the footsteps of previous researchers and modeling an 1D single isothermal Stirling cooler with an ideal gas as its working medium. It is the opinion of the author that such a model, while it has been repeatedly published by researchers working on SSRs is deeply flawed and offers little valuable information, as it can be seen when its results are compared to later and much more accurate models of this study. The reason that it has been included in this study has merely been as a starting point, where the initial data could be compared to previous attempts. Following this, the deviations between the adiabatic and isothermal models of a Stirling cooler at these temperatures are investigated where it was shown that very little difference exists between them and as such the isothermal model will be used from that step onward.

Due to the lack of the data for the regenerative properties of the materials at such low temperatures a different design of Stirling cooler is used where two opposed Stirling coolers are used connected with a heat exchanger replacing the regenerator. Based on this design models, the SSR's behavior has been presented initiating with the ideal gas model followed by the first published model of a CFD simulation using the full equation of state for the Helium 3-4 mixture. During these models the optimal phase difference has been found as well as the efficiency and the cooling power of each apparatus.

In the last part of the study this simulation was moved even more forward where a full 3D CFD model was designed and simulated in ANSYS Fluent. To our knowledge this has been the first published model of any superfluid ever being modeled in a CFD software. Within this model phenomena that have been previously impossible to describe are shown, for instance the effects of the osmotic pressure and the mixing properties. Also based on this simulation, the first cooling power-to-rpm and efficiency-to-rpm curves have been derived and presented finding the optimal working points for such a cooler.

Overall, it is hoped that the reader will have gained an in-depth understanding about the working of cryogenic Helium and this work can serve as a reference point for equations of state, data points as well as methodologies for working with Helium and superfluids in general. Additionally, through the application of the full model of cryogenic Helium to the SSRs hopefully the reader will have a complete understanding of these apparatuses, while in parallel they will have understood how cryogenic Helium and superfluid can be worked with and included in simulations of other applications as well.

Chapter 12

Future work

This being a dissertation focused on basic research, it has countless possibilities for further elaboration and future applications. Some of the key points that are suggested to be followed by anyone reading this research and seeking to move it forward are the following.

- Utilize the partition function method further on Helium-3 and based on the Debye's theory attempt to theoretically describe all the thermodynamic variable of superfluid Helium-3 without the need for experimental data. When experimental data become available verify the results and use this data to produce directly all the thermodynamic values and interatomic potential through the partition function approach as in Helium-4.
- Utilize the partition function method in Helium-4 to find the exact function of the interatomic potential and then try to derive the total energies of the excitations based on both the ideal and non-ideal part as to create the spectrum of energies for the excitations and compare that to the quasiparticle energy spectrum.
- Use the provided equations of states for other types of cryocoolers like dilution refrigerators and attempt to create models that reach temperatures as close to absolute zero as possible by using Helium.
- Create a model for a hybrid Stirling cryocooler where it utilizes a superleak on the cold side, with the heater temperature being below the lambda line, and a standard piston on the hot side with the cooler being just below the liquefaction temperate of Helium, as to be able to cool industrially bought liquid Helium to very low temperatures.

During the latest parts of this research, I have been selected as the lead researcher for NTUA's basic research program (PEVE) through which in the following years all of the above will be addressed. Through this program the aim for the future of this research is to utilize the gathered knowledge from the equations of state and the Stirling cryocoolers to create closed cooling system able to initiate from the temperature of 4K of industrially bought liquid Helium and reach temperatures in the range of 0.001K, used to cool the chipsets of quantum computers, adding a final stage of dilution cooling and a possible Joule-Thomson expansion cooler after the Stirling cryocoolers in order to reach this temperature. Thus, it is seen that this dissertation has provided a very solid foundation and has set the most important points for continuing and applying this knowledge into cryogenic engineering applications at temperatures near absolute zero.

Appendix A

Appendix of Physics of Superfluidity

Bose-Einstein Statistics
The Bose-Einstein distribution function is:

$$f(E) = \frac{1}{Ae^{\frac{E}{kT}} - 1}$$

with f being the probability of a particle having energy E, and A a constant based on the nature of the particles described.

Maxwell-Boltzmann Statistics
The Bose-Einstein distribution function is:

$$f(E) = \frac{1}{Ae^{\frac{E}{kT}}}$$

with f being the probability of a particle having energy E, and A a constant based on the nature of the particles described.

Fermi-Dirac Statistics
The Fermi-Dirac distribution function is:

$$f(E) = \frac{1}{e^{\frac{E-E_F}{kT}} + 1}$$

with f being the probability of a particle having energy E.

Temperature of Bose-Einstein Condensation

Assume an ideal gas obeying Bose-Einstein statistics in a finite closed box. For the volume of the box one can the Hamiltonian:

$$H = \frac{\hbar^2}{2m}\frac{d^2}{dV^2}$$

given this the time independent Schrodinger equation of the particles of the gas will be of the form:

$$H\Psi(r) - V_o\Psi(0) = E\Psi(r)$$

Given the closed nature of the box one assumes the wavefuntions of the particles to be stationary waves, with Dirichlet boundary conditions. Thus, the solution of the differential equation will be:

$$\Psi(r) = \frac{e^{irk_r}}{\sqrt{V}}$$

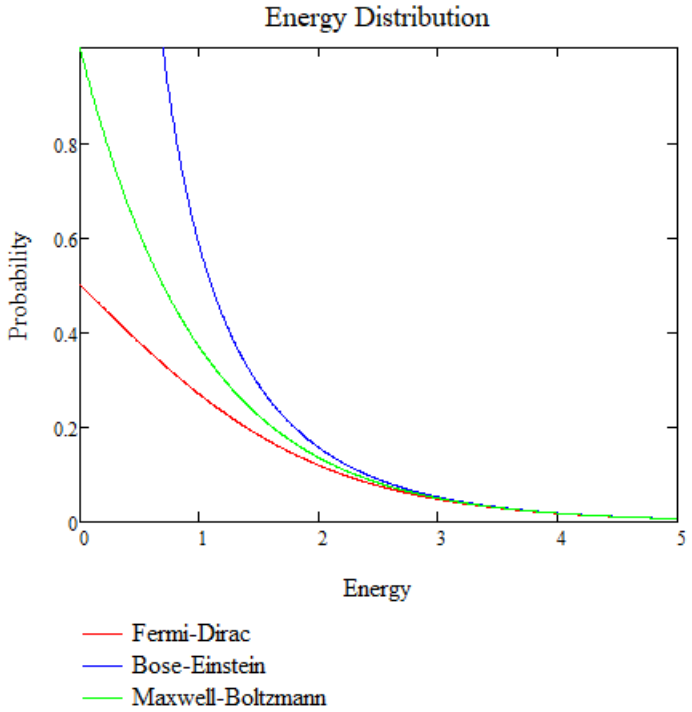

FIGURE A.1: The probabilities for the three distribution functions

with $k_r = \frac{2\pi m}{L}$ (L being the length of the box) and by applying the boundary conditions the energy can be found to be:

$$E_{k_r} = \frac{\hbar^2 k_r}{2m}$$

The Bose-Einstein distribution function for the particles will be:

$$N = \sum_{n=0}^{\infty} \frac{1}{e^{\frac{E_{k_r}-\mu}{kT}}-1}$$

So the thermodynamical limit for the box:

$$N = \frac{V}{(2\pi)^2} \int_{-\infty}^{\infty} \int_{-\infty}^{\infty} \int_{-\infty}^{\infty} \frac{1}{e^{\frac{E_{k_r}-\mu}{kT}}-1} dk_x dk_y dk_z$$

Now assuming the box being spherical the equation above will be transformed into:

$$\frac{N}{V} = \frac{1}{(4\pi)^2} (\frac{2m}{\hbar^2})^{\frac{3}{2}} \int_0^{\infty} \frac{\sqrt{E_{k_r}}}{e^{\frac{E_{k_r}-\mu}{kT}}-1} dE_{k_r}$$

The phase density will:

$$\rho_{ph} = \frac{N}{V} \lambda_T^3$$

with λ_T being the de Broglie wavelength $\lambda_T = \sqrt{\frac{2\pi\hbar^2}{mT}}$. So overall the phase density can be calculated to be:

$$\rho_{ph} = \frac{2}{\sqrt{\pi}} \int_0^\infty \frac{\sqrt{E_{k_r}}}{e^{\frac{E_{k_r}-\mu}{kT}}-1} dE_{k_r}$$

the limit of this phase density for the ideal gas with $\mu = 0$ will be:

$$\rho_{ph} = \frac{2}{\sqrt{\pi}} \int_0^\infty \frac{\sqrt{E_{k_r}}}{e^{\frac{E_{k_r}}{kT}}-1} dE_{k_r} = \zeta(\frac{3}{2})$$

with ζ being the Riemann ζ-function. The number of particles given their distribution will can be written as:

$$N = N_0 + \sum_{n=1}^{\infty} \frac{1}{e^{\frac{E_{k_r}}{kT}}-1}$$

with N_0 the number of particles in the ground state. Thus, using the de Broglie wavelength for a phase density $\rho_{ph} > \zeta(\frac{3}{2})$:

$$N = N_0 + \frac{2V}{\sqrt{\pi}\lambda_T^3} \int_0^\infty \frac{\sqrt{E_{k_r}}}{e^{\frac{E_{k_r}}{kT}} - 1} dE_{k_r}$$

or

$$N_0 = N - V(\frac{mkT}{2\pi\hbar^2})^{\frac{3}{2}} \zeta(\frac{3}{2})$$

The transition to from BEC will happen for the first time (looking through an increasing temperature arrow starting from absolute zero) when not all the particle will be in their ground state. Solving for the temperature, one derives the eq.2.1:

$$Tc = \frac{h^2}{2\pi mk}(\frac{N}{2.612V})^{\frac{2}{3}}. \tag{A.1}$$

Appendix B

Appendix for Helium 4

Table for eq.3.3

1.123408	0.1902787	-0.01761074	0.001091368	-4.59351E-05	1.13375E-06	-1.19834E-08
0.023223	-0.00711	0.003685531	-0.00068585	5.56792E-05	-2.06339E-06	2.86518E-08
-0.10864	0.0304943	-0.0153843	0.002837224	-0.000229825	8.52232E-06	-1.1856E-07
0.233912	-0.056693	0.027787271	-0.00507474	0.000410349	-1.52402E-05	2.1262E-07
-0.26255	0.04906	-0.02397552	0.004381054	-0.000355565	1.3273E-05	-1.86174E-07
0.15944	-0.019591	0.009828061	-0.00181317	0.000148341	-5.5807E-06	7.88448E-08
-0.04973	0.0027587	-0.00153111	0.000288909	-2.39296E-05	9.09228E-07	-1.29554E-08

TABLE B.1: Values for 3.3

B.1 Vapor pressure appendix

Summarizing the work of of Donnelly and Barenghi [32] the equations for the vapor pressure for liquid Helium-4 are given by:

$$a' = \begin{bmatrix} -7.57537 \\ 6.87483 \end{bmatrix} \times 10^{-3}$$

$$b' = \begin{bmatrix} 3.79937 \\ 1.86557 \\ 4.88345 \\ 0 \\ 0 \\ 0 \\ 0 \end{bmatrix} \times 10^{-3}$$

$$m = \begin{bmatrix} -1.26935 \\ 7.12413 \\ -16.7461 \\ 8.75342 \end{bmatrix} \times 10^{-5}$$

$$a'' = \begin{bmatrix} -7.94605 \\ 5.07051 \end{bmatrix} \times 10^{-3}$$

$$b' = \begin{bmatrix} -30.3511 \\ -10.2326 \\ -3.00636 \\ 0.240720 \\ -2.45749 \\ 1.53454 \\ -0.308182 \end{bmatrix} \times 10^{-3}$$

The density at 0 is: $\rho_o = 0.1451397$ and at lambda $\rho_\lambda = 0.1461087$ at $T_\lambda = 2.1768$.

$$\rho(T) = \rho_o + \sum_{i=1}^{4}(m_i T^{+1})$$

$$\rho'(T) = \rho_\lambda + \rho_\lambda(\sum_{i=1}^{2}(a'_i(T - T_\lambda)^i ln(|T - T_\lambda)) + \sum_{i=1}^{7}(b'_i(T - T_\lambda)^i$$

$$\rho''(T) = \rho_\lambda + \rho_\lambda(\sum_{i=1}^{2}(a''_i(T - T_\lambda)^i ln(|T - T_\lambda)) + \sum_{i=1}^{7}(b''_i(T - T_\lambda)^i$$

So according to the work of Donnelly and Barenghi [32] the density of the vapor pressure for the different areas is given by:

$$\rho_{vp} = \begin{cases} \rho_o(T) \times 10^3 \, if \, T \leq 1.344 \\ \rho'(T) \times 10^3 \, if \, 1.344 < T \leq T_\lambda \\ \rho''(T) \times 10^3 \, if \, T_\lambda < T \leq 5 \end{cases} \tag{B.1}$$

Following the isobaric expansion coefficient is calculated as:

$$s = \begin{bmatrix} -0.117818 \\ 1.64045 \\ -6.18750 \\ 13.4293 \\ -11.3971 \\ 1.53454 \\ 2.94176 \end{bmatrix} \times 10^{-3}$$

$$a_o(T) = \sum_{i=1}^{6}(s_i T^i) \tag{B.2}$$

$$\begin{aligned} a'(T) = \frac{-\rho_\lambda}{\rho'(T)}(a'_1 + b'_1 + a'_1 ln(|T - T_\lambda) \\ + (a'_2 + 2b'_2)(T - T_\lambda) + 2a'_2(T - T_\lambda) ln(|T - T_\lambda) \\ + \sum_{i=3}^{7} i \, b'_i (T - T_\lambda)^{i-1} \end{aligned} \tag{B.3}$$

$$
\begin{aligned}
a''(T) = \frac{-\rho_\lambda}{\rho'(T)}(a_1'' + b_1'' + a_1'' ln(|T - T_\lambda) \\
+ (a_2'' + 2b_2'')(T - T_\lambda) + 2a_2''(T - T_\lambda) ln(|T - T_\lambda) \\
+ \sum_{i=3}^{7} i\, b_i''(T - T_\lambda)^{i-1}
\end{aligned}
\tag{B.4}
$$

$$
a_{vp} = \begin{cases} a_o(T)\, if\ T \leq 1.344 \\ a'(T)\, if\ 1.344 < T \leq T_\lambda \\ a''(T)\, if\ T_\lambda < T \leq 5 \end{cases}
\tag{B.5}
$$

B.2 Superfluid EOS code

The code used for create the different variables of the EOS for superfluid Helium-4 is presented below.

The code is written in the computing software Mathcad 15. Two needed functions are defined: $RegN(x, X) = -e^{(interp(RN(X), X^{\langle 1 \rangle}, X^{\langle 2 \rangle}, x)}$ and $RN(X) = regress(X^{\langle 1 \rangle}, ln(-X^{\langle 2 \rangle}), 15)$, with x being the variable, X being the a two column input matrix, with the temperature in the first column and the wanted variable (entropy, enthalpy etc) in the second column. "Regress" is the regression function in Mathcad and 15 stands for a 15th degree polynomial. "Interp" is the Mathcad function that takes the result of "regress" and puts it in an equation form.

The first variable to be describe is the Gibbs free energy as the temperature and the pressure are its natural values and as such it is a fundamental equation.

$$
\begin{aligned}
G(T,P) := \;& tmp \leftarrow linear\left[P, \begin{pmatrix} 0 \\ 2.5 \end{pmatrix}, \begin{pmatrix} RegN(T, augment(T0, G0)) \\ RegN(T, augment(T25, G25)) \end{pmatrix}\right] \text{ if } P \le 2.5 \\
& tmp \leftarrow linear\left[P, \begin{pmatrix} 2.5 \\ 5 \end{pmatrix}, \begin{pmatrix} RegN(T, augment(T25, G25)) \\ RegN(T, augment(T5, G5)) \end{pmatrix}\right] \text{ if } P > 2.5 \wedge P \le 5 \\
& tmp \leftarrow linear\left[P, \begin{pmatrix} 5 \\ 7.5 \end{pmatrix}, \begin{pmatrix} RegN(T, augment(T5, G5)) \\ RegN(T, augment(T75, G75)) \end{pmatrix}\right] \text{ if } P > 5 \wedge P \le 7.5 \\
& tmp \leftarrow linear\left[P, \begin{pmatrix} 7.5 \\ 10 \end{pmatrix}, \begin{pmatrix} RegN(T, augment(T75, G75)) \\ RegN(T, augment(T10, G10)) \end{pmatrix}\right] \text{ if } P > 7.5 \wedge P \le 10 \\
& tmp \leftarrow linear\left[P, \begin{pmatrix} 10 \\ 12.5 \end{pmatrix}, \begin{pmatrix} RegN(T, augment(T10, G10)) \\ RegN(T, augment(T125, G125)) \end{pmatrix}\right] \text{ if } P > 10 \wedge P \le 12.5 \\
& tmp \leftarrow linear\left[P, \begin{pmatrix} 12.5 \\ 15 \end{pmatrix}, \begin{pmatrix} RegN(T, augment(T125, G125)) \\ RegN(T, augment(T15, G15)) \end{pmatrix}\right] \text{ if } P > 12.5 \wedge P \le 15 \\
& tmp \leftarrow linear\left[P, \begin{pmatrix} 15 \\ 17.5 \end{pmatrix}, \begin{pmatrix} RegN(T, augment(T15, G15)) \\ RegN(T, augment(T175, G175)) \end{pmatrix}\right] \text{ if } P > 15 \wedge P \le 17.5 \\
& tmp \leftarrow linear\left[P, \begin{pmatrix} 17.5 \\ 20 \end{pmatrix}, \begin{pmatrix} RegN(T, augment(T175, G175)) \\ RegN(T, augment(T20, G20)) \end{pmatrix}\right] \text{ if } P > 17.5 \wedge P \le 20 \\
& tmp \leftarrow linear\left[P, \begin{pmatrix} 20 \\ 22.5 \end{pmatrix}, \begin{pmatrix} RegN(T, augment(T20, G20)) \\ RegN(T, augment(T225, G225)) \end{pmatrix}\right] \text{ if } P > 20 \wedge P \le 22.5 \\
& tmp \leftarrow linear\left[P, \begin{pmatrix} 22.5 \\ 25 \end{pmatrix}, \begin{pmatrix} RegN(T, augment(T225, G225)) \\ RegN(T, augment(T250, G250)) \end{pmatrix}\right] \text{ if } P > 22.5 \wedge P \le 25 \\
& tmp
\end{aligned}
$$

FIGURE B.1: Gibbs free energy code for superfluid region

Then the entropy is calculated.

$$
\begin{aligned}
S(T,P) := \;& \mathrm{tmp} \leftarrow \mathrm{linear}\left[P, \begin{pmatrix} 0 \\ 2.5 \end{pmatrix}, \begin{pmatrix} \mathrm{Reg}(T, \mathrm{augment}(T0, S0)) \\ \mathrm{Reg}(T, \mathrm{augment}(T25, S25)) \end{pmatrix}\right] \text{ if } P \le 2.5 \\
& \mathrm{tmp} \leftarrow \mathrm{linear}\left[P, \begin{pmatrix} 2.5 \\ 5 \end{pmatrix}, \begin{pmatrix} \mathrm{Reg}(T, \mathrm{augment}(T25, S25)) \\ \mathrm{Reg}(T, \mathrm{augment}(T5, S5)) \end{pmatrix}\right] \text{ if } P > 2.5 \wedge P \le 5 \\
& \mathrm{tmp} \leftarrow \mathrm{linear}\left[P, \begin{pmatrix} 5 \\ 7.5 \end{pmatrix}, \begin{pmatrix} \mathrm{Reg}(T, \mathrm{augment}(T5, S5)) \\ \mathrm{Reg}(T, \mathrm{augment}(T75, S75)) \end{pmatrix}\right] \text{ if } P > 5 \wedge P \le 7.5 \\
& \mathrm{tmp} \leftarrow \mathrm{linear}\left[P, \begin{pmatrix} 7.5 \\ 10 \end{pmatrix}, \begin{pmatrix} \mathrm{Reg}(T, \mathrm{augment}(T75, S75)) \\ \mathrm{Reg}(T, \mathrm{augment}(T10, S10)) \end{pmatrix}\right] \text{ if } P > 7.5 \wedge P \le 10 \\
& \mathrm{tmp} \leftarrow \mathrm{linear}\left[P, \begin{pmatrix} 10 \\ 12.5 \end{pmatrix}, \begin{pmatrix} \mathrm{Reg}(T, \mathrm{augment}(T10, S10)) \\ \mathrm{Reg}(T, \mathrm{augment}(T125, S125)) \end{pmatrix}\right] \text{ if } P > 10 \wedge P \le 12.5 \\
& \mathrm{tmp} \leftarrow \mathrm{linear}\left[P, \begin{pmatrix} 12.5 \\ 15 \end{pmatrix}, \begin{pmatrix} \mathrm{Reg}(T, \mathrm{augment}(T125, S125)) \\ \mathrm{Reg}(T, \mathrm{augment}(T15, S15)) \end{pmatrix}\right] \text{ if } P > 12.5 \wedge P \le 15 \\
& \mathrm{tmp} \leftarrow \mathrm{linear}\left[P, \begin{pmatrix} 15 \\ 17.5 \end{pmatrix}, \begin{pmatrix} \mathrm{Reg}(T, \mathrm{augment}(T15, S15)) \\ \mathrm{Reg}(T, \mathrm{augment}(T175, S175)) \end{pmatrix}\right] \text{ if } P > 15 \wedge P \le 17.5 \\
& \mathrm{tmp} \leftarrow \mathrm{linear}\left[P, \begin{pmatrix} 17.5 \\ 20 \end{pmatrix}, \begin{pmatrix} \mathrm{Reg}(T, \mathrm{augment}(T175, S175)) \\ \mathrm{Reg}(T, \mathrm{augment}(T20, S20)) \end{pmatrix}\right] \text{ if } P > 17.5 \wedge P \le 20 \\
& \mathrm{tmp} \leftarrow \mathrm{linear}\left[P, \begin{pmatrix} 20 \\ 22.5 \end{pmatrix}, \begin{pmatrix} \mathrm{Reg}(T, \mathrm{augment}(T20, S20)) \\ \mathrm{Reg}(T, \mathrm{augment}(T225, S225)) \end{pmatrix}\right] \text{ if } P > 20 \wedge P \le 22.5 \\
& \mathrm{tmp} \leftarrow \mathrm{linear}\left[P, \begin{pmatrix} 22.5 \\ 25 \end{pmatrix}, \begin{pmatrix} \mathrm{Reg}(T, \mathrm{augment}(T225, S225)) \\ \mathrm{Reg}(T, \mathrm{augment}(T250, S250)) \end{pmatrix}\right] \text{ if } P > 22.5 \wedge P \le 25 \\
& \mathrm{tmp}
\end{aligned}
$$

FIGURE B.2: Entropy code for superfluid region

The code for the enthalpy:

$$
\begin{aligned}
H(T,P) := \;& tmp \leftarrow \text{linear}\left[P, \begin{pmatrix} 0 \\ 2.5 \end{pmatrix}, \begin{pmatrix} \text{Reg}(T, \text{augment}(T0, H0)) \\ \text{Reg}(T, \text{augment}(T25, H25)) \end{pmatrix}\right] \text{ if } P \le 2.5 \\
& tmp \leftarrow \text{linear}\left[P, \begin{pmatrix} 2.5 \\ 5 \end{pmatrix}, \begin{pmatrix} \text{Reg}(T, \text{augment}(T25, H25)) \\ \text{Reg}(T, \text{augment}(T5, H5)) \end{pmatrix}\right] \text{ if } P > 2.5 \wedge P \le 5 \\
& tmp \leftarrow \text{linear}\left[P, \begin{pmatrix} 5 \\ 7.5 \end{pmatrix}, \begin{pmatrix} \text{Reg}(T, \text{augment}(T5, H5)) \\ \text{Reg}(T, \text{augment}(T75, H75)) \end{pmatrix}\right] \text{ if } P > 5 \wedge P \le 7.5 \\
& tmp \leftarrow \text{linear}\left[P, \begin{pmatrix} 7.5 \\ 10 \end{pmatrix}, \begin{pmatrix} \text{Reg}(T, \text{augment}(T75, H75)) \\ \text{Reg}(T, \text{augment}(T10, H10)) \end{pmatrix}\right] \text{ if } P > 7.5 \wedge P \le 10 \\
& tmp \leftarrow \text{linear}\left[P, \begin{pmatrix} 10 \\ 12.5 \end{pmatrix}, \begin{pmatrix} \text{Reg}(T, \text{augment}(T10, H10)) \\ \text{Reg}(T, \text{augment}(T125, H125)) \end{pmatrix}\right] \text{ if } P > 10 \wedge P \le 12.5 \\
& tmp \leftarrow \text{linear}\left[P, \begin{pmatrix} 12.5 \\ 15 \end{pmatrix}, \begin{pmatrix} \text{Reg}(T, \text{augment}(T125, H125)) \\ \text{Reg}(T, \text{augment}(T15, H15)) \end{pmatrix}\right] \text{ if } P > 12.5 \wedge P \le 15 \\
& tmp \leftarrow \text{linear}\left[P, \begin{pmatrix} 15 \\ 17.5 \end{pmatrix}, \begin{pmatrix} \text{Reg}(T, \text{augment}(T15, H15)) \\ \text{Reg}(T, \text{augment}(T175, H175)) \end{pmatrix}\right] \text{ if } P > 15 \wedge P \le 17.5 \\
& tmp \leftarrow \text{linear}\left[P, \begin{pmatrix} 17.5 \\ 20 \end{pmatrix}, \begin{pmatrix} \text{Reg}(T, \text{augment}(T175, H175)) \\ \text{Reg}(T, \text{augment}(T20, H20)) \end{pmatrix}\right] \text{ if } P > 17.5 \wedge P \le 20 \\
& tmp \leftarrow \text{linear}\left[P, \begin{pmatrix} 20 \\ 22.5 \end{pmatrix}, \begin{pmatrix} \text{Reg}(T, \text{augment}(T20, H20)) \\ \text{Reg}(T, \text{augment}(T225, H225)) \end{pmatrix}\right] \text{ if } P > 20 \wedge P \le 22.5 \\
& tmp \leftarrow \text{linear}\left[P, \begin{pmatrix} 22.5 \\ 25 \end{pmatrix}, \begin{pmatrix} \text{Reg}(T, \text{augment}(T225, H225)) \\ \text{Reg}(T, \text{augment}(T250, H250)) \end{pmatrix}\right] \text{ if } P > 22.5 \wedge P \le 25 \\
& tmp
\end{aligned}
$$

FIGURE B.3: Enthalpy code for superfluid region

The code for the density:

$$
\rho(T,P) := \left|
\begin{array}{ll}
\text{tmp} \leftarrow \text{linear}\left[P, \begin{pmatrix} 0 \\ 2.5 \end{pmatrix}, \begin{pmatrix} \text{Reg}\rho(T, \text{augment}(T0, \rho 0)) \\ \text{Reg}\rho(T, \text{augment}(T25, \rho 25)) \end{pmatrix}\right] & \text{if } P \le 2.5 \\
\text{tmp} \leftarrow \text{linear}\left[P, \begin{pmatrix} 2.5 \\ 5 \end{pmatrix}, \begin{pmatrix} \text{Reg}\rho(T, \text{augment}(T25, \rho 25)) \\ \text{Reg}\rho(T, \text{augment}(T5, \rho 5)) \end{pmatrix}\right] & \text{if } P > 2.5 \wedge P \le 5 \\
\text{tmp} \leftarrow \text{linear}\left[P, \begin{pmatrix} 5 \\ 7.5 \end{pmatrix}, \begin{pmatrix} \text{Reg}\rho(T, \text{augment}(T5, \rho 5)) \\ \text{Reg}\rho(T, \text{augment}(T75, \rho 75)) \end{pmatrix}\right] & \text{if } P > 5 \wedge P \le 7.5 \\
\text{tmp} \leftarrow \text{linear}\left[P, \begin{pmatrix} 7.5 \\ 10 \end{pmatrix}, \begin{pmatrix} \text{Reg}\rho(T, \text{augment}(T75, \rho 75)) \\ \text{Reg}\rho(T, \text{augment}(T10, \rho 10)) \end{pmatrix}\right] & \text{if } P > 7.5 \wedge P \le 10 \\
\text{tmp} \leftarrow \text{linear}\left[P, \begin{pmatrix} 10 \\ 12.5 \end{pmatrix}, \begin{pmatrix} \text{Reg}\rho(T, \text{augment}(T10, \rho 10)) \\ \text{Reg}\rho(T, \text{augment}(T125, \rho 125)) \end{pmatrix}\right] & \text{if } P > 10 \wedge P \le 12.5 \\
\text{tmp} \leftarrow \text{linear}\left[P, \begin{pmatrix} 12.5 \\ 15 \end{pmatrix}, \begin{pmatrix} \text{Reg}\rho(T, \text{augment}(T125, \rho 125)) \\ \text{Reg}\rho(T, \text{augment}(T15, \rho 15)) \end{pmatrix}\right] & \text{if } P > 12.5 \wedge P \le 15 \\
\text{tmp} \leftarrow \text{linear}\left[P, \begin{pmatrix} 15 \\ 17.5 \end{pmatrix}, \begin{pmatrix} \text{Reg}\rho(T, \text{augment}(T15, \rho 15)) \\ \text{Reg}\rho(T, \text{augment}(T175, \rho 175)) \end{pmatrix}\right] & \text{if } P > 15 \wedge P \le 17.5 \\
\text{tmp} \leftarrow \text{linear}\left[P, \begin{pmatrix} 17.5 \\ 20 \end{pmatrix}, \begin{pmatrix} \text{Reg}\rho(T, \text{augment}(T175, \rho 175)) \\ \text{Reg}\rho(T, \text{augment}(T20, \rho 20)) \end{pmatrix}\right] & \text{if } P > 17.5 \wedge P \le 20 \\
\text{tmp} \leftarrow \text{linear}\left[P, \begin{pmatrix} 20 \\ 22.5 \end{pmatrix}, \begin{pmatrix} \text{Reg}\rho(T, \text{augment}(T20, \rho 20)) \\ \text{Reg}\rho(T, \text{augment}(T225, \rho 225)) \end{pmatrix}\right] & \text{if } P > 20 \wedge P \le 22.5 \\
\text{tmp} \leftarrow \text{linear}\left[P, \begin{pmatrix} 22.5 \\ 25 \end{pmatrix}, \begin{pmatrix} \text{Reg}\rho(T, \text{augment}(T225, \rho 225)) \\ \text{Reg}\rho(T, \text{augment}(T250, \rho 250)) \end{pmatrix}\right] & \text{if } P > 22.5 \wedge P \le 25 \\
\text{tmp} &
\end{array}
\right.
$$

FIGURE B.4: Density code for superfluid region

The code for the specific heat under constant volume:

$$
\begin{aligned}
Cv(T,P) := \;
&\left| \begin{array}{ll}
tmp \leftarrow linear\left[P, \begin{pmatrix} 0 \\ 2.5 \end{pmatrix}, \begin{pmatrix} Reg(T, augment(T0, Cv0)) \\ Reg(T, augment(T25, Cv25)) \end{pmatrix}\right] & \text{if } P \le 2.5 \\
tmp \leftarrow linear\left[P, \begin{pmatrix} 2.5 \\ 5 \end{pmatrix}, \begin{pmatrix} Reg(T, augment(T25, Cv25)) \\ Reg(T, augment(T5, Cv5)) \end{pmatrix}\right] & \text{if } P > 2.5 \wedge P \le 5 \\
tmp \leftarrow linear\left[P, \begin{pmatrix} 5 \\ 7.5 \end{pmatrix}, \begin{pmatrix} Reg(T, augment(T5, Cv5)) \\ Reg(T, augment(T75, Cv75)) \end{pmatrix}\right] & \text{if } P > 5 \wedge P \le 7.5 \\
tmp \leftarrow linear\left[P, \begin{pmatrix} 7.5 \\ 10 \end{pmatrix}, \begin{pmatrix} Reg(T, augment(T75, Cv75)) \\ Reg(T, augment(T10, Cv10)) \end{pmatrix}\right] & \text{if } P > 7.5 \wedge P \le 10 \\
tmp \leftarrow linear\left[P, \begin{pmatrix} 10 \\ 12.5 \end{pmatrix}, \begin{pmatrix} Reg(T, augment(T10, Cv10)) \\ Reg(T, augment(T125, Cv125)) \end{pmatrix}\right] & \text{if } P > 10 \wedge P \le 12.5 \\
tmp \leftarrow linear\left[P, \begin{pmatrix} 12.5 \\ 15 \end{pmatrix}, \begin{pmatrix} Reg(T, augment(T125, Cv125)) \\ Reg(T, augment(T15, Cv15)) \end{pmatrix}\right] & \text{if } P > 12.5 \wedge P \le 15 \\
tmp \leftarrow linear\left[P, \begin{pmatrix} 15 \\ 17.5 \end{pmatrix}, \begin{pmatrix} Reg(T, augment(T15, Cv15)) \\ Reg(T, augment(T175, Cv175)) \end{pmatrix}\right] & \text{if } P > 15 \wedge P \le 17.5 \\
tmp \leftarrow linear\left[P, \begin{pmatrix} 17.5 \\ 20 \end{pmatrix}, \begin{pmatrix} Reg(T, augment(T175, Cv175)) \\ Reg(T, augment(T20, Cv20)) \end{pmatrix}\right] & \text{if } P > 17.5 \wedge P \le 20 \\
tmp \leftarrow linear\left[P, \begin{pmatrix} 20 \\ 22.5 \end{pmatrix}, \begin{pmatrix} Reg(T, augment(T20, Cv20)) \\ Reg(T, augment(T225, Cv225)) \end{pmatrix}\right] & \text{if } P > 20 \wedge P \le 22.5 \\
tmp \leftarrow linear\left[P, \begin{pmatrix} 22.5 \\ 25 \end{pmatrix}, \begin{pmatrix} Reg(T, augment(T225, Cv225)) \\ Reg(T, augment(T250, Cv250)) \end{pmatrix}\right] & \text{if } P > 22.5 \wedge P \le 25 \\
tmp &
\end{array} \right.
\end{aligned}
$$

FIGURE B.5: Cv code for superfluid region

The code for the specific heat under constant pressure:

$$
\begin{aligned}
Cp(T,P) := \;& tmp \leftarrow linear\left[P, \begin{pmatrix} 0 \\ 2.5 \end{pmatrix}, \begin{pmatrix} RegCp(T, augment(T0, Cp0)) \\ RegCp(T, augment(T25, Cp25)) \end{pmatrix}\right] \text{ if } P \le 2.5 \\
& tmp \leftarrow linear\left[P, \begin{pmatrix} 2.5 \\ 5 \end{pmatrix}, \begin{pmatrix} RegCp(T, augment(T25, Cp25)) \\ RegCp(T, augment(T5, Cp5)) \end{pmatrix}\right] \text{ if } P > 2.5 \wedge P \le 5 \\
& tmp \leftarrow linear\left[P, \begin{pmatrix} 5 \\ 7.5 \end{pmatrix}, \begin{pmatrix} RegCp(T, augment(T5, Cp5)) \\ RegCp(T, augment(T75, Cp75)) \end{pmatrix}\right] \text{ if } P > 5 \wedge P \le 7.5 \\
& tmp \leftarrow linear\left[P, \begin{pmatrix} 7.5 \\ 10 \end{pmatrix}, \begin{pmatrix} RegCp(T, augment(T75, Cp75)) \\ RegCp(T, augment(T10, Cp10)) \end{pmatrix}\right] \text{ if } P > 7.5 \wedge P \le 10 \\
& tmp \leftarrow linear\left[P, \begin{pmatrix} 10 \\ 12.5 \end{pmatrix}, \begin{pmatrix} RegCp(T, augment(T10, Cp10)) \\ RegCp(T, augment(T125, Cp125)) \end{pmatrix}\right] \text{ if } P > 10 \wedge P \le 12.5 \\
& tmp \leftarrow linear\left[P, \begin{pmatrix} 12.5 \\ 15 \end{pmatrix}, \begin{pmatrix} RegCp(T, augment(T125, Cp125)) \\ RegCp(T, augment(T15, Cp15)) \end{pmatrix}\right] \text{ if } P > 12.5 \wedge P \le 15 \\
& tmp \leftarrow linear\left[P, \begin{pmatrix} 15 \\ 17.5 \end{pmatrix}, \begin{pmatrix} RegCp(T, augment(T15, Cp15)) \\ RegCp(T, augment(T175, Cp175)) \end{pmatrix}\right] \text{ if } P > 15 \wedge P \le 17.5 \\
& tmp \leftarrow linear\left[P, \begin{pmatrix} 17.5 \\ 20 \end{pmatrix}, \begin{pmatrix} RegCp(T, augment(T175, Cp175)) \\ RegCp(T, augment(T20, Cp20)) \end{pmatrix}\right] \text{ if } P > 17.5 \wedge P \le 20 \\
& tmp \leftarrow linear\left[P, \begin{pmatrix} 20 \\ 22.5 \end{pmatrix}, \begin{pmatrix} RegCp(T, augment(T20, Cp20)) \\ RegCp(T, augment(T225, Cp225)) \end{pmatrix}\right] \text{ if } P > 20 \wedge P \le 22.5 \\
& tmp \leftarrow linear\left[P, \begin{pmatrix} 22.5 \\ 25 \end{pmatrix}, \begin{pmatrix} RegCp(T, augment(T225, Cp225)) \\ RegCp(T, augment(T250, Cp250)) \end{pmatrix}\right] \text{ if } P > 22.5 \wedge P \le 25 \\
& tmp
\end{aligned}
$$

FIGURE B.6: Cp code for superfluid region

The code for the superfluid ratio:

$$
\begin{aligned}
\text{ratio}(T,P) := \;& \text{tmp} \leftarrow \text{linear}\left[P, \begin{pmatrix} 0 \\ 2.5 \end{pmatrix}, \begin{pmatrix} \text{Reg}(T, \text{augment}(T0, \text{ratio0})) \\ \text{Reg}(T, \text{augment}(T25, \text{ratio25})) \end{pmatrix}\right] \text{ if } P \le 2.5 \\
& \text{tmp} \leftarrow \text{linear}\left[P, \begin{pmatrix} 2.5 \\ 5 \end{pmatrix}, \begin{pmatrix} \text{Reg}(T, \text{augment}(T25, \text{ratio25})) \\ \text{Reg}(T, \text{augment}(T5, \text{ratio5})) \end{pmatrix}\right] \text{ if } P > 2.5 \wedge P \le 5 \\
& \text{tmp} \leftarrow \text{linear}\left[P, \begin{pmatrix} 5 \\ 7.5 \end{pmatrix}, \begin{pmatrix} \text{Reg}(T, \text{augment}(T5, \text{ratio5})) \\ \text{Reg}(T, \text{augment}(T75, \text{ratio75})) \end{pmatrix}\right] \text{ if } P > 5 \wedge P \le 7.5 \\
& \text{tmp} \leftarrow \text{linear}\left[P, \begin{pmatrix} 7.5 \\ 10 \end{pmatrix}, \begin{pmatrix} \text{Reg}(T, \text{augment}(T75, \text{ratio75})) \\ \text{Reg}(T, \text{augment}(T10, \text{ratio10})) \end{pmatrix}\right] \text{ if } P > 7.5 \wedge P \le 10 \\
& \text{tmp} \leftarrow \text{linear}\left[P, \begin{pmatrix} 10 \\ 12.5 \end{pmatrix}, \begin{pmatrix} \text{Reg}(T, \text{augment}(T10, \text{ratio10})) \\ \text{Reg}(T, \text{augment}(T125, \text{ratio125})) \end{pmatrix}\right] \text{ if } P > 10 \wedge P \le 12.5 \\
& \text{tmp} \leftarrow \text{linear}\left[P, \begin{pmatrix} 12.5 \\ 15 \end{pmatrix}, \begin{pmatrix} \text{Reg}(T, \text{augment}(T125, \text{ratio125})) \\ \text{Reg}(T, \text{augment}(T15, \text{ratio15})) \end{pmatrix}\right] \text{ if } P > 12.5 \wedge P \le 15 \\
& \text{tmp} \leftarrow \text{linear}\left[P, \begin{pmatrix} 15 \\ 17.5 \end{pmatrix}, \begin{pmatrix} \text{Reg}(T, \text{augment}(T15, \text{ratio15})) \\ \text{Reg}(T, \text{augment}(T175, \text{ratio175})) \end{pmatrix}\right] \text{ if } P > 15 \wedge P \le 17.5 \\
& \text{tmp} \leftarrow \text{linear}\left[P, \begin{pmatrix} 17.5 \\ 20 \end{pmatrix}, \begin{pmatrix} \text{Reg}(T, \text{augment}(T175, \text{ratio175})) \\ \text{Reg}(T, \text{augment}(T20, \text{ratio20})) \end{pmatrix}\right] \text{ if } P > 17.5 \wedge P \le 20 \\
& \text{tmp} \leftarrow \text{linear}\left[P, \begin{pmatrix} 20 \\ 22.5 \end{pmatrix}, \begin{pmatrix} \text{Reg}(T, \text{augment}(T20, \text{ratio20})) \\ \text{Reg}(T, \text{augment}(T225, \text{ratio225})) \end{pmatrix}\right] \text{ if } P > 20 \wedge P \le 22.5 \\
& \text{tmp} \leftarrow \text{linear}\left[P, \begin{pmatrix} 22.5 \\ 25 \end{pmatrix}, \begin{pmatrix} \text{Reg}(T, \text{augment}(T225, \text{ratio225})) \\ \text{Reg}(T, \text{augment}(T250, \text{ratio250})) \end{pmatrix}\right] \text{ if } P > 22.5 \wedge P \le 25 \\
& \text{tmp}
\end{aligned}
$$

FIGURE B.7: Superfluid ratio percentage code

B.3 Normal fluid EOS code

The code used for create the different variables of the EOS for normal fluid region of Helium-4 is presented below.

The internal energy is calculated as:

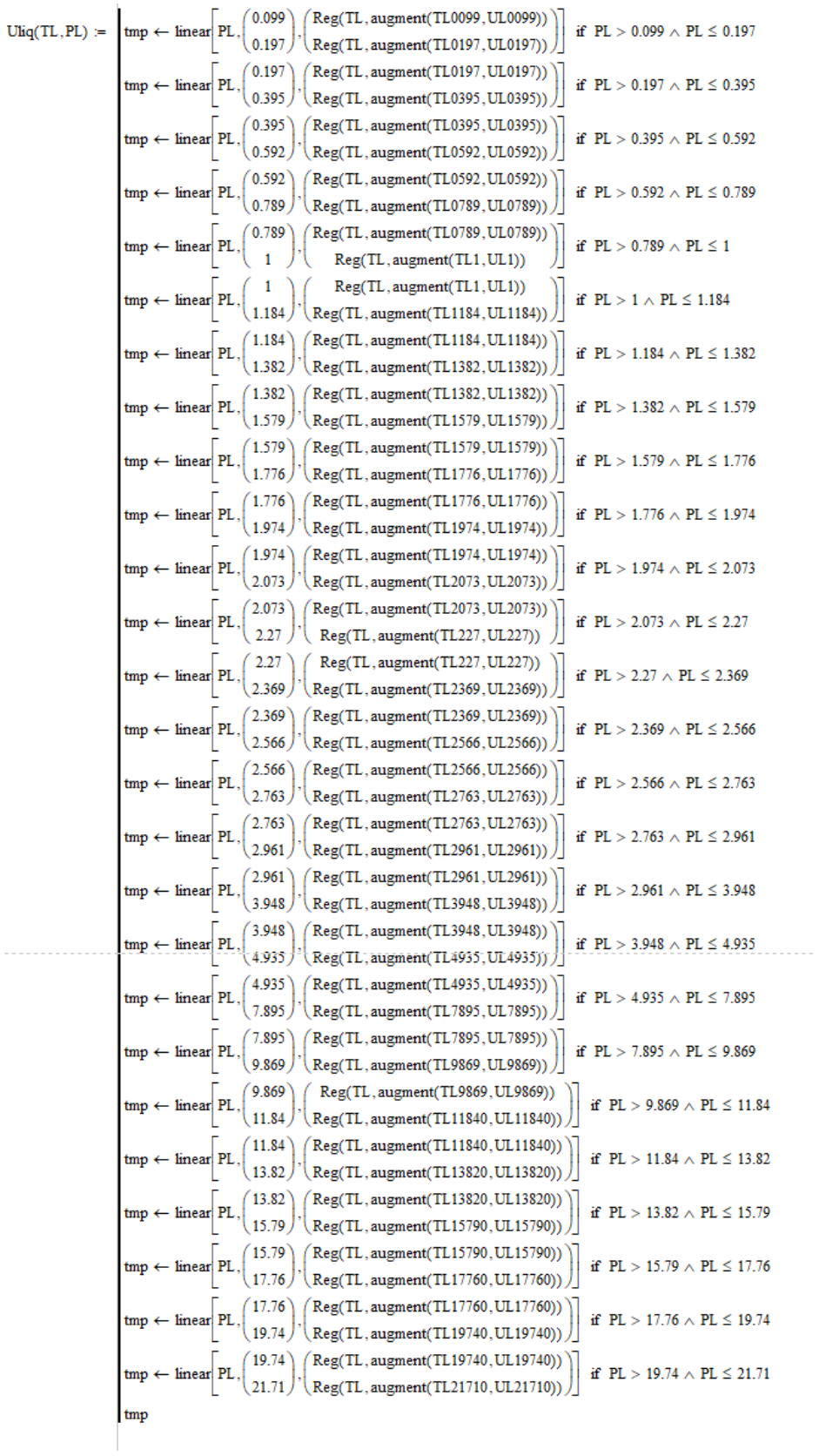

FIGURE B.8: Internal energy code for normal fluid region

Then the entropy is calculated.

$$
\begin{aligned}
\mathrm{Sliq}(TL,PL) := \;
&\mathrm{tmp} \leftarrow \mathrm{linear}\left[PL,\begin{pmatrix}0.099\\0.197\end{pmatrix},\begin{pmatrix}\mathrm{Reg}(TL,\mathrm{augment}(TL0099,SL0099))\\\mathrm{Reg}(TL,\mathrm{augment}(TL0197,SL0197))\end{pmatrix}\right] \text{ if } PL > 0.099 \wedge PL \le 0.197\\
&\mathrm{tmp} \leftarrow \mathrm{linear}\left[PL,\begin{pmatrix}0.197\\0.395\end{pmatrix},\begin{pmatrix}\mathrm{Reg}(TL,\mathrm{augment}(TL0197,SL0197))\\\mathrm{Reg}(TL,\mathrm{augment}(TL0395,SL0395))\end{pmatrix}\right] \text{ if } PL > 0.197 \wedge PL \le 0.395\\
&\mathrm{tmp} \leftarrow \mathrm{linear}\left[PL,\begin{pmatrix}0.395\\0.592\end{pmatrix},\begin{pmatrix}\mathrm{Reg}(TL,\mathrm{augment}(TL0395,SL0395))\\\mathrm{Reg}(TL,\mathrm{augment}(TL0592,SL0592))\end{pmatrix}\right] \text{ if } PL > 0.395 \wedge PL \le 0.592\\
&\mathrm{tmp} \leftarrow \mathrm{linear}\left[PL,\begin{pmatrix}0.592\\0.789\end{pmatrix},\begin{pmatrix}\mathrm{Reg}(TL,\mathrm{augment}(TL0592,SL0592))\\\mathrm{Reg}(TL,\mathrm{augment}(TL0789,SL0789))\end{pmatrix}\right] \text{ if } PL > 0.592 \wedge PL \le 0.789\\
&\mathrm{tmp} \leftarrow \mathrm{linear}\left[PL,\begin{pmatrix}0.789\\1\end{pmatrix},\begin{pmatrix}\mathrm{Reg}(TL,\mathrm{augment}(TL0789,SL0789))\\\mathrm{Reg}(TL,\mathrm{augment}(TL1,SL1))\end{pmatrix}\right] \text{ if } PL > 0.789 \wedge PL \le 1\\
&\mathrm{tmp} \leftarrow \mathrm{linear}\left[PL,\begin{pmatrix}1\\1.184\end{pmatrix},\begin{pmatrix}\mathrm{Reg}(TL,\mathrm{augment}(TL1,SL1))\\\mathrm{Reg}(TL,\mathrm{augment}(TL1184,SL1184))\end{pmatrix}\right] \text{ if } PL > 1 \wedge PL \le 1.184\\
&\mathrm{tmp} \leftarrow \mathrm{linear}\left[PL,\begin{pmatrix}1.184\\1.382\end{pmatrix},\begin{pmatrix}\mathrm{Reg}(TL,\mathrm{augment}(TL1184,SL1184))\\\mathrm{Reg}(TL,\mathrm{augment}(TL1382,SL1382))\end{pmatrix}\right] \text{ if } PL > 1.184 \wedge PL \le 1.382\\
&\mathrm{tmp} \leftarrow \mathrm{linear}\left[PL,\begin{pmatrix}1.382\\1.579\end{pmatrix},\begin{pmatrix}\mathrm{Reg}(TL,\mathrm{augment}(TL1382,SL1382))\\\mathrm{Reg}(TL,\mathrm{augment}(TL1579,SL1579))\end{pmatrix}\right] \text{ if } PL > 1.382 \wedge PL \le 1.579\\
&\mathrm{tmp} \leftarrow \mathrm{linear}\left[PL,\begin{pmatrix}1.579\\1.776\end{pmatrix},\begin{pmatrix}\mathrm{Reg}(TL,\mathrm{augment}(TL1579,SL1579))\\\mathrm{Reg}(TL,\mathrm{augment}(TL1776,SL1776))\end{pmatrix}\right] \text{ if } PL > 1.579 \wedge PL \le 1.776\\
&\mathrm{tmp} \leftarrow \mathrm{linear}\left[PL,\begin{pmatrix}1.776\\1.974\end{pmatrix},\begin{pmatrix}\mathrm{Reg}(TL,\mathrm{augment}(TL1776,SL1776))\\\mathrm{Reg}(TL,\mathrm{augment}(TL1974,SL1974))\end{pmatrix}\right] \text{ if } PL > 1.776 \wedge PL \le 1.974\\
&\mathrm{tmp} \leftarrow \mathrm{linear}\left[PL,\begin{pmatrix}1.974\\2.073\end{pmatrix},\begin{pmatrix}\mathrm{Reg}(TL,\mathrm{augment}(TL1974,SL1974))\\\mathrm{Reg}(TL,\mathrm{augment}(TL2073,SL2073))\end{pmatrix}\right] \text{ if } PL > 1.974 \wedge PL \le 2.073\\
&\mathrm{tmp} \leftarrow \mathrm{linear}\left[PL,\begin{pmatrix}2.073\\2.27\end{pmatrix},\begin{pmatrix}\mathrm{Reg}(TL,\mathrm{augment}(TL2073,SL2073))\\\mathrm{Reg}(TL,\mathrm{augment}(TL227,SL227))\end{pmatrix}\right] \text{ if } PL > 2.073 \wedge PL \le 2.27\\
&\mathrm{tmp} \leftarrow \mathrm{linear}\left[PL,\begin{pmatrix}2.27\\2.369\end{pmatrix},\begin{pmatrix}\mathrm{Reg}(TL,\mathrm{augment}(TL227,SL227))\\\mathrm{Reg}(TL,\mathrm{augment}(TL2369,SL2369))\end{pmatrix}\right] \text{ if } PL > 2.27 \wedge PL \le 2.369\\
&\mathrm{tmp} \leftarrow \mathrm{linear}\left[PL,\begin{pmatrix}2.369\\2.566\end{pmatrix},\begin{pmatrix}\mathrm{Reg}(TL,\mathrm{augment}(TL2369,SL2369))\\\mathrm{Reg}(TL,\mathrm{augment}(TL2566,SL2566))\end{pmatrix}\right] \text{ if } PL > 2.369 \wedge PL \le 2.566\\
&\mathrm{tmp} \leftarrow \mathrm{linear}\left[PL,\begin{pmatrix}2.566\\2.763\end{pmatrix},\begin{pmatrix}\mathrm{Reg}(TL,\mathrm{augment}(TL2566,SL2566))\\\mathrm{Reg}(TL,\mathrm{augment}(TL2763,SL2763))\end{pmatrix}\right] \text{ if } PL > 2.566 \wedge PL \le 2.763\\
&\mathrm{tmp} \leftarrow \mathrm{linear}\left[PL,\begin{pmatrix}2.763\\2.961\end{pmatrix},\begin{pmatrix}\mathrm{Reg}(TL,\mathrm{augment}(TL2763,SL2763))\\\mathrm{Reg}(TL,\mathrm{augment}(TL2961,SL2961))\end{pmatrix}\right] \text{ if } PL > 2.763 \wedge PL \le 2.961\\
&\mathrm{tmp} \leftarrow \mathrm{linear}\left[PL,\begin{pmatrix}2.961\\3.948\end{pmatrix},\begin{pmatrix}\mathrm{Reg}(TL,\mathrm{augment}(TL2961,SL2961))\\\mathrm{Reg}(TL,\mathrm{augment}(TL3948,SL3948))\end{pmatrix}\right] \text{ if } PL > 2.961 \wedge PL \le 3.948\\
&\mathrm{tmp} \leftarrow \mathrm{linear}\left[PL,\begin{pmatrix}3.948\\4.935\end{pmatrix},\begin{pmatrix}\mathrm{Reg}(TL,\mathrm{augment}(TL3948,SL3948))\\\mathrm{Reg}(TL,\mathrm{augment}(TL4935,SL4935))\end{pmatrix}\right] \text{ if } PL > 3.948 \wedge PL \le 4.935\\
&\mathrm{tmp} \leftarrow \mathrm{linear}\left[PL,\begin{pmatrix}4.935\\7.895\end{pmatrix},\begin{pmatrix}\mathrm{Reg}(TL,\mathrm{augment}(TL4935,SL4935))\\\mathrm{Reg}(TL,\mathrm{augment}(TL7895,SL7895))\end{pmatrix}\right] \text{ if } PL > 4.935 \wedge PL \le 7.895\\
&\mathrm{tmp} \leftarrow \mathrm{linear}\left[PL,\begin{pmatrix}7.895\\9.869\end{pmatrix},\begin{pmatrix}\mathrm{Reg}(TL,\mathrm{augment}(TL7895,SL7895))\\\mathrm{Reg}(TL,\mathrm{augment}(TL9869,SL9869))\end{pmatrix}\right] \text{ if } PL > 7.895 \wedge PL \le 9.869\\
&\mathrm{tmp} \leftarrow \mathrm{linear}\left[PL,\begin{pmatrix}9.869\\11.84\end{pmatrix},\begin{pmatrix}\mathrm{Reg}(TL,\mathrm{augment}(TL9869,SL9869))\\\mathrm{Reg}(TL,\mathrm{augment}(TL11840,SL11840))\end{pmatrix}\right] \text{ if } PL > 9.869 \wedge PL \le 11.84\\
&\mathrm{tmp} \leftarrow \mathrm{linear}\left[PL,\begin{pmatrix}11.84\\13.82\end{pmatrix},\begin{pmatrix}\mathrm{Reg}(TL,\mathrm{augment}(TL11840,SL11840))\\\mathrm{Reg}(TL,\mathrm{augment}(TL13820,SL13820))\end{pmatrix}\right] \text{ if } PL > 11.84 \wedge PL \le 13.82\\
&\mathrm{tmp} \leftarrow \mathrm{linear}\left[PL,\begin{pmatrix}13.82\\15.79\end{pmatrix},\begin{pmatrix}\mathrm{Reg}(TL,\mathrm{augment}(TL13820,SL13820))\\\mathrm{Reg}(TL,\mathrm{augment}(TL15790,SL15790))\end{pmatrix}\right] \text{ if } PL > 13.82 \wedge PL \le 15.79\\
&\mathrm{tmp} \leftarrow \mathrm{linear}\left[PL,\begin{pmatrix}15.79\\17.76\end{pmatrix},\begin{pmatrix}\mathrm{Reg}(TL,\mathrm{augment}(TL15790,SL15790))\\\mathrm{Reg}(TL,\mathrm{augment}(TL17760,SL17760))\end{pmatrix}\right] \text{ if } PL > 15.79 \wedge PL \le 17.76\\
&\mathrm{tmp} \leftarrow \mathrm{linear}\left[PL,\begin{pmatrix}17.76\\19.74\end{pmatrix},\begin{pmatrix}\mathrm{Reg}(TL,\mathrm{augment}(TL17760,SL17760))\\\mathrm{Reg}(TL,\mathrm{augment}(TL19740,SL19740))\end{pmatrix}\right] \text{ if } PL > 17.76 \wedge PL \le 19.74\\
&\mathrm{tmp} \leftarrow \mathrm{linear}\left[PL,\begin{pmatrix}19.74\\21.71\end{pmatrix},\begin{pmatrix}\mathrm{Reg}(TL,\mathrm{augment}(TL19740,SL19740))\\\mathrm{Reg}(TL,\mathrm{augment}(TL21710,SL21710))\end{pmatrix}\right] \text{ if } PL > 19.74 \wedge PL \le 21.71\\
&\mathrm{tmp}
\end{aligned}
$$

FIGURE B.9: Entropy code for normal fluid region

The code for the enthalpy:

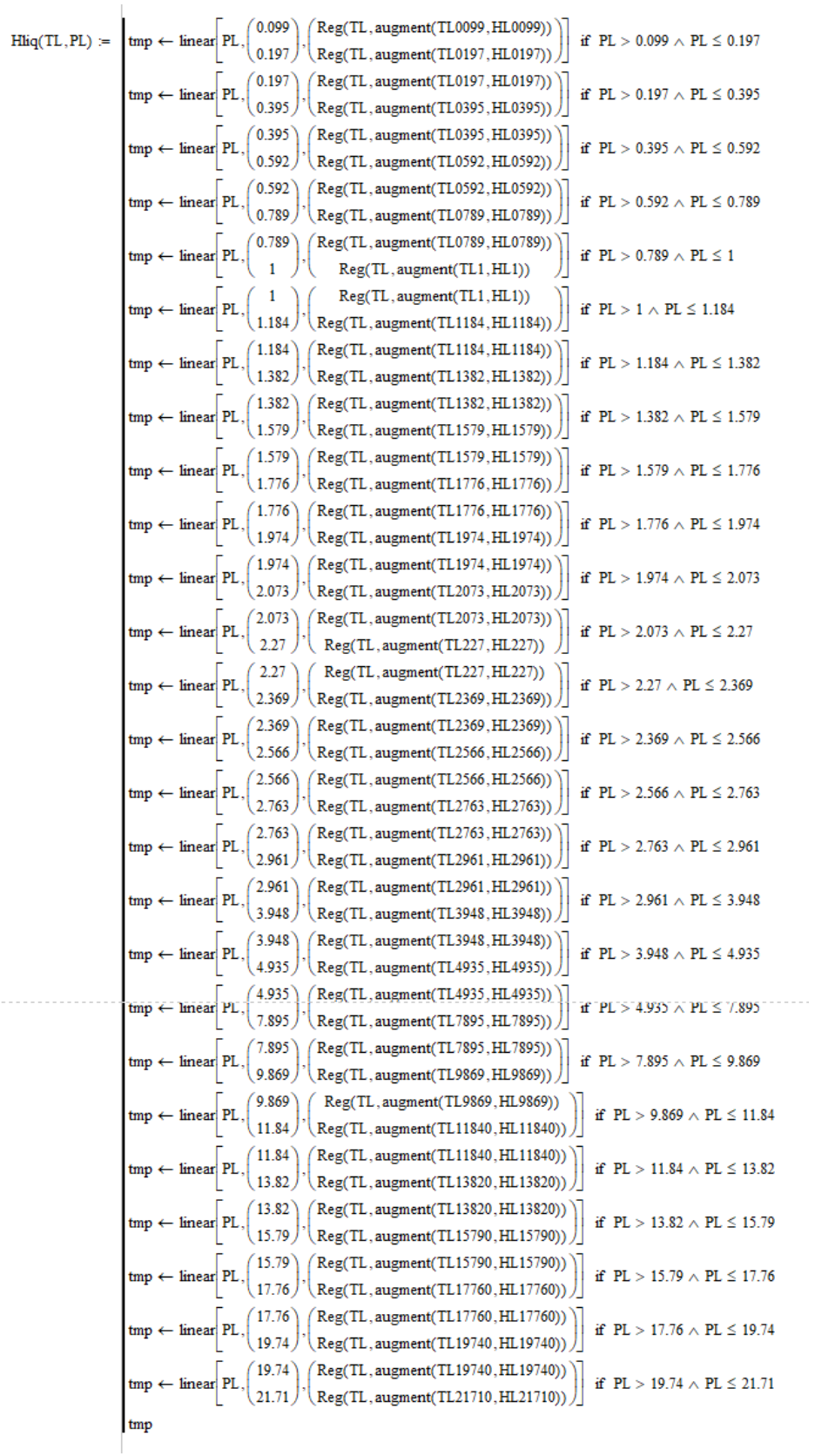

FIGURE B.10: Enthalpy code for normal fluid region

The code for the density:

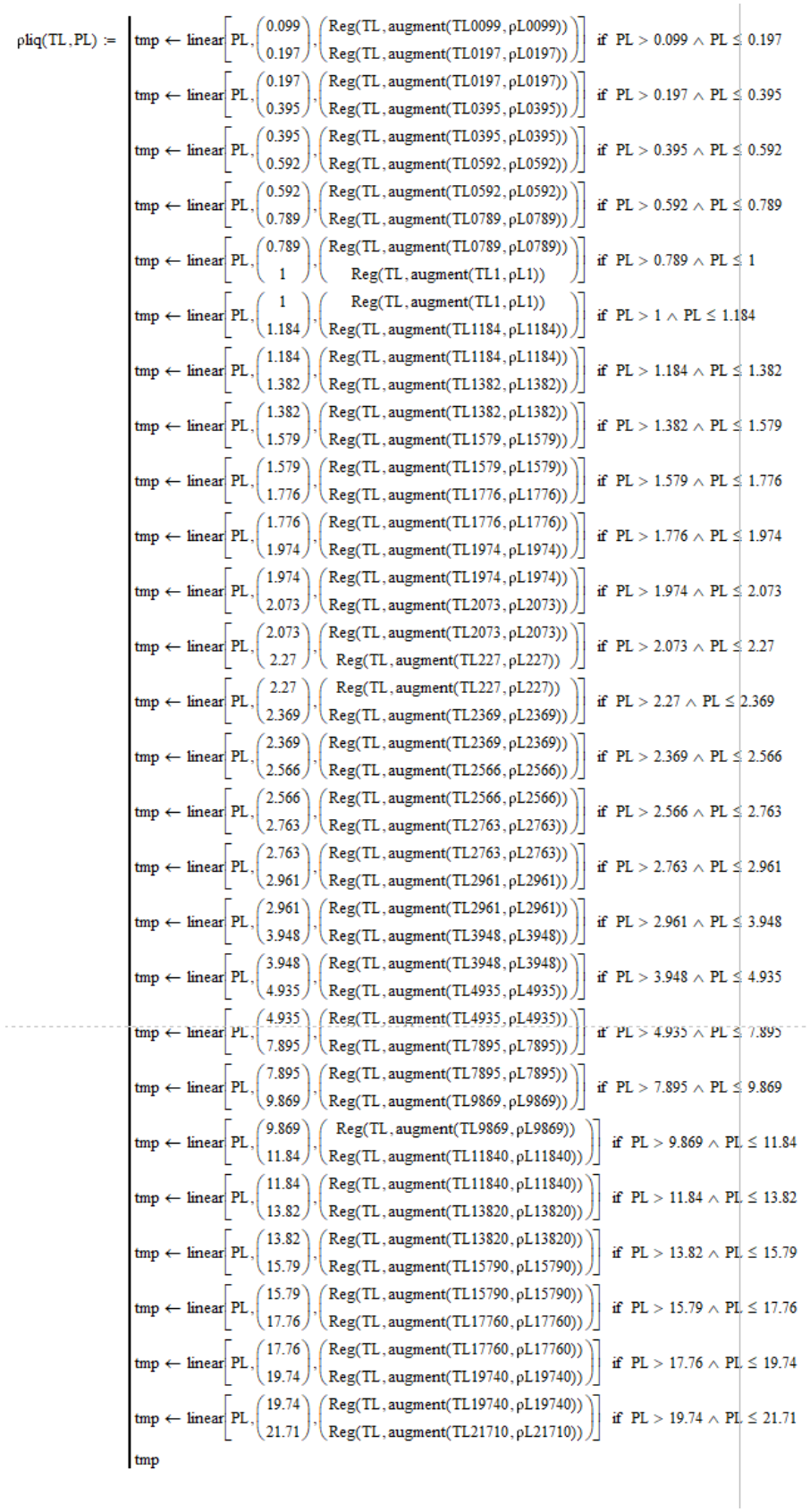

FIGURE B.11: Density code for normal fluid region

The code for the specific heat under constant volume:

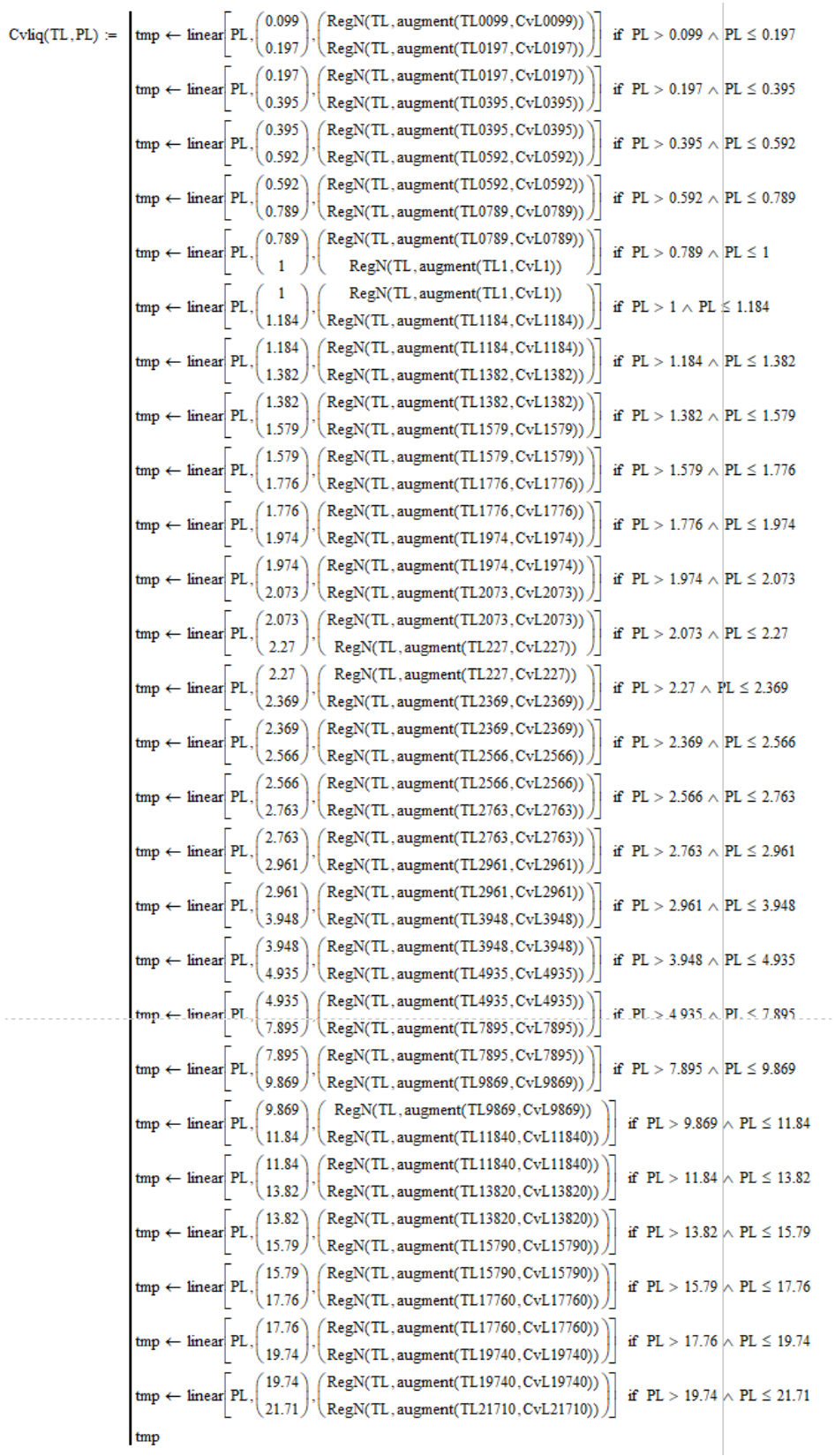

FIGURE B.12: Cv code for normal fluid region

The code for the specific heat under constant pressure:

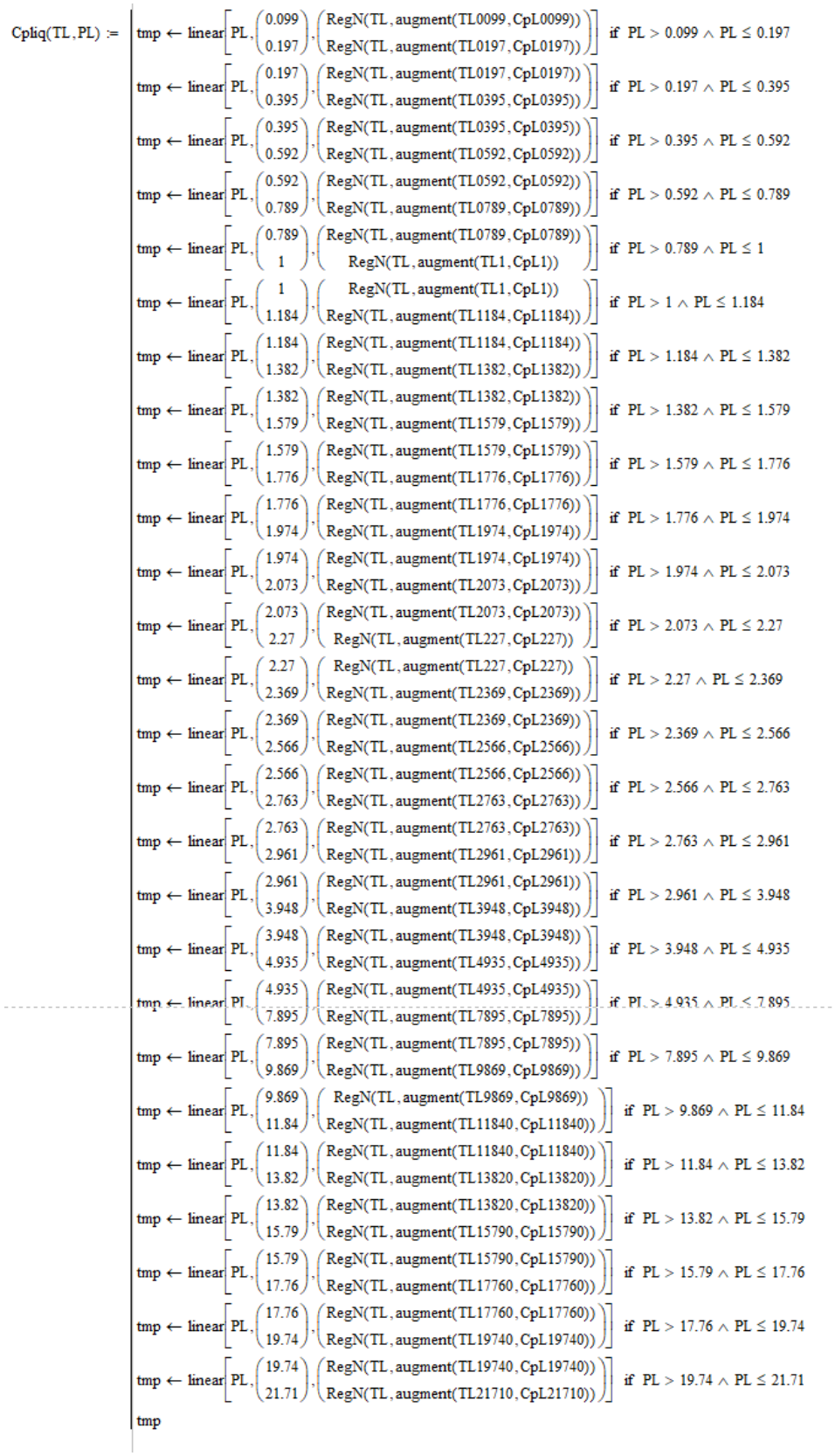

FIGURE B.13: Cp code for normal fluid region

B.4 Lambda line bridging code

B.4.1 Density lambda unification

A third degree polynomial is used for the modelling between the the fluid and the superfluid.

$$d\rho(T,P) = \frac{\partial \rho(T,P)}{\partial T} \tag{B.6}$$

$$d\rho_{liq}(T,P) = \frac{\partial \rho_{liq}(T,P)}{\partial T} \tag{B.7}$$

To solve the equation of the values and the differentials above and below the lambda line the following system is used:

$$A\rho(T_{low},T_{high}) = \begin{bmatrix} T_{low}^3 & T_{low}^2 & T_{low} & 1 \\ 3T_{low}^2 & 2T_{low} & 1 & 0 \\ T_{high}^3 & T_{high}^2 & T_{high} & 1 \\ 3T_{high}^2 & 2T_{high} & 1 & 0 \end{bmatrix}$$

$$B(T_{low},T_{high},P) = \begin{bmatrix} \rho(T_{low},P) \\ d\rho(T_{low},P) \\ \rho_{liq}(T_{high},P) \\ d\rho_{liq}(T_{high},P) \end{bmatrix}$$

$$sol(T_{low},T_{high},P) = A\rho(T_{low},T_{high})^{-1}\, B(T_{low},T_{high},P) \tag{B.8}$$

Using the above the following code is used for the different pressures.

```
ρ_unified(T,P) :=
    if P ≤ 2.5
        m ← 2.1
        tmp ← ρ(T,P)  if T < m − 0.1
        tmp ← sol(m − 0.1,m + 0.05,P)_1·T^3 + sol(m − 0.1,m + 0.05,P)_2·T^2 + sol(m − 0.1,m + 0.05,P)_3·T + sol(m − 0.1,m + 0.05,P)_4  if T ≥ m − 0.1 ∧ T ≤ m + 0.05
        tmp ← ρliq(T,P)  if T > m + 0.05
    if P > 2.5 ∧ P ≤ 5
        m ← 2.05
        tmp ← ρ(T,P)  if T < m − 0.1
        tmp ← sol(m − 0.1,m + 0.1,P)_1·T^3 + sol(m − 0.1,m + 0.1,P)_2·T^2 + sol(m − 0.1,m + 0.1,P)_3·T + sol(m − 0.1,m + 0.1,P)_4  if T ≥ m − 0.1 ∧ T ≤ m + 0.1
        tmp ← ρliq(T,P)  if T > m + 0.1
    if P > 5 ∧ P ≤ 7.5
        m ← 2
        tmp ← ρ(T,P)  if T < m − 0.1
        tmp ← sol(m − 0.1,m + 0.2,P)_1·T^3 + sol(m − 0.1,m + 0.2,P)_2·T^2 + sol(m − 0.1,m + 0.2,P)_3·T + sol(m − 0.1,m + 0.2,P)_4  if T ≥ m − 0.1 ∧ T ≤ m + 0.2
        tmp ← ρliq(T,P)  if T > m + 0.2
    if P > 7.5 ∧ P ≤ 15
        m ← 1.95
        tmp ← ρ(T,P)  if T < m − 0.1
        tmp ← sol(m − 0.1,m + 0.2,P)_1·T^3 + sol(m − 0.1,m + 0.2,P)_2·T^2 + sol(m − 0.1,m + 0.2,P)_3·T + sol(m − 0.1,m + 0.2,P)_4  if T ≥ m − 0.1 ∧ T ≤ m + 0.2
        tmp ← ρliq(T,P)  if T > m + 0.2
    if P > 15 ∧ P ≤ 17.5
        m ← 1.9
        tmp ← ρ(T,P)  if T < m − 0.1
        tmp ← sol(m − 0.1,m + 0.2,P)_1·T^3 + sol(m − 0.1,m + 0.2,P)_2·T^2 + sol(m − 0.1,m + 0.2,P)_3·T + sol(m − 0.1,m + 0.2,P)_4  if T ≥ m − 0.1 ∧ T ≤ m + 0.2
        tmp ← ρliq(T,P)  if T > m + 0.2
    if P > 17.5 ∧ P ≤ 22.5
        m ← 1.85
        tmp ← ρ(T,P)  if T < m − 0.1
        tmp ← sol(m − 0.1,m + 0.2,P)_1·T^3 + sol(m − 0.1,m + 0.2,P)_2·T^2 + sol(m − 0.1,m + 0.2,P)_3·T + sol(m − 0.1,m + 0.2,P)_4  if T ≥ m − 0.1 ∧ T ≤ m + 0.2
        tmp ← ρliq(T,P)  if T > m + 0.2
    if P > 22.5
        m ← 1.8
        tmp ← ρ(T,P)  if T < m − 0.1
        tmp ← sol(m − 0.1,m + 0.2,P)_1·T^3 + sol(m − 0.1,m + 0.2,P)_2·T^2 + sol(m − 0.1,m + 0.2,P)_3·T + sol(m − 0.1,m + 0.2,P)_4  if T ≥ m − 0.1 ∧ T ≤ m + 0.2
        tmp ← ρliq(T,P)  if T > m + 0.2
    tmp
```

FIGURE B.14: code for unifying the density above and below the lambda line

The reasoning behind splitting the code code into different section for the pressures is to assure a greater accuracy on the lambda line which is heavily dependent on the pressure. One can observe the continuous and differentiable behavior of the provided equation in the figure below.

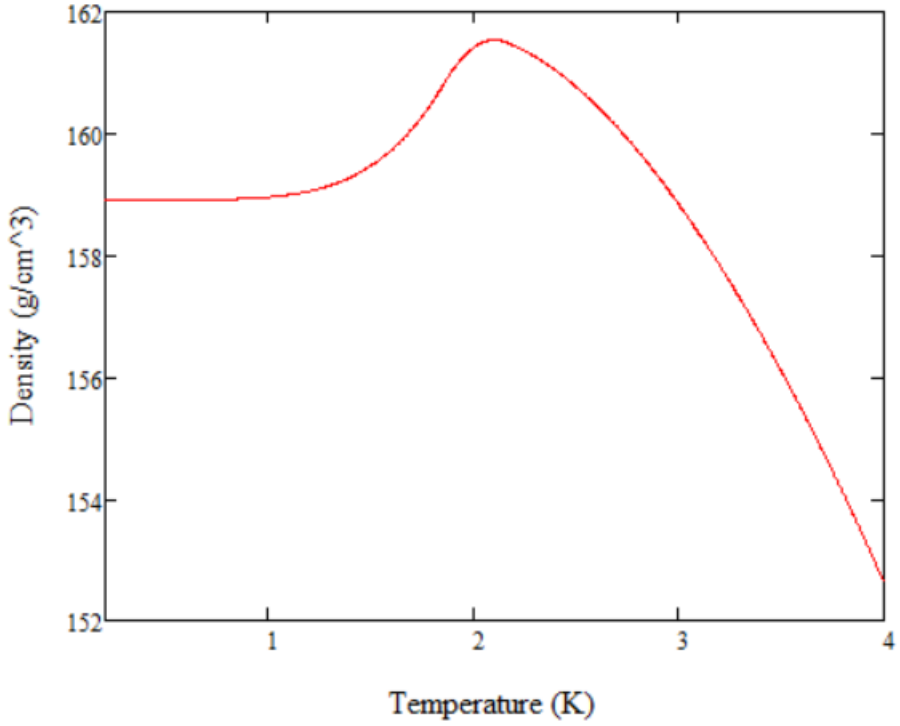

FIGURE B.15: Density of Helium-4 for 10 atm

B.4.2 Entropy lambda unification

A third degree polynomial is used for the modelling between the the fluid and the superfluid.

$$dS(T,P) = \frac{\partial S(T,P)}{\partial T} \tag{B.9}$$

$$dS_{liq}(T,P) = \frac{\partial S_{liq}(T,P)}{\partial T} \tag{B.10}$$

To solve the equation of the values and the differentials above and below the lambda line the following system is used:

$$AS(T_{low},T_{high}) = \begin{bmatrix} T_{low}^3 & T_{low}^2 & T_{low} & 1 \\ 3T_{low}^2 & 2T_{low} & 1 & 0 \\ T_{high}^3 & T_{high}^2 & T_{high} & 1 \\ 3T_{high}^2 & 2T_{high} & 1 & 0 \end{bmatrix}$$

$$B(T_{low},T_{high},P) = \begin{bmatrix} S(T_{low},P) \\ dS(T_{low},P) \\ S_{liq}(T_{high},P) \\ dS_{liq}(T_{high},P) \end{bmatrix}$$

$$sol(T_{low},T_{high},P) = AS(T_{low},T_{high})^{-1}\, B(T_{low},T_{high},P) \tag{B.11}$$

Using the above the following code is used for the different pressures.

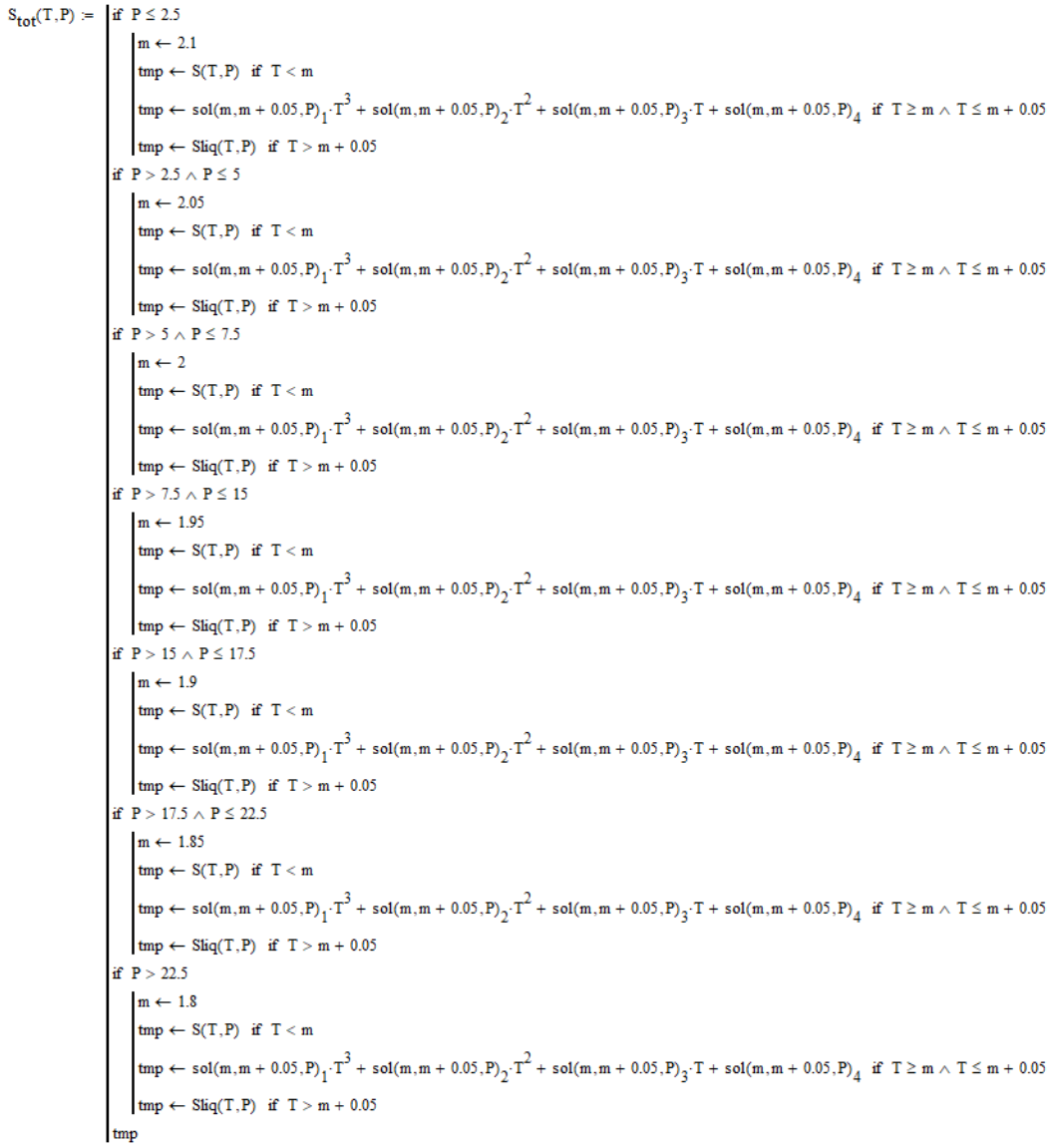

FIGURE B.16: code for unifying the entropy above and below the lambda line

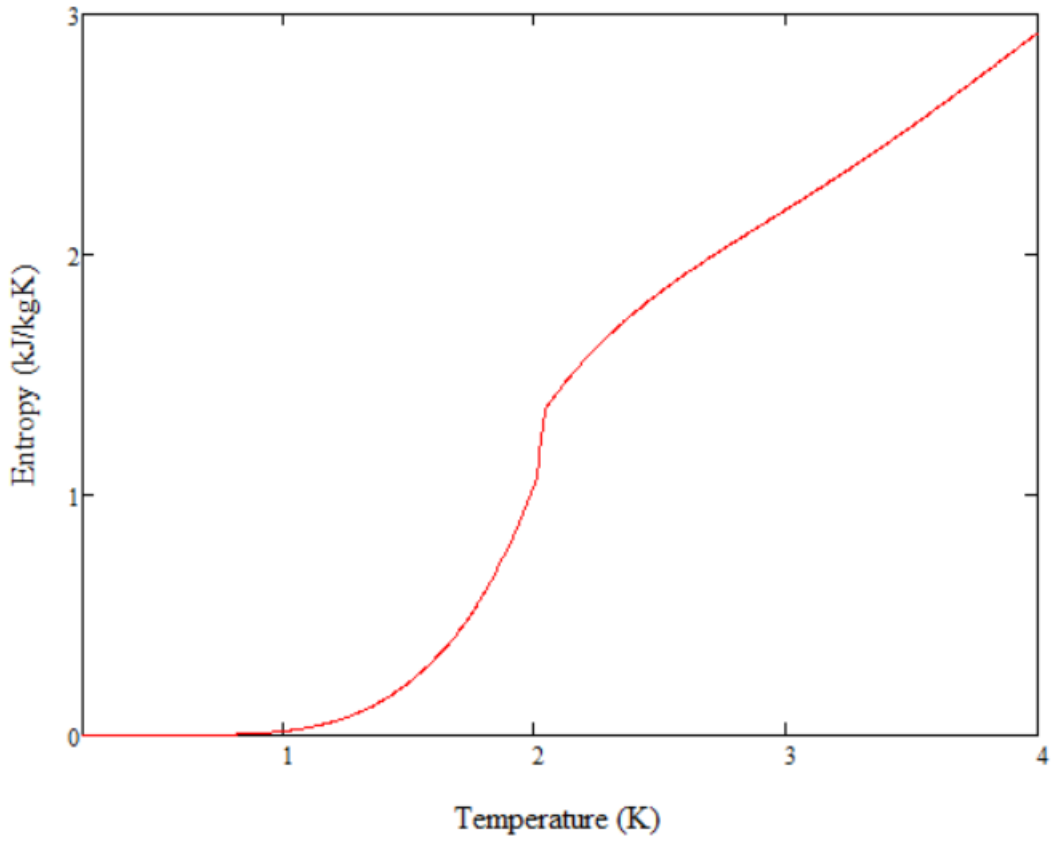

FIGURE B.17: Density of Helium-4 for 10 atm

B.4.3 Specific Heat under constant volume lambda unification

A third degree polynomial is used for the modelling between the the fluid and the superfluid.

$$dCv(T,P) = \frac{\partial Cv(T,P)}{\partial T} \tag{B.12}$$

$$dCv_{liq}(T,P) = \frac{\partial Cv_{liq}(T,P)}{\partial T} \tag{B.13}$$

To solve the equation of the values and the differentials above and below the lambda line the following system is used:

$$ACv(T_{low},T_{high}) = \begin{bmatrix} T_{low}^3 & T_{low}^2 & T_{low} & 1 \\ 3T_{low}^2 & 2T_{low} & 1 & 0 \\ T_{high}^3 & T_{high}^2 & T_{high} & 1 \\ 3T_{high}^2 & 2T_{high} & 1 & 0 \end{bmatrix}$$

$$B(T_{low},T_{high},P) = \begin{bmatrix} Cv(T_{low},P) \\ dCv(T_{low},P) \\ Cv_{liq}(T_{high},P) \\ dCv_{liq}(T_{high},P) \end{bmatrix}$$

$$sol(T_{low}, T_{high}, P) = ACv(T_{low}, T_{high})^{-1}\, B(T_{low}, T_{high}, P) \tag{B.14}$$

Using the above the following code is used for the different pressures.

```
Cv_tot(T,P) := if P ≤ 2.5
                 m ← 2.1
                 tmp ← Cv(T,P) if T < m
                 tmp ← sol(m,m + 0.1,P)_1·T^3 + sol(m,m + 0.1,P)_2·T^2 + sol(m,m + 0.1,P)_3·T + sol(m,m + 0.1,P)_4 if T ≥ m ∧ T ≤ m + 0.1
                 tmp ← Cvliq(T,P) if T > m + 0.1
               if P > 2.5 ∧ P ≤ 5
                 m ← 2.05
                 tmp ← Cv(T,P) if T < m
                 tmp ← sol(m,m + 0.1,P)_1·T^3 + sol(m,m + 0.1,P)_2·T^2 + sol(m,m + 0.1,P)_3·T + sol(m,m + 0.1,P)_4 if T ≥ m ∧ T ≤ m + 0.1
                 tmp ← Cvliq(T,P) if T > m + 0.1
               if P > 5 ∧ P ≤ 7.5
                 m ← 2
                 tmp ← Cv(T,P) if T < m
                 tmp ← sol(m,m + 0.1,P)_1·T^3 + sol(m,m + 0.1,P)_2·T^2 + sol(m,m + 0.1,P)_3·T + sol(m,m + 0.1,P)_4 if T ≥ m ∧ T ≤ m + 0.1
                 tmp ← Cvliq(T,P) if T > m + 0.1
               if P > 7.5 ∧ P ≤ 15
                 m ← 1.95
                 tmp ← Cv(T,P) if T < m
                 tmp ← sol(m,m + 0.1,P)_1·T^3 + sol(m,m + 0.1,P)_2·T^2 + sol(m,m + 0.1,P)_3·T + sol(m,m + 0.1,P)_4 if T ≥ m ∧ T ≤ m + 0.1
                 tmp ← Cvliq(T,P) if T > m + 0.1
               if P > 15 ∧ P ≤ 17.5
                 m ← 1.9
                 tmp ← Cv(T,P) if T < m
                 tmp ← sol(m,m + 0.1,P)_1·T^3 + sol(m,m + 0.1,P)_2·T^2 + sol(m,m + 0.1,P)_3·T + sol(m,m + 0.1,P)_4 if T ≥ m ∧ T ≤ m + 0.1
                 tmp ← Cvliq(T,P) if T > m + 0.1
               if P > 17.5 ∧ P ≤ 22.5
                 m ← 1.85
                 tmp ← Cv(T,P) if T < m
                 tmp ← sol(m,m + 0.1,P)_1·T^3 + sol(m,m + 0.1,P)_2·T^2 + sol(m,m + 0.1,P)_3·T + sol(m,m + 0.1,P)_4 if T ≥ m ∧ T ≤ m + 0.1
                 tmp ← Cvliq(T,P) if T > m + 0.1
               if P > 22.5
                 m ← 1.8
                 tmp ← Cv(T,P) if T < m
                 tmp ← sol(m,m + 0.1,P)_1·T^3 + sol(m,m + 0.1,P)_2·T^2 + sol(m,m + 0.1,P)_3·T + sol(m,m + 0.1,P)_4 if T ≥ m ∧ T ≤ m + 0.1
                 tmp ← Cvliq(T,P) if T > m + 0.1
               tmp
```

FIGURE B.18: code for unifying the Cv above and below the lambda line

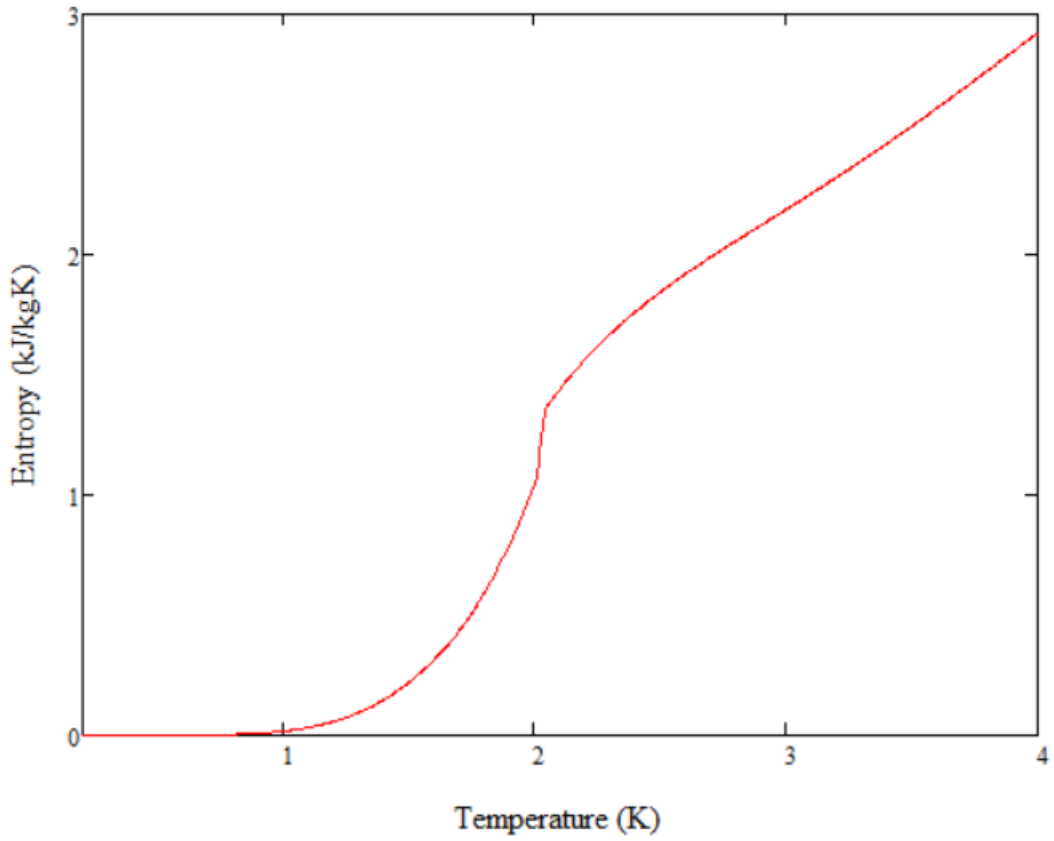

FIGURE B.19: Density of Helium-4 for 15 atm

B.4.4 Specific Heat lambda under constant pressure unification

A third degree polynomial is used for the modelling between the the fluid and the superfluid.

$$dCp(T,P) = \frac{\partial Cp(T,P)}{\partial T} \tag{B.15}$$

$$dCp_{liq}(T,P) = \frac{\partial Cp_{liq}(T,P)}{\partial T} \tag{B.16}$$

To solve the equation of the values and the differentials above and below the lambda line the following system is used:

$$ACp(T_{low},T_{high}) = \begin{bmatrix} T_{low}^3 & T_{low}^2 & T_{low} & 1 \\ 3T_{low}^2 & 2T_{low} & 1 & 0 \\ T_{high}^3 & T_{high}^2 & T_{high} & 1 \\ 3T_{high}^2 & 2T_{high} & 1 & 0 \end{bmatrix}$$

$$B(T_{low},T_{high},P) = \begin{bmatrix} Cp(T_{low},P) \\ dCp(T_{low},P) \\ Cp_{liq}(T_{high},P) \\ dCp_{liq}(T_{high},P) \end{bmatrix}$$

$$sol(T_{low}, T_{high}, P) = ACp(T_{low}, T_{high})^{-1}\, B(T_{low}, T_{high}, P) \tag{B.17}$$

Using the above the following code is used for the different pressures.

```
Cp_tot(T,P) := if P ≤ 2.5
                 m ← 2.1
                 tmp ← Cp(T,P) if T < m
                 tmp ← sol(m,m + 0.1,P)_1·T^3 + sol(m,m + 0.1,P)_2·T^2 + sol(m,m + 0.1,P)_3·T + sol(m,m + 0.1,P)_4 if T ≥ m ∧ T ≤ m + 0.1
                 tmp ← Cpliq(T,P) if T > m + 0.1
               if P > 2.5 ∧ P ≤ 5
                 m ← 2.05
                 tmp ← Cp(T,P) if T < m
                 tmp ← sol(m,m + 0.1,P)_1·T^3 + sol(m,m + 0.1,P)_2·T^2 + sol(m,m + 0.1,P)_3·T + sol(m,m + 0.1,P)_4 if T ≥ m ∧ T ≤ m + 0.1
                 tmp ← Cpliq(T,P) if T > m + 0.1
               if P > 5 ∧ P ≤ 7.5
                 m ← 2
                 tmp ← Cp(T,P) if T < m
                 tmp ← sol(m,m + 0.1,P)_1·T^3 + sol(m,m + 0.1,P)_2·T^2 + sol(m,m + 0.1,P)_3·T + sol(m,m + 0.1,P)_4 if T ≥ m ∧ T ≤ m + 0.1
                 tmp ← Cpliq(T,P) if T > m + 0.1
               if P > 7.5 ∧ P ≤ 15
                 m ← 1.95
                 tmp ← Cp(T,P) if T < m
                 tmp ← sol(m,m + 0.1,P)_1·T^3 + sol(m,m + 0.1,P)_2·T^2 + sol(m,m + 0.1,P)_3·T + sol(m,m + 0.1,P)_4 if T ≥ m ∧ T ≤ m + 0.1
                 tmp ← Cpliq(T,P) if T > m + 0.1
               if P > 15 ∧ P ≤ 17.5
                 m ← 1.9
                 tmp ← Cp(T,P) if T < m
                 tmp ← sol(m,m + 0.1,P)_1·T^3 + sol(m,m + 0.1,P)_2·T^2 + sol(m,m + 0.1,P)_3·T + sol(m,m + 0.1,P)_4 if T ≥ m ∧ T ≤ m + 0.1
                 tmp ← Cpliq(T,P) if T > m + 0.1
               if P > 17.5 ∧ P ≤ 22.5
                 m ← 1.85
                 tmp ← Cp(T,P) if T < m
                 tmp ← sol(m,m + 0.1,P)_1·T^3 + sol(m,m + 0.1,P)_2·T^2 + sol(m,m + 0.1,P)_3·T + sol(m,m + 0.1,P)_4 if T ≥ m ∧ T ≤ m + 0.1
                 tmp ← Cpliq(T,P) if T > m + 0.1
               if P > 22.5
                 m ← 1.8
                 tmp ← Cp(T,P) if T < m
                 tmp ← sol(m,m + 0.1,P)_1·T^3 + sol(m,m + 0.1,P)_2·T^2 + sol(m,m + 0.1,P)_3·T + sol(m,m + 0.1,P)_4 if T ≥ m ∧ T ≤ m + 0.1
                 tmp ← Cpliq(T,P) if T > m + 0.1
               tmp
```

FIGURE B.20: code for unifying the Cp above and below the lambda line

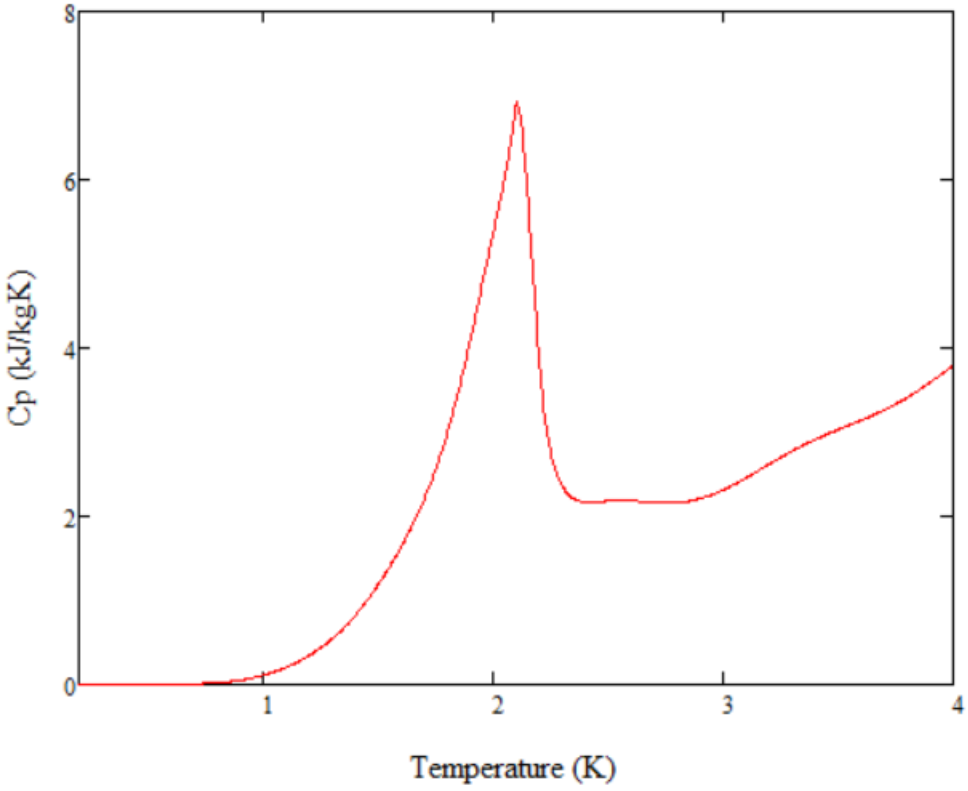

FIGURE B.21: Density of Helium-4 for 2.5 atm

B.4.5 Enthalpy lambda unification

A third degree polynomial is used for the modelling between the the fluid and the superfluid.

$$dH(T,P) = \frac{\partial H(T,P)}{\partial T} \tag{B.18}$$

$$dH_{liq}(T,P) = \frac{\partial H_{liq}(T,P)}{\partial T} \tag{B.19}$$

To solve the equation of the values and the differentials above and below the lambda line the following system is used:

$$AH(T_{low},T_{high}) = \begin{bmatrix} T_{low}^3 & T_{low}^2 & T_{low} & 1 \\ 3T_{low}^2 & 2T_{low} & 1 & 0 \\ T_{high}^3 & T_{high}^2 & T_{high} & 1 \\ 3T_{high}^2 & 2T_{high} & 1 & 0 \end{bmatrix}$$

$$B(T_{low},T_{high},P) = \begin{bmatrix} H(T_{low},P) \\ dH(T_{low},P) \\ H_{liq}(T_{high},P) \\ dH_{liq}(T_{high},P) \end{bmatrix}$$

$$sol(T_{low},T_{high},P) = AH(T_{low},T_{high})^{-1}\, B(T_{low},T_{high},P) \tag{B.20}$$

Using the above the following code is used for the different pressures.

```
H_tot(T,P) :=
  if P ≤ 2.5
    m ← 2.1
    tmp ← H(T,P)  if  T < m − 0.05
    tmp ← sol(m − 0.05,m,P)_1·T^3 + sol(m − 0.05,m,P)_2·T^2 + sol(m − 0.05,m,P)_3·T + sol(m − 0.05,m,P)_4  if  T ≥ m − 0.05 ∧ T ≤ m
    tmp ← Hliq(T,P)  if  T > m
  if  P > 2.5 ∧ P ≤ 5
    m ← 2.05
    tmp ← H(T,P)  if  T < m − 0.05
    tmp ← sol(m − 0.05,m,P)_1·T^3 + sol(m − 0.05,m,P)_2·T^2 + sol(m − 0.05,m,P)_3·T + sol(m − 0.05,m,P)_4  if  T ≥ m − 0.05 ∧ T ≤ m
    tmp ← Hliq(T,P)  if  T > m
  if  P > 5 ∧ P ≤ 7.5
    m ← 2
    tmp ← H(T,P)  if  T < m − 0.05
    tmp ← sol(m − 0.05,m,P)_1·T^3 + sol(m − 0.05,m,P)_2·T^2 + sol(m − 0.05,m,P)_3·T + sol(m − 0.05,m,P)_4  if  T ≥ m − 0.05 ∧ T ≤ m
    tmp ← Hliq(T,P)  if  T > m
  if  P > 7.5 ∧ P ≤ 15
    m ← 1.95
    tmp ← H(T,P)  if  T < m − 0.05
    tmp ← sol(m − 0.05,m,P)_1·T^3 + sol(m − 0.05,m,P)_2·T^2 + sol(m − 0.05,m,P)_3·T + sol(m − 0.05,m,P)_4  if  T ≥ m − 0.05 ∧ T ≤ m
    tmp ← Hliq(T,P)  if  T > m
  if  P > 15 ∧ P ≤ 17.5
    m ← 1.9
    tmp ← H(T,P)  if  T < m − 0.05
    tmp ← sol(m − 0.05,m,P)_1·T^3 + sol(m − 0.05,m,P)_2·T^2 + sol(m − 0.05,m,P)_3·T + sol(m − 0.05,m,P)_4  if  T ≥ m − 0.05 ∧ T ≤ m
    tmp ← Hliq(T,P)  if  T > m
  if  P > 17.5 ∧ P ≤ 22.5
    m ← 1.85
    tmp ← H(T,P)  if  T < m − 0.05
    tmp ← sol(m − 0.05,m,P)_1·T^3 + sol(m − 0.05,m,P)_2·T^2 + sol(m − 0.05,m,P)_3·T + sol(m − 0.05,m,P)_4  if  T ≥ m − 0.05 ∧ T ≤ m
    tmp ← Hliq(T,P)  if  T > m
  if  P > 22.5
    m ← 1.8
    tmp ← H(T,P)  if  T < m − 0.05
    tmp ← sol(m − 0.05,m,P)_1·T^3 + sol(m − 0.05,m,P)_2·T^2 + sol(m − 0.05,m,P)_3·T + sol(m − 0.05,m,P)_4  if  T ≥ m − 0.05 ∧ T ≤ m
    tmp ← Hliq(T,P)  if  T > m
  tmp
```

FIGURE B.22: code for unifying the enthalpy above and below the lambda line

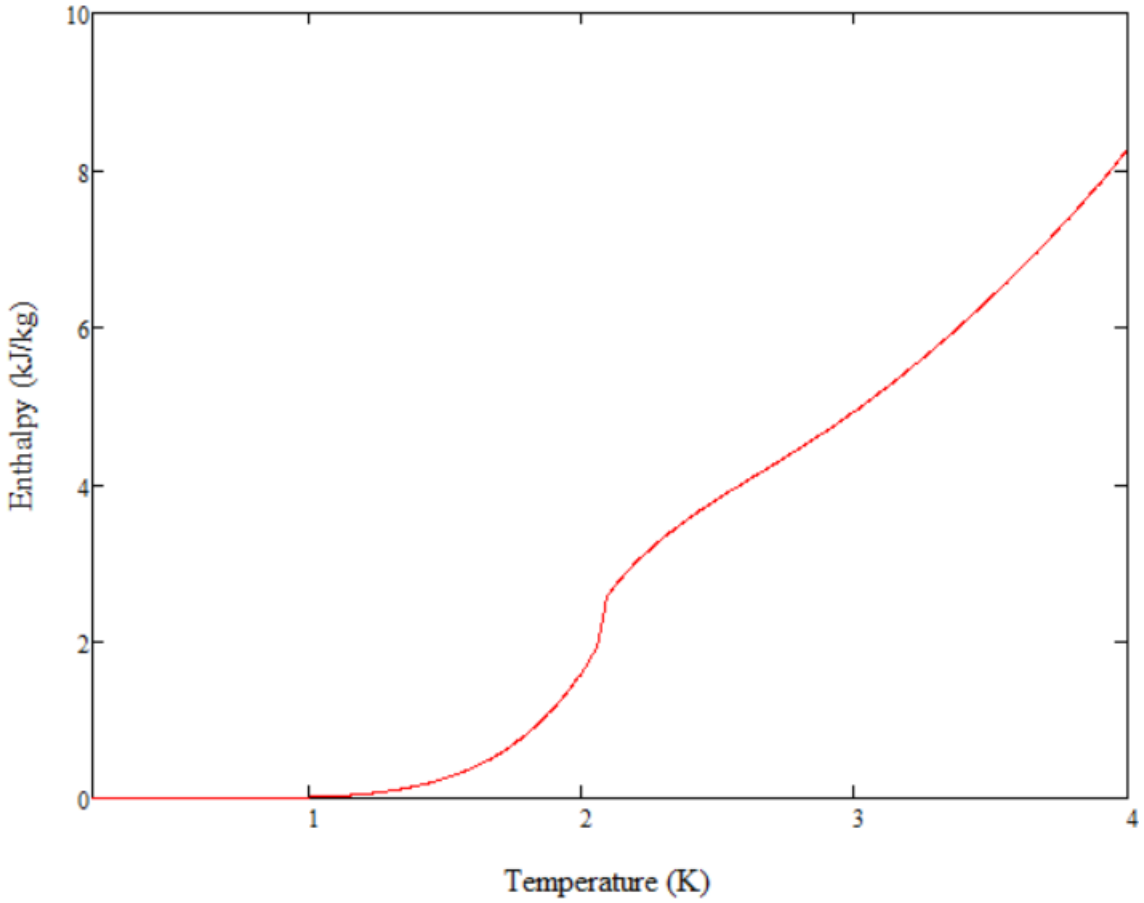

FIGURE B.23: Density of Helium-4 for 1 atm

Below the rest of the graphs for the pressure spectrum of the equations of Helium-4 as continued from Chapter 3 are presented.

For the pressure of 10 atm

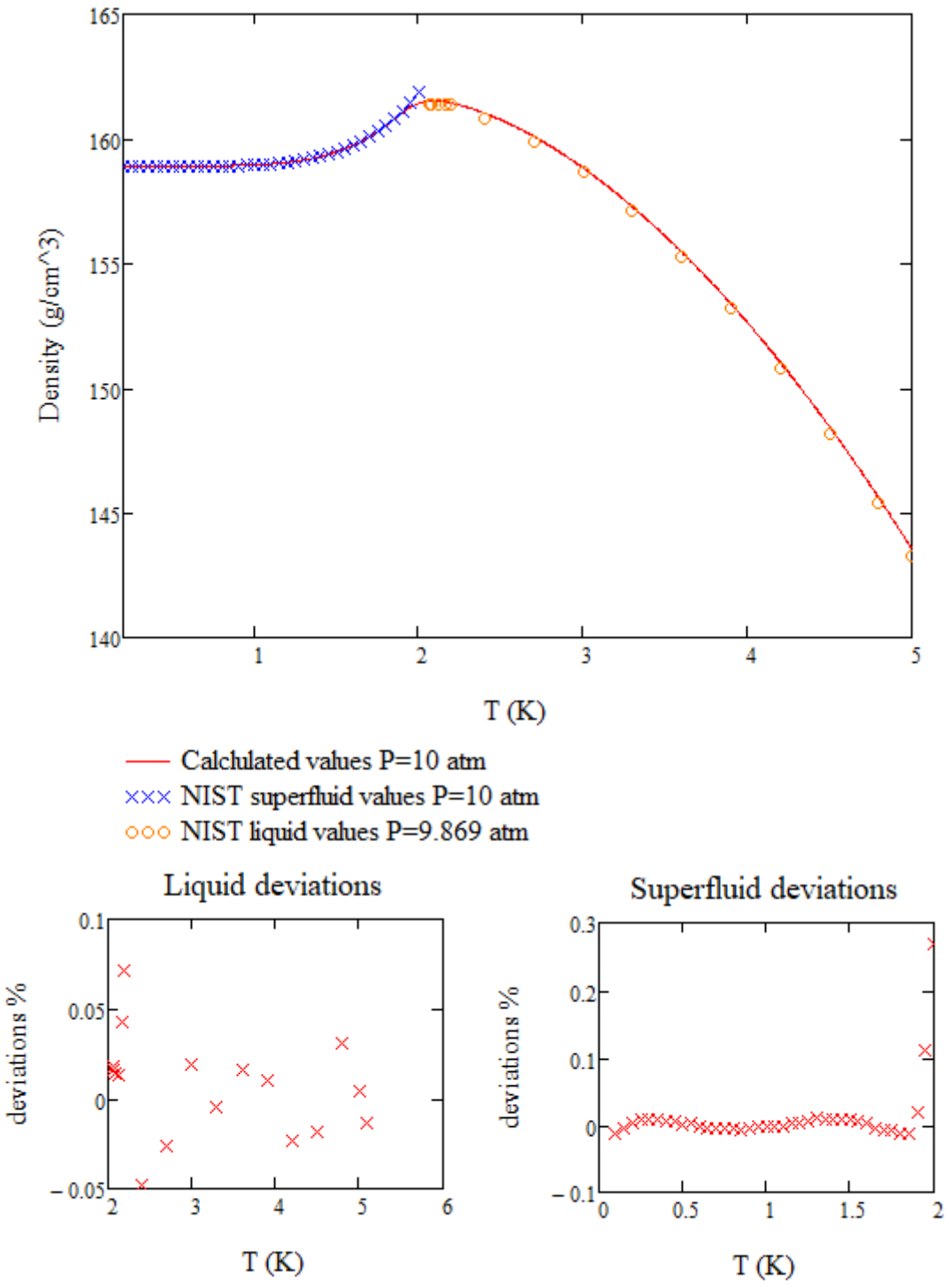

FIGURE B.24: Calculated density compared to the NIST values

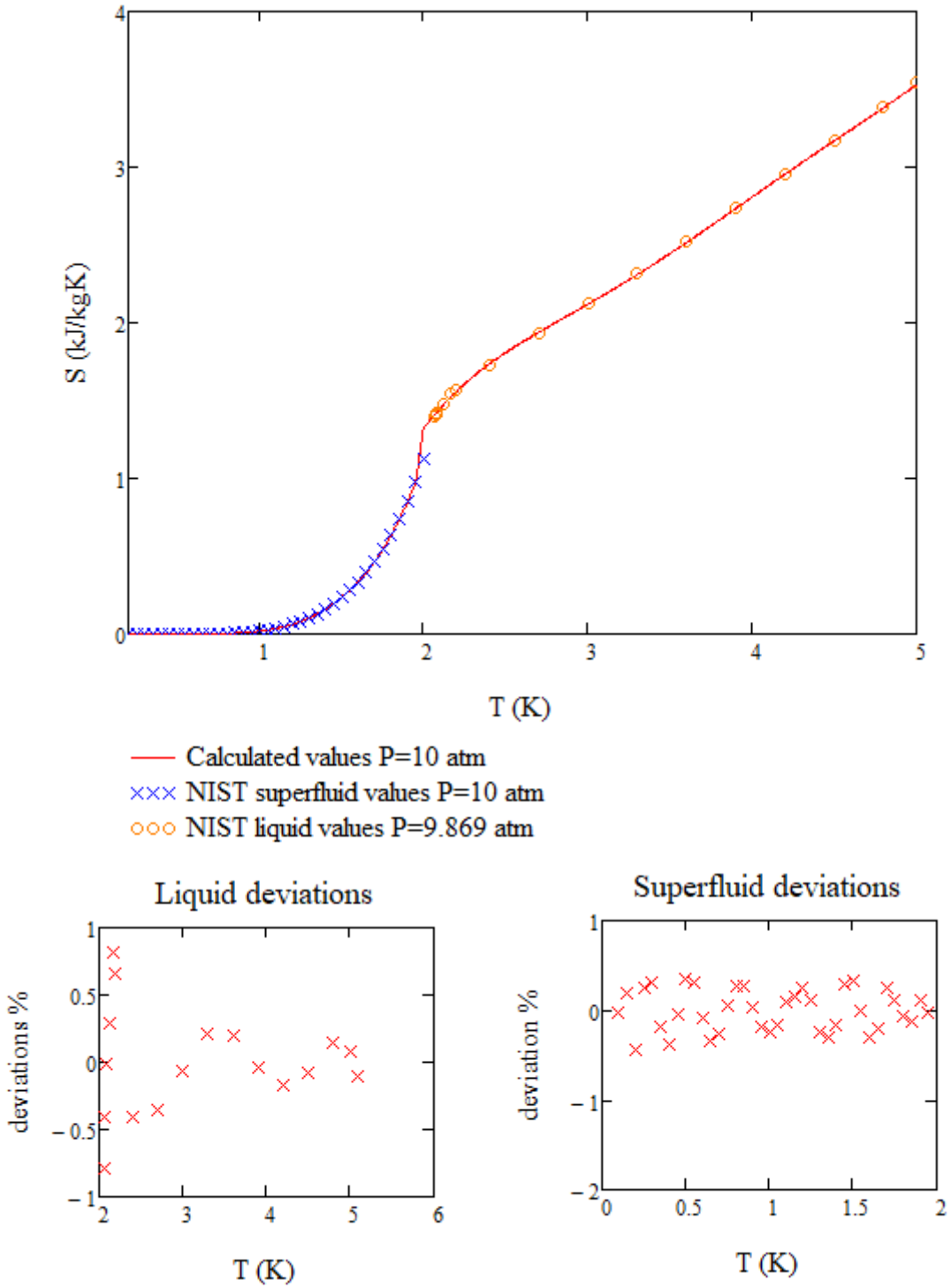

FIGURE B.25: Calculated entropy compared to the NIST values

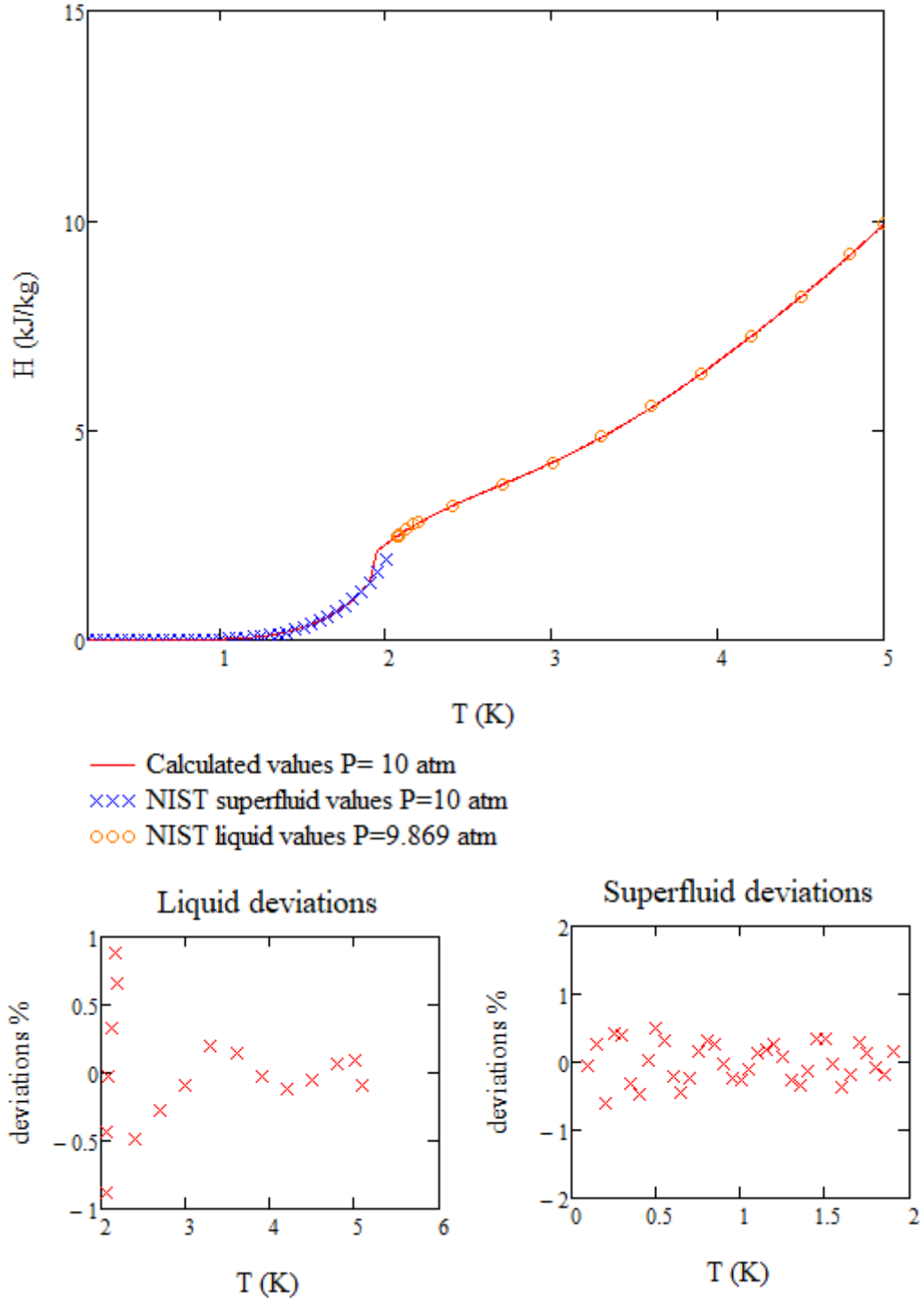

FIGURE B.26: Calculated enthalpy compared to the NIST values

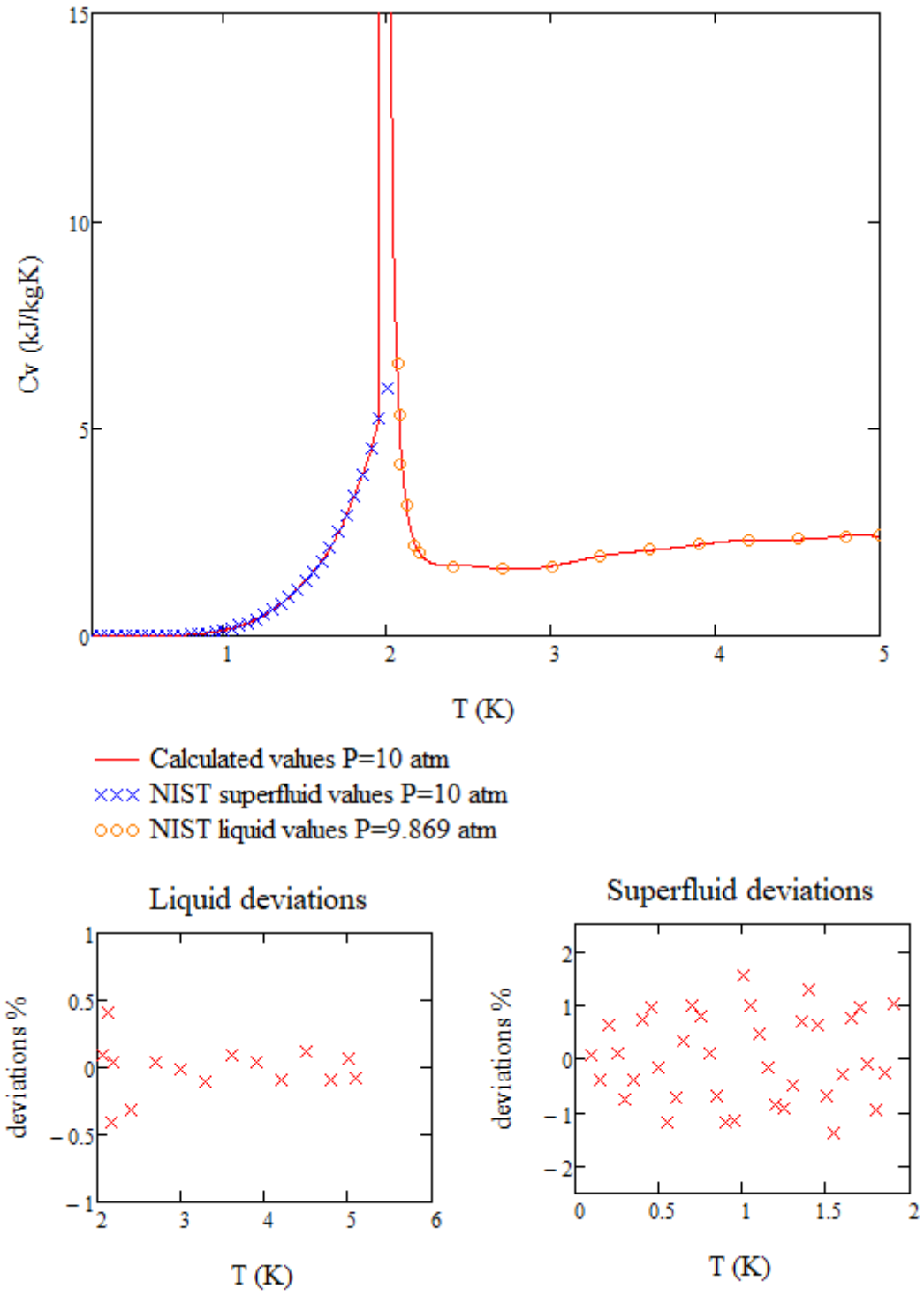

FIGURE B.27: Calculated Cv compared to the NIST values

For the pressure of 17.5 atm

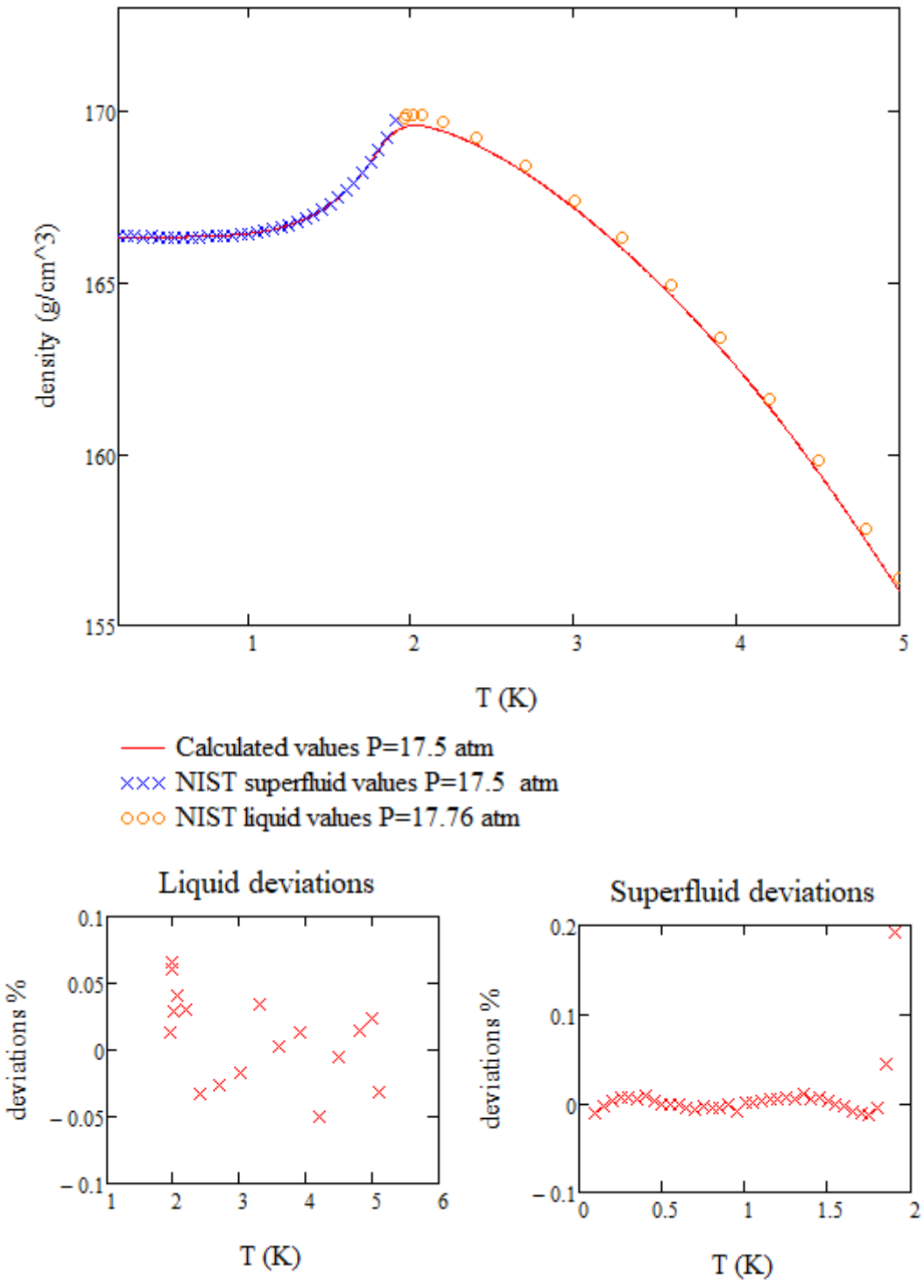

FIGURE B.28: Calculated density compared to the NIST values

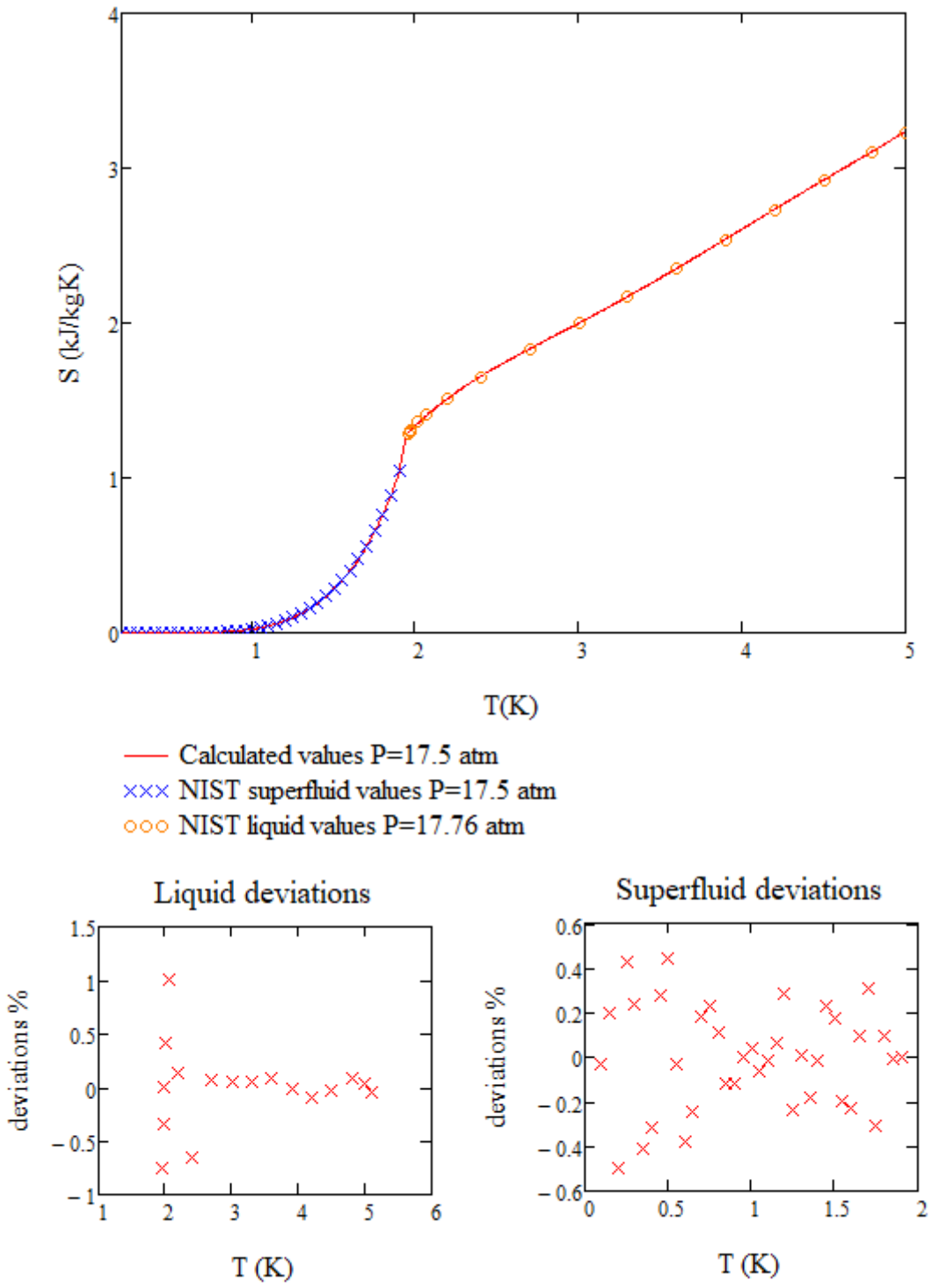

FIGURE B.29: Calculated entropy compared to the NIST values

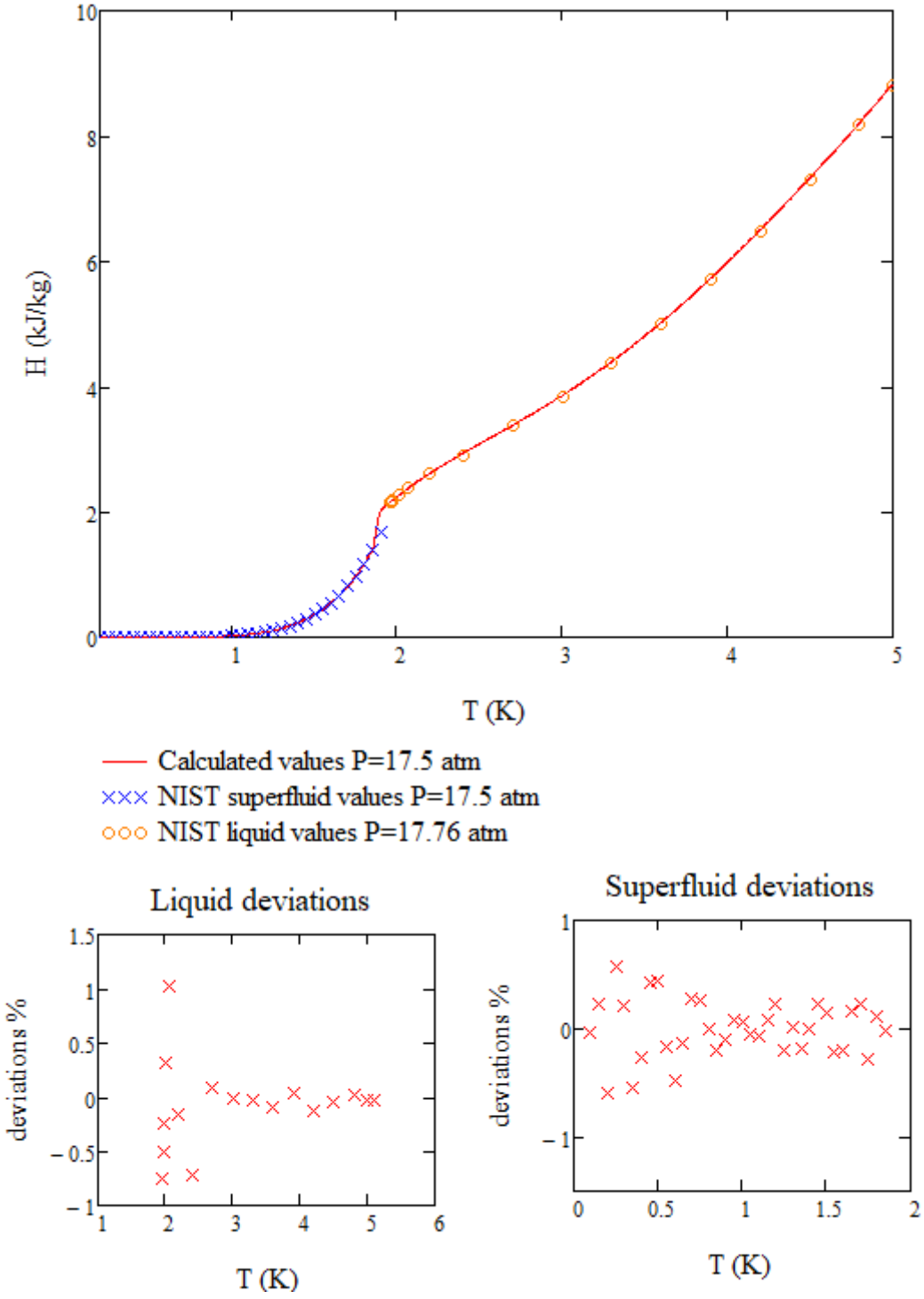

FIGURE B.30: Calculated enthalpy compared to the NIST values

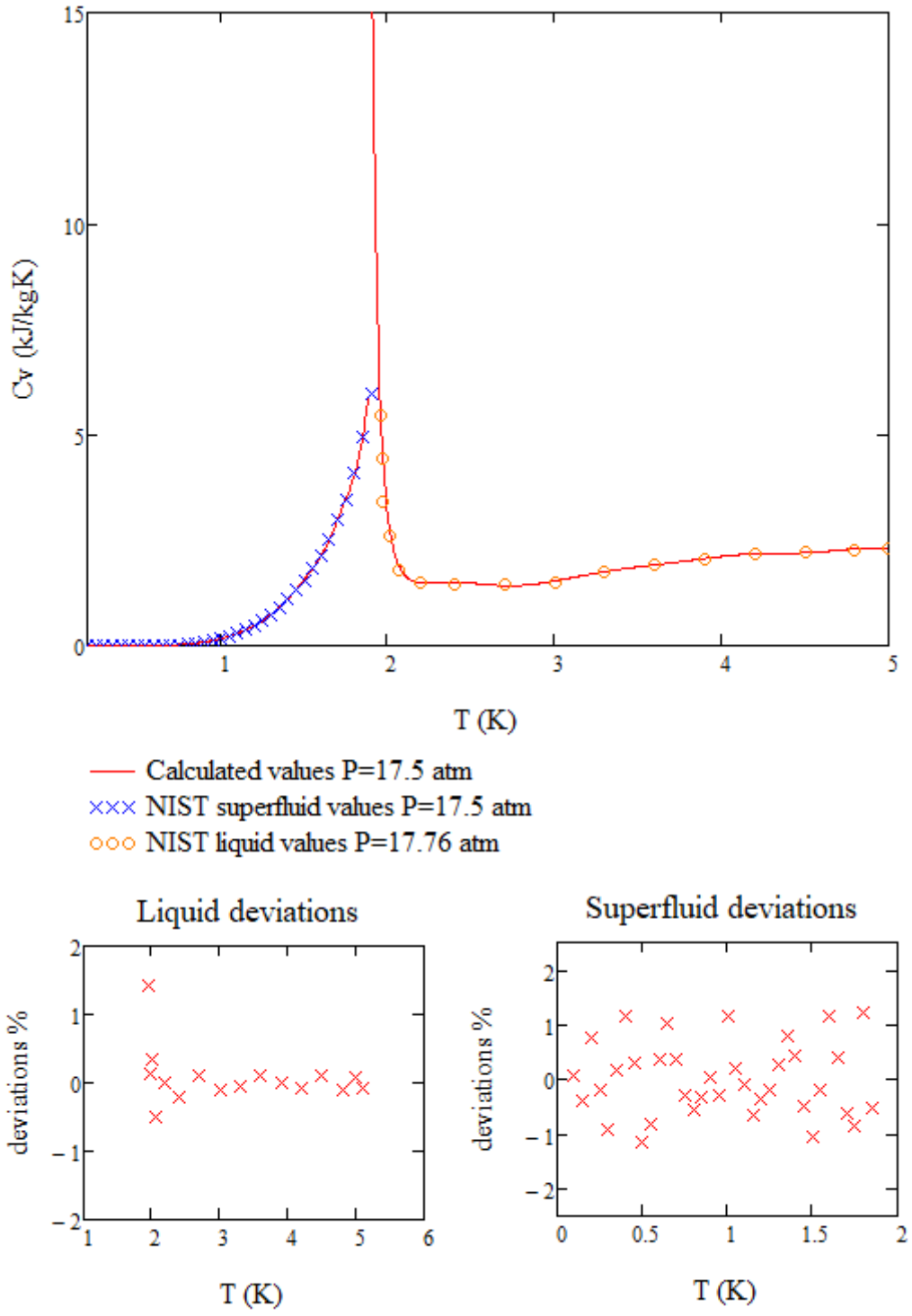

FIGURE B.31: Calculated Cv compared to the NIST values

Coefficients A, B, C for equations 3.30,3.31,3.32.

A	1	2	3	4
1	1.0412277277778E-01	-2.4034933851993E-01	8.3420461018326E-02	-1.3067751932983E-02
2	-4.2024128116990E-01	2.2147290494175E+00	-7.5954548090200E-01	1.1808622774893E-01
3	-1.8008327680543E-02	-4.6623082782179E+00	1.5777521759029E+00	-2.4409535120981E-01
4	3.1677074801942E-01	3.9658021221151E+00	-1.3227378988727E+00	2.0389721497284E-01
5	2.1693492776641E-02	-1.5955770110885E+00	5.2412055176278E-01	-8.0411575271253E-02
6	-4.6329216676061E-02	3.0342211687491E-01	-9.8251944905298E-02	1.4988565125295E-02
7	6.5493480253451E-03	-2.2017962183576E-02	7.0344906396709E-03	-1.0662535672353E-03

Table B.2: Eq. 3.30 coefficients

A	5	6	7
1	1.0315470478363E-03	-3.9845530153053E-05	5.9868188679111E-07
2	-9.2750822997147E-03	3.5690990290860E-04	-5.3462399853747E-06
3	1.9125773602930E-02	-7.3490383775172E-04	1.0997723133852E-05
4	-1.5953832063294E-02	6.1272302211458E-04	-9.1684391765032E-06
5	6.2768817903458E-03	-2.4076570344077E-04	3.6001532163667E-06
6	-1.1660717729045E-03	4.4633304579506E-05	-6.6646406884662E-07
7	8.2609264865491E-05	-3.1532052673936E-06	4.6991052967232E-08

Table B.3: Eq. 3.31 coefficients

B	1	2	3	4
1	1.4328199251724E+02	2.4995182375956E+00	-1.9691702007769E-01	1.4131158408264E-02
2	1.5246809650510E+01	-4.9905708275271E+00	8.0860946946091E-01	-4.7309787217245E-02
3	-3.5463444458474E+01	9.9869388349003E+00	-1.3232801491867E+00	2.9586598515696E-02
4	3.3588281392551E+01	-8.7491781510819E+00	9.6909536730676E-01	1.6566209162436E-02
5	-1.4635531338950E+01	3.8959603262452E+00	-4.0976388795732E-01	-1.1897752626895E-02
6	2.9377340295461E+00	-8.5576640491163E-01	9.8107559496876E-02	7.0079896038729E-04
7	-2.2531934915833E-01	7.3727962093781E-02	-9.7744627718597E-03	2.4994169031560E-04

Table B.4: Eq. 3.32 coefficients

B	5	6	7
1	-4.8810989574191E-04	5.4456493846956E-06	2.4775287775952E-08
2	1.1268019904603E-05	7.7803412170458E-05	-1.7094203667516E-06
3	5.4533860540646E-03	-3.6130216627714E-04	6.3098524998090E-06
4	-8.3649481042780E-03	4.5293008011676E-04	-7.4885240804019E-06
5	4.0849423106936E-03	-2.1573530624796E-04	3.5580031254531E-06
6	-7.2454695792515E-04	4.0734059020416E-05	-6.9006411568451E-07
7	3.4576496875657E-05	-2.4193932229523E-06	4.3861314027288E-08

C	1	2	3	4
1	-1.7697638754163E-01	-4.7534858770845E-02	7.6844591319251E-03	-9.8042324943453E-07
2	2.3901960784721E+00	6.2877945111706E-01	-1.1054768669661E-01	4.2247641419138E-03
3	-6.0059837182230E+00	-1.8183422908258E+00	3.5547564968312E-01	-2.6225406188548E-02
4	4.9161826205907E+00	2.0290829674619E+00	-4.2950443004419E-01	4.1589064818976E-02
5	-1.4183603969816E+00	-1.0164525745529E+00	2.2604466746005E-01	-2.4713508724054E-02
6	1.4732212320390E-01	2.3010527934455E-01	-5.2901530525594E-02	6.1501667545121E-03
7	-1.7518592443086E-03	-1.9320062576618E-02	4.5462035567394E-03	-5.4715845570318E-04

C	5	6	7
1	-6.6457497218259E-05	4.5071431055277E-06	-9.0647515101144E-08
2	3.6121066524305E-04	-3.3678548553402E-05	7.3462240505830E-07
3	5.7793594208609E-04	1.8775464638763E-05	-7.4819311886524E-07
4	-2.0441693903292E-03	4.6080113182283E-05	-3.2971050592579E-07
5	1.4533865417391E-03	-4.3342591896604E-05	5.1362521802549E-07
6	-3.8805088189195E-04	1.2534639933226E-05	-1.6243159310253E-07
7	3.5727267699850E-05	-1.1941551136084E-06	1.6003152059373E-08

Appendix C

Appendix Helium 3-4 Mixture

C.1 Numerical Equations of Thermodynamic Mix data

The form of the equation used for the polynomial for the different thermodynamic variables is given by the following code:

```
Eq(deg) := | count ← 0
           | tmp ← ""
           | for i ∈ 0.. deg
           |   for j ∈ 0.. deg
           |     for k ∈ 0.. deg
           |       | count ← count + 1
           |       | tmp ← concat(tmp,"+c",num2str(count),"*x1^",num2str(i),"*x2^",num2str(j),"*x3^",num2str(k))
           | tmp
```

a)

```
H(T,P,x) = | count ← 0
           | tmp ← 0
           | for i ∈ 0..5
           |   for j ∈ 0..5
           |     for k ∈ 0..5
           |       | count ← count + 1
           |       | tmp ← tmp + C_count · T^i · P^j · x^k
           | tmp
```

b)

FIGURE C.1: Code for the polynomial: subfigure (a) gives the text form, subfigure (b) gives the Mathcad equation form for the enthalpy. C is the table of coefficients.

where the deg refers to the degree of the polynomial with x1, x2, x3 being the variables used, in this case being x, T ,P.

The overall code for a 5 degree polynomial will be presented in general to showcase it in general. For space and repetition reasons only the code for the enthalpy is to be presented. For the rest of the variables the reader can use the provided code in C.1 combined with the tables given for the coefficients for each of the variables. The coefficients are at each time derived using the CurveExpert software by inserting the equation and the wanted data.

General Equation Form:

$Eq(5) = +c1*x1^0*x2^0*x3^0+c2*x1^0*x2^0*x3^1+c3*x1^0*x2^0*x3^2+c4*x1^0*x2^0*x3^3+c5*x1^0*x2^0*x3^4+c6*x1^0*x2^0*x3^5+c7*x1^0*x2^1*x3^0+c8*x1^0*x2^1*x3^1+c9*x1^0*x2^1*x3^2+$

$$c10*x1^0*x2^1*x3^3+c11*x1^0*x2^1*x3^4+c12*x1^0*x2^1*x3^5+c13*x1^0*x2^2*x3^0+c14*x1^0*x2^2*x3^1+c15*x1^0*x2^2*x3^2+c16*x1^0*x2^2*x3^3+c17*x1^0*x2^2*x3^4+c18*x1^0*x2^2*x3^5+c19*x1^0*x2^3*x3^0+c20*x1^0*x2^3*x3^1+c21*x1^0*x2^3*x3^2+c22*x1^0*x2^3*x3^3+c23*x1^0*x2^3*x3^4+c24*x1^0*x2^3*x3^5+c25*x1^0*x2^4*x3^0+c26*x1^0*x2^4*x3^1+c27*x1^0*x2^4*x3^2+c28*x1^0*x2^4*x3^3+c29*x1^0*x2^4*x3^4+c30*x1^0*x2^4*x3^5+c31*x1^0*x2^5*x3^0+c32*x1^0*x2^5*x3^1+c33*x1^0*x2^5*x3^2+c34*x1^0*x2^5*x3^3+c35*x1^0*x2^5*x3^4+c36*x1^0*x2^5*x3^5+c37*x1^1*x2^0*x3^0+c38*x1^1*x2^0*x3^1+c39*x1^1*x2^0*x3^2+c40*x1^1*x2^0*x3^3+c41*x1^1*x2^0*x3^4+c42*x1^1*x2^0*x3^5+c43*x1^1*x2^1*x3^0+c44*x1^1*x2^1*x3^1+c45*x1^1*x2^1*x3^2+c46*x1^1*x2^1*x3^3+c47*x1^1*x2^1*x3^4+c48*x1^1*x2^1*x3^5+c49*x1^1*x2^2*x3^0+c50*x1^1*x2^2*x3^1+c51*x1^1*x2^2*x3^2+c52*x1^1*x2^2*x3^3+c53*x1^1*x2^2*x3^4+c54*x1^1*x2^2*x3^5+c55*x1^1*x2^3*x3^0+c56*x1^1*x2^3*x3^1+c57*x1^1*x2^3*x3^2+c58*x1^1*x2^3*x3^3+c59*x1^1*x2^3*x3^4+c60*x1^1*x2^3*x3^5+c61*x1^1*x2^4*x3^0+c62*x1^1*x2^4*x3^1+c63*x1^1*x2^4*x3^2+c64*x1^1*x2^4*x3^3+c65*x1^1*x2^4*x3^4+c66*x1^1*x2^4*x3^5+c67*x1^1*x2^5*x3^0+c68*x1^1*x2^5*x3^1+c69*x1^1*x2^5*x3^2+c70*x1^1*x2^5*x3^3+c71*x1^1*x2^5*x3^4+c72*x1^1*x2^5*x3^5+c73*x1^2*x2^0*x3^0+c74*x1^2*x2^0*x3^1+c75*x1^2*x2^0*x3^2+c76*x1^2*x2^0*x3^3+c77*x1^2*x2^0*x3^4+c78*x1^2*x2^0*x3^5+c79*x1^2*x2^1*x3^0+c80*x1^2*x2^1*x3^1+c81*x1^2*x2^1*x3^2+c82*x1^2*x2^1*x3^3+c83*x1^2*x2^1*x3^4+c84*x1^2*x2^1*x3^5+c85*x1^2*x2^2*x3^0+c86*x1^2*x2^2*x3^1+c87*x1^2*x2^2*x3^2+c88*x1^2*x2^2*x3^3+c89*x1^2*x2^2*x3^4+c90*x1^2*x2^2*x3^5+c91*x1^2*x2^3*x3^0+c92*x1^2*x2^3*x3^1+c93*x1^2*x2^3*x3^2+c94*x1^2*x2^3*x3^3+c95*x1^2*x2^3*x3^4+c96*x1^2*x2^3*x3^5+c97*x1^2*x2^4*x3^0+c98*x1^2*x2^4*x3^1+c99*x1^2*x2^4*x3^2+c100*x1^2*x2^4*x3^3+c101*x1^2*x2^4*x3^4+c102*x1^2*x2^4*x3^5+c103*x1^2*x2^5*x3^0+c104*x1^2*x2^5*x3^1+c105*x1^2*x2^5*x3^2+c106*x1^2*x2^5*x3^3+c107*x1^2*x2^5*x3^4+c108*x1^2*x2^5*x3^5+c109*x1^3*x2^0*x3^0+c110*x1^3*x2^0*x3^1+c111*x1^3*x2^0*x3^2+c112*x1^3*x2^0*x3^3+c113*x1^3*x2^0*x3^4+c114*x1^3*x2^0*x3^5+c115*x1^3*x2^1*x3^0+c116*x1^3*x2^1*x3^1+c117*x1^3*x2^1*x3^2+c118*x1^3*x2^1*x3^3+c119*x1^3*x2^1*x3^4+c120*x1^3*x2^1*x3^5+c121*x1^3*x2^2*x3^0+c122*x1^3*x2^2*x3^1+c123*x1^3*x2^2*x3^2+c124*x1^3*x2^2*x3^3+c125*x1^3*x2^2*x3^4+c126*x1^3*x2^2*x3^5+c127*x1^3*x2^3*x3^0+c128*x1^3*x2^3*x3^1+c129*x1^3*x2^3*x3^2+c130*x1^3*x2^3*x3^3+c131*x1^3*x2^3*x3^4+c132*x1^3*x2^3*x3^5+c133*x1^3*x2^4*x3^0+c134*x1^3*x2^4*x3^1+c135*x1^3*x2^4*x3^2+c136*x1^3*x2^4*x3^3+c137*x1^3*x2^4*x3^4+c138*x1^3*x2^4*x3^5+c139*x1^3*x2^5*x3^0+c140*x1^3*x2^5*x3^1+c141*x1^3*x2^5*x3^2+c142*x1^3*x2^5*x3^3+c143*x1^3*x2^5*x3^4+c144*x1^3*x2^5*x3^5+c145*x1^4*x2^0*x3^0+c146*x1^4*x2^0*x3^1+c147*x1^4*x2^0*x3^2+c148*x1^4*x2^0*x3^3+c149*x1^4*x2^0*x3^4+c150*x1^4*x2^0*x3^5+c151*x1^4*x2^1*x3^0+c152*x1^4*x2^1*x3^1+c153*x1^4*x2^1*x3^2+c154*x1^4*x2^1*x3^3+c155*x1^4*x2^1*x3^4+c156*x1^4*x2^1*x3^5+c157*x1^4*x2^2*x3^0+c158*x1^4*x2^2*x3^1+c159*x1^4*x2^2*x3^2+c160*x1^4*x2^2*x3^3+c161*x1^4*x2^2*x3^4+c162*x1^4*x2^2*x3^5+c163*x1^4*x2^3*x3^0+c164*x1^4*x2^3*x3^1+c165*x1^4*x2^3*x3^2+c166*x1^4*x2^3*x3^3+c167*x1^4*x2^3*x3^4+c168*x1^4*x2^3*x3^5+c169*x1^4*x2^4*x3^0+c170*x1^4*x2^4*x3^1+c171*x1^4*x2^4*x3^2+c172*x1^4*x2^4*x3^3+c173*x1^4*x2^4*x3^4+c174*x1^4*x2^4*x3^5+c175*x1^4*x2^5*x3^0+c176*x1^4*x2^5*x3^1+c177*x1^4*x2^5*x3^2+c178*x1^4*x2^5*x3^3+c179*x1^4*x2^5*x3^4+c180*x1^4*x2^5*x3^5+c181*x1^5*x2^0*x3^0+c182*x1^5*x2^0*x3^1+c183*x1^5*x2^0*x3^2+c184*x1^5*x2^0*x3^3+c185*x1^5*x2^0*x3^4+c186*x1^5*x2^0*x3^5+c187*x1^5*x2^1*x3^0+c188*x1^5*x2^1*x3^1+c189*x1^5*x2^1*x3^2+c190*x1^5*x2^1*x3^3+c191*x1^5*x2^1*x3^4+c192*x1^5*x2^1*x3^5+c193*x1^5*x2^2*x3^0+c194*x1^5*x2^2*x3^1+c195*x1^5*x2^2*x3^2+c196*x1^5*x2^2*x3^3+c197*x1^5*x2^2*x3^4+c198*x1^5*x2^2*x3^5+c199*x1^5*x2^3*x3^0+c200*x1^5*x2^3*x3^1+c201*x1^5*x2^3*x3^2+c202*x1^5*x2^3*x3^3+c203*x1^5*x2^3*x3^4+c204*x1^5*x2^3*x3^5+c205*x1^5*x2^4*x3^0+c206*x1^5*x2^4*x3^1+c207*x1^5*x2^4*x3^2+c208*x1^5*x2^4*x3^3+c209*x1^5*x2^4*x3^4+c210*x1^5*x2^4*x3^5+c211*x1^5*x2^5*x3^0+c212*x1^5*x2^5*x3^1+c213*x1^5*x2^5*x3^2+c214*x1^5*x2^5*x3^3+c215*x1^5*x2^5*x3^4+c216*x1^5*x2^5*x3^5$$

For the enthalpy specifically the specific equation used, including the coefficients, is:

$$H(x,T,P) = -0.079284*T^0*P^0*x^0+10.076656*T^0*P^0*x^1+-69.72213*T^0*P^0*x^2+210.402783*T^0*P^0*x^3+-253.924167*T^0*P^0*x^4+103.314602*T^0*P^0*x^5+3.27498*T^0*P^1*x^0+0.475766*T^0*P^1*x^1+23.087939*T^0*P^1*x^2+-132.136613*T^0*P^1*x^3+218.028038*T^0*P^1*x^4+-110.221046*T^0*P^1*x^5+-0.555089*T^0*P^2*x^0+-0.546722*T^0*P^2*x^1+-3.233962*T^0*P^2*x^2+45.810516*T^0*P^2*x^3+-91.815686*T^0*P^2*x^4+51.072871*T^0*P^2*x^5+0.166067*T^0*P^3*x^0+-0.145248*T^0*P^3*x^1+1.027247*T^0*P^3*x^2+-8.419012*T^0*P^3*x^3+16.431625*T^0*P^3*x^4+-9.251559*T^0*P^3*x^5+-0.019757*T^0*P^4*x^0+0.039605*T^0*P^4*x^1+-0.112447*T^0*P^4*x^2+0.546657*T^0*P^4*x^3+-1.045255*T^0*P^4*x^4+0.610878*T^0*P^4*x^5+0.000807*T^0*P^5*x^0+-0.002163*T^0*P^5*x^1+0.003462*T^0*P^5*x^2+-0.006848*T^0*P^5*x^3+0.013863*T^0*P^5*x^4+-0.009835*T^0*P^5*x^5+0.546297*T^1*P^0*x^0+-68.5214*T^1*P^0*x^1+356.118375*T^1*P^0*x^2+-1012.988417*T^1*P^0*x^3+1194.1079*T^1*P^0*x^4+-469.13684*T^1*P^0*x^5+-4.060499*T^1*P^1*x^0+-14.1703*T^1*P^1*x^1+-4.107869*T^1*P^1*x^2+454.639331*T^1*P^1*x^3+-951.712527*T^1*P^1*x^4+527.557268*T^1*P^1*x^5+4.559952*T^1*P^2*x^0+8.258493*T^1*P^2*x^1+-48.958289*T^1*P^2*x^2+-54.317628*T^1*P^2*x^3+271.294431*T^1*P^2*x^4+-186.054291*T^1*P^2*x^5+-1.452354*T^1*P^3*x^0+2.467917*T^1*P^3*x^1+-4.419436*T^1*P^3*x^2+21.954008*T^1*P^3*x^3+-44.189293*T^1*P^3*x^4+26.868989*T^1*P^3*x^5+0.17689*T^1*P^4*x^0+-0.673862*T^1*P^4*x^1+1.912354*T^1*P^4*x^2+-2.725658*T^1*P^4*x^3+1.974614*T^1*P^4*x^4+-0.785359*T^1*P^4*x^5+-0.007337*T^1*P^5*x^0+0.037736*T^1*P^5*x^1+-0.110572*T^1*P^5*x^2+0.092039*T^1*P^5*x^3+0.040545*T^1*P^5*x^4+-0.048188*T^1*P^5*x^5+-1.232049*T^2*P^0*x^0+174.776938*T^2*P^0*x^1+-345.489429*T^2*P^0*x^2+460.321047*T^2*P^0*x^3+-259.8126*T^2*P^0*x^4+-19.773507*T^2*P^0*x^5+13.816402*T^2*P^1*x^0+47.009207*T^2*P^1*x^1+-351.97022*T^2*P^1*x^2+229.928713*T^2*P^1*x^3+549.352738*T^2*P^1*x^4+-507.465776*T^2*P^1*x^5+-15.583572*T^2*P^2*x^0+-6.529397*T^2*P^2*x^1+265.353853*T^2*P^2*x^2+-638.737366*T^2*P^2*x^3+508.399383*T^2*P^2*x^4+-101.421966*T^2*P^2*x^5+4.986333*T^2*P^3*x^0+-17.568207*T^2*P^3*x^1+20.888305*T^2*P^3*x^2+45.844374*T^2*P^3*x^3+-111.390473*T^2*P^3*x^4+54.671768*T^2*P^3*x^5+-0.609887*T^2*P^4*x^0+3.628525*T^2*P^4*x^1+-10.201071*T^2*P^4*x^2+5.328177*T^2*P^4*x^3+10.827429*T^2*P^4*x^4+-8.733605*T^2*P^4*x^5+0.025379*T^2*P^5*x^0+-0.190862*T^2*P^5*x^1+0.61817*T^2*P^5*x^2+-0.459637*T^2*P^5*x^3+-0.458156*T^2*P^5*x^4+0.457227*T^2*P^5*x^5+1.351115*T^3*P^0*x^0+-167.914114*T^3*P^0*x^1+-211.856654*T^3*P^0*x^2+1669.493892*T^3*P^0*x^3+-2506.656131*T^3*P^0*x^4+1203.321462*T^3*P^0*x^5+-22.656113*T^3*P^1*x^0+-25.16501*T^3*P^1*x^1+671.107627*T^3*P^1*x^2+-1638.496256*T^3*P^1*x^3+1381.524549*T^3*P^1*x^4+-345.888277*T^3*P^1*x^5+24.860501*T^3*P^2*x^0+-43.02926*T^3*P^2*x^1+-347.974872*T^3*P^2*x^2+1466.157599*T^3*P^2*x^3+-1880.771412*T^3*P^2*x^4+769.656786*T^3*P^2*x^5+-7.880647*T^3*P^3*x^0+42.994526*T^3*P^3*x^1+-72.187477*T^3*P^3*x^2+-112.664053*T^3*P^3*x^3+348.359525*T^3*P^3*x^4+-196.309867*T^3*P^3*x^5+0.960076*T^3*P^4*x^0+-7.52529*T^3*P^4*x^1+22.485926*T^3*P^4*x^2+-12.001286*T^3*P^4*x^3+-24.986067*T^3*P^4*x^4+20.86821*T^3*P^4*x^5+-0.039865*T^3*P^5*x^0+0.375448*T^3*P^5*x^1+-1.294318*T^3*P^5*x^2+1.132764*T^3*P^5*x^3+0.663992*T^3*P^5*x^4+-0.832172*T^3*P^5*x^5+-1.025378*T^4*P^0*x^0+78.003436*T^4*P^0*x^1+316.070743*T^4*P^0*x^2+-1542.77666*T^4*P^0*x^3+2085.808375*T^4*P^0*x^4+-927.600404*T^4*P^0*x^5+16.778198*T^4*P^1*x^0+-19.76783*T^4*P^1*x^1+-427.45675*T^4*P^1*x^2+1478.072768*T^4*P^1*x^3+-1705.050059*T^4*P^1*x^4+647.381441*T^4*P^1*x^5+-17.901959*T^4*P^2*x^0+64.116094*T^4*P^2*x^1+153.213347*T^4*P^2*x^2+-1081.945179*T^4*P^2*x^3+1628.229158*T^4*P^2*x^4+-740.855775*T^4*P^2*$$

$$x^5 + 5.612295 * T^4 * P^3 * x^0 + -39.178278 * T^4 * P^3 * x^1 + 80.982682 * T^4 * P^3 * x^2 + 62.554425 * T^4 * P^3 * x^3 + -279.545571 * T^4 * P^3 * x^4 + 168.662986 * T^4 * P^3 * x^5 + -0.679971 * T^4 * P^4 * x^0 + 6.281515 * T^4 * P^4 * x^1 + -19.80332 * T^4 * P^4 * x^2 + 13.39954 * T^4 * P^4 * x^3 + 16.705611 * T^4 * P^4 * x^4 + -15.835904 * T^4 * P^4 * x^5 + 0.02814 * T^4 * P^5 * x^0 + -0.302971 * T^4 * P^5 * x^1 + 1.089293 * T^4 * P^5 * x^2 + -1.096423 * T^4 * P^5 * x^3 + -0.276605 * T^4 * P^5 * x^4 + 0.557039 * T^4 * P^5 * x^5 + 0.489816 * T^5 * P^0 * x^0 + -15.962987 * T^5 * P^0 * x^1 + -64.635971 * T^5 * P^0 * x^2 + 297.946578 * T^5 * P^0 * x^3 + -385.747103 * T^5 * P^0 * x^4 + 165.800722 * T^5 * P^0 * x^5 + -4.481864 * T^5 * P^1 * x^0 + 13.469388 * T^5 * P^1 * x^1 + 88.202119 * T^5 * P^1 * x^2 + -398.658555 * T^5 * P^1 * x^3 + 522.151594 * T^5 * P^1 * x^4 + -218.821857 * T^5 * P^1 * x^5 + 4.681183 * T^5 * P^2 * x^0 + -23.389649 * T^5 * P^2 * x^1 + -15.746118 * T^5 * P^2 * x^2 + 263.807135 * T^5 * P^2 * x^3 + -442.511328 * T^5 * P^2 * x^4 + 212.379534 * T^5 * P^2 * x^5 + -1.453789 * T^5 * P^3 * x^0 + 11.794221 * T^5 * P^3 * x^1 + -27.536012 * T^5 * P^3 * x^2 + -8.126265 * T^5 * P^3 * x^3 + 70.874497 * T^5 * P^3 * x^4 + -45.428218 * T^5 * P^3 * x^5 + 0.175263 * T^5 * P^4 * x^0 + -1.796194 * T^5 * P^4 * x^1 + 5.895694 * T^5 * P^4 * x^2 + -4.77108 * T^5 * P^4 * x^3 + -3.436153 * T^5 * P^4 * x^4 + 3.925871 * T^5 * P^4 * x^5 + -0.007231 * T^5 * P^5 * x^0 + 0.084741 * T^5 * P^5 * x^1 + -0.313966 * T^5 * P^5 * x^2 + 0.349259 * T^5 * P^5 * x^3 + 0.01235 * T^5 * P^5 * x^4 + -0.125135 * T^5 * P^5 * x^5$$

Coefficients for the enthalpy equation:

i	C	i	C	i	C	i	C	i	C
1	-0.0790	51	-48.9580	101	10.8270	151	16.7780	201	-27.5360
2	10.0770	52	-54.3180	102	-8.7340	152	-19.7680	202	-8.1260
3	-69.7220	53	271.2940	103	0.0250	153	-427.4570	203	70.8740
4	210.4030	54	-186.0540	104	-0.1910	154	1478.0000	204	-45.4280
5	-253.9240	55	-1.4520	105	0.6180	155	-1705.0000	205	0.1750
6	103.3150	56	2.4680	106	-0.4600	156	647.3810	206	-1.7960
7	3.2750	57	-4.4190	107	-0.4580	157	-17.9020	207	5.8960
8	0.4760	58	21.9540	108	0.4570	158	64.1160	208	-4.7710
9	23.0880	59	-44.1890	109	1.3510	159	153.2130	209	-3.4360
10	-132.1370	60	26.8690	110	-167.9140	160	-1082.0000	210	3.9260
11	218.0280	61	0.1770	111	-211.8570	161	1628.0000	211	-0.0072
12	-110.2210	62	-0.6740	112	1669.0000	162	-740.8560	212	0.0850
13	-0.5550	63	1.9120	113	-2507.0000	163	5.6120	213	-0.3140
14	-0.5470	64	-2.7260	114	1203.0000	164	-39.1780	214	0.3490
15	-3.2340	65	1.9750	115	-22.6560	165	80.9830	215	0.0120
16	45.8110	66	-0.7850	116	-25.1650	166	62.5540	216	-0.1250
17	-91.8160	67	-0.0073	117	671.1080	167	-279.5460		
18	51.0730	68	0.0380	118	-1638.0000	168	168.6630		
19	0.1660	69	-0.1110	119	1382.0000	169	-0.6800		
20	-0.1450	70	0.0920	120	-345.8880	170	6.2820		
21	1.0270	71	0.0410	121	24.8610	171	-19.8030		
22	-8.4190	72	-0.0480	122	-43.0290	172	13.4000		
23	16.4320	73	-1.2320	123	-347.9750	173	16.7060		
24	-9.2520	74	174.7770	124	1466.0000	174	-15.8360		
25	-0.0200	75	-345.4890	125	-1881.0000	175	0.0280		
26	0.0400	76	460.3210	126	769.6570	176	-0.3030		
27	-0.1120	77	-259.8130	127	-7.8810	177	1.0890		
28	0.5470	78	-19.7740	128	42.9950	178	-1.0960		
29	-1.0450	79	13.8160	129	-72.1870	179	-0.2770		
30	0.6110	80	47.0090	130	-112.6640	180	0.5570		
31	0.0008	81	-351.9700	131	348.3600	181	0.4900		
32	-0.0022	82	229.9290	132	-196.3100	182	-15.9630		
33	0.0035	83	549.3530	133	0.9600	183	-64.6360		
34	-0.0068	84	-507.4660	134	-7.5250	184	297.9470		
35	0.0140	85	-15.5840	135	22.4860	185	-385.7470		
36	-0.0098	86	-6.5290	136	-12.0010	186	165.8010		
37	0.5460	87	265.3540	137	-24.9860	187	-4.4820		
38	-68.5210	88	-638.7370	138	20.8680	188	13.4690		
39	356.1180	89	508.3990	139	-0.0400	189	88.2020		
40	-1013.0000	90	-101.4220	140	0.3750	190	-398.6590		
41	1194.0000	91	4.9860	141	-1.2940	191	522.1520		
42	-469.1370	92	-17.5680	142	1.1330	192	-218.8220		
43	-4.0600	93	20.8880	143	0.6640	193	4.6810		
44	-14.1700	94	45.8440	144	-0.8320	194	-23.3900		
45	-4.1080	95	-111.3900	145	-1.0250	195	-15.7460		
46	454.6390	96	54.6720	146	78.0030	196	263.8070		
47	-951.7130	97	-0.6100	147	316.0710	197	-442.5110		
48	527.5570	98	3.6290	148	-1543.0000	198	212.3800		
49	4.5600	99	-10.2010	149	2086.0000	199	-1.4540		
50	8.2580	100	5.3280	150	-927.6000	200	11.7940		

Table C.1: Enthalpy coefficients

For the entropy and the molar volume a similar approach has been used, using the *regress* and *interp* functions of Mathcad for initial results and the equation from the code provided above for even better accuracy.

For the entropy the coefficients are:

i	C	i	C	i	C	i	C
1	343.276	51	1329	101	-0.046	151	-6.706
2	3.939	52	-3193	102	0.278	152	20.084
3	-264.222	53	3586	103	-0.728	153	-31.463
4	1032	54	-750.051	104	0.36	154	26.934
5	3.207	55	-66.186	105	-0.039	155	-11.918
6	-0.413	56	-33.338	106	-0.078	156	2.137
7	-11.186	57	-0.0001141	107	3.281	157	-1.023
8	-2040	58	-0.00007891	108	-20.245	158	15.273
9	-240.64	59	0.002574	109	41.512	159	-89.065
10	-656.874	60	-0.023	110	-37.608	160	279.199
11	-0.369	61	-0.003118	111	16.071	161	-511.754
12	-0.064	62	0.0005922	112	-2.676	162	560.462
13	2.482	63	0.043	113	24.439	163	-358.779
14	-0.643	64	0.149	114	20.98	164	123.342
15	13.441	65	-0.065	115	-79.032	165	-17.515
16	-10.918	66	0.006797	116	279.411		
17	2846	67	-0.038	117	-433.714		
18	-2665	68	-1.593	118	329.333		
19	3915	69	1.16	119	-110.647		
20	-738.833	70	0.006516	120	10.99		
21	0.006037	71	-0.146	121	1.814E-06		
22	0.004283	72	-0.901	122	8.048E-07		
23	0.064	73	18.334	123	-3.508E-05		
24	-3.8	74	-32.885	124	0.0005604		
25	1.207	75	18.142	125	1.088E-05		
26	-0.474	76	-2.167	126	-0.0000211		
27	19.105	77	-0.707	127	-0.003921		
28	-32.388	78	-309.412	128	-0.001366		
29	18.258	79	623.838	129	0.000629		
30	0.571	80	-534.428	130	9.527E-06		
31	-2616	81	-160.454	131	0.008997		
32	5122	82	308.639	132	0.02		
33	-6242	83	-174.354	133	-0.008818		
34	1418	84	51.04	134	0.001297		
35	77.037	85	-0.00004701	135	-0.0004738		
36	0.004062	86	0.000003629	136	0.025		
37	-0.0001269	87	0.00003144	137	-0.131		
38	-0.007496	88	-0.003078	138	0.075		
39	0.072	89	0.001572	139	-0.032		
40	-0.122	90	-0.00000692	140	0.011		
41	0.028	91	0.042	141	-2.284E-05		
42	1.649	92	-0.019	142	-0.148		
43	0.377	93	0.0001269	143	0.456		
44	-0.531	94	-0.0001914	144	-0.534		
45	0.279	95	-0.215	145	0.612		
46	-11.141	96	0.07	146	-0.506		
47	1.253	97	0.025	147	0.247		
48	21.537	98	-0.003012	148	-0.055		
49	-19.803	99	-0.0001055	149	0.058		
50	4.628	100	0.409	150	0.8		

TABLE C.2: Entropy coefficients

And the coefficients for the molar volume are:

i	C	i	C	i	C	i	C
1	-14.734	51	-130.646	101	-1.486	151	3.522
2	-1.509	52	324.984	102	-2.692	152	-7.869
3	8.315	53	-84.007	103	-0.181	153	8.848
4	-8.523	54	-94.816	104	-0.038	154	-5.443
5	1.417	55	50.064	105	0.019	155	1.725
6	0.15	56	-3.38	106	11.028	156	-0.211
7	1.691	57	-4.31E-04	107	-1.121	157	17.151
8	-3.811	58	4.07E-05	108	8.315	158	3.88
9	16.255	59	1.04E-03	109	-6.387	159	-28.074
10	12.281	60	-0.05	110	7.729	160	82.14
11	2.218	61	5.45E-03	111	-3.206	161	-139.093
12	0.038	62	1.57E-03	112	0.394	162	144.054
13	-2.112	63	0.593	113	-2.831	163	-89.712
14	22.597	64	-0.049	114	12.345	164	30.878
15	-46.516	65	0.023	115	-40.362	165	-4.521
16	10.578	66	-6.62E-03	116	96.664		
17	-75.352	67	-2.315	117	-133.254		
18	257.197	68	-0.079	118	93.604		
19	-216.581	69	-1.993	119	-34.051		
20	48.142	70	0.688	120	5.302		
21	-0.027	71	-0.081	121	3.59E-05		
22	4.99E-04	72	-4.922	122	-2.16E-05		
23	-0.089	73	15.767	123	9.11E-04		
24	4.301	74	12.096	124	-0.017		
25	-4.305	75	-6.914	125	-1.04E-03		
26	-0.67	76	-0.19	126	-1.19E-04		
27	-51.928	77	0.716	127	0.174		
28	98.271	78	33.826	128	0.011		
29	-22.294	79	-61.817	129	3.37E-03		
30	3.352	80	-69.168	130	4.65E-05		
31	177.521	81	113.887	131	-1.133		
32	-518.717	82	-50.596	132	-0.062		
33	333.005	83	10.599	133	-0.034		
34	-37.601	84	-1.878	134	-1.11E-03		
35	-16.307	85	-4.43E-04	135	-1.26E-04		
36	4.04E-03	86	1.03E-04	136	4.698		
37	-1.45E-03	87	-3.77E-03	137	0.211		
38	0.04	88	0.057	138	0.152		
39	-0.373	89	0.013	139	-1.89E-03		
40	-0.013	90	1.62E-03	140	9.37E-03		
41	-0.037	91	-0.47	141	-1.39E-03		
42	-0.994	92	-0.146	142	-11.978		
43	2.737	93	-0.051	143	-0.563		
44	2.126	94	6.90E-06	144	-0.47		
45	-0.251	95	2.273	145	0.483		
46	35.529	96	0.714	146	-0.454		
47	-69.88	97	0.586	147	0.185		
48	3.284	98	-3.20E-03	148	-0.032		
49	2.412	99	2.73E-03	149	16.701		
50	-1.379	100	-6.581	150	0.582		

Table C.3: Molar volume coefficients

Lastly the coefficients for the chemical potential equation are:

-1.76200E+05	-2.26900E+03	2.40816E+02	-6.76900E+03
-4.70700E+04	-4.10400E+03	-1.33389E+02	1.32400E+04
5.41300E+05	-1.88000E+05	-2.96923E+02	-1.36500E+04
-1.45400E+06	1.83500E+05	3.58298E+02	7.47200E+03
1.05400E+04	-7.36700E+04	-1.02074E+02	-1.97100E+03
2.04600E+03	1.59500E+04	-5.82668E+02	1.78494E+02
1.12300E+05	-2.80000E-02	4.09600E+03	-7.90930E+01
1.41200E+06	-3.90000E-02	-1.35900E+04	1.12200E+03
5.83600E+05	9.13000E-01	2.14100E+04	-6.76900E+03
-6.20900E+04	-7.22900E+00	-1.73800E+04	2.24900E+04
-7.48560E+01	-2.04200E+00	6.88300E+03	-4.42200E+04
-1.14220E+01	1.83000E-01	-1.02600E+03	5.22700E+04
-5.24600E+03	7.00070E+01	8.29261E+02	-3.62400E+04
-8.84700E+04	-3.63000E+00	-1.09300E+04	1.35400E+04
-2.84700E+04	8.50200E+00	4.99800E+04	-2.09700E+03
5.91841E+02	5.12200E+00	-1.07200E+05	
-5.63400E+05	-4.42553E+02	1.17900E+05	
-7.49800E+05	1.21900E+03	-6.70100E+04	
1.48200E+05	-1.24100E+03	1.75000E+04	
5.99600E+03	3.97245E+02	-1.31100E+03	
-2.94780E+01	1.14350E+01	2.86100E-04	
-4.10800E+00	2.87113E+02	9.79000E-05	
1.51129E+02	-2.59400E+03	-4.12200E-03	
3.79700E+03	8.84800E+03	6.00000E-02	
2.55347E+02	-7.50300E+03	5.33900E-03	
2.75626E+02	2.43500E+03	-1.20000E-02	
2.08600E+04	-3.37801E+02	-2.78000E-01	
4.05300E+04	5.00500E+03	-4.48000E-01	
-1.66900E+04	-4.08800E+04	5.22000E-01	
4.59200E+03	1.14500E+05	-7.10000E-02	
6.52300E+04	-1.18400E+05	-1.13400E+00	
3.80300E+05	5.55200E+04	7.47500E+00	
-3.51900E+03	-6.86800E+03	-8.87700E+00	
-6.98300E+04	-2.39400E+03	2.47300E+00	
6.69300E+03	4.84400E-03	-2.47000E-01	
1.89900E+00	-6.71700E-04	1.36920E+01	
2.22000E-01	6.00000E-02	-3.72090E+01	
-8.84000E-01	-1.33600E+00	2.44190E+01	
-1.41784E+02	-1.81000E-01	3.08150E+01	
3.94240E+01	4.40000E-02	-3.20010E+01	
-1.92640E+01	1.18760E+01	8.58500E+00	
-3.96657E+02	5.93000E+00	-1.39540E+01	
-1.25400E+03	-4.26600E+00	-1.78313E+02	
8.72989E+02	1.09000E+00	9.09071E+02	
-3.94670E+02	-4.40760E+01	-1.73500E+03	
2.24500E+03	-9.34960E+01	1.53200E+03	
-2.11100E+04	1.03365E+02	-6.45349E+02	
1.00500E+04	-4.30110E+01	1.03802E+02	
-1.69371E+02	3.46000E+00	-1.19807E+02	
-8.52011E+02	1.00482E+02	1.64800E+03	

Table C.4: Chemical potential coefficients

C.2 Osmotic Pressure Coefficients

The coefficients for the 4th degree polynomial for the equation of the osmotic pressure are:

i	C	i	C
1	-9.01E-11	18	1.71E-10
2	5.16E-08	19	0
3	-5.34E-08	20	0.054
4	9.57E-12	21	0.025
5	-2.15E-12	22	-0.388
6	9.03E-11	23	2.294
7	2.07E-08	24	-1.825
8	7.87E-11	25	2.624
9	-3.33E-10	26	-3.334
10	-5.36E-15	27	13.924
11	-1.23E-15	28	36.478
12	1.15E-12	29	-55.704
13	-2.88E-11	30	2.39
14	-5.27E-12	31	5.735
15	7.75E-13	32	-16.822
16	-3.56E-09	33	6.815
17	-3.99E-11	34	45.397

Appendix D

Appendix 1D Superfluid Stirling Refregerator

D.1 Mathcad code for 1D isothermal ideal SSR

$$
\begin{aligned}
t(X) := \;& \varphi \leftarrow 720 \\
& TH_1 \leftarrow Th \\
& TH^*_1 \leftarrow Th \\
& TK_1 \leftarrow Tk \\
& TK^*_1 \leftarrow Tk \\
& Tr_1 \leftarrow \frac{Tk - Th}{\ln\left(\frac{Tk}{Th}\right)} \\
& Tr^*_1 \leftarrow \frac{Tk - Th}{\ln\left(\frac{Tk}{Th}\right)} \\
& TH_2 \leftarrow Thout2 \\
& TH^*_2 \leftarrow Th \\
& TK_2 \leftarrow Tk \\
& TK^*_2 \leftarrow Tk \\
& Tr_2 \leftarrow \frac{Tk - Thout2}{\ln\left(\frac{Tk}{Thout2}\right)} \\
& Tr^*_2 \leftarrow \frac{Tk - Th}{\ln\left(\frac{Tk}{Th}\right)}
\end{aligned}
$$

"a Tr3 is set to enter the if the first time "

$Tr_3 \leftarrow Tr_2$

$N \leftarrow \text{floor}\left(\frac{\varphi}{360}\right)$

$n \leftarrow 0$

$gA_{all} \leftarrow gAr_{kr}(\theta, Tr_2, Tr_3) + gAr_{rh}(\theta, Tr_3, Tr_3)$

for $\theta \in 3..\varphi$

$Tr_p \leftarrow Tr_{\theta-1}$

$Tr^*_p \leftarrow Tr^*_{\theta-1}$

if $gA^*_{all} > 0 \wedge gA_{all} < 0 \vee \theta = 3$

$Tr_p \leftarrow Tr_{\theta-1}$

"assume m<m*"

$TH^*_{out} \leftarrow Th_{out^*}(\theta, X, Tr^*_p, Thout^*)$

$TH^*_{out} \leftarrow Re(TH^*_{out})$ if $Im(TH^*_{out}) < 10^{-5}$

if $(TH^*_{out}) \geq Th$

$TH_\theta \leftarrow Th$

$TH^*_\theta \leftarrow TH^*_{out}$

$TK_\theta \leftarrow Tk$

$TK^*_\theta \leftarrow Tk$

otherwise

"means that m>m*"

$TK_{out} \leftarrow Tk_{out}(\theta, X, Tr_p, Tkout)$

$TH_\theta \leftarrow Th$

$TH^*_\theta \leftarrow Th$

$TK_\theta \leftarrow TK_{out}$

$TK^*_\theta \leftarrow Tk$

$$Tr_\theta \leftarrow \frac{TK_\theta - TH_\theta}{\ln\left(\frac{TK_\theta}{TH_\theta}\right)}$$

$$Tr^*_\theta \leftarrow \frac{TK^*_\theta - TH^*_\theta}{\ln\left(\frac{TK^*_\theta}{TH^*_\theta}\right)}$$

if $gA^*_{all} < 0 \wedge gA_{all} > 0$

$Tr_p \leftarrow Tr_{\theta-1}$

"assume m<m*"

$TK^*_{out} \leftarrow Tk_{out^*}(\theta, X, Tr^*_p, Tkout^*)$

if $(TK^*_{out}) \le Tk$

$TH_\theta \leftarrow Th$

$TH^*_\theta \leftarrow Th$

$TK_\theta \leftarrow Tk$

$TK^*_\theta \leftarrow TK^*_{out}$

otherwise

"means that m>m*"

$TH_{out} \leftarrow Th_{out}(\theta, X, Tr_p, Thout)$

$TH_\theta \leftarrow TH_{out}$

$TH_\theta \leftarrow Re(TH_{out})$ if $Im(TH_{out}) < 10^{-5}$

$TH^*_\theta \leftarrow Th$

$TK_\theta \leftarrow Tk$

$TK^*_\theta \leftarrow Tk$

$$Tr_\theta \leftarrow \frac{TK_\theta - TH_\theta}{\ln\left(\frac{TK_\theta}{TH_\theta}\right)}$$

$$Tr^*_\theta \leftarrow \frac{TK^*_\theta - TH^*_\theta}{\ln\left(\frac{TK^*_\theta}{TH^*_\theta}\right)}$$

if $gA_{all} < 0 \wedge gA^*_{all} < 0 \vee gA_{all} > 0 \wedge gA^*_{all} > 0$

$kk \leftarrow kk + 1$ if $gA_{all} > 0 \wedge gA^*_{all} > 0$

$TH_\theta \leftarrow Th$

$TH^*_\theta \leftarrow Th$

$TK_\theta \leftarrow Tk$

$TK^*_\theta \leftarrow Tk$

$$Tr_\theta \leftarrow \frac{TK_\theta - TH_\theta}{\ln\left(\frac{TK_\theta}{TH_\theta}\right)}$$

$$Tr^*_\theta \leftarrow \frac{TK^*_\theta - TH^*_\theta}{\ln\left(\frac{TK^*_\theta}{TH^*_\theta}\right)}$$

$gA_{all} \leftarrow gAr_{kr}(\theta, Tr_p, Tr_\theta) + gAr_{rh}(\theta, Tr_p, Tr_\theta)$

$gA^*_{all} \leftarrow gAr^*_{kr}(\theta, X, Tr^*_p, Tr^*_\theta) + gAr^*_{rh}(\theta, X, Tr^*_p, Tr^*_\theta)$

$T^{\langle 1 \rangle} \leftarrow TH$

$T^{\langle 2 \rangle} \leftarrow TK$

$T^{\langle 3 \rangle} \leftarrow TH^*$

$T^{\langle 4 \rangle} \leftarrow TK^*$

$T^{\langle 5 \rangle} \leftarrow kk$

T

FIGURE D.1: Mathcad code for 1D isothermal ideal SSR

D.2 1D mix Single Stirling Mathcad code

$$
\begin{aligned}
&\text{loop}(N,\theta,M4_{in},err) = \\
&\quad P \leftarrow 1 \\
&\quad \text{for } i \in 1..N \\
&\qquad m_{oc} \leftarrow \frac{Voc(\theta)}{v_{40}(Tk,P)} \\
&\qquad m_{oe} \leftarrow \frac{Voe(\theta)}{v_{40}(Tk,P)} \\
&\qquad m_{c3} \leftarrow \frac{Vc(\theta)+Vk}{v_{30}(Tk,P)} \\
&\qquad m_{c4} \leftarrow \frac{Vc(\theta)+Vk}{v_{40}(Tk,P)} \\
&\qquad m_{e3} \leftarrow \frac{Ve(\theta)+Vh}{v_{30}(Tk,P)} \\
&\qquad m_{e4} \leftarrow \frac{Ve(\theta)+Vh}{v_{40}(Tk,P)} \\
&\qquad m_{r3} \leftarrow m3 - m_{c3} - m_{e3} \\
&\qquad m_{r4} \leftarrow m4 - m_{c4} - m_{e4} - m_{oc} - m_{oe} \\
&\qquad xr \leftarrow \frac{m_{r3}}{m_{r3}+m_{r4}} \\
&\qquad xc \leftarrow \frac{m_{c3}}{m_{c3}+m_{c4}} \\
&\qquad xe \leftarrow \frac{m_{e3}}{m_{e3}+m_{e4}} \\
&\qquad P \leftarrow \text{findP}(\theta,xc,xr,xe,M4_{in},err) \\
&\quad \text{return}(P,xc,xr,xe)
\end{aligned}
$$

$$
\begin{aligned}
\text{runs} = \;& M \leftarrow m3 + m4 \\
& p_1 \leftarrow P_1 \\
& XC_1 \leftarrow xc_1 \\
& XR_1 \leftarrow xr_1 \\
& XE_1 \leftarrow xe_1 \\
& MOC_1 \leftarrow \frac{Voc(1)}{v_{40}(Tk, p_1)} \\
& MC4_1 \leftarrow \frac{Vc(1)}{v_{40}(Tk, p_1)} \\
& MC3_1 \leftarrow \frac{Vc(1)}{v_{30}(Tk, p_1)} \\
& MR4_1 \leftarrow \frac{Vr}{v_{40}(Tr, p_1)} \\
& MR3_1 \leftarrow \frac{Vr}{v_{30}(Tr, p_1)} \\
& ME4_1 \leftarrow \frac{Ve(1)}{v_{40}(Th, p_1)} \\
& ME3_1 \leftarrow \frac{Ve(1)}{v_{30}(Th, p_1)} \\
& MOE_1 \leftarrow \frac{Voe(1)}{v_{40}(Th, p_1)} \\
& MC_1 \leftarrow MC3_1 + MC4_1 \\
& MR_1 \leftarrow MR3_1 + MR4_1 \\
& ME_1 \leftarrow ME3_1 + ME4_1
\end{aligned}
$$

for $\theta \in 2..360 \cdot N$

$dVoc \leftarrow Voc(\theta) - Voc(\theta - 1)$

$dVc \leftarrow Vc(\theta) - Vc(\theta - 1)$

$dVe \leftarrow Ve(\theta) - Ve(\theta - 1)$

$dVoe \leftarrow Voe(\theta) - Voe(\theta - 1)$

$$dmoc_{\theta} \leftarrow \frac{p_{\theta-1} \cdot 10^{5} \cdot dVoc}{H\left(0, Tk, p_{\theta-1} - Posm\left(XC_{\theta-1}, Th, p_{\theta-1}\right)\right)}$$

$$dmoe_{\theta} \leftarrow \frac{p_{\theta-1} \cdot 10^{5} \cdot dVoe}{H\left(0, Th, p_{\theta-1} - Posm\left(XE_{\theta-1}, Th, p_{\theta-1}\right)\right)}$$

$$dmc_{\theta} \leftarrow \frac{p_{\theta-1} \cdot 10^{5} \cdot dVc}{H\left(XC_{\theta-1}, Tk, p_{\theta-1} - Posm\left(XC_{\theta-1}, Th, p_{\theta-1}\right)\right)}$$

$$dmr_{\theta} \leftarrow \frac{p_{\theta-1} \cdot 10^{5} \cdot dVoc}{H\left(XR_{\theta-1}, Tr, p_{\theta-1} - Posm\left(XR_{\theta-1}, Tr, p_{\theta-1}\right)\right)}$$

$$dme_{\theta} \leftarrow \frac{p_{\theta-1} \cdot 10^{5} \cdot dVoc}{H\left(XE_{\theta-1}, Th, p_{\theta-1} - Posm\left(XE_{\theta-1}, Th, p_{\theta-1}\right)\right)}$$

$MOC_{\theta} \leftarrow MOC_{\theta-1} + dmoc_{\theta}$

$MOE_{\theta} \leftarrow MOE_{\theta-1} - dmoe_{\theta}$

$MC_{\theta} \leftarrow MC_{\theta-1} + dmc_{\theta}$

$ME_{\theta} \leftarrow ME_{\theta-1} - dme_{\theta}$

$M4_{in} \leftarrow m4 - \left(MOC_{\theta} + MOE_{\theta}\right)$

$MR_{\theta} \leftarrow m3 + m4 - \left(ME_{\theta} + MC_{\theta} + MOE_{\theta} + MOC_{\theta}\right)$

```
    k ← Pxcxrxe(10, θ, M, 0.5)
    p_θ ← k_1
    XC_θ ← k_2
    XR_θ ← k_3
    XE_θ ← k_4
    MC_θ ← mc(XC_θ, Tk, p_θ)
    MR_θ ← mr(XR_θ, Tr, p_θ)
    ME_θ ← me(XE_θ, Th, p_θ)
tmp_1 ← p
tmp_2 ← XC
tmp_3 ← XR
tmp_4 ← XE
tmp_5 ← MOC
tmp_6 ← MC
tmp_7 ← MR
tmp_8 ← ME
tmp_9 ← MOE
tmp
```

FIGURE D.2: Mathcad code for 1D single Stirling with Helium 3-4 mix

D.3 Mathcad code for 1D dual mix SSR

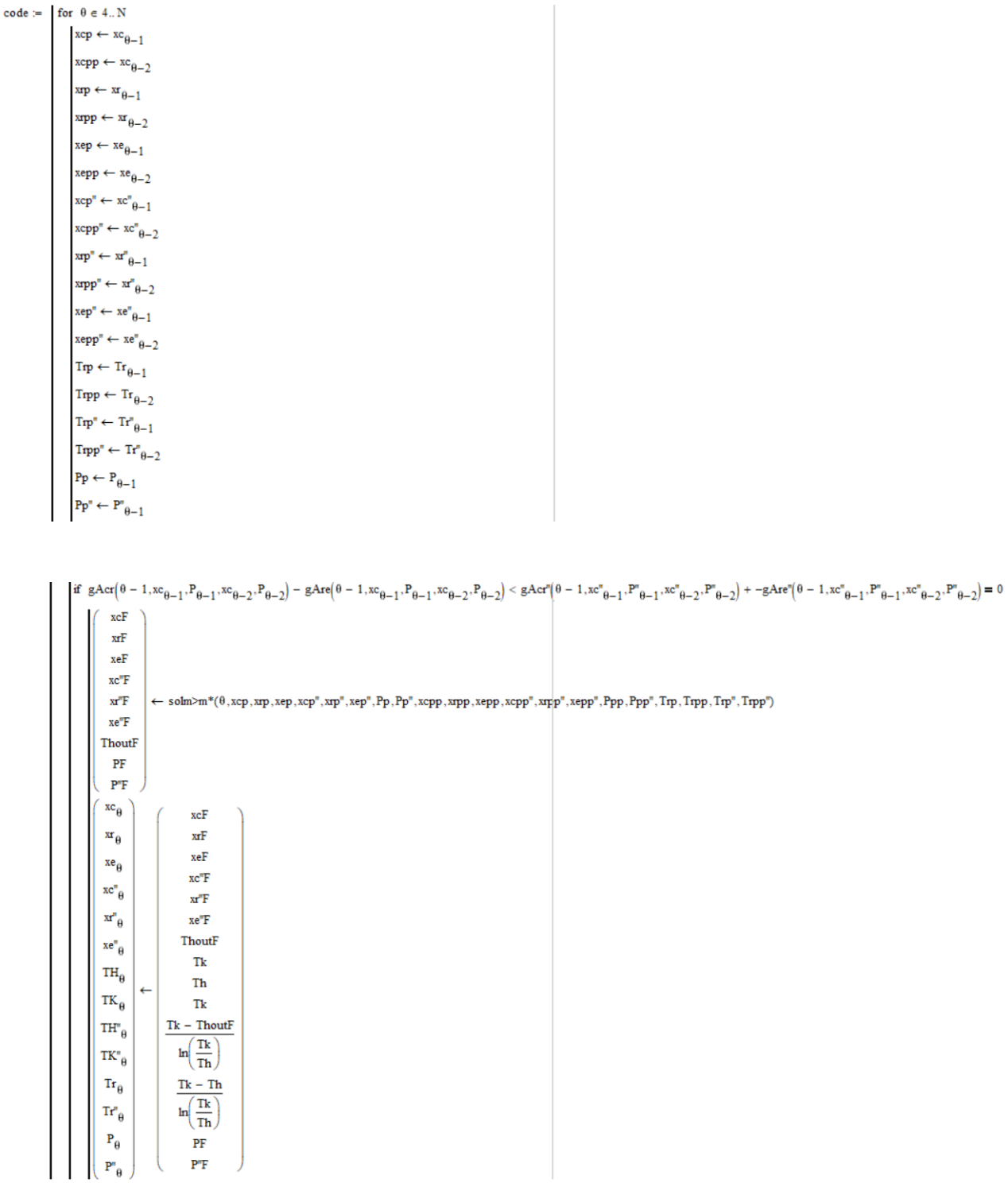

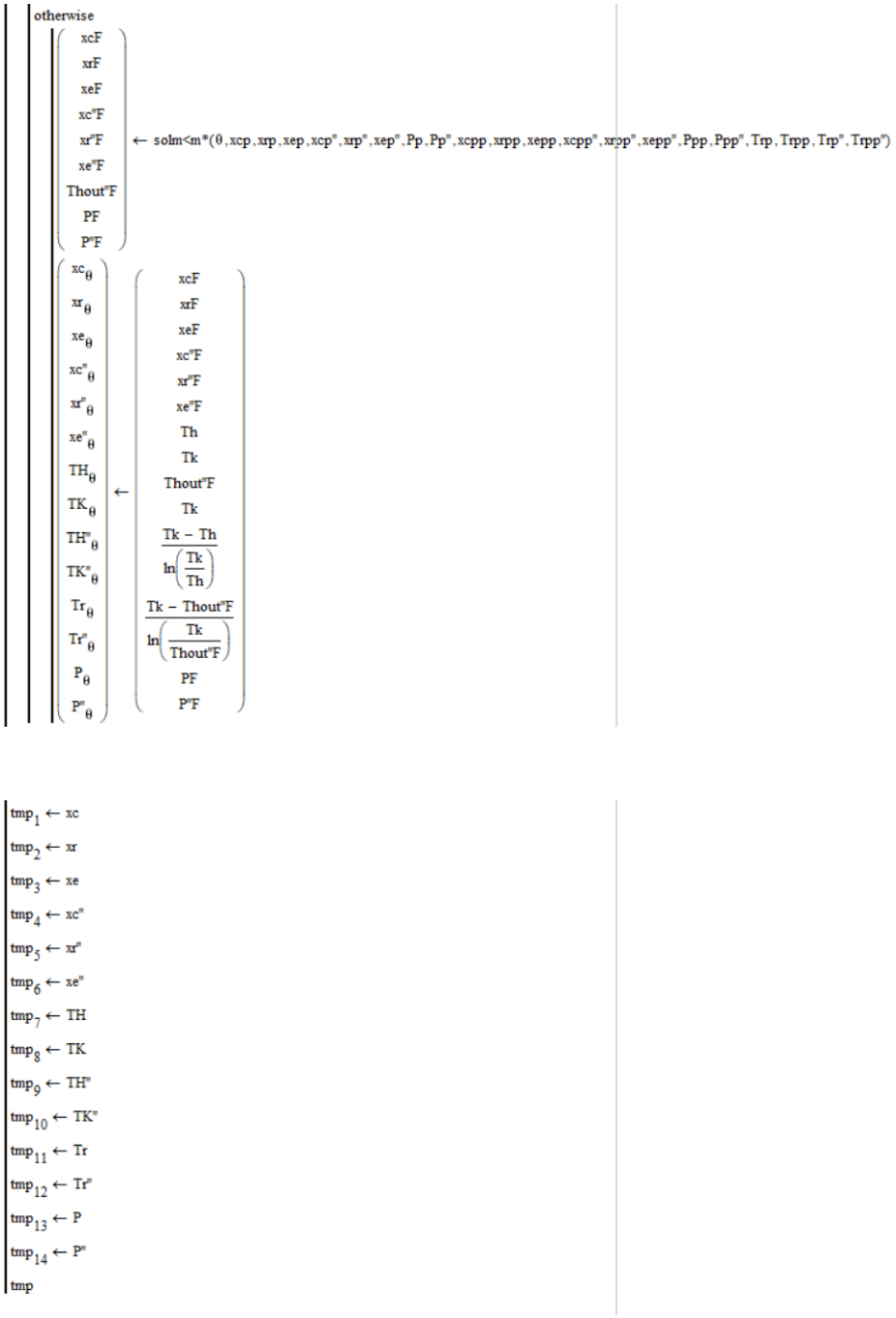

FIGURE D.3: code for 1D dual SSR with Helium 3-4 mix

Appendix E

Appendix for 3D Superfluid Stirling Refrigerator

User defined functions for the movements of the pistons used in the ANSYS Fluent software.

```
All UDFs
140 1Hz
#include "udf.h"
#include "math.h"
DEFINE_CG_MOTION(piston_comp_1_new,dt,vel,omega,time,dtime)
{
        real pi,w,hz;
        pi=3.14159265358979323846264338327 9;
        hz=1;
        w=2*pi*hz;


        real Vswc,Apc;
        Vswc=17.74*pow(10,-6);
        Apc=17.74*pow(10,-4);


        real Ve;
        Ve=(Vswc*w/(2*Apc))*sin(w*time);
;

        vel[0]=Ve;
        vel[1]=0;
        vel[2]=0;

}
#include "udf.h"
#include "math.h"
DEFINE_CG_MOTION(piston_comp_2_140,dt,vel,omega,time,dtime)
{
        real pi,w,hz,T;
        pi=3.14159265358979323846264338327 9;
        hz=1;
```

```
        w=2*pi*hz;
        T=1/hz;


        real Vswc,Apc;
        Vswc=17.74*pow(10,-6);
        Apc=17.74*pow(10,-4);


        real Ve;
        Ve=-(Vswc*w/(2*Apc))*sin(w*(time+T/2.57142));
;

        vel[0]=Ve;
        vel[1]=0;
        vel[2]=0;

}
#include "udf.h"
#include "math.h"
DEFINE_CG_MOTION(piston_exp_1a_new,dt,vel,omega,time,dtime)
{
        real pi,w,hz,T;
        pi=3.14159265358979323846264338327 9;
        hz=1;
        T=1/hz;
        w=2*pi*hz;


        real Vswe,Ape;
        Vswe=9.39*pow(10,-6);
        Ape=13.61*pow(10,-4);


        real Ve;
        Ve=(Vswe*w/(2*Ape))*sin(w*(time+T/4));
;

        vel[0]=Ve;
        vel[1]=0;
        vel[2]=0;

}
#include "udf.h"
#include "math.h"
DEFINE_CG_MOTION(piston_exp_2a_140,dt,vel,omega,time,dtime)
{
```

```
        real pi,w,hz,T;
        pi=3.14159265358979323846264338327 9;
        hz=1;
        T=1/hz;
        w=2*pi*hz;


        real Vswe,Ape;
        Vswe=9.39*pow(10,-6);
        Ape=13.61*pow(10,-4);


        real Ve;
        Ve=-(Vswe*w/(2*Ape))*sin(w*(time+T/2.5714+T/4));
;

        vel[0]=Ve;
        vel[1]=0;
        vel[2]=0;

}

160 1Hz
#include "udf.h"
#include "math.h"
DEFINE_CG_MOTION(piston_comp_1_new,dt,vel,omega,time,dtime)
{
        real pi,w,hz;
        pi=3.14159265358979323846264338327 9;
        hz=1;
        w=2*pi*hz;


        real Vswc,Apc;
        Vswc=17.74*pow(10,-6);
        Apc=17.74*pow(10,-4);


        real Ve;
        Ve=(Vswc*w/(2*Apc))*sin(w*time);
;

        vel[0]=Ve;
        vel[1]=0;
        vel[2]=0;

}
```

```
#include "udf.h"
#include "math.h"
DEFINE_CG_MOTION(piston_comp_2_140,dt,vel,omega,time,dtime)
{
        real pi,w,hz,T;
        pi=3.14159265358979323846264338327 9;
        hz=1;
        w=2*pi*hz;
        T=1/hz;


        real Vswc,Apc;
        Vswc=17.74*pow(10,-6);
        Apc=17.74*pow(10,-4);


        real Ve;
        Ve=-(Vswc*w/(2*Apc))*sin(w*(time+T/2.57142));
;

        vel[0]=Ve;
        vel[1]=0;
        vel[2]=0;

}
#include "udf.h"
#include "math.h"
DEFINE_CG_MOTION(piston_exp_1a_new,dt,vel,omega,time,dtime)
{
        real pi,w,hz,T;
        pi=3.14159265358979323846264338327 9;
        hz=1;
        T=1/hz;
        w=2*pi*hz;


        real Vswe,Ape;
        Vswe=9.39*pow(10,-6);
        Ape=13.61*pow(10,-4);


        real Ve;
        Ve=(Vswe*w/(2*Ape))*sin(w*(time+T/4));
;

        vel[0]=Ve;
        vel[1]=0;
```

```
        vel[2]=0;

}
#include "udf.h"
#include "math.h"
DEFINE_CG_MOTION(piston_exp_2a_140,dt,vel,omega,time,dtime)
{
        real pi,w,hz,T;
        pi=3.14159265358979323846264338327 9;
        hz=1;
        T=1/hz;
        w=2*pi*hz;


        real Vswe,Ape;
        Vswe=9.39*pow(10,-6);
        Ape=13.61*pow(10,-4);


        real Ve;
        Ve=-(Vswe*w/(2*Ape))*sin(w*(time+T/2.5714+T/4));
;

        vel[0]=Ve;
        vel[1]=0;
        vel[2]=0;

}

180 1Hz
#include "udf.h"
#include "math.h"
DEFINE_CG_MOTION(piston_comp_1_new,dt,vel,omega,time,dtime)
{
        real pi,w,hz;
        pi=3.14159265358979323846264338327 9;
        hz=1;
        w=2*pi*hz;


        real Vswc,Apc;
        Vswc=17.74*pow(10,-6);
        Apc=17.74*pow(10,-4);


        real Ve;
        Ve=(Vswc*w/(2*Apc))*sin(w*time);
```

```
;

        vel[0]=Ve;
        vel[1]=0;
        vel[2]=0;

}
#include "udf.h"
#include "math.h"
DEFINE_CG_MOTION(piston_comp_2_140,dt,vel,omega,time,dtime)
{
        real pi,w,hz,T;
        pi=3.14159265358979323846264338327 9;
        hz=1;
        w=2*pi*hz;
        T=1/hz;


        real Vswc,Apc;
        Vswc=17.74*pow(10,-6);
        Apc=17.74*pow(10,-4);


        real Ve;
        Ve=-(Vswc*w/(2*Apc))*sin(w*(time+T/2.57142));
;

        vel[0]=Ve;
        vel[1]=0;
        vel[2]=0;

}
#include "udf.h"
#include "math.h"
DEFINE_CG_MOTION(piston_exp_1a_new,dt,vel,omega,time,dtime)
{
        real pi,w,hz,T;
        pi=3.14159265358979323846264338327 9;
        hz=1;
        T=1/hz;
        w=2*pi*hz;


        real Vswe,Ape;
        Vswe=9.39*pow(10,-6);
        Ape=13.61*pow(10,-4);
```

```
        real Ve;
        Ve=(Vswe*w/(2*Ape))*sin(w*(time+T/4));
;

        vel[0]=Ve;
        vel[1]=0;
        vel[2]=0;

}

#include "udf.h"
#include "math.h"
DEFINE_CG_MOTION(piston_exp_2a_140,dt,vel,omega,time,dtime)
{
        real pi,w,hz,T;
        pi=3.14159265358979323846264338327 9;
        hz=1;
        T=1/hz;
        w=2*pi*hz;


        real Vswe,Ape;
        Vswe=9.39*pow(10,-6);
        Ape=13.61*pow(10,-4);


        real Ve;
        Ve=-(Vswe*w/(2*Ape))*sin(w*(time+T/2.5714+T/4));
;

        vel[0]=Ve;
        vel[1]=0;
        vel[2]=0;

}

160 10Hz
#include "udf.h"
#include "math.h"
DEFINE_CG_MOTION(piston_comp_1_new,dt,vel,omega,time,dtime)
{
        real pi,w,hz;
        pi=3.14159265358979323846264338327 9;
        hz=1;
        w=2*pi*hz;
```

```
        real Vswc,Apc;
        Vswc=17.74*pow(10,-6);
        Apc=17.74*pow(10,-4);


        real Ve;
        Ve=(Vswc*w/(2*Apc))*sin(w*time);
;

        vel[0]=Ve;
        vel[1]=0;
        vel[2]=0;

}
#include "udf.h"
#include "math.h"
DEFINE_CG_MOTION(piston_comp_2_140,dt,vel,omega,time,dtime)
{
        real pi,w,hz,T;
        pi=3.14159265358979323846264338327 9;
        hz=1;
        w=2*pi*hz;
        T=1/hz;


        real Vswc,Apc;
        Vswc=17.74*pow(10,-6);
        Apc=17.74*pow(10,-4);


        real Ve;
        Ve=-(Vswc*w/(2*Apc))*sin(w*(time+T/2.57142));
;

        vel[0]=Ve;
        vel[1]=0;
        vel[2]=0;

}
#include "udf.h"
#include "math.h"
DEFINE_CG_MOTION(piston_exp_1a_new,dt,vel,omega,time,dtime)
{
        real pi,w,hz,T;
        pi=3.14159265358979323846264338327 9;
        hz=1;
```

```
        T=1/hz;
        w=2*pi*hz;


        real Vswe,Ape;
        Vswe=9.39*pow(10,-6);
        Ape=13.61*pow(10,-4);


        real Ve;
        Ve=(Vswe*w/(2*Ape))*sin(w*(time+T/4));
;

        vel[0]=Ve;
        vel[1]=0;
        vel[2]=0;

}
#include "udf.h"
#include "math.h"
DEFINE_CG_MOTION(piston_exp_2a_140,dt,vel,omega,time,dtime)
{
        real pi,w,hz,T;
        pi=3.14159265358979323846264338327 9;
        hz=1;
        T=1/hz;
        w=2*pi*hz;


        real Vswe,Ape;
        Vswe=9.39*pow(10,-6);
        Ape=13.61*pow(10,-4);


        real Ve;
        Ve=-(Vswe*w/(2*Ape))*sin(w*(time+T/2.5714+T/4));
;

        vel[0]=Ve;
        vel[1]=0;
        vel[2]=0;

}
```

Appendix F

Appendix Helium 4 Data

In this appendix the calculated data for Helium-4 based on the equation of state of chapter 3 are presented.
SF stands for Superfluid phase, NF stands for Normal Fluid phase.

T(K)	P(atm)	S(kJ/kgK)	H(kJ/kg)	ρ(kg/m3)	Phase	-	T (K)	P (atm)	S (kJ/kgK)	H (kJ/kg)	ρ (kg/m3)	Phase.
0	0	4.49E-06	2.37E-05	2.23E-08	SF		2.6	10	1.88E+00	3.54E+00	1.65E+00	NF
0.05	0	1.94E-06	5.19E-06	2.42E-06	SF		2.65	10	1.91E+00	3.62E+00	1.63E+00	NF
0.1	0	6.89E-06	4.18E-06	2.06E-05	SF		2.7	10	1.94E+00	3.71E+00	1.61E+00	NF
0.15	0	2.31E-05	6.25E-06	6.90E-05	SF		2.75	10	1.97E+00	3.79E+00	1.60E+00	NF
0.2	0	5.47E-05	1.18E-05	1.61E-04	SF		2.8	10	2.00E+00	3.88E+00	1.60E+00	NF
0.25	0	1.04E-04	2.33E-05	3.11E-04	SF		2.85	10	2.03E+00	3.96E+00	1.61E+00	NF
0.3	0	1.80E-04	4.41E-05	5.34E-04	SF		2.9	10	2.06E+00	4.05E+00	1.62E+00	NF
0.35	0	2.87E-04	7.80E-05	8.36E-04	SF		2.95	10	2.09E+00	4.14E+00	1.65E+00	NF
0.4	0	4.27E-04	1.29E-04	1.23E-03	SF		3	10	2.12E+00	4.23E+00	1.68E+00	NF
0.45	0	5.91E-04	2.03E-04	1.72E-03	SF		3.05	10	2.15E+00	4.32E+00	1.72E+00	NF
0.5	0	7.75E-04	3.04E-04	2.37E-03	SF		3.1	10	2.18E+00	4.42E+00	1.76E+00	NF
0.55	0	9.96E-04	4.43E-04	3.23E-03	SF		3.15	10	2.21E+00	4.52E+00	1.80E+00	NF
0.6	0	1.29E-03	6.33E-04	4.47E-03	SF		3.2	10	2.24E+00	4.62E+00	1.84E+00	NF
0.65	0	1.69E-03	8.99E-04	6.31E-03	SF		3.25	10	2.28E+00	4.73E+00	1.88E+00	NF
0.7	0	2.28E-03	1.28E-03	9.17E-03	SF		3.3	10	2.31E+00	4.83E+00	1.92E+00	NF
0.75	0	3.12E-03	1.85E-03	1.40E-02	SF		3.35	10	2.34E+00	4.95E+00	1.95E+00	NF
0.8	0	4.31E-03	2.70E-03	2.10E-02	SF		3.4	10	2.38E+00	5.06E+00	1.98E+00	NF
0.85	0	5.95E-03	3.99E-03	3.20E-02	SF		3.45	10	2.41E+00	5.18E+00	2.00E+00	NF
0.9	0	8.19E-03	5.96E-03	4.80E-02	SF		3.5	10	2.45E+00	5.30E+00	2.02E+00	NF
0.95	0	1.10E-02	8.89E-03	7.20E-02	SF		0	11	2.72E-07	2.65E-04	4.95E-08	SF
1	0	1.50E-02	1.30E-02	1.04E-01	SF		0.05	11	6.30E-07	3.37E-06	1.19E-06	SF
1.05	0	2.10E-02	1.90E-02	1.45E-01	SF		0.1	11	2.93E-06	1.78E-06	8.77E-06	SF
1.1	0	2.90E-02	2.80E-02	1.97E-01	SF		0.15	11	9.86E-06	2.66E-06	2.98E-05	SF
1.15	0	3.90E-02	3.90E-02	2.60E-01	SF		0.2	11	2.36E-05	5.10E-06	7.00E-05	SF
1.2	0	5.20E-02	5.30E-02	3.36E-01	SF		0.25	11	4.57E-05	1.01E-05	1.38E-04	SF
1.25	0	6.70E-02	7.20E-02	4.26E-01	SF		0.3	11	7.91E-05	1.93E-05	2.41E-04	SF
1.3	0	8.60E-02	9.50E-02	5.34E-01	SF		0.35	11	1.27E-04	3.48E-05	3.82E-04	SF
1.35	0	1.07E-01	1.25E-01	6.58E-01	SF		0.4	11	1.90E-04	5.86E-05	5.69E-04	SF
1.4	0	1.33E-01	1.61E-01	7.99E-01	SF		0.45	11	2.71E-04	9.31E-05	8.30E-04	SF
1.45	0	1.63E-01	2.05E-01	9.56E-01	SF		0.5	11	3.77E-04	1.44E-04	1.24E-03	SF
1.5	0	1.99E-01	2.57E-01	1.13E+00	SF		0.55	11	5.24E-04	2.21E-04	1.95E-03	SF
1.55	0	2.40E-01	3.18E-01	1.33E+00	SF		0.6	11	7.44E-04	3.48E-04	3.24E-03	SF
1.6	0	2.88E-01	3.90E-01	1.57E+00	SF		0.65	11	1.09E-03	5.64E-04	5.58E-03	SF
1.65	0	3.39E-01	4.74E-01	1.85E+00	SF		0.7	11	1.65E-03	9.40E-04	9.74E-03	SF
1.7	0	3.96E-01	5.72E-01	2.17E+00	SF		0.75	11	2.54E-03	1.59E-03	1.70E-02	SF
1.75	0	4.60E-01	6.89E-01	2.53E+00	SF		0.8	11	3.94E-03	2.68E-03	2.80E-02	SF
1.8	0	5.37E-01	8.26E-01	2.93E+00	SF		0.85	11	6.08E-03	4.45E-03	4.40E-02	SF
1.85	0	6.29E-01	9.84E-01	3.36E+00	SF		0.9	11	9.19E-03	7.18E-03	6.70E-02	SF
1.9	0	7.29E-01	1.16E+00	3.86E+00	SF		0.95	11	1.40E-02	1.10E-02	9.70E-02	SF
1.95	0	8.29E-01	1.37E+00	4.48E+00	SF		1	11	1.90E-02	1.70E-02	1.36E-01	SF
2	0	9.38E-01	1.60E+00	5.21E+00	SF		1.05	11	2.70E-02	2.50E-02	1.85E-01	SF
2.05	0	1.10E+00	1.89E+00	5.90E+00	SF		1.1	11	3.70E-02	3.50E-02	2.45E-01	SF
0	1	2.71E-06	2.56E-05	2.39E-08	SF		1.15	11	4.90E-02	4.90E-02	3.18E-01	SF
0.05	1	1.50E-06	4.83E-06	2.23E-06	SF		1.2	11	6.40E-02	6.70E-02	4.05E-01	SF
0.1	1	6.26E-06	3.80E-06	1.87E-05	SF		1.25	11	8.20E-02	8.90E-02	5.10E-01	SF
0.15	1	2.10E-05	5.69E-06	6.29E-05	SF		1.3	11	1.04E-01	1.17E-01	6.35E-01	SF
0.2	1	4.98E-05	1.08E-05	1.47E-04	SF		1.35	11	1.31E-01	1.53E-01	7.82E-01	SF
0.25	1	9.55E-05	2.13E-05	2.85E-04	SF		1.4	11	1.63E-01	1.96E-01	9.53E-01	SF
0.3	1	1.64E-04	4.03E-05	4.90E-04	SF		1.45	11	1.99E-01	2.49E-01	1.14E+00	SF
0.35	1	2.62E-04	7.14E-05	7.69E-04	SF		1.5	11	2.42E-01	3.11E-01	1.35E+00	SF
0.4	1	3.90E-04	1.19E-04	1.13E-03	SF		1.55	11	2.90E-01	3.85E-01	1.58E+00	SF
0.45	1	5.44E-04	1.86E-04	1.59E-03	SF		1.6	11	3.44E-01	4.70E-01	1.84E+00	SF
0.5	1	7.24E-04	2.81E-04	2.20E-03	SF		1.65	11	4.05E-01	5.69E-01	2.15E+00	SF
0.55	1	9.44E-04	4.10E-04	3.03E-03	SF		1.7	11	4.75E-01	6.88E-01	2.54E+00	SF
0.6	1	1.23E-03	5.89E-04	4.23E-03	SF		1.75	11	5.57E-01	8.29E-01	2.99E+00	SF
0.65	1	1.63E-03	8.42E-04	6.06E-03	SF		1.8	11	6.50E-01	9.94E-01	3.46E+00	SF
0.7	1	2.19E-03	1.21E-03	8.94E-03	SF		1.85	11	7.53E-01	1.18E+00	3.96E+00	SF
0.75	1	2.99E-03	1.77E-03	1.40E-02	SF		1.9	11	8.68E-01	1.40E+00	4.62E+00	SF
0.8	1	4.14E-03	2.62E-03	2.10E-02	SF		2.05	11	1.39E+00	2.43E+00	6.12E+00	SF
0.85	1	5.76E-03	3.92E-03	3.20E-02	SF		2.1	11	1.45E+00	2.55E+00	3.23E+00	NF

T(K)	P(atm)	S(kJ/kgK)	H(kJ/kg)	ρ(kg/m3)	Phase	-	T (K)	P (atm)	S (kJ/kgK)	H (kJ/kg)	ρ (kg/m3)	Phase.
0.9	1	8.02E-03	5.90E-03	4.90E-02	SF		2.15	11	1.50E+00	2.67E+00	2.26E+00	NF
0.95	1	1.10E-02	8.88E-03	7.30E-02	SF		2.2	11	1.55E+00	2.78E+00	1.88E+00	NF
1	1	1.60E-02	1.30E-02	1.05E-01	SF		2.25	11	1.60E+00	2.88E+00	1.73E+00	NF
1.05	1	2.10E-02	1.90E-02	1.47E-01	SF		2.3	11	1.65E+00	2.98E+00	1.68E+00	NF
1.1	1	2.90E-02	2.80E-02	1.99E-01	SF		2.35	11	1.69E+00	3.07E+00	1.66E+00	NF
1.15	1	3.90E-02	3.90E-02	2.63E-01	SF		2.4	11	1.72E+00	3.16E+00	1.66E+00	NF
1.2	1	5.20E-02	5.40E-02	3.40E-01	SF		2.45	11	1.76E+00	3.25E+00	1.66E+00	NF
1.25	1	6.80E-02	7.30E-02	4.32E-01	SF		2.5	11	1.80E+00	3.33E+00	1.65E+00	NF
1.3	1	8.60E-02	9.70E-02	5.40E-01	SF		2.55	11	1.83E+00	3.41E+00	1.63E+00	NF
1.35	1	1.09E-01	1.26E-01	6.66E-01	SF		2.6	11	1.86E+00	3.50E+00	1.61E+00	NF
1.4	1	1.35E-01	1.63E-01	8.08E-01	SF		2.65	11	1.89E+00	3.58E+00	1.59E+00	NF
1.45	1	1.65E-01	2.07E-01	9.67E-01	SF		2.7	11	1.92E+00	3.66E+00	1.58E+00	NF
1.5	1	2.01E-01	2.60E-01	1.14E+00	SF		2.75	11	1.95E+00	3.74E+00	1.57E+00	NF
1.55	1	2.43E-01	3.22E-01	1.35E+00	SF		2.8	11	1.98E+00	3.83E+00	1.57E+00	NF
1.6	1	2.90E-01	3.94E-01	1.58E+00	SF		2.85	11	2.01E+00	3.91E+00	1.58E+00	NF
1.65	1	3.42E-01	4.79E-01	1.86E+00	SF		2.9	11	2.04E+00	4.00E+00	1.60E+00	NF
1.7	1	4.00E-01	5.79E-01	2.19E+00	SF		2.95	11	2.07E+00	4.08E+00	1.63E+00	NF
1.75	1	4.66E-01	6.97E-01	2.56E+00	SF		3	11	2.10E+00	4.17E+00	1.66E+00	NF
1.8	1	5.44E-01	8.35E-01	2.96E+00	SF		3.05	11	2.13E+00	4.27E+00	1.70E+00	NF
1.85	1	6.35E-01	9.95E-01	3.40E+00	SF		3.1	11	2.16E+00	4.36E+00	1.74E+00	NF
1.9	1	7.34E-01	1.18E+00	3.91E+00	SF		3.15	11	2.19E+00	4.46E+00	1.78E+00	NF
1.95	1	8.38E-01	1.38E+00	4.52E+00	SF		3.2	11	2.22E+00	4.56E+00	1.82E+00	NF
2	1	9.53E-01	1.62E+00	5.25E+00	SF		3.25	11	2.26E+00	4.66E+00	1.86E+00	NF
2.05	1	1.11E+00	1.92E+00	5.97E+00	SF		3.3	11	2.29E+00	4.77E+00	1.89E+00	NF
2.15	1	1.54E+00	2.84E+00	1.03E+01	SF		3.35	11	2.32E+00	4.88E+00	1.92E+00	NF
2.2	1	1.62E+00	3.02E+00	4.59E+00	NF		3.4	11	2.35E+00	4.99E+00	1.95E+00	NF
2.25	1	1.69E+00	3.18E+00	3.07E+00	NF		3.45	11	2.39E+00	5.10E+00	1.98E+00	NF
2.3	1	1.76E+00	3.33E+00	2.54E+00	NF		3.5	11	2.42E+00	5.22E+00	2.00E+00	NF
2.35	1	1.82E+00	3.46E+00	2.33E+00	NF		0	12	3.78E-07	3.82E-04	6.70E-08	SF
2.4	1	1.87E+00	3.59E+00	2.23E+00	NF		0.05	12	6.31E-07	3.40E-06	1.18E-06	SF
2.45	1	1.92E+00	3.71E+00	2.17E+00	NF		0.1	12	2.77E-06	1.68E-06	8.30E-06	SF
2.5	1	1.97E+00	3.82E+00	2.12E+00	NF		0.15	12	9.33E-06	2.51E-06	2.82E-05	SF
2.55	1	2.01E+00	3.93E+00	2.07E+00	NF		0.2	12	2.23E-05	4.83E-06	6.63E-05	SF
2.6	1	2.05E+00	4.04E+00	2.03E+00	NF		0.25	12	4.33E-05	9.56E-06	1.30E-04	SF
2.65	1	2.09E+00	4.14E+00	2.00E+00	NF		0.3	12	7.49E-05	1.83E-05	2.28E-04	SF
2.7	1	2.13E+00	4.25E+00	1.99E+00	NF		0.35	12	1.20E-04	3.30E-05	3.62E-04	SF
2.75	1	2.17E+00	4.35E+00	1.98E+00	NF		0.4	12	1.80E-04	5.55E-05	5.39E-04	SF
2.8	1	2.21E+00	4.46E+00	1.99E+00	NF		0.45	12	2.57E-04	8.83E-05	7.91E-04	SF
2.85	1	2.25E+00	4.58E+00	2.00E+00	NF		0.5	12	3.59E-04	1.37E-04	1.20E-03	SF
2.9	1	2.29E+00	4.69E+00	2.01E+00	NF		0.55	12	5.02E-04	2.12E-04	1.91E-03	SF
2.95	1	2.33E+00	4.81E+00	2.03E+00	NF		0.6	12	7.20E-04	3.38E-04	3.23E-03	SF
3	1	2.37E+00	4.93E+00	2.04E+00	NF		0.65	12	1.07E-03	5.56E-04	5.67E-03	SF
3.05	1	2.41E+00	5.06E+00	2.06E+00	NF		0.7	12	1.64E-03	9.40E-04	1.00E-02	SF
3.1	1	2.45E+00	5.19E+00	2.08E+00	NF		0.75	12	2.56E-03	1.61E-03	1.70E-02	SF
3.15	1	2.50E+00	5.32E+00	2.10E+00	NF		0.8	12	4.01E-03	2.74E-03	2.90E-02	SF
3.2	1	2.54E+00	5.46E+00	2.12E+00	NF		0.85	12	6.23E-03	4.57E-03	4.60E-02	SF
3.25	1	2.58E+00	5.61E+00	2.15E+00	NF		0.9	12	9.46E-03	7.41E-03	6.90E-02	SF
3.3	1	2.63E+00	5.75E+00	2.18E+00	NF		0.95	12	1.40E-02	1.20E-02	1.00E-01	SF
3.35	1	2.68E+00	5.91E+00	2.21E+00	NF		1	12	2.00E-02	1.80E-02	1.40E-01	SF
3.4	1	2.72E+00	6.06E+00	2.25E+00	NF		1.05	12	2.80E-02	2.60E-02	1.90E-01	SF
3.45	1	2.77E+00	6.22E+00	2.28E+00	NF		1.1	12	3.80E-02	3.60E-02	2.52E-01	SF
3.5	1	2.82E+00	6.38E+00	2.32E+00	NF		1.15	12	5.10E-02	5.10E-02	3.26E-01	SF
0	2	9.30E-07	2.75E-05	2.56E-08	SF		1.2	12	6.60E-02	6.90E-02	4.14E-01	SF
0.05	2	1.05E-06	4.47E-06	2.05E-06	SF		1.25	12	8.50E-02	9.20E-02	5.20E-01	SF
0.1	2	5.64E-06	3.42E-06	1.69E-05	SF		1.3	12	1.07E-01	1.20E-01	6.47E-01	SF
0.15	2	1.89E-05	5.13E-06	5.68E-05	SF		1.35	12	1.34E-01	1.56E-01	7.98E-01	SF
0.2	2	4.48E-05	9.74E-06	1.33E-04	SF		1.4	12	1.66E-01	2.01E-01	9.74E-01	SF
0.25	2	8.67E-05	1.92E-05	2.58E-04	SF		1.45	12	2.04E-01	2.54E-01	1.17E+00	SF
0.3	2	1.49E-04	3.65E-05	4.46E-04	SF		1.5	12	2.47E-01	3.19E-01	1.38E+00	SF
0.35	2	2.37E-04	6.49E-05	7.02E-04	SF		1.55	12	2.96E-01	3.94E-01	1.61E+00	SF

T(K)	P(atm)	S(kJ/kgK)	H(kJ/kg)	ρ(kg/m3)	Phase	-	T (K)	P (atm)	S (kJ/kgK)	H (kJ/kg)	ρ (kg/m3)	Phase.
0.4	2	3.52E-04	1.08E-04	1.04E-03	SF		1.6	12	3.52E-01	4.80E-01	1.88E+00	SF
0.45	2	4.97E-04	1.70E-04	1.46E-03	SF		1.65	12	4.14E-01	5.82E-01	2.20E+00	SF
0.5	2	6.73E-04	2.57E-04	2.03E-03	SF		1.7	12	4.87E-01	7.04E-01	2.60E+00	SF
0.55	2	8.92E-04	3.77E-04	2.82E-03	SF		1.75	12	5.70E-01	8.49E-01	3.06E+00	SF
0.6	2	1.18E-03	5.44E-04	3.99E-03	SF		1.8	12	6.65E-01	1.02E+00	3.52E+00	SF
0.65	2	1.56E-03	7.86E-04	5.81E-03	SF		1.85	12	7.70E-01	1.21E+00	4.02E+00	SF
0.7	2	2.09E-03	1.15E-03	8.72E-03	SF		1.9	12	8.89E-01	1.43E+00	4.78E+00	SF
0.75	2	2.86E-03	1.69E-03	1.30E-02	SF		2	12	1.33E+00	2.29E+00	1.17E+01	SF
0.8	2	3.97E-03	2.54E-03	2.10E-02	SF		2.05	12	1.39E+00	2.42E+00	4.74E+00	NF
0.85	2	5.57E-03	3.85E-03	3.20E-02	SF		2.1	12	1.45E+00	2.54E+00	2.78E+00	NF
0.9	2	7.85E-03	5.85E-03	5.00E-02	SF		2.15	12	1.50E+00	2.65E+00	2.07E+00	NF
0.95	2	1.10E-02	8.87E-03	7.40E-02	SF		2.2	12	1.55E+00	2.76E+00	1.78E+00	NF
1	2	1.60E-02	1.30E-02	1.07E-01	SF		2.25	12	1.59E+00	2.86E+00	1.67E+00	NF
1.05	2	2.20E-02	2.00E-02	1.49E-01	SF		2.3	12	1.64E+00	2.95E+00	1.63E+00	NF
1.1	2	3.00E-02	2.80E-02	2.02E-01	SF		2.35	12	1.68E+00	3.04E+00	1.63E+00	NF
1.15	2	4.00E-02	4.00E-02	2.66E-01	SF		2.4	12	1.71E+00	3.13E+00	1.63E+00	NF
1.2	2	5.30E-02	5.40E-02	3.44E-01	SF		2.45	12	1.75E+00	3.21E+00	1.63E+00	NF
1.25	2	6.80E-02	7.40E-02	4.37E-01	SF		2.5	12	1.78E+00	3.30E+00	1.62E+00	NF
1.3	2	8.70E-02	9.80E-02	5.47E-01	SF		2.55	12	1.82E+00	3.38E+00	1.60E+00	NF
1.35	2	1.10E-01	1.28E-01	6.74E-01	SF		2.6	12	1.85E+00	3.46E+00	1.58E+00	NF
1.4	2	1.36E-01	1.65E-01	8.17E-01	SF		2.65	12	1.88E+00	3.54E+00	1.56E+00	NF
1.45	2	1.68E-01	2.10E-01	9.77E-01	SF		2.7	12	1.91E+00	3.62E+00	1.55E+00	NF
1.5	2	2.04E-01	2.63E-01	1.16E+00	SF		2.75	12	1.94E+00	3.70E+00	1.54E+00	NF
1.55	2	2.45E-01	3.25E-01	1.36E+00	SF		2.8	12	1.97E+00	3.78E+00	1.55E+00	NF
1.6	2	2.92E-01	3.99E-01	1.60E+00	SF		2.85	12	2.00E+00	3.86E+00	1.56E+00	NF
1.65	2	3.45E-01	4.84E-01	1.88E+00	SF		2.9	12	2.02E+00	3.95E+00	1.58E+00	NF
1.7	2	4.04E-01	5.85E-01	2.21E+00	SF		2.95	12	2.05E+00	4.03E+00	1.60E+00	NF
1.75	2	4.72E-01	7.04E-01	2.58E+00	SF		3	12	2.08E+00	4.12E+00	1.64E+00	NF
1.8	2	5.51E-01	8.44E-01	2.99E+00	SF		3.05	12	2.11E+00	4.21E+00	1.67E+00	NF
1.85	2	6.41E-01	1.01E+00	3.44E+00	SF		3.1	12	2.14E+00	4.31E+00	1.72E+00	NF
1.9	2	7.40E-01	1.19E+00	3.95E+00	SF		3.15	12	2.17E+00	4.40E+00	1.76E+00	NF
1.95	2	8.46E-01	1.40E+00	4.57E+00	SF		3.2	12	2.20E+00	4.50E+00	1.80E+00	NF
2	2	9.68E-01	1.64E+00	5.30E+00	SF		3.25	12	2.24E+00	4.60E+00	1.83E+00	NF
2.05	2	1.12E+00	1.94E+00	6.04E+00	SF		3.3	12	2.27E+00	4.71E+00	1.87E+00	NF
2.15	2	1.54E+00	2.72E+00	8.17E+00	SF		3.35	12	2.30E+00	4.81E+00	1.90E+00	NF
2.2	2	1.61E+00	2.90E+00	4.17E+00	NF		3.4	12	2.33E+00	4.92E+00	1.93E+00	NF
2.25	2	1.68E+00	3.07E+00	2.89E+00	NF		3.45	12	2.36E+00	5.04E+00	1.95E+00	NF
2.3	2	1.75E+00	3.21E+00	2.40E+00	NF		3.5	12	2.40E+00	5.15E+00	1.97E+00	NF
2.35	2	1.80E+00	3.35E+00	2.21E+00	NF		0	13	4.96E-07	4.77E-04	6.19E-08	SF
2.4	2	1.85E+00	3.47E+00	2.13E+00	NF		0.05	13	6.26E-07	3.36E-06	1.09E-06	SF
2.45	2	1.90E+00	3.58E+00	2.10E+00	NF		0.1	13	2.63E-06	1.60E-06	7.87E-06	SF
2.5	2	1.95E+00	3.69E+00	2.08E+00	NF		0.15	13	8.85E-06	2.39E-06	2.67E-05	SF
2.55	2	1.99E+00	3.79E+00	2.06E+00	NF		0.2	13	2.12E-05	4.58E-06	6.29E-05	SF
2.6	2	2.03E+00	3.89E+00	2.03E+00	NF		0.25	13	4.11E-05	9.07E-06	1.24E-04	SF
2.65	2	2.07E+00	3.99E+00	2.00E+00	NF		0.3	13	7.11E-05	1.74E-05	2.17E-04	SF
2.7	2	2.11E+00	4.08E+00	1.96E+00	NF		0.35	13	1.14E-04	3.14E-05	3.44E-04	SF
2.75	2	2.15E+00	4.18E+00	1.94E+00	NF		0.4	13	1.71E-04	5.28E-05	5.13E-04	SF
2.8	2	2.18E+00	4.28E+00	1.92E+00	NF		0.45	13	2.45E-04	8.40E-05	7.57E-04	SF
2.85	2	2.22E+00	4.39E+00	1.91E+00	NF		0.5	13	3.42E-04	1.30E-04	1.16E-03	SF
2.9	2	2.26E+00	4.50E+00	1.92E+00	NF		0.55	13	4.82E-04	2.04E-04	1.88E-03	SF
2.95	2	2.29E+00	4.61E+00	1.94E+00	NF		0.6	13	6.99E-04	3.29E-04	3.24E-03	SF
3	2	2.33E+00	4.72E+00	1.97E+00	NF		0.65	13	1.05E-03	5.50E-04	5.78E-03	SF
3.05	2	2.37E+00	4.84E+00	2.00E+00	NF		0.7	13	1.64E-03	9.44E-04	1.00E-02	SF
3.1	2	2.41E+00	4.97E+00	2.04E+00	NF		0.75	13	2.59E-03	1.64E-03	1.80E-02	SF
3.15	2	2.45E+00	5.10E+00	2.08E+00	NF		0.8	13	4.10E-03	2.81E-03	3.00E-02	SF
3.2	2	2.49E+00	5.24E+00	2.11E+00	NF		0.85	13	6.39E-03	4.71E-03	4.70E-02	SF
3.25	2	2.54E+00	5.38E+00	2.15E+00	NF		0.9	13	9.74E-03	7.64E-03	7.10E-02	SF
3.3	2	2.58E+00	5.52E+00	2.18E+00	NF		0.95	13	1.40E-02	1.20E-02	1.03E-01	SF
3.35	2	2.62E+00	5.67E+00	2.20E+00	NF		1	13	2.10E-02	1.80E-02	1.44E-01	SF
3.4	2	2.67E+00	5.82E+00	2.23E+00	NF		1.05	13	2.90E-02	2.60E-02	1.96E-01	SF

T(K)	P(atm)	S(kJ/kgK)	H(kJ/kg)	ρ(kg/m3)	Phase	-	T (K)	P (atm)	S (kJ/kgK)	H (kJ/kg)	ρ (kg/m3)	Phase.
3.45	2	2.71E+00	5.98E+00	2.24E+00	NF		1.1	13	3.90E-02	3.80E-02	2.59E-01	SF
3.5	2	2.76E+00	6.14E+00	2.26E+00	NF		1.15	13	5.20E-02	5.20E-02	3.34E-01	SF
0	3	4.45E-08	3.42E-05	3.15E-08	SF		1.2	13	6.80E-02	7.10E-02	4.24E-01	SF
0.05	3	8.14E-07	4.23E-06	1.92E-06	SF		1.25	13	8.70E-02	9.40E-02	5.31E-01	SF
0.1	3	5.12E-06	3.11E-06	1.53E-05	SF		1.3	13	1.10E-01	1.23E-01	6.60E-01	SF
0.15	3	1.72E-05	4.66E-06	5.17E-05	SF		1.35	13	1.37E-01	1.60E-01	8.15E-01	SF
0.2	3	4.08E-05	8.87E-06	1.21E-04	SF		1.4	13	1.70E-01	2.05E-01	9.95E-01	SF
0.25	3	7.92E-05	1.75E-05	2.36E-04	SF		1.45	13	2.09E-01	2.61E-01	1.20E+00	SF
0.3	3	1.36E-04	3.33E-05	4.08E-04	SF		1.5	13	2.53E-01	3.26E-01	1.42E+00	SF
0.35	3	2.16E-04	5.94E-05	6.45E-04	SF		1.55	13	3.04E-01	4.03E-01	1.65E+00	SF
0.4	3	3.22E-04	9.92E-05	9.54E-04	SF		1.6	13	3.60E-01	4.92E-01	1.92E+00	SF
0.45	3	4.57E-04	1.57E-04	1.35E-03	SF		1.65	13	4.24E-01	5.96E-01	2.25E+00	SF
0.5	3	6.26E-04	2.37E-04	1.89E-03	SF		1.7	13	4.98E-01	7.21E-01	2.66E+00	SF
0.55	3	8.38E-04	3.48E-04	2.65E-03	SF		1.75	13	5.85E-01	8.71E-01	3.13E+00	SF
0.6	3	1.11E-03	5.07E-04	3.80E-03	SF		1.8	13	6.82E-01	1.04E+00	3.60E+00	SF
0.65	3	1.48E-03	7.40E-04	5.64E-03	SF		1.85	13	7.88E-01	1.24E+00	4.12E+00	SF
0.7	3	2.00E-03	1.09E-03	8.61E-03	SF		1.9	13	9.12E-01	1.47E+00	4.96E+00	SF
0.75	3	2.76E-03	1.64E-03	1.30E-02	SF		2	13	1.33E+00	2.28E+00	8.97E+00	SF
0.8	3	3.86E-03	2.49E-03	2.10E-02	SF		2.05	13	1.39E+00	2.41E+00	3.99E+00	NF
0.85	3	5.47E-03	3.82E-03	3.30E-02	SF		2.1	13	1.45E+00	2.52E+00	2.49E+00	NF
0.9	3	7.80E-03	5.87E-03	5.10E-02	SF		2.15	13	1.50E+00	2.63E+00	1.94E+00	NF
0.95	3	1.10E-02	8.95E-03	7.50E-02	SF		2.2	13	1.54E+00	2.73E+00	1.71E+00	NF
1	3	1.60E-02	1.30E-02	1.09E-01	SF		2.25	13	1.59E+00	2.83E+00	1.63E+00	NF
1.05	3	2.20E-02	2.00E-02	1.51E-01	SF		2.3	13	1.63E+00	2.92E+00	1.60E+00	NF
1.1	3	3.00E-02	2.90E-02	2.05E-01	SF		2.35	13	1.67E+00	3.01E+00	1.60E+00	NF
1.15	3	4.00E-02	4.00E-02	2.70E-01	SF		2.4	13	1.70E+00	3.09E+00	1.60E+00	NF
1.2	3	5.30E-02	5.50E-02	3.49E-01	SF		2.45	13	1.74E+00	3.17E+00	1.60E+00	NF
1.25	3	6.90E-02	7.50E-02	4.44E-01	SF		2.5	13	1.77E+00	3.25E+00	1.59E+00	NF
1.3	3	8.80E-02	9.90E-02	5.55E-01	SF		2.55	13	1.80E+00	3.33E+00	1.57E+00	NF
1.35	3	1.11E-01	1.30E-01	6.83E-01	SF		2.6	13	1.83E+00	3.41E+00	1.55E+00	NF
1.4	3	1.39E-01	1.67E-01	8.28E-01	SF		2.65	13	1.86E+00	3.49E+00	1.53E+00	NF
1.45	3	1.70E-01	2.13E-01	9.90E-01	SF		2.7	13	1.89E+00	3.57E+00	1.52E+00	NF
1.5	3	2.07E-01	2.67E-01	1.17E+00	SF		2.75	13	1.92E+00	3.65E+00	1.52E+00	NF
1.55	3	2.48E-01	3.30E-01	1.38E+00	SF		2.8	13	1.95E+00	3.73E+00	1.52E+00	NF
1.6	3	2.95E-01	4.04E-01	1.61E+00	SF		2.85	13	1.98E+00	3.81E+00	1.53E+00	NF
1.65	3	3.48E-01	4.90E-01	1.90E+00	SF		2.9	13	2.01E+00	3.90E+00	1.55E+00	NF
1.7	3	4.09E-01	5.92E-01	2.23E+00	SF		2.95	13	2.04E+00	3.98E+00	1.58E+00	NF
1.75	3	4.79E-01	7.13E-01	2.61E+00	SF		3	13	2.07E+00	4.07E+00	1.62E+00	NF
1.8	3	5.59E-01	8.54E-01	3.03E+00	SF		3.05	13	2.10E+00	4.16E+00	1.65E+00	NF
1.85	3	6.49E-01	1.02E+00	3.49E+00	SF		3.1	13	2.13E+00	4.25E+00	1.69E+00	NF
1.9	3	7.48E-01	1.20E+00	4.00E+00	SF		3.15	13	2.16E+00	4.35E+00	1.74E+00	NF
1.95	3	8.57E-01	1.42E+00	4.61E+00	SF		3.2	13	2.19E+00	4.44E+00	1.77E+00	NF
2	3	9.83E-01	1.66E+00	5.34E+00	SF		3.25	13	2.22E+00	4.54E+00	1.81E+00	NF
2.15	3	1.53E+00	2.82E+00	6.56E+00	NF		3.3	13	2.25E+00	4.65E+00	1.85E+00	NF
2.2	3	1.60E+00	2.97E+00	3.67E+00	NF		3.35	13	2.28E+00	4.75E+00	1.88E+00	NF
2.25	3	1.67E+00	3.11E+00	2.66E+00	NF		3.4	13	2.31E+00	4.86E+00	1.91E+00	NF
2.3	3	1.72E+00	3.25E+00	2.26E+00	NF		3.45	13	2.34E+00	4.97E+00	1.93E+00	NF
2.35	3	1.78E+00	3.37E+00	2.10E+00	NF		3.5	13	2.38E+00	5.08E+00	1.95E+00	NF
2.4	3	1.83E+00	3.49E+00	2.05E+00	NF		0	14	6.27E-07	5.50E-04	3.42E-08	SF
2.45	3	1.88E+00	3.60E+00	2.03E+00	NF		0.05	14	6.15E-07	3.26E-06	9.18E-07	SF
2.5	3	1.92E+00	3.71E+00	2.01E+00	NF		0.1	14	2.50E-06	1.52E-06	7.50E-06	SF
2.55	3	1.96E+00	3.81E+00	2.00E+00	NF		0.15	14	8.43E-06	2.27E-06	2.55E-05	SF
2.6	3	2.00E+00	3.91E+00	1.97E+00	NF		0.2	14	2.02E-05	4.37E-06	5.98E-05	SF
2.65	3	2.04E+00	4.01E+00	1.94E+00	NF		0.25	14	3.91E-05	8.64E-06	1.18E-04	SF
2.7	3	2.08E+00	4.11E+00	1.91E+00	NF		0.3	14	6.78E-05	1.66E-05	2.07E-04	SF
2.75	3	2.12E+00	4.22E+00	1.88E+00	NF		0.35	14	1.09E-04	2.99E-05	3.28E-04	SF
2.8	3	2.15E+00	4.32E+00	1.86E+00	NF		0.4	14	1.63E-04	5.03E-05	4.89E-04	SF
2.85	3	2.19E+00	4.42E+00	1.86E+00	NF		0.45	14	2.33E-04	8.02E-05	7.26E-04	SF
2.9	3	2.23E+00	4.53E+00	1.86E+00	NF		0.5	14	3.28E-04	1.25E-04	1.13E-03	SF
2.95	3	2.26E+00	4.63E+00	1.88E+00	NF		0.55	14	4.65E-04	1.98E-04	1.86E-03	SF

T(K)	P(atm)	S(kJ/kgK)	H(kJ/kg)	ρ(kg/m3)	Phase	-	T (K)	P (atm)	S (kJ/kgK)	H (kJ/kg)	ρ (kg/m3)	Phase.
3	3	2.30E+00	4.74E+00	1.90E+00	NF		0.6	14	6.82E-04	3.22E-04	3.27E-03	SF
3.05	3	2.34E+00	4.86E+00	1.94E+00	NF		0.65	14	1.04E-03	5.47E-04	5.91E-03	SF
3.1	3	2.37E+00	4.97E+00	1.98E+00	NF		0.7	14	1.64E-03	9.51E-04	1.10E-02	SF
3.15	3	2.41E+00	5.09E+00	2.02E+00	NF		0.75	14	2.62E-03	1.67E-03	1.90E-02	SF
3.2	3	2.45E+00	5.22E+00	2.06E+00	NF		0.8	14	4.19E-03	2.89E-03	3.10E-02	SF
3.25	3	2.49E+00	5.34E+00	2.10E+00	NF		0.85	14	6.57E-03	4.86E-03	4.90E-02	SF
3.3	3	2.53E+00	5.47E+00	2.14E+00	NF		0.9	14	1.00E-02	7.89E-03	7.40E-02	SF
3.35	3	2.57E+00	5.61E+00	2.17E+00	NF		0.95	14	1.50E-02	1.20E-02	1.07E-01	SF
3.4	3	2.61E+00	5.75E+00	2.19E+00	NF		1	14	2.10E-02	1.90E-02	1.49E-01	SF
3.45	3	2.65E+00	5.89E+00	2.21E+00	NF		1.05	14	3.00E-02	2.70E-02	2.02E-01	SF
3.5	3	2.69E+00	6.04E+00	2.23E+00	NF		1.1	14	4.00E-02	3.90E-02	2.66E-01	SF
0	4	5.48E-08	4.55E-05	4.19E-08	SF		1.15	14	5.40E-02	5.40E-02	3.43E-01	SF
0.05	4	7.79E-07	4.09E-06	1.85E-06	SF		1.2	14	7.00E-02	7.30E-02	4.34E-01	SF
0.1	4	4.71E-06	2.87E-06	1.41E-05	SF		1.25	14	8.90E-02	9.70E-02	5.43E-01	SF
0.15	4	1.59E-05	4.29E-06	4.77E-05	SF		1.3	14	1.13E-01	1.27E-01	6.75E-01	SF
0.2	4	3.76E-05	8.18E-06	1.12E-04	SF		1.35	14	1.41E-01	1.64E-01	8.33E-01	SF
0.25	4	7.31E-05	1.62E-05	2.18E-04	SF		1.4	14	1.75E-01	2.11E-01	1.02E+00	SF
0.3	4	1.26E-04	3.08E-05	3.78E-04	SF		1.45	14	2.14E-01	2.67E-01	1.22E+00	SF
0.35	4	2.00E-04	5.50E-05	5.99E-04	SF		1.5	14	2.60E-01	3.34E-01	1.45E+00	SF
0.4	4	2.98E-04	9.20E-05	8.86E-04	SF		1.55	14	3.11E-01	4.13E-01	1.69E+00	SF
0.45	4	4.24E-04	1.45E-04	1.26E-03	SF		1.6	14	3.69E-01	5.04E-01	1.97E+00	SF
0.5	4	5.81E-04	2.20E-04	1.77E-03	SF		1.65	14	4.34E-01	6.11E-01	2.30E+00	SF
0.55	4	7.81E-04	3.25E-04	2.51E-03	SF		1.7	14	5.11E-01	7.39E-01	2.73E+00	SF
0.6	4	1.04E-03	4.77E-04	3.66E-03	SF		1.75	14	6.00E-01	8.93E-01	3.21E+00	SF
0.65	4	1.41E-03	7.03E-04	5.53E-03	SF		1.8	14	6.99E-01	1.07E+00	3.70E+00	SF
0.7	4	1.92E-03	1.05E-03	8.60E-03	SF		1.85	14	8.08E-01	1.27E+00	4.25E+00	SF
0.75	4	2.68E-03	1.60E-03	1.40E-02	SF		1.9	14	9.37E-01	1.51E+00	5.15E+00	SF
0.8	4	3.80E-03	2.47E-03	2.20E-02	SF		2	14	1.33E+00	2.28E+00	6.54E+00	SF
0.85	4	5.46E-03	3.84E-03	3.40E-02	SF		2.05	14	1.39E+00	2.39E+00	3.29E+00	NF
0.9	4	7.87E-03	5.96E-03	5.20E-02	SF		2.1	14	1.44E+00	2.50E+00	2.22E+00	NF
0.95	4	1.10E-02	9.13E-03	7.80E-02	SF		2.15	14	1.49E+00	2.61E+00	1.81E+00	NF
1	4	1.60E-02	1.40E-02	1.11E-01	SF		2.2	14	1.54E+00	2.71E+00	1.64E+00	NF
1.05	4	2.20E-02	2.00E-02	1.55E-01	SF		2.25	14	1.58E+00	2.80E+00	1.59E+00	NF
1.1	4	3.10E-02	2.90E-02	2.08E-01	SF		2.3	14	1.62E+00	2.89E+00	1.57E+00	NF
1.15	4	4.10E-02	4.10E-02	2.75E-01	SF		2.35	14	1.66E+00	2.97E+00	1.58E+00	NF
1.2	4	5.40E-02	5.60E-02	3.55E-01	SF		2.4	14	1.69E+00	3.06E+00	1.58E+00	NF
1.25	4	7.00E-02	7.60E-02	4.51E-01	SF		2.45	14	1.73E+00	3.14E+00	1.58E+00	NF
1.3	4	9.00E-02	1.01E-01	5.63E-01	SF		2.5	14	1.76E+00	3.22E+00	1.56E+00	NF
1.35	4	1.13E-01	1.32E-01	6.93E-01	SF		2.55	14	1.79E+00	3.29E+00	1.54E+00	NF
1.4	4	1.41E-01	1.70E-01	8.40E-01	SF		2.6	14	1.82E+00	3.37E+00	1.53E+00	NF
1.45	4	1.73E-01	2.16E-01	1.00E+00	SF		2.65	14	1.85E+00	3.45E+00	1.51E+00	NF
1.5	4	2.10E-01	2.71E-01	1.19E+00	SF		2.7	14	1.88E+00	3.53E+00	1.50E+00	NF
1.55	4	2.52E-01	3.35E-01	1.39E+00	SF		2.75	14	1.91E+00	3.61E+00	1.49E+00	NF
1.6	4	3.00E-01	4.10E-01	1.63E+00	SF		2.8	14	1.94E+00	3.69E+00	1.50E+00	NF
1.65	4	3.53E-01	4.97E-01	1.92E+00	SF		2.85	14	1.96E+00	3.77E+00	1.51E+00	NF
1.7	4	4.15E-01	6.00E-01	2.25E+00	SF		2.9	14	1.99E+00	3.85E+00	1.53E+00	NF
1.75	4	4.86E-01	7.23E-01	2.64E+00	SF		2.95	14	2.02E+00	3.93E+00	1.56E+00	NF
1.8	4	5.67E-01	8.67E-01	3.07E+00	SF		3	14	2.05E+00	4.02E+00	1.59E+00	NF
1.85	4	6.58E-01	1.03E+00	3.54E+00	SF		3.05	14	2.08E+00	4.11E+00	1.63E+00	NF
1.9	4	7.59E-01	1.22E+00	4.06E+00	SF		3.1	14	2.11E+00	4.20E+00	1.67E+00	NF
1.95	4	8.70E-01	1.44E+00	4.67E+00	SF		3.15	14	2.14E+00	4.29E+00	1.71E+00	NF
2	4	9.99E-01	1.69E+00	5.40E+00	SF		3.2	14	2.17E+00	4.39E+00	1.75E+00	NF
2.15	4	1.53E+00	2.79E+00	5.57E+00	NF		3.25	14	2.20E+00	4.49E+00	1.79E+00	NF
2.2	4	1.59E+00	2.94E+00	3.39E+00	NF		3.3	14	2.23E+00	4.59E+00	1.83E+00	NF
2.25	4	1.65E+00	3.07E+00	2.56E+00	NF		3.35	14	2.26E+00	4.69E+00	1.86E+00	NF
2.3	4	1.71E+00	3.20E+00	2.20E+00	NF		3.4	14	2.29E+00	4.80E+00	1.88E+00	NF
2.35	4	1.76E+00	3.32E+00	2.05E+00	NF		3.45	14	2.32E+00	4.91E+00	1.91E+00	NF
2.4	4	1.81E+00	3.43E+00	1.98E+00	NF		3.5	14	2.36E+00	5.02E+00	1.93E+00	NF
2.45	4	1.86E+00	3.54E+00	1.96E+00	NF		0	15	7.58E-07	6.24E-04	6.51E-09	SF
2.5	4	1.90E+00	3.65E+00	1.94E+00	NF		0.05	15	6.05E-07	3.17E-06	7.47E-07	SF

T(K)	P(atm)	S(kJ/kgK)	H(kJ/kg)	ρ(kg/m3)	Phase	-	T (K)	P (atm)	S (kJ/kgK)	H (kJ/kg)	ρ (kg/m3)	Phase.
2.55	4	1.94E+00	3.75E+00	1.92E+00	NF		0.1	15	2.38E-06	1.44E-06	7.13E-06	SF
2.6	4	1.98E+00	3.85E+00	1.90E+00	NF		0.15	15	8.02E-06	2.16E-06	2.43E-05	SF
2.65	4	2.02E+00	3.95E+00	1.88E+00	NF		0.2	15	1.92E-05	4.15E-06	5.68E-05	SF
2.7	4	2.05E+00	4.05E+00	1.85E+00	NF		0.25	15	3.72E-05	8.22E-06	1.13E-04	SF
2.75	4	2.09E+00	4.14E+00	1.83E+00	NF		0.3	15	6.45E-05	1.58E-05	1.97E-04	SF
2.8	4	2.13E+00	4.24E+00	1.82E+00	NF		0.35	15	1.03E-04	2.85E-05	3.12E-04	SF
2.85	4	2.16E+00	4.34E+00	1.82E+00	NF		0.4	15	1.55E-04	4.79E-05	4.65E-04	SF
2.9	4	2.20E+00	4.45E+00	1.83E+00	NF		0.45	15	2.22E-04	7.64E-05	6.96E-04	SF
2.95	4	2.23E+00	4.55E+00	1.84E+00	NF		0.5	15	3.13E-04	1.20E-04	1.10E-03	SF
3	4	2.27E+00	4.66E+00	1.87E+00	NF		0.55	15	4.48E-04	1.91E-04	1.84E-03	SF
3.05	4	2.30E+00	4.77E+00	1.90E+00	NF		0.6	15	6.65E-04	3.16E-04	3.29E-03	SF
3.1	4	2.34E+00	4.88E+00	1.94E+00	NF		0.65	15	1.03E-03	5.43E-04	6.03E-03	SF
3.15	4	2.37E+00	4.99E+00	1.98E+00	NF		0.7	15	1.64E-03	9.59E-04	1.10E-02	SF
3.2	4	2.41E+00	5.11E+00	2.02E+00	NF		0.75	15	2.66E-03	1.70E-03	1.90E-02	SF
3.25	4	2.45E+00	5.23E+00	2.05E+00	NF		0.8	15	4.28E-03	2.96E-03	3.20E-02	SF
3.3	4	2.49E+00	5.36E+00	2.09E+00	NF		0.85	15	6.75E-03	5.00E-03	5.10E-02	SF
3.35	4	2.52E+00	5.49E+00	2.12E+00	NF		0.9	15	1.00E-02	8.14E-03	7.60E-02	SF
3.4	4	2.56E+00	5.62E+00	2.15E+00	NF		0.95	15	1.50E-02	1.30E-02	1.10E-01	SF
3.45	4	2.60E+00	5.76E+00	2.17E+00	NF		1	15	2.20E-02	1.90E-02	1.53E-01	SF
3.5	4	2.64E+00	5.90E+00	2.19E+00	NF		1.05	15	3.10E-02	2.80E-02	2.07E-01	SF
0	5	6.51E-08	5.69E-05	5.22E-08	SF		1.1	15	4.20E-02	4.00E-02	2.73E-01	SF
0.05	5	7.44E-07	3.96E-06	1.78E-06	SF		1.15	15	5.50E-02	5.50E-02	3.51E-01	SF
0.1	5	4.31E-06	2.62E-06	1.29E-05	SF		1.2	15	7.20E-02	7.50E-02	4.44E-01	SF
0.15	5	1.45E-05	3.92E-06	4.36E-05	SF		1.25	15	9.20E-02	9.90E-02	5.56E-01	SF
0.2	5	3.45E-05	7.49E-06	1.03E-04	SF		1.3	15	1.16E-01	1.30E-01	6.90E-01	SF
0.25	5	6.70E-05	1.48E-05	2.00E-04	SF		1.35	15	1.45E-01	1.68E-01	8.51E-01	SF
0.3	5	1.16E-04	2.82E-05	3.48E-04	SF		1.4	15	1.79E-01	2.16E-01	1.04E+00	SF
0.35	5	1.84E-04	5.05E-05	5.52E-04	SF		1.45	15	2.20E-01	2.74E-01	1.25E+00	SF
0.4	5	2.75E-04	8.47E-05	8.19E-04	SF		1.5	15	2.66E-01	3.42E-01	1.48E+00	SF
0.45	5	3.91E-04	1.34E-04	1.17E-03	SF		1.55	15	3.19E-01	4.23E-01	1.73E+00	SF
0.5	5	5.37E-04	2.04E-04	1.65E-03	SF		1.6	15	3.77E-01	5.15E-01	2.01E+00	SF
0.55	5	7.24E-04	3.02E-04	2.37E-03	SF		1.65	15	4.45E-01	6.25E-01	2.36E+00	SF
0.6	5	9.75E-04	4.47E-04	3.52E-03	SF		1.7	15	5.23E-01	7.57E-01	2.79E+00	SF
0.65	5	1.33E-03	6.67E-04	5.42E-03	SF		1.75	15	6.15E-01	9.16E-01	3.28E+00	SF
0.7	5	1.84E-03	1.01E-03	8.60E-03	SF		1.8	15	7.17E-01	1.10E+00	3.79E+00	SF
0.75	5	2.60E-03	1.57E-03	1.40E-02	SF		1.85	15	8.28E-01	1.30E+00	4.38E+00	SF
0.8	5	3.75E-03	2.46E-03	2.20E-02	SF		1.9	15	9.63E-01	1.56E+00	5.34E+00	SF
0.85	5	5.45E-03	3.86E-03	3.50E-02	SF		2	15	1.34E+00	2.27E+00	5.26E+00	SF
0.9	5	7.93E-03	6.04E-03	5.40E-02	SF		2.05	15	1.39E+00	2.38E+00	2.86E+00	NF
0.95	5	1.10E-02	9.32E-03	8.00E-02	SF		2.1	15	1.44E+00	2.49E+00	2.04E+00	NF
1	5	1.60E-02	1.40E-02	1.14E-01	SF		2.15	15	1.49E+00	2.59E+00	1.72E+00	NF
1.05	5	2.30E-02	2.10E-02	1.58E-01	SF		2.2	15	1.53E+00	2.68E+00	1.59E+00	NF
1.1	5	3.10E-02	3.00E-02	2.12E-01	SF		2.25	15	1.57E+00	2.77E+00	1.55E+00	NF
1.15	5	4.20E-02	4.20E-02	2.79E-01	SF		2.3	15	1.61E+00	2.86E+00	1.55E+00	NF
1.2	5	5.50E-02	5.70E-02	3.60E-01	SF		2.35	15	1.65E+00	2.94E+00	1.56E+00	NF
1.25	5	7.10E-02	7.70E-02	4.57E-01	SF		2.4	15	1.68E+00	3.02E+00	1.56E+00	NF
1.3	5	9.10E-02	1.03E-01	5.72E-01	SF		2.45	15	1.71E+00	3.10E+00	1.55E+00	NF
1.35	5	1.15E-01	1.34E-01	7.03E-01	SF		2.5	15	1.75E+00	3.18E+00	1.54E+00	NF
1.4	5	1.43E-01	1.73E-01	8.52E-01	SF		2.55	15	1.78E+00	3.26E+00	1.52E+00	NF
1.45	5	1.76E-01	2.20E-01	1.02E+00	SF		2.6	15	1.81E+00	3.33E+00	1.50E+00	NF
1.5	5	2.14E-01	2.75E-01	1.20E+00	SF		2.65	15	1.84E+00	3.41E+00	1.48E+00	NF
1.55	5	2.56E-01	3.40E-01	1.41E+00	SF		2.7	15	1.87E+00	3.49E+00	1.47E+00	NF
1.6	5	3.04E-01	4.16E-01	1.65E+00	SF		2.75	15	1.89E+00	3.56E+00	1.47E+00	NF
1.65	5	3.59E-01	5.04E-01	1.94E+00	SF		2.8	15	1.92E+00	3.64E+00	1.48E+00	NF
1.7	5	4.21E-01	6.09E-01	2.28E+00	SF		2.85	15	1.95E+00	3.72E+00	1.49E+00	NF
1.75	5	4.92E-01	7.33E-01	2.67E+00	SF		2.9	15	1.98E+00	3.80E+00	1.51E+00	NF
1.8	5	5.75E-01	8.79E-01	3.12E+00	SF		2.95	15	2.01E+00	3.89E+00	1.54E+00	NF
1.85	5	6.68E-01	1.05E+00	3.60E+00	SF		3	15	2.04E+00	3.97E+00	1.58E+00	NF
1.9	5	7.70E-01	1.24E+00	4.12E+00	SF		3.05	15	2.06E+00	4.06E+00	1.61E+00	NF
1.95	5	8.83E-01	1.46E+00	4.72E+00	SF		3.1	15	2.09E+00	4.15E+00	1.65E+00	NF

T(K)	P(atm)	S(kJ/kgK)	H(kJ/kg)	ρ(kg/m3)	Phase	-	T (K)	P (atm)	S (kJ/kgK)	H (kJ/kg)	ρ (kg/m3)	Phase.
2	5	1.01E+00	1.72E+00	5.46E+00	SF		3.15	15	2.12E+00	4.24E+00	1.69E+00	NF
2.05	5	1.16E+00	2.37E+00	2.33E+00	SF		3.2	15	2.15E+00	4.34E+00	1.73E+00	NF
2.1	5	1.41E+00	2.53E+00	4.41E+00	SF		3.25	15	2.18E+00	4.43E+00	1.77E+00	NF
2.15	5	1.48E+00	2.68E+00	5.22E+00	NF		3.3	15	2.21E+00	4.53E+00	1.80E+00	NF
2.2	5	1.55E+00	2.82E+00	4.61E+00	NF		3.35	15	2.24E+00	4.63E+00	1.84E+00	NF
2.25	5	1.61E+00	2.96E+00	3.60E+00	NF		3.4	15	2.27E+00	4.74E+00	1.86E+00	NF
2.3	5	1.66E+00	3.08E+00	2.75E+00	NF		3.45	15	2.30E+00	4.85E+00	1.89E+00	NF
2.35	5	1.72E+00	3.20E+00	2.19E+00	NF		3.5	15	2.34E+00	4.96E+00	1.91E+00	NF
2.4	5	1.77E+00	3.32E+00	1.85E+00	NF		0	16	8.67E-07	7.00E-04	1.85E-08	SF
2.45	5	1.81E+00	3.43E+00	1.67E+00	NF		0.05	16	5.89E-07	3.07E-06	7.85E-07	SF
2.5	5	1.86E+00	3.54E+00	1.60E+00	NF		0.1	16	2.28E-06	1.38E-06	6.83E-06	SF
2.55	5	1.90E+00	3.65E+00	1.60E+00	NF		0.15	16	7.68E-06	2.07E-06	2.32E-05	SF
2.6	5	1.94E+00	3.75E+00	1.64E+00	NF		0.2	16	1.84E-05	3.97E-06	5.44E-05	SF
2.65	5	1.98E+00	3.86E+00	1.71E+00	NF		0.25	16	3.56E-05	7.87E-06	1.08E-04	SF
2.7	5	2.02E+00	3.96E+00	1.79E+00	NF		0.3	16	6.18E-05	1.51E-05	1.89E-04	SF
2.75	5	2.06E+00	4.06E+00	1.87E+00	NF		0.35	16	9.91E-05	2.73E-05	2.98E-04	SF
2.8	5	2.10E+00	4.16E+00	1.92E+00	NF		0.4	16	1.49E-04	4.59E-05	4.47E-04	SF
2.85	5	2.13E+00	4.26E+00	1.95E+00	NF		0.45	16	2.13E-04	7.33E-05	6.73E-04	SF
2.9	5	2.17E+00	4.37E+00	1.96E+00	NF		0.5	16	3.02E-04	1.16E-04	1.07E-03	SF
2.95	5	2.21E+00	4.47E+00	1.96E+00	NF		0.55	16	4.36E-04	1.86E-04	1.84E-03	SF
3	5	2.24E+00	4.58E+00	1.93E+00	NF		0.6	16	6.55E-04	3.12E-04	3.34E-03	SF
3.05	5	2.28E+00	4.69E+00	1.91E+00	NF		0.65	16	1.03E-03	5.45E-04	6.21E-03	SF
3.1	5	2.31E+00	4.80E+00	1.89E+00	NF		0.7	16	1.66E-03	9.74E-04	1.10E-02	SF
3.15	5	2.35E+00	4.91E+00	1.87E+00	NF		0.75	16	2.72E-03	1.74E-03	2.00E-02	SF
3.2	5	2.38E+00	5.03E+00	1.87E+00	NF		0.8	16	4.40E-03	3.05E-03	3.30E-02	SF
3.25	5	2.42E+00	5.15E+00	1.89E+00	NF		0.85	16	6.96E-03	5.17E-03	5.30E-02	SF
3.3	5	2.46E+00	5.27E+00	1.92E+00	NF		0.9	16	1.10E-02	8.42E-03	7.90E-02	SF
3.35	5	2.49E+00	5.39E+00	1.96E+00	NF		0.95	16	1.60E-02	1.30E-02	1.14E-01	SF
3.4	5	2.53E+00	5.52E+00	2.01E+00	NF		1	16	2.30E-02	2.00E-02	1.58E-01	SF
3.45	5	2.57E+00	5.65E+00	2.08E+00	NF		1.05	16	3.20E-02	2.90E-02	2.14E-01	SF
3.5	5	2.61E+00	5.78E+00	2.15E+00	NF		1.1	16	4.30E-02	4.10E-02	2.81E-01	SF
0	6	7.60E-08	6.82E-05	1.02E-07	SF		1.15	16	5.70E-02	5.70E-02	3.61E-01	SF
0.05	6	7.14E-07	3.81E-06	1.77E-06	SF		1.2	16	7.40E-02	7.70E-02	4.55E-01	SF
0.1	6	4.03E-06	2.45E-06	1.21E-05	SF		1.25	16	9.40E-02	1.02E-01	5.68E-01	SF
0.15	6	1.36E-05	3.66E-06	4.08E-05	SF		1.3	16	1.19E-01	1.33E-01	7.06E-01	SF
0.2	6	3.23E-05	7.00E-06	9.60E-05	SF		1.35	16	1.49E-01	1.73E-01	8.72E-01	SF
0.25	6	6.27E-05	1.39E-05	1.88E-04	SF		1.4	16	1.84E-01	2.21E-01	1.07E+00	SF
0.3	6	1.08E-04	2.64E-05	3.26E-04	SF		1.45	16	2.25E-01	2.81E-01	1.28E+00	SF
0.35	6	1.72E-04	4.74E-05	5.18E-04	SF		1.5	16	2.73E-01	3.51E-01	1.51E+00	SF
0.4	6	2.58E-04	7.95E-05	7.69E-04	SF		1.55	16	3.27E-01	4.33E-01	1.76E+00	SF
0.45	6	3.67E-04	1.26E-04	1.10E-03	SF		1.6	16	3.87E-01	5.29E-01	2.06E+00	SF
0.5	6	5.05E-04	1.91E-04	1.56E-03	SF		1.65	16	4.56E-01	6.41E-01	2.42E+00	SF
0.55	6	6.83E-04	2.86E-04	2.28E-03	SF		1.7	16	5.37E-01	7.78E-01	2.87E+00	SF
0.6	6	9.26E-04	4.26E-04	3.44E-03	SF		1.75	16	6.31E-01	9.40E-01	3.37E+00	SF
0.65	6	1.27E-03	6.43E-04	5.41E-03	SF		1.8	16	7.36E-01	1.13E+00	3.89E+00	SF
0.7	6	1.79E-03	9.92E-04	8.74E-03	SF		1.85	16	8.51E-01	1.34E+00	4.61E+00	SF
0.75	6	2.57E-03	1.56E-03	1.40E-02	SF		1.95	16	1.28E+00	2.15E+00	9.78E+00	SF
0.8	6	3.75E-03	2.48E-03	2.30E-02	SF		2	16	1.34E+00	2.26E+00	4.10E+00	NF
0.85	6	5.52E-03	3.94E-03	3.70E-02	SF		2.05	16	1.39E+00	2.37E+00	2.46E+00	NF
0.9	6	8.10E-03	6.21E-03	5.60E-02	SF		2.1	16	1.44E+00	2.47E+00	1.87E+00	NF
0.95	6	1.20E-02	9.60E-03	8.20E-02	SF		2.15	16	1.48E+00	2.57E+00	1.63E+00	NF
1	6	1.70E-02	1.50E-02	1.17E-01	SF		2.2	16	1.52E+00	2.66E+00	1.54E+00	NF
1.05	6	2.30E-02	2.10E-02	1.62E-01	SF		2.25	16	1.56E+00	2.75E+00	1.52E+00	NF
1.1	6	3.20E-02	3.10E-02	2.17E-01	SF		2.3	16	1.60E+00	2.83E+00	1.53E+00	NF
1.15	6	4.30E-02	4.30E-02	2.85E-01	SF		2.35	16	1.64E+00	2.91E+00	1.53E+00	NF
1.2	6	5.60E-02	5.90E-02	3.67E-01	SF		2.4	16	1.67E+00	2.99E+00	1.54E+00	NF
1.25	6	7.30E-02	7.90E-02	4.65E-01	SF		2.45	16	1.70E+00	3.07E+00	1.53E+00	NF
1.3	6	9.30E-02	1.05E-01	5.81E-01	SF		2.5	16	1.74E+00	3.15E+00	1.52E+00	NF
1.35	6	1.17E-01	1.37E-01	7.15E-01	SF		2.55	16	1.77E+00	3.22E+00	1.50E+00	NF
1.4	6	1.46E-01	1.76E-01	8.67E-01	SF		2.6	16	1.80E+00	3.30E+00	1.48E+00	NF

T(K)	P(atm)	S(kJ/kgK)	H(kJ/kg)	ρ(kg/m3)	Phase	-	T (K)	P (atm)	S (kJ/kgK)	H (kJ/kg)	ρ (kg/m3)	Phase.
1.45	6	1.79E-01	2.24E-01	1.04E+00	SF		2.65	16	1.82E+00	3.37E+00	1.46E+00	NF
1.5	6	2.18E-01	2.81E-01	1.23E+00	SF		2.7	16	1.85E+00	3.45E+00	1.45E+00	NF
1.55	6	2.61E-01	3.47E-01	1.44E+00	SF		2.75	16	1.88E+00	3.52E+00	1.45E+00	NF
1.6	6	3.10E-01	4.24E-01	1.68E+00	SF		2.8	16	1.91E+00	3.60E+00	1.46E+00	NF
1.65	6	3.65E-01	5.14E-01	1.96E+00	SF		2.85	16	1.94E+00	3.68E+00	1.47E+00	NF
1.7	6	4.28E-01	6.20E-01	2.31E+00	SF		2.9	16	1.96E+00	3.76E+00	1.49E+00	NF
1.75	6	5.01E-01	7.46E-01	2.72E+00	SF		2.95	16	1.99E+00	3.84E+00	1.52E+00	NF
1.8	6	5.85E-01	8.95E-01	3.17E+00	SF		3	16	2.02E+00	3.93E+00	1.56E+00	NF
1.85	6	6.80E-01	1.07E+00	3.65E+00	SF		3.05	16	2.05E+00	4.01E+00	1.59E+00	NF
1.9	6	7.84E-01	1.26E+00	4.17E+00	SF		3.1	16	2.08E+00	4.10E+00	1.63E+00	NF
1.95	6	8.99E-01	1.49E+00	4.82E+00	SF		3.15	16	2.11E+00	4.19E+00	1.67E+00	NF
2.05	6	1.36E+00	2.39E+00	6.35E+00	SF		3.2	16	2.14E+00	4.29E+00	1.71E+00	NF
2.1	6	1.43E+00	2.54E+00	4.74E+00	SF		3.25	16	2.16E+00	4.38E+00	1.75E+00	NF
2.15	6	1.49E+00	2.69E+00	4.48E+00	NF		3.3	16	2.19E+00	4.48E+00	1.78E+00	NF
2.2	6	1.56E+00	2.82E+00	3.80E+00	NF		3.35	16	2.22E+00	4.58E+00	1.81E+00	NF
2.25	6	1.61E+00	2.95E+00	3.03E+00	NF		3.4	16	2.26E+00	4.68E+00	1.84E+00	NF
2.3	6	1.67E+00	3.07E+00	2.44E+00	NF		3.45	16	2.29E+00	4.79E+00	1.87E+00	NF
2.35	6	1.72E+00	3.19E+00	2.05E+00	NF		3.5	16	2.32E+00	4.90E+00	1.89E+00	NF
2.4	6	1.76E+00	3.30E+00	1.83E+00	NF		0	17	9.76E-07	7.76E-04	3.06E-08	SF
2.45	6	1.81E+00	3.40E+00	1.71E+00	NF		0.05	17	5.73E-07	2.97E-06	8.23E-07	SF
2.5	6	1.85E+00	3.51E+00	1.66E+00	NF		0.1	17	2.18E-06	1.32E-06	6.53E-06	SF
2.55	6	1.89E+00	3.61E+00	1.65E+00	NF		0.15	17	7.34E-06	1.98E-06	2.22E-05	SF
2.6	6	1.93E+00	3.71E+00	1.67E+00	NF		0.2	17	1.76E-05	3.80E-06	5.21E-05	SF
2.65	6	1.97E+00	3.80E+00	1.71E+00	NF		0.25	17	3.41E-05	7.53E-06	1.03E-04	SF
2.7	6	2.01E+00	3.90E+00	1.76E+00	NF		0.3	17	5.91E-05	1.45E-05	1.81E-04	SF
2.75	6	2.04E+00	4.00E+00	1.80E+00	NF		0.35	17	9.48E-05	2.61E-05	2.85E-04	SF
2.8	6	2.08E+00	4.10E+00	1.83E+00	NF		0.4	17	1.42E-04	4.39E-05	4.28E-04	SF
2.85	6	2.11E+00	4.19E+00	1.85E+00	NF		0.45	17	2.04E-04	7.02E-05	6.51E-04	SF
2.9	6	2.15E+00	4.29E+00	1.87E+00	NF		0.5	17	2.91E-04	1.11E-04	1.05E-03	SF
2.95	6	2.18E+00	4.39E+00	1.87E+00	NF		0.55	17	4.23E-04	1.81E-04	1.83E-03	SF
3	6	2.21E+00	4.50E+00	1.87E+00	NF		0.6	17	6.44E-04	3.08E-04	3.39E-03	SF
3.05	6	2.25E+00	4.60E+00	1.86E+00	NF		0.65	17	1.02E-03	5.46E-04	6.39E-03	SF
3.1	6	2.28E+00	4.71E+00	1.86E+00	NF		0.7	17	1.68E-03	9.89E-04	1.20E-02	SF
3.15	6	2.32E+00	4.82E+00	1.87E+00	NF		0.75	17	2.77E-03	1.79E-03	2.10E-02	SF
3.2	6	2.35E+00	4.93E+00	1.88E+00	NF		0.8	17	4.52E-03	3.15E-03	3.50E-02	SF
3.25	6	2.39E+00	5.05E+00	1.91E+00	NF		0.85	17	7.18E-03	5.34E-03	5.40E-02	SF
3.3	6	2.42E+00	5.17E+00	1.94E+00	NF		0.9	17	1.10E-02	8.70E-03	8.10E-02	SF
3.35	6	2.46E+00	5.29E+00	1.98E+00	NF		0.95	17	1.60E-02	1.40E-02	1.17E-01	SF
3.4	6	2.50E+00	5.41E+00	2.02E+00	NF		1	17	2.30E-02	2.10E-02	1.64E-01	SF
3.45	6	2.53E+00	5.54E+00	2.07E+00	NF		1.05	17	3.30E-02	3.00E-02	2.21E-01	SF
3.5	6	2.57E+00	5.67E+00	2.12E+00	NF		1.1	17	4.40E-02	4.30E-02	2.90E-01	SF
0	7	8.69E-08	7.96E-05	1.52E-07	SF		1.15	17	5.90E-02	5.90E-02	3.71E-01	SF
0.05	7	6.83E-07	3.66E-06	1.77E-06	SF		1.2	17	7.60E-02	7.90E-02	4.66E-01	SF
0.1	7	3.74E-06	2.28E-06	1.12E-05	SF		1.25	17	9.70E-02	1.05E-01	5.81E-01	SF
0.15	7	1.26E-05	3.41E-06	3.79E-05	SF		1.3	17	1.22E-01	1.37E-01	7.22E-01	SF
0.2	7	3.00E-05	6.52E-06	8.95E-05	SF		1.35	17	1.52E-01	1.77E-01	8.94E-01	SF
0.25	7	5.83E-05	1.29E-05	1.75E-04	SF		1.4	17	1.89E-01	2.27E-01	1.09E+00	SF
0.3	7	1.01E-04	2.46E-05	3.04E-04	SF		1.45	17	2.31E-01	2.88E-01	1.31E+00	SF
0.35	7	1.61E-04	4.42E-05	4.84E-04	SF		1.5	17	2.80E-01	3.60E-01	1.55E+00	SF
0.4	7	2.40E-04	7.42E-05	7.19E-04	SF		1.55	17	3.35E-01	4.44E-01	1.80E+00	SF
0.45	7	3.43E-04	1.18E-04	1.03E-03	SF		1.6	17	3.97E-01	5.42E-01	2.10E+00	SF
0.5	7	4.73E-04	1.79E-04	1.48E-03	SF		1.65	17	4.68E-01	6.58E-01	2.49E+00	SF
0.55	7	6.43E-04	2.69E-04	2.18E-03	SF		1.7	17	5.51E-01	7.98E-01	2.96E+00	SF
0.6	7	8.78E-04	4.05E-04	3.36E-03	SF		1.75	17	6.48E-01	9.65E-01	3.45E+00	SF
0.65	7	1.22E-03	6.20E-04	5.39E-03	SF		1.8	17	7.55E-01	1.16E+00	3.98E+00	SF
0.7	7	1.74E-03	9.71E-04	8.87E-03	SF		1.85	17	8.75E-01	1.38E+00	4.84E+00	SF
0.75	7	2.54E-03	1.55E-03	1.50E-02	SF		1.95	17	1.28E+00	2.14E+00	7.45E+00	SF
0.8	7	3.76E-03	2.50E-03	2.40E-02	SF		2	17	1.34E+00	2.25E+00	3.43E+00	NF
0.85	7	5.59E-03	4.01E-03	3.80E-02	SF		2.05	17	1.39E+00	2.36E+00	2.20E+00	NF
0.9	7	8.28E-03	6.37E-03	5.80E-02	SF		2.1	17	1.43E+00	2.45E+00	1.74E+00	NF

T(K)	P(atm)	S(kJ/kgK)	H(kJ/kg)	ρ(kg/m3)	Phase	-	T (K)	P (atm)	S (kJ/kgK)	H (kJ/kg)	ρ (kg/m3)	Phase.
0.95	7	1.20E-02	9.89E-03	8.50E-02	SF		2.15	17	1.48E+00	2.55E+00	1.56E+00	NF
1	7	1.70E-02	1.50E-02	1.21E-01	SF		2.2	17	1.52E+00	2.63E+00	1.50E+00	NF
1.05	7	2.40E-02	2.20E-02	1.66E-01	SF		2.25	17	1.56E+00	2.72E+00	1.49E+00	NF
1.1	7	3.30E-02	3.10E-02	2.22E-01	SF		2.3	17	1.59E+00	2.80E+00	1.50E+00	NF
1.15	7	4.40E-02	4.40E-02	2.91E-01	SF		2.35	17	1.63E+00	2.88E+00	1.51E+00	NF
1.2	7	5.80E-02	6.00E-02	3.74E-01	SF		2.4	17	1.66E+00	2.96E+00	1.52E+00	NF
1.25	7	7.50E-02	8.10E-02	4.73E-01	SF		2.45	17	1.69E+00	3.03E+00	1.51E+00	NF
1.3	7	9.50E-02	1.07E-01	5.90E-01	SF		2.5	17	1.72E+00	3.11E+00	1.49E+00	NF
1.35	7	1.20E-01	1.40E-01	7.26E-01	SF		2.55	17	1.75E+00	3.18E+00	1.47E+00	NF
1.4	7	1.49E-01	1.80E-01	8.82E-01	SF		2.6	17	1.78E+00	3.26E+00	1.46E+00	NF
1.45	7	1.83E-01	2.28E-01	1.06E+00	SF		2.65	17	1.81E+00	3.33E+00	1.44E+00	NF
1.5	7	2.22E-01	2.86E-01	1.25E+00	SF		2.7	17	1.84E+00	3.41E+00	1.43E+00	NF
1.55	7	2.66E-01	3.53E-01	1.46E+00	SF		2.75	17	1.87E+00	3.48E+00	1.43E+00	NF
1.6	7	3.16E-01	4.32E-01	1.70E+00	SF		2.8	17	1.90E+00	3.56E+00	1.44E+00	NF
1.65	7	3.72E-01	5.23E-01	1.99E+00	SF		2.85	17	1.92E+00	3.64E+00	1.45E+00	NF
1.7	7	4.36E-01	6.31E-01	2.34E+00	SF		2.9	17	1.95E+00	3.72E+00	1.47E+00	NF
1.75	7	5.10E-01	7.59E-01	2.76E+00	SF		2.95	17	1.98E+00	3.80E+00	1.50E+00	NF
1.8	7	5.96E-01	9.11E-01	3.23E+00	SF		3	17	2.01E+00	3.88E+00	1.54E+00	NF
1.85	7	6.92E-01	1.09E+00	3.71E+00	SF		3.05	17	2.03E+00	3.97E+00	1.58E+00	NF
1.9	7	7.98E-01	1.29E+00	4.22E+00	SF		3.1	17	2.06E+00	4.05E+00	1.61E+00	NF
1.95	7	9.16E-01	1.51E+00	4.93E+00	SF		3.15	17	2.09E+00	4.14E+00	1.65E+00	NF
2.05	7	1.37E+00	2.42E+00	1.04E+01	SF		3.2	17	2.12E+00	4.24E+00	1.69E+00	NF
2.1	7	1.44E+00	2.57E+00	5.07E+00	SF		3.25	17	2.15E+00	4.33E+00	1.73E+00	NF
2.15	7	1.51E+00	2.70E+00	3.73E+00	NF		3.3	17	2.18E+00	4.43E+00	1.76E+00	NF
2.2	7	1.56E+00	2.83E+00	2.99E+00	NF		3.35	17	2.21E+00	4.53E+00	1.79E+00	NF
2.25	7	1.62E+00	2.96E+00	2.46E+00	NF		3.4	17	2.24E+00	4.63E+00	1.82E+00	NF
2.3	7	1.67E+00	3.07E+00	2.12E+00	NF		3.45	17	2.27E+00	4.73E+00	1.85E+00	NF
2.35	7	1.72E+00	3.18E+00	1.92E+00	NF		3.5	17	2.30E+00	4.84E+00	1.87E+00	NF
2.4	7	1.76E+00	3.28E+00	1.81E+00	NF		0	18	1.16E-06	8.63E-04	4.70E-08	SF
2.45	7	1.81E+00	3.38E+00	1.75E+00	NF		0.05	18	5.60E-07	2.88E-06	8.45E-07	SF
2.5	7	1.85E+00	3.48E+00	1.72E+00	NF		0.1	18	2.09E-06	1.27E-06	6.26E-06	SF
2.55	7	1.88E+00	3.57E+00	1.71E+00	NF		0.15	18	7.04E-06	1.89E-06	2.12E-05	SF
2.6	7	1.92E+00	3.67E+00	1.71E+00	NF		0.2	18	1.68E-05	3.64E-06	5.00E-05	SF
2.65	7	1.96E+00	3.76E+00	1.71E+00	NF		0.25	18	3.26E-05	7.21E-06	9.90E-05	SF
2.7	7	1.99E+00	3.85E+00	1.72E+00	NF		0.3	18	5.67E-05	1.39E-05	1.73E-04	SF
2.75	7	2.02E+00	3.94E+00	1.73E+00	NF		0.35	18	9.09E-05	2.50E-05	2.73E-04	SF
2.8	7	2.06E+00	4.04E+00	1.74E+00	NF		0.4	18	1.36E-04	4.20E-05	4.12E-04	SF
2.85	7	2.09E+00	4.13E+00	1.75E+00	NF		0.45	18	1.96E-04	6.74E-05	6.31E-04	SF
2.9	7	2.12E+00	4.22E+00	1.77E+00	NF		0.5	18	2.80E-04	1.08E-04	1.03E-03	SF
2.95	7	2.16E+00	4.32E+00	1.78E+00	NF		0.55	18	4.12E-04	1.77E-04	1.84E-03	SF
3	7	2.19E+00	4.42E+00	1.80E+00	NF		0.6	18	6.36E-04	3.06E-04	3.45E-03	SF
3.05	7	2.22E+00	4.52E+00	1.82E+00	NF		0.65	18	1.03E-03	5.50E-04	6.60E-03	SF
3.1	7	2.25E+00	4.63E+00	1.84E+00	NF		0.7	18	1.70E-03	1.01E-03	1.20E-02	SF
3.15	7	2.29E+00	4.73E+00	1.86E+00	NF		0.75	18	2.84E-03	1.84E-03	2.20E-02	SF
3.2	7	2.32E+00	4.84E+00	1.89E+00	NF		0.8	18	4.66E-03	3.25E-03	3.60E-02	SF
3.25	7	2.36E+00	4.95E+00	1.92E+00	NF		0.85	18	7.41E-03	5.53E-03	5.60E-02	SF
3.3	7	2.39E+00	5.07E+00	1.96E+00	NF		0.9	18	1.10E-02	9.00E-03	8.40E-02	SF
3.35	7	2.43E+00	5.19E+00	1.99E+00	NF		0.95	18	1.70E-02	1.40E-02	1.21E-01	SF
3.4	7	2.46E+00	5.31E+00	2.03E+00	NF		1	18	2.40E-02	2.10E-02	1.69E-01	SF
3.45	7	2.50E+00	5.44E+00	2.06E+00	NF		1.05	18	3.40E-02	3.10E-02	2.28E-01	SF
3.5	7	2.54E+00	5.56E+00	2.10E+00	NF		1.1	18	4.60E-02	4.40E-02	2.98E-01	SF
0	8	1.07E-07	9.80E-05	1.48E-07	SF		1.15	18	6.10E-02	6.10E-02	3.81E-01	SF
0.05	8	6.60E-07	3.53E-06	1.65E-06	SF		1.2	18	7.80E-02	8.20E-02	4.77E-01	SF
0.1	8	3.50E-06	2.13E-06	1.05E-05	SF		1.25	18	1.00E-01	1.08E-01	5.95E-01	SF
0.15	8	1.18E-05	3.18E-06	3.55E-05	SF		1.3	18	1.26E-01	1.41E-01	7.40E-01	SF
0.2	8	2.81E-05	6.10E-06	8.37E-05	SF		1.35	18	1.57E-01	1.82E-01	9.17E-01	SF
0.25	8	5.46E-05	1.21E-05	1.64E-04	SF		1.4	18	1.94E-01	2.33E-01	1.12E+00	SF
0.3	8	9.43E-05	2.31E-05	2.85E-04	SF		1.45	18	2.38E-01	2.96E-01	1.35E+00	SF
0.35	8	1.50E-04	4.14E-05	4.54E-04	SF		1.5	18	2.88E-01	3.70E-01	1.58E+00	SF
0.4	8	2.25E-04	6.96E-05	6.75E-04	SF		1.55	18	3.44E-01	4.56E-01	1.84E+00	SF

T(K)	P(atm)	S(kJ/kgK)	H(kJ/kg)	ρ(kg/m3)	Phase	-	T (K)	P (atm)	S (kJ/kgK)	H (kJ/kg)	ρ (kg/m3)	Phase.
0.45	8	3.22E-04	1.10E-04	9.72E-04	SF		1.6	18	4.07E-01	5.56E-01	2.15E+00	SF
0.5	8	4.44E-04	1.69E-04	1.41E-03	SF		1.65	18	4.80E-01	6.75E-01	2.56E+00	SF
0.55	8	6.07E-04	2.55E-04	2.11E-03	SF		1.7	18	5.66E-01	8.20E-01	3.04E+00	SF
0.6	8	8.37E-04	3.87E-04	3.31E-03	SF		1.75	18	6.65E-01	9.91E-01	3.53E+00	SF
0.65	8	1.18E-03	6.01E-04	5.40E-03	SF		1.8	18	7.76E-01	1.19E+00	4.12E+00	SF
0.7	8	1.71E-03	9.57E-04	9.04E-03	SF		1.95	18	1.29E+00	2.14E+00	5.42E+00	SF
0.75	8	2.52E-03	1.55E-03	1.50E-02	SF		2	18	1.34E+00	2.24E+00	2.83E+00	NF
0.8	8	3.78E-03	2.53E-03	2.50E-02	SF		2.05	18	1.39E+00	2.34E+00	1.97E+00	NF
0.85	8	5.69E-03	4.11E-03	3.90E-02	SF		2.1	18	1.43E+00	2.43E+00	1.63E+00	NF
0.9	8	8.47E-03	6.55E-03	6.00E-02	SF		2.15	18	1.47E+00	2.52E+00	1.50E+00	NF
0.95	8	1.20E-02	1.00E-02	8.80E-02	SF		2.2	18	1.51E+00	2.61E+00	1.47E+00	NF
1	8	1.80E-02	1.50E-02	1.24E-01	SF		2.25	18	1.55E+00	2.69E+00	1.47E+00	NF
1.05	8	2.50E-02	2.30E-02	1.70E-01	SF		2.3	18	1.59E+00	2.77E+00	1.48E+00	NF
1.1	8	3.40E-02	3.20E-02	2.27E-01	SF		2.35	18	1.62E+00	2.85E+00	1.49E+00	NF
1.15	8	4.50E-02	4.50E-02	2.97E-01	SF		2.4	18	1.65E+00	2.92E+00	1.50E+00	NF
1.2	8	5.90E-02	6.20E-02	3.81E-01	SF		2.45	18	1.68E+00	3.00E+00	1.49E+00	NF
1.25	8	7.60E-02	8.30E-02	4.81E-01	SF		2.5	18	1.71E+00	3.07E+00	1.47E+00	NF
1.3	8	9.70E-02	1.09E-01	6.00E-01	SF		2.55	18	1.74E+00	3.14E+00	1.45E+00	NF
1.35	8	1.22E-01	1.43E-01	7.39E-01	SF		2.6	18	1.77E+00	3.22E+00	1.43E+00	NF
1.4	8	1.52E-01	1.84E-01	8.98E-01	SF		2.65	18	1.80E+00	3.29E+00	1.42E+00	NF
1.45	8	1.87E-01	2.33E-01	1.08E+00	SF		2.7	18	1.83E+00	3.37E+00	1.41E+00	NF
1.5	8	2.26E-01	2.92E-01	1.27E+00	SF		2.75	18	1.86E+00	3.44E+00	1.41E+00	NF
1.55	8	2.71E-01	3.60E-01	1.49E+00	SF		2.8	18	1.88E+00	3.52E+00	1.42E+00	NF
1.6	8	3.22E-01	4.40E-01	1.73E+00	SF		2.85	18	1.91E+00	3.60E+00	1.43E+00	NF
1.65	8	3.79E-01	5.34E-01	2.02E+00	SF		2.9	18	1.94E+00	3.67E+00	1.46E+00	NF
1.7	8	4.45E-01	6.44E-01	2.38E+00	SF		2.95	18	1.97E+00	3.76E+00	1.49E+00	NF
1.75	8	5.21E-01	7.74E-01	2.81E+00	SF		3	18	1.99E+00	3.84E+00	1.52E+00	NF
1.8	8	6.08E-01	9.29E-01	3.29E+00	SF		3.05	18	2.02E+00	3.92E+00	1.56E+00	NF
1.85	8	7.06E-01	1.11E+00	3.76E+00	SF		3.1	18	2.05E+00	4.01E+00	1.60E+00	NF
1.9	8	8.14E-01	1.31E+00	4.29E+00	SF		3.15	18	2.08E+00	4.10E+00	1.64E+00	NF
2.1	8	1.45E+00	2.59E+00	5.28E+00	NF		3.2	18	2.11E+00	4.19E+00	1.67E+00	NF
2.15	8	1.52E+00	2.72E+00	3.04E+00	NF		3.25	18	2.13E+00	4.28E+00	1.71E+00	NF
2.2	8	1.57E+00	2.84E+00	2.25E+00	NF		3.3	18	2.16E+00	4.38E+00	1.74E+00	NF
2.25	8	1.62E+00	2.96E+00	1.95E+00	NF		3.35	18	2.19E+00	4.48E+00	1.77E+00	NF
2.3	8	1.67E+00	3.07E+00	1.83E+00	NF		3.4	18	2.22E+00	4.58E+00	1.80E+00	NF
2.35	8	1.72E+00	3.17E+00	1.79E+00	NF		3.45	18	2.25E+00	4.68E+00	1.83E+00	NF
2.4	8	1.76E+00	3.27E+00	1.79E+00	NF		3.5	18	2.28E+00	4.78E+00	1.86E+00	NF
2.45	8	1.80E+00	3.36E+00	1.78E+00	NF		0	19	1.42E-06	9.62E-04	6.77E-08	SF
2.5	8	1.84E+00	3.46E+00	1.77E+00	NF		0.05	19	5.51E-07	2.80E-06	8.50E-07	SF
2.55	8	1.87E+00	3.54E+00	1.76E+00	NF		0.1	19	2.01E-06	1.22E-06	6.01E-06	SF
2.6	8	1.91E+00	3.63E+00	1.73E+00	NF		0.15	19	6.76E-06	1.82E-06	2.04E-05	SF
2.65	8	1.94E+00	3.72E+00	1.70E+00	NF		0.2	19	1.62E-05	3.49E-06	4.81E-05	SF
2.7	8	1.97E+00	3.81E+00	1.68E+00	NF		0.25	19	3.14E-05	6.93E-06	9.51E-05	SF
2.75	8	2.01E+00	3.89E+00	1.66E+00	NF		0.3	19	5.45E-05	1.33E-05	1.66E-04	SF
2.8	8	2.04E+00	3.98E+00	1.66E+00	NF		0.35	19	8.74E-05	2.40E-05	2.63E-04	SF
2.85	8	2.07E+00	4.07E+00	1.66E+00	NF		0.4	19	1.31E-04	4.04E-05	3.97E-04	SF
2.9	8	2.10E+00	4.16E+00	1.68E+00	NF		0.45	19	1.89E-04	6.50E-05	6.14E-04	SF
2.95	8	2.13E+00	4.25E+00	1.70E+00	NF		0.5	19	2.72E-04	1.04E-04	1.02E-03	SF
3	8	2.16E+00	4.35E+00	1.73E+00	NF		0.55	19	4.04E-04	1.74E-04	1.85E-03	SF
3.05	8	2.19E+00	4.45E+00	1.77E+00	NF		0.6	19	6.31E-04	3.05E-04	3.54E-03	SF
3.1	8	2.23E+00	4.55E+00	1.81E+00	NF		0.65	19	1.03E-03	5.56E-04	6.84E-03	SF
3.15	8	2.26E+00	4.65E+00	1.86E+00	NF		0.7	19	1.74E-03	1.03E-03	1.30E-02	SF
3.2	8	2.29E+00	4.76E+00	1.90E+00	NF		0.75	19	2.92E-03	1.90E-03	2.30E-02	SF
3.25	8	2.32E+00	4.87E+00	1.94E+00	NF		0.8	19	4.81E-03	3.37E-03	3.70E-02	SF
3.3	8	2.36E+00	4.98E+00	1.97E+00	NF		0.85	19	7.67E-03	5.73E-03	5.80E-02	SF
3.35	8	2.39E+00	5.10E+00	2.00E+00	NF		0.9	19	1.20E-02	9.32E-03	8.70E-02	SF
3.4	8	2.43E+00	5.22E+00	2.03E+00	NF		0.95	19	1.70E-02	1.50E-02	1.25E-01	SF
3.45	8	2.46E+00	5.34E+00	2.05E+00	NF		1	19	2.50E-02	2.20E-02	1.74E-01	SF
3.5	8	2.50E+00	5.46E+00	2.07E+00	NF		1.05	19	3.50E-02	3.20E-02	2.35E-01	SF
0	9	1.36E-07	1.23E-04	8.98E-08	SF		1.1	19	4.70E-02	4.50E-02	3.07E-01	SF

T(K)	P(atm)	S(kJ/kgK)	H(kJ/kg)	ρ(kg/m3)	Phase	-	T (K)	P (atm)	S (kJ/kgK)	H (kJ/kg)	ρ (kg/m3)	Phase.
0.05	9	6.45E-07	3.44E-06	1.43E-06	SF		1.15	19	6.20E-02	6.30E-02	3.91E-01	SF
0.1	9	3.29E-06	2.00E-06	9.86E-06	SF		1.2	19	8.10E-02	8.40E-02	4.89E-01	SF
0.15	9	1.11E-05	2.99E-06	3.34E-05	SF		1.25	19	1.03E-01	1.11E-01	6.10E-01	SF
0.2	9	2.65E-05	5.74E-06	7.87E-05	SF		1.3	19	1.29E-01	1.45E-01	7.59E-01	SF
0.25	9	5.14E-05	1.14E-05	1.54E-04	SF		1.35	19	1.61E-01	1.87E-01	9.42E-01	SF
0.3	9	8.88E-05	2.17E-05	2.69E-04	SF		1.4	19	1.99E-01	2.40E-01	1.15E+00	SF
0.35	9	1.42E-04	3.90E-05	4.28E-04	SF		1.45	19	2.44E-01	3.04E-01	1.38E+00	SF
0.4	9	2.13E-04	6.56E-05	6.37E-04	SF		1.5	19	2.96E-01	3.80E-01	1.61E+00	SF
0.45	9	3.03E-04	1.04E-04	9.20E-04	SF		1.55	19	3.53E-01	4.68E-01	1.88E+00	SF
0.5	9	4.20E-04	1.60E-04	1.35E-03	SF		1.6	19	4.18E-01	5.71E-01	2.21E+00	SF
0.55	9	5.77E-04	2.42E-04	2.05E-03	SF		1.65	19	4.94E-01	6.94E-01	2.63E+00	SF
0.6	9	8.03E-04	3.73E-04	3.27E-03	SF		1.7	19	5.82E-01	8.42E-01	3.11E+00	SF
0.65	9	1.15E-03	5.87E-04	5.45E-03	SF		1.75	19	6.83E-01	1.02E+00	3.62E+00	SF
0.7	9	1.68E-03	9.48E-04	9.25E-03	SF		1.8	19	7.99E-01	1.22E+00	4.31E+00	SF
0.75	9	2.52E-03	1.56E-03	1.60E-02	SF		1.9	19	1.24E+00	2.02E+00	1.14E+01	SF
0.8	9	3.83E-03	2.57E-03	2.60E-02	SF		1.95	19	1.29E+00	2.12E+00	4.34E+00	NF
0.85	9	5.81E-03	4.21E-03	4.10E-02	SF		2	19	1.34E+00	2.22E+00	2.46E+00	NF
0.9	9	8.70E-03	6.75E-03	6.20E-02	SF		2.05	19	1.38E+00	2.32E+00	1.80E+00	NF
0.95	9	1.30E-02	1.10E-02	9.10E-02	SF		2.1	19	1.43E+00	2.41E+00	1.55E+00	NF
1	9	1.80E-02	1.60E-02	1.28E-01	SF		2.15	19	1.47E+00	2.49E+00	1.45E+00	NF
1.05	9	2.60E-02	2.30E-02	1.75E-01	SF		2.2	19	1.51E+00	2.58E+00	1.44E+00	NF
1.1	9	3.50E-02	3.30E-02	2.33E-01	SF		2.25	19	1.54E+00	2.66E+00	1.45E+00	NF
1.15	9	4.60E-02	4.60E-02	3.03E-01	SF		2.3	19	1.58E+00	2.73E+00	1.46E+00	NF
1.2	9	6.10E-02	6.30E-02	3.89E-01	SF		2.35	19	1.61E+00	2.81E+00	1.48E+00	NF
1.25	9	7.80E-02	8.50E-02	4.91E-01	SF		2.4	19	1.64E+00	2.89E+00	1.48E+00	NF
1.3	9	1.00E-01	1.12E-01	6.12E-01	SF		2.45	19	1.67E+00	2.96E+00	1.47E+00	NF
1.35	9	1.25E-01	1.46E-01	7.53E-01	SF		2.5	19	1.70E+00	3.03E+00	1.45E+00	NF
1.4	9	1.55E-01	1.87E-01	9.15E-01	SF		2.55	19	1.73E+00	3.10E+00	1.43E+00	NF
1.45	9	1.91E-01	2.38E-01	1.10E+00	SF		2.6	19	1.76E+00	3.18E+00	1.42E+00	NF
1.5	9	2.31E-01	2.98E-01	1.30E+00	SF		2.65	19	1.79E+00	3.25E+00	1.40E+00	NF
1.55	9	2.77E-01	3.68E-01	1.52E+00	SF		2.7	19	1.82E+00	3.32E+00	1.39E+00	NF
1.6	9	3.29E-01	4.50E-01	1.77E+00	SF		2.75	19	1.84E+00	3.40E+00	1.39E+00	NF
1.65	9	3.88E-01	5.45E-01	2.07E+00	SF		2.8	19	1.87E+00	3.47E+00	1.40E+00	NF
1.7	9	4.54E-01	6.57E-01	2.43E+00	SF		2.85	19	1.90E+00	3.55E+00	1.42E+00	NF
1.75	9	5.32E-01	7.91E-01	2.86E+00	SF		2.9	19	1.93E+00	3.63E+00	1.44E+00	NF
1.8	9	6.21E-01	9.50E-01	3.34E+00	SF		2.95	19	1.95E+00	3.71E+00	1.47E+00	NF
1.85	9	7.21E-01	1.13E+00	3.83E+00	SF		3	19	1.98E+00	3.79E+00	1.50E+00	NF
1.9	9	8.31E-01	1.34E+00	4.38E+00	SF		3.05	19	2.01E+00	3.88E+00	1.54E+00	NF
2.05	9	1.39E+00	2.44E+00	1.05E+01	SF		3.1	19	2.04E+00	3.96E+00	1.58E+00	NF
2.1	9	1.45E+00	2.57E+00	4.47E+00	NF		3.15	19	2.06E+00	4.05E+00	1.62E+00	NF
2.15	9	1.51E+00	2.70E+00	2.74E+00	NF		3.2	19	2.09E+00	4.14E+00	1.65E+00	NF
2.2	9	1.57E+00	2.82E+00	2.12E+00	NF		3.25	19	2.12E+00	4.23E+00	1.69E+00	NF
2.25	9	1.62E+00	2.93E+00	1.87E+00	NF		3.3	19	2.15E+00	4.33E+00	1.72E+00	NF
2.3	9	1.66E+00	3.04E+00	1.77E+00	NF		3.35	19	2.18E+00	4.42E+00	1.76E+00	NF
2.35	9	1.71E+00	3.14E+00	1.75E+00	NF		3.4	19	2.21E+00	4.52E+00	1.79E+00	NF
2.4	9	1.75E+00	3.23E+00	1.74E+00	NF		3.45	19	2.24E+00	4.62E+00	1.81E+00	NF
2.45	9	1.79E+00	3.32E+00	1.74E+00	NF		3.5	19	2.27E+00	4.73E+00	1.84E+00	NF
2.5	9	1.82E+00	3.41E+00	1.73E+00	NF		0	20	1.67E-06	1.06E-03	8.85E-08	SF
2.55	9	1.86E+00	3.50E+00	1.71E+00	NF		0.05	20	5.41E-07	2.72E-06	8.55E-07	SF
2.6	9	1.89E+00	3.58E+00	1.69E+00	NF		0.1	20	1.92E-06	1.16E-06	5.76E-06	SF
2.65	9	1.92E+00	3.67E+00	1.67E+00	NF		0.15	20	6.49E-06	1.74E-06	1.96E-05	SF
2.7	9	1.96E+00	3.75E+00	1.65E+00	NF		0.2	20	1.55E-05	3.35E-06	4.61E-05	SF
2.75	9	1.99E+00	3.84E+00	1.63E+00	NF		0.25	20	3.01E-05	6.64E-06	9.13E-05	SF
2.8	9	2.02E+00	3.93E+00	1.63E+00	NF		0.3	20	5.23E-05	1.28E-05	1.59E-04	SF
2.85	9	2.05E+00	4.01E+00	1.63E+00	NF		0.35	20	8.39E-05	2.31E-05	2.52E-04	SF
2.9	9	2.08E+00	4.10E+00	1.65E+00	NF		0.4	20	1.26E-04	3.87E-05	3.82E-04	SF
2.95	9	2.11E+00	4.19E+00	1.67E+00	NF		0.45	20	1.82E-04	6.25E-05	5.97E-04	SF
3	9	2.14E+00	4.29E+00	1.71E+00	NF		0.5	20	2.63E-04	1.01E-04	1.01E-03	SF
3.05	9	2.17E+00	4.38E+00	1.75E+00	NF		0.55	20	3.95E-04	1.71E-04	1.86E-03	SF
3.1	9	2.20E+00	4.48E+00	1.79E+00	NF		0.6	20	6.26E-04	3.03E-04	3.62E-03	SF

T(K)	P(atm)	S(kJ/kgK)	H(kJ/kg)	ρ(kg/m3)	Phase	-	T (K)	P (atm)	S (kJ/kgK)	H (kJ/kg)	ρ (kg/m3)	Phase.
3.15	9	2.24E+00	4.58E+00	1.83E+00	NF		0.65	20	1.04E-03	5.62E-04	7.08E-03	SF
3.2	9	2.27E+00	4.69E+00	1.87E+00	NF		0.7	20	1.77E-03	1.06E-03	1.30E-02	SF
3.25	9	2.30E+00	4.79E+00	1.91E+00	NF		0.75	20	3.00E-03	1.95E-03	2.30E-02	SF
3.3	9	2.33E+00	4.90E+00	1.95E+00	NF		0.8	20	4.97E-03	3.48E-03	3.90E-02	SF
3.35	9	2.37E+00	5.02E+00	1.98E+00	NF		0.85	20	7.93E-03	5.93E-03	6.00E-02	SF
3.4	9	2.40E+00	5.13E+00	2.00E+00	NF		0.9	20	1.20E-02	9.64E-03	9.00E-02	SF
3.45	9	2.44E+00	5.25E+00	2.03E+00	NF		0.95	20	1.80E-02	1.50E-02	1.29E-01	SF
3.5	9	2.47E+00	5.38E+00	2.05E+00	NF		1	20	2.60E-02	2.30E-02	1.80E-01	SF
0	10	1.65E-07	1.49E-04	3.20E-08	SF		1.05	20	3.60E-02	3.30E-02	2.43E-01	SF
0.05	10	6.29E-07	3.35E-06	1.20E-06	SF		1.1	20	4.90E-02	4.70E-02	3.16E-01	SF
0.1	10	3.08E-06	1.88E-06	9.24E-06	SF		1.15	20	6.40E-02	6.40E-02	4.01E-01	SF
0.15	10	1.04E-05	2.80E-06	3.14E-05	SF		1.2	20	8.30E-02	8.70E-02	5.01E-01	SF
0.2	10	2.48E-05	5.38E-06	7.37E-05	SF		1.25	20	1.06E-01	1.14E-01	6.25E-01	SF
0.25	10	4.82E-05	1.07E-05	1.45E-04	SF		1.3	20	1.33E-01	1.49E-01	7.79E-01	SF
0.3	10	8.33E-05	2.04E-05	2.53E-04	SF		1.35	20	1.66E-01	1.93E-01	9.67E-01	SF
0.35	10	1.33E-04	3.67E-05	4.02E-04	SF		1.4	20	2.05E-01	2.47E-01	1.18E+00	SF
0.4	10	2.00E-04	6.17E-05	5.98E-04	SF		1.45	20	2.51E-01	3.12E-01	1.41E+00	SF
0.45	10	2.85E-04	9.80E-05	8.69E-04	SF		1.5	20	3.03E-01	3.90E-01	1.65E+00	SF
0.5	10	3.96E-04	1.51E-04	1.29E-03	SF		1.55	20	3.62E-01	4.80E-01	1.92E+00	SF
0.55	10	5.47E-04	2.30E-04	1.99E-03	SF		1.6	20	4.29E-01	5.86E-01	2.26E+00	SF
0.6	10	7.68E-04	3.58E-04	3.24E-03	SF		1.65	20	5.07E-01	7.12E-01	2.71E+00	SF
0.65	10	1.11E-03	5.72E-04	5.49E-03	SF		1.7	20	5.97E-01	8.65E-01	3.19E+00	SF
0.7	10	1.65E-03	9.39E-04	9.45E-03	SF		1.75	20	7.02E-01	1.05E+00	3.70E+00	SF
0.75	10	2.52E-03	1.57E-03	1.60E-02	SF		1.8	20	8.21E-01	1.26E+00	4.50E+00	SF
0.8	10	3.87E-03	2.62E-03	2.70E-02	SF		1.9	20	1.24E+00	2.01E+00	7.59E+00	SF
0.85	10	5.92E-03	4.32E-03	4.30E-02	SF		1.95	20	1.29E+00	2.11E+00	3.40E+00	NF
0.9	10	8.93E-03	6.95E-03	6.50E-02	SF		2	20	1.34E+00	2.21E+00	2.13E+00	NF
0.95	10	1.30E-02	1.10E-02	9.40E-02	SF		2.05	20	1.38E+00	2.30E+00	1.65E+00	NF
1	10	1.90E-02	1.60E-02	1.32E-01	SF		2.1	20	1.42E+00	2.39E+00	1.47E+00	NF
1.05	10	2.60E-02	2.40E-02	1.79E-01	SF		2.15	20	1.46E+00	2.47E+00	1.41E+00	NF
1.1	10	3.60E-02	3.40E-02	2.38E-01	SF		2.2	20	1.50E+00	2.55E+00	1.41E+00	NF
1.15	10	4.80E-02	4.80E-02	3.10E-01	SF		2.25	20	1.54E+00	2.63E+00	1.43E+00	NF
1.2	10	6.20E-02	6.50E-02	3.96E-01	SF		2.3	20	1.57E+00	2.71E+00	1.45E+00	NF
1.25	10	8.00E-02	8.70E-02	5.00E-01	SF		2.35	20	1.60E+00	2.78E+00	1.46E+00	NF
1.3	10	1.02E-01	1.15E-01	6.23E-01	SF		2.4	20	1.63E+00	2.85E+00	1.46E+00	NF
1.35	10	1.28E-01	1.49E-01	7.67E-01	SF		2.45	20	1.66E+00	2.93E+00	1.45E+00	NF
1.4	10	1.59E-01	1.91E-01	9.32E-01	SF		2.5	20	1.69E+00	3.00E+00	1.43E+00	NF
1.45	10	1.95E-01	2.43E-01	1.12E+00	SF		2.55	20	1.72E+00	3.07E+00	1.41E+00	NF
1.5	10	2.36E-01	3.04E-01	1.32E+00	SF		2.6	20	1.75E+00	3.14E+00	1.40E+00	NF
1.55	10	2.83E-01	3.76E-01	1.55E+00	SF		2.65	20	1.78E+00	3.21E+00	1.38E+00	NF
1.6	10	3.36E-01	4.59E-01	1.80E+00	SF		2.7	20	1.81E+00	3.29E+00	1.38E+00	NF
1.65	10	3.96E-01	5.56E-01	2.11E+00	SF		2.75	20	1.83E+00	3.36E+00	1.38E+00	NF
1.7	10	4.64E-01	6.71E-01	2.48E+00	SF		2.8	20	1.86E+00	3.43E+00	1.39E+00	NF
1.75	10	5.43E-01	8.08E-01	2.91E+00	SF		2.85	20	1.89E+00	3.51E+00	1.40E+00	NF
1.8	10	6.34E-01	9.70E-01	3.40E+00	SF		2.9	20	1.91E+00	3.59E+00	1.42E+00	NF
1.85	10	7.36E-01	1.16E+00	3.90E+00	SF		2.95	20	1.94E+00	3.67E+00	1.45E+00	NF
1.9	10	8.48E-01	1.37E+00	4.46E+00	SF		3	20	1.97E+00	3.75E+00	1.49E+00	NF
2.05	10	1.39E+00	2.43E+00	7.62E+00	SF		3.05	20	2.00E+00	3.83E+00	1.52E+00	NF
2.1	10	1.45E+00	2.56E+00	3.71E+00	NF		3.1	20	2.02E+00	3.92E+00	1.56E+00	NF
2.15	10	1.51E+00	2.68E+00	2.46E+00	NF		3.15	20	2.05E+00	4.00E+00	1.60E+00	NF
2.2	10	1.56E+00	2.80E+00	1.98E+00	NF		3.2	20	2.08E+00	4.09E+00	1.64E+00	NF
2.25	10	1.61E+00	2.91E+00	1.79E+00	NF		3.25	20	2.11E+00	4.18E+00	1.67E+00	NF
2.3	10	1.65E+00	3.01E+00	1.72E+00	NF		3.3	20	2.14E+00	4.28E+00	1.71E+00	NF
2.35	10	1.70E+00	3.10E+00	1.70E+00	NF		3.35	20	2.16E+00	4.37E+00	1.74E+00	NF
2.4	10	1.74E+00	3.20E+00	1.70E+00	NF		3.4	20	2.19E+00	4.47E+00	1.77E+00	NF
2.45	10	1.77E+00	3.29E+00	1.70E+00	NF		3.45	20	2.22E+00	4.57E+00	1.79E+00	NF
2.5	10	1.81E+00	3.37E+00	1.69E+00	NF		3.5	20	2.25E+00	4.67E+00	1.82E+00	NF
2.55	10	1.84E+00	3.46E+00	1.67E+00	NF							

Appendix G

Appendix Helium 3-4 Mixture Data

In this appendix the calculated data for Helium 3-4 based on the equation of state of chapter 6 are presented.

x	T(K)	P(bar)	S(J/molK)	H(J/mol)	V(cm3/mol)	-	x.	T (K)	P (bar)	S (J/molK)	H (J/mol)	V (cm3/mol)
0.05	0.1	1	0.649	3.6	26.076		0.95	1.5	5	11.385	22.295	32.302
0.1	0.1	1	0.802	3.514	26.399		1	1.5	5	10.335	21.987	32.693
0.15	0.1	1	0.705	3.387	26.75		0.05	0.1	6	0.497	16.754	26.275
0.2	0.1	1	0.587	3.297	27.107		0.1	0.1	6	0.668	16.841	26.579
0.25	0.1	1	0.559	3.267	27.454		0.15	0.1	6	0.566	16.9	26.874
0.3	0.1	1	0.653	3.29	27.784		0.2	0.1	6	0.421	16.999	27.164
0.35	0.1	1	0.853	3.35	28.097		0.25	0.1	6	0.348	17.152	27.453
0.4	0.1	1	1.116	3.431	28.396		0.3	0.1	6	0.381	17.344	27.742
0.45	0.1	1	1.391	3.52	28.688		0.35	0.1	6	0.512	17.559	28.034
0.5	0.1	1	1.626	3.608	28.983		0.4	0.1	6	0.702	17.782	28.33
0.55	0.1	1	1.781	3.687	29.286		0.45	0.1	6	0.908	18.006	28.632
0.6	0.1	1	1.835	3.748	29.604		0.5	0.1	6	1.086	18.228	28.939
0.65	0.1	1	1.787	3.784	29.941		0.55	0.1	6	1.201	18.448	29.251
0.7	0.1	1	1.661	3.794	30.294		0.6	0.1	6	1.237	18.66	29.566
0.75	0.1	1	1.504	3.791	30.657		0.65	0.1	6	1.194	18.859	29.883
0.8	0.1	1	1.38	3.808	31.019		0.7	0.1	6	1.092	19.044	30.197
0.85	0.1	1	1.362	3.896	31.364		0.75	0.1	6	0.97	19.226	30.505
0.9	0.1	1	1.515	4.113	31.676		0.8	0.1	6	0.879	19.437	30.803
0.95	0.1	1	1.866	4.469	31.934		0.85	0.1	6	0.874	19.73	31.089
1	0.1	1	2.369	4.839	32.123		0.9	0.1	6	0.993	20.155	31.362
0	0.2	1	0.046	2.99	25.841		0.95	0.1	6	1.235	20.717	31.629
0.05	0.2	1	0.994	3.147	26.112		1	0.1	6	1.522	21.265	31.901
0.1	0.2	1	1.39	3.189	26.432		0.05	0.2	6	0.981	16.354	26.286
0.15	0.2	1	1.54	3.202	26.778		0.1	0.2	6	1.419	16.566	26.588
0.2	0.2	1	1.614	3.229	27.132		0.15	0.2	6	1.601	16.759	26.885
0.25	0.2	1	1.696	3.279	27.482		0.2	0.2	6	1.7	16.973	27.18
0.3	0.2	1	1.818	3.345	27.821		0.25	0.2	6	1.799	17.212	27.476
0.35	0.2	1	1.978	3.416	28.149		0.3	0.2	6	1.93	17.464	27.773
0.4	0.2	1	2.162	3.486	28.467		0.35	0.2	6	2.093	17.715	28.072
0.45	0.2	1	2.349	3.551	28.778		0.4	0.2	6	2.277	17.96	28.374
0.5	0.2	1	2.523	3.614	29.087		0.45	0.2	6	2.465	18.198	28.678
0.55	0.2	1	2.67	3.674	29.399		0.5	0.2	6	2.642	18.435	28.984
0.6	0.2	1	2.786	3.731	29.719		0.55	0.2	6	2.8	18.674	29.291
0.65	0.2	1	2.877	3.778	30.048		0.6	0.2	6	2.937	18.916	29.598
0.7	0.2	1	2.957	3.812	30.386		0.65	0.2	6	3.057	19.154	29.903
0.75	0.2	1	3.045	3.833	30.732		0.7	0.2	6	3.171	19.383	30.206
0.8	0.2	1	3.164	3.854	31.082		0.75	0.2	6	3.296	19.6	30.506
0.85	0.2	1	3.329	3.896	31.429		0.8	0.2	6	3.444	19.817	30.801
0.9	0.2	1	3.535	3.982	31.77		0.85	0.2	6	3.619	20.055	31.094
0.95	0.2	1	3.731	4.093	32.102		0.9	0.2	6	3.801	20.334	31.388
1	0.2	1	3.792	4.093	32.429		0.95	0.2	6	3.926	20.631	31.695
0	0.3	1	0.057	2.994	25.813		1	0.2	6	3.855	20.788	32.031
0.05	0.3	1	1.132	3.136	26.091		0	0.3	6	9.42E-03	16.02	25.977
0.1	0.3	1	1.732	3.244	26.402		0.05	0.3	6	1.126	16.349	26.279
0.15	0.3	1	2.094	3.339	26.733		0.1	0.3	6	1.765	16.625	26.575
0.2	0.3	1	2.345	3.432	27.071		0.15	0.3	6	2.164	16.894	26.87
0.25	0.3	1	2.549	3.522	27.408		0.2	0.3	6	2.453	17.17	27.165
0.3	0.3	1	2.733	3.603	27.741		0.25	0.3	6	2.692	17.45	27.461
0.35	0.3	1	2.908	3.671	28.067		0.3	0.3	6	2.909	17.722	27.76
0.4	0.3	1	3.076	3.726	28.385		0.35	0.3	6	3.113	17.979	28.06
0.45	0.3	1	3.239	3.772	28.699		0.4	0.3	6	3.305	18.219	28.362
0.5	0.3	1	3.401	3.818	29.009		0.45	0.3	6	3.49	18.451	28.664
0.55	0.3	1	3.567	3.873	29.319		0.5	0.3	6	3.673	18.683	28.966
0.6	0.3	1	3.746	3.94	29.631		0.55	0.3	6	3.859	18.926	29.268
0.65	0.3	1	3.943	4.018	29.948		0.6	0.3	6	4.058	19.185	29.568
0.7	0.3	1	4.163	4.101	30.27		0.65	0.3	6	4.275	19.454	29.866
0.75	0.3	1	4.408	4.181	30.598		0.7	0.3	6	4.513	19.728	30.162
0.8	0.3	1	4.667	4.255	30.933		0.75	0.3	6	4.772	19.996	30.456
0.85	0.3	1	4.916	4.327	31.276		0.8	0.3	6	5.036	20.256	30.749
0.9	0.3	1	5.105	4.396	31.633		0.85	0.3	6	5.279	20.512	31.043

x	T(K)	P(bar)	S(J/molK)	H(J/mol)	V(cm3/mol)	-	x.	T (K)	P (bar)	S (J/molK)	H (J/mol)	V (cm3/mol)
0.95	0.3	1	5.136	4.431	32.014		0.9	0.3	6	5.443	20.767	31.345
1	0.3	1	4.846	4.305	32.437		0.95	0.3	6	5.432	20.987	31.665
0	0.4	1	0.051	3.027	25.783		1	0.3	6	5.082	21.032	32.02
0.05	0.4	1	1.244	3.166	26.068		0	0.4	6	7.17E-03	16.046	25.979
0.1	0.4	1	2.019	3.339	26.37		0.05	0.4	6	1.231	16.381	26.274
0.15	0.4	1	2.565	3.509	26.683		0.1	0.4	6	2.034	16.72	26.566
0.2	0.4	1	2.981	3.665	27.001		0.15	0.4	6	2.61	17.06	26.858
0.25	0.4	1	3.317	3.8	27.321		0.2	0.4	6	3.059	17.395	27.151
0.3	0.4	1	3.596	3.91	27.641		0.25	0.4	6	3.429	17.717	27.447
0.35	0.4	1	3.831	3.993	27.957		0.3	0.4	6	3.74	18.017	27.744
0.4	0.4	1	4.038	4.056	28.27		0.35	0.4	6	4.006	18.291	28.043
0.45	0.4	1	4.229	4.107	28.579		0.4	0.4	6	4.238	18.541	28.344
0.5	0.4	1	4.422	4.158	28.886		0.45	0.4	6	4.451	18.778	28.645
0.55	0.4	1	4.633	4.224	29.192		0.5	0.4	6	4.66	19.014	28.945
0.6	0.4	1	4.873	4.31	29.497		0.55	0.4	6	4.88	19.264	29.245
0.65	0.4	1	5.149	4.417	29.804		0.6	0.4	6	5.125	19.534	29.544
0.7	0.4	1	5.457	4.536	30.114		0.65	0.4	6	5.4	19.821	29.842
0.75	0.4	1	5.782	4.655	30.429		0.7	0.4	6	5.701	20.118	30.138
0.8	0.4	1	6.095	4.761	30.753		0.75	0.4	6	6.012	20.411	30.433
0.85	0.4	1	6.347	4.842	31.094		0.8	0.4	6	6.305	20.69	30.728
0.9	0.4	1	6.46	4.887	31.461		0.85	0.4	6	6.532	20.947	31.025
0.95	0.4	1	6.318	4.864	31.873		0.9	0.4	6	6.621	21.178	31.328
1	0.4	1	5.747	4.672	32.359		0.95	0.4	6	6.464	21.354	31.645
0	0.5	1	0.05	3.029	25.761		1	0.4	6	5.902	21.367	31.991
0.05	0.5	1	1.354	3.193	26.053		0	0.5	6	0.017	16.046	25.981
0.1	0.5	1	2.273	3.438	26.347		0.05	0.5	6	1.346	16.409	26.27
0.15	0.5	1	2.973	3.686	26.643		0.1	0.5	6	2.285	16.82	26.559
0.2	0.5	1	3.538	3.91	26.943		0.15	0.5	6	3.006	17.234	26.849
0.25	0.5	1	4.007	4.102	27.245		0.2	0.5	6	3.594	17.635	27.141
0.3	0.5	1	4.398	4.26	27.549		0.25	0.5	6	4.087	18.012	27.436
0.35	0.5	1	4.728	4.387	27.854		0.3	0.5	6	4.504	18.359	27.732
0.4	0.5	1	5.013	4.487	28.159		0.35	0.5	6	4.855	18.672	28.031
0.45	0.5	1	5.273	4.572	28.464		0.4	0.5	6	5.158	18.957	28.331
0.5	0.5	1	5.529	4.655	28.768		0.45	0.5	6	5.429	19.224	28.631
0.55	0.5	1	5.802	4.749	29.07		0.5	0.5	6	5.689	19.486	28.933
0.6	0.5	1	6.102	4.861	29.372		0.55	0.5	6	5.956	19.755	29.235
0.65	0.5	1	6.433	4.991	29.674		0.6	0.5	6	6.243	20.039	29.538
0.7	0.5	1	6.785	5.128	29.978		0.65	0.5	6	6.552	20.336	29.841
0.75	0.5	1	7.132	5.256	30.287		0.7	0.5	6	6.873	20.637	30.144
0.8	0.5	1	7.432	5.354	30.607		0.75	0.5	6	7.184	20.925	30.446
0.85	0.5	1	7.623	5.402	30.946		0.8	0.5	6	7.444	21.184	30.748
0.9	0.5	1	7.62	5.384	31.319		0.85	0.5	6	7.6	21.403	31.049
0.95	0.5	1	7.307	5.276	31.75		0.9	0.5	6	7.576	21.576	31.351
1	0.5	1	6.521	5.017	32.273		0.95	0.5	6	7.275	21.688	31.657
0	0.6	1	0.043	3.02	25.745		1	0.5	6	6.561	21.678	31.975
0.05	0.6	1	1.446	3.229	26.044		0	0.6	6	0.021	16.036	25.982
0.1	0.6	1	2.478	3.545	26.33		0.05	0.6	6	1.45	16.445	26.264
0.15	0.6	1	3.299	3.866	26.612		0.1	0.6	6	2.497	16.926	26.551
0.2	0.6	1	3.988	4.156	26.895		0.15	0.6	6	3.332	17.411	26.84
0.25	0.6	1	4.58	4.411	27.18		0.2	0.6	6	4.035	17.876	27.131
0.3	0.6	1	5.091	4.631	27.47		0.25	0.6	6	4.642	18.312	27.425
0.35	0.6	1	5.533	4.82	27.764		0.3	0.6	6	5.167	18.718	27.721
0.4	0.6	1	5.921	4.983	28.062		0.35	0.6	6	5.62	19.091	28.02
0.45	0.6	1	6.275	5.128	28.362		0.4	0.6	6	6.015	19.435	28.319
0.5	0.6	1	6.615	5.264	28.664		0.45	0.6	6	6.369	19.756	28.621
0.55	0.6	1	6.958	5.402	28.966		0.5	0.6	6	6.701	20.064	28.926
0.6	0.6	1	7.315	5.547	29.268		0.55	0.6	6	7.027	20.368	29.233
0.65	0.6	1	7.682	5.695	29.57		0.6	0.6	6	7.355	20.675	29.542
0.7	0.6	1	8.044	5.836	29.874		0.65	0.6	6	7.685	20.98	29.854
0.75	0.6	1	8.369	5.947	30.182		0.7	0.6	6	8	21.272	30.168

x	T(K)	P(bar)	S(J/molK)	H(J/mol)	V(cm3/mol)	-	x.	T (K)	P (bar)	S (J/molK)	H (J/mol)	V (cm3/mol)
0.8	0.6	1	8.609	6.005	30.501		0.75	0.6	6	8.274	21.534	30.482
0.85	0.6	1	8.701	5.986	30.841		0.8	0.6	6	8.463	21.745	30.793
0.9	0.6	1	8.561	5.875	31.217		0.85	0.6	6	8.515	21.895	31.101
0.95	0.6	1	8.089	5.664	31.655		0.9	0.6	6	8.363	21.981	31.4
1	0.6	1	7.152	5.339	32.19		0.95	0.6	6	7.93	22.011	31.69
0	0.7	1	0.031	3.014	25.734		1	0.6	6	7.121	21.974	31.97
0.05	0.7	1	1.52	3.275	26.036		0	0.7	6	9.65E-03	16.03	25.981
0.1	0.7	1	2.631	3.654	26.315		0.05	0.7	6	1.531	16.49	26.256
0.15	0.7	1	3.538	4.033	26.584		0.1	0.7	6	2.657	17.031	26.54
0.2	0.7	1	4.325	4.379	26.851		0.15	0.7	6	3.573	17.572	26.829
0.25	0.7	1	5.024	4.693	27.121		0.2	0.7	6	4.364	18.089	27.121
0.3	0.7	1	5.649	4.979	27.398		0.25	0.7	6	5.069	18.581	27.416
0.35	0.7	1	6.208	5.242	27.682		0.3	0.7	6	5.698	19.05	27.712
0.4	0.7	1	6.711	5.483	27.973		0.35	0.7	6	6.258	19.493	28.009
0.45	0.7	1	7.171	5.704	28.27		0.4	0.7	6	6.758	19.91	28.31
0.5	0.7	1	7.603	5.908	28.572		0.45	0.7	6	7.209	20.302	28.613
0.55	0.7	1	8.02	6.099	28.876		0.5	0.7	6	7.625	20.673	28.919
0.6	0.7	1	8.425	6.279	29.182		0.55	0.7	6	8.015	21.025	29.231
0.65	0.7	1	8.811	6.441	29.488		0.6	0.7	6	8.384	21.36	29.548
0.7	0.7	1	9.159	6.573	29.795		0.65	0.7	6	8.726	21.673	29.87
0.75	0.7	1	9.433	6.653	30.106		0.7	0.7	6	9.02	21.951	30.196
0.8	0.7	1	9.587	6.653	30.426		0.75	0.7	6	9.237	22.175	30.522
0.85	0.7	1	9.56	6.551	30.766		0.8	0.7	6	9.336	22.326	30.846
0.9	0.7	1	9.284	6.338	31.141		0.85	0.7	6	9.271	22.391	31.16
0.95	0.7	1	8.68	6.028	31.574		0.9	0.7	6	8.992	22.381	31.458
1	0.7	1	7.657	5.659	32.102		0.95	0.7	6	8.45	22.325	31.73
0	0.8	1	0.028	3.015	25.728		1	0.7	6	7.595	22.273	31.968
0.05	0.8	1	1.593	3.333	26.03		0.05	0.8	6	1.603	16.547	26.248
0.1	0.8	1	2.756	3.761	26.3		0.1	0.8	6	2.781	17.135	26.53
0.15	0.8	1	3.717	4.18	26.556		0.15	0.8	6	3.745	17.713	26.82
0.2	0.8	1	4.572	4.569	26.809		0.2	0.8	6	4.598	18.268	27.114
0.25	0.8	1	5.36	4.934	27.066		0.25	0.8	6	5.381	18.807	27.409
0.3	0.8	1	6.089	5.287	27.331		0.3	0.8	6	6.103	19.336	27.706
0.35	0.8	1	6.762	5.629	27.606		0.35	0.8	6	6.767	19.853	28.004
0.4	0.8	1	7.379	5.956	27.892		0.4	0.8	6	7.373	20.351	28.304
0.45	0.8	1	7.947	6.261	28.187		0.45	0.8	6	7.925	20.823	28.607
0.5	0.8	1	8.471	6.537	28.49		0.5	0.8	6	8.427	21.263	28.915
0.55	0.8	1	8.955	6.783	28.797		0.55	0.8	6	8.883	21.668	29.23
0.6	0.8	1	9.399	6.993	29.108		0.6	0.8	6	9.29	22.034	29.553
0.65	0.8	1	9.791	7.162	29.42		0.65	0.8	6	9.636	22.353	29.883
0.7	0.8	1	10.107	7.275	29.733		0.7	0.8	6	9.9	22.612	30.219
0.75	0.8	1	10.315	7.311	30.048		0.75	0.8	6	10.053	22.792	30.558
0.8	0.8	1	10.371	7.246	30.371		0.8	0.8	6	10.058	22.877	30.892
0.85	0.8	1	10.225	7.06	30.709		0.85	0.8	6	9.879	22.858	31.214
0.9	0.8	1	9.828	6.755	31.076		0.9	0.8	6	9.487	22.756	31.511
0.95	0.8	1	9.13	6.37	31.495		0.95	0.8	6	8.863	22.628	31.768
1	0.8	1	8.082	5.996	31.997		1	0.8	6	8.004	22.582	31.967
0	0.9	1	0.051	3.03	25.729		0	0.9	6	0.014	16.055	25.983
0.05	0.9	1	1.687	3.408	26.024		0.05	0.9	6	1.695	16.626	26.242
0.1	0.9	1	2.882	3.877	26.285		0.1	0.9	6	2.903	17.251	26.522
0.15	0.9	1	3.874	4.326	26.528		0.15	0.9	6	3.891	17.853	26.815
0.2	0.9	1	4.778	4.748	26.768		0.2	0.9	6	4.782	18.435	27.112
0.25	0.9	1	5.637	5.163	27.013		0.25	0.9	6	5.624	19.015	27.411
0.3	0.9	1	6.458	5.583	27.268		0.3	0.9	6	6.427	19.602	27.709
0.35	0.9	1	7.236	6.007	27.536		0.35	0.9	6	7.185	20.194	28.007
0.4	0.9	1	7.961	6.423	27.818		0.4	0.9	6	7.891	20.775	28.306
0.45	0.9	1	8.629	6.813	28.113		0.45	0.9	6	8.538	21.327	28.608
0.5	0.9	1	9.235	7.159	28.417		0.5	0.9	6	9.121	21.836	28.915
0.55	0.9	1	9.777	7.452	28.729		0.55	0.9	6	9.636	22.29	29.23
0.6	0.9	1	10.246	7.682	29.046		0.6	0.9	6	10.073	22.68	29.555

x	T(K)	P(bar)	S(J/molK)	H(J/mol)	V(cm3/mol)	-	x.	T (K)	P (bar)	S (J/molK)	H (J/mol)	V (cm3/mol)
0.65	0.9	1	10.63	7.843	29.364		0.65	0.9	6	10.417	22.998	29.89
0.7	0.9	1	10.903	7.923	29.684		0.7	0.9	6	10.647	23.232	30.233
0.75	0.9	1	11.038	7.905	30.004		0.75	0.9	6	10.734	23.365	30.581
0.8	0.9	1	10.998	7.771	30.328		0.8	0.9	6	10.651	23.384	30.925
0.85	0.9	1	10.747	7.508	30.661		0.85	0.9	6	10.373	23.289	31.254
0.9	0.9	1	10.256	7.13	31.016		0.9	0.9	6	9.891	23.11	31.552
0.95	0.9	1	9.503	6.702	31.41		0.95	0.9	6	9.214	22.931	31.798
1	0.9	1	8.483	6.366	31.871		1	0.9	6	8.382	22.913	31.968
0	1	1	0.101	3.064	25.737		0	1	6	0.068	16.098	25.985
0.05	1	1	1.814	3.511	26.021		0.05	1	6	1.827	16.737	26.235
0.1	1	1	3.035	4.021	26.269		0.1	1	6	3.055	17.398	26.517
0.15	1	1	4.048	4.5	26.5		0.15	1	6	4.052	18.022	26.814
0.2	1	1	4.989	4.958	26.728		0.2	1	6	4.966	18.628	27.117
0.25	1	1	5.909	5.426	26.962		0.25	1	6	5.854	19.248	27.421
0.3	1	1	6.813	5.919	27.21		0.3	1	6	6.725	19.895	27.722
0.35	1	1	7.685	6.432	27.473		0.35	1	6	7.566	20.563	28.021
0.4	1	1	8.507	6.939	27.753		0.4	1	6	8.36	21.226	28.319
0.45	1	1	9.262	7.41	28.048		0.45	1	6	9.09	21.856	28.617
0.5	1	1	9.935	7.817	28.356		0.5	1	6	9.741	22.426	28.921
0.55	1	1	10.517	8.142	28.673		0.55	1	6	10.301	22.919	29.233
0.6	1	1	10.996	8.374	28.996		0.6	1	6	10.757	23.321	29.555
0.65	1	1	11.357	8.507	29.322		0.65	1	6	11.091	23.625	29.89
0.7	1	1	11.579	8.536	29.647		0.7	1	6	11.284	23.823	30.235
0.75	1	1	11.64	8.454	29.971		0.75	1	6	11.312	23.904	30.587
0.8	1	1	11.514	8.248	30.294		0.8	1	6	11.154	23.862	30.937
0.85	1	1	11.179	7.918	30.62		0.85	1	6	10.799	23.701	31.273
0.9	1	1	10.625	7.489	30.956		0.9	1	6	10.252	23.462	31.575
0.95	1	1	9.855	7.046	31.317		0.95	1	6	9.548	23.25	31.82
1	1	1	8.899	6.779	31.726		1	1	6	8.755	23.271	31.976
0	1.1	1	0.167	3.12	25.751		0	1.1	6	0.154	16.164	25.983
0.05	1.1	1	1.972	3.648	26.018		0.05	1.1	6	1.999	16.883	26.227
0.1	1.1	1	3.227	4.206	26.252		0.1	1.1	6	3.25	17.586	26.511
0.15	1.1	1	4.263	4.724	26.471		0.15	1.1	6	4.255	18.236	26.816
0.2	1.1	1	5.242	5.23	26.689		0.2	1.1	6	5.189	18.873	27.129
0.25	1.1	1	6.222	5.764	26.916		0.25	1.1	6	6.117	19.54	27.44
0.3	1.1	1	7.203	6.343	27.158		0.3	1.1	6	7.048	20.253	27.747
0.35	1.1	1	8.162	6.951	27.419		0.35	1.1	6	7.962	20.999	28.047
0.4	1.1	1	9.067	7.55	27.699		0.4	1.1	6	8.829	21.742	28.342
0.45	1.1	1	9.89	8.096	27.996		0.45	1.1	6	9.624	22.441	28.636
0.5	1.1	1	10.61	8.551	28.309		0.5	1.1	6	10.324	23.06	28.933
0.55	1.1	1	11.211	8.887	28.632		0.55	1.1	6	10.911	23.574	29.237
0.6	1.1	1	11.678	9.096	28.962		0.6	1.1	6	11.369	23.971	29.551
0.65	1.1	1	12	9.178	29.295		0.65	1.1	6	11.683	24.245	29.878
0.7	1.1	1	12.163	9.137	29.625		0.7	1.1	6	11.836	24.396	30.219
0.75	1.1	1	12.151	8.979	29.951		0.75	1.1	6	11.811	24.423	30.57
0.8	1.1	1	11.952	8.702	30.271		0.8	1.1	6	11.597	24.325	30.923
0.85	1.1	1	11.558	8.316	30.585		0.85	1.1	6	11.189	24.112	31.264
0.9	1.1	1	10.971	7.856	30.897		0.9	1.1	6	10.605	23.832	31.575
0.95	1.1	1	10.214	7.421	31.218		0.95	1.1	6	9.89	23.599	31.83
1	1.1	1	9.334	7.23	31.565		1	1.1	6	9.126	23.649	31.994
0	1.2	1	0.238	3.207	25.769		0	1.2	6	0.252	16.263	25.976
0.05	1.2	1	2.152	3.822	26.017		0.05	1.2	6	2.196	17.068	26.214
0.1	1.2	1	3.455	4.438	26.237		0.1	1.2	6	3.481	17.819	26.504
0.15	1.2	1	4.53	5.008	26.445		0.15	1.2	6	4.505	18.504	26.82
0.2	1.2	1	5.559	5.578	26.655		0.2	1.2	6	5.466	19.181	27.145
0.25	1.2	1	6.605	6.196	26.877		0.25	1.2	6	6.439	19.904	27.467
0.3	1.2	1	7.664	6.873	27.118		0.3	1.2	6	7.427	20.689	27.781
0.35	1.2	1	8.702	7.583	27.379		0.35	1.2	6	8.403	21.513	28.084
0.4	1.2	1	9.676	8.273	27.661		0.4	1.2	6	9.328	22.33	28.377
0.45	1.2	1	10.547	8.883	27.964		0.45	1.2	6	10.166	23.085	28.664

x	T(K)	P(bar)	S(J/molK)	H(J/mol)	V(cm3/mol)	-	x.	T (K)	P (bar)	S (J/molK)	H (J/mol)	V (cm3/mol)
0.5	1.2	1	11.288	9.363	28.282		0.5	1.2	6	10.89	23.734	28.95
0.55	1.2	1	11.879	9.686	28.613		0.55	1.2	6	11.48	24.247	29.24
0.6	1.2	1	12.311	9.844	28.95		0.6	1.2	6	11.921	24.616	29.539
0.65	1.2	1	12.575	9.85	29.289		0.65	1.2	6	12.201	24.843	29.853
0.7	1.2	1	12.669	9.723	29.623		0.7	1.2	6	12.312	24.94	30.181
0.75	1.2	1	12.589	9.482	29.948		0.75	1.2	6	12.245	24.914	30.524
0.8	1.2	1	12.332	9.141	30.261		0.8	1.2	6	11.993	24.774	30.874
0.85	1.2	1	11.901	8.717	30.558		0.85	1.2	6	11.56	24.532	31.221
0.9	1.2	1	11.309	8.247	30.842		0.9	1.2	6	10.962	24.232	31.546
0.95	1.2	1	10.58	7.832	31.117		0.95	1.2	6	10.243	23.983	31.825
1	1.2	1	9.76	7.697	31.394		1	1.2	6	9.474	24.027	32.021
0	1.3	1	0.326	3.359	25.79		0	1.3	6	0.356	16.434	25.964
0.05	1.3	1	2.354	4.06	26.019		0.05	1.3	6	2.404	17.322	26.198
0.1	1.3	1	3.722	4.74	26.225		0.1	1.3	6	3.737	18.123	26.497
0.15	1.3	1	4.853	5.375	26.425		0.15	1.3	6	4.796	18.847	26.827
0.2	1.3	1	5.949	6.024	26.631		0.2	1.3	6	5.799	19.572	27.168
0.25	1.3	1	7.074	6.739	26.852		0.25	1.3	6	6.825	20.357	27.504
0.3	1.3	1	8.215	7.523	27.094		0.3	1.3	6	7.871	21.214	27.826
0.35	1.3	1	9.326	8.334	27.359		0.35	1.3	6	8.9	22.109	28.133
0.4	1.3	1	10.352	9.102	27.648		0.4	1.3	6	9.865	22.984	28.423
0.45	1.3	1	11.247	9.754	27.958		0.45	1.3	6	10.722	23.772	28.701
0.5	1.3	1	11.979	10.232	28.285		0.5	1.3	6	11.442	24.422	28.972
0.55	1.3	1	12.531	10.508	28.624		0.55	1.3	6	12.006	24.906	29.242
0.6	1.3	1	12.898	10.585	28.968		0.6	1.3	6	12.406	25.222	29.52
0.65	1.3	1	13.086	10.491	29.312		0.65	1.3	6	12.639	25.387	29.81
0.7	1.3	1	13.102	10.266	29.648		0.7	1.3	6	12.706	25.426	30.117
0.75	1.3	1	12.957	9.947	29.969		0.75	1.3	6	12.607	25.362	30.444
0.8	1.3	1	12.66	9.563	30.27		0.8	1.3	6	12.342	25.207	30.786
0.85	1.3	1	12.218	9.132	30.545		0.85	1.3	6	11.913	24.971	31.137
0.9	1.3	1	11.642	8.681	30.793		0.9	1.3	6	11.325	24.679	31.482
0.95	1.3	1	10.943	8.293	31.015		0.95	1.3	6	10.598	24.417	31.799
1	1.3	1	10.14	8.166	31.216		1	1.3	6	9.768	24.397	32.058
0	1.4	1	0.488	3.634	25.811		0	1.4	6	0.52	16.744	25.952
0.05	1.4	1	2.606	4.422	26.022		0.05	1.4	6	2.651	17.71	26.185
0.1	1.4	1	4.037	5.175	26.218		0.1	1.4	6	4.03	18.563	26.494
0.15	1.4	1	5.235	5.887	26.414		0.15	1.4	6	5.134	19.333	26.841
0.2	1.4	1	6.412	6.628	26.621		0.2	1.4	6	6.191	20.11	27.2
0.25	1.4	1	7.625	7.446	26.846		0.25	1.4	6	7.276	20.955	27.553
0.3	1.4	1	8.851	8.332	27.095		0.3	1.4	6	8.379	21.873	27.887
0.35	1.4	1	10.026	9.229	27.37		0.35	1.4	6	9.45	22.819	28.197
0.4	1.4	1	11.087	10.048	27.669		0.4	1.4	6	10.433	23.721	28.484
0.45	1.4	1	11.98	10.704	27.99		0.45	1.4	6	11.281	24.503	28.75
0.5	1.4	1	12.671	11.137	28.327		0.5	1.4	6	11.964	25.113	29.002
0.55	1.4	1	13.152	11.324	28.676		0.55	1.4	6	12.472	25.529	29.246
0.6	1.4	1	13.429	11.284	29.027		0.6	1.4	6	12.806	25.763	29.493
0.65	1.4	1	13.523	11.068	29.374		0.65	1.4	6	12.979	25.851	29.75
0.7	1.4	1	13.459	10.742	29.708		0.7	1.4	6	13.006	25.838	30.026
0.75	1.4	1	13.262	10.365	30.02		0.75	1.4	6	12.895	25.761	30.327
0.8	1.4	1	12.949	9.975	30.303		0.8	1.4	6	12.649	25.637	30.655
0.85	1.4	1	12.528	9.586	30.549		0.85	1.4	6	12.261	25.459	31.008
0.9	1.4	1	11.991	9.198	30.754		0.9	1.4	6	11.711	25.219	31.377
0.95	1.4	1	11.318	8.842	30.914		0.95	1.4	6	10.971	24.944	31.749
1	1.4	1	10.469	8.651	31.031		1	1.4	6	10.007	24.774	32.101
0	1.5	1	0.834	3.994	25.81		0	1.5	6	0.901	17.144	25.933
0.05	1.5	1	2.961	4.909	26.012		0.05	1.5	6	3.039	18.223	26.167
0.1	1.5	1	4.412	5.774	26.207		0.1	1.5	6	4.426	19.161	26.49
0.15	1.5	1	5.66	6.597	26.407		0.15	1.5	6	5.557	20.004	26.858
0.2	1.5	1	6.914	7.451	26.622		0.2	1.5	6	6.661	20.849	27.239
0.25	1.5	1	8.214	8.378	26.859		0.25	1.5	6	7.8	21.755	27.61
0.3	1.5	1	9.518	9.356	27.122		0.3	1.5	6	8.947	22.719	27.958

x	T(K)	P(bar)	S(J/molK)	H(J/mol)	V(cm3/mol)	-	x.	T (K)	P (bar)	S (J/molK)	H (J/mol)	V (cm3/mol)
0.35	1.5	1	10.746	10.307	27.412		0.35	1.5	6	10.04	23.683	28.275
0.4	1.5	1	11.821	11.13	27.728		0.4	1.5	6	11.013	24.564	28.558
0.45	1.5	1	12.684	11.732	28.065		0.45	1.5	6	11.817	25.284	28.81
0.5	1.5	1	13.306	12.056	28.416		0.5	1.5	6	12.429	25.795	29.038
0.55	1.5	1	13.689	12.095	28.776		0.55	1.5	6	12.849	26.089	29.251
0.6	1.5	1	13.857	11.893	29.134		0.6	1.5	6	13.098	26.202	29.458
0.65	1.5	1	13.853	11.531	29.482		0.65	1.5	6	13.207	26.196	29.673
0.7	1.5	1	13.721	11.107	29.81		0.7	1.5	6	13.208	26.141	29.908
0.75	1.5	1	13.503	10.704	30.106		0.75	1.5	6	13.121	26.09	30.173
0.8	1.5	1	13.221	10.367	30.363		0.8	1.5	6	12.946	26.056	30.478
0.85	1.5	1	12.872	10.09	30.569		0.85	1.5	6	12.656	26.005	30.83
0.9	1.5	1	12.418	9.822	30.719		0.9	1.5	6	12.19	25.868	31.228
0.95	1.5	1	11.777	9.505	30.806		0.95	1.5	6	11.446	25.576	31.671
1	1.5	1	10.814	9.147	30.829		1	1.5	6	10.277	25.139	32.148
0.05	0.1	2	0.59	6.117	27.243		0.05	0.1	7	0.457	19.366	25.99
0.1	0.1	2	0.758	6.07	27.608		0.1	0.1	7	0.633	19.48	26.29
0.15	0.1	2	0.672	5.984	27.995		0.15	0.1	7	0.529	19.572	26.579
0.2	0.1	2	0.557	5.935	28.388		0.2	0.1	7	0.379	19.706	26.86
0.25	0.1	2	0.525	5.944	28.778		0.25	0.1	7	0.298	19.892	27.14
0.3	0.1	2	0.608	6.005	29.16		0.3	0.1	7	0.323	20.116	27.421
0.35	0.1	2	0.793	6.101	29.534		0.35	0.1	7	0.445	20.358	27.706
0.4	0.1	2	1.038	6.217	29.901		0.4	0.1	7	0.627	20.605	27.995
0.45	0.1	2	1.294	6.342	30.267		0.45	0.1	7	0.827	20.852	28.291
0.5	0.1	2	1.512	6.466	30.636		0.5	0.1	7	1	21.097	28.592
0.55	0.1	2	1.654	6.584	31.013		0.55	0.1	7	1.114	21.341	28.898
0.6	0.1	2	1.701	6.687	31.401		0.6	0.1	7	1.152	21.578	29.206
0.65	0.1	2	1.653	6.768	31.8		0.65	0.1	7	1.113	21.803	29.516
0.7	0.1	2	1.532	6.826	32.207		0.7	0.1	7	1.017	22.016	29.822
0.75	0.1	2	1.385	6.874	32.618		0.75	0.1	7	0.902	22.228	30.121
0.8	0.1	2	1.271	6.943	33.023		0.8	0.1	7	0.816	22.47	30.411
0.85	0.1	2	1.261	7.088	33.41		0.85	0.1	7	0.811	22.794	30.688
0.9	0.1	2	1.41	7.365	33.769		0.9	0.1	7	0.92	23.252	30.953
0.95	0.1	2	1.74	7.787	34.087		0.95	0.1	7	1.138	23.844	31.212
1	0.1	2	2.196	8.229	34.36		1	0.1	7	1.379	24.416	31.476
0.05	0.2	2	0.961	5.644	27.295		0.05	0.2	7	0.97	18.999	26.007
0.1	0.2	2	1.377	5.727	27.657		0.1	0.2	7	1.416	19.237	26.302
0.15	0.2	2	1.55E+00	5.782	28.04		0.15	0.2	7	1.602	19.46	26.59
0.2	0.2	2	1.635	5.853	28.432		0.2	0.2	7	1.702	19.707	26.876
0.25	0.2	2	1.728	5.947	28.825		0.25	0.2	7	1.802	19.978	27.162
0.3	0.2	2	1.856	6.057	29.214		0.3	0.2	7	1.933	20.262	27.45
0.35	0.2	2	2.019	6.173	29.6		0.35	0.2	7	2.098	20.543	27.74
0.4	0.2	2	2.204	6.286	29.981		0.4	0.2	7	2.283	20.817	28.033
0.45	0.2	2	2.39	6.396	30.359		0.45	0.2	7	2.473	21.084	28.328
0.5	0.2	2	2.564	6.505	30.738		0.5	0.2	7	2.653	21.35	28.625
0.55	0.2	2	2.712	6.612	31.118		0.55	0.2	7	2.814	21.619	28.923
0.6	0.2	2	2.833	6.718	31.503		0.6	0.2	7	2.955	21.891	29.221
0.65	0.2	2	2.931	6.816	31.892		0.65	0.2	7	3.081	22.161	29.518
0.7	0.2	2	3.02	6.902	32.285		0.7	0.2	7	3.202	22.422	29.812
0.75	0.2	2	3.119	6.975	32.68		0.75	0.2	7	3.333	22.673	30.103
0.8	0.2	2	3.247	7.047	33.072		0.8	0.2	7	3.485	22.923	30.39
0.85	0.2	2	3.417	7.141	33.46		0.85	0.2	7	3.663	23.195	30.675
0.9	0.2	2	3.617	7.28	33.841		0.9	0.2	7	3.842	23.509	30.961
0.95	0.2	2	3.793	7.446	34.219		0.95	0.2	7	3.958	23.84	31.258
1	0.2	2	3.816	7.504	34.605		1	0.2	7	3.867	24.025	31.581
0	0.3	2	0.011	5.44	26.969		0.05	0.3	7	1.117	18.994	26.008
0.05	0.3	2	1.101	5.626	27.299		0.1	0.3	7	1.763	19.298	26.296
0.1	0.3	2	1.721	5.775	27.653		0.15	0.3	7	2.166	19.596	26.582
0.15	0.3	2	2.102	5.913	28.024		0.2	0.3	7	2.458	19.903	26.868
0.2	0.3	2	2.371	6.051	28.404		0.25	0.3	7	2.7	20.214	27.155
0.25	0.3	2	2.591	6.188	28.789		0.3	0.3	7	2.921	20.517	27.444

x	T(K)	P(bar)	S(J/molK)	H(J/mol)	V(cm3/mol)	-	x.	T (K)	P (bar)	S (J/molK)	H (J/mol)	V (cm3/mol)
0.3	0.3	2	2.788	6.318	29.174		0.35	0.3	7	3.128	20.805	27.735
0.35	0.3	2	2.973	6.433	29.557		0.4	0.3	7	3.324	21.076	28.026
0.4	0.3	2	3.148	6.535	29.939		0.45	0.3	7	3.512	21.338	28.319
0.45	0.3	2	3.317	6.629	30.318		0.5	0.3	7	3.697	21.601	28.611
0.5	0.3	2	3.485	6.724	30.696		0.55	0.3	7	3.886	21.875	28.903
0.55	0.3	2	3.657	6.828	31.074		0.6	0.3	7	4.087	22.165	29.194
0.6	0.3	2	3.841	6.947	31.451		0.65	0.3	7	4.306	22.466	29.484
0.65	0.3	2	4.046	7.076	31.829		0.7	0.3	7	4.546	22.771	29.771
0.7	0.3	2	4.274	7.21	32.207		0.75	0.3	7	4.806	23.07	30.057
0.75	0.3	2	4.524	7.34	32.586		0.8	0.3	7	5.072	23.362	30.342
0.8	0.3	2	4.788	7.463	32.966		0.85	0.3	7	5.315	23.652	30.628
0.85	0.3	2	5.036	7.583	33.35		0.9	0.3	7	5.48	23.942	30.92
0.9	0.3	2	5.216	7.701	33.743		0.95	0.3	7	5.469	24.199	31.228
0.95	0.3	2	5.23	7.787	34.157		1	0.3	7	5.12	24.278	31.565
1	0.3	2	4.91	7.717	34.613		0.05	0.4	7	1.222	19.023	26.009
0	0.4	2	9.36E-03	5.471	26.966		0.1	0.4	7	2.03	19.391	26.293
0.05	0.4	2	1.215	5.654	27.299		0.15	0.4	7	2.609	19.759	26.577
0.1	0.4	2	2.005	5.868	27.647		0.2	0.4	7	3.061	20.125	26.862
0.15	0.4	2	2.57E+00	6.081	28.006		0.25	0.4	7	3.433	20.478	27.149
0.2	0.4	2	3.001	6.284	28.373		0.3	0.4	7	3.748	20.809	27.437
0.25	0.4	2	3.352	6.467	28.745		0.35	0.4	7	4.017	21.114	27.727
0.3	0.4	2	3.644	6.626	29.122		0.4	0.4	7	4.252	21.395	28.018
0.35	0.4	2	3.891	6.759	29.499		0.45	0.4	7	4.466	21.662	28.309
0.4	0.4	2	4.106	6.869	29.877		0.5	0.4	7	4.676	21.929	28.6
0.45	0.4	2	4.305	6.968	30.254		0.55	0.4	7	4.896	22.209	28.891
0.5	0.4	2	4.504	7.069	30.63		0.6	0.4	7	5.139	22.508	29.18
0.55	0.4	2	4.719	7.183	31.005		0.65	0.4	7	5.411	22.825	29.47
0.6	0.4	2	4.964	7.318	31.378		0.7	0.4	7	5.707	23.151	29.758
0.65	0.4	2	5.243	7.475	31.749		0.75	0.4	7	6.015	23.472	30.045
0.7	0.4	2	5.553	7.643	32.119		0.8	0.4	7	6.305	23.779	30.332
0.75	0.4	2	5.879	7.809	32.49		0.85	0.4	7	6.53	24.069	30.62
0.8	0.4	2	6.19	7.961	32.863		0.9	0.4	7	6.621	24.335	30.912
0.85	0.4	2	6.436	8.088	33.245		0.95	0.4	7	6.471	24.551	31.213
0.9	0.4	2	6.539	8.181	33.645		1	0.4	7	5.925	24.605	31.535
0.95	0.4	2	6.383	8.209	34.079		0	0.5	7	8.81E-04	18.648	25.732
1	0.4	2	5.793	8.076	34.575		0.05	0.5	7	1.34	19.05	26.011
0	0.5	2	0.014	5.471	26.965		0.1	0.5	7	2.283	19.491	26.292
0.05	0.5	2	1.329	5.679	27.304		0.15	0.5	7	3.006	19.935	26.574
0.1	0.5	2	2.26	5.965	27.647		0.2	0.5	7	3.596	20.365	26.859
0.15	0.5	2	2.975	6.257	27.996		0.25	0.5	7	4.091	20.773	27.145
0.2	0.5	2	3.554	6.529	28.352		0.3	0.5	7	4.509	21.15	27.433
0.25	0.5	2	4.035	6.771	28.714		0.35	0.5	7	4.863	21.495	27.722
0.3	0.5	2	4.438	6.978	29.081		0.4	0.5	7	5.167	21.811	28.012
0.35	0.5	2	4.777	7.153	29.453		0.45	0.5	7	5.439	22.109	28.304
0.4	0.5	2	5.069	7.301	29.828		0.5	0.5	7	5.698	22.4	28.596
0.45	0.5	2	5.334	7.433	30.204		0.55	0.5	7	5.962	22.699	28.889
0.5	0.5	2	5.594	7.563	30.58		0.6	0.5	7	6.243	23.011	29.183
0.55	0.5	2	5.868	7.704	30.955		0.65	0.5	7	6.545	23.335	29.478
0.6	0.5	2	6.169	7.862	31.328		0.7	0.5	7	6.859	23.662	29.774
0.65	0.5	2	6.499	8.038	31.7		0.75	0.5	7	7.161	23.975	30.069
0.7	0.5	2	6.848	8.221	32.069		0.8	0.5	7	7.414	24.261	30.363
0.75	0.5	2	7.191	8.393	32.439		0.85	0.5	7	7.566	24.51	30.654
0.8	0.5	2	7.484	8.535	32.812		0.9	0.5	7	7.545	24.719	30.943
0.85	0.5	2	7.667	8.627	33.195		0.95	0.5	7	7.256	24.874	31.229
0.9	0.5	2	7.654	8.657	33.599		1	0.5	7	6.57	24.91	31.517
0.95	0.5	2	7.331	8.605	34.043		0	0.6	7	8.45E-03	18.636	25.738
1	0.5	2	6.538	8.411	34.555		0.05	0.6	7	1.449	19.086	26.011
0	0.6	2	0.013	5.46	26.964		0.1	0.6	7	2.5	19.599	26.288
0.05	0.6	2	1.426	5.712	27.308		0.15	0.6	7	3.336	20.112	26.569
0.1	0.6	2	2.469	6.071	27.649		0.2	0.6	7	4.04	20.606	26.853

x	T(K)	P(bar)	S(J/molK)	H(J/mol)	V(cm3/mol)	-	x.	T (K)	P (bar)	S (J/molK)	H (J/mol)	V (cm3/mol)
0.15	0.6	2	3.302	6.437	27.991		0.25	0.6	7	4.648	21.074	27.139
0.2	0.6	2	4.002	6.776	28.339		0.3	0.6	7	5.174	21.51	27.426
0.25	0.6	2	4.604	7.081	28.693		0.35	0.6	7	5.629	21.915	27.715
0.3	0.6	2	5.123	7.35	29.054		0.4	0.6	7	6.025	22.29	28.006
0.35	0.6	2	5.571	7.587	29.422		0.45	0.6	7	6.379	22.642	28.298
0.4	0.6	2	5.964	7.796	29.796		0.5	0.6	7	6.708	22.98	28.593
0.45	0.6	2	6.32	7.986	30.173		0.55	0.6	7	7.029	23.314	28.891
0.5	0.6	2	6.66	8.166	30.552		0.6	0.6	7	7.351	23.648	29.193
0.55	0.6	2	7.002	8.348	30.931		0.65	0.6	7	7.672	23.978	29.497
0.6	0.6	2	7.355	8.536	31.31		0.7	0.6	7	7.977	24.295	29.804
0.65	0.6	2	7.717	8.727	31.687		0.75	0.6	7	8.24	24.581	30.111
0.7	0.6	2	8.073	8.91	32.062		0.8	0.6	7	8.42	24.818	30.415
0.75	0.6	2	8.39	9.064	32.437		0.85	0.6	7	8.467	24.997	30.712
0.8	0.6	2	8.621	9.163	32.815		0.9	0.6	7	8.318	25.119	30.997
0.85	0.6	2	8.702	9.188	33.201		0.95	0.6	7	7.9	25.192	31.264
0.9	0.6	2	8.555	9.126	33.608		1	0.6	7	7.124	25.206	31.509
0.95	0.6	2	8.079	8.974	34.053		0.05	0.7	7	1.532	19.132	26.007
1	0.6	2	7.149	8.722	34.562		0.1	0.7	7	2.663	19.704	26.282
0	0.7	2	4.35E-03	5.453	26.962		0.15	0.7	7	3.579	20.273	26.563
0.05	0.7	2	1.505	5.757	27.311		0.2	0.7	7	4.371	20.819	26.846
0.1	0.7	2	2.626	6.179	27.65		0.25	0.7	7	5.076	21.341	27.132
0.15	0.7	2	3.54E+00	6.604	27.988		0.3	0.7	7	5.706	21.841	27.418
0.2	0.7	2	4.338	7	28.33		0.35	0.7	7	6.268	22.317	27.706
0.25	0.7	2	5.045	7.364	28.68		0.4	0.7	7	6.769	22.766	27.997
0.3	0.7	2	5.675	7.7	29.038		0.45	0.7	7	7.22	23.19	28.29
0.35	0.7	2	6.237	8.009	29.404		0.5	0.7	7	7.634	23.592	28.588
0.4	0.7	2	6.741	8.295	29.779		0.55	0.7	7	8.02	23.973	28.891
0.45	0.7	2	7.2	8.558	30.159		0.6	0.7	7	8.383	24.337	29.2
0.5	0.7	2	7.629	8.803	30.544		0.65	0.7	7	8.716	24.676	29.515
0.55	0.7	2	8.041	9.035	30.931		0.7	0.7	7	9	24.978	29.834
0.6	0.7	2	8.44	9.255	31.318		0.75	0.7	7	9.206	25.226	30.153
0.65	0.7	2	8.818	9.458	31.705		0.8	0.7	7	9.296	25.402	30.469
0.7	0.7	2	9.157	9.63	32.09		0.85	0.7	7	9.225	25.496	30.772
0.75	0.7	2	9.421	9.749	32.474		0.9	0.7	7	8.948	25.521	31.054
0.8	0.7	2	9.564	9.79	32.859		0.95	0.7	7	8.42	25.508	31.302
0.85	0.7	2	9.528	9.731	33.251		1	0.7	7	7.6	25.504	31.504
0.9	0.7	2	9.247	9.568	33.657		0.05	0.8	7	1.604	19.188	26.004
0.95	0.7	2	8.646	9.319	34.094		0.1	0.8	7	2.786	19.807	26.276
1	0.7	2	7.642	9.029	34.585		0.15	0.8	7	3.751	20.411	26.557
0	0.8	2	3.03E-03	5.456	26.959		0.2	0.8	7	4.604	20.994	26.841
0.05	0.8	2	1.581	5.816	27.31		0.25	0.8	7	5.386	21.563	27.127
0.1	0.8	2	2.754	6.288	27.649		0.3	0.8	7	6.11	22.124	27.413
0.15	0.8	2	3.72E+00	6.756	27.985		0.35	0.8	7	6.775	22.673	27.7
0.2	0.8	2	4.586	7.194	28.325		0.4	0.8	7	7.383	23.204	27.989
0.25	0.8	2	5.378	7.61	28.673		0.45	0.8	7	7.936	23.709	28.282
0.3	0.8	2	6.109	8.01	29.031		0.5	0.8	7	8.438	24.182	28.581
0.35	0.8	2	6.781	8.397	29.398		0.55	0.8	7	8.892	24.618	28.887
0.4	0.8	2	7.396	8.766	29.776		0.6	0.8	7	9.295	25.014	29.202
0.45	0.8	2	7.959	9.11	30.162		0.65	0.8	7	9.635	25.361	29.525
0.5	0.8	2	8.477	9.426	30.554		0.7	0.8	7	9.891	25.647	29.854
0.55	0.8	2	8.954	9.709	30.95		0.75	0.8	7	10.034	25.853	30.185
0.6	0.8	2	9.39	9.958	31.349		0.8	0.8	7	10.03	25.963	30.511
0.65	0.8	2	9.771	10.165	31.748		0.85	0.8	7	9.845	25.974	30.822
0.7	0.8	2	10.077	10.316	32.145		0.9	0.8	7	9.453	25.905	31.102
0.75	0.8	2	10.274	10.39	32.54		0.95	0.8	7	8.84	25.816	31.335
0.8	0.8	2	10.319	10.364	32.934		1	0.8	7	8.012	25.811	31.498
0.85	0.8	2	10.166	10.221	33.33		0	0.9	7	2.03E-03	18.652	25.752
0.9	0.8	2	9.767	9.965	33.733		0.05	0.9	7	1.695	19.266	26.002
0.95	0.8	2	9.078	9.643	34.155		0.1	0.9	7	2.906	19.921	26.273
1	0.8	2	8.059	9.353	34.615		0.15	0.9	7	3.893	20.549	26.555

x	T(K)	P(bar)	S(J/molK)	H(J/mol)	V(cm3/mol)	-	x.	T (K)	P (bar)	S (J/molK)	H (J/mol)	V (cm3/mol)
0	0.9	2	0.026	5.474	26.959		0.2	0.9	7	4.782	21.156	26.841
0.05	0.9	2	1.678	5.895	27.308		0.25	0.9	7	5.623	21.764	27.128
0.1	0.9	2	2.883	6.409	27.647		0.3	0.9	7	6.426	22.383	27.414
0.15	0.9	2	3.882	6.907	27.984		0.35	0.9	7	7.186	23.006	27.7
0.2	0.9	2	4.79	7.38	28.324		0.4	0.9	7	7.895	23.621	27.987
0.25	0.9	2	5.65	7.843	28.674		0.45	0.9	7	8.545	24.209	28.278
0.3	0.9	2	6.47	8.309	29.034		0.5	0.9	7	9.131	24.753	28.575
0.35	0.9	2	7.243	8.775	29.406		0.55	0.9	7	9.647	25.242	28.881
0.4	0.9	2	7.963	9.23	29.789		0.6	0.9	7	10.084	25.666	29.197
0.45	0.9	2	8.622	9.656	30.182		0.65	0.9	7	10.427	26.017	29.524
0.5	0.9	2	9.22	10.038	30.583		0.7	0.9	7	10.652	26.28	29.86
0.55	0.9	2	9.753	10.366	30.99		0.75	0.9	7	10.734	26.442	30.199
0.6	0.9	2	10.212	10.633	31.401		0.8	0.9	7	10.643	26.489	30.534
0.65	0.9	2	10.584	10.831	31.813		0.85	0.9	7	10.359	26.422	30.852
0.7	0.9	2	10.847	10.948	32.223		0.9	0.9	7	9.873	26.272	31.134
0.75	0.9	2	10.971	10.968	32.63		0.95	0.9	7	9.2	26.124	31.358
0.8	0.9	2	10.921	10.872	33.032		1	0.9	7	8.388	26.136	31.495
0.85	0.9	2	10.665	10.652	33.431		0	1	7	0.058	18.694	25.756
0.9	0.9	2	10.174	10.323	33.828		0.05	1	7	1.827	19.377	25.999
0.95	0.9	2	9.435	9.958	34.23		0.1	1	7	3.056	20.067	26.271
1	0.9	2	8.451	9.707	34.649		0.15	1	7	4.05	20.714	26.557
0	1	2	0.078	5.513	26.96		0.2	1	7	4.959	21.344	26.848
0.05	1	2	1.808	6.004	27.306		0.25	1	7	5.844	21.99	27.138
0.1	1	2	3.04	6.56	27.645		0.3	1	7	6.714	22.667	27.425
0.15	1	2	4.058	7.088	27.984		0.35	1	7	7.557	23.366	27.71
0.2	1	2	5	7.594	28.329		0.4	1	7	8.355	24.064	27.994
0.25	1	2	5.917	8.109	28.683		0.45	1	7	9.09	24.731	28.28
0.3	1	2	6.815	8.645	29.05		0.5	1	7	9.748	25.34	28.572
0.35	1	2	7.679	9.195	29.429		0.55	1	7	10.315	25.872	28.873
0.4	1	2	8.491	9.737	29.82		0.6	1	7	10.776	26.314	29.186
0.45	1	2	9.234	10.241	30.222		0.65	1	7	11.114	26.656	29.511
0.5	1	2	9.896	10.681	30.634		0.7	1	7	11.308	26.89	29.847
0.55	1	2	10.467	11.039	31.053		0.75	1	7	11.334	27.005	30.19
0.6	1	2	10.935	11.305	31.476		0.8	1	7	11.172	26.993	30.531
0.65	1	2	11.284	11.475	31.901		0.85	1	7	10.81	26.86	30.855
0.7	1	2	11.496	11.542	32.323		0.9	1	7	10.255	26.645	31.143
0.75	1	2	11.547	11.498	32.741		0.95	1	7	9.544	26.453	31.369
0.8	1	2	11.413	11.332	33.151		1	1	7	8.753	26.484	31.5
0.85	1	2	11.075	11.044	33.55		0	1.1	7	0.151	18.762	25.755
0.9	1	2	10.524	10.663	33.938		0.05	1.1	7	2.003	19.525	25.994
0.95	1	2	9.772	10.283	34.316		0.1	1.1	7	3.251	20.255	26.269
1	1	2	8.854	10.101	34.691		0.15	1.1	7	4.249	20.927	26.562
0	1.1	2	0.148	5.574	26.962		0.2	1.1	7	5.175	21.584	26.86
0.05	1.1	2	1.971	6.146	27.303		0.25	1.1	7	6.098	22.275	27.155
0.1	1.1	2	3.235	6.751	27.642		0.3	1.1	7	7.026	23.015	27.446
0.15	1.1	2	4.273	7.316	27.987		0.35	1.1	7	7.94	23.792	27.73
0.2	1.1	2	5.249	7.868	28.339		0.4	1.1	7	8.813	24.57	28.01
0.25	1.1	2	6.221	8.444	28.703		0.45	1.1	7	9.616	25.309	28.289
0.3	1.1	2	7.192	9.06	29.08		0.5	1.1	7	10.326	25.971	28.572
0.35	1.1	2	8.137	9.701	29.469		0.55	1.1	7	10.926	26.531	28.863
0.4	1.1	2	9.028	10.329	29.872		0.6	1.1	7	11.397	26.974	29.166
0.45	1.1	2	9.837	10.903	30.286		0.65	1.1	7	11.722	27.294	29.482
0.5	1.1	2	10.543	11.386	30.71		0.7	1.1	7	11.884	27.49	29.812
0.55	1.1	2	11.13	11.754	31.141		0.75	1.1	7	11.864	27.556	30.152
0.6	1.1	2	11.586	11.997	31.576		0.8	1.1	7	11.648	27.492	30.494
0.65	1.1	2	11.897	12.116	32.013		0.85	1.1	7	11.233	27.307	30.825
0.7	1.1	2	12.051	12.115	32.447		0.9	1.1	7	10.634	27.044	31.124
0.75	1.1	2	12.032	11.997	32.874		0.95	1.1	7	9.9	26.816	31.366
0.8	1.1	2	11.827	11.762	33.288		1	1.1	7	9.114	26.85	31.514
0.85	1.1	2	11.432	11.419	33.686		0	1.2	7	0.258	18.864	25.747

x	T(K)	P(bar)	S(J/molK)	H(J/mol)	V(cm3/mol)	-	x.	T (K)	P (bar)	S (J/molK)	H (J/mol)	V (cm3/mol)
0.9	1.1	2	10.851	11.008	34.063		0.05	1.2	7	2.205	19.713	25.983
0.95	1.1	2	10.113	10.634	34.416		0.1	1.2	7	3.483	20.49	26.264
1	1.1	2	9.272	10.525	34.745		0.15	1.2	7	4.496	21.193	26.567
0	1.2	2	0.224	5.665	26.963		0.2	1.2	7	5.446	21.887	26.875
0.05	1.2	2	2.154	6.325	27.298		0.25	1.2	7	6.409	22.63	27.18
0.1	1.2	2	3.465	6.986	27.641		0.3	1.2	7	7.392	23.44	27.475
0.15	1.2	2	4.538	7.601	27.993		0.35	1.2	7	8.368	24.294	27.759
0.2	1.2	2	5.559	8.212	28.358		0.4	1.2	7	9.299	25.146	28.035
0.25	1.2	2	6.592	8.866	28.735		0.45	1.2	7	10.149	25.944	28.305
0.3	1.2	2	7.635	9.573	29.127		0.5	1.2	7	10.889	26.641	28.575
0.35	1.2	2	8.654	10.308	29.531		0.55	1.2	7	11.498	27.207	28.849
0.4	1.2	2	9.608	11.019	29.948		0.6	1.2	7	11.959	27.632	29.134
0.45	1.2	2	10.461	11.651	30.376		0.65	1.2	7	12.261	27.915	29.434
0.5	1.2	2	11.185	12.157	30.814		0.7	1.2	7	12.389	28.066	29.749
0.55	1.2	2	11.761	12.508	31.258		0.75	1.2	7	12.333	28.089	30.078
0.6	1.2	2	12.181	12.701	31.706		0.8	1.2	7	12.085	27.988	30.416
0.65	1.2	2	12.436	12.746	32.153		0.85	1.2	7	11.644	27.773	30.753
0.7	1.2	2	12.524	12.661	32.596		0.9	1.2	7	11.026	27.481	31.07
0.75	1.2	2	12.439	12.464	33.03		0.95	1.2	7	10.27	27.219	31.343
0.8	1.2	2	12.18	12.168	33.446		1	1.2	7	9.452	27.217	31.539
0.85	1.2	2	11.752	11.79	33.84		0	1.3	7	0.37	19.039	25.734
0.9	1.2	2	11.168	11.369	34.204		0.05	1.3	7	2.418	19.971	25.969
0.95	1.2	2	10.458	11.014	34.531		0.1	1.3	7	3.74	20.795	26.259
1	1.2	2	9.675	10.958	34.815		0.15	1.3	7	4.784	21.535	26.575
0	1.3	2	0.314	5.822	26.964		0.2	1.3	7	5.772	22.273	26.896
0.05	1.3	2	2.357	6.568	27.294		0.25	1.3	7	6.784	23.073	27.212
0.1	1.3	2	3.729	7.292	27.643		0.3	1.3	7	7.823	23.95	27.513
0.15	1.3	2	4.855	7.967	28.008		0.35	1.3	7	8.851	24.874	27.799
0.2	1.3	2	5.937	8.651	28.389		0.4	1.3	7	9.823	25.785	28.069
0.25	1.3	2	7.042	9.392	28.786		0.45	1.3	7	10.694	26.619	28.327
0.3	1.3	2	8.16	10.196	29.197		0.5	1.3	7	11.436	27.323	28.579
0.35	1.3	2	9.245	11.021	29.62		0.55	1.3	7	12.026	27.869	28.831
0.4	1.3	2	10.246	11.803	30.056		0.6	1.3	7	12.456	28.253	29.09
0.45	1.3	2	11.118	12.469	30.501		0.65	1.3	7	12.72	28.487	29.362
0.5	1.3	2	11.83	12.967	30.954		0.7	1.3	7	12.816	28.592	29.652
0.55	1.3	2	12.366	13.27	31.411		0.75	1.3	7	12.738	28.587	29.962
0.6	1.3	2	12.722	13.382	31.87		0.8	1.3	7	12.482	28.478	30.291
0.65	1.3	2	12.903	13.33	32.327		0.85	1.3	7	12.045	28.268	30.631
0.7	1.3	2	12.917	13.151	32.777		0.9	1.3	7	11.43	27.976	30.972
0.75	1.3	2	12.772	12.881	33.212		0.95	1.3	7	10.65	27.679	31.294
0.8	1.3	2	12.478	12.546	33.628		1	1.3	7	9.738	27.574	31.57
0.85	1.3	2	12.043	12.164	34.014		0	1.4	7	0.536	19.353	25.72
0.9	1.3	2	11.478	11.766	34.363		0.05	1.4	7	2.667	20.363	25.956
0.95	1.3	2	10.798	11.436	34.663		0.1	1.4	7	4.034	21.236	26.257
1	1.3	2	10.029	11.386	34.906		0.15	1.4	7	5.119	22.017	26.588
0	1.4	2	0.478	6.107	26.962		0.2	1.4	7	6.156	22.801	26.926
0.05	1.4	2	2.61	6.939	27.292		0.25	1.4	7	7.225	23.656	27.255
0.1	1.4	2	4.04	7.733	27.652		0.3	1.4	7	8.317	24.591	27.565
0.15	1.4	2	5.227	8.479	28.036		0.35	1.4	7	9.386	25.563	27.851
0.2	1.4	2	6.383	9.245	28.44		0.4	1.4	7	10.376	26.502	28.115
0.25	1.4	2	7.57	10.078	28.861		0.45	1.4	7	11.241	27.335	28.358
0.3	1.4	2	8.763	10.972	29.297		0.5	1.4	7	11.951	28.007	28.587
0.35	1.4	2	9.906	11.872	29.745		0.55	1.4	7	12.493	28.496	28.809
0.4	1.4	2	10.935	12.693	30.203		0.6	1.4	7	12.868	28.811	29.033
0.45	1.4	2	11.799	13.356	30.668		0.65	1.4	7	13.084	28.983	29.268
0.5	1.4	2	12.468	13.802	31.138		0.7	1.4	7	13.15	29.052	29.522
0.55	1.4	2	12.931	14.014	31.61		0.75	1.4	7	13.07	29.046	29.802
0.6	1.4	2	13.198	14.009	32.079		0.8	1.4	7	12.841	28.975	30.114
0.65	1.4	2	13.287	13.838	32.542		0.85	1.4	7	12.448	28.823	30.456
0.7	1.4	2	13.225	13.563	32.994		0.9	1.4	7	11.863	28.572	30.827

x	T(K)	P(bar)	S(J/molK)	H(J/mol)	V(cm3/mol)	-	x.	T (K)	P (bar)	S (J/molK)	H (J/mol)	V (cm3/mol)
0.75	1.4	2	13.035	13.241	33.428		0.95	1.4	7	11.051	28.236	31.216
0.8	1.4	2	12.732	12.907	33.837		1	1.4	7	9.971	27.939	31.607
0.85	1.4	2	12.324	12.572	34.211		0	1.5	7	0.917	19.76	25.701
0.9	1.4	2	11.803	12.239	34.54		0.05	1.5	7	3.059	20.88	25.94
0.95	1.4	2	11.15	11.942	34.813		0.1	1.5	7	4.434	21.833	26.254
1	1.4	2	10.33	11.826	35.017		0.15	1.5	7	5.545	22.68	26.603
0	1.5	2	0.839	6.48	26.941		0.2	1.5	7	6.626	23.526	26.96
0.05	1.5	2	2.977	7.439	27.28		0.25	1.5	7	7.744	24.436	27.304
0.1	1.5	2	4.424	8.34	27.659		0.3	1.5	7	8.877	25.412	27.625
0.15	1.5	2	5.655	9.189	28.07		0.35	1.5	7	9.965	26.401	27.914
0.2	1.5	2	6.879	10.058	28.505		0.4	1.5	7	10.944	27.321	28.17
0.25	1.5	2	8.143	10.988	28.959		0.45	1.5	7	11.767	28.098	28.396
0.3	1.5	2	9.406	11.96	29.428		0.5	1.5	7	12.41	28.681	28.598
0.35	1.5	2	10.591	12.9	29.907		0.55	1.5	7	12.872	29.062	28.783
0.4	1.5	2	11.625	13.714	30.393		0.6	1.5	7	13.171	29.272	28.963
0.45	1.5	2	12.453	14.313	30.883		0.65	1.5	7	13.335	29.367	29.15
0.5	1.5	2	13.047	14.645	31.373		0.7	1.5	7	13.387	29.411	29.357
0.55	1.5	2	13.41	14.705	31.859		0.75	1.5	7	13.342	29.445	29.597
0.6	1.5	2	13.568	14.538	32.338		0.8	1.5	7	13.192	29.473	29.882
0.65	1.5	2	13.563	14.225	32.805		0.85	1.5	7	12.9	29.448	30.224
0.7	1.5	2	13.439	13.858	33.254		0.9	1.5	7	12.392	29.286	30.63
0.75	1.5	2	13.234	13.516	33.68		0.95	1.5	7	11.556	28.904	31.104
0.8	1.5	2	12.97	13.241	34.074		1	1.5	7	10.234	28.289	31.646
0.85	1.5	2	12.643	13.023	34.428		0.05	0.1	8	0.455	21.877	25.851
0.9	1.5	2	12.21	12.812	34.732		0.1	0.1	8	0.633	22.021	26.14
0.95	1.5	2	11.592	12.555	34.973		0.15	0.1	8	0.526	22.148	26.415
1	1.5	2	10.655	12.27	35.14		0.2	0.1	8	0.369	22.32	26.682
0.05	0.1	3	0.549	8.813	27.004		0.25	0.1	8	0.279	22.541	26.946
0.1	0.1	3	0.722	8.803	27.353		0.3	0.1	8	0.294	22.796	27.21
0.15	0.1	3	0.637	8.753	27.714		0.35	0.1	8	0.405	23.065	27.477
0.2	0.1	3	0.519	8.742	28.078		0.4	0.1	8	0.579	23.336	27.749
0.25	0.1	3	0.479	8.787	28.44		0.45	0.1	8	0.771	23.606	28.026
0.3	0.1	3	0.551	8.882	28.798		0.5	0.1	8	0.939	23.873	28.308
0.35	0.1	3	0.721	9.01	29.152		0.55	0.1	8	1.051	24.139	28.595
0.4	0.1	3	0.95	9.155	29.505		0.6	0.1	8	1.088	24.399	28.885
0.45	0.1	3	1.19	9.307	29.858		0.65	0.1	8	1.052	24.648	29.175
0.5	0.1	3	1.395	9.46	30.216		0.7	0.1	8	0.962	24.884	29.462
0.55	0.1	3	1.528	9.608	30.58		0.75	0.1	8	0.852	25.118	29.742
0.6	0.1	3	1.57	9.743	30.952		0.8	0.1	8	0.771	25.381	30.014
0.65	0.1	3	1.522	9.859	31.331		0.85	0.1	8	0.764	25.725	30.273
0.7	0.1	3	1.406	9.955	31.715		0.9	0.1	8	0.863	26.201	30.521
0.75	0.1	3	1.267	10.042	32.098		0.95	0.1	8	1.054	26.811	30.761
0.8	0.1	3	1.161	10.154	32.473		1	0.1	8	1.244	27.395	31.005
0.85	0.1	3	1.154	10.342	32.833		0.05	0.2	8	0.994	21.56	25.858
0.9	0.1	3	1.299	10.665	33.171		0.1	0.2	8	1.443	21.824	26.139
0.95	0.1	3	1.609	11.133	33.484		0.15	0.2	8	1.629	22.078	26.413
1	0.1	3	2.022	11.619	33.773		0.2	0.2	8	1.728	22.357	26.684
0.05	0.2	3	0.948	8.341	27.047		0.25	0.2	8	1.825	22.661	26.953
0.1	0.2	3	1.375	8.458	27.394		0.3	0.2	8	1.955	22.974	27.223
0.15	0.2	3	1.553	8.551	27.753		0.35	0.2	8	2.117	23.284	27.495
0.2	0.2	3	1.65	8.659	28.117		0.4	0.2	8	2.301	23.584	27.768
0.25	0.2	3	1.749	8.792	28.483		0.45	0.2	8	2.49	23.878	28.043
0.3	0.2	3	1.881	8.941	28.849		0.5	0.2	8	2.67	24.171	28.32
0.35	0.2	3	2.045	9.094	29.213		0.55	0.2	8	2.833	24.468	28.598
0.4	0.2	3	2.23	9.244	29.575		0.6	0.2	8	2.976	24.768	28.876
0.45	0.2	3	2.417	9.391	29.938		0.65	0.2	8	3.105	25.065	29.153
0.5	0.2	3	2.591	9.536	30.3		0.7	0.2	8	3.23	25.353	29.428
0.55	0.2	3	2.741	9.682	30.665		0.75	0.2	8	3.366	25.629	29.701
0.6	0.2	3	2.866	9.827	31.032		0.8	0.2	8	3.523	25.904	29.971
0.65	0.2	3	2.971	9.966	31.4		0.85	0.2	8	3.703	26.2	30.239

x	T(K)	P(bar)	S(J/molK)	H(J/mol)	V(cm3/mol)	-	x.	T (K)	P (bar)	S (J/molK)	H (J/mol)	V (cm3/mol)
0.7	0.2	3	3.068	10.093	31.77		0.9	0.2	8	3.88	26.539	30.51
0.75	0.2	3	3.175	10.208	32.138		0.95	0.2	8	3.986	26.894	30.79
0.8	0.2	3	3.31	10.321	32.504		1	0.2	8	3.875	27.1	31.094
0.85	0.2	3	3.482	10.456	32.865		0	0.3	8	1.27E-03	21.183	25.57
0.9	0.2	3	3.677	10.635	33.224		0.05	0.3	8	1.139	21.565	25.851
0.95	0.2	3	3.838	10.841	33.587		0.1	0.3	8	1.786	21.894	26.126
1	0.2	3	3.832	10.936	33.97		0.15	0.3	8	2.19	22.22	26.398
0.05	0.3	3	1.091	8.321	27.052		0.2	0.3	8	2.48	22.556	26.669
0.1	0.3	3	1.72	8.504	27.392		0.25	0.3	8	2.722	22.897	26.94
0.15	0.3	3	2.111	8.678	27.742		0.3	0.3	8	2.943	23.229	27.212
0.2	0.3	3	2.391	8.855	28.098		0.35	0.3	8	3.15	23.544	27.484
0.25	0.3	3	2.621	9.032	28.458		0.4	0.3	8	3.346	23.843	27.757
0.3	0.3	3	2.83E+00	9.201	28.82		0.45	0.3	8	3.534	24.132	28.03
0.35	0.3	3	3.019	9.356	29.182		0.5	0.3	8	3.719	24.422	28.302
0.4	0.3	3	3.201	9.497	29.544		0.55	0.3	8	3.907	24.724	28.574
0.45	0.3	3	3.375	9.631	29.906		0.6	0.3	8	4.106	25.041	28.846
0.5	0.3	3	3.548	9.765	30.267		0.65	0.3	8	4.324	25.369	29.116
0.55	0.3	3	3.725	9.91	30.627		0.7	0.3	8	4.564	25.699	29.385
0.6	0.3	3	3.914	10.069	30.986		0.75	0.3	8	4.824	26.023	29.654
0.65	0.3	3	4.124	10.239	31.344		0.8	0.3	8	5.091	26.339	29.923
0.7	0.3	3	4.356	10.414	31.701		0.85	0.3	8	5.336	26.653	30.193
0.75	0.3	3	4.611	10.584	32.057		0.9	0.3	8	5.503	26.97	30.471
0.8	0.3	3	4.876	10.746	32.412		0.95	0.3	8	5.494	27.256	30.761
0.85	0.3	3	5.123	10.905	32.771		1	0.3	8	5.147	27.364	31.077
0.9	0.3	3	5.297	11.061	33.139		0.05	0.4	8	1.239	21.596	25.846
0.95	0.3	3	5.299	11.186	33.529		0.1	0.4	8	2.048	21.99	26.117
1	0.3	3	4.962	11.153	33.963		0.15	0.4	8	2.626	22.385	26.388
0.05	0.4	3	1.204	8.348	27.056		0.2	0.4	8	3.076	22.778	26.659
0.1	0.4	3	2.002	8.595	27.389		0.25	0.4	8	3.447	23.159	26.93
0.15	0.4	3	2.573	8.844	27.73		0.3	0.4	8	3.762	23.518	27.203
0.2	0.4	3	3.016	9.084	28.076		0.35	0.4	8	4.031	23.85	27.475
0.25	0.4	3	3.376	9.308	28.427		0.4	0.4	8	4.265	24.158	27.748
0.3	0.4	3	3.677	9.507	28.783		0.45	0.4	8	4.478	24.452	28.021
0.35	0.4	3	3.93E+00	9.68	29.14		0.5	0.4	8	4.684	24.745	28.293
0.4	0.4	3	4.153	9.83	29.499		0.55	0.4	8	4.9	25.051	28.565
0.45	0.4	3	4.357	9.969	29.858		0.6	0.4	8	5.138	25.376	28.836
0.5	0.4	3	4.56	10.108	30.217		0.65	0.4	8	5.403	25.716	29.108
0.55	0.4	3	4.779	10.262	30.574		0.7	0.4	8	5.694	26.064	29.379
0.6	0.4	3	5.025	10.437	30.929		0.75	0.4	8	5.997	26.407	29.65
0.65	0.4	3	5.306	10.631	31.282		0.8	0.4	8	6.283	26.736	29.922
0.7	0.4	3	5.616	10.838	31.633		0.85	0.4	8	6.508	27.048	30.195
0.75	0.4	3	5.94	11.041	31.983		0.9	0.4	8	6.602	27.343	30.471
0.8	0.4	3	6.248	11.23	32.335		0.95	0.4	8	6.463	27.591	30.754
0.85	0.4	3	6.488	11.394	32.692		1	0.4	8	5.936	27.681	31.052
0.9	0.4	3	6.584	11.525	33.065		0	0.5	8	0.013	21.195	25.576
0.95	0.4	3	6.422	11.595	33.467		0.05	0.5	8	1.357	21.627	25.842
1	0.4	3	5.829	11.507	33.923		0.1	0.5	8	2.3	22.094	26.111
0	0.5	3	1.46E-03	8.123	26.734		0.15	0.5	8	3.021	22.564	26.38
0.05	0.5	3	1.319	8.37	27.062		0.2	0.5	8	3.609	23.021	26.651
0.1	0.5	3	2.256	8.69	27.391		0.25	0.5	8	4.103	23.455	26.923
0.15	0.5	3	2.977	9.017	27.723		0.3	0.5	8	4.52	23.86	27.195
0.2	0.5	3	3.563	9.327	28.062		0.35	0.5	8	4.873	24.232	27.468
0.25	0.5	3	4.052	9.608	28.406		0.4	0.5	8	5.175	24.575	27.742
0.3	0.5	3	4.461	9.856	28.755		0.45	0.5	8	5.444	24.898	28.016
0.35	0.5	3	4.81E+00	10.071	29.109		0.5	0.5	8	5.698	25.216	28.291
0.4	0.5	3	5.102	10.258	29.465		0.55	0.5	8	5.955	25.538	28.567
0.45	0.5	3	5.371	10.428	29.823		0.6	0.5	8	6.228	25.874	28.845
0.5	0.5	3	5.632	10.596	30.182		0.65	0.5	8	6.52	26.219	29.124
0.55	0.5	3	5.906	10.773	30.54		0.7	0.5	8	6.823	26.565	29.404
0.6	0.5	3	6.205	10.968	30.896		0.75	0.5	8	7.116	26.897	29.684

x	T(K)	P(bar)	S(J/molK)	H(J/mol)	V(cm3/mol)	-	x.	T (K)	P (bar)	S (J/molK)	H (J/mol)	V (cm3/mol)
0.65	0.5	3	6.532	11.18	31.251		0.8	0.5	8	7.363	27.203	29.963
0.7	0.5	3	6.877	11.398	31.603		0.85	0.5	8	7.512	27.475	30.239
0.75	0.5	3	7.213	11.605	31.955		0.9	0.5	8	7.496	27.712	30.511
0.8	0.5	3	7.498	11.781	32.309		0.95	0.5	8	7.222	27.903	30.777
0.85	0.5	3	7.673	11.909	32.668		1	0.5	8	6.565	27.981	31.039
0.9	0.5	3	7.655	11.979	33.043		0	0.6	8	0.021	21.186	25.575
0.95	0.5	3	7.331	11.973	33.447		0.05	0.6	8	1.467	21.668	25.836
1	0.5	3	6.548	11.834	33.903		0.1	0.6	8	2.519	22.206	26.102
0	0.6	3	2.93E-03	8.11	26.737		0.15	0.6	8	3.353	22.744	26.371
0.05	0.6	3	1.42	8.4	27.066		0.2	0.6	8	4.055	23.264	26.641
0.1	0.6	3	2.466	8.793	27.392		0.25	0.6	8	4.661	23.758	26.913
0.15	0.6	3	3.303	9.194	27.72		0.3	0.6	8	5.187	24.222	27.185
0.2	0.6	3	4.009	9.571	28.053		0.35	0.6	8	5.64	24.654	27.458
0.25	0.6	3	4.616	9.914	28.392		0.4	0.6	8	6.034	25.056	27.733
0.3	0.6	3	5.139	10.224	28.738		0.45	0.6	8	6.384	25.434	28.009
0.35	0.6	3	5.59E+00	10.5	29.089		0.5	0.6	8	6.708	25.797	28.289
0.4	0.6	3	5.984	10.747	29.445		0.55	0.6	8	7.021	26.155	28.571
0.45	0.6	3	6.34	10.973	29.804		0.6	0.6	8	7.333	26.51	28.858
0.5	0.6	3	6.679	11.189	30.165		0.65	0.6	8	7.642	26.861	29.148
0.55	0.6	3	7.018	11.406	30.528		0.7	0.6	8	7.935	27.196	29.44
0.6	0.6	3	7.366	11.628	30.89		0.75	0.6	8	8.187	27.499	29.733
0.65	0.6	3	7.721	11.852	31.251		0.8	0.6	8	8.359	27.756	30.023
0.7	0.6	3	8.068	12.068	31.612		0.85	0.6	8	8.402	27.957	30.304
0.75	0.6	3	8.375	12.253	31.971		0.9	0.6	8	8.257	28.109	30.571
0.8	0.6	3	8.596	12.386	32.331		0.95	0.6	8	7.856	28.22	30.817
0.85	0.6	3	8.669	12.446	32.695		1	0.6	8	7.116	28.277	31.033
0.9	0.6	3	8.519	12.426	33.07		0	0.7	8	0.01	21.181	25.574
0.95	0.6	3	8.049	12.325	33.467		0.05	0.7	8	1.551	21.716	25.829
1	0.6	3	7.141	12.137	33.907		0.1	0.7	8	2.682	22.313	26.093
0.05	0.7	3	1.5	8.443	27.066		0.15	0.7	8	3.596	22.905	26.36
0.1	0.7	3	2.625	8.898	27.39		0.2	0.7	8	4.387	23.476	26.63
0.15	0.7	3	3.545	9.359	27.716		0.25	0.7	8	5.09	24.024	26.9
0.2	0.7	3	4.343	9.792	28.047		0.3	0.7	8	5.719	24.551	27.171
0.25	0.7	3	5.052	10.194	28.384		0.35	0.7	8	6.28	25.054	27.444
0.3	0.7	3	5.683	10.569	28.729		0.4	0.7	8	6.779	25.531	27.719
0.35	0.7	3	6.246	10.917	29.08		0.45	0.7	8	7.228	25.982	27.997
0.4	0.7	3	6.75E+00	11.239	29.437		0.5	0.7	8	7.637	26.409	28.281
0.45	0.7	3	7.205	11.537	29.799		0.55	0.7	8	8.016	26.815	28.57
0.5	0.7	3	7.63	11.816	30.165		0.6	0.7	8	8.37	27.201	28.866
0.55	0.7	3	8.037	12.081	30.535		0.65	0.7	8	8.692	27.561	29.168
0.6	0.7	3	8.428	12.333	30.906		0.7	0.7	8	8.965	27.883	29.473
0.65	0.7	3	8.797	12.567	31.277		0.75	0.7	8	9.16	28.149	29.78
0.7	0.7	3	9.125	12.77	31.648		0.8	0.7	8	9.241	28.344	30.081
0.75	0.7	3	9.378	12.919	32.018		0.85	0.7	8	9.165	28.462	30.368
0.8	0.7	3	9.51	12.992	32.387		0.9	0.7	8	8.892	28.515	30.631
0.85	0.7	3	9.466	12.969	32.756		0.95	0.7	8	8.38	28.539	30.856
0.9	0.7	3	9.184	12.848	33.13		1	0.7	8	7.595	28.577	31.028
0.95	0.7	3	8.595	12.655	33.515		0.05	0.8	8	1.62	21.774	25.824
1	0.7	3	7.624	12.437	33.927		0.1	0.8	8	2.803	22.415	26.085
0.05	0.8	3	1.577	8.5	27.062		0.15	0.8	8	3.765	23.041	26.352
0.1	0.8	3	2.754	9.006	27.387		0.2	0.8	8	4.616	23.647	26.62
0.15	0.8	3	3.725	9.508	27.713		0.25	0.8	8	5.397	24.241	26.89
0.2	0.8	3	4.588	9.983	28.044		0.3	0.8	8	6.119	24.828	27.159
0.25	0.8	3	5.379	10.437	28.382		0.35	0.8	8	6.785	25.405	27.43
0.3	0.8	3	6.109	10.875	28.728		0.4	0.8	8	7.392	25.964	27.704
0.35	0.8	3	6.778	11.299	29.081		0.45	0.8	8	7.944	26.497	27.983
0.4	0.8	3	7.39	11.702	29.441		0.5	0.8	8	8.444	26.997	28.269
0.45	0.8	3	7.95E+00	12.08	29.808		0.55	0.8	8	8.894	27.46	28.562
0.5	0.8	3	8.46	12.428	30.181		0.6	0.8	8	9.291	27.881	28.865
0.55	0.8	3	8.93	12.743	30.558		0.65	0.8	8	9.623	28.252	29.176

x	T(K)	P(bar)	S(J/molK)	H(J/mol)	V(cm3/mol)	-	x.	T (K)	P (bar)	S (J/molK)	H (J/mol)	V (cm3/mol)
0.6	0.8	3	9.356	13.022	30.939		0.7	0.8	8	9.871	28.559	29.493
0.65	0.8	3	9.728	13.259	31.322		0.75	0.8	8	10.004	28.786	29.811
0.7	0.8	3	10.023	13.44	31.705		0.8	0.8	8	9.992	28.918	30.123
0.75	0.8	3	10.208	13.545	32.086		0.85	0.8	8	9.802	28.952	30.417
0.8	0.8	3	10.243	13.55	32.465		0.9	0.8	8	9.411	28.911	30.678
0.85	0.8	3	10.084	13.442	32.839		0.95	0.8	8	8.81	28.854	30.888
0.9	0.8	3	9.687	13.231	33.21		1	0.8	8	8.009	28.884	31.022
0.95	0.8	3	9.014	12.967	33.579		0	0.9	8	6.83E-03	21.207	25.576
1	0.8	3	8.036	12.753	33.953		0.05	0.9	8	1.707	21.852	25.82
0	0.9	3	0.014	8.122	26.736		0.1	0.9	8	2.917	22.527	26.08
0.05	0.9	3	1.674	8.579	27.058		0.15	0.9	8	3.901	23.175	26.347
0.1	0.9	3	2.883	9.126	27.382		0.2	0.9	8	4.787	23.803	26.616
0.15	0.9	3	3.883	9.659	27.711		0.25	0.9	8	5.625	24.434	26.885
0.2	0.9	3	4.789	10.167	28.046		0.3	0.9	8	6.428	25.078	27.154
0.25	0.9	3	5.645	10.666	28.388		0.35	0.9	8	7.188	25.729	27.422
0.3	0.9	3	6.46	11.168	28.738		0.4	0.9	8	7.898	26.373	27.694
0.35	0.9	3	7.228	11.669	29.096		0.45	0.9	8	8.55	26.99	27.971
0.4	0.9	3	7.941	12.157	29.461		0.5	0.9	8	9.137	27.564	28.255
0.45	0.9	3	8.594	12.614	29.834		0.55	0.9	8	9.654	28.083	28.55
0.5	0.9	3	9.184	13.027	30.213		0.6	0.9	8	10.09	28.537	28.855
0.55	0.9	3	9.708	13.386	30.599		0.65	0.9	8	10.43	28.916	29.171
0.6	0.9	3	10.158	13.683	30.989		0.7	0.9	8	10.651	29.206	29.495
0.65	0.9	3	10.52	13.911	31.383		0.75	0.9	8	10.727	29.393	29.821
0.7	0.9	3	10.773	14.059	31.777		0.8	0.9	8	10.63	29.464	30.142
0.75	0.9	3	10.886	14.11	32.17		0.85	0.9	8	10.34	29.421	30.442
0.8	0.9	3	10.828	14.046	32.558		0.9	0.9	8	9.851	29.297	30.705
0.85	0.9	3	10.567	13.861	32.936		0.95	0.9	8	9.182	29.174	30.906
0.9	0.9	3	10.081	13.577	33.302		1	0.9	8	8.383	29.205	31.018
0.95	0.9	3	9.362	13.27	33.652		0	1	8	0.063	21.253	25.578
1	0.9	3	8.422	13.097	33.986		0.05	1	8	1.836	21.964	25.818
0	1	3	0.067	8.162	26.736		0.1	1	8	3.063	22.673	26.079
0.05	1	3	1.807	8.689	27.052		0.15	1	8	4.051	23.336	26.348
0.1	1	3	3.041	9.278	27.377		0.2	1	8	4.955	23.984	26.619
0.15	1	3	4.057	9.838	27.711		0.25	1	8	5.836	24.651	26.889
0.2	1	3	4.994	10.379	28.054		0.3	1	8	6.704	25.352	27.157
0.25	1	3	5.904	10.927	28.404		0.35	1	8	7.548	26.078	27.424
0.3	1	3	6.793	11.495	28.761		0.4	1	8	8.348	26.805	27.692
0.35	1	3	7.648	12.077	29.126		0.45	1	8	9.088	27.504	27.964
0.4	1	3	8.451	12.649	29.499		0.5	1	8	9.751	28.147	28.244
0.45	1	3	9.185	13.182	29.878		0.55	1	8	10.324	28.714	28.534
0.5	1	3	9.839	13.652	30.265		0.6	1	8	10.791	29.191	28.836
0.55	1	3	10.401	14.04	30.658		0.65	1	8	11.134	29.569	29.151
0.6	1	3	10.859	14.338	31.057		0.7	1	8	11.33	29.836	29.475
0.65	1	3	11.2	14.54	31.46		0.75	1	8	11.356	29.982	29.805
0.7	1	3	11.403	14.639	31.865		0.8	1	8	11.19	29.999	30.13
0.75	1	3	11.446	14.627	32.267		0.85	1	8	10.821	29.891	30.436
0.8	1	3	11.306	14.495	32.661		0.9	1	8	10.258	29.697	30.705
0.85	1	3	10.965	14.243	33.042		0.95	1	8	9.539	29.518	30.911
0.9	1	3	10.42	13.907	33.402		1	1	8	8.742	29.548	31.02
0.95	1	3	9.689	13.584	33.733		0	1.1	8	0.16	21.324	25.575
1	1	3	8.815	13.477	34.028		0.05	1.1	8	2.014	22.115	25.814
0	1.1	3	0.141	8.223	26.734		0.1	1.1	8	3.255	22.862	26.078
0.05	1.1	3	1.973	8.832	27.044		0.15	1.1	8	4.244	23.547	26.352
0.1	1.1	3	3.237	9.468	27.372		0.2	1.1	8	5.161	24.219	26.628
0.15	1.1	3	4.271	10.064	27.714		0.25	1.1	8	6.077	24.928	26.901
0.2	1.1	3	5.238	10.646	28.068		0.3	1.1	8	7.002	25.689	27.17
0.25	1.1	3	6.198	11.252	28.43		0.35	1.1	8	7.917	26.492	27.435
0.3	1.1	3	7.156	11.896	28.799		0.4	1.1	8	8.794	27.3	27.698
0.35	1.1	3	8.089	12.563	29.174		0.45	1.1	8	9.605	28.073	27.963
0.4	1.1	3	8.967	13.218	29.556		0.5	1.1	8	10.327	28.774	28.235

x	T(K)	P(bar)	S(J/molK)	H(J/mol)	V(cm3/mol)	-	x.	T (K)	P (bar)	S (J/molK)	H (J/mol)	V (cm3/mol)
0.45	1.1	3	9.764	13.819	29.944		0.55	1.1	8	10.939	29.375	28.515
0.5	1.1	3	10.46	14.331	30.338		0.6	1.1	8	11.423	29.861	28.807
0.55	1.1	3	11.039	14.729	30.738		0.65	1.1	8	11.761	30.226	29.112
0.6	1.1	3	11.487	15.005	31.144		0.7	1.1	8	11.933	30.464	29.43
0.65	1.1	3	11.792	15.159	31.554		0.75	1.1	8	11.92	30.57	29.755
0.7	1.1	3	11.939	15.194	31.966		0.8	1.1	8	11.704	30.54	30.08
0.75	1.1	3	11.916	15.111	32.374		0.85	1.1	8	11.282	30.381	30.393
0.8	1.1	3	11.708	14.912	32.773		0.9	1.1	8	10.669	30.133	30.673
0.85	1.1	3	11.313	14.608	33.155		0.95	1.1	8	9.91	29.903	30.897
0.9	1.1	3	10.739	14.24	33.509		1	1.1	8	9.093	29.908	31.032
0.95	1.1	3	10.019	13.92	33.824		0	1.2	8	0.274	21.429	25.565
1	1.1	3	9.218	13.884	34.085		0.05	1.2	8	2.22	22.307	25.805
0	1.2	3	0.221	8.315	26.729		0.1	1.2	8	3.488	23.098	26.075
0.05	1.2	3	2.159	9.011	27.033		0.15	1.2	8	4.487	23.811	26.357
0.1	1.2	3	3.468	9.702	27.366		0.2	1.2	8	5.424	24.517	26.641
0.15	1.2	3	4.532	10.344	27.721		0.25	1.2	8	6.377	25.274	26.92
0.2	1.2	3	5.539	10.981	28.09		0.3	1.2	8	7.355	26.102	27.191
0.25	1.2	3	6.556	11.658	28.468		0.35	1.2	8	8.331	26.981	27.455
0.3	1.2	3	7.58	12.387	28.852		0.4	1.2	8	9.268	27.864	27.713
0.35	1.2	3	8.582	13.142	29.241		0.45	1.2	8	10.129	28.699	27.969
0.4	1.2	3	9.52	13.875	29.635		0.5	1.2	8	10.885	29.439	28.227
0.45	1.2	3	10.359	14.53	30.032		0.55	1.2	8	11.515	30.055	28.491
0.5	1.2	3	11.072	15.063	30.434		0.6	1.2	8	11.999	30.534	28.765
0.55	1.2	3	11.641	15.446	30.841		0.65	1.2	8	12.323	30.873	29.052
0.6	1.2	3	12.055	15.674	31.251		0.7	1.2	8	12.472	31.078	29.353
0.65	1.2	3	12.307	15.757	31.666		0.75	1.2	8	12.431	31.151	29.665
0.7	1.2	3	12.392	15.713	32.081		0.8	1.2	8	12.188	31.091	29.985
0.75	1.2	3	12.307	15.557	32.492		0.85	1.2	8	11.741	30.904	30.302
0.8	1.2	3	12.05	15.302	32.893		0.9	1.2	8	11.1	30.62	30.6
0.85	1.2	3	11.624	14.964	33.274		0.95	1.2	8	10.303	30.337	30.859
0.9	1.2	3	11.047	14.588	33.622		1	1.2	8	9.422	30.271	31.051
0.95	1.2	3	10.354	14.284	33.923		0	1.3	8	0.392	21.608	25.551
1	1.2	3	9.603	14.295	34.159		0.05	1.3	8	2.437	22.569	25.794
0	1.3	3	0.313	8.474	26.722		0.1	1.3	8	3.746	23.405	26.072
0.05	1.3	3	2.362	9.255	27.021		0.15	1.3	8	4.772	24.151	26.366
0.1	1.3	3	3.729	10.006	27.364		0.2	1.3	8	5.743	24.895	26.661
0.15	1.3	3	4.841	10.703	27.735		0.25	1.3	8	6.741	25.705	26.948
0.2	1.3	3	5.904	11.405	28.123		0.3	1.3	8	7.772	26.598	27.224
0.25	1.3	3	6.986	12.162	28.522		0.35	1.3	8	8.799	27.544	27.487
0.3	1.3	3	8.08	12.979	28.927		0.4	1.3	8	9.778	28.486	27.738
0.35	1.3	3	9.143	13.818	29.333		0.45	1.3	8	10.665	29.361	27.981
0.4	1.3	3	10.124	14.614	29.741		0.5	1.3	8	11.429	30.117	28.221
0.45	1.3	3	10.98	15.3	30.149		0.55	1.3	8	12.048	30.723	28.461
0.5	1.3	3	11.68	15.823	30.559		0.6	1.3	8	12.511	31.173	28.708
0.55	1.3	3	12.209	16.159	30.97		0.65	1.3	8	12.81	31.476	28.967
0.6	1.3	3	12.562	16.309	31.383		0.7	1.3	8	12.937	31.651	29.24
0.65	1.3	3	12.744	16.301	31.798		0.75	1.3	8	12.884	31.708	29.531
0.7	1.3	3	12.761	16.169	32.212		0.8	1.3	8	12.641	31.648	29.837
0.75	1.3	3	12.622	15.947	32.621		0.85	1.3	8	12.198	31.468	30.157
0.8	1.3	3	12.334	15.659	33.019		0.9	1.3	8	11.553	31.176	30.479
0.85	1.3	3	11.906	15.321	33.397		0.95	1.3	8	10.712	30.835	30.792
0.9	1.3	3	11.349	14.967	33.74		1	1.3	8	9.703	30.625	31.076
0.95	1.3	3	10.682	14.686	34.032		0	1.4	8	0.558	21.927	25.539
1	1.3	3	9.935	14.697	34.254		0.05	1.4	8	2.687	22.964	25.786
0	1.4	3	0.477	8.764	26.712		0.1	1.4	8	4.039	23.846	26.075
0.05	1.4	3	2.612	9.63	27.011		0.15	1.4	8	5.104	24.628	26.382
0.1	1.4	3	4.034	10.445	27.367		0.2	1.4	8	6.12	25.413	26.69
0.15	1.4	3	5.202	11.207	27.76		0.25	1.4	8	7.171	26.272	26.987
0.2	1.4	3	6.333	11.982	28.174		0.3	1.4	8	8.253	27.218	27.269
0.25	1.4	3	7.49	12.821	28.599		0.35	1.4	8	9.319	28.212	27.532

x	T(K)	P(bar)	S(J/molK)	H(J/mol)	V(cm3/mol)	-	x.	T (K)	P (bar)	S (J/molK)	H (J/mol)	V (cm3/mol)
0.3	1.4	3	8.653	13.719	29.028		0.4	1.4	8	10.317	29.183	27.776
0.35	1.4	3	9.768	14.622	29.456		0.45	1.4	8	11.201	30.062	28.004
0.4	1.4	3	10.772	15.451	29.881		0.5	1.4	8	11.939	30.794	28.219
0.45	1.4	3	11.616	16.129	30.302		0.55	1.4	8	12.519	31.356	28.429
0.5	1.4	3	12.272	16.599	30.719		0.6	1.4	8	12.938	31.752	28.639
0.55	1.4	3	12.729	16.843	31.134		0.65	1.4	8	13.201	32.011	28.858
0.6	1.4	3	12.995	16.882	31.546		0.7	1.4	8	13.311	32.165	29.092
0.65	1.4	3	13.091	16.761	31.956		0.75	1.4	8	13.268	32.237	29.349
0.7	1.4	3	13.039	16.541	32.364		0.8	1.4	8	13.06	32.226	29.634
0.75	1.4	3	12.861	16.275	32.765		0.85	1.4	8	12.663	32.106	29.953
0.8	1.4	3	12.571	15.994	33.155		0.9	1.4	8	12.041	31.843	30.306
0.85	1.4	3	12.175	15.709	33.525		0.95	1.4	8	11.149	31.438	30.691
0.9	1.4	3	11.665	15.421	33.862		1	1.4	8	9.934	30.988	31.103
0.95	1.4	3	11.022	15.171	34.15		0	1.5	8	0.935	22.345	25.524
1	1.4	3	10.214	15.107	34.369		0.05	1.5	8	3.08	23.487	25.775
0	1.5	3	0.847	9.143	26.686		0.1	1.5	8	4.441	24.443	26.076
0.05	1.5	3	2.988	10.133	26.993		0.15	1.5	8	5.531	25.284	26.398
0.1	1.5	3	4.422	11.051	27.37		0.2	1.5	8	6.588	26.124	26.722
0.15	1.5	3	5.628	11.907	27.791		0.25	1.5	8	7.685	27.032	27.033
0.2	1.5	3	6.82	12.776	28.238		0.3	1.5	8	8.804	28.015	27.323
0.25	1.5	3	8.046	13.7	28.696		0.35	1.5	8	9.887	29.024	27.587
0.3	1.5	3	9.27	14.664	29.156		0.4	1.5	8	10.874	29.98	27.824
0.35	1.5	3	10.42	15.598	29.611		0.45	1.5	8	11.717	30.809	28.034
0.4	1.5	3	11.422	16.412	30.057		0.5	1.5	8	12.394	31.462	28.222
0.45	1.5	3	12.225	17.021	30.493		0.55	1.5	8	12.902	31.93	28.393
0.5	1.5	3	12.803	17.374	30.919		0.6	1.5	8	13.256	32.24	28.558
0.55	1.5	3	13.16	17.47	31.335		0.65	1.5	8	13.479	32.442	28.725
0.6	1.5	3	13.322	17.351	31.743		0.7	1.5	8	13.589	32.592	28.907
0.65	1.5	3	13.327	17.096	32.144		0.75	1.5	8	13.593	32.721	29.119
0.7	1.5	3	13.22	16.792	32.539		0.8	1.5	8	13.473	32.82	29.374
0.75	1.5	3	13.036	16.515	32.925		0.85	1.5	8	13.179	32.827	29.688
0.8	1.5	3	12.794	16.301	33.3		0.9	1.5	8	12.627	32.642	30.077
0.85	1.5	3	12.485	16.137	33.656		0.95	1.5	8	11.69	32.159	30.554
0.9	1.5	3	12.066	15.972	33.985		1	1.5	8	10.194	31.337	31.132
0.95	1.5	3	11.454	15.757	34.271		0.05	0.1	9	0.487	24.148	26.078
1	1.5	3	10.518	15.516	34.497		0.1	0.1	9	0.661	24.325	26.34
0.05	0.1	4	0.542	11.507	26.732		0.15	0.1	9	0.546	24.491	26.588
0.1	0.1	4	0.713	11.532	27.061		0.2	0.1	9	0.38	24.7	26.826
0.15	0.1	4	0.621	11.52	27.392		0.25	0.1	9	0.28	24.954	27.061
0.2	0.1	4	0.494	11.546	27.722		0.3	0.1	9	0.285	25.237	27.294
0.25	0.1	4	0.442	11.628	28.051		0.35	0.1	9	0.387	25.529	27.529
0.3	0.1	4	0.499	11.757	28.377		0.4	0.1	9	0.553	25.821	27.766
0.35	0.1	4	0.654	11.914	28.703		0.45	0.1	9	0.737	26.11	28.009
0.4	0.1	4	0.868	12.086	29.029		0.5	0.1	9	0.9	26.398	28.255
0.45	0.1	4	1.094	12.264	29.358		0.55	0.1	9	1.008	26.683	28.506
0.5	0.1	4	1.287	12.441	29.691		0.6	0.1	9	1.045	26.963	28.759
0.55	0.1	4	1.411	12.613	30.031		0.65	0.1	9	1.01	27.231	29.013
0.6	0.1	4	1.449	12.775	30.376		0.7	0.1	9	0.924	27.483	29.264
0.65	0.1	4	1.401	12.92	30.725		0.75	0.1	9	0.819	27.729	29.51
0.7	0.1	4	1.289	13.046	31.076		0.8	0.1	9	0.74	28.001	29.747
0.75	0.1	4	1.155	13.165	31.423		0.85	0.1	9	0.73	28.35	29.973
0.8	0.1	4	1.055	13.311	31.763		0.9	0.1	9	0.816	28.829	30.187
0.85	0.1	4	1.05	13.534	32.089		0.95	0.1	9	0.976	29.439	30.393
0.9	0.1	4	1.187	13.891	32.399		1	0.1	9	1.11	30.021	30.597
0.95	0.1	4	1.476	14.392	32.693		0	0.2	9	0.021	23.499	25.788
1	0.1	4	1.848	14.9	32.98		0.05	0.2	9	1.047	23.896	26.053
0.05	0.2	4	0.967	11.053	26.758		0.1	0.2	9	1.492	24.188	26.306
0.1	0.2	4	1.397	11.205	27.085		0.15	0.2	9	1.673	24.472	26.553
0.15	0.2	4	1.577	11.332	27.417		0.2	0.2	9	1.767	24.781	26.795
0.2	0.2	4	1.675	11.477	27.75		0.25	0.2	9	1.861	25.112	27.034

x	T(K)	P(bar)	S(J/molK)	H(J/mol)	V(cm3/mol)	-	x.	T (K)	P (bar)	S (J/molK)	H (J/mol)	V (cm3/mol)
0.25	0.2	4	1.775	11.647	28.085		0.3	0.2	9	1.987	25.45	27.273
0.3	0.2	4	1.906	11.832	28.419		0.35	0.2	9	2.146	25.783	27.511
0.35	0.2	4	2.07	12.019	28.754		0.4	0.2	9	2.327	26.105	27.75
0.4	0.2	4	2.253	12.202	29.089		0.45	0.2	9	2.514	26.42	27.99
0.45	0.2	4	2.44	12.381	29.425		0.5	0.2	9	2.692	26.736	28.23
0.5	0.2	4	2.614	12.558	29.761		0.55	0.2	9	2.853	27.055	28.471
0.55	0.2	4	2.766	12.736	30.099		0.6	0.2	9	2.995	27.379	28.713
0.6	0.2	4	2.894	12.914	30.438		0.65	0.2	9	3.125	27.699	28.953
0.65	0.2	4	3.003	13.087	30.777		0.7	0.2	9	3.253	28.006	29.193
0.7	0.2	4	3.106	13.249	31.116		0.75	0.2	9	3.392	28.299	29.432
0.75	0.2	4	3.219	13.399	31.452		0.8	0.2	9	3.552	28.587	29.67
0.8	0.2	4	3.359	13.546	31.785		0.85	0.2	9	3.734	28.894	29.908
0.85	0.2	4	3.532	13.715	32.115		0.9	0.2	9	3.909	29.244	30.149
0.9	0.2	4	3.722	13.926	32.446		0.95	0.2	9	4.004	29.61	30.399
0.95	0.2	4	3.87	14.161	32.786		1	0.2	9	3.87	29.827	30.67
1	0.2	4	3.84	14.275	33.154		0	0.3	9	0.05	23.517	25.763
0	0.3	4	9.36E-03	10.778	26.436		0.05	0.3	9	1.185	23.918	26.017
0.05	0.3	4	1.11	11.04	26.754		0.1	0.3	9	1.828	24.271	26.266
0.1	0.3	4	1.742	11.256	27.076		0.15	0.3	9	2.225	24.623	26.511
0.15	0.3	4	2.137	11.462	27.402		0.2	0.3	9	2.511	24.984	26.755
0.2	0.3	4	2.42	11.674	27.73		0.25	0.3	9	2.75	25.349	26.997
0.25	0.3	4	2.654	11.886	28.062		0.3	0.3	9	2.968	25.703	27.238
0.3	0.3	4	2.864	12.092	28.395		0.35	0.3	9	3.173	26.04	27.479
0.35	0.3	4	3.061	12.283	28.729		0.4	0.3	9	3.367	26.359	27.718
0.4	0.3	4	3.246	12.459	29.064		0.45	0.3	9	3.552	26.669	27.957
0.45	0.3	4	3.424	12.626	29.399		0.5	0.3	9	3.733	26.982	28.194
0.5	0.3	4	3.599	12.795	29.733		0.55	0.3	9	3.917	27.306	28.431
0.55	0.3	4	3.78E+00	12.974	30.066		0.6	0.3	9	4.112	27.644	28.667
0.6	0.3	4	3.972	13.167	30.398		0.65	0.3	9	4.326	27.992	28.902
0.65	0.3	4	4.185	13.372	30.729		0.7	0.3	9	4.563	28.34	29.138
0.7	0.3	4	4.42	13.58	31.057		0.75	0.3	9	4.821	28.679	29.375
0.75	0.3	4	4.676	13.784	31.384		0.8	0.3	9	5.088	29.008	29.613
0.8	0.3	4	4.941	13.978	31.711		0.85	0.3	9	5.334	29.334	29.855
0.85	0.3	4	5.186	14.169	32.04		0.9	0.3	9	5.504	29.665	30.104
0.9	0.3	4	5.355	14.356	32.379		0.95	0.3	9	5.498	29.969	30.367
0.95	0.3	4	5.35	14.511	32.741		1	0.3	9	5.153	30.098	30.654
1	0.3	4	5.005	14.502	33.147		0	0.4	9	0.041	23.539	25.738
0	0.4	4	8.06E-03	10.81	26.436		0.05	0.4	9	1.277	23.957	25.986
0.05	0.4	4	1.22	11.07	26.752		0.1	0.4	9	2.079	24.372	26.233
0.1	0.4	4	2.018	11.349	27.068		0.15	0.4	9	2.651	24.79	26.479
0.15	0.4	4	2.591	11.629	27.387		0.2	0.4	9	3.096	25.205	26.724
0.2	0.4	4	3.037	11.902	27.71		0.25	0.4	9	3.464	25.608	26.968
0.25	0.4	4	3.401	12.16	28.036		0.3	0.4	9	3.776	25.988	27.211
0.3	0.4	4	3.706	12.395	28.365		0.35	0.4	9	4.042	26.34	27.454
0.35	0.4	4	3.965	12.603	28.696		0.4	0.4	9	4.272	26.667	27.695
0.4	0.4	4	4.191	12.788	29.028		0.45	0.4	9	4.48	26.981	27.935
0.45	0.4	4	4.398	12.96	29.361		0.5	0.4	9	4.68	27.294	28.175
0.5	0.4	4	4.603	13.134	29.693		0.55	0.4	9	4.887	27.619	28.413
0.55	0.4	4	4.82E+00	13.321	30.024		0.6	0.4	9	5.116	27.962	28.652
0.6	0.4	4	5.069	13.528	30.353		0.65	0.4	9	5.372	28.319	28.891
0.65	0.4	4	5.348	13.755	30.681		0.7	0.4	9	5.654	28.681	29.131
0.7	0.4	4	5.656	13.993	31.006		0.75	0.4	9	5.949	29.036	29.372
0.75	0.4	4	5.976	14.227	31.33		0.8	0.4	9	6.232	29.376	29.614
0.8	0.4	4	6.279	14.445	31.656		0.85	0.4	9	6.457	29.701	29.859
0.85	0.4	4	6.514	14.64	31.986		0.9	0.4	9	6.557	30.011	30.109
0.9	0.4	4	6.606	14.803	32.328		0.95	0.4	9	6.429	30.283	30.365
0.95	0.4	4	6.442	14.907	32.697		1	0.4	9	5.922	30.401	30.635
1	0.4	4	5.855	14.851	33.111		0	0.5	9	0.051	23.541	25.713
0	0.5	4	0.016	10.811	26.439		0.05	0.5	9	1.391	23.995	25.958
0.05	0.5	4	1.334	11.095	26.752		0.1	0.5	9	2.328	24.482	26.204

x	T(K)	P(bar)	S(J/molK)	H(J/mol)	V(cm3/mol)	-	x.	T (K)	P (bar)	S (J/molK)	H (J/mol)	V (cm3/mol)
0.1	0.5	4	2.27	11.445	27.064		0.15	0.5	9	3.042	24.971	26.451
0.15	0.5	4	2.991	11.802	27.378		0.2	0.5	9	3.625	25.449	26.697
0.2	0.5	4	3.578	12.143	27.695		0.25	0.5	9	4.115	25.904	26.942
0.25	0.5	4	4.069	12.458	28.017		0.3	0.5	9	4.529	26.329	27.187
0.3	0.5	4	4.481	12.74	28.342		0.35	0.5	9	4.879	26.721	27.432
0.35	0.5	4	4.828	12.989	28.67		0.4	0.5	9	5.176	27.082	27.676
0.4	0.5	4	5.126	13.21	29.001		0.45	0.5	9	5.437	27.424	27.92
0.45	0.5	4	5.396	13.413	29.333		0.5	0.5	9	5.682	27.759	28.165
0.5	0.5	4	5.657	13.613	29.665		0.55	0.5	9	5.928	28.099	28.411
0.55	0.5	4	5.929	13.822	29.998		0.6	0.5	9	6.189	28.45	28.659
0.6	0.5	4	6.224	14.048	30.329		0.65	0.5	9	6.467	28.809	28.908
0.65	0.5	4	6.546	14.29	30.66		0.7	0.5	9	6.758	29.166	29.158
0.7	0.5	4	6.883	14.536	30.989		0.75	0.5	9	7.04	29.508	29.41
0.75	0.5	4	7.211	14.771	31.318		0.8	0.5	9	7.279	29.822	29.661
0.8	0.5	4	7.488	14.974	31.647		0.85	0.5	9	7.427	30.107	29.911
0.85	0.5	4	7.655	15.133	31.98		0.9	0.5	9	7.418	30.362	30.156
0.9	0.5	4	7.634	15.236	32.324		0.95	0.5	9	7.161	30.579	30.396
0.95	0.5	4	7.314	15.269	32.689		1	0.5	9	6.535	30.69	30.63
1	0.5	4	6.551	15.173	33.092		0	0.6	9	0.056	23.54	25.687
0	0.6	4	0.017	10.8	26.44		0.05	0.6	9	1.499	24.042	25.931
0.05	0.6	4	1.434	11.127	26.75		0.1	0.6	9	2.545	24.598	26.177
0.1	0.6	4	2.479	11.548	27.06		0.15	0.6	9	3.373	25.154	26.423
0.15	0.6	4	3.315	11.977	27.371		0.2	0.6	9	4.071	25.693	26.669
0.2	0.6	4	4.02	12.384	27.685		0.25	0.6	9	4.674	26.207	26.914
0.25	0.6	4	4.627	12.76	28.003		0.3	0.6	9	5.196	26.69	27.16
0.3	0.6	4	5.15	13.103	28.326		0.35	0.6	9	5.646	27.142	27.406
0.35	0.6	4	5.602	13.412	28.653		0.4	0.6	9	6.034	27.562	27.653
0.4	0.6	4	5.996	13.692	28.983		0.45	0.6	9	6.377	27.958	27.902
0.45	0.6	4	6.351	13.95	29.316		0.5	0.6	9	6.692	28.339	28.155
0.5	0.6	4	6.687	14.197	29.651		0.55	0.6	9	6.993	28.712	28.411
0.55	0.6	4	7.021	14.444	29.988		0.6	0.6	9	7.291	29.081	28.67
0.6	0.6	4	7.362	14.694	30.325		0.65	0.6	9	7.585	29.444	28.933
0.65	0.6	4	7.709	14.947	30.663		0.7	0.6	9	7.864	29.789	29.199
0.7	0.6	4	8.046	15.188	31.002		0.75	0.6	9	8.103	30.1	29.465
0.75	0.6	4	8.342	15.4	31.339		0.8	0.6	9	8.266	30.366	29.727
0.8	0.6	4	8.552	15.559	31.677		0.85	0.6	9	8.306	30.58	29.982
0.85	0.6	4	8.618	15.65	32.016		0.9	0.6	9	8.168	30.751	30.222
0.9	0.6	4	8.466	15.665	32.359		0.95	0.6	9	7.786	30.889	30.441
0.95	0.6	4	8.006	15.608	32.714		1	0.6	9	7.082	30.982	30.63
1	0.6	4	7.129	15.473	33.091		0	0.7	9	0.039	23.542	25.664
0	0.7	4	6.43E-03	10.792	26.439		0.05	0.7	9	1.579	24.094	25.906
0.05	0.7	4	1.514	11.17	26.746		0.1	0.7	9	2.705	24.706	26.151
0.1	0.7	4	2.638	11.652	27.053		0.15	0.7	9	3.615	25.314	26.396
0.15	0.7	4	3.556	12.139	27.362		0.2	0.7	9	4.402	25.902	26.64
0.2	0.7	4	4.351	12.601	27.676		0.25	0.7	9	5.102	26.469	26.884
0.25	0.7	4	5.057	13.035	27.994		0.3	0.7	9	5.729	27.015	27.129
0.3	0.7	4	5.687	13.442	28.316		0.35	0.7	9	6.287	27.537	27.375
0.35	0.7	4	6.248	13.822	28.643		0.4	0.7	9	6.782	28.033	27.625
0.4	0.7	4	6.748	14.176	28.974		0.45	0.7	9	7.224	28.502	27.878
0.45	0.7	4	7.202	14.505	29.309		0.5	0.7	9	7.624	28.946	28.138
0.5	0.7	4	7.623	14.814	29.648		0.55	0.7	9	7.993	29.369	28.403
0.55	0.7	4	8.02E+00	15.108	29.99		0.6	0.7	9	8.334	29.769	28.675
0.6	0.7	4	8.406	15.387	30.336		0.65	0.7	9	8.643	30.141	28.953
0.65	0.7	4	8.766	15.648	30.683		0.7	0.7	9	8.901	30.473	29.234
0.7	0.7	4	9.082	15.876	31.033		0.75	0.7	9	9.084	30.748	29.515
0.75	0.7	4	9.323	16.051	31.382		0.8	0.7	9	9.155	30.954	29.79
0.8	0.7	4	9.444	16.15	31.73		0.85	0.7	9	9.077	31.085	30.051
0.85	0.7	4	9.393	16.157	32.075		0.9	0.7	9	8.809	31.159	30.287
0.9	0.7	4	9.112	16.075	32.417		0.95	0.7	9	8.315	31.21	30.485
0.95	0.7	4	8.539	15.93	32.757		1	0.7	9	7.564	31.28	30.629

x	T(K)	P(bar)	S(J/molK)	H(J/mol)	V(cm3/mol)	-	x.	T (K)	P (bar)	S (J/molK)	H (J/mol)	V (cm3/mol)
1	0.7	4	7.607	15.773	33.099		0	0.8	9	0.018	23.55	25.645
0	0.8	4	2.09E-04	10.795	26.439		0.05	0.8	9	1.642	24.152	25.885
0.05	0.8	4	1.589	11.227	26.739		0.1	0.8	9	2.821	24.805	26.129
0.1	0.8	4	2.764	11.758	27.045		0.15	0.8	9	3.779	25.445	26.372
0.15	0.8	4	3.732	12.285	27.355		0.2	0.8	9	4.626	26.066	26.615
0.2	0.8	4	4.591	12.788	27.67		0.25	0.8	9	5.404	26.677	26.857
0.25	0.8	4	5.378	13.271	27.989		0.3	0.8	9	6.124	27.282	27.099
0.3	0.8	4	6.104	13.74	28.313		0.35	0.8	9	6.788	27.878	27.345
0.35	0.8	4	6.77	14.195	28.641		0.4	0.8	9	7.393	28.457	27.595
0.4	0.8	4	7.378	14.63	28.974		0.45	0.8	9	7.94	29.009	27.851
0.45	0.8	4	7.932	15.038	29.312		0.5	0.8	9	8.435	29.527	28.115
0.5	0.8	4	8.438	15.415	29.655		0.55	0.8	9	8.877	30.008	28.388
0.55	0.8	4	8.90E+00	15.758	30.003		0.6	0.8	9	9.265	30.445	28.67
0.6	0.8	4	9.32	16.066	30.356		0.65	0.8	9	9.586	30.831	28.96
0.65	0.8	4	9.681	16.33	30.714		0.7	0.8	9	9.823	31.151	29.255
0.7	0.8	4	9.965	16.536	31.074		0.75	0.8	9	9.947	31.391	29.549
0.75	0.8	4	10.139	16.666	31.435		0.8	0.8	9	9.926	31.536	29.835
0.8	0.8	4	10.164	16.699	31.794		0.85	0.8	9	9.733	31.585	30.102
0.85	0.8	4	9.998	16.622	32.145		0.9	0.8	9	9.345	31.564	30.336
0.9	0.8	4	9.604	16.45	32.484		0.95	0.8	9	8.756	31.531	30.517
0.95	0.8	4	8.95	16.235	32.807		1	0.8	9	7.982	31.584	30.625
1	0.8	4	8.016	16.086	33.11		0	0.9	9	0.021	23.574	25.63
0	0.9	4	0.019	10.815	26.44		0.05	0.9	9	1.721	24.23	25.87
0.05	0.9	4	1.684	11.306	26.733		0.1	0.9	9	2.928	24.913	26.113
0.1	0.9	4	2.891	11.877	27.038		0.15	0.9	9	3.906	25.571	26.355
0.15	0.9	4	3.886	12.433	27.351		0.2	0.9	9	4.787	26.212	26.596
0.2	0.9	4	4.786	12.966	27.669		0.25	0.9	9	5.622	26.859	26.836
0.25	0.9	4	5.636	13.493	27.993		0.3	0.9	9	6.423	27.52	27.076
0.3	0.9	4	6.445	14.024	28.32		0.35	0.9	9	7.182	28.189	27.32
0.35	0.9	4	7.207	14.554	28.652		0.4	0.9	9	7.891	28.852	27.568
0.4	0.9	4	7.914	15.071	28.987		0.45	0.9	9	8.541	29.49	27.825
0.45	0.9	4	8.562	15.559	29.328		0.5	0.9	9	9.127	30.085	28.091
0.5	0.9	4	9.147	16.001	29.674		0.55	0.9	9	9.641	30.625	28.368
0.55	0.9	4	9.664	16.39	30.027		0.6	0.9	9	10.073	31.099	28.655
0.6	0.9	4	10.107	16.716	30.386		0.65	0.9	9	10.408	31.497	28.953
0.65	0.9	4	10.461	16.973	30.752		0.7	0.9	9	10.623	31.806	29.256
0.7	0.9	4	10.704	17.148	31.122		0.75	0.9	9	10.693	32.01	29.56
0.75	0.9	4	10.808	17.226	31.493		0.8	0.9	9	10.591	32.099	29.855
0.8	0.9	4	10.741	17.191	31.86		0.85	0.9	9	10.297	32.074	30.128
0.85	0.9	4	10.476	17.038	32.216		0.9	0.9	9	9.807	31.968	30.362
0.9	0.9	4	9.994	16.792	32.552		0.95	0.9	9	9.141	31.861	30.536
0.95	0.9	4	9.294	16.535	32.858		1	0.9	9	8.355	31.9	30.623
1	0.9	4	8.398	16.427	33.123		0	1	9	0.073	23.623	25.618
0	1	4	0.071	10.856	26.441		0.05	1	9	1.846	24.342	25.858
0.05	1	4	1.816	11.416	26.726		0.1	1	9	3.066	25.055	26.102
0.1	1	4	3.047	12.027	27.031		0.15	1	9	4.046	25.726	26.345
0.15	1	4	4.056	12.608	27.35		0.2	1	9	4.944	26.384	26.586
0.2	1	4	4.984	13.172	27.676		0.25	1	9	5.819	27.064	26.825
0.25	1	4	5.885	13.744	28.006		0.3	1	9	6.685	27.78	27.063
0.3	1	4	6.765	14.338	28.34		0.35	1	9	7.528	28.523	27.304
0.35	1	4	7.612	14.947	28.676		0.4	1	9	8.329	29.27	27.55
0.4	1	4	8.408	15.547	29.015		0.45	1	9	9.071	29.99	27.804
0.45	1	4	9.136	16.109	29.359		0.5	1	9	9.737	30.657	28.069
0.5	1	4	9.784	16.609	29.707		0.55	1	9	10.313	31.249	28.344
0.55	1	4	10.341	17.029	30.063		0.6	1	9	10.783	31.753	28.632
0.6	1	4	10.795	17.358	30.426		0.65	1	9	11.128	32.157	28.93
0.65	1	4	11.13	17.592	30.797		0.7	1	9	11.326	32.451	29.236
0.7	1	4	11.327	17.722	31.173		0.75	1	9	11.351	32.623	29.543
0.75	1	4	11.363	17.741	31.551		0.8	1	9	11.183	32.662	29.842
0.8	1	4	11.217	17.639	31.925		0.85	1	9	10.81	32.574	30.12

x	T(K)	P(bar)	S(J/molK)	H(J/mol)	V(cm3/mol)	-	x.	T (K)	P (bar)	S (J/molK)	H (J/mol)	V (cm3/mol)
0.85	1	4	10.874	17.421	32.284		0.9	1	9	10.241	32.396	30.36
0.9	1	4	10.333	17.123	32.618		0.95	1	9	9.513	32.222	30.537
0.95	1	4	9.618	16.847	32.91		1	1	9	8.706	32.237	30.626
1	1	4	8.784	16.802	33.144		0	1.1	9	0.171	23.698	25.604
0	1.1	4	0.148	10.919	26.441		0.05	1.1	9	2.022	24.494	25.846
0.05	1.1	4	1.983	11.559	26.717		0.1	1.1	9	3.254	25.243	26.094
0.1	1.1	4	3.243	12.215	27.025		0.15	1.1	9	4.232	25.931	26.34
0.15	1.1	4	4.267	12.829	27.352		0.2	1.1	9	5.139	26.61	26.583
0.2	1.1	4	5.221	13.43	27.689		0.25	1.1	9	6.047	27.328	26.823
0.25	1.1	4	6.169	14.057	28.03		0.3	1.1	9	6.967	28.103	27.061
0.3	1.1	4	7.114	14.723	28.373		0.35	1.1	9	7.881	28.921	27.3
0.35	1.1	4	8.036	15.413	28.716		0.4	1.1	9	8.761	29.749	27.543
0.4	1.1	4	8.905	16.094	29.06		0.45	1.1	9	9.577	30.546	27.792
0.45	1.1	4	9.696	16.724	29.406		0.5	1.1	9	10.307	31.274	28.05
0.5	1.1	4	10.387	17.266	29.756		0.55	1.1	9	10.929	31.907	28.319
0.55	1.1	4	10.962	17.698	30.112		0.6	1.1	9	11.425	32.428	28.599
0.6	1.1	4	11.408	18.01	30.475		0.65	1.1	9	11.775	32.829	28.89
0.65	1.1	4	11.711	18.2	30.847		0.7	1.1	9	11.957	33.104	29.19
0.7	1.1	4	11.857	18.271	31.225		0.75	1.1	9	11.951	33.245	29.492
0.75	1.1	4	11.831	18.224	31.606		0.8	1.1	9	11.738	33.245	29.791
0.8	1.1	4	11.621	18.06	31.983		0.85	1.1	9	11.312	33.109	30.073
0.85	1.1	4	11.224	17.79	32.345		0.9	1.1	9	10.685	32.872	30.322
0.9	1.1	4	10.654	17.459	32.678		0.95	1.1	9	9.902	32.633	30.519
0.95	1.1	4	9.947	17.183	32.963		1	1.1	9	9.049	32.594	30.636
1	1.1	4	9.176	17.2	33.176		0	1.2	9	0.291	23.806	25.585
0	1.2	4	0.232	11.012	26.437		0.05	1.2	9	2.231	24.688	25.833
0.05	1.2	4	2.172	11.738	26.706		0.1	1.2	9	3.486	25.479	26.087
0.1	1.2	4	3.473	12.448	27.019		0.15	1.2	9	4.47	26.191	26.34
0.15	1.2	4	4.523	13.104	27.357		0.2	1.2	9	5.392	26.899	26.588
0.2	1.2	4	5.514	13.754	27.709		0.25	1.2	9	6.334	27.662	26.831
0.25	1.2	4	6.513	14.445	28.065		0.3	1.2	9	7.305	28.499	27.071
0.3	1.2	4	7.521	15.191	28.42		0.35	1.2	9	8.279	29.392	27.308
0.35	1.2	4	8.509	15.966	28.773		0.4	1.2	9	9.219	30.295	27.546
0.4	1.2	4	9.436	16.721	29.123		0.45	1.2	9	10.09	31.156	27.788
0.45	1.2	4	10.268	17.404	29.471		0.5	1.2	9	10.86	31.93	28.036
0.5	1.2	4	10.977	17.969	29.821		0.55	1.2	9	11.508	32.585	28.291
0.55	1.2	4	11.545	18.389	30.174		0.6	1.2	9	12.013	33.109	28.555
0.6	1.2	4	11.96	18.658	30.534		0.65	1.2	9	12.36	33.497	28.83
0.65	1.2	4	12.216	18.784	30.902		0.7	1.2	9	12.529	33.751	29.113
0.7	1.2	4	12.305	18.783	31.277		0.75	1.2	9	12.505	33.871	29.402
0.75	1.2	4	12.222	18.669	31.656		0.8	1.2	9	12.271	33.851	29.692
0.8	1.2	4	11.967	18.454	32.032		0.85	1.2	9	11.82	33.69	29.976
0.85	1.2	4	11.543	18.153	32.395		0.9	1.2	9	11.159	33.411	30.242
0.9	1.2	4	10.968	17.813	32.729		0.95	1.2	9	10.32	33.101	30.474
0.95	1.2	4	10.28	17.546	33.013		1	1.2	9	9.371	32.955	30.652
1	1.2	4	9.547	17.601	33.221		0	1.3	9	0.413	23.987	25.566
0	1.3	4	0.327	11.174	26.431		0.05	1.3	9	2.451	24.95	25.821
0.05	1.3	4	2.375	11.984	26.693		0.1	1.3	9	3.744	25.783	26.083
0.1	1.3	4	3.731	12.749	27.014		0.15	1.3	9	4.751	26.524	26.345
0.15	1.3	4	4.824	13.455	27.368		0.2	1.3	9	5.703	27.266	26.601
0.2	1.3	4	5.866	14.164	27.739		0.25	1.3	9	6.686	28.076	26.851
0.25	1.3	4	6.926	14.929	28.113		0.3	1.3	9	7.706	28.974	27.093
0.3	1.3	4	7.999	15.755	28.484		0.35	1.3	9	8.731	29.933	27.331
0.35	1.3	4	9.044	16.608	28.849		0.4	1.3	9	9.714	30.895	27.564
0.4	1.3	4	10.012	17.423	29.206		0.45	1.3	9	10.613	31.8	27.795
0.45	1.3	4	10.86	18.135	29.557		0.5	1.3	9	11.397	32.595	28.027
0.5	1.3	4	11.557	18.692	29.904		0.55	1.3	9	12.044	33.251	28.262
0.55	1.3	4	12.088	19.069	30.252		0.6	1.3	9	12.539	33.758	28.501
0.6	1.3	4	12.448	19.267	30.604		0.65	1.3	9	12.872	34.126	28.748
0.65	1.3	4	12.639	19.31	30.962		0.7	1.3	9	13.033	34.366	29.003

x	T(K)	P(bar)	S(J/molK)	H(J/mol)	V(cm3/mol)	-	x.	T (K)	P (bar)	S (J/molK)	H (J/mol)	V (cm3/mol)
0.7	1.3	4	12.666	19.23	31.327		0.75	1.3	9	13.008	34.484	29.268
0.75	1.3	4	12.537	19.059	31.698		0.8	1.3	9	12.781	34.476	29.542
0.8	1.3	4	12.257	18.817	32.07		0.85	1.3	9	12.338	34.326	29.825
0.85	1.3	4	11.833	18.52	32.431		0.9	1.3	9	11.665	34.032	30.111
0.9	1.3	4	11.277	18.2	32.769		0.95	1.3	9	10.762	33.642	30.396
0.95	1.3	4	10.609	17.951	33.061		1	1.3	9	9.649	33.31	30.671
1	1.3	4	9.863	17.992	33.281		0	1.4	9	0.576	24.31	25.552
0	1.4	4	0.489	11.47	26.422		0.05	1.4	9	2.7	25.346	25.815
0.05	1.4	4	2.623	12.363	26.683		0.1	1.4	9	4.035	26.22	26.087
0.1	1.4	4	4.03	13.188	27.015		0.15	1.4	9	5.078	26.992	26.36
0.15	1.4	4	5.176	13.951	27.39		0.2	1.4	9	6.072	27.768	26.627
0.2	1.4	4	6.279	14.725	27.783		0.25	1.4	9	7.104	28.622	26.885
0.25	1.4	4	7.408	15.563	28.18		0.3	1.4	9	8.172	29.569	27.133
0.3	1.4	4	8.546	16.463	28.571		0.35	1.4	9	9.233	30.572	27.371
0.35	1.4	4	9.638	17.373	28.95		0.4	1.4	9	10.236	31.565	27.599
0.4	1.4	4	10.626	18.217	29.316		0.45	1.4	9	11.135	32.477	27.818
0.45	1.4	4	11.461	18.919	29.669		0.5	1.4	9	11.9	33.258	28.029
0.5	1.4	4	12.114	19.425	30.012		0.55	1.4	9	12.516	33.881	28.236
0.55	1.4	4	12.577	19.716	30.35		0.6	1.4	9	12.979	34.351	28.44
0.6	1.4	4	12.856	19.809	30.688		0.65	1.4	9	13.29	34.692	28.647
0.65	1.4	4	12.968	19.75	31.03		0.7	1.4	9	13.448	34.931	28.862
0.7	1.4	4	12.934	19.593	31.379		0.75	1.4	9	13.446	35.082	29.09
0.75	1.4	4	12.774	19.387	31.734		0.8	1.4	9	13.263	35.134	29.338
0.8	1.4	4	12.499	19.161	32.094		0.85	1.4	9	12.867	35.049	29.615
0.85	1.4	4	12.111	18.92	32.452		0.9	1.4	9	12.211	34.778	29.927
0.9	1.4	4	11.601	18.666	32.794		0.95	1.4	9	11.238	34.297	30.284
0.95	1.4	4	10.949	18.439	33.104		1	1.4	9	9.881	33.677	30.692
1	1.4	4	10.124	18.391	33.355		0	1.5	9	0.943	24.739	25.539
0	1.5	4	0.864	11.856	26.403		0.05	1.5	9	3.089	25.875	25.809
0.05	1.5	4	3.003	12.868	26.666		0.1	1.5	9	4.437	26.816	26.092
0.1	1.5	4	4.42	13.79	27.017		0.15	1.5	9	5.504	27.639	26.378
0.15	1.5	4	5.599	14.64	27.417		0.2	1.5	9	6.535	28.461	26.658
0.2	1.5	4	6.758	15.498	27.839		0.25	1.5	9	7.609	29.358	26.928
0.25	1.5	4	7.95	16.412	28.264		0.3	1.5	9	8.71	30.337	27.184
0.3	1.5	4	9.141	17.369	28.678		0.35	1.5	9	9.785	31.352	27.425
0.35	1.5	4	10.262	18.303	29.075		0.4	1.5	9	10.776	32.331	27.649
0.4	1.5	4	11.244	19.128	29.452		0.45	1.5	9	11.637	33.2	27.854
0.45	1.5	4	12.036	19.761	29.807		0.5	1.5	9	12.345	33.912	28.041
0.5	1.5	4	12.612	20.153	30.146		0.55	1.5	9	12.897	34.457	28.213
0.55	1.5	4	12.977	20.301	30.471		0.6	1.5	9	13.306	34.859	28.373
0.6	1.5	4	13.155	20.247	30.79		0.65	1.5	9	13.591	35.165	28.529
0.65	1.5	4	13.184	20.064	31.109		0.7	1.5	9	13.763	35.421	28.689
0.7	1.5	4	13.104	19.835	31.432		0.75	1.5	9	13.821	35.649	28.868
0.75	1.5	4	12.948	19.63	31.764		0.8	1.5	9	13.736	35.826	29.08
0.8	1.5	4	12.728	19.478	32.106		0.85	1.5	9	13.448	35.874	29.346
0.85	1.5	4	12.432	19.363	32.454		0.9	1.5	9	12.856	35.67	29.688
0.9	1.5	4	12.014	19.23	32.802		0.95	1.5	9	11.816	35.081	30.134
0.95	1.5	4	11.385	19.028	33.136		1	1.5	9	10.137	34.032	30.714
1	1.5	4	10.414	18.784	33.437		0.05	0.1	10	0.403	26.887	25.464
0.05	0.1	5	0.533	14.138	26.518		0.1	0.1	10	0.582	27.105	25.735
0.1	0.1	5	0.701	14.197	26.831		0.15	0.1	10	0.473	27.311	25.997
0.15	0.1	5	0.602	14.222	27.14		0.2	0.1	10	0.314	27.555	26.252
0.2	0.1	5	0.465	14.285	27.445		0.25	0.1	10	0.221	27.838	26.505
0.25	0.1	5	0.401	14.404	27.748		0.3	0.1	10	0.235	28.145	26.758
0.3	0.1	5	0.445	14.565	28.051		0.35	0.1	10	0.346	28.459	27.012
0.35	0.1	5	0.586	14.752	28.354		0.4	0.1	10	0.519	28.772	27.269
0.4	0.1	5	0.786	14.95	28.661		0.45	0.1	10	0.711	29.084	27.529
0.45	0.1	5	1.001	15.151	28.972		0.5	0.1	10	0.882	29.399	27.794
0.5	0.1	5	1.184	15.351	29.288		0.55	0.1	10	0.998	29.716	28.062
0.55	0.1	5	1.303	15.547	29.609		0.6	0.1	10	1.044	30.031	28.333

x	T(K)	P(bar)	S(J/molK)	H(J/mol)	V(cm3/mol)	-	x.	T (K)	P (bar)	S (J/molK)	H (J/mol)	V (cm3/mol)
0.6	0.1	5	1.339	15.734	29.934		0.65	0.1	10	1.02	30.335	28.604
0.65	0.1	5	1.292	15.906	30.261		0.7	0.1	10	0.944	30.623	28.874
0.7	0.1	5	1.184	16.061	30.588		0.75	0.1	10	0.849	30.902	29.138
0.75	0.1	5	1.056	16.211	30.91		0.8	0.1	10	0.777	31.202	29.393
0.8	0.1	5	0.96	16.39	31.223		0.85	0.1	10	0.767	31.575	29.637
0.85	0.1	5	0.955	16.647	31.523		0.9	0.1	10	0.839	32.077	29.868
0.9	0.1	5	1.083	17.037	31.81		0.95	0.1	10	0.966	32.712	30.085
0.95	0.1	5	1.35	17.567	32.088		1	0.1	10	1.036	33.321	30.295
1	0.1	5	1.68	18.093	32.368		0.05	0.2	10	1.001	26.68	25.47
0.05	0.2	5	0.986	13.712	26.531		0.1	0.2	10	1.451	27.006	25.729
0.1	0.2	5	1.418	13.895	26.842		0.15	0.2	10	1.638	27.324	25.985
0.15	0.2	5	1.598	14.056	27.153		0.2	0.2	10	1.742	27.664	26.24
0.2	0.2	5	1.696	14.237	27.463		0.25	0.2	10	1.846	28.023	26.493
0.25	0.2	5	1.794	14.442	27.773		0.3	0.2	10	1.984	28.385	26.746
0.3	0.2	5	1.924	14.661	28.085		0.35	0.2	10	2.156	28.74	26.999
0.35	0.2	5	2.087	14.882	28.397		0.4	0.2	10	2.348	29.087	27.251
0.4	0.2	5	2.27	15.096	28.712		0.45	0.2	10	2.545	29.43	27.504
0.45	0.2	5	2.456	15.305	29.027		0.5	0.2	10	2.731	29.777	27.757
0.5	0.2	5	2.631	15.513	29.344		0.55	0.2	10	2.9	30.133	28.01
0.55	0.2	5	2.786	15.722	29.663		0.6	0.2	10	3.05	30.496	28.263
0.6	0.2	5	2.917	15.931	29.981		0.65	0.2	10	3.187	30.856	28.517
0.65	0.2	5	3.03E+00	16.137	30.299		0.7	0.2	10	3.322	31.204	28.77
0.7	0.2	5	3.14	16.332	30.614		0.75	0.2	10	3.469	31.534	29.023
0.75	0.2	5	3.259	16.515	30.927		0.8	0.2	10	3.636	31.856	29.276
0.8	0.2	5	3.402	16.696	31.236		0.85	0.2	10	3.822	32.196	29.529
0.85	0.2	5	3.576	16.899	31.542		0.9	0.2	10	3.996	32.579	29.785
0.9	0.2	5	3.762	17.142	31.851		0.95	0.2	10	4.08	32.982	30.05
0.95	0.2	5	3.898	17.405	32.171		1	0.2	10	3.92	33.242	30.332
1	0.2	5	3.846	17.538	32.522		0	0.3	10	0.012	26.266	25.211
0	0.3	5	0.023	13.408	26.21		0.05	0.3	10	1.146	26.699	25.464
0.05	0.3	5	1.129	13.705	26.52		0.1	0.3	10	1.791	27.085	25.717
0.1	0.3	5	1.763	13.952	26.827		0.15	0.3	10	2.194	27.468	25.971
0.15	0.3	5	2.159	14.19	27.134		0.2	0.3	10	2.489	27.86	26.225
0.2	0.3	5	2.444	14.435	27.443		0.25	0.3	10	2.739	28.252	26.478
0.25	0.3	5	2.68	14.682	27.753		0.3	0.3	10	2.969	28.632	26.73
0.3	0.3	5	2.894	14.921	28.064		0.35	0.3	10	3.185	28.993	26.981
0.35	0.3	5	3.093	15.146	28.378		0.4	0.3	10	3.389	29.339	27.231
0.4	0.3	5	3.282	15.355	28.692		0.45	0.3	10	3.582	29.678	27.479
0.45	0.3	5	3.463	15.555	29.007		0.5	0.3	10	3.767	30.022	27.726
0.5	0.3	5	3.641	15.756	29.321		0.55	0.3	10	3.954	30.382	27.972
0.55	0.3	5	3.824	15.967	29.634		0.6	0.3	10	4.15	30.759	28.217
0.6	0.3	5	4.02	16.193	29.947		0.65	0.3	10	4.365	31.146	28.462
0.65	0.3	5	4.234	16.43	30.257		0.7	0.3	10	4.602	31.531	28.707
0.7	0.3	5	4.471	16.671	30.565		0.75	0.3	10	4.863	31.906	28.954
0.75	0.3	5	4.728	16.906	30.871		0.8	0.3	10	5.133	32.269	29.205
0.8	0.3	5	4.993	17.133	31.176		0.85	0.3	10	5.384	32.631	29.46
0.85	0.3	5	5.236	17.355	31.483		0.9	0.3	10	5.558	33	29.723
0.9	0.3	5	5.402	17.575	31.8		0.95	0.3	10	5.557	33.348	30.001
0.95	0.3	5	5.393	17.759	32.138		1	0.3	10	5.212	33.53	30.301
1	0.3	5	5.044	17.774	32.516		0	0.4	10	6.93E-03	26.276	25.211
0	0.4	5	0.02	13.441	26.207		0.05	0.4	10	1.242	26.727	25.461
0.05	0.4	5	1.235	13.739	26.512		0.1	0.4	10	2.045	27.176	25.713
0.1	0.4	5	2.034	14.048	26.815		0.15	0.4	10	2.621	27.626	25.965
0.15	0.4	5	2.608	14.358	27.118		0.2	0.4	10	3.074	28.073	26.218
0.2	0.4	5	3.055	14.663	27.423		0.25	0.4	10	3.453	28.505	26.471
0.25	0.4	5	3.421	14.953	27.73		0.3	0.4	10	3.775	28.913	26.723
0.3	0.4	5	3.729	15.221	28.04		0.35	0.4	10	4.051	29.292	26.974
0.35	0.4	5	3.991	15.462	28.352		0.4	0.4	10	4.288	29.647	27.224
0.4	0.4	5	4.22	15.68	28.664		0.45	0.4	10	4.5	29.991	27.472
0.45	0.4	5	4.429	15.885	28.978		0.5	0.4	10	4.7	30.336	27.72

x	T(K)	P(bar)	S(J/molK)	H(J/mol)	V(cm3/mol)	-	x.	T (K)	P (bar)	S (J/molK)	H (J/mol)	V (cm3/mol)
0.5	0.4	5	4.636	16.091	29.29		0.55	0.4	10	4.905	30.695	27.966
0.55	0.4	5	4.856	16.309	29.602		0.6	0.4	10	5.129	31.073	28.212
0.6	0.4	5	5.102	16.548	29.913		0.65	0.4	10	5.378	31.465	28.458
0.65	0.4	5	5.379	16.805	30.221		0.7	0.4	10	5.655	31.86	28.706
0.7	0.4	5	5.683	17.072	30.529		0.75	0.4	10	5.946	32.248	28.955
0.75	0.4	5	5.999	17.336	30.834		0.8	0.4	10	6.227	32.62	29.207
0.8	0.4	5	6.296	17.583	31.141		0.85	0.4	10	6.455	32.979	29.463
0.85	0.4	5	6.527	17.808	31.45		0.9	0.4	10	6.563	33.329	29.724
0.9	0.4	5	6.616	18.004	31.77		0.95	0.4	10	6.449	33.649	29.993
0.95	0.4	5	6.454	18.141	32.109		1	0.4	10	5.961	33.827	30.276
1	0.4	5	5.878	18.117	32.487		0	0.5	10	0.022	26.27	25.209
0	0.5	5	0.028	13.443	26.206		0.05	0.5	10	1.362	26.758	25.459
0.05	0.5	5	1.348	13.767	26.507		0.1	0.5	10	2.3	27.28	25.711
0.1	0.5	5	2.284	14.147	26.806		0.15	0.5	10	3.02	27.804	25.963
0.15	0.5	5	3.004	14.532	27.106		0.2	0.5	10	3.611	28.316	26.215
0.2	0.5	5	3.591	14.903	27.409		0.25	0.5	10	4.11	28.803	26.466
0.25	0.5	5	4.082	15.249	27.714		0.3	0.5	10	4.535	29.259	26.717
0.3	0.5	5	4.496	15.564	28.022		0.35	0.5	10	4.892	29.681	26.969
0.35	0.5	5	4.845	15.845	28.332		0.4	0.5	10	5.194	30.072	27.221
0.4	0.5	5	5.145	16.098	28.644		0.45	0.5	10	5.457	30.445	27.473
0.45	0.5	5	5.415	16.334	28.956		0.5	0.5	10	5.699	30.811	27.725
0.5	0.5	5	5.675	16.564	29.27		0.55	0.5	10	5.939	31.183	27.978
0.55	0.5	5	5.945	16.803	29.584		0.6	0.5	10	6.189	31.566	28.233
0.6	0.5	5	6.236	17.058	29.898		0.65	0.5	10	6.457	31.956	28.489
0.65	0.5	5	6.551	17.328	30.211		0.7	0.5	10	6.737	32.343	28.746
0.7	0.5	5	6.88	17.601	30.524		0.75	0.5	10	7.01	32.714	29.004
0.75	0.5	5	7.199	17.862	30.836		0.8	0.5	10	7.244	33.059	29.262
0.8	0.5	5	7.468	18.093	31.148		0.85	0.5	10	7.394	33.376	29.519
0.85	0.5	5	7.629	18.281	31.462		0.9	0.5	10	7.393	33.672	29.773
0.9	0.5	5	7.605	18.418	31.782		0.95	0.5	10	7.156	33.94	30.023
0.95	0.5	5	7.294	18.489	32.114		1	0.5	10	6.561	34.113	30.269
1	0.5	5	6.554	18.434	32.471		0	0.6	10	0.032	26.263	25.204
0	0.6	5	0.029	13.435	26.204		0.05	0.6	10	1.477	26.801	25.457
0.05	0.6	5	1.449	13.802	26.5		0.1	0.6	10	2.526	27.393	25.708
0.1	0.6	5	2.494	14.252	26.797		0.15	0.6	10	3.361	27.986	25.958
0.15	0.6	5	3.328	14.708	27.095		0.2	0.6	10	4.067	28.562	26.207
0.2	0.6	5	4.031	15.144	27.396		0.25	0.6	10	4.68	29.111	26.456
0.25	0.6	5	4.637	15.55	27.7		0.3	0.6	10	5.212	29.629	26.706
0.3	0.6	5	5.16	15.924	28.007		0.35	0.6	10	5.669	30.113	26.957
0.35	0.6	5	5.612	16.265	28.316		0.4	0.6	10	6.062	30.566	27.211
0.4	0.6	5	6.006	16.576	28.628		0.45	0.6	10	6.405	30.994	27.468
0.45	0.6	5	6.36	16.866	28.942		0.5	0.6	10	6.715	31.406	27.728
0.5	0.6	5	6.694	17.143	29.259		0.55	0.6	10	7.008	31.81	27.992
0.55	0.6	5	7.023	17.418	29.577		0.6	0.6	10	7.294	32.21	28.259
0.6	0.6	5	7.358	17.697	29.897		0.65	0.6	10	7.575	32.602	28.53
0.65	0.6	5	7.696	17.975	30.219		0.7	0.6	10	7.841	32.975	28.801
0.7	0.6	5	8.022	18.242	30.542		0.75	0.6	10	8.068	33.314	29.072
0.75	0.6	5	8.306	18.478	30.865		0.8	0.6	10	8.224	33.608	29.339
0.8	0.6	5	8.506	18.664	31.187		0.85	0.6	10	8.264	33.855	29.598
0.85	0.6	5	8.564	18.783	31.507		0.9	0.6	10	8.136	34.065	29.844
0.9	0.6	5	8.412	18.833	31.826		0.95	0.6	10	7.775	34.255	30.069
0.95	0.6	5	7.965	18.819	32.145		1	0.6	10	7.108	34.407	30.269
1	0.6	5	7.121	18.733	32.469		0	0.7	10	0.018	26.262	25.2
0	0.7	5	0.017	13.43	26.201		0.05	0.7	10	1.562	26.849	25.455
0.05	0.7	5	1.529	13.846	26.491		0.1	0.7	10	2.694	27.498	25.705
0.1	0.7	5	2.652	14.357	26.785		0.15	0.7	10	3.611	28.144	25.952
0.15	0.7	5	3.567	14.869	27.084		0.2	0.7	10	4.407	28.771	26.197
0.2	0.7	5	4.36	15.358	27.385		0.25	0.7	10	5.118	29.378	26.441
0.25	0.7	5	5.064	15.821	27.689		0.3	0.7	10	5.755	29.961	26.687
0.3	0.7	5	5.692	16.258	27.996		0.35	0.7	10	6.32	30.519	26.937

x	T(K)	P(bar)	S(J/molK)	H(J/mol)	V(cm3/mol)	-	x.	T (K)	P (bar)	S (J/molK)	H (J/mol)	V (cm3/mol)
0.35	0.7	5	6.252	16.669	28.305		0.4	0.7	10	6.82	31.049	27.193
0.4	0.7	5	6.751	17.054	28.618		0.45	0.7	10	7.262	31.551	27.454
0.45	0.7	5	7.203	17.414	28.933		0.5	0.7	10	7.659	32.028	27.723
0.5	0.7	5	7.62	17.754	29.253		0.55	0.7	10	8.02	32.482	27.998
0.55	0.7	5	8.015	18.076	29.576		0.6	0.7	10	8.35	32.913	28.279
0.6	0.7	5	8.39	18.383	29.904		0.65	0.7	10	8.645	33.314	28.564
0.65	0.7	5	8.74	18.669	30.236		0.7	0.7	10	8.891	33.673	28.852
0.7	0.7	5	9.045	18.922	30.57		0.75	0.7	10	9.062	33.976	29.137
0.75	0.7	5	9.274	19.121	30.906		0.8	0.7	10	9.126	34.21	29.414
0.8	0.7	5	9.384	19.246	31.239		0.85	0.7	10	9.046	34.374	29.676
0.85	0.7	5	9.326	19.282	31.567		0.9	0.7	10	8.786	34.487	29.913
0.9	0.7	5	9.046	19.235	31.884		0.95	0.7	10	8.312	34.586	30.115
0.95	0.7	5	8.488	19.135	32.187		1	0.7	10	7.596	34.709	30.268
1	0.7	5	7.596	19.032	32.472		0.05	0.8	10	1.627	26.903	25.455
0	0.8	5	6.92E-03	13.434	26.2		0.1	0.8	10	2.812	27.593	25.704
0.05	0.8	5	1.601	13.904	26.482		0.15	0.8	10	3.779	28.272	25.947
0.1	0.8	5	2.776	14.462	26.774		0.2	0.8	10	4.635	28.934	26.186
0.15	0.8	5	3.741	15.013	27.073		0.25	0.8	10	5.424	29.586	26.425
0.2	0.8	5	4.596	15.541	27.377		0.3	0.8	10	6.155	30.232	26.666
0.25	0.8	5	5.379	16.051	27.683		0.35	0.8	10	6.826	30.866	26.914
0.3	0.8	5	6.102	16.55	27.991		0.4	0.8	10	7.436	31.481	27.17
0.35	0.8	5	6.766	17.035	28.301		0.45	0.8	10	7.986	32.068	27.435
0.4	0.8	5	7.371	17.5	28.614		0.5	0.8	10	8.478	32.621	27.71
0.45	0.8	5	7.923	17.939	28.931		0.55	0.8	10	8.915	33.134	27.994
0.5	0.8	5	8.426	18.347	29.253		0.6	0.8	10	9.295	33.604	28.288
0.55	0.8	5	8.885	18.72	29.58		0.65	0.8	10	9.606	34.02	28.587
0.6	0.8	5	9.296	19.056	29.915		0.7	0.8	10	9.832	34.37	28.888
0.65	0.8	5	9.65E+00	19.347	30.255		0.75	0.8	10	9.947	34.639	29.186
0.7	0.8	5	9.922	19.579	30.601		0.8	0.8	10	9.92	34.814	29.472
0.75	0.8	5	10.085	19.734	30.948		0.85	0.8	10	9.724	34.896	29.737
0.8	0.8	5	10.1	19.792	31.292		0.9	0.8	10	9.341	34.912	29.968
0.85	0.8	5	9.928	19.745	31.627		0.95	0.8	10	8.767	34.921	30.15
0.9	0.8	5	9.536	19.608	31.943		1	0.8	10	8.019	35.014	30.265
0.95	0.8	5	8.898	19.438	32.229		0.05	0.9	10	1.707	26.978	25.46
1	0.8	5	8.004	19.345	32.475		0.1	0.9	10	2.92	27.698	25.708
0	0.9	5	0.023	13.456	26.2		0.15	0.9	10	3.906	28.395	25.946
0.05	0.9	5	1.694	13.983	26.474		0.2	0.9	10	4.796	29.079	26.179
0.1	0.9	5	2.9	14.579	26.765		0.25	0.9	10	5.64	29.768	26.412
0.15	0.9	5	3.89	15.157	27.067		0.3	0.9	10	6.45	30.47	26.649
0.2	0.9	5	4.784	15.713	27.375		0.35	0.9	10	7.218	31.179	26.893
0.25	0.9	5	5.629	16.266	27.684		0.4	0.9	10	7.933	31.88	27.148
0.3	0.9	5	6.433	16.824	27.995		0.45	0.9	10	8.588	32.555	27.414
0.35	0.9	5	7.192	17.384	28.307		0.5	0.9	10	9.174	33.186	27.693
0.4	0.9	5	7.897	17.931	28.621		0.55	0.9	10	9.687	33.761	27.985
0.45	0.9	5	8.542	18.45	28.938		0.6	0.9	10	10.115	34.271	28.286
0.5	0.9	5	9.124	18.924	29.261		0.65	0.9	10	10.445	34.703	28.595
0.55	0.9	5	9.639	19.344	29.59		0.7	0.9	10	10.655	35.046	28.906
0.6	0.9	5	10.077	19.701	29.928		0.75	0.9	10	10.72	35.284	29.212
0.65	0.9	5	10.425	19.988	30.275		0.8	0.9	10	10.613	35.406	29.505
0.7	0.9	5	10.661	20.191	30.629		0.85	0.9	10	10.317	35.415	29.773
0.75	0.9	5	10.756	20.296	30.985		0.9	0.9	10	9.827	35.343	30.001
0.8	0.9	5	10.681	20.288	31.339		0.95	0.9	10	9.167	35.268	30.171
0.85	0.9	5	10.41	20.165	31.68		1	0.9	10	8.391	35.327	30.264
0.9	0.9	5	9.929	19.954	31.995		0	1	10	0.054	26.339	25.201
0.95	0.9	5	9.243	19.738	32.268		0.05	1	10	1.833	27.09	25.466
1	0.9	5	8.384	19.682	32.48		0.1	1	10	3.058	27.839	25.714
0	1	5	0.075	13.498	26.202		0.15	1	10	4.044	28.55	25.95
0.05	1	5	1.825	14.094	26.466		0.2	1	10	4.948	29.25	26.179
0.1	1	5	3.054	14.728	26.758		0.25	1	10	5.831	29.972	26.407
0.15	1	5	4.056	15.329	27.065		0.3	1	10	6.704	30.73	26.639

x	T(K)	P(bar)	S(J/molK)	H(J/mol)	V(cm3/mol)	-	x.	T (K)	P (bar)	S (J/molK)	H (J/mol)	V (cm3/mol)
0.2	1	5	4.975	15.912	27.38		0.35	1	10	7.555	31.513	26.88
0.25	1	5	5.868	16.507	27.696		0.4	1	10	8.364	32.3	27.133
0.3	1	5	6.742	17.127	28.011		0.45	1	10	9.112	33.059	27.399
0.35	1	5	7.584	17.763	28.326		0.5	1	10	9.783	33.764	27.679
0.4	1	5	8.377	18.393	28.64		0.55	1	10	10.363	34.396	27.973
0.45	1	5	9.103	18.987	28.957		0.6	1	10	10.836	34.94	28.277
0.5	1	5	9.751	19.521	29.278		0.65	1	10	11.183	35.384	28.589
0.55	1	5	10.307	19.975	29.607		0.7	1	10	11.382	35.718	28.903
0.6	1	5	10.76	20.339	29.945		0.75	1	10	11.408	35.929	29.212
0.65	1	5	11.093	20.607	30.293		0.8	1	10	11.239	36.007	29.507
0.7	1	5	11.286	20.77	30.651		0.85	1	10	10.864	35.954	29.776
0.75	1	5	11.317	20.819	31.013		0.9	1	10	10.29	35.805	30.005
0.8	1	5	11.165	20.747	31.373		0.95	1	10	9.554	35.649	30.175
0.85	1	5	10.817	20.558	31.719		1	1	10	8.736	35.658	30.267
0.9	1	5	10.275	20.292	32.036		0	1.1	10	0.159	26.415	25.199
0.95	1	5	9.57	20.053	32.302		0.05	1.1	10	2.015	27.244	25.471
1	1	5	8.764	20.05	32.492		0.1	1.1	10	3.249	28.028	25.722
0	1.1	5	0.156	13.563	26.202		0.15	1.1	10	4.229	28.756	25.958
0.05	1.1	5	1.995	14.239	26.457		0.2	1.1	10	5.138	29.476	26.185
0.1	1.1	5	3.249	14.916	26.752		0.25	1.1	10	6.05	30.235	26.41
0.15	1.1	5	4.262	15.546	27.067		0.3	1.1	10	6.976	31.051	26.64
0.2	1.1	5	5.205	16.163	27.391		0.35	1.1	10	7.896	31.909	26.878
0.25	1.1	5	6.141	16.808	27.717		0.4	1.1	10	8.783	32.777	27.129
0.3	1.1	5	7.077	17.496	28.04		0.45	1.1	10	9.608	33.614	27.393
0.35	1.1	5	7.992	18.213	28.358		0.5	1.1	10	10.348	34.384	27.671
0.4	1.1	5	8.858	18.922	28.674		0.55	1.1	10	10.98	35.061	27.961
0.45	1.1	5	9.648	19.584	28.989		0.6	1.1	10	11.487	35.629	28.262
0.5	1.1	5	10.341	20.163	29.306		0.65	1.1	10	11.848	36.079	28.569
0.55	1.1	5	10.919	20.633	29.63		0.7	1.1	10	12.04	36.403	28.878
0.6	1.1	5	11.368	20.985	29.963		0.75	1.1	10	12.042	36.592	29.182
0.65	1.1	5	11.675	21.216	30.308		0.8	1.1	10	11.833	36.637	29.473
0.7	1.1	5	11.822	21.326	30.663		0.85	1.1	10	11.405	36.538	29.741
0.75	1.1	5	11.796	21.315	31.026		0.9	1.1	10	10.768	36.324	29.974
0.8	1.1	5	11.583	21.184	31.389		0.95	1.1	10	9.962	36.085	30.159
0.85	1.1	5	11.182	20.944	31.74		1	1.1	10	9.07	36.006	30.278
0.9	1.1	5	10.608	20.642	32.061		0	1.2	10	0.289	26.525	25.191
0.95	1.1	5	9.903	20.394	32.328		0.05	1.2	10	2.233	27.439	25.473
1	1.1	5	9.145	20.44	32.512		0.1	1.2	10	3.487	28.265	25.73
0	1.2	5	0.246	13.659	26.197		0.15	1.2	10	4.468	29.016	25.968
0.05	1.2	5	2.187	14.42	26.445		0.2	1.2	10	5.388	29.764	26.197
0.1	1.2	5	3.479	15.148	26.745		0.25	1.2	10	6.329	30.566	26.423
0.15	1.2	5	4.515	15.816	27.071		0.3	1.2	10	7.301	31.442	26.652
0.2	1.2	5	5.489	16.478	27.409		0.35	1.2	10	8.279	32.373	26.89
0.25	1.2	5	6.473	17.183	27.748		0.4	1.2	10	9.227	33.316	27.138
0.3	1.2	5	7.469	17.946	28.08		0.45	1.2	10	10.109	34.219	27.398
0.35	1.2	5	8.448	18.743	28.404		0.5	1.2	10	10.894	35.039	27.67
0.4	1.2	5	9.371	19.527	28.721		0.55	1.2	10	11.559	35.745	27.952
0.45	1.2	5	10.203	20.243	29.033		0.6	1.2	10	12.085	36.324	28.241
0.5	1.2	5	10.916	20.846	29.344		0.65	1.2	10	12.453	36.772	28.534
0.55	1.2	5	11.491	21.31	29.658		0.7	1.2	10	12.644	37.087	28.827
0.6	1.2	5	11.916	21.626	29.981		0.75	1.2	10	12.637	37.266	29.116
0.65	1.2	5	12.181	21.801	30.316		0.8	1.2	10	12.414	37.298	29.395
0.7	1.2	5	12.278	21.847	30.663		0.85	1.2	10	11.963	37.177	29.66
0.75	1.2	5	12.202	21.776	31.021		0.9	1.2	10	11.284	36.915	29.903
0.8	1.2	5	11.948	21.599	31.382		0.95	1.2	10	10.405	36.584	30.117
0.85	1.2	5	11.521	21.33	31.736		1	1.2	10	9.385	36.357	30.294
0.9	1.2	5	10.939	21.014	32.065		0	1.3	10	0.42	26.704	25.182
0.95	1.2	5	10.243	20.766	32.345		0.05	1.3	10	2.462	27.7	25.476
1	1.2	5	9.504	20.832	32.544		0.1	1.3	10	3.751	28.568	25.741
0	1.3	5	0.344	13.827	26.189		0.15	1.3	10	4.751	29.345	25.985

x	T(K)	P(bar)	S(J/molK)	H(J/mol)	V(cm3/mol)	-	x.	T (K)	P (bar)	S (J/molK)	H (J/mol)	V (cm3/mol)
0.05	1.3	5	2.391	14.67	26.432		0.2	1.3	10	5.695	30.124	26.218
0.1	1.3	5	3.734	15.45	26.739		0.25	1.3	10	6.672	30.97	26.448
0.15	1.3	5	4.81	16.162	27.081		0.3	1.3	10	7.689	31.904	26.68
0.2	1.3	5	5.831	16.877	27.436		0.35	1.3	10	8.715	32.899	26.919
0.25	1.3	5	6.871	17.649	27.79		0.4	1.3	10	9.705	33.9	27.165
0.3	1.3	5	7.928	18.488	28.134		0.45	1.3	10	10.618	34.849	27.42
0.35	1.3	5	8.962	19.359	28.466		0.5	1.3	10	11.421	35.695	27.682
0.4	1.3	5	9.925	20.201	28.784		0.55	1.3	10	12.094	36.41	27.949
0.45	1.3	5	10.773	20.947	29.091		0.6	1.3	10	12.62	36.985	28.217
0.5	1.3	5	11.478	21.547	29.392		0.65	1.3	10	12.987	37.425	28.485
0.55	1.3	5	12.021	21.973	29.693		0.7	1.3	10	13.181	37.74	28.751
0.6	1.3	5	12.396	22.227	29.999		0.75	1.3	10	13.185	37.932	29.013
0.65	1.3	5	12.605	22.328	30.316		0.8	1.3	10	12.978	37.986	29.271
0.7	1.3	5	12.649	22.306	30.647		0.85	1.3	10	12.537	37.879	29.528
0.75	1.3	5	12.533	22.187	30.992		0.9	1.3	10	11.841	37.594	29.784
0.8	1.3	5	12.261	21.989	31.347		0.95	1.3	10	10.879	37.158	30.044
0.85	1.3	5	11.836	21.725	31.703		1	1.3	10	9.661	36.699	30.314
0.9	1.3	5	11.27	21.427	32.044		0	1.4	10	0.584	27.026	25.178
0.95	1.3	5	10.581	21.183	32.349		0.05	1.4	10	2.714	28.094	25.484
1	1.3	5	9.808	21.215	32.586		0.1	1.4	10	4.045	29	25.758
0	1.4	5	0.506	14.13	26.18		0.15	1.4	10	5.078	29.804	26.011
0.05	1.4	5	2.638	15.054	26.42		0.2	1.4	10	6.059	30.612	26.252
0.1	1.4	5	4.03	15.889	26.738		0.25	1.4	10	7.079	31.497	26.489
0.15	1.4	5	5.153	16.653	27.098		0.3	1.4	10	8.139	32.475	26.728
0.2	1.4	5	6.232	17.426	27.474		0.35	1.4	10	9.198	33.511	26.97
0.25	1.4	5	7.336	18.264	27.847		0.4	1.4	10	10.206	34.542	27.216
0.3	1.4	5	8.453	19.169	28.207		0.45	1.4	10	11.12	35.502	27.465
0.35	1.4	5	9.531	20.093	28.546		0.5	1.4	10	11.909	36.34	27.713
0.4	1.4	5	10.513	20.962	28.866		0.55	1.4	10	12.559	37.032	27.958
0.45	1.4	5	11.349	21.7	29.167		0.6	1.4	10	13.064	37.583	28.197
0.5	1.4	5	12.013	22.253	29.455		0.65	1.4	10	13.421	38.013	28.428
0.55	1.4	5	12.492	22.601	29.736		0.7	1.4	10	13.628	38.345	28.653
0.6	1.4	5	12.794	22.761	30.019		0.75	1.4	10	13.668	38.585	28.875
0.65	1.4	5	12.932	22.771	30.31		0.8	1.4	10	13.516	38.713	29.102
0.7	1.4	5	12.925	22.684	30.616		0.85	1.4	10	13.126	38.675	29.344
0.75	1.4	5	12.788	22.541	30.94		0.9	1.4	10	12.442	38.404	29.616
0.8	1.4	5	12.527	22.367	31.282		0.95	1.4	10	11.39	37.85	29.939
0.85	1.4	5	12.142	22.161	31.636		1	1.4	10	9.89	37.048	30.337
0.9	1.4	5	11.618	21.923	31.994		0	1.5	10	0.937	27.469	25.172
0.95	1.4	5	10.934	21.688	32.336		0.05	1.5	10	3.098	28.631	25.49
1	1.4	5	10.057	21.605	32.637		0.1	1.5	10	4.445	29.598	25.774
0	1.5	5	0.885	14.524	26.164		0.15	1.5	10	5.501	30.446	26.038
0.05	1.5	5	3.021	15.563	26.404		0.2	1.5	10	6.516	31.292	26.29
0.1	1.5	5	4.422	16.489	26.738		0.25	1.5	10	7.572	32.211	26.539
0.15	1.5	5	5.575	17.332	27.121		0.3	1.5	10	8.659	33.215	26.789
0.2	1.5	5	6.705	18.181	27.521		0.35	1.5	10	9.727	34.26	27.039
0.25	1.5	5	7.867	19.087	27.917		0.4	1.5	10	10.721	35.276	27.287
0.3	1.5	5	9.033	20.043	28.295		0.45	1.5	10	11.596	36.195	27.53
0.35	1.5	5	10.136	20.987	28.645		0.5	1.5	10	12.332	36.972	27.763
0.4	1.5	5	11.108	21.835	28.967		0.55	1.5	10	12.925	37.599	27.981
0.45	1.5	5	11.9	22.506	29.261		0.6	1.5	10	13.386	38.098	28.182
0.5	1.5	5	12.489	22.951	29.532		0.65	1.5	10	13.731	38.513	28.365
0.55	1.5	5	12.875	23.167	29.79		0.7	1.5	10	13.966	38.883	28.537
0.6	1.5	5	13.083	23.19	30.042		0.75	1.5	10	14.08	39.219	28.706
0.65	1.5	5	13.147	23.091	30.299		0.8	1.5	10	14.037	39.486	28.889
0.7	1.5	5	13.104	22.946	30.57		0.85	1.5	10	13.76	39.585	29.109
0.75	1.5	5	12.979	22.816	30.863		0.9	1.5	10	13.135	39.371	29.4
0.8	1.5	5	12.782	22.725	31.184		0.95	1.5	10	11.998	38.677	29.801
0.85	1.5	5	12.493	22.647	31.534		1	1.5	10	10.136	37.386	30.364
0.9	1.5	5	12.058	22.523	31.91							

List of Figures

List of Tables

Bibliography

[1] Lord Kelvin. "On an Absolute Thermometric Scale". In: *Phil. Mag* (1848).

[2] P Kapitza. "Viscosity of liquid helium below the λ-point". In: *Nature* 141.3558 (1938), pp. 74–74.

[3] John F Allen and AD Misener. "Flow of liquid helium II". In: *Nature* 141.3558 (1938), pp. 75–75.

[4] Mike H Anderson et al. "Observation of Bose-Einstein condensation in a dilute atomic vapor". In: *science* 269.5221 (1995), pp. 198–201.

[5] Christian Deppner et al. "Collective-mode enhanced matter-wave optics". In: *Physical Review Letters* 127.10 (2021), p. 100401.

[6] Toshiya Kinoshita, Trevor Wenger, and David S Weiss. "All-optical Bose-Einstein condensation using a compressible crossed dipole trap". In: *Physical Review A* 71.1 (2005), p. 011602.

[7] Laszlo Tisza. "Transport phenomena in helium II". In: *Nature* 141.3577 (1938), pp. 913–913.

[8] Boris Aleksandrovich Mamyrin and Igor Nesterovich Tolstikhin. *Helium isotopes in nature*. Elsevier, 2013.

[9] H Suhl, BT Matthias, and LR Walker. "Bardeen-Cooper-Schrieffer theory of superconductivity in the case of overlapping bands". In: *Physical Review Letters* 3.12 (1959), p. 552.

[10] R Span et al. "A reference quality equation of state for nitrogen". In: *International Journal of Thermophysics* 19.4 (1998), pp. 1121–1132.

[11] JR Roebuck and Harold Osterberg. "The Joule-Thomson effect in helium". In: *Physical Review* 43.1 (1933), p. 60.

[12] Yu Hou et al. "Developments in reverse Brayton cycle cryocooler in China". In: *Cryogenics* 46.5 (2006), pp. 403–407.

[13] TK Nandi and S Sarangi. "Performance and optimization of hydrogen liquefaction cycles". In: *International journal of hydrogen energy* 18.2 (1993), pp. 131–139.

[14] James S Brooks and Russell J Donnelly. "The calculated thermodynamic properties of superfluid helium-4". In: *Journal of Physical and Chemical Reference Data* 6.1 (1977), pp. 51–104.

[15] Eunseong Kim and Moses Hung-Wai Chan. "Probable observation of a supersolid helium phase". In: *Nature* 427.6971 (2004).

[16] Zhi Gang Cheng and John Beamish. "Mass Flow through Solid He 3 in the bcc Phase". In: *Physical Review Letters* 121.22 (2018), p. 225304.

[17] Fritz London. "The λ-phenomenon of liquid helium and the Bose-Einstein degeneracy". In: *Nature* 141.3571 (1938), pp. 643–644.

[18] Laszlo Tisza. "Sur la théorie des liquides quantiques. Application a l'hélium liquide". In: *Journal de Physique et le Radium* 1.5 (1940), pp. 164–172.

[19] L Tisza. "Sur la théorie des liquides quantiques. Application à l'hélium liquide. II". In: *Journal de Physique et le Radium* 1.8 (1940), pp. 350–358.

[20] Fritz London. *Superfluids*. Vol. 1. Dover Publications, 1961.

[21] Fritz London. *Macroscopic Theory of Superfluid Helium*. Dover Publications, 1964.

[22] L Landau. "On the theory of superfluidity". In: *Physical Review* 75.5 (1949), p. 884.

[23] Lev Landau. "The theory of superfluidity of helium II". In: *An Introduction to the Theory of Superfluidity*. CRC Press, 2018, pp. 185–204.

[24] Atsushi Togo and Isao Tanaka. "First principles phonon calculations in materials science". In: *Scripta Materialia* 108 (2015), pp. 1–5.

[25] Alexander L Fetter. "Quantum theory of superfluid vortices. I. Liquid helium II". In: *Physical Review* 162.1 (1967), p. 143.

[26] Robert D McCarty. *Thermophysical Properties of Helium-4 from 2 to 1500 K with Pressures to 1000 Atmospheres*. Vol. 631. US Government Printing Office, 1972.

[27] Robert D McCarty. *The Thermodynamic Properties of Helium II from OK to the Lambda Transitions*. Vol. 1029. US Department of Commerce, National Bureau of Standards, 1981.

[28] Vincent D Arp and Robert D McCarty. *Thermophysical Properties of Helium-4 from 0.8 to 1500 K with Pressures to 2000 MPa*. Tech. rep. National Inst. of Standards and Technology, 1989.

[29] Vincent D Arp. "State equation of liquid helium-4 from 0.8 to 2.5 K". In: *Journal of low temperature physics* 79.1 (1990), pp. 93–114.

[30] VK Samaranayake and G Wilk. *S'-AND D-STATE EFFECTS IN sup3 He FORM FACTORS AND IN p–sup3 He ELASTIC SCATTERING CROSS-SECTION*. Tech. rep. International Centre for Theoretical Physics, Trieste, Italy, 1972.

[31] VD Arp, RD McCarty, and DG Friend. *Thermophysical Properties of Helium-4 from 0.8 to 1500 K with Pressures to 2000 MPa. Tech*. Tech. rep. Note 1334, NIST, Boulder, 1998.

[32] Russell J Donnelly and Carlo F Barenghi. "The observed properties of liquid helium at the saturated vapor pressure". In: *Journal of physical and chemical reference data* 27.6 (1998), pp. 1217–1274.

[33] JL Yarnell et al. "Excitations in liquid helium: neutron scattering measurements". In: *Physical Review* 113.6 (1959), p. 1379.

[34] HW Jackson and E Feenberg. "Perturbation method for low states of a many-particle boson system". In: *Annals of Physics* 15.2 (1961), pp. 266–295.

[35] OW Dietrich et al. "Neutron scattering by rotons in liquid helium". In: *Physical Review A* 5.3 (1972), p. 1377.

[36] V Arp, RD McCarty, and BA Hands. "Computer code HEPAK ver 3.30". In: *CRYODATA, Niwot, CO* (1994).

[37] GR Domenikos, E Rogdakis, and I Koronaki. "Continuous Equation of State and Thermodynamic Maps for Cryogenic Helium 4". In: *ASME International Mechanical Engineering Congress and Exposition*. Vol. 85642. American Society of Mechanical Engineers. 2021, V08BT08A009.

[38] GR Domenikos, E Rogdakis, and I Koronaki. "Studying the Superfluid Transformation in Helium 4 Through the Partition Function and Entropic Behavior". In: *ASME International Mechanical Engineering Congress and Exposition*. Vol. 85642. American Society of Mechanical Engineers. 2021, V08BT08A008.

[39] Diego O Ortiz Vega. "A new wide range equation of state for helium-4". PhD thesis. 2013.

[40] Alessandro Vetere. "Predicting the vapor pressures of pure compounds by using the wagner equation". In: *Fluid Phase Equilibria* 62.1-2 (1991), pp. 1–10.

[41] C.G. Kuper. "On the properties of helium films and superleaks". In: *Physica* 24.6 (1958), pp. 1009–1017. ISSN: 0031-8914. DOI: https://doi.org/10.1016/S0031-8914(58)80118-4. URL: https://www.sciencedirect.com/science/article/pii/S0031891458801184.

[42] G-R Domenikos, P Bitsikas, and E Rogdakis. "Computational Analysis of Cryogenic Stirling Refrigerator". In: *ASME 2019 International Mechanical Engineering Congress and Exposition*. American Society of Mechanical Engineers Digital Collection. 2019.

[43] G-R Domenikos, P Bitsikas, and E Rogdakis. "Thermodynamic Modelling of Superfluid Stirling Cryocoolers". In: *ASME International Mechanical Engineering Congress and Exposition*. Vol. 59438. American Society of Mechanical Engineers. 2019, V006T06A069.

[44] John C Slater. "The normal state of helium". In: *Physical Review* 32.3 (1928), p. 349.

[45] Eunseong Kim and Moses HW Chan. "Observation of superflow in solid helium". In: *Science* 305.5692 (2004), pp. 1941–1944.

[46] Seth J Putterman. "Superfluid hydrodynamics". In: *Amsterdam* 3 (1974).

[47] Jianhua Lin. "Divergence measures based on the Shannon entropy". In: *IEEE Transactions on Information theory* 37.1 (1991), pp. 145–151.

[48] Moochan B Kim et al. "Entropy of the Bose-Einstein-condensate ground state: Correlation versus ground-state entropy". In: *Physical Review A* 97.1 (2018), p. 013605.

[49] Anatoly Svidzinsky et al. "Canonical ensemble ground state and correlation entropy of Bose–Einstein condensate". In: *New Journal of Physics* 20.1 (2018), p. 013002.

[50] Marlan O Scully. "Condensation of N bosons and the laser phase transition analogy". In: *Physical review letters* 82.20 (1999), p. 3927.

[51] Víctor Romero-Rochín and Vanderlei S Bagnato. "Thermodynamics of an ideal gas of bosons harmonically trapped: equation of state and susceptibilities". In: *Brazilian journal of physics* 35 (2005), pp. 607–613.

[52] Bias Cabrera and ME Peskin. "Cooper-pair mass". In: *Physical Review B* 39.10 (1989), p. 6425.

[53] M Mahdavi and B Kaleji. "Deuterium/helium-3 fusion reactors with lithium seeding". In: *Plasma Physics and Controlled Fusion* 51.8 (2009), p. 085003.

[54] YH Huang, GB Chen, and VD Arp. "Equation of state for fluid helium-3 based on Debye phonon model". In: *Applied physics letters* 88.9 (2006), p. 091905.

[55] Yonghua Huang, Guobang Chen, and Vincent Arp. "Debye equation of state for fluid helium-3". In: *The Journal of chemical physics* 125.5 (2006), p. 054505.

[56] RH Sherman and FJ Edeskuty. "Pressure-Volume-Temperature relations of liquid He3 from 1.00 to 3.30° K". In: *Annals of Physics* 9.4 (1960), pp. 522–547.

[57] Thomas R Roberts and Stephen G Sydoriak. "Thermomolecular pressure ratios for He 3 and He 4". In: *Physical Review* 102.2 (1956), p. 304.

[58] Henry L Laquer, Stephen G Sydoriak, and Thomas R Roberts. "Sound velocity and adiabatic compressibility of liquid helium three". In: *Physical Review* 113.2 (1959), p. 417.

[59] KR Atkins and H Flicker. "VELOCITY OF SOUND IN LIQUID He *sup3*". In: *Physical Review (US) Superseded in part by Phys. Rev. A, Phys. Rev. B: Solid State, Phys. Rev. C, and Phys. Rev. D* 113 (1959).

[60] V.V. Tolmachev. "Superconducting Bose–Einstein condensates of Cooper pairs interacting with electrons". In: *Physics Letters A* 266.4 (2000), pp. 400–408. ISSN: 0375-9601. DOI: https://doi.org/10.1016/S0375-9601(00)00079-7. URL: https://www.sciencedirect.com/science/article/pii/S0375960100000797.

[61] Dieter Vollhardt and Peter Wolfle. *The superfluid phases of helium 3*. Courier Corporation, 2013.

[62] Masayuki Matsuo. "Spatial structure of neutron Cooper pair in low density uniform matter". In: *Physical Review C* 73.4 (2006), p. 044309.

[63] R Baquero, D Quesada, and C Trallero-Giner. "BCS-universal ratios within the Van Hove scenario". In: *Physica C: Superconductivity* 271.1-2 (1996), pp. 122–126.

[64] JA Lipa and TCP Chui. "Very high-resolution heat-capacity measurements near the lambda point of helium". In: *Physical review letters* 51.25 (1983), p. 2291.

[65] GR Domenikos, E Rogdakis, and I Koronaki. "Thermodynamic Correlation of the Entropy of Bose-Einstein Condensation transition to the lambda points of Superfluids". In: *Journal of Energy Resources Technology* (2022). (in press), to appear.

[66] Athina STEGOU-SAGİA and M Damanakis. "Thermophysical property formulations for R32/R134a mixtures". In: *International Journal of Thermodynamics* 2.3 (1999), pp. 139–143.

[67] J Del Cueto et al. "Experiments in 3He-4He liquid mixtures near the tricritical point". In: *Le Journal de Physique Colloques* 41.C7 (1980), pp. C7–133.

[68] Shinichi Yorozu et al. "Phase-separation curve of- 4 3 He mixtures under pressure". In: *Physical Review B* 45.22 (1992), p. 12942.

[69] C Boghosian and H Meyer. "Density of a dilute 3He-4He solution under pressure". In: *Physics Letters A* 25.5 (1967), pp. 352–353.

[70] J Landau et al. "Temperature, Pressure, and Concentration Dependence of the Osmotic Pressure of Dilute He 3-He 4 Mixtures". In: *Physical Review A* 2.6 (1970), p. 2472.

[71] Gunaranjan Chaudhry and JG Brisson. "Thermodynamic properties of liquid 3he-4he mixtures between 0.15 k and 1.8 k". In: *Journal of Low Temperature Physics* 155.5 (2009), pp. 235–289.

[72] Anssi Salmela et al. "Osmotic pressure of He 3/He 4 mixtures at the crystallization pressure and at millikelvin temperatures". In: *Physical Review B* 83.13 (2011), p. 134510.

[73] CG Kuper. "On the properties of helium films and superleaks". In: *Physica* 24.6-10 (1958), pp. 1009–1017.

[74] Ray Radebaugh. *Thermodynamic properties of HE3-HE4 solutions with applications to the HE3-HE4 dilution refrigerator*. Vol. 362. US Department of Commerce, National Bureau of Standards, 1967.

[75] OV Lounasmaa. "Dilution refrigeration". In: *Journal of Physics E: Scientific Instruments* 12.8 (1979), p. 668.

[76] SB Trickey, WP Kirk, and ED Adams. "Thermodynamic, elastic, and magnetic properties of solid helium". In: *Reviews of Modern Physics* 44.4 (1972), p. 668.

[77] John Beamish. "Supersolid helium". In: *Nature* 427.6971 (2004), pp. 204–205.

[78] RA Aziz et al. "An accurate intermolecular potential for helium". In: *The Journal of Chemical Physics* 70.9 (1979), pp. 4330–4342.

[79] HR Glyde. "Relation of vacancy formation and migration energies to the Debye temperature in solids". In: *Journal of Physics and Chemistry of Solids* 28.10 (1967), pp. 2061–2065.

[80] JG Brisson and GW Swift. "A recuperative superfluid Stirling refrigerator". In: *Advances in cryogenic engineering*. Springer, 1994, pp. 1393–1397.

[81] JG Brisson and AB Patel. "A simple model for a superfluid Stirling refrigerator at high operating temperature". In: *Journal of low temperature physics* 116.5 (1999), pp. 443–475.

[82] Ashok B Patel and JG Brisson. "Experimental performance of a single stage superfluid Stirling refrigerator using a small plastic recuperator". In: *Journal of low temperature physics* 111.1 (1998), pp. 201–212.

[83] V Kotsubo and GW Swift. "Superfluid Stirling-cycle refrigeration below 1 Kelvin". In: *Journal of low temperature physics* 83.3 (1991), pp. 217–224.

[84] Israel Urieli and David M Berchowitz. "Stirling cycle engine analysis". In: (1984).

[85] E Rogdakis, P Bitsikas, and G Dogkas. "Numerical Simulation of Prime Mover Stirling Engine by Finite Volume Method". In: *International Stirling Engine Conference, Newcastle, UK, pp451-464*. 2016.

[86] E Rogdakis, P Bitsikas, and G Dogkas. "Three-Dimensional CFD Simulation of Prime Mover Stirling Engine". In: *ASME International Mechanical Engineering Congress and Exposition*. Vol. 58417. American Society of Mechanical Engineers. 2017, V006T08A071.

[87] N Borbilas. "Thermodynamic analysis of Stirling cycle". PhD thesis. 2004.

[88] F Rondeaux, Ph Bredy, and JM Rey. "Thermal conductivity measurements of epoxy systems at low temperature". In: *AIP Conference Proceedings*. Vol. 614. 1. American Institute of Physics. 2002, pp. 197–203.

[89] Marco Barucci et al. "Low temperature thermal conductivity of Kapton and Upilex". In: *Cryogenics* 40.2 (2000), pp. 145–147.

[90] GR Domenikos, E Rogdakis, and I Koronaki. "Thermodynamic Behavior and Equation of State for Cryogenic Helium 3-4 Mixtures". In: *ASME International Mechanical Engineering Congress and Exposition*. Vol. 85642. American Society of Mechanical Engineers. 2021, V08BT08A010.

[91] Jorge J Moré. "The Levenberg-Marquardt algorithm: implementation and theory". In: *Numerical analysis*. Springer, 1978, pp. 105–116.

[92] A Stegou-Sagia and N Paignigiannis. "Evaluation of mixtures efficiency in refrigerating systems". In: *Energy Conversion and Management* 46.17 (2005), pp. 2787–2802.

[93] A Stegou-Sagia. "A computational method for the methyl amine/H {sub 2} gas mixture concentrations in methyl amine H {sub 2} O/H {sub 2} absorption refrigeration units". In: *Applied Thermal Engineering* 16 (1996).

[94] E Rogdakis et al. "Three-dimensional CFD study of a β-type Stirling Engine". In: *Thermal Science and Engineering Progress* 11 (2019), pp. 302–316.